



Proceedings of the 14th International Congress of the International Radiation Protection Association

Cape Town, South Africa
9 – 13 May 2016

Volume 2 of 5

3- Medical

4- General Ionising Radiation Protection

Organised in collaboration with:



International Labour Office



INTERNATIONAL SOCIETY OF
RADIOGRAPHERS &
RADIOLOGICAL
TECHNOLOGISTS



Pan American
Health
Organization



United Nations Scientific Committee
on the Effects of Atomic Radiation



World Health
Organization

The Proceedings of the 14th International Congress of the International Radiation Protection Association are divided into 5 volumes, as follows:

Volume 1 of 5

Area 1: Fundamental Science
Area 2: Policy, Standards and Culture

Volume 2 of 5

Area 3: Medical
Area 4: General Ionising Radiation Protection

Volume 3 of 5

Area 5: Optimisation and Design of New Facilities
Area 6: Radiation Detection and Dosimetry

Volume 4 of 5

Area 7: Environment and Natural Background
Area 8: Transport / Sealed Source Management
Area 9: Non-ionising Radiation

Volume 5 of 5

Area 10: Emergency Preparedness and Management
Area 11: Decommissioning, Waste Management and Remediation
Area 12: Societies

Proceedings of the 14th International Congress of the International Radiation Protection Association

EDITORIAL TEAM

Christopher Clement, Jack Valentin,
Haruyuki Ogino, Devon Foote, Julie Reyjal,
Laila Omar-Nazir

Published by
The International Radiation Protection Association



www.irpa.net

© 2017 International Radiation Protection Association

ISBN 978-0-9989666-2-5

Table of Contents

VOLUME 1

IRPA14 Membership List

Editorial

Preface

How to Protect the Public When You Can't Measure the Risk -- The Role of Radiation Epidemiology Author: John D. Boice, Jr.....	1
What Can We Learn from Studies of Nuclear Workers? Author: Ethel Gilbert.....	2
Area 1: Fundamental Science	3
Attenuation Coefficients of Some Species of Wood Authors: Chioma Nwankwo, Olatunde Oni, Folorunso Ogundare.....	4
Scoping Study of Possible Chronic Health Effects for Workers at the Rössing Uranium Mine Authors: Douglas Chambers, Gunhild von Oertzen, Paul J. Villeneuve, Ron Stager, Sylvain Saint Pierre	11
Pregnancy Outcomes in Women Exposed Along the Techa River Authors: Elena Pastukhova, Sergey Shalaginov, Alexander Akleyev.....	18
Amelioration of radiation-induced DNA damage in human and animal cells mediated by natural compounds of plant and animal origin Authors: Goran Gajski, Marko Gerić, Branka Mihaljević, Saveta Miljanić, Vera Garaj-Vrhovac	26
Ionizing Radiation and Metastasis: The Dark Side of a Keystone Treatment in Cancer Authors: Guadalupe Vedoya, Nora Mohamad, Mónica Táquez Delgado, Tamara Galarza, Rosa Bergoc, Ernesto Crescenti, Graciela Cricco, Gabriela Martín	31
Concentrations of Radiocesium and ⁹⁰Sr in Agricultural Plants Collected from Local Markets and Experimental Fields before Resuming Agriculture in Fukushima Prefecture Authors: Hirofumi Tsukada, Tomoyuki Takahashi, Satoshi Fukutani, Makoto Akashi	37
The Detriment in Radiation Protection Authors: Jonas Buermeyer, Samaneh Emami, Kaija Spruck, Joachim Breckow.....	43
Establishment of Concentration Ratios Riparian and Shrub Steppe Areas of the Eastern Washington Columbia Basin Authors: Jonathan Napier, Elizabeth Reudig, Leah Minc, David Bytwerk, Kathryn Higley	48
Development of a Standard Procedure for the Irradiation of Biomolecules Authors: Marc Benjamin Hahn, Tihomir Solomun, Susan Meyer, Hans-Jörg Kunte, Maria-Astrid Schröter, Heinz Sturm.....	56
Modelling the decrease in ambient dose rate from the Chernobyl fallout using data from the Swedish municipality measurement system Authors: Mattias Jönsson, Martin Tondel, Mats Isaksson, Robert Finck, Robert Wälinder, Afrah Mamour, Christopher Rääf	60
Reconstruction of the Montenegro territory contamination with ²³⁸Pu using ²³⁸Pu/²³⁹⁺²⁴⁰Pu activity ratio Authors: Nevenka M. Antović, Perko Vukotić, Nikola Svrkota	66
A probabilistic/stochastic model for contamination levels of Cs-137 in wild boars Authors: Philipp Hartmann, Laura Urso, Ulrich Fielitz, Martin Steiner	74
Results of proficiency test using radioactive brown rice sample contaminated by the accident at Fukushima Daiichi Nuclear Power Plant Authors: Rio Furukawa, Yasuhiro Unno, Akira Yunoki, Shioka Hamamatsu, Mayumi Hachinohe, Tsutomu Miura, Masayuki Mizui, Hidesuke Itadzu	81
The non-linear effects of low dose ionizing radiation on the eye lens and the tools needed to determine Authors: Roy A. Quinlan; Alexia Kalligeraki, Miguel Jarrin, Robert Pal.....	89
Shielding design for reducing secondary neutron doses to paediatric patients during intracranial proton therapy: Monte Carlo simulation of the neutron energy spectrum and its organ doses Authors: Shinnosuke Matsumoto, Koba Yusuke, Kohno Ryosuke, Choonsik Lee, Wesley E. Bolch, Michiaki Kai.....	96
A Study on UF₆ Transportation Accident Scenarios and Diffusion Model Authors: Shutang Sun, Guoqiang Li, Hongchao Sun, Feng Yan, Jiangang Zhang.....	102

Optimization of Sr/Y-90 measurement instrument for contaminated mixture sample without chemical separation	
<i>Authors: Yasuhiro Unno, Toshiya Sanami, Shinichi Sasaki, Masayuki Hagiwara, Akira Yunoki</i>	108
Development of Integrated Nuclear Emergency Command and Decision Support System for Nuclear Power Plant	
<i>Authors: Yang Yapeng, Zhang Jiangang, Feng Zongyang, Tang Rongyao, Jia Linsheng, Xu Xiaoxiao</i>	114
Cognitive and Cerebrovascular Effects Induced by Low Dose Ionizing Radiation 'CEREBRAD' (Grant agreement: 295552)	
<i>Author: Abderrafi Benotmane</i>	121
Evaluation of the Effect of Low and Intermediate Frequency Electromagnetic Waves on Radiosensitivity	
<i>Authors: Angela Chinhengo, Antonio Serafin, Bianca Hamman, John Akudugu</i>	122
Educational and Occupational Outcomes of Childhood Cancer Survivors 30 Years after Irradiation	
<i>Authors: Agnes Dumas, Claire Berger, Pascal Auquier, Gérard Michel, Brice Fresneau, Rodrigue Allodji, Nadia Haddy, Carole Rubino, Gilles Vassal, Dominique Valteau- Couanet, Sandrine Thouvenin-Doulet, Leonie Casagrande, H�el�ene Pacquement, Chiraz El-Fayech, Odile Oberlin, Catherine Guibout, Florent De Vathaire</i>	123
Radiation Survival Curve for Paediatrics Rhabdomyosarcoma Cells	
<i>Authors: Alexander F. Ibrahim, Siddig T. Kafi, Omer F. Idris</i>	124
How Nuclear Issues are Imagined: Social Perception in Relation to Radiation Protection	
<i>Author: Alejandro Igor Margetic</i>	125
Chromosomal Aberrations and Telomere Dysfunction Induced by Low Dose- irradiation Measured by Telomere and Centromere Staining	
<i>Authors: Akram Kaddour, Bruno Colicchio, Luc Morat, Corina Cuceu, Elie El Malouf, Monika Frenzel, Leonhard Heidingsfelder, Eric Laplagne, William Hempel, Mich�ele Elmay, Laure Sabatier, Radhia M'kacher</i>	126
Transmission of Induced Chromosomal Aberrations and Telomere Dysfunction through Successive Mitotic Divisions in Human Lymphocytes after In Vitro Exposure Measured by Telomere and Centromere Staining	
<i>Authors: Akram Kaddour, Bruno Colicchio, Diane Baron, Corina Cuceu, Monika Frenzel, Luc Morat, Eric Laplane, William Hempel, Laure Sabatier, Radhia M'kacher</i>	127
EPI-CT - European Cohort Study of Paediatric CT Risks: Challenges, Achievements and Perspectives	
<i>Authors: Ausrele Kesminiene, Sarah Baatout, Elisabeth Cardis, Michael Hauptmann, Andreas Jahnen, Magnus Kaijser, Carlo Maccia, Mark Pearce, Isabelle Thierry-Chef</i>	128
DNA Double Strand Break Formation and Repair in Human Fibroblasts Continuously Exposed to X-ray Radiation	
<i>Authors: Andreyan Osipov, Anna Grekhova, Margarita Pustovalova, Ivan Ozerov, Petr Eremin, Natalia Vorobyeva, Dmitry Klovok</i>	129
DNA Double-strand Break Repair in Mammalian Cells Exposed to Low-LET Radiation at Low Doses: The Controversy Continues	
<i>Authors: Andreyan Osipov, Aleksandr Samoylov, Andrey Bushmanov, Dmitry Klovok</i>	130
The ANDANTE Project: A Multidisciplinary Evaluation of the Risk from Neutrons Relative to Photons	
<i>Authors: Andrea Ottolenghi, Giorgio Baiocco, Vere Smyth, Klaus Trott</i>	131
Morphological and Molecular Analysis of Radiation-Induced Posterior Capsule Opacification (PCO) of the Lens	
<i>Authors: Andr�es Rossini, Severino Michelin, Marta Bouchez, Ana Julia Molinari, Diana Dubner, Marina DiGiorgio</i>	132
Muscular Pathology due to High Dose Irradiation in Human Muscle	
<i>Authors: Alhondra Solares-P�erez, Val�erie Allamand, Ga�etan Gruel, Fran�ois Trompier, Gillian Butler-Browne, Vincent Mouly, Marc Benderitter, Eric Bey, St�ephane Flamant, Radia Tamarat</i>	133
Alveolar Macrophages as a Key Target for Decorporating Agents Following Pulmonary Contamination with Moderately Soluble Actinides	
<i>Authors: Anne Van der Meeren, Olivier Gr�emy, Agn�es Moureau, David Laurent, Nina Griffiths, Pierre Laroche, Jaime F. Angulo-Mora</i>	134

Refinement of In Vitro Approaches for Radiotoxicological Studies to Predict Actinide Bioavailability In Vivo <i>Authors: Anne Van der Meeren, Olivier Grémy, Pierre Laroche, Jaime Angulo, Nina Griffiths</i>	135
Effect of Natural Chronic Low Dose Radiation on Human Population Residing in High Background Radiation Areas of Kerala Coast, in Southwest India <i>Author: Birajlaxmi Das</i>	136
Radiomodifying Effects of Medicinal Plants <i>Centella asiatica</i> and <i>Withania somnifera</i> <i>Authors: Bianca Hamman, Antonio Serafin, Angela Chinhengo, Vikash Sewram, John Akudugu</i>	137
R Highlights of the Russian Health Studies Program and Updated Research Findings <i>Author: Barrett N. Fountos</i>	138
Modifying the Cytokinesis-Block Micronucleus Assay for Triage Biodosimetry <i>Authors: Christina Beinke, Matthias Port, Armin Riecke, Christian Ruf, Michael Abend, Harry Scherthan</i>	139
Ionising Radiation Biological Markers for Health Risk Prediction <i>Author: Coretchi Liuba</i>	140
Sustainable Development and Nuclear Law in Argentina <i>Authors: Cecilia Tula, Mariana Arias</i>	141
Design, Development and Application of a Desk-Top Laser Produced Plasma X- Ray Source for Radiobiology Studies <i>Authors: Daniel Adjei, Anna Wiechec, Przemyslaw Wachulak, Mesfin Getachew Ayele, Janusz Lekki Wojciech M. Kwiatek, Marie Davidková, Andrzej Bartnik, Henryk Fiedorowicz, Ladislav Pina, Jakub Svobod</i>	142
Low Dose Effect Research at the Electric Power Research Institute <i>Author: Donald Cool</i>	143
Role of Radiation Dose in Cardiac and Cerebrovascular Disease Risk following Childhood Cancer: Results from CEREBRAD and PROCARDIO FP7-European Projects <i>Authors: Florent de Vathaire, Rodrigue Allodji, Giao Vu-Bezin, Florent Dayet, Damien Llanas, Cristina Veres, Mohamedamine Benadjaoud, Rafi Benotmane, Mike Atkinson, Mike Hawkins, Leontien Kremer, Elisabeth Cardis, David Winter, Lieke Feijen, Elisa Pasqual, Nadia Haddy, Ibrahima Diallo</i>	144
Dose-related Effects of Long-term Radiation Exposure on Aquatic Biota within the Chernobyl Exclusion Zone: 30 years after accident <i>Authors: Dmitri Gudkov, Natalia Shevtsova, Natalia Pomortseva, Elena Dzyubenko, Alexander Kaglyan, Alexander Nazarov</i>	145
R The International Nuclear Workers Study (INWORKS): a collaborative epidemiological study to improve knowledge about health effects of protracted low dose exposure <i>Authors: Dominique Laurier, David B Richardson, Elisabeth Cardis, Robert D Daniels, Michael Gillies, Jackie O'Hagan, Ghassan B Hamra, Richard Haylock, Klervi Leuraud, Monika Moissonnier, Mary K Schubauer-Berigan, Isabelle Thierry-Chef, Ausrele Kesminiene</i>	146
R Estimates of Radiation Effects on Cancer Risks in The Mayak Worker, Techa River and Atomic Bomb Survivor Studies <i>Authors: Dale L. Preston, Mikhail E. Sokolnikov, Lyudmila Yu. Krestinina, Daniel O. Stram</i>	147
Study on Cytotoxic Effects of the Auger Electron Emitter Technetium-99m in Functional Rat Thyroid Cells <i>Authors: Dominik Oskamp, Marcus Unverricht-Yeboah, Anugrah Gawai, Roshni Murali, Ekkehard Pomplun, Ralf Kriehuber</i>	148
R The Growth of Biostatistics and Estimation of Cancer Risk Estimates: Past, Current, and Future Challenges <i>Authors: Daniel O. Stram, Dale Preston</i>	149
External Irradiation of the Thyroid Results in Non-Targeted Transcriptional Response in the Kidneys and Liver <i>Authors: Eva Forssell-Aronsson, Britta Langen, Nils Rudqvist, Johan Spetz, Johan Swanpalmer, Khalil Helou</i>	150

Genome-wide Transcriptional Response in Normal Tissues are Influenced by Time of Day of I.V. Injection of ¹³¹I in Mice <i>Authors: Eva Forssell-Aronsson, Britta Langen, Nils Rudqvist, Toshima Z Parris, Khalil Helou</i>	151
R The potential impact of circadian rhythms on paediatric medical imaging and radiotherapy <i>Authors: Eva Forssell-Aronsson, Roy A Quinlan</i>	152
DS02R1: Improvements to Atomic Bomb Survivors' Input Data and Implementation of Dosimetry System 2002 (DS02) and Resulting Changes in Estimated Doses <i>Authors: Eric Grant, Kotaro Ozasa, Harry Cullings</i>	153
Solid cancer incidence among the Life Span Study of atomic bomb survivors: 1958-2009 <i>Authors: Eric J. Grant, Kotaro Ozasa</i>	154
Protein Status in Atomic Workers in Distant Period after Long-term Occupational Combined Low-dose Exposure <i>Authors: Evgeniia Kirillova, Maria Zakharova, Taisa Uryadnitskaya, Christopher Loffredo</i>	155
Cancer Incidence among Mayak Workers <i>Authors: Elena Labutina, Nezahat Hunter, Irina Kuznetsova</i>	156
Comparison of Total Antioxidant Capacity level between radiation workers in diagnostic radiology and other staffs of hospital in Zahedan <i>Authors: Fatemeh Ramrodi, Farnaz Farifteh, Amir Hossein Zarghami, AliReza Nakhaee, Dariush Askari, Jalal Ordoni, Yazdan Salimi, Mohammad Hossein Jamshidi, Hamed Dehghani</i>	157
Effects of Radon Inhalation on Biophysical Properties of Blood in Rats <i>Authors: Fayez Shahin, Omar Abdel-Salam</i>	158
Assessment of Respiratory Toxicity of ITER-like Tungsten Metal Nanoparticles using an in vitro 3D Human Airway Epithelium Model <i>Authors: George Isabelle, Hagege Agnès, Herlin Nathalie, Vrel Dominique, Rose Jérôme, Sanles Marcos, Orsiere Thierry, Uboldi Chiara, Grisolia Christian, Rousseau Bernard, Malard Véronique</i>	159
Beyond Paternalism and Strategy: Understanding Radiological Risks as a Mutual Learning Experience <i>Authors: Gaston Meskens, Tanja Perko</i>	160
Survey of the Effect of Ionizing Radiation Energy on the Blood Indices of Occupationally Exposed Staff (radiologic technologists and radiologists) <i>Authors: Hamid Behrozi, Mohammad Hossein Jamshidi, Kimia Benabbas, Marziyeh Daemolzeqr, Yazdan Salimi, Dariush Askari, Jalal Ordoni, Hamed Dehghani</i>	161
Development of Radiological Protection Powder <i>Authors: Hiroki Ohtani, Yuya Ishita</i>	162
Risk of Thyroid Cancer Incidence due to Living Close to Atomic Facility in Childhood <i>Authors: Irina Martinenko, Mikhail Sokolnikov</i>	163
Retrospective Estimation of Organ Doses for an Epidemiology Study of CT Scanning in Paediatric Patients (EPI-CT) <i>Authors: Isabelle Thierry-Chef, Jérémie Dabin, Joahannes Hermen, Tore S. Istad, Andreas Jahnen, Lucian Krille, Choonsik Lee, Carlo Maccia, Arvid Nordenskjöld, Hilde Olerud, Steven L Simon, Lara Struelens, Ausrele Kesminiene</i>	164
Biological Dosimetry after Total Body Irradiation (TBI) for Hematologic Malignancy Patients using Premature Chromosomal Condensation in Combination with Fluorescence in Situ Hybridization <i>Authors: Julien Dossou, Dominique Violot, Theodore Girinsky, Patrice Carde, Jean-Henri Bourhis, Claude Parmentier, Radhia M'kacher</i>	165
Doses and risks from radon and other internal emitters and their control <i>Author: John Harrison</i>	166

Synthesis of Novel Psammaplin A-based Radiosensitizers <i>Authors: Jin Ho Kim, Chan Woo Wee, Hak Jae Kim, Soo Youn Suh, Eun Sook Ma, Boom Soo Shin, Il Han Kim</i>	167
Responses to Radiation and Fate of Cells <i>Authors: Jin Kyu Kim, Mi Young Kang, Remigius A. Kawala, Tae Ho Ryu, Jin-Hong Kim</i>	168
Radiation-Induced p53 Level Determines Radiosensitivity of Cells <i>Authors: Jin Kyu Kim, Min Young Kang, Yun-Jong Lee, Jin-Hong Kim, Jacobus P. Slabbert</i>	169
Development and Validation of a Multivariate Calibration Strategy for Direct Analysis of Trace Elements in Soft Tissue Utilizing Chemometric Energy Dispersive X-Ray Fluorescence and Scattering (EDXRFS) Spectroscopy <i>Authors: Justus Okonda, Angeyo Kalambuka, Seth Kisia, Michael Mangala</i>	170
Radiation Shielding perfection at Design and construction Stages <i>Author: Joseph Rugut</i>	171
Application of the Spencer-Attix Cavity Theory for Determination of Conversion Coefficient for Ambient Equivalent Dose with TLD-100 Dosimeters Calibrated in Air Kerma <i>Authors: Jose T Alvarez Romero, Fernando Gonzalez Jimenez</i>	172
Evaluation of Fission Energy Deposition in the SAFARI-I Nuclear Reactor <i>Authors: Linina Jurbandam, Oscar Zamonsky</i>	173
Lung Cancer Risk from Radon and Smoking – Additive or Multiplicative Effect <i>Author: Ladislav Tomasek</i>	174
Risk of Leukemia in Uranium Miners <i>Author: Ladislav Tomasek</i>	175
Chronic Bronchitis Incidence in the Cohort of Mayak Production Association Workers Occupationally Exposed to Radiation <i>Authors: Tamara Azizova, Galina Zhuntova, Richard Haylock, Maria Moseeva, Evgenia Grigorieva, Maria Bannikova, Zinaida Belyaeva, Evgeniy Bragin</i>	176
Microdosimetric Measurements for Electron Irradiation of DNA under Physiological Conditions: Low Energy Electrons vs. Radicals <i>Authors: Marc Benjamin Hahn, Tihomir Solomun, Susan Meyer, Hans-Joerg Kunte, Heinz Sturm</i>	177
Markers of Neural Degeneration and Regeneration in Blood of Cardiac Catheterization Personals <i>Authors: Mohamed ElKhafif, Soheir Korraa, Nevine Noussier, Walid Elhammady, Eman El Gazzar, Hanan Diab</i>	178
Regulatory Culture and its Role in Radiation Protection <i>Authors: Marcela Ermacora, Chris Englefield</i>	179
The Hybrid Analytical – Voxel Head Phantom for Activity Measurement of ²⁴¹Am in Cranial Bone <i>Author: Marko Fulop</i>	180
Occupational and Medical Exposure: The Contribution to Carcinogenic Risk In Mayak Worker Cohort <i>Authors: Mikhail Osipov, Mikhail Sokolnikov</i>	181
Baseline Lifetime Mortality Risk from Circulatory Disease in Japan <i>Authors: Michiya Sasaki, Haruyuki Ogino, Takatoshi Hattori</i>	182
DNA Repair Genes XRCC1 and XRCC3 Polymorphisms and the Level of Micronuclei in Industrial Radiographers <i>Authors: Mahsa Shakeri, Farideh Zakeri, Vahid Changizi, Mohammad Reza Farshidpour, Mohammad Reza Rajabpour</i>	183
Mayak Worker Cancer Mortality <i>Authors: Mikhail Sokolnikov, Dale Preston, Dan Stram</i>	184

Repair of Ionizing Radiation-Induced DNA Damage and Risk of Second Cancer in Childhood Cancer Survivors <i>Authors: Nadia Haddy, Laurence Tartier, Serge Koscielny, Elisabeth Adjadj, Carole Rubino, Laurence Brugières, Hélène Pacquement, Ibrahima Diallo, Florent de Vathaire, Dietrich Aeverbeck, Janet Hall, Simone Benhamou...</i>	
The Role of the Scientific Review Group in the Russian Health Studies Programs: Key Contributions and Influence and Impact on Radiation Protection <i>Author: Nolan Hertel</i>	186
A Comprehensive Study on Tritium Release from Nuclear Accidents and Impact of Tritiated Water on Postnatal Development of Mouse Cerebellum <i>Authors: Narendra Jain, A. L. Bhati</i>	187
Current State of Pharmacologic Radioprotection for Clinical Exposure to Ionizing Radiation <i>Authors: Nivethan Vela, Joe Barfett, Kieran Murphy, David Mikulis</i>	188
Ameliorating Effects of Bone Marrow Transplantation and Zinc Supplementation on Physiological and Immunological Changes in γ-Irradiated Rats <i>Authors: Omaima Ashry, Maha Soliman, Mervat Ahmed, Yasmin Abd El Naby</i>	189
Occupational Exposure to ^7Be – A Case Study <i>Authors: Ofer Aviv, Hanan Datz, Shlomi Halfon, Zohar Yungrais, Erez Daniely</i>	190
Early and Late Alterations of Neurochemical, Behavioral, and Somatic Criteria in Rats Exposed to ^{12}C ions and γ-rays <i>Authors: Oleg Belov, Ksenia Belokopytova, Ara Bazyan, Vladimir Kudrin, Viktor Narkevich, Aleksandr Ivanov, Gennady Timoshenko, Eugene Krasavin</i>	191
Integrating Dosimetry, Radiobiology and Epidemiology to study the Effects of Occupational Exposure to Uranium in Europe: the CURE Project <i>Authors: Olivier Laurent, Maria Gomolka, Richard Haylock, Eric Blanchardon, Augusto Giussani, Will Atkinson, Derek Bingham, Sarah Baatout, Ladislav Tomasek, Elisabeth Cardis, Janet Hall, Dominique Laurier</i>	192
Investigations of radiation exposures in the aftermath of the Chernobyl accident <i>Author: Rolf Michel</i>	193
A New Tool for Genotoxic Risk Assessment: Re-evaluation of Cytokinesis-Block Micronucleus Assay using Semi-Automated Scoring following Telomere and Centromere Staining <i>Authors: Radhia M'kacher, Narjes Zaguia, Francis Finot, Luc Morat, André Essahli, Corina Cuceu, Bruno Colicchio, Leonhard Heidingsfelder, Eric Laplagne, William Hempel, Laure Sabatier</i>	194
Change in Peripheral Blood Lymphocyte Telomere Length and the Occurrence of Secondary Cancers in Hodgkin Lymphoma Patients <i>Authors: Radhia M'kacher, Theodore Girinsky, Bruno Colicchio, Michelle Ricoul, Corina Cuceu, Luc Morat, Monika Frenzel, Aude Lenain, Leonhard Heidingsfelder, William Hempel, Alain Dieterlen, Laure Sabatier, Patrice Carde</i>	195
Radiation Dose to the Eyes in the Risk of Cataract after Non-Retinoblastoma Solid Childhood Cancers <i>Authors: Rodrigue Sètchéou Allodji, Chiraz El-Fayech, Amar Kahlouche, Boris Schwartz, Odile Oberlin, Mohamed Benadjaoud, Julien Bullet, Ibrahima Diallo, Carole Rubino, Nadia Haddy, Florent de Vathaire</i>	196
Risk of Subsequent Leukaemia after a Solid Tumour in Childhood: Radiotherapy and Chemotherapy Side Effects <i>Authors: Rodrigue Sètchéou Allodji, Boris Schwartz, Cristina Veres, Nadia Haddy, Carole Rubino, Marie-Cécile Le Deley, Jérémie Vu Bezin, Jean Chavaudra, Dimitri Lefkopoulos, Eric Deutsch, Odile Oberlin, Ibrahima Diallo, Florent de Vathaire</i>	197
Simulation-extrapolation Method to Address Errors in Atomic Bomb Survivor Dosimetry on Solid Cancer and Leukaemia Mortality Risk Estimates, 1950-2003 <i>Authors: Rodrigue Sètchéou Allodji, Boris Schwartz, Ibrahima Diallo, Dominique Laurier, Florent de Vathaire</i>	198
Chernobyl, 30 Years on – Health Effects <i>Author: Richard Wakeford</i>	199
Immunological Monitoring of the Personnel at Radiation Hazardous Facilities <i>Authors: S.M. Kiselev, M.E. Sokolnikov, L.V. Lyss, N. I. Ilyina</i>	200

Raman Spectroscopy as an Analytical Tool for Ionizing Effect Studies in Pig Lens “Ex Vivo” and “In Vitro” <i>Authors: Severino Michelin, Andres Rossini, Emilia Halac, Diana Dubner, Ana Molinari</i>	201
Current Status of the Biological Study on Low-Dose Ionizing Radiation Effects in KHNP-RHI, Korea <i>Authors: Seon Young Nam, Kwang Hee Yang</i>	202
Role of AKT and ERK Pathway in Controlling Radio-Sensitivity and Adaptive Response by Low-Dose Radiation in Human Immune Cells <i>Authors: Seon Young Nam, Hyung Sun Park, Ga Eun You, Kwang Hee Yang, Ji Young Kim</i>	203
Non-cancer Effects in the Cohort of Mayak PA Workers Occupationally Exposed to Radiation <i>Authors: Tamara Azizova, Evgeniya Grigorieva, Maria Bannikova, Richard Haylock, Nazahat Hunter</i>	204
Micro- and Mesocosms for Assessing Ecosystem Effects of Radiation – A Review <i>Authors: Tanya Hevroy, Clare Bradshaw, Hallvard Haanes, Elisabeth Hansen, Runhild Gjelsvik, Alicja Jaworska, Louise Jensen, Emmanuel Lapied, Deborah Oughton</i>	205
An Update on a Rapid Method of Biological Dosimetry to Assist in the Event of a Nuclear Emergency <i>Authors: Timothy Sebeela, JP Slabbert, V.V. Vandersickel, D. Serfontein</i>	206
Radioiodine Transfer from Seaweed to Abalone <i>Authors: Toshihiro Shibata, Yoshio Ishikawa, Yuichi Takaku, Shun-ichi Hisamatsu</i>	207
Clinical Features of Subacute Radiation Syndrome <i>Authors: Valeriy Krasnyuk, Anastasia Ustyugova</i>	208
The Frequency of Chromosome Aberrations in Peripheral Blood Lymphocyte Cultures and Risk of Disease Development after Radiation Exposure <i>Authors: Vladimir Nugis, Maria Kozlova</i>	209
Airborne I-131 detection on Internal Surface of Buildings using Common Household Products <i>Authors: Yung-Chang Lai, Ying-Fong Huang, Yu-Wen Chen, Mei-Ling Chung</i>	210
History of Ultra-Sonography Examination for Thyroid in the Residents Near Nuclear Power Plants <i>Authors: Young-Khi Lim, Kwang-Pil Ko, Keun-Young Yoo, Sue K. Park, Aesun Shin, Keon Wook Kang</i>	211
Pu isotopes in Surface Soils in China: Its Concentration and Isotopic Ratio <i>Authors: Youyi Ni, Wenting Bu, Wei Dong, Qiuju Guo</i>	212
Development and Application of High Intensity D-T Fusion Neutron Generator (HINEG) <i>Authors: Yican Wu, Song Gang, Yongfeng Wang, Taosheng Li, Xiang Ji, Chao Liu, Jieqiong Jiang</i>	213
ESR Dosimetry with Ceramic and Glass Materials from Electronic Components for Dose Assessment in Radiation Accident <i>Authors: Zhe Liu, Zhiping Luo, Jinfeng Huang, Guowen Zheng</i>	214
  Results of RELID Study 2014 - Buenos Aires, Argentina Retrospective Evaluation of Lens Injuries and Dose <i>Authors: Papp, C., Romano-Miller, M.; Descalzo, A., Michelin, S., Molinari, A., Rossini, A., Plotkin, C.; Bodino, G., Esperanza, G., Di Giorgio, M., Touzet, R.</i>	215
Area 2: Policy, Standards and Culture	216
Integration of radiation safety in management systems in Swedish health care – success or distress <i>Author: Anja Almén</i>	217
Some Suggestions to Adequate the IAEA Safety Standards Series No. 49 According to the General Safety Requirements Part 3 from IAEA <i>Authors: Adelia Sahyun, Carlos N. Ghobril, Clarice F. Perez, Gian Maria Sordi</i>	224
Restoring the “R” in ALARA <i>Author: Brant A. Ulsh</i>	228
De minimis non curat lex or endless optimization? <i>Author: Bernd Lorenz</i>	236

Ethics and radiation protection in biomedical research in the post-Fukushima era: <i>up to date</i> <i>Author: Chieko Kurihara</i>	244
e-Learning – Radiation Safety Training Course <i>Author: Carolyn Mac Kenzie</i>	253
The Romanian Society for Radiological Protection – 25 years as Associate Society to IRPA <i>Authors: Constantin Milu, Ion Chiosila, Nicolae-Mihail Mocanu</i>	256
Radiation Safety Climate in a University Setting <i>Authors: Caitlin Root, Robert Sinclair, Konstantin Povod, Nicole Martinez</i>	259
Young Scientists and Professionals (YSP) – Austria’s Young Generation as best practice example <i>Authors: Ch. Stettner, F. Kabrt, E. Langegger, N. Baumgartner</i>	267
Carbon Molecular Sieves used in the Sampling and Monitoring Technology of Krypton in the Atmosphere <i>Authors: Deng Achang, Ma Xiongnan, Zhu Jun, Xiao Xiangzhong, Zhang Aiming</i>	270
Public Acceptance of Nuclear Technology: education and communication to transform old prejudices and inspire new thoughts <i>Author: Denise S. Levy</i>	277
Enhancing communication on Radiological Protection throughout Brazil <i>Authors: Denise S. Levy, Gian M. A. A. Sordi, Demerval L. Rodrigues, Janete C. G. Carneiro</i>	284
Radiation Protection Culture in Waste Management <i>Authors: G. Hampel, J. Feinhals, H. Völkle</i>	291
Comments on the General IAEA Safety Requirements – Part 3 – and Suggestions for the Next Publications <i>Author: Gian Maria Sordi</i>	298
5th European IRPA Congress (4-8 June 2018): <i>Encouraging Sustainability in Radiation Protection</i> <i>Authors: Hielke Freerk Boersma, Bert Gerritsen, Gert Jonkers, Jan Kops, Lars Roobol, Carel Thijssen</i>	304
L Band EPR Tooth Dosimetry for neutron <i>Authors: Ichiro Yamaguchi, Hitoshi Sato, Hiraku Kawamura, Tuyoshi Hamano, Hiroshi Yoshii, Mituru Suda, Minoru Miyake, Naoki Kunugita</i>	309
Promoting Radiation Safety Culture in the UK: General Users Sector <i>Authors: J. R. Croft, A. MacDonald, R. Fannin, R. Hill, P. Boulton, D. Orr, A. Bannon</i>	316
Promoting Radiation Safety Culture in the UK <i>Authors: J. R. Croft, R. Coates, C. Edwards, C.-L. Chapple, K. Davies, A. MacDonald</i>	324
Radiation Protection Quantities for the Assessment of Stochastic Effects: <i>Should we be more Papal than the Pope?</i> <i>Authors: Jozef Sabol, Jana Hudzietzová, Bedřich Šesták</i>	331
"A North-American first: a state-of-the-art fully functional Linac for teaching to the next generations of therapists and physicists in a college" <i>Authors: Mathieu Bergeron, Louis Archambault, Luc Beaulieu</i>	336
2015 IRPA survey of professionals on the new dose limit to the lens of the eye, and wider issues associated with tissue reactions <i>Authors: Marie Claire Cantone, Merce Ginjaume, Saveta Miljanić, Colin J. Martin, Keiichi Akahane, Louisa Mpete, Severino C. Michelin, Cinthia M. Flannery, Lawrence T. Dauer, Stephen Balter</i>	342
Introducing on-line modules in the Swedish Master’s Degree Programme for Applied Radiation Protection 14 <i>Authors: Mattias Jönsson, Mats Isaksson, Robert Finck, Christopher Rääf</i>	349
Management of Radioactive Waste: Public Perceptions Versus Scientific Views <i>Author: Mogwera Khoathane</i>	355

New EU-Regulations for Radon at Workplaces and their Consequences on the Regulatory Radiation Protection in Bavaria <i>Authors: Markus Trautmannsheimer, Simone Körner</i>	364
Contributions from Women to the Radiation Sciences <i>Authors: Nicole Martinez, Elizabeth Gillenwalters</i>	370
Argentine Plan for strengthening occupational radiation protection infrastructure framed in the RLA 9075 IAEA Project <i>Authors: Nancy Puerta Yepes, Ana Rojo, Adrián Discacciatti, Marina Di Giorgio, Laura Castro, Fabio López, Analía Canoba</i>	379
Activities of EUTERP, the European Training and Education in Radiation Protection Foundation <i>Authors: Richard Paynter, Folkert Draaisma, Penelope Allisy, Michèle Coeck, Friedrich Hoyler, Marcel Schouwenburg, Joanne Stewart</i>	387
A model for determining risk constraints for potential exposures of the public and limitations of the activity of radionuclides released by accidents in nuclear facilities <i>Author: Robert R. Finck</i>	391
The Advantages of Creating a Positive Radiation Protection Safety Culture in the Higher Education and Research Sectors <i>A report from the Working Group on Culture in Research and Teaching</i> <i>Authors: T. Coldwell, P. Coleb, C. Edwards, J. Makepeace, C. Murdock, H. Odams, R. Whitcher, S. Willis, L. Yates</i>	399
Education and Training of Workers for Development of a Safety Culture in a Radioactive Facility <i>Authors: Zayda Haydeé Amador Balbona, Miguel Antonio Soria Guevara</i>	409
Assessment of radiation science studies in 4 successive years <i>Authors: Banafsheh Zeinali-Rafsanjani, Mahdi Haghghatafshar, Mahdi Saeedi-Moghadam, Mohammad-Amin Mosleh-Shirazi</i>	415
Y Gender demographics in radiation protection <i>Authors: Elizabeth Gillenwalters, Nicole Martinez</i>	419
The FORO Project on Safety Culture in Organizations, Facilities, and Activities with Sources of Ionizing Radiation <i>Authors: Rubén Ferro Fernández, Jorge Arciniegas Torres, Ana Blanes Tabernero, Ana M. Bomben, Rodolfo Cruz Suárez, Claudia Da Silva Silveira, E. Ordoñez Gutiérrez, Jorge F. Perera Meas, Renán Ramírez Quijada, Ricardo Videla Valdebenito</i>	427
The Intersection of Public Health and Radiation Protection in Radiation Emergencies <i>Author: Armin Ansari</i>	435
Assessment of the Safety Culture at Facilities Involved in Management of the Spent Nuclear Fuel and Radioactive Waste <i>Authors: Alexander Bobrov, Sergey Kiselev, Malgorzata Sneve, Victor Scheblanov</i>	436
The Decision Threshold and Other Characteristic Limits: An Approach to Re- evaluating the Current Computational Paradigm <i>Authors: Alexander Brandl, Jenelle Mann</i>	437
Lessons learned from 4th African Regional Congress of the International Radiation Protection Association (AFRIRPA04) held in Morocco <i>Authors: Abdelmajid Choukri, Oum Keltoum Hakam</i>	438
Safety Culture Issues in Nuclear Fusion Activities <i>Author: Altair de Assis</i>	439
Communication in an Organization within a Framework of Social Responsibility <i>Authors: Andrea Docters, Maria B. Lucuix</i>	440
Interdisciplinary Approach to Radiation and Nuclear Safety Education <i>Author: Andrejs Dreimanis</i>	441

Education and Training in Radiopharmacy: The INSTN Approach <i>Author: Akli Hammadi</i>	442
Experience of Belarus to the Introduction of International Radiation Safety Standards to the National System <i>Authors: Alena Nikalayenka, Sergey Sychik, Viktoia Kliaus</i>	443
R The Evaluation of the Real Alpha Value in Brazil and Its Projection until the Year 2050 <i>Authors: Adelia Sahyun, Carlos N. Ghobril, Clarice F. Perez, Gian Maria Sordi</i>	444
Radiation Protection in Medical Field in Cameroon <i>Authors: Augustin Simo, Maurice Ndontchueng Moyo, Yolande Huguette Ebele Yigbedeck, Richard Samba Ndi</i>	445
EURADOS IDEAS Guidelines Spanish Translation: A New Tool for Training Activities from the Collaboration between SEPR-SAR Radiation Protection Societies <i>Authors: Borja Bravo, Eduardo Sollet, Ana Maria Rojo, Inés Gomez</i>	446
Engaging Communities to Discuss Nuclear Power Options for the Future <i>Author: Barbara L. Hamrick</i>	447
An IRPA, WHO, IOMP Initiative on Radiation Protection Culture in Medicine <i>Authors: Bernard Le Guen, María Del Rosario Perez, Madan M. Rehani</i>	448
Regulating the Security of Radioactive Sources in South Africa and Institutionalising Nuclear Security Culture and Effective Physical Protection <i>Author: Boikanyo Ntuane</i>	449
Fraudulent Exams in the Training of Reactor Supervisors at the Laguna Verde Nuclear Power <i>Author: Bernardo Salas</i>	450
R Plenary Panel International Standards – RP in Medicine <i>Author: Claire Cousins</i>	451
R Radiation Safety Culture in the UK Medical Sector: A top to bottom strategy <i>Authors: Claire-Louise Chapple, Andy Bradley, Maria Murray, Phil Orr, Jill Reay, Peter Riley, Andy Rogers, Navneet Sandhu, Jim Thurston</i>	452
Implementation in the Republic of Moldova the Requirements of Directive 2013/59 / Euratom on Indoor Radon Concentrations <i>Authors: Coretchi Liuba, Bahnarel Ion</i>	453
Workshop on Radiopathology and Radiation Protection at the Annual Rotating Internship, School of Medicine at the University of Buenos Aires <i>Authors: Cinthia Papp, Mónica Gardey, Gerardo Rank, Roberto Agüero, Mara Scarabino, Adriana Cascón</i>	454
Implications of ICRP 103, the International and the European Basic Safety Standards on the use of Dose Constraints in the Management and Disposal of Radioactive Waste, Including Waste Containing Elevated Levels of Naturally Occurring Radionuclides in France <i>Authors: Marie-Odile Gallerand, Christophe Serres, Didier Gay, François Besnus, Jérôme Guillevic</i>	455
Dose Limits in Radioactive Waste Management: Interdisciplinary Perspectives from the German ENTRIA Project <i>Authors: Clemens Walther, Achim Brunnengräber, Peter Hocke, Karena Kalmbach, Claudia König, Sophie Kuppler, Klaus-Jürgen Röhlig, Ulrich Smeddinck</i>	456
The ICRP System of Protection for Existing Exposure Situations: The Work of Committee 4 to Elaborate the Framework for Protection <i>Author: Donald Cool</i>	457
Policy Standards and Culture <i>Author: David Crawford</i>	458
The UK Ministry of Defence Radon Safety Programme <i>Authors: Dee Emerson, Dean Williams</i>	459

R Certified Training for Nuclear and Radioactive Source Security <i>Authors: Daniel Johnson, Brunelle Battistella, Pierre Legoux</i>	460
Radiation Safety Culture at United States Nuclear Power Plants <i>Author: Ellen Anderson</i>	461
43 Years of Experience in Training in Radiation Protection <i>Author: Eduardo Medina-Gironzini</i>	462
Experience in the Use of Social Networks in Radiation Protection <i>Author: Eduardo Medina-Gironzini</i>	463
Nuclear regulators need to adopt international standards applicable to radiation measuring instruments into their national legislation <i>Author: Emma Snyman</i>	464
ICNIRP: Preliminary Thoughts on Protection Principles for Non-Ionizing Radiation <i>Author: Eric van Rongen</i>	465
Ethical Considerations on the Empowerment of People Living in Contaminated Areas after a Nuclear Accident <i>Authors: François Rollinger, Jacques Lochard, Thierry Schneider</i>	466
The Inter-Agency Committee on Radiation Safety – 25 years of Cooperation Efforts to Harmonize International Radiation Protection and Safety <i>Authors: Ferid Shannoun, Miroslav Pinak, Ted Lazo, Carl Blackburn, Stephan Mundigl, Malcolm Crick, Shengli Niu, Pablo Jimenez, María Pérez, Hans Menzel, Christopher Clement, Miroslav Voytchev, Renate Czarwinski, Alain Rannou</i>	467
Lessons Learned from the Fukushima Event: The Radiation Protection Emergency Preparedness <i>Authors: Giorgio Cucchi, Lorenzo Isolan, Federico Rocchi, Marco Sumini</i>	468
Interplay of Nuclear Power on Earth and in Space: Nuclear Energy as Sustainable Energy <i>Author: Gordana Lastovicka-Medin</i>	469
Scientific Issues, Emerging Challenges and Emerging Digital Social Innovations for Radiation and Radiological Protection <i>Author: Gordana Lastovicka-Medin</i>	470
Workers' Knowledge on Radiation Protection. A Survey at Mongi Slim Hospital <i>Author: Hager Kamoun</i>	471
R Importance to Engage in Dialogue with the Affected Population after the Acute Phase of an Accident <i>Author: Hans Vanmarcke</i>	472
Establishing Radiation Protection Culture for Local Residents Left in the outside Boundary of Fukushima and Challenges facing Mothers and Children <i>Author: Hiroko Yoshida</i>	473
Scientific, Societal, Implementation and Regulatory Challenges of Radiological Protection <i>Authors: Ingemar Lund, Ted Lazo</i>	474
Radiation Protection in a Mixed Contaminant Context, Risk Assessment Methodologies <i>Authors: Ivica Prlic, Hrvoje Mesic, Mladen Hajdinjak, Jerko Sisko, Domagoj Kosmina, Tomislav Bituh</i>	475
OPERRA-HARMONE: Harmonising Modelling Strategies of European Decision Support Systems for Nuclear Emergencies <i>Authors: Jan Christian Kaiser, Shan Bai, Johan Camps, Thomas Charnock, Damien Didier, Fabricio Fiengo, Laurent Garcia-Sanchez, Jérôme Groell, Christophe Gueibe, Kerstin Hürkamp, Olivier Isnard, Anne Nisbet, Wolfgang Raskob, Marie Simon Cornu, Christian Staudt, Lieve Sweeck, Jochen Tschiersch, Jordi Vives i Batlle, Samantha Watson, Mark Zheleznyak</i>	476
How to Develop and Maintain an Effective Training Program in Radiation Protection <i>Authors: Joe Cortese, Liz Krivonosov</i>	477

Delineation of Radon Prone Areas for Mandatory Radon Measurement in Workplaces in the Czech Republic <i>Authors: Jana Davidková, Karla Petrová</i>	478
Nuclear Security Consideration for Radiation Protection Professionals <i>Authors: Jason Harris, Edward Waller</i>	479
Communicating Risk to the Public: An Important Element in Mitigating the Impact of a Radiological Terrorist Attack <i>Authors: Jozef Sabol, Bedrich Sestak, Ivo Petr</i>	480
Improvement in Radioactive Waste Management over the Past 40 Years in the U.S <i>Author: J. Scott Kirk</i>	481
Current Discussions in Japan Health Physics Society regarding Radiation Protection of the Lens of the Eye <i>Authors: Keiichi Akahane, Takeshi Iimoto, Takeshi Ichiji, Satoshi Iwai, Hiroyuki Ohguchi, Kazuko Ohno, Tadahiro Kurosawa, Chiyo Yamauchi-Kawaura, Hideo Tatsuzaki, Norio Tsujimura, Nobuyuki Hamada, Toshiyuki Hayashida, Yutaka Hotta, Tadashi Yamasaki, Sumi Yokoyama</i>	482
 The Ethical Foundations of the Radiological Protection System <i>Author: Kunwoo Cho</i>	483
Assessing and Promoting Radiation Safety Culture in the UK Nuclear Sector <i>Authors: Karl Davies, John Croft, Ellie Krukowski, John Bradshaw</i>	484
Managing Suitably Qualified and Experienced Persons (SQEP) Requirements to Meet Business Need <i>Authors: Kenneth Gibbs, Robin Wells</i>	485
The Selected Issues Related to the Development of National Legislation Based on ICRP103, IAEA BSS and EU BSS <i>Authors: Karla Petrová, Jana Davidková</i>	486
Updating the Radiation Protection Guidance for the United States <i>Authors: Kenneth Kase, Michael Boyd, John Boice, Armin Ansari</i>	487
Unification of Legal and Procedural Documentation for Emergency Response in the FMBA of Russia <i>Authors: Liudmila Bogdanova, Yuriy Salenko</i>	488
Development of Nuclear Security infrastructure in Nigeria: Achievements Challenges and prospects <i>Author: Mbet Akpanowo</i>	489
Practical Aspects of Applying Ethics to Occupational Exposures within the Nuclear Sector <i>Author: Marie Barnes</i>	490
Stakeholder Dialogue Webinar: Experience and Lessons for Young and Old Experts and Researchers <i>Authors: Mike Boyda, Ted Lazob</i>	491
Goals and Intermediate Results of the 7FP ENETRAP III Project <i>Authors: Michèle Coeck, Joanne Stewart, Annemarie Schmitt-Hannig, Paul Livolsid, Sascha Trumm, Marisa Marco</i>	492
Problems Associated with Radiation Protection Training Programs <i>Author: Mohamed Gomaa</i>	493
The INEX 5 Exercise: Notification, Communication and Interfaces for Catastrophic Radiological Events <i>Authors: Mike Griffiths, Olvido Guzman</i>	494
Mini UAS based Gamma Spectrometry Measurements in case of Emergency <i>Author: Markku Kettunen</i>	495
Radon occupancy factor for the public areas, needs for revision <i>Authors: Mohsen Shafiee, Sajad Borzoueisileh, Razieh Rashidfar</i>	496
An Insight into the Nuclear Security Science and Policy Institute at Texas A&M University <i>Author: Mani D. Shah</i>	497

Education Standards and Standards Education (ESSE) Process in Radiation Protection in a National Education Cycle <i>Author: Mehdi Sohrabi</i>	498
The URPS Hypothesis for Universal Radiation Protection Standardization <i>Author: Mehdi Sohrabi</i>	499
Lessons from Fukushima Daiichi Nuclear Accident and Efforts of Nuclear Regulation Authority <i>Author: Nobuhiko Ban</i>	500
Balancing Theory and Practicality: Engaging Non-Philosophers in Ethical Decision Making <i>Authors: Nicole Martinez, Daniel Wueste</i>	501
The 4th Workshop on Science and Values in Radiological Protection Decision Making <i>Authors: Nataliya Shandala, Aleksandr Rakhuba, Ted Lazo</i>	502
Cs-137 Contamination Incident at Scrap Yard in South Africa <i>Author: Nico van der Merwe</i>	503
Evaluation of the National Legislative & the Regulatory Framework of Security of Sealed Radioactive Sources in interim Storage <i>Authors: Oumkeltoum Hakam, Mohamed Maital, Assia Lasfar</i>	504
South African Perspective for Radon in Dwellings and the Anticipated Regulatory Control Measures <i>Author: Obusitse John Pule</i>	505
Contribution of a Master Program in Radiation Protection to Building Competencies in Morocco and Regionally <i>Authors: Oum Keltoum Hakam, Abdelmajid Choukri</i>	506
Promoting Nuclear Security Culture through the International Nuclear Security Education Network (INSEN) <i>Authors: Oum Keltoum Hakam, Guido Gluschke, Dmitriy Nikonov</i>	507
 Nuclear New Build – Integrating Cultural Differences in Radiation Protection <i>Authors: Peter A Bryant, Valentin Haemmerli, Peter Cole</i>	508
What to Say to the General Public: CT Doses are Safe or Causing Cancer? <i>Author: Pradip Deb</i>	509
The IAEA Safety Standards – Current and Future Perspectives <i>Author: Peter Johnston</i>	510
1,200 High School Students Involved in Radiation Protection Actions: Eight Years of Experience Feedback in Dissemination of Radiation Protection Culture. <i>Authors: Paul Livolsi, Thierry Schneider, Lucie D'Ascenzo, Sylvie Charron, Emmanuel Bouchot, Pascal Remond</i>	511
 Prudence in Radiation Protection - How Much? A Case Study <i>Author: Roger Coates</i>	512
Ethical Basis of Radiation Protection <i>Author: Richard Toohey</i>	513
The 1980 Sievert Lecturer: Lauriston S. Taylor <i>Author: Richard Toohey</i>	514
Management of Contaminated Goods in Post Accidental Situation: Synthesis of European Stakeholders' Panels <i>Authors: Sylvie Charron, Sandra Lafage, Jean-François Lecomte, Thierry Schneider, Pascal Crouail, Christophe Murith, Bruno Cessac, Vanessa Parache</i>	515
Establishment of a New Nuclear Regulatory Authority in Ghana <i>Authors: Stephen Inkoom, Geoffrey Emi-Reynolds, Emmanuel O. Darko, Abdel Razak Awudu, Joseph K. Amoako, Augustine Faanu, Margaret Ahiadeke, Ebenezer O. Appiah, Ann Mensah, Daniel N. Adjei, Adriana Nkansah</i>	516

Lessons learned from the Fukushima Dai-ichi accident and safety enhancements for the restart of nuclear power plants in Japan <i>Author: Shinichi Kawamura</i>	517
Accreditation Model of Courses in Radiation Protection in Medicine: One proposal to Latin America countries <i>Authors: Simone Kodlulovich Renha, Lidia Vasconcellos de Sá</i>	518
Development of Practical Guidance's for Workplace Monitoring in Nuclear and Radiation Facilities - an IAEA TECDOC Project <i>Authors: Suriya Murthy Nagamani, Jizeng Ma, Miraslov Pinak</i>	519
Management of Malaysian Nuclear Agency's License: Experiences and Challenges <i>Authors: Suzilawati Muhd Sarowi, Azimawati Ahmad, Mohd Fazlie Abdul Rashid, Noor Fadilla Ismail, Hairul Nizam Idris</i>	520
Microdistribution of Plutonium in Human Skeleton. Should we Change the ICRP Model? <i>Authors: Sergey Romanov, Ekaterina Lyovkina, Elena Labutina</i>	521
A Tool for Implementing the UNSCEAR Methodology for Estimating Human Exposures from Radioactive Discharges <i>Authors: Tracey Anderson, Kelly Jones, Helen Grogan, Ed Waller, Lynn Hubbard, Jane Simmonds</i>	522
International Standards for Managing Radionuclides in Food and Drinking Water <i>Authors: Tony Colgan, Carl Michael Blackburn, Maria Perez del Rosario, Igor Gusev</i>	523
Transition of Public Awareness and Its Factor Analysis Concerning Nuclear Energy and Radiation Application Based on Japanese Nationwide Fixed-Points Poll <i>Authors: Takeshi Iimoto, Kazuhisa Kawakami, Hiroshi Kimura, Masayuki Tomiyama, Makoto Funakoshi, Noriaki Sakai, Itaru Takahashi, Yumiko Kawasaki</i>	524
Communicating Radiological Concepts in Plain Language: The Value of International Consistency <i>Authors: Ted Lazo, Maria Perez, Shengli Niu, Miroslav Pinak, Carl Blackburn, Pablo Jimenez, Stephan Mundigl, Malcolm Crick, Chris Clement, Renate Czarwinski</i>	525
ICRP Stakeholder Dialogues: Lessons for the International Community <i>Author: Ted Lazo</i>	526
Management of Protection through Prevailing Circumstances: Interpretation of the ICRP System of Radiological Protection <i>Author: Ted Lazo</i>	527
Plain Language We Can All Understand <i>Author: Ted Lazo</i>	528
Developing Radiation Protection Culture at School: The Experience of the 2015 France-Japan High School Students Radiation Protection Workshop in Fukushima <i>Authors: Thierry Schneider, Daniel Ayrault, Sylvie Charron, Takashi Hara, Ryugo Hayano, Claire Schneider, Hiroyuki Takano</i>	529
Measurement and Data Analysis Concepts Combined with Data Assimilation Techniques for Source Term Reconstruction and Dose Assessment <i>Authors: Ulrich Stoehlker, Martin Bleher, Florian Gering</i>	530
Optimizing a Commercial Radiation Portal Monitor for Spot Traffic Controls <i>Authors: Udo Strauch, Reto Linder, Eike Hohmann, Rouven Philipp, Sabine Mayer</i>	531
Training as Awareness Factor and Dissemination of the Brazilian Nuclear Area <i>Authors: Valéria Pastura, Antonio Carlos Mol, Ana Paula Legey, Eugenio Marins</i>	532
INSTN: The Most Complete Training Centre for First Time Nuclear Plant Workers <i>Author: Vial Thierry</i>	533
Comparison between Brazilian Radiation Protection Norm and the Basic Safety Standards Published in 2014 <i>Authors: Wagner De Souza Pereira, Alphonse Kelecom, Ademir Xavier Da Silva</i>	534

Licensing of Nuclear Facilities in Brazil: Radiological Aspects <i>Authors: Wagner de Souza Pereira^{a,b}, Ana Cristina Lorençob, Alphonse Kelecomc, Ademir Xavier da Silva</i>	535
The Principle of Low Risk and Optimization and the Connection with the ALARA concept. Exemption, Exclusion and Clearance <i>Authors: Wagner De Souza Pereira, Alphonse Kelecom, Ademir Xavier Da Silva</i>	536
The State of the Art about the Radiation Protection System in the World <i>Authors: Wagner de Souza Pereira, Alphonse Kelecom, Ademir Xavier da Silva</i>	537
The Importance of Including the Human Error Factor and Decision Making in Training and Education Programs to Avoid Radiological Incidents of Accidents <i>Author: Walter Truppa</i>	538
Individual Monitoring for External Exposure of Users at Synchrotron Radiation Facilities and New Solutions <i>Authors: Xiaobin Xia, Guanghong Wang, Jianzhong Zhou, Pingan Fei, Sixin Liu</i>	539
VOLUME 2	
Area 3: Medical	540
Pediatric Head CT examination doses in two university teaching Hospitals in Tunisia <i>Authors: Bouaoun Abir, Latifa Ben Omrane, Azza Hammou</i>	541
Spanish Radiation Protection Association (SEPR) Working Groups in Radiation Protection in Medicine <i>Authors: Gil-Agudo, Antonio; Ruiz-Cruces, Rafael; Almansa-López, Julio; Torres-Cabrera, Ricardo; Martí-Climent, Josep María; Sanjuanbenito-Ruiz de Alda, Waldo; Prieto-Martín, Carlos; Macías-Dominguez, Maria Teresa</i>	545
Regulatory T cells (Tregs) as a possible prognostic marker in radiation skin injury <i>Authors: Ana Julia Molinari, Mercedes Portas, Andrés Rossini, Severino Michelin, Diana Dubnera</i>	549
Head and Neck Immobilization Masks: Increase in Dose Surface evaluated by EBT3, TLD-100 and PBC Method <i>Authors: Arnie Verde Nolasco, Luiz Oliveira Faria</i>	555
MCNPX versus DOSXYZnrc in patient specific voxel-based phantom calculations <i>Authors: Banafsheh Zeinali-Rafsanjani, Kamal Hadad, Mahdi Saeedi-Moghadam, Reza Jalli</i>	563
Justification of CT examinations <i>National surveys in Sweden</i> <i>Authors: Carl Bladh, Torsten Cederlund, Sven Richter</i>	566
The transposition and the practical implementation of the Council Directive 2013/59/Euratom in the medical field in Romania <i>Author: Constantin Milu</i>	569
Level 2 justification is now part of the national system for introduction of new health technologies within the specialist health service in Norway <i>Authors: Eva G. Friberg, Reidun Silkosef, Ingrid E. Heikkilä, Jan F. Unhjem</i>	576
Proposed diagnostic reference levels for coronary angiography, left ventriculography and pacemaker placement in South Africa: 3-year improvement from 2012-2015 <i>Authors: Hendrik Johannes de Vos, Christoph Jan Trauernicht</i>	583
Procedure for measurement of Intrinsic Efficiency of a High Energy Collimator Gamma camera <i>Authors: Hugo Pérez-García, Raquel Barquero, Monica Gómez-Incio</i>	592
Simulation of a High Energy Collimator Gamma camera with MCNPX <i>Authors: Hugo Pérez-García, Raquel Barquero, Monica Gómez-Incio</i>	597
Local Computed Tomography Dose Index and Dose Length Product Values Agree with Published European DRLs <i>Authors: I. Garba, A. M. Tabari, A. Dare, M. Yahuza, M. Barde, M. Abba</i>	602
A Review of Occupational Radiation Exposure among Medical Professionals in Canada (1985-2006) <i>Author: Jing Chen</i>	607

The use of the Monte Carlo simulation method for assessing the radiation burden of the hands of workers during some risky manipulations with radiopharmaceuticals <i>Authors: Jana Hudzietzová, Marko Fülöp, Pavol Ragan, Jozef Sabol, P. Povinec,</i>	613
Y Radiation dose optimization in paediatric conventional imaging using automatic dose data management software <i>Authors: Luis Alejo, Eva Corredoira, Zulima Aza, Rodrigo Plaza-Núñez, Antonio Serrada</i>	618
Practical Lessons for a Dosimetry Program <i>Authors: Michelle Baca, Chad Hopponen</i>	627
Large scale multi-national studies on radiation protection of children in CT <i>Author: Madan M. Rehani</i>	635
Extension of the IAEA-International Nuclear and Radiological Event Scale (INES) for Medical Events <i>Authors: Marc Valero, Maria Luisa Ramirez Vera, Nera Belamaric</i>	640
Control of Radiation Exposure to Pediatric Patients at Conventional Radiology and Cardiac Centers at Dubai Hospital <i>Authors: Najlaa K. Almazrouei, Jamila S. Alsuwaidi, Adel H. Hashish</i>	649
Radioprotection in Radiosynovectomy Concerning Accompanying Persons and the Public <i>Authors: Susie Medeiros Oliveira Ramos, Sylvia Thomas, Mônica Araújo Pinheiro, Mirta Bárbara Torres Berdeguez, Lidia Vasconcellos de Sá, Sergio Augusto Lopes de Souza</i>	657
Physicians' Knowledge about patient Radiation Exposure from CT Examinations: Case of Hassan II Hospital Agadir-Morocco <i>Authors: Slimane Semghouli, Bouchra Amaoui, Abdelmajid Choukri, Oum Keltoum Hakam</i>	663
Changes in patients' radiation doses during CT exams in Japan (1997-2014) <i>Authors: Shoichi Suzuki, Yuuta Matsunaga, Ai Kawaguchi, Kazuyuki Minami, Masanao Kobayashi, Yasutaka Takei, Yasuki Asada</i>	669
Estimation of response characteristics for radiophotoluminescent glass dosimeters in X-ray diagnosis by using Monte Carlo simulation method <i>Authors: Toshioh Fujibuchi, Emi Ishibashi</i>	674
Small size OSL dosimeter to measure patient exposure dose in X-ray diagnosis - Evaluation of invisibility <i>Authors: Tohru Okazaki, Hiroaki Hayashi, Kazuki Takegami, Yoshiki Mihara, Natsumi Kimoto, Yuki Kanazawa, Takuya Hashizume, Ikuo Kobayashi</i>	678
Analysis of reasons for the multiple scans of paediatric CT examinations: Finding whether there is possible confounding by indication. <i>Authors: Takayasu Yoshitake, Koji Ono, Tsuneo Ishiguchi, Michiaki Kai</i>	684
A Multi-Center Study on Eye Lens Radiation Doses for Medical Staff Performing Non-Vascular Interventional Procedures in Japan <i>Authors: Kosuke Matsubara, Yasutaka Takei, Ikuo Kobayashi, Hiroshige Mori, Kimiya Noto, Shoichi Suzuki, Takayuki Igarashi, Keichi Akahane</i>	686
FTS (Fused Toes Homolog) can be a Target to Modulate Radiosensitivity in Uterine Cervix Cancer Cells and Normal Cells <i>Authors: Arunkumar Anandharaj, Senthilkumar Cinghu, Won-Dong Kim, Jae-Ran Yu, Woo-Yoon Park</i>	687
Standardized and Automated Risk Assessment Forms for a Dutch Radiation Organization <i>Authors: Arjanka Bandstra, Marcel Wiegman</i>	688
Bonn Conference 2012 - Implementation of Results <i>Author: Axel Böttger</i>	689
Radiological Zoning and Radiation Exposure Assessment of External Staff in the CHU-Ibn Rochd-Casablanca Nuclear Medicine Service <i>Authors: Abdelmajid Choukri, Said Ouzouh, Oum Keltoum Hakam, Rachida El Gamoussi, Amal Guensi</i>	690
Multistep Optimization Approach in Medical Radiology - The Patient Imperative <i>Author: Andrejs Dreimanis</i>	691

R Y Advanced aspects of radiation protection in the use of particle accelerators in the medical field <i>Authors: Angelo Infantino, Gianfranco Cicoria, Giulia Lucconi, Davide Pancaldi, Sara Vichi, Federico Zagari, Domiziano Mostacci, Mario Marengo</i>	692
French Recommendations on the Conditions of Implementation of “New Techniques and Practices” in Radiotherapy <i>Authors: Aurelie Isambert, Eric Lartigau, Albert Lisbona, Philippe Cadot, Sylvie Derreumaux, Olivier Dupuis, Jean-Pierre Gérard, Dominique Ledu, Marc-André Mahé, Vincent Marchesi, Jocelyne Mazurier, Aurelien De Oliveira, Olivier Pharé, Marc Valero, Bernard Aubert</i>	693
A Cross-sectional Study of Nuclear Cardiology Practices and Radiation Exposure in Africa: Results from the IAEA Nuclear Cardiology Protocols study (INCAPS) <i>Authors: Andrew J. Einstein, Salah Bouyoucef, Thomas Pascual, Mathew Mercuri, Mboyo D.T.W. Vangu, Adel Allam, Madan Rehani, Ravi Kashyap, Maurizio Dondi, Diana Paez</i>	694
Quality Control of Radiography X-ray Generators in Kerman Province, South-Eastern Iran <i>Authors: Ali Jomehzadeh, Zahra Jomehzadeh, Mohammadbagher Tavakoli</i>	695
Occupational Dose Profiles of Radiation Workers in Oman Hospitals: A 5-year Dose Analysis <i>Authors: Arun Kumar L. S., Jamal Al-Shanfari, Saeed Al-Kalbani</i>	696
Investigation of Potential Use of ¹²⁴Xe-incorporated Amorphous Si Films in Brachytherapy <i>Authors: Alexandre Leal, Telma Fonseca, Lucas Reis</i>	697
Evaluation of Patient Dose in Interventional Cardiology <i>Authors: Ayoub Momivand, Reza Zohdiaghdam, Zhaleh Behrouzki, Ebrahim Khayati Shal</i>	698
Review of Radiation Safety in Medical Diagnosis in Kenya <i>Author: Arthur Omondi Koteng</i>	699
Study on Incidence of Radiation Induced Cataract among Radiographers in Interventional Fluoroscopy <i>Authors: Aruna Pallewatte, Suvini Karunaratne, MPN Piyasena</i>	700
The Impact of Fluoroscopic Technique on Incidence of Radiation Injuries in Neurointervention <i>Author: Aruna Pallewatte</i>	701
Tandem KAP Meters Calibration Parameters by Monte Carlo Simulation using Reference RQR Radiation Qualities <i>Authors: Ademar Potiens Jr., Nathalia Costa, Eduardo Correa, Lucas Santos, Vitor Vivolo, Marie Da Penha Potiens</i>	702
The IAEA Latin American Working Group on Internal Dosimetry of Radionuclides in Human Body <i>Authors: Ana Rojo, Nancy Puerta, Bernardo Dantas, Arlene Reis, Mariella Teran, Rodolfo Cruz Suarez</i>	703
The Effect of Single Catheter on Patient and Operator Radiation Dose during Trans-radial Coronary Angiography <i>Authors: Ali Tarighatnia, Amirhossein Mohammadalian, Alireza Farajollahi, Morteza Ghojzade</i>	704
The Impact of Both Radial & Pelvic Lead Shields on Operator Radiation Exposure during Trans-radial Coronary Procedures <i>Authors: Ali Tarighatnia, Aida Khaleghifard, Amirhossein Mohammadalian, Alireza Farajollahi, Morteza Ghojzade</i>	705
R Establishing Diagnostic Reference Levels for Conventional X-ray Procedures in the Russian Federation <i>Author: Aleksandr Vodovatov</i>	706
Computing Calibration Factor with Visual Monte Carlo – VMC simulations of an Accident Contamination with ^{99m}Tc <i>Authors: Bruno Mendes, Fernanda Paiva, Marco Aurelio Lacerda, John Hunt, Telma Fonseca</i>	707
Establishing the Quality Management Baseline in the use of Computed Tomography Machines in Kenya <i>Authors: Bernard Ochieng, Geoffrey Korir, Jeska Wambani</i>	708
Radiation Exposure in Interventional Procedures <i>Authors: Bernard Ochieng, Geoffrey Korir, Jeska Wambani</i>	709

Study on the Effects of Gorkha Earthquake in Radiological Facilities (Nepal) <i>Authors: Buddha Ram Shah, Shanta Lal Shrestha, Kanchan Prasad Adhikary</i>	710
Evaluation of Important Physical Parameters in Micro Beam Radiotherapy of Lung Tumors <i>Authors: Banafsheh Zeinali-Rafsanjani, Mohammad-Amin Mosleh-Shirazi, Mahdi Haghatafshar, Mahdi Saeedi-Moghadam</i>	711
Dicentric Assay in DTC Patients with High Dose Radioiodine Therapy <i>Authors: Chung Mei-Ling, Huang Ying-Fong, Chen Yu-Wen, Jong Shiang-Bin, Lai Yung-Chang</i>	712
Animal Sporting Events and Radioprotection Management <i>Authors: Roy Catherine, Audigie Fabrice, Coudry Virginie, Malet Christophe, Sgro Geraldine</i>	713
Occupational Exposure Observations at Groote Schuur Hospital <i>Authors: Christoph Trauernicht, Tobie Kotzé</i>	714
 Comparison of Primary Doses Obtained in Three 6 MV Photon Beams Using a Small Attenuator <i>Author: C Trauernicht</i>	715
Detector Dependence of the Measured Spectra of the OncoSeed IMC6711 Iodine-125 Seed <i>Authors: Christoph Trauernicht, Paul Papka, Peane Maleka, Egbert Hering, Freek Du Plessis</i>	716
Measured Anisotropy of the OncoSeed IMC 6711 Iodine-125 Seed <i>Authors: Christoph Trauernicht, Paul Papka, Egbert Hering, Freek Du Plessis</i>	717
The Monte Carlo Simulation Study of Secondary Neutron Dose for Proton Therapy at Samsung Medical Center using FLUKA <i>Authors: Chae Young Lee, Jin Sung Kim, Yong Hyun Chung, Sungkoo Cho, Dae-Hyun Kim, Youngyih Han, Jongho Kim, Yunho Kim, Sangmin Lee, Chan Woo Park</i>	718
Biological Effects of Radioactive Hot Particles on the Human Lung. Assessment of the Cancer Risk <i>Authors: Diana Apostolova, Zdravko Paskalev</i>	719
Mathematical Modeling of Dose Profile of a Dental Facilities <i>Authors: Deise Diana Lava, Diogo da Silva Borges, Maria de Lourdes Moreira, Antonio Cesar Ferreira Guimaraes</i>	720
In Young Women: Justification of Breast Ultrasound Rather than Combined Breast Ultrasound and Mammography. Radiation Protection Perspective <i>Authors: Dina Salama, Hanan Gewfel</i>	721
Cone Beam CT Patient Dose in Paediatric Cardiac Catheterization Procedures <i>Authors: Eva Corredoira Silva, Luis Alejo Luque, Eliseo Vañó Carruana, Cristina Koren, Rodrigo Plaza, Antonio Serrada, Carlos Huerga Cabrerizo</i>	722
Proposal of a spreadsheet to monitor units verification for intracranial radiosurgery treatments <i>Authors: Erick Hernandez, Ricardo Contreras, Miguel Ortega</i>	723
Establishment of National Dose Reference Levels (DRLs) for Digital Mammography Practices at the UAE <i>Authors: Fatima Al Kaabi, Najla Al Mazrouei, Jamila AlSuwaidi, Jacek Janaczek, Alfani Al Ameri, Sara Booz, Wadha AlShamsi</i>	724
Risk of a Second Kidney Carcinoma Following Childhood Cancer: Role of Chemotherapy and Radiation Dose to Kidneys <i>Authors: Florent de Vathaire, Boris Schwartz, Chiraz El-Fayech, Rodrigue Allodji, Bernard Escudier, Mike Hawkins, Ibrahima Diallo, Nadia Haddy</i>	725
Developing Light Nano-Composites with Improved Mechanical Properties for Neutron Shielding <i>Authors: Fatemeh Jamali, SMJ Mortazavi, MR Kardan, Sedigheh Sina, MA Mosleh-Shirazi, Jila Rahpeyma</i>	726
Evaluation of the Scattered Radiation Field in an Interventional Radiology Room <i>Authors: Francesca Mariotti, Paolo Ferrari, Lorenzo Campani, Elena Fantuzzi, Luisa Pierotti, Pier Luca Rossi</i>	727
In Vivo Dosimetry for the Measurement of Doses to Breast Cancer Patients During External Beam Radiotherapy Treatment, using the Optically Stimulated Luminescence (OSL) Dosimeters at the Douala General Hospital, Cameroon <i>Authors: Fokou Mvoufo, Samba Richard</i>	728

UNSCEAR's Assessment of Medical Exposure	729
<i>Author: Ferid Shannoun</i>	
Radiation Dose in Childhood Cancer Management: Challenges and Recommendations for Dose Reduction	730
<i>Author: Hamid Abdollahi</i>	
Review and Evaluation of Imaging Methods and Analysis of Images Obtained by Magnetic Resonance Imaging to Determine the Absorbed Dose in the Phantom by Polymer Gel Dosimetry	731
<i>Authors: Hamed Dehghani, Amin Farzadnia, Saeed Shanehsazzadeh, Yazdan Salimi, Jalal Ordoni, Dariush Askari, Mohammad Hossein Jamshidi</i>	
Standard Calibration of Ionization Chambers Used in Radiation Therapy Dosimetry and Evaluation of Uncertainties	732
<i>Authors: HyoJin Kim, Sung Jin Noh, Hyun Kim, Sang koo Kang, Manwoo Lee, Dong Hyeok Jeong, Kwangmo Yang, Yeong-Rok Kang</i>	
Radiological Risk Assessment in Tunisian University Hospital	733
<i>Authors: Hager Kamoun, Samar Kallela, Mohamed Faouzi Ben Slimane</i>	
An Automated Mechanical Quality Assurance System for Medical Accelerators using a Smartphone	734
<i>Authors: Hwiyoung Kim, Il Han Kim, Hyunseok Lee, Sangmin Lee, Sung-Joon Ye</i>	
Patient Doses in a Hybrid Operating Room	735
<i>Authors: Hugo Perez-Garcia, Carlos Andrés Rodríguez, Manuel Agulla Otero, Ricardo Torres Cabrera, Raquel Barquero Sanz</i>	
Comparison of Patients CTDI from Two Different "Make" 16-SLICE CT Scanners in Maiduguri North Eastern Nigeria	736
<i>Authors: Idris Garba, Aisha Abba Kato, Auwal Abubakar, Chogozie Nwobi, Mansur Yahuza, Nasiru Isha Fagge</i>	
Hearing Radiation and its Application to in Vivo Radiation Dosimetry during Radiation Treatment	737
<i>Authors: I.J. Kima, J.H. Kim, C.Y. Yi, C.H. Kim, J.S. Kim, E.Y. Park, Y.H. Jung</i>	
Effectiveness of Dose Modulation Technique of CT scan on Organ Dose	738
<i>Authors: Il Park, Seung Cheol Oh, Kwang Pyo Kim</i>	
Application of Prospective Approaches in Preventing Accidental Exposure in Radiotherapy: A Review of Italian Experiences	739
<i>Authors: Ivan Veronese, Marie Claire Cantone, Luisa Begnozzi</i>	
Survey of Radiation Protection in Patients Undergoing X-ray Medical Examination	740
<i>Authors: Justina Achuka, Mojisola Usikalu</i>	
Long Half-Life Isotopes Europium-152 and Europium-154 Found in Hospital Waste	741
<i>Authors: Janneke Ansems, Bunna Damink, Jelle van Riet, Corinne Valk, Ruud Hack</i>	
Prospective Risk Assessment of the Use of Radioactive Iodine-125 Seeds for the Localisation of Impalpable Breast Lesions	742
<i>Authors: Janneke Ansems, Bunna Damink, Jelle van Riet, Pieter Buijs, Els Vanaert</i>	
Global Developments in DRLs and Assessment of Medical Exposures	743
<i>Author: John Damilakis</i>	
Persistence of Dicentric Chromosomes associated with Telomere Dysfunction: A Biomarker of Prognosis in Patients Undergoing Total Body Irradiation	744
<i>Authors: Julien Dossou, Theodore Girinsky, Dominique Violot, Jean-Henri Bourhis, Eric Lartigaux, Luc Morat, Claude Parmentier, Radhia M'kacher</i>	
Dosimetric Analysis with the Specifically Selected Low-Dose Threshold on Gamma Evaluation for VMAT QA	745
<i>Authors: Ji-Hye Song, Min-Joo Kim, So-Hyun Park, Seu-Ran Lee, Min-Young Lee, Dong Soo Lee, Tae Suk Suh</i>	

Y	The Influence of the Dose Calculation Resolution of VMAT Plans on the Calculated Dose for Eye Lens and Optic Apparatus	
	<i>Authors: Jong Min Park, So-Yeon Park, Jung-in Kim, Hong-Gyun Wu, Jin Ho Kim</i>	746
R	Monte Carlo Estimation of Effective Dose to Patients Undergoing Contrast Based X-Ray Fluoroscopy Procedures	
	<i>Authors: J. E Ngaile, P. Msaki, R. Kazema</i>	747
	An Assessment of Radiographers' Technical and Protective Performance in Hospitals Affiliated to Birjand University of Medical Sciences in 2012	
	<i>Authors: Jalal Ordoni, Saeid Ghasemi, Dariush Askari, Yazdan Salimi, Fatemeh Ramrodi, Mohammad Hossein Jamshidi, Hamed Dehghani</i>	748
	Patient Radiation Safety Control in Nuclear Medicine Practices in View of the New Basic Safety Standards (BSS)	
	<i>Authors: Jamila S AlSuwaidi, Priyank Gupta, Shabna Miyath</i>	749
	New X-ray Technology Results in 70% Dose Reduction in Pacemaker and Implantable Cardioverter Defibrillator (ICD) Implantations	
	<i>Authors: Joris van Dijk, Jan Paul Ottervanger, Peter Paul Delnoy, Martine Lagerweij, Siert Knollema, Cornelis Slump, Piet Jager</i>	750
	The Study on the Interspace Materials of Radiographic Anti-Scattering Grid with Monte Carlo Calculation	
	<i>Authors: Jun Woo Bae, Hee Reyoung Kim</i>	751
	¹³¹I Activity in the Thyroid in Members of the Nuclear Medicine Medical Personnel	
	<i>Authors: Kamil Brudecki, Aldona Kowalska, Pawel Zagrodzki, Artur Szczodry, Tomasz Mroz, Pawel Janowski, Jerzy Wojciech Mietelski</i>	752
	Impact of Earthquake on Radiological Facilities in Kathmandu Valley	
	<i>Authors: Kanchan P. Adhikari, Yaduram Panthi, Deepak Subedi</i>	753
	Radiation Dose from Whole Body F-18 FDG PET/CT: Nationwide Survey in Korea	
	<i>Authors: Keon Wook Kang, Hyun Woo Kwon, Jong Phil Kim, Jin Chul Paeng, Hong Jae Lee, Jae Sung Lee, Gi Jeong Cheon, Dong Soo Lee, June-Key Chung</i>	754
	Using I-125 Seeds for Localisation; a Retrospective Overview of Radiation Safety Issues	
	<i>Author: Linda Janssen-Pinkse</i>	755
	Activimeter Response Behaviour Analysis Related to Well Depth	
	<i>Authors: Lilian Kuahara, Eduardo Corrêa, Maria da Penha Potiens</i>	756
	Digital Breast Tomosynthesis: Preliminary Results of Patient Radiation Dose Survey in a Brazilian Facility	
	<i>Authors: Larissa Oliveira, Fernando Mecca, Simone Renha</i>	757
	Measurement of Entrance Skin Dose for Pediatric Patients during Cardiac IVR	
	<i>Authors: Lue Sun, Yusuke Mizuno, Takashi Moritake</i>	758
	New Concept: Reduction of Dose of the Lens	
	<i>Authors: Lue Sun, Yuji Matsumaru, Takashi Moritake</i>	759
	Development of a Specialization Program in Radiation Protection: Proposal to CPLP	
	<i>Authors: Lidia V. Sá, Simone K. Renha</i>	760
	Diagnostic Reference Levels in CT: First Experience in one Major Hospital in Algeria	
	<i>Authors: Merad Ahmed, Khelassi-Toutaoui Nadia, Mansouri Boudjema</i>	761
	Occupational Radiation Exposure in Nuclear Medicine	
	<i>Authors: Mashari Alnaaimi, Mohammed Alkhoryaf, Fareda Alkandri, Mousa Aldouij, Mohamed Omer, Nawaf Abughaith, Talal Salhudeen</i>	762
	High Voltage Consideration to Determine the Dose Received by Patient in Conventional Radiology	
	<i>Authors: Mbolatiana Anjarasoa Luc Ralaivelo, Andriambololona Raelina, Edmond Randrianarivony, Solofonirina Ravelomanantsoa, Hery Fanja Randriantseheno, Ralainirina Dina Randriantsizafy, Tiana Harimalala Randriamora, Veroniaina Raharimboangy, Tahiry Razakarimanana, Hary Andrianarimanana Razafindramiandra</i>	763

Diagnostic Reference Levels for Fluoroscopically Guided Interventions at a Major Australian Hospital <i>Authors: Mohamed Badawy, Tegan Clark</i>	764
Image Quality and Patient Dose Assessment in Simple Radiographic Examinations in Ghana <i>Authors: Mary Boadu, Stephen Inkoom, Cyril Schandorf, Geoffrey Emi-Reynold, Emmanuel Akrobortu</i>	765
Determination of attenuation properties of lead glasses used in the catheterization laboratory <i>Authors: Marcin Brodecki, Marek Zmyslony</i>	766
Dose Reassessment Applied in Routine TL Dosimetry by using the PTTL method in LADIS Laboratory <i>Authors: Maciej Budzanowski, Renata Kopec, Anna Bieniarz-Sas</i>	767
Occupational Doses of Medical Staff in Interventional Cardiology Procedures and Correlations with Patient Dose Levels <i>Authors: Maciej Budzanowski, Agnieszka Szumska, Renata Kopec</i>	768
Out-of-field Dose and Risk of Radiogenic Second Cancer for children Treated with Craniospinal 3D-Conformal Radiotherapy or TomoTherapy <i>Authors: Marijke De Saint-Hubert, Željka Knežević, Natalia Adamek, Marija Majer, Liliana Stolarczyk, Remy Savelli, Vedran Rajevac, Saveta Miljanić, Pawel Olko, Roger M. Harrison, Filip Vanhavere, Dirk Verellen, Lara Struelens</i>	769
Evaluation of Thyroid Function after Radiotherapy for Patients with Breast Cancer <i>Authors: Masomeh Dorri Gav, Seyed Mahmood Reza Aghamiri, Mohammd Hossien Bahreini Toosi</i>	770
Preliminary Diagnostic References Levels of Audit CT at Aristide LeDantec National Hospital <i>Authors: Magatte Diagne, Fama Gning, Mamadou Moustapha Dieng, Latifatou Gueye</i>	771
Frequency of Overscan in Standard CT Protocols <i>Authors: Michael Galea, Mohamed Badawy</i>	772
Overview of the Activities on Eye Lens Dosimetry within EURADOS WG 12 (Dosimetry in medical imaging) <i>Authors: Merce Ginjaume, Isabelle Clairand, Eleftheria Carinou, Olivera Ciraj Bjelac, Paolo Ferrari, Marta Sans-Merce, Jad Farah, Frank Becker, Vadim Chumak, Josiane Daures, Joanna Domienik, Zoran Jovanovic, Renata Kopec, Dragana Krstic, Agnieszka Szumska, Denisa Nikodemova, Pedro Teles, Sara Principi, Filip Vanhavere, Željka Knežević</i>	773
Imaging for Saving Kids - Improving Radiation Safety in Paediatric Radiology <i>Authors: Donald Frush, Lawrence Lau, Maria del Rosario Perez, Michael G Kawooya</i>	774
Evaluation of Survived Neuronal Tissue Area around Brain Tumor Lesions Post Radiation Therapy by Diffusion-weighted Imaging (DWI) <i>Authors: Mohammad Hossein Jamshidi, Alireza Eftekhari Moqadam, Jafar Fatahi, Hamid Behrozi, Yavar Shahvali, Jalal Ordoni, Yazdan Salimi, Dariush Askari, Hamed Dehghani</i>	775
Surveying the Relationship between Brain CT Scan Findings in Children with a Clinical Signs and Determining the Appropriate Indications for Requesting CT Scan <i>Authors: Mohammad Hossein Jamshidi, Hamid Behrozi, Dariush Askari, Jalal Ordoni, Yazdan Salimi, Hamed Dehghani</i>	776
Radiation Emergency Medicine Preparedness: Web-Based Reporting of News and Events from SREMC to Target Expert Groups <i>Authors: Marita Lagergren Lindberg, Karin Lindberg, Rolf Lewensohn, Giuseppe V., Masucci, Jack Valentin, Leif Stenke</i>	777
Evaluation of Organ Doses and Cancer Risk from Paediatric Head CT Examination – Phantom Study <i>Authors: Marija Majer, Željka Knezevic, Saveta Miljanic, Liu Haikuan, Weihai Zhuo</i>	778
Radiation Protection Optimization in I-131 Therapy of Thyroid Cancer to Ablate Postthyroidectomy Remnants or Destroy Residual or Recurrent Tumour <i>Author: Mario Medvedec</i>	779
Operational Radiation Safety with Y-90 Microspheres <i>Authors: Mark Miller, Charles Martin III</i>	780


In-Vivo Tooth Dosimetry Using L Band EPR. The Research Involving Human Subjects Related to Fukushima Nuclear Power Plant Accident <i>Authors: Minoru Miyake, Ichiro Yamaguchi, Yasuhiro Nakai, Hiroshi Hirata, Naoki Kunugita, Harold Swartz</i>	781
Establishment of Local DRLs on Standard Radiographic Examinations and Estimation of Cancer Risk for Paediatric and Adult Patients at Two Tunisian Hospitals <i>Authors: Mohamed Mogaadi, Latifa Ben Omrane, Azza Hammou</i>	782
Audit of Clinical Image Quality in Chest Radiography using Visual Grading Analysis <i>Authors: Michael Sandborg, Jonas Nilsson Althen, Erik Tesselaar</i>	783
Radiation Protection in Medical Imaging and Radiation Oncology: A Cooperative Effort between IOMP and IRPA <i>Authors: Magdalena Stoeva, Richard Vetter, K.Y. Cheung, Renate Czarwinski, Francesca McGopwan</i>	784
Monte Carlo Calculation of Neutron Doses to Organs of a Female Undergoing A Pelvic 18 MV Irradiation <i>Authors: Mansour Zabihzadeh, Seyyed Rabi Mahdavi, Mohammad Reza Ay, Zahra Shakarami</i>	785
Study of the Radiation Effect on the Biological Cellule DNA by Determination Bragg Peak Position of the Proton Beams <i>Authors: Noura Harakat, Jamal Inchaouh, Abdenbi Khouaja, Mohammed Benjelloun, Hamid Chakir, Said Boudhaim, Zouhair Housni, Mohamed Lhadi Bouhssa, Abdellatif Kartouni, Mohamed Reda Mesradi, Sara Stimade, Meriem Fiak, Mustapha Krim</i>	786
 Internal dose assessment of new ¹⁷⁷Lu-radiopharmaceuticals and its role in radiation protection of patients <i>Authors: Nancy Puerta Yepes, Ana Rojo, Sebastián Gossio, José Luis Crudo</i>	787
Design Shielding Assessment for a Nuclear Medicine Service <i>Authors: Osvaldo Brígido-Flores, José Hernández-García, Orlando Fabelo-Bonet, Adelmo Montalván-Estrada</i> 788	
Performance Study of Hybride Imaging SPECT/CT: Case of Nuclear Medicine Service - Ibn Sina Hospital in Rabat-Morocco <i>Authors: Oum Keltoum Hakam, Abdelmajid Choukri, Rajaa Sebihi, Youness Esserhir El Fassi</i>	789
Comprehensive quality audits in radiation oncology, diagnostic and interventional radiology <i>Authors: Ahmed Meghzifene, Ola Holmberg</i>	790
International Response to the Bonn Call for Action – from the Viewpoint of the Organizers of the Bonn Conference: the IAEA <i>Author: Ola Holmberg</i>	791
Assessment of the Practice of Optimizing Paediatric Doses in Conventional Radiography in Cameroon <i>Authors: Odette Ngano Samba, Jean Bernard Kamgang, Ariane Lynda Kengne Fonkam, Emmanuel Chi, Lukong Cornelius Fai, Jean Yomi</i>	792
Can Standard CT be replaced by Contrast Enhanced Ultra-low-dose CT with Iterative Reconstruction for the Screening of Patients Admitted with Acute Abdominal Pain? A Comparative Study <i>Authors: Pierre-Alexandre Poletti, Minerva Becker, Thomas Perneger, Christoph D Becker, Alexandra Platon</i>	793
Radiological and Dosimetrical Aspects of CO₂ Peripheral DSA: Optimization of X-ray Spectrum <i>Authors: Pier Luca Rossi, David Bianchini, Alessandro Lombi, Giacomo Feliciani, Manami Zanzi, Romano Zannoli, Ivan Corazza</i>	794
Establishment of National Diagnostic Reference Levels for Nuclear Medicine in Australia <i>Authors: Paul Marks, Toby Beveridge, Peter Thomas, Anna Hayton, Anthony Wallace</i>	795
Survey of Knowledge about Radiation Dose in Radiological Investigation in Kermanshah Hospitals, Iran <i>Authors: Rasool Azmoonfar, Hosein Faghimavaz, Edalat Morovati, Hosein Younesi</i>	796
Measurement of ¹³¹I activity with a High Energy Gamma Camera <i>Authors: Raquel Barquero, Hugo Perez-Garcia, Monica Gomez-Incio</i>	797
Situation of Radiation Therapy, Cancer Diagnosis and Radiation Protection of Patients in Cameroon <i>Authors: Richard Ndi Samba, Augustin Simo, Ernest C. Nwabueze Okonkwo</i>	798

R Promoting Fluoroscopic Personal Radiation Protection Equipment: Unfamiliarity, Facts, and Fears <i>Author: Stephen Balter</i>	799
Traceability of the KAP-Meters Used for Patient Dosimetry in Radiodiagnostic <i>Authors: Sorin Bercea, Constantin Cenusă, Ioan Cenusă, Aurelia Celarel, Elena Iliescu</i>	800
Radiation Dose Assessment for Abdominal Computed Tomography <i>Authors: Seung Cheol Oh, Il Park, Kwang Pyo Kim</i>	801
Implementation on Methodology for the Calibration of well type chambers used in ¹⁹²Ir-Brachytherapy Sources <i>Authors: Stefan Gutierrez Lores, Gonzalo Walwyn Salas, Jorge Luis Morales</i>	802
Study of the ¹³¹I Thyroid Monitoring Measurements Using MCNP Simulations <i>Authors: Sebastián Gossio, Nancy Puerta, Ana Rojo</i>	803
Dosimetric Studies of Radionuclide Therapy of Neuroendocrine Tumors with ¹⁷⁷Lu-Dotatate <i>Authors: Santosh Kumar Gupta, Suhas Singla, Chandrasekhar Bal</i>	804
Managing the Gaseous Waste in Nuclear Medicine: A Novel Approach <i>Authors: Shahed Khan, Eleonora Santos</i>	805
Monitoring and Evaluating the Air Concentration of Radionuclides in the Vicinity of a Nuclear Medicine Facility <i>Authors: Shahed Khan, Eleanora Santos</i>	806
Neutron Measurement for Proton Therapy Facility at Samsung Medical Center with Wobbling and Line Scanning Mode using WENDI-2 <i>Authors: Sangmin Lee, Jin Sung Kim, Sungkoo Cho, Dae-Hyun Kim, Jungho Kim, Yunho Kim, Youngyih Han, Sung-Joon Ye, Chae Young Lee, Yong Hyun Chang</i>	807
Utilizing 3D Scanner/Printer for a Dummy Shield: Monte Carlo Dose Calculations on Artefact-free CT Images of a Metallic Shield for Electron Radiation Therapy <i>Authors: Jong In Park, Il Han Kim, Jaegi Lee, Hyeonseok Lee, Sung-Joon Ye, Sangmin Lee</i>	808
Comparison of Cadmium Zinc Telluride (CZT) with Photomultiplier Tube (PMT) Detectors in SPECT and Bismuth Germanate (BGO) in PET <i>Authors: Seyed Mohsen Zahraei-Moghadam, Mehdi Saeedi –Moghadam, Banafsheh Zenali –Rafsenjani, Masoumeh Dorri-Gev, Fatemeh Shekoochi –Shooli</i>	809
Nurses Knowledge of Ionizing Radiation and Radiation Protection during Mobile Radiodiagnostic Examinations <i>Author: Samuel Opoku</i>	810
Personal Radiation Monitoring of Occupationally Exposed Radiographers in the Biggest Tertiary Referral Hospital in Ghana <i>Author: Samuel Opoku</i>	811
Health Physicist Monitors Own Medical Dose from Radioiodine Thyroid Ablation Procedure <i>Authors: Sander Perle, Kip Bennett, Chad Hopponen, Michael Lantz</i>	812
R Evaluation of Eye Lens Doses of Interventional Cardiologists <i>Authors: Sumi Yokoyama, Shoichi Suzuki, Hiroshi Toyama, Shinji Arakawa, Satoshi Inoue, Yutaka Kinomura, Ikuo Kobayashi</i>	813
Development of Thermoplastic Mask set up Monitoring System using Force Sensing Resistor (FSR) Sensor <i>Authors: Tae Ho Kim, Siyong Kim, Min-Seok Cho, Seong-Hee Kang, Dong-Su Kim, Kyeong-Hyun Kim, Dong-Seok Shin, Tae-Suk Suh</i>	814
Measurements of Photon Spectra around IVR for the Evaluation of Eye-lens Dose <i>Authors: Tadahiro Kurosawa, Masahiro Kato, Sumi Yokoyama</i>	815
RADIREC: System for Mapping and Collecting Entrance Skin Dose during Neurointerventional Radiology <i>Authors: Takashi Moritake, Lue Sun, Koichiro Futatsuya, Satoru Kawauchi, Yasuhiro Koguchi, Mikito Hayakawa, Yuji Matsumaru</i>	816

Diagnostic Reference Levels (DRLs) for CT Examinations in Adults in Cameroon <i>Authors: Thierry Ndzana Ndah, Boniface Moifo, Mathurin Neossi Nguena</i>	817
The Dose Kernels for Pencil Beam and Differential Pencil Beam of Photons with Spectrum of Treatment Machine with ⁶⁰Co Source and their Analytical Approximations <i>Authors: Vladimir Klimanov, Alexey Moiseev, Maria Kolyvanova</i>	818
Radiation Protection of the Public and of the Immediate Family of a Patient Following the Therapy with Iodine-131 <i>Author: Youssef Ech Chaykhy</i>	819
A Study Evaluating the Dependence of the Patient Dose on the CT Dose Change in a SPECT/CT Scan <i>Authors: Young-Hwan Ryu, Ho-Sung Kim, Kyung-Rae Dong, Chang-Bok Kim, Yun-Jong Lee</i>	820
A Study on Quantitative Analysis of Exposure Dose Caused by Patient Depending on Time and Distance in Nuclear Medicine Examination <i>Authors: Young-Hwan Ryu, Ho-Sung Kim, Yun-Jong Lee, Kyung-Rae Dong, Jin-Kyu Kim, Chang-Bok Kim</i>	821
Medical Personnel Radiation Safety in Autopsies for Radiation Accidents <i>Author: Yulia Kvacheva</i>	822
Evaluating Patient Dose in Conventional Radiology for Ten Routine Projections in Tehran, Iran: Recommendation for Local Diagnostic Reference Levels <i>Authors: Yazdan Salimi, Mohammad Reza Deevband, Dariush Askari, Jalal Ordoni, Mohammad Hossein Jamshidi, Isaac Shiri, Hamed Dehghani, Hamid Behrozi</i>	823
Eye Lens Dosimetry: Measurement in Hospitals <i>Authors: Zina Cemusova, Daniela Ekendahl, Lucie Sukupova, Michael Zelizko, Martin Mates, Kamil Sedlacek, Jiri Novotny, Iva Krulova</i>	824
A National Audit Programme for Radiotherapy Centres <i>Author: Zakithi Msimang</i>	825
Calculation of Organs Doses and Secondary Cancer Risk during Mantle Field Radiotherapy for Hodgkin's Lymphoma <i>Authors: Zahra Shakarami, Mansour Zabihzadeh, Mohammad Javad Tahmasebi Birgani, MohammadAli Behrooz, Hojatollah Shahbazian</i>	826
Organ doses and associated cancer risks for CT examinations of thorax <i>Authors: Marija Majer, Željka Knežević, Jelena Popić Ramač, Hrvoje Hršak, Saveta Miljanić</i>	827
 Optimization of image quality and patient dose in radiographs of paediatric extremities using direct digital radiography <i>Authors: Jones A., Ansell C., Jerrom C., Honey Id</i>	828
Area 4: General Ionising Radiation Protection	829
Side by Side Monitoring Test for Radon Emissions from an Underground Uranium Mine <i>Authors: Douglas Chambers, David Frydenlund, Jaime Massey, Ron Stager, Kathy Weinel</i>	830
From Radiation Solutions for Engineering Problems to Engineering Solutions for Radiation Problems: the uses of industrial radiation <i>Author: Edward Waller</i>	838
 Patrimonial management of source term in French nuclear power plants <i>Authors: François Drouet, Serge Blond, Alain Rocher, Charlotte Dabat-Blondeau, François Renard, Samir Ider</i>	847
Public Dose Assessments for Atmospheric Pathways at Rössing Uranium Mine, Utilising Direct Monitoring Data <i>Author: Gunhild von Oertzen</i>	853
Health impact assessment of recovery/disposal options of sewage sludge: methodology and critical parameters <i>Authors: Hélène Caplin, Alain Thomassin</i>	862
Criticality Safety and Control System for Nuclear Fuel Fabrication Plant <i>Authors: H. A. Elsayed, M. K. Shaat, M. E. Nagy, S. A. Agamy</i>	869

Study on the transfer of Polonium-210 from soil and sediment to cattle in a catchment area influenced by gold mining <i>Author: Immanda Louw</i>	876
Release Fractions from Airborne Fluid and Slurry Spills <i>Authors: Judith Ann Bamberger, John A. Glissmeyer</i>	884
Basic Characterization of a Radioactive Facility and Evaluation of Risk Agents <i>Authors: Carneiro, J. C. G. G., Alves, A. S., Sanches, M. P., Rodrigues D. L., Levy, D. S, Sordi, G. M. A. A</i>	892
Supervision of German miners at small underground construction sites of old mining to prevent high radon exposures <i>Author: Jörg Dehnert</i>	900
Analysis of Gamma-Ray Skyshine Contribution to Dose Rates Exterior to an Above-Ground Waste Storage Facility Using Radiation Transport Models <i>Authors: Jenelle Mann, Norbert Zoeger, Roman Koppitsch, Alexander Brandl</i>	905
Use of Real-Time Radon Progeny Monitors in Uranium Mines <i>Authors: John Takala, Andre Boucher, Mikhail Ioffe, Kari Toews</i>	912
Verification of main shielding bodies at Atucha-2 during full power operation <i>Authors: Martin Brizuela, Felipe Alborno, Elianna Cuello</i>	917
Newcomers, new build – the industry view <i>Author: Marcel Lips</i>	921
Lanthanides Patterns as a Nuclear Forensic Signature from a Uranium Mine in South Africa <i>Authors: Manny Mathuthu, Ntokozo Khumalo, Malayita M. Baloyi, Refilwe N. Maretela</i>	925
A Review of Gamma Cell 220 Research Irradiator External Dose Rates <i>Authors: Michael Shannon, Ryan Howell, Spencer Mickum, Robert Rushton</i>	931
Interpretation of Data Collected During Individual Monitoring of Uranium Dioxide Exposure: Collective Dose Assessment <i>Authors: N. Blanchin, E. Davesne, E. Blanchardon, E. Chojnacki, D. Franck, M. Ruffin</i>	936
Monte Carlo analyses for BNCT using near-threshold $^7\text{Li}(p,n)$ neutrons <i>Radiation source, shielding, activation, and external exposure</i> <i>Authors: Noriaki Nakao, Kazuaki Kosako, Noriyosu Hayashizaki, Tatsuya Katabuchi, Tooru Kobayashi</i>	943
Nuclear New Build – Disseminating Radiation Safety Culture in the Supply Chain <i>Authors: Peter A. Bryant, Peter Cole</i>	952
On the ingestion of Cs-137 at Volincy municipality in Belarus about 30 years after the Chernobyl accident <i>Authors: Peter Hill, Petro Zoriy, Herbert Dederichs, Burkhard Heuel-Fabianek, Jürgen Pillath</i>	960
In preparation for future reduction of the dose limit for the lens of the eye – an assessment at Swedish nuclear facilities <i>Author: V. Nilsson</i>	968
Findings of radiological events in the Centre of Isotopes in Cuba <i>Author: Zayda Haydeé Amador Balbona</i>	974
Occupational Exposure in Production of Radiopharmaceuticals and Labeled Compounds in Cuba <i>Authors: Zayda Haydeé Amador Balbona, Miguel Antonio Soria Guevara</i>	984
Estimation of air born radioactivity induced by 8GeV class electron LINAC accelerator <i>Author: Yoshihiro Asano</i>	993
Principles of Formation of Risk Groups for Occupational Diseases for Workers of Facilities Using Nuclear Energy during Obligatory Medical Examinations in the Russian Federation <i>Authors: Andrey Kretov, Andrey Bushmanov, Alexander Samoilov</i>	1002

PREDO – A Strengthened Dose Assessment for Routine Discharges by Swedish Nuclear Installations <i>Authors: Anna Maria Blixt Buhr, Helene Alpfjord, Rodolfo Avila, Roman Bezhenar, Robert Broed, Anna Fermvik, Eva Grusell, Kenneth Häggkvist, Vladimir Maderich, Veronika Rensfeldt, Synnöve Sundell-Bergman, Cor W.M Timmermans, Stefan Willemsen, Govert deWith</i>	1003
Improvement of the Dose Estimation in Case of an Occupational ²⁴¹Am Incorporation Event <i>Authors: Anna Pántya, Andor Andrási, Tamás Pázmándi, Péter Zagyvai</i>	1004
Argentinian Intercomparison on Interpretation of Data from Internal Exposure Sceneries for Dose Assessment <i>Authors: Ana Rojo, Nancy Puerta, Sebastian Gossio, Inés Gomez Parada</i>	1005
Economic Losses of the Nuclear Industry Related to Loss of Workers Occupational Disability for Medical Reasons <i>Authors: Alexander Samoilov, Andrey Bushmanov, Andrey Kretov</i>	1006
3A vii Safety and Risk Assessment Safety Assessment for Non-Reactor Facilities <i>Author: Bethany Louise Cawood</i>	1007
RadProtect® Increases Survival Rate in Novel Murine Slow and Low (S&L) Irradiation Model <i>Authors: Chia-Hung Chen, Jen-Ling Wang, Wei-Chuan Liao, Chau-Hui Wang, Tzu-ying Hung, Alan Liss</i>	1008
Development of Mesh-Type ICRP Reference Phantoms and its Implications <i>Author: Chan Hyeong Kim</i>	1009
Devaluation of Rhinoceros Horn through Nuclear Techniques <i>Authors: Charles Kros, Jan Rijn Zeevaart, Arnaud Faanhof, Frikkie de Beer, Deon Kotze, Dave Hudson-Lamb, Frederik Botha, Gawie Nothnagel</i>	1010
The Radiological and Health Impacts to the Residents of the Tudor Shaft Informal Settlement <i>Authors: Dawid de Villiers, Gert Liebenberg, Rean Swart, Rietha Oosthuizen, Juanette John, Hanlie Liebenberg-Enslin, Didintle Modisamongwe, Grant Walters</i>	1011
Mathematical Modeling of the Aging Process of the Containment Spray Injection System using the Fault Tree Method <i>Authors: Diogo da Silva Borges, Deise Diana Lava, Maria de Lourdes Moreira, Antonio Cesar Ferreira Guimarães</i>	1012
Determination of the Detection Efficiency of ¹³¹I in Thiroid using Monte Carlo Method <i>Authors: Dayana Ramos Machado, Yoan Yera Simanca, Gladys M. López Bejerano, Nancy Acosta Rodriguez</i>	1013
Uranium Aerosols in Nuclear Fuel Manufacturing <i>Authors: Edvin Hansson, Håkan Pettersson, Christine Fortin, Mats Eriksson</i>	1014
The Future Free Electron Laser Facility SwissFEL from a Radiation Protection Point of View <i>Authors: Eike Hohmann, Roland Luescher, Elisa Musto, Albert Fuchs, Sabine Mayer</i>	1015
Assessment of Beam Dump Activation for RAON Heavy Ion Accelerator in Korea <i>Authors: Eunjoong Lee, Cheolwoo Lee, Sungchul Yang, Young-Ouk Lee, Kyeongjin Park, Gyuseong Cho</i>	1016
Area Monitoring on Nuclear Fuel Cycle Facilities <i>Authors: Elizabeth Renteria, Paula Nuñez, Analia Saavedra, Nestor Fruttero, Allan Segato</i>	1017
How Spanish Nuclear Power Plant have Implemented Lessons Learned from the Fukushima Accident in the Radiation Protection Field <i>Author: Eduardo Sollet</i>	1018
Setting up an Occupational Radiation Protection Program in NORM Industry: A Case Study in Mining Industry in the Democratic Republic of the Congo <i>Authors: Francois Kazadi Kabuya, Vincent Lukanda Mwamba, Leonard Woto Makontsh, Robert Lwamba Ilonda</i>	1019

Monitoring and Mapping of Radon Concentration within Ghana Atomic Energy Commission <i>Authors: Francis Otoo, Emmanuel Ofori Darko, Massimo Garavaglia, Concettina Giovani, Silvia Pividore, Bentil Aba Andam, Geoffrey Emi-Reynolds, Lucas Piccini</i>	1020
GIS Mapping and Background Ionizing Radiation (BIR) Assessment of Solid Mineral Mining Sites in Enugu State, Nigeria <i>Authors: Avwiri Gregory, Agbalagba Ezekiel, Osimobi Jude, Ononugbo Patience</i>	1021
Using a Portable Neutron Generator in an Open Field: The Radiation Protection Assessment <i>Authors: Gian Marco Contessa, Nadia Cherubini, Alessandro Dodaro, Luigi Lepore, Giuseppe Augusto Marzo, Sandro Sandri</i>	1022
Testing of Burn-up Calculation Method based on Chebyshev Rational Approximation with IAEA-ADS Benchmark <i>Authors: Guangyao Sun, Wending Fan, Lijuan Hao, Binhang Zhang, Jing Song, Pengcheng Long, Liqin Hu</i> ..	1023
Assessment of Occupational Exposure of ‘Conflict Mineral’ Artisanal Mine Workers via Radiogenic and Dosimetric Characterization of High Background Radiation Area (HBRA) Columbite-Tantalite (Coltan) <i>Authors: Hudson Angeyo Kalambuka, Leon Ntihakose, Jayanti Patel, David Maina</i>	1024
 Towards a Novel Modular Architecture for CERN Radiation Monitoring <i>Authors: Hamza Boukabache, Michel Pangallo, Nicola Cardines, Gael Ducos, Antonio Bellotta, Ciarán Toner, Daniel Perrin, Doris Forkel-Wirth</i>	1025
Assessment of Internal Dose due to Intake of Food for Determination of Representative Person in Normal Operation of Nuclear Power Plant <i>Authors: Hyungjoon Yu, Insu Chang, Jungil Lee, Jang-Lyul Kim, Bonghwan Kim</i>	1026
Practical use of Graph Theory to Reduce the Individual Doses of the Employees Working in Areas with High Background Radiation <i>Authors: Iliia Kudrin, Ivan Mazur, Konstantin Chizhov, Victor Kryuchkov</i>	1027
Development and Implementation Experience of Information-Analytical System of Radiation Safety of Workers <i>Authors: Ivan Mazur, Iliia Kudrin, Chizhov Konstantin, Kryuchkov Viktor</i>	1028
Recent Developments in Occupational Exposure Reduction in Nuclear Power Plants <i>Authors: Jason Harris, David Miller</i>	1029
Practical Impacts of NORM Standards on Mining and Minerals Processing <i>Author: Jim Hondros</i>	1030
Radiation Protection in the South African Mining and Minerals Extraction Industries <i>Author: James Larkin</i>	1031
Improved Approach to Estimate Fission Product Inventory using TRITON in SCALE 6.1 for a Nuclear Reactor with Gadolinium Burnable Poison <i>Authors: Jaehoon Song, Kyoyoun Kim</i>	1032
The Field Characterization Around the High Energy X-ray Cargo Screenings <i>Authors: Kamil Szewczak, Katarzyna Woloszczuk</i>	1033
Occupational Exposure during Fusion Research on PF-1000 Unit <i>Authors: Kamil Szewczak, Slawomir Jednorog</i>	1034
Room Submersion Calculations of Noble Gas Dose Rate Coefficients <i>Authors: Ken Veinot, Shaheen Dewji, Michael Bellamy, Keith Eckerman, Nolan Hertel, Mauritius Hiller</i>	1035
Residual Activity in Lead and Bismuth Materials induced by 100-40 MeV Protons <i>Authors: Leila Mokhtari Oranj, Nam-Suk Jung, Joo-Hee Oh, Hee-Seock Lee</i>	1036
Security of Radioactive Materials in Oil & Gas Industry (Compliance & Challenges) <i>Author: Mohammad Aref</i>	1037
Egypt Experience with Research Reactors Operation, Nuclear and Radiological Activities Law as a Step for Building Nuclear Power Reactors <i>Author: Mohamed Gomaa</i>	1038

Direct Measurement of Radium Levels in Waste Water Samples using Portable Medium Resolution Gamma Spectrometers <i>Authors: Michael Iwatschenko-Borho, Scott Masiella, Richard Oxford, James Williams</i>	1039
Practical Application Illustrating Excellence in Radiological Protection at the Koeberg Nuclear Power Station <i>Author: Marc Maree</i>	1040
Improvement of Underground Radon Concentrations at a South African Gold Mine <i>Author: Marc Vermeijs</i>	1041
Building Nuclear Security Culture in Morocco <i>Authors: Oumkeltoum Hakam, Abdelmajid Choukri, Taha Laghouazi</i>	1042
The Role of Radiation Protection in Nuclear Forensics: From the Crime Scene to the Laboratory <i>Authors: Philemon Magampa, Gedion Nkosi</i>	1043
EcoMine – A Software Package based on Ecolego to Assess the Radiological Impact of Mining Sites and Activities <i>Authors: Rodolfo Avila, Erik Johansson, Japie van Blerk</i>	1044
U and Th Source Term Characterisation in Selected Gold Tailings of the Witwatersrand (South Africa): A Geochemical Modelling and Reaction Network Approach <i>Authors: Robert Hansen, Japie Van Blerk</i>	1045
Radiation Protection Research <i>Author: Rebecca Tadesse</i>	1046
Radiation Protection Aspects of Uranium In Situ Recovery / In Situ Leach Facilities <i>Author: Steven Brown</i>	1047
Worker Protection Implications of the Solubility and Human Metabolism of Modern Uranium Mill Products <i>Authors: Steve Brown, Douglas Chambers</i>	1048
Dust Management on Tailings Storage Facilities at a South African Gold Mine <i>Authors: SJ van Wyk, CF Human</i>	1049
Risk of Radon Induced Health Effect: Evaluation Methods and Practical Application <i>Authors: Sergey Kiselev, Vladimir Demin</i>	1050
Comparison of the Efficacy of Neutron Shielding of Aluminum and Polyethylene Composites Containing Micro and Nano-Sized B₄C and Carbon Nanotubes <i>Authors: SMJ Mortazavi, Fatemeh Jamali, MR Kardan, Sedigheh Sina, MA Mosleh-Shirazi, Jila Rahpeyma</i>	1051
Assessment on Occupational Exposure in Malaysia: Practices and Trends <i>Authors: Suzilawati Muhd Sarowi, John Konsoh, Ahmad Bazlie Abdul Kadir</i>	1052
Advance Determination of Respiratory Protection Needs when Performing Destructive Work on Structural Materials <i>Author: Scott Schwahn</i>	1053
Reduction in Doses and Lung Cancer Risks among Canadian Uranium Miners between 1930s and 2013 <i>Authors: Tristan Barr, Pascale Reinhardt, Patsy Thompson, Douglas Chambers, Ron Stager, Occupational Cancer Research Center</i>	1054
Operational Health Physics Development Activities Related to Fast Reactor Fuel Fabrication and Pyro-Processing <i>Authors: Ravi T, Akhila R, Krishnakumar D N, Rajagopal V, Jose M T, Venkatraman B, Satyamurthy S A V</i>	1055
The Information System on Occupational Exposure (ISOE): Trends and Lessons <i>Authors: Tae-Won Hwang, Olvido Guzman</i>	1056
Protecting Humans and the Environment the Next Hundred Thousands of Years <i>Authors: Ulrik Kautsky, Eva Andersson, Tobias Lindborg, Anders Löfgren, Sara Nordén, Peter Saetre</i>	1057


Assessment of Belarusian NPP for Protection of the Public <i>Author: Viktoryia Kliaus</i>	1058
Development of a Dose Assessment Code for the Radiation Protection of Representative Person in Korea <i>Authors: Won Tae Hwang, Eun Han Kim, Moon Hee Han, Hae Sun Jeong</i>	1059
Effect of Particle Size and Percentages of Boron Carbide on the Thermal Neutron Radiation Shielding Properties of HDPE/B4C Composite: Experimental and Simulation Studies <i>Authors: Zahra Soltani, Farhood Ziaie</i>	1060

JC@ A9

Area 5: Optimisation and Design of New Facilities	1061
Monte Carlo Modeling and Verification of the Shielding for an Ionizing Radiation Test Laboratory <i>Authors: C. Stettner, N. Baumgartner, M. Blaickner, C. Hranitzky</i>	1062
Preconcentration of cobalt metal ions onto imprinted polymer hydrogels <i>Authors: Ghada A. Mahmoud, Hegazy E. A, S. M. Elbakery</i>	1065
Dose Constraint – a Mysterious Concept of Radiation Protection <i>Author: Helena Janžekovič</i>	1072
Establishment of a Laboratory for Gamma-ray Spectrometry of Environmental Samples Collected in Fukushima <i>Authors: Jun Saegusa, Tomoyuki Yoda, Satoshi Maeda, Tsutomu Okazaki, Shuichi Otani, Toshio Yamaguchi, Yoshiyuki Kurita, Atsushi Hasumi, Chushiro Yonezawa, Minoru Takeishi</i>	1078
New Remote Controlled Experiments in Nuclear Chemistry <i>Authors: Jan-Willem Vahlbruch, Wolfgang Schulz, Claudia Fournier, Paul Hanemann, Sebastian Büchner, Clemens Walther</i>	1086
Introduction and assessment of new heavy weight concrete shields using Monte Carlo simulation <i>Authors: Mahdi Saeedi-Moghadam, Mahdi Kazempour, Sedigheh Sina, Reza Jalli, Banafsheh Zeinali-Rafsanjani</i>	1094
Exposure Rate Assessment From Selected Cathode Ray Tube Devices <i>Authors: Ife-Adediran O. O., Arogunjo A. M.</i>	1100
Case Study: Radiation Protection measures when designing an extension of a Nuclear Medicine Department <i>Authors: Youness Esserhir El Fassi, Jean-Élie Fontaine, Mathieu Valla, Siham El Moghni, Youness Haddoudi, Paul Livolsi, Abdelmajid Choukri, Oum Keltoum Hakam</i>	1108
Optimization of occupational exposure during first operations with ¹⁸F in Cuba <i>Author: Zayda Haydeé Amador Balbona</i>	1117
The Role of the Radiological Protection Team as a Stakeholder in the Design Phase of a Nuclear Facility: the Case of Brazilian Conversion Plant <i>Authors: Ana Cristina Lourenço, Wagner de Souza Pereira</i>	1126
Design Study of ELI-NP Beam Dumps: Radioprotection Issues and Monte-Carlo Simulations <i>Authors: Adolfo Esposito, Oscar Frasciello, Maurizio Pelliccioni</i>	1127
Preliminary Thermo-mechanical Design of the Main Dump for the High Energy Electron Beam Lines in ELI-NP <i>Authors: Adolfo Esposito, Lina Quintieri</i>	1128
Radioprotection Issues for the STAR Project <i>Authors: Adolfo Esposito, Oscar Frasciello, Fiorello Martire, Maurizio Pelliccioni</i>	1129
Cyclotron Production of Sc and V Radionuclides from Natural Titanium for Medical Applications <i>Authors: Ahmed Rufai Usman, Mayeen Uddin Khandaker, Hiromitsu Haba, Naohiko Otuka</i>	1130
Design Approval and Registration for Radiation Devices <i>Authors: BokHyoung Lee, SangEun Han, KiWon Jang, JongRae Kim, WooRan Kim, KyungWha Kim, Younjin Park</i>	1131

Preliminary Analysis of Radiation Characteristic for 250 MeV Proton Accelerator Driven Sub-critical System	
<i>Authors: Bin Li, Qi Yang, Bo Chang, Chao Liu, Liqin Hu</i>	1132
New CZT (H3D) Technology Employed at Cook Nuclear Plant Achieves Immediate Individual Isotopic Identification and Verifies Adequacy of Temporary Shielding	
<i>Author: David Miller</i>	1133
Radiation Protection for NORM Industries – Results of the European Joint Research Project ‘Metrology for Processing Materials with High Natural Radioactivity (MetroNORM)	
<i>Authors: Franz Josef Maringer, Sylvie Pierre, Teresa Crespo Vazquez, Monika Mazanova, Pierino De Felice, Branko Vodenik, Mario Reis, Mikael Hult, Laszlo Szücs, Simon Jerome, Alexander Muring, Roy Pöllänen, Andreas Baumgartner, Boris Bulanek, Boguslaw Michalik, Nathalie Michielsen, Julian Dean, Philippe Cassette, Franz Kabrt, Hannah Moser</i>	1134
Effectiveness of the Shielding Mechanism in Rooms Housing X-ray Diagnostic Equipment - A Case Study of Mulago Hospital	
<i>Authors: Festo Kiragga, Rebecca Nakatudde, Akisophel Kisolo</i>	1135
KIRDI’S Role in the Project “Promoting Safety, Self-reliance and Sustainability of Non-Destructive (NDT) Testing Facilities”	
<i>Author: Humphrey Lumadede</i>	1136
Requirements for Specific Safety Issues - Fire, Earthquake, and Flooding – at Large Particle Accelerator Facilities	
<i>Authors: Hee-Seock Lee, Arim Lee, Nam-suk Jung, Joohee Oh, Leila Mokhtari Oranj</i>	1137
Modernisation of the Radiation Monitoring Systems at Research and Training Reactors in Hungary	
<i>Authors: János Petrányi, Dénes Elter, Imre Szalóki, Máté Solymosi, László Manga</i>	1138
Environmental Radiation and Meteorological Monitoring Systems of a Greenfield Nuclear Power Plant	
<i>Authors: Juho Rissanen, Jussi Huotilainen</i>	1139
Evaluation of Carbon -14 Released from Small Power Reactor	
<i>Authors: Kyo-Youn Kim, Ha-Young Kim, Jae Hoon Song</i>	1140
Development of a Methodology to Correlate Safety Classification of Components to the Maintenance Programme of a Facility	
<i>Author: Muhammad Akbar</i>	1141
Applicability of Lessons Learned from the Fukushima Accident to Radioactive Material Users	
<i>Authors: Shawn Smith, Catherine Haney</i>	1142
Local Shield Model around Beam Target Stations using Radiation Transport Code MCNPX	
<i>Authors: Tebogo Kupi, Johann van Rooyen, Raymond Njinga</i>	1143
Validation of Experimental Measurements of Activity for Radioisotopes in SAFARI-1 Reactor	
<i>Author: Tholakele Ngeleka</i>	1144
Robotic HPGe Spectrometer for Radionuclide Analysis	
<i>Authors: Vladimir Gostilo, Alexander Sokolov</i>	1145
Area 6: Radiation Detection and Dosimetry	1146
A New Approach to Worker Internal Dosimetry and its Impact on Radiation Protection	
<i>Authors: Alan Birchall, Vadim Vostrotin, Matthew Puncher, Alexander Efimov, Bruce Napier</i>	1147
Approach to uncertainties in exposure, dose and risk estimates for uranium workers within the CURE project	
<i>Authors: Augusto Giussani, Sophie Ancelet, Derek Bingham, Eric Blanchardon, Richard Bull, Estelle Davesne, James Grellier, Olivier Laurent, Dominique Laurier, Matthew Puncher, Tony Riddell</i>	1155
Joint Coordinating Committee on Radiation Effects Research Project 1.1: Techa River Population Dosimetry	
<i>Authors: Bruce A Napier, Marina O Degteva, Evgenia I Tolstykh, Natalia B Shagina, Elena A Shishkina, Marina I Vorobiova, Nickolay G Bougrov, Lynn R Anspaugh</i>	1162

Joint Coordinating Committee on Radiation Effects Research Project 2.4: Mayak Worker Dosimetry <i>Authors: Bruce Napier, Alexander Efimov, Alan Birchall, Vadim Vostrotin, Matthew Puncher, Alexandra Sokolova, Klara Suslova, Scott Miller, Alexay Zhdanov, Evgeney Vasilenko</i>	1168
Waterfowl-specific Computational Models for use in Internal Dosimetry <i>Authors: Dawn Montgomery, Jennifer Paloni, Nicole Martinez</i>	1174
Project 1.2b: Techa River Population Cancer Morbidity and Mortality <i>Authors: Daniel O. Stram, Lyudmila Krestinina, Dale Preston, Alexander Akleyev</i>	1182
Assessment of equivalent dose of the lens of the eyes and the extremities to workers under nonhomogeneous exposure situation in nuclear and accelerator facilities by means of measurements using a phantom coupled with Monte Carlo simulation <i>Authors: Hiroshi Yoshitomi, Masayuki Hagiwara, Munehiko Kowatari, Sho Nishino, Toshiya Sanami, Hiroshi Iwase</i>	1188
Implementation of Co-worker Models for the Reconstruction of Dose under an Occupational Radiation Exposure Compensation Program <i>Author: James W. Neton</i>	1196
Experience with Wound Dosimetry in Uranium Mining and Processing <i>Authors: John Takala, Kari Toews</i>	1204
Response of $^{10}\text{B}+\text{ZnS}(\text{Ag})$ as neutron detector in Radiation Portal Monitors <i>Authors: Karen A. Guzmán-García, H.R. Vega-Carrillo, Eduardo Gallego, Alfredo Lorente, Juan A. González</i>	1213
Wrist, finger, and crystalline dosimetry study with radiopharmacists and nursing technicians for various applications and tests, using various radiopharmaceuticals, for adjustment of a percentage factor between difference values obtained at the extremities to optimize the dosimetry in nuclear medicine services. <i>Authors: Maria Inês Calil Cury Guimarães, Sato, Karen A. K., Leandro F. Souza, Leia R. Santo, Elaine C. Santo, Ivani B. Melo, Heber S. Videira, Julia A. Gonzalez, Carlos A. Buchpiguel, Josefina da Silva Santos, Adélia Sahyun</i>	1221
Direct Surface Contamination Measurement of Low Energy Beta and Electron Capture Isotopes <i>Authors: Michael Iwatschenko-Borho, Reinhard Loew</i>	1224
The Facility of Radiation Standards in Japan Atomic Energy Agency, present status and its research works on dosimetry <i>Authors: Munehiko Kowatari, Hiroshi Yoshitomi, Sho Nishino, Yoshihiko Tanimura, Tetsuya Ohishi, Michio Yoshizawa</i>	1230
Evaluation of radiation detectors for a possible integration into the automated survey system TIM in the Large Hadron Collider (LHC) <i>Authors: Markus Widorski, Frédéric Aberle, Cristina Adoriso, Daniel Perrin</i>	1239
Investigations into Radiation Dose Distribution in a Computed Tomography Fluoroscopy Room: Monte Carlo Studies <i>Authors: Prince Kwabena Gyekye, Frank Becker, Geoffrey Emi-Reynolds</i>	1245
PIMAL: A GUI-Driven Software Package To Conduct Radiation Dose Assessments Using Realistic Phantom Postures <i>Authors: Shaheen Dewji, Mauritius Hiller, Nolan Hertel, Sami Sherbini, Mohammad Saba</i>	1251
Comprehensive Study on the Response of Neutron Dosimeters in Various Simulated Workplace Neutron Calibration Fields <i>Authors: Sho Nishino, Katsuya Hoshi, Norio Tsujimura, Munehiko Kowatari, Tadayoshi Yoshida</i>	1258
Estimation of basic characteristics about scintillation type survey meter using multi pixel photon counter <i>Author: Toshioh Fujibuchi</i>	1264
Comparison of dose rate measurements of commercially available hand- held gamma detectors with radiation protection dose meter <i>Authors: Theo Köble, Hermann Friedrich</i>	1268
Estimation of detective efficiency of CdZnTe semiconductor detector and NaI(Tl) scintillation detector <i>Authors: Takatoshi Toyoda, Toshioh Fujibuchi</i>	1273

A study of Energy-Compensating Metal Filter of Semiconductor Detector for Personal Dosimetry in X-ray Diagnosis <i>Authors: Kento Terasaki, Toshioh Fujibuchi, Hiroo Murazakic, Taku Kuramoto, Yoshiyuki Umezu, Yang Ishigaki, Yoshinori Matsumoto</i>	1279
Determination of fission radionuclides activities in a real fission gamma-ray field <i>Authors: Žlebčík P. , Malá H., Huml O.</i>	1285
Radiation-induced Color Bleaching of Methyl Red in Polyvinyl Alcohol (PVA) Film Dosimeter <i>Authors: Awad Alzahrany, Ahmed Basfar, Khalid Rabaeh</i>	1293
Characterization of HPGe Detectors using Computed Tomography <i>Authors: Angelica Hedman, Jalil Bahar Gogani, Micael Granström, Lennart Johansson, Jonas Andersson, Henrik Ramebäck</i>	1294
Optimized Detector for in Situ Low Energy Gamma Spectrometry in Close Geometries <i>Authors: Angelica Hedman, Göran Ågren, Lennart Johansson, Jalil Bahar Gogani, Henrik Ramebäck</i>	1295
Delineation of Radiation Dose Pattern in Radiation Workers and Dose Optimization Using Dose Reduction Methodologies <i>Authors: Ajai Kumar Shukla, Dhiraj Kumar Tewari</i>	1296
Establishment of a National Dose Register in South Africa <i>Authors: Alan Muller, Nthabiseng Mohlala</i>	1297
Public In Vivo Thyroid Monitoring for Dose Estimation after Accidental Intake of I-131. Experiences from Scandinavia <i>Authors: Asser Nyander Poulsen, Henrik Roed, Lilián del Risco Norrlid, Mats Isaksson, Bjorn Lind, Óskar Halldórson Holm, Jussi Huikari</i>	1298
Comparison of Radiation Dose Assessment Methodology used for the Public Living in the Area Contaminated with Radioactive Materials <i>Authors: A Ra Go, Min Jun Kim, Kwang Pyo Kim</i>	1299
Argentinian Intercomparison Exercise on Internal Dosimetry: ¹³¹I Thyroid Monitoring <i>Authors: Ana Rojo, Nancy Puerta, Sebastian Gossio, Ines Gomez Parada</i>	1300
Performance Comparison of OSLD (Al₂O₃:C) and TLD (LiF:Mg,Cu,P) in Accreditation Proficiency Testing <i>Authors: Alexander Romanyukha, Mathew Grypp, Anthony Williams</i>	1301
Test of Ring, Eye Lens and Whole Body Dosemeters for the Dose Quantity Hp(3) to be used in Interventional Radiology <i>Authors: Agnieszka Szumska, Renata Kopeć, Maciej Budzanowski</i>	1302
From Filter Swipe Test to Bioavailability: A Rapid Experimental Approach to Assess Actinide Behaviour Following Internal Contamination <i>Authors: Anne Van der Meeren, Agnès Moureau, Sylvie Coudert, Pierre Laroche, Jaime Angulo, Nina Griffiths</i>	1303
Microphotonics Approaches to Nuclear Forensics Analysis <i>Authors: Bobby Bhatt, Hudson Angeyo, Alix Dehayem-Massop</i>	1304
Determination of Scattering Factors Associated to the In Vivo Monitoring of Iodine-131 in the Thyroid <i>Authors: Bernardo Dantas, Fabiana Lima, Ana Leticia Dantas, Eder Lucena, Rodrigo Gontijo, Carlaine Carvalho, Clovis Hazin</i>	1305
μ-TPC: A New Recoil Nuclei Telescope for Low Energy Neutron Fields characterization <i>Authors: Benjamin Tampon, Daniel Santos, Olivier Guillaudin, Jean-François Muraz, Lena Lebreton, Thibaut Vinchon, Nadine Sauzet</i>	1306
A Passive Neutron Dosimeter for Measurement in Mixed Neutron-Photon Fields <i>Authors: Sören Mattsson, Maria Christiansson, Christian Bernhardsson</i>	1307
 The Russian Human Radiobiological Tissue Repository: A Unique Resource for Studies of Plutonium-Exposed Workers <i>Authors: Christopher Loffredo, David Goerlitz, Svetlana Sokolova, Leonidas Leondaridis, Mariya Zakharova, Valentina Revina, Evgeniya Kirillova</i>	1308

Characterization and Measurement of Dosimetry X-ray Bean on Kenya <i>Authors: Collins Omondi, David Otwoma</i>	1309
R International Standards on Radioactivity Measurement for Radiological Protection: Status and Perspectives <i>Authors: Dominique Calmet, Roselyne Ameon, Aude Bombard, Stephane Brun, Francois Byrde, Jing Chen, Jean-Marie Duda, Maurizio Forte, Marc Fournier, Ales Fronka, Thomas Haug, Margarita Herranz, Amir Husain, Simon Jerome, Martin Jiranek, Steven Judge, Sang Bog Kim, Pieter Kwakman, Jeanne Loyen, Montse LLaurado, Rolf Michel, David Porterfield, Andry Ratsirahonana, Anthony Richards, Katerina Rovenska, Tetsuya Sanada, Christoph Schuler, Laurence Thomas, Shinji Tokonami, Andrey Tsapalov, Takahiro Yamada</i>	1310
A Method for Response Time Measurement of Ionization Chamber Type Survey Meter <i>Authors: Dehong Li, Bin Guo, Jianwei Wang, Di Wu, Xingdong Li</i>	1312
The Primary Standard for Air Kerma at the NIM for the Gamma Radiation of 137Cs <i>Authors: Dehong Li, Peiwai Wang, Jianwei Huang, Bin Guo, Di Wu</i>	1313
Dosimetry for Radiological Protection at the New Research Facility, ELI-NP <i>Authors: Elena Iliescu, Sorin Bercea, Iani Mitu, Aurelia Celarel, Constantin Cenusu</i>	1314
Determination of a Urine Reference Level for an Individual Monitoring Programme for Uranium <i>Author: Frik Beeslaar</i>	1315
Data Recording Regarding the Dose Assessment due to X-ray Generator Sources and the ²⁴¹Am Calibration Curve Usefulness <i>Authors: Felicia Mihai, Ana Stochioiu, Catalina Tuca</i>	1316
R Integrated Operational Dosimetry System at CERN <i>Authors: Gérald Dumont, Fernando Baltasar Dos Santos Pedrosa, Pierre Carbonez, Doris Forkel- Wirth, Pierre Ninin, Eloy Reguero Fuentes, Stefan Roesler, Joachim Vollaire</i>	1317
Biodosimetry of in Vitro Human Lymphocytes exposed to ⁶⁰Co γ-rays and DNA Incorporated ¹²³I <i>Authors: Hein Fourie, Jacobus Slabbert, Richard Newman, Philip Beukes, Neil Rossouw</i>	1318
Development of Radiation Portal Monitoring System based on Energy Weighted Algorithm for Gamma Spectroscopy <i>Authors: Hyuncheol Lee, Wook-Geun Shin, Han Rim Lee, Chang-Il Choi, Chang-Su Park, Hong- Suk Kim, Chul Hee Min</i>	1319
Results of the EURADOS Intercomparisons IC2014 on Whole Body Dosimeters for Photons <i>Authors: Hannes Stadtmann, Tom Grimbergen, Andrew McWhan, Ana Maria Romero, Markus Figel, Christian Gärtner</i>	1320
Improving Potential in a Retrospective Dosimetry using Common Plastics by Extracting Inorganic Materials <i>Authors: Insu Chang, Jang-Lyul Kim, Jungil Lee, Tae-Hyoung Kim, Seung-Kyu Lee, Bong-Hwan Kim</i>	1321
Performance of Eye Lens Dosimeters in use in Europe <i>Authors: Isabelle Clairand, Merce Ginjaume, Filip Vanhavere, Eleftheria Carinou, Josiane Dures, Marc Denoziere, Edilaine Honorio da Silva, Maria Roig, Sara Principi, Laurent Van Rychehem</i>	1322
Contemporary Radiation Protection Trends – Do we need a New Yype of Digital Personal Dosimeters to be used in Medicine, Homeland Security, Environmental Protection and Emergencies? <i>Authors: Ivica Prlic, Marija Suric Mihic, Mladen Hajdinjak, Tomislav Mestrovic, Zdravko Cerovac</i>	1323
Rare-earth Doped Silica Fibres for Dosimetry Applications in Medicine <i>Authors: Ivan Veronese, Mauro Fasoli, Norberto Chiodini, Eleonora Mones, Cristina De Mattia, Eduardo D'Ippolito, Marie Claire Cantone, Anna Vedda</i>	1324
DosiKit, Innovative Solution for On-site External Radiation Biodosimetry <i>Authors : Julie Bensimon, Caroline Bettencourt, Sandrine Altmeyer, Arnaud Tupinier, Nicolas Ugolin, Sylvie Chevillard</i>	1325
Analysis of Photon Energy Distribution at the Working Places in Nuclear Power Plants Using In-situ CZT Detectors <i>Authors: Jeongin Kim, Seokon Kang, Meeseon Jeong</i>	1326

Monte Carlo Approach to Accidental Dose Reconstruction Based on the EPR Measurements of Absorbed Dose to Human Teeth <i>Authors: Jeongin Kim, Hoon Choi, Byoungil Lee</i>	1327
R Development of two new single-exposure, multi-detector neutron spectrometers for radiation protection applications in workplace monitoring <i>Authors: J.M. Gómez-Ros, R. Bedogni, D. Bortot, C. Domingo, A. Esposito, M.V. Introini, M. Lorenzoli, G. Mazzitelli, M. Moraleda, A. Pola, D. Sacco</i>	1328
The Influence of the Dose Calculation Resolution of VMAT Plans on the Calculated Dose for Eye Lens and Optic Apparatus <i>Authors: Jong Min Park, So-Yeon Park, Jung-in Kim, Hong-Gyun Wu, Jin Ho Kim</i>	1329
Dosimetry Aspects for the Development of an Irradiator for Cross-linking of Cables using ⁶⁰Co Gamma Rays <i>Authors: Jain Reji George, B K Pathak</i>	1330
Development and Applications of Super Monte Carlo Simulation Program for Advanced Nuclear Energy Systems <i>Authors: Jing Song, Liqin Hu, Pengcheng Long, Tao He, Lijuan Hao, Mengyun Cheng, Huaqing Zheng, Shengpeng Yu, Guangyao Sun, Tongqiang Dang, Qi Yang, Bin Wu, Chaobin Chen, Ling Fang, Yican Wu, FDS Team</i>	1331
Study of Eye Lens Dose at the Nuclear Industries in Sweden <i>Authors: Lisa Bäckström, Karin Andgren</i>	1332
Direct Ion Storage Dosimetry Roadmap <i>Authors: Kip Bennett, Michael Lantz, Matti Vuotilla, Jani Rakkola</i>	1333
Implementation of a New BeOSL Dosimetry Platform Utilizing Lean Manufacturing Tools <i>Authors: Kip Bennett, Mike Lantz, Joel White, Gordon Sturm, Reiner Esser, Timo Wiedenmann, Jay Thomas</i>	1334
R Y Monte Carlo calibration of the whole body counting detection system for β ⁹⁰Sr measurement of people internally contaminated with ⁹⁰Sr <i>Authors: Karin Fantinová, Pavel Fojtík, Irena Malátová</i>	1335
Backscatter Response of Different Personal Dosimeter Detectors for Water Slab and Cylindrical Calibration Phantoms <i>Authors: Kristine Marie Romallosa, Hiroshi Yoshitomi</i>	1336
Dosimetric Uncertainty Analysis of the Optically Stimulated Luminescence Dosimeter System in the Philippines <i>Authors: Kristine Marie Romallosa, Marianna Lourdes Grande, Estrella Caseria</i>	1337
Development of the Electronic Personal Dosimeter Based on Scintillator for a Mobile Phone Application <i>Authors: Kyeongjin Park, Daehee Lee, Hyunjun Yoo, Eunjoong Lee, Hyunduk Kim, Hojong Chang, Gyuseong Cho, Alexander Solodov</i>	1338
Salty Nuts and Snacks for Retrospective Dosimetry <i>Authors: Maria Christiansson, Christian Bernhardsson, Therese Geber-Bergstrand, Sören Mattsson, Christopher Rääf</i>	1339
Dosimetric Evaluation of a Radiological Accident involving a Gammagraphy Industrial Source of ¹⁹²Ir (44 Ci)-Multidisciplinary Approach <i>Authors: Marina Di Giorgio, Analía Radl, Adrian Discacciatti, Diana Dubner, Sebastian Gossio, Francois Trompier, Ezequiel Soppe, Adriana Coppola, Mayra Deminge, Julieta Rearte, Ana Molinari, Ignacio Menchaca, Fabio Lopez, Gaston Castro, Mariana Egan, Mercedes Portas</i>	1340
In Light Optically Stimulated Luminescence Dosimetry for Occupational Workers in the Philippines <i>Authors: Marianna Grande, Kristine Romallosa, Estrella Caseria, Ahmad Bazlie</i>	1341
Particle Size Distributions of Radioactive Aerosols in the Atmosphere <i>Authors: Miroslav Hýža, Petr Rulík, Helena Malá, Vera Beckova</i>	1342
Optical Stimulated luminescence from Citrine for High-Doses Dosimetry <i>Authors: Maria Ines Teixeira, Linda V.E. Caldas</i>	1343

Performance Data of a new Active Personal Dosimeter in Respect to Gamma, Beta and Pulsed X-ray Radiation	
<i>Authors: Michael Iwatschenko-Borho, Alan Laing, Ling Luo, Cassidy McKee, Greg Nelson, Ralf Pijahn, Norbert Trost</i>	1344
Calibration of Conventional Survey Meters for Soft X-ray Below 5 keV	
<i>Authors: Masahiro Kato, Tadahiro Kurosawa, Toshihiko Hino, Yoshinori Inagaki</i>	1345
Retrospective Review of Dosimeter Film Processing	
<i>Authors: Mirela Kirr, Christopher Passmore</i>	1346
Design of Long Counter Having Flat Response from Few keV up to 150 MeV	
<i>Authors: Mohamed Mazunga, Taosheng Li, Yanan Li, Jieqiong Jiang, Yican Wu</i>	1347
Measurement of Occupational Doses of Ionising Radiation to the Whole body of Diagnosis Radiologists	
<i>Author: Maryam Pourkaveh</i>	1348
Calculation of 2D Dose Distribution in an Inhomogeneous Phantom using Artificial Neural Network with Best Training Method	
<i>Authors: Mahdi Saeedi-Moghadam, Banafsheh Zeinali-Rafsanjani, Kamal Hadad, Sepideh Sefidbakht</i>	1349
Photoneutron Secondary Cancer Risk Estimation by a Novel Position-Sensitive Detection Method	
<i>Authors: Mehdi Sohrabi, Amir Hakimi</i>	1350
A New Method for Effective Dose Calculation based on the Ambient Dose Height Distribution	
<i>Authors: Niroojiny Sangarapillai, Mario Liebmann, Bjoern Poppe, Heiner von Boetticher</i>	1351
Development of a New Optical Reading Technique for Dosimetric Gels based on the Analysis of the Scattering Light	
<i>Authors: Olivier Bleuse, Régine Gschwind, Yannick Bailly</i>	1352
Performance Assessment of the Criticality Dosimetry System at The Belgian Nuclear Research Centre SCK•CEN	
<i>Authors: Olivier Van Hoey, Filip Vanhavere, Marcel Reginatto</i>	1353
PROCORAD's International Proficiency Testing for Radio-Bioassays	
<i>Authors: Robert Fottorino, Bernadette Peleau, Christian Hurtgen</i>	1354
Assessment of Dose Calibrators Performance in Nuclear Medicine Department in Sudan	
<i>Author: Suhaib Alameen</i>	1355
A Simple, Reliable and Inexpensive Microscopy-Based Method for Radiation Biodosimetry	
<i>Authors: Sudhir Chandna, Shwetanjali Nimker, Kanupriya Sharma, Vijaypal Singh</i>	1356
Secondary Neutron Dose Assessment from Proton Therapy Using Passive Scattering at The National Cancer Centre (NCC)	
<i>Authors: Sang Eun Han, Se Byeong Lee, Gyuseong Cho, Kyeongjin Park</i>	1357
Traceable Measurements for Radiation Protection Industry in South Africa	
<i>Author: Sibusiso Jozela</i>	1358
Development of the Performance Testing Procedure for the New Proposed Portable Gamma Irradiation System	
<i>Authors: Seung Kyu Lee, Hyungjoon Yu, Insu Chang, Hyoungtaek Kim, Jungil Lee, Jang-Lyul Kim, Bong-Hwan Kim</i>	1359
Development of the Probabilistic Internal Dosimetry Code	
<i>Authors: Siwan Noh, Jai-Ki Lee, Jong-Il Lee, Jang-Lyul Kim</i>	1360
Effect of Radon Progeny on Real Time Alpha-CAM Monitoring in Uranium Facility	
<i>Authors: TaeHyoungh Kim, JunBok Lee, Jong Il Lee, Bong Hwan Kim</i>	1361
PoCAMon – All in one Personal Online Continuous Air Monitor, Gamma Dose Meter and Gas warner	
<i>Author: Thomas Strel</i>	1362

R	Implementation of ICRP 116 Dose Conversion Coefficients for Reconstructing Organ Dose in a Radiation Compensation Program	
	<i>Authors: Timothy Taulbee, Keith McCartney, Richard Traub, Matthew Smith, James Neton</i>	1363
	Tracking System for Radiation Works Using Passive RFID Technology to Enhance Radiation Protection	
	<i>Authors: Yunjong Lee, Jin Kyu Kim, Jinwoo Lee, Young-Hwan Ryu, Ho-Sung Kim, Kyung-Rae Dong, Eun-Jin Choi</i>	1364
	Capability Study of Multi-function Dose Rate Meter Based on Hemisphere CdZnTe Detector	
	<i>Authors: Ying Wang, Wenjun Xiong, Zhiping Luo, Jizeng Ma, Ling Chen</i>	1365
	Combination of Automated Chromatographic Separation and Off-line Cherenkov Counting in Determination of Low Level Activity of Sr-90	
	<i>Authors: Željko Grahek, Ivana Coha</i>	1366
	VOLUME 4	
	Area 7: Environment and Natural Background	1367
	Health Detriment Associated with Exposure to Natural Radioactivity from the Soil of Ondo and Ekiti States South Western, Nigeria.	
	<i>Authors: A.E. Ayodele, A. M. Arogunjo, J. I. Ajisafe, O.T. Arije</i>	1368
	Radioactivity Level of Drilled Well Water across Selected Cities in Ondo and Ekiti States, Southwestern Nigeria and its Radiological Implications	
	<i>Authors: A. E. Ayodele, A. M. Arongunjo, J. I. Ajisafe, O. T. Arije</i>	1376
T	Dating of a sediment core from Lake Biel (Switzerland) and source characterization of fallout Pu	
	<i>Author: Anja Pregler</i>	1382
	Preliminary survey of radon population exposure in east Romanian region	
	<i>Authors: Andreea Teodor, Irina Anca Popescu, Constantin Milu</i>	1390
	Excess Lifetime Cancer Risk of Cosmetic Powders	
	<i>Authors: Chioma Nwankwo, Damilola Folley, Olawunmi Gbolagade</i>	1397
	Monitoring of ambient dose equivalent at the boundary of nuclear sites to verify compliance with the regulations	
	<i>Authors: Cristina P. Tanzi, M. Farahmand, P. Kwakman, R.B. Tax, A.P.P.A. van Lunenburg, G.J.E Slagt, L.P. Roobol</i>	1404
	Determination of the activity concentrations of natural occurring radionuclides in foodstuffs for public dose assessments	
	<i>Authors: Deon Kotze, Immanda Louw, Charles Krös</i>	1409
	Monitoring the environmental radiation by using a new gas-filled proportional counter probe as a quasi-spectroscopic system	
	<i>Authors: Dirk Peter Schmalfuß, Uwe Hoffmann, Julia Glück, Andreas Meister</i>	1416
	Radiological assessment of natural radioactivity in groundwater from Greater Accra Region of Ghana: Gross alpha and gross beta measurements and annual committed effective dose evaluation.	
	<i>Authors: E.J.M.Nguelem, M.Ndontchueng, E.O.Darko</i>	1422
T	Correlations of Radon Measurements in Soil Gas and Indoor for Improving the Prediction of an Area's Radon Potential	
	<i>Authors: Franz Kabrt, Andreas Baumgartner, Harry Friedmann, Valeria Gruber, Wolfgang Ringer, Franz Josef Maringer</i>	1429
	Radiation Measurement Systems and Experiences in Japan after the Fukushima Accident	
	<i>Author: Frazier L. Bronson</i>	1437
T	Environmental radiation monitoring in the gold mining region East Cameroon	
	<i>Authors: Dallou G. B., Ngoa Engola L., Ndjana Nkoulou II, J.Emmanuel, Saïdou, Kwato Njock M. G.</i>	1446

Environmental Dosimetry of Mining Areas: Case of Abandoned Uranium Site, Vinaninkarena- Antsirabe, Madagascar	
<i>Authors: Hary A. Razafindramiandra, Tiana h. Randriamora , Elijaona H. Rakotomalala Anja, Raelina Andriambololona, R. Dina Randriantsizafy, Mbolatiana A. L. Ralaivelo , Edmond Randrianarivony, Solofonirina D. Ravelomanantsoa, Joseph L. R. Zafimanjato, H. Fanja Randriantseheno</i>	1454
The European Radioecology Alliance: Encouraging the Coordination and Integration of Research Activities in Radioecology	
<i>Authors: Hildegard Vandenhove, Jacqueline Garnier-Laplace, Almudena Real, Maarit Muikku, Catherine Lecomte-Pradines, Åste Søvik, Brenda J. Howard, Pere Masque, Rafael Tenorio</i>	1461
A cancer risk due to natural radiation on the Coast of Montenegro	
<i>Authors: Ivanka Antović, Nikola Svrkota, Danko Živković, Nevenka M. Antović</i>	1470
A Survey of Indoor Gamma Dose Rates in Selected Dwellings and Offices in Abeokuta, South Western Nigeria	
<i>Authors: Okeyode, I.C., Oladotun, I.C., Mustapha, A.O., Alatise, O.O., Bada, B.S., Makinde V., Akinboro, F.G., Al-Azmi, D.</i>	1478
Natural radioactivity of samples from the building industry in South Africa	
<i>Authors: I. Ramathhape, D. Kotze, I. Louw</i>	1486
The ICRP Publication 126 on Radiological Protection against Radon Exposure	
<i>Authors: Jean-François Lecomte, Stephen Solomon, John Takala, Thomas Jung, Per Strand, Christophe Murith, Sergey Kiselev, Weihai Zhuo, Ferrid Shannoun, Augustin Janssens</i>	1492
Curies Contaminated Notebook	
<i>An analysis of a notebook and papers, originally belonging to Marie Curie, which are now retained by the Wellcome Collection, London</i>	
<i>Authors: Lindsey Simcox, Jon Taylor</i>	1497
Comparison of Federal Guidance Reports 12 and 15: External Exposure to Radionuclides in Soil, Air, and Water	
<i>Authors: M.B. Bellamy, K.G. Veinot, M.M. Hiller, S.A. Dewji, K.F. Eckerman, C.E. Easterly, N.E. Hertel, R.W. Leggett</i>	1504
Thoron Exhalation Rate and ²³²Th Content in Traditional Building Materials Used in the Coastal Region of Kenya	
<i>Authors: Margaret Chege, Nadir Hashim, Abdallah Merenga, Oliver Meisenberg, Jochen Tschiersch</i>	1511
A comparison of a commercial and specifically developed (CTBTO-VGSL) software packages used in high-resolution gamma-spectrometry on their applicability and accuracy in NORM analysis of environmental samples, which includes optimization of spectrum analysis parameter settings and sum-coincidence and self-absorption corrections	
<i>Authors: Monnicca M. Rapetsoa, Arnaud Faanhofa, Deon Kotze, Robert Lindsay</i>	1515
K-40 levels in the South Adriatic Sea environment (Montenegro)	
<i>Authors: N. M. Antović, I. Antović, N. Svrkota</i>	1520
Would Radiation Deter Space Exploration	
<i>Author: Nicholas Sion</i>	1528
Development of absolute measurement instrument for radioactivity of Radon gas	
<i>Authors: Rio Furukawa, Yasuhiro Unno, Akira Yunoki, Yasushi Sato</i>	1538
Determination of radon emission rate regarding to constructional energy- saving-measures	
<i>Authors: Thomas Neugebauer, Hans Hingmann, Jonas Buermeyer, Anna-Lisa Grund, Volker Grimmf, Joachim Breckow</i>	1543
Selection of Potassium Fertilizer Application Method to Reduce Uptake of Cs-137 in Brown Rice	
<i>Authors: Takashi Saito, Kazuhira Takahashi, Takeshi Ota, Tomoyuki Makino</i>	1550
Findings of the control and monitoring of liquid releases from the Centre of Isotopes of Cuba	
<i>Authors: Zayda Haydeé Amador Balbona, Pilar Oropesa Verdecia</i>	1557
Findings of the control and monitoring of airborne releases from the Centre of Isotopes of Cuba	
<i>Authors: Zayda Haydeé Amador Balbona*, Miguel Antonio Soria Guevara</i>	1564

Radiation Ecology and Human Health. Regional and Global Problems <i>Authors: Z.Paskalev, G.Vassilev, V.Baduline, D.Apostolova</i>	1570
Potassium-40 determination in NPK fertilizer by CZT-500s gamma spectrometry in the LPNPE Lab <i>Authors: A. Justinien Franck Ratovonjanahary, Hery Tiana Rakotondramanana, Haritiana L. Ralalarisoa, H. Léonce Randria-Mampianina, Solofonirina D. Ravelomanantsoa</i>	1572
Characterization of Airborne Particulates Containing Naturally Occurring Radioactive Materials in Investment Casting Facilities <i>Authors: Yong Gun Kim, Cheol Kyu Choi, Boncheol Goo, Kwang Pyo Kim</i>	1578
Spatial Distribution of Naturally Occurring Radioactive Materials (^{235}U, ^{238}U, ^{228}Th, ^{230}Th, ^{232}Th, ^{226}Ra, ^{228}Ra and ^{40}K) in the Marine Sediment Samples Along the Red Sea Coast of Saudi Arabia <i>Authors: A. A. Alzahrany, M. A. Farouk, E. I. Shabana, A. A. Al-Yousef, K. N. Alnajem, F. I. Al-Masoud</i>	1584
Radon Mass Exhalation Rates of Selected Building Materials in Tanzania <i>Authors: Aloyce Amasi, Kelvin Mark Mtei, Pawel Jodlowski, Chau Nguyen Dinh</i>	1585
Assessment of Natural Radionuclide Content of Some Public Well Water within Ondo and Ekiti States, South-western Nigeria <i>Authors: Adeolu Ayodele, Adeseye Arogunjo, Olubodun Arije</i>	1586
Study of Particular Problems Appearing in NORM Samples and Recommendations for Best Practice Gamma-ray Spectrometry <i>Authors: Andreas Baumgartner, Michael Stietka, Franz Kabrt, Hannah Moser, Franz Josef Maringer</i>	1587
Public Exposure due to Radon and External Radiation from Ornamental Rock Indoors <i>Authors: André Luiz do Carmo Leal, Dejanira da Costa Lauria</i>	1588
Outdoor Thoron and Thoron Progeny in a Thorium-rich Area in Norway <i>Authors: Anne Liv Rudjord, Hallvard Haanes, Trine Kolstad, Alexander Mauring, Ingvild Finne, Sven Dahlgren</i>	1589
Advanced Approach to Assessment of Potential Radon Hazard of Building Sites in Russia <i>Authors: Albert Marennyy, Peter Miklyaev, Andrey Tsapalov, Tatyana Petrovac, Sergey Kiselev</i>	1590
Complex Monitoring Study of Radon Field Generation in Soils under Various Geological and Climatic Conditions in Russia (2011 – 2015) <i>Authors: Albert Marennyy, Peter Miklyaev, Andrey Tsapalov, Andrey Penezhev, Sergey Kiselev</i>	1591
Ⓡ Area Monitoring of Ambient Dose rates in some parts of South Western Nigeria using a GPS integrated Dosimetric System <i>Authors: A.O. Mustapha, O.O. Alatise, I.C. Okeyode, V. Makinde, F.G. Akinboro, D. Al-Azmi</i>	1592
Dose Assessment from Groundwater Water Consumption in Central Portugal <i>Authors: Alcides Pereira, Luis Neves</i>	1593
Experimental and Numerical Studies for Understanding of Radon Emanation in Environmental Materials <i>Authors: Akihiro Sakoda, Yuu Ishimori</i>	1594
The Principle of Uncertainty Assessment of the Average Annual Radon Indoor based on Measurement Results of Different Duration <i>Authors: Andrey Tsapalov, Albert Marennyy, Peter Miklyaev, Sergey Kiselev</i>	1595
The Effect of Relative Humidity and Temperature Variability on Continuous Environmental Radon Monitoring <i>Author: Bashir Muhammad</i>	1596
Forecast and Analysis of Atmospheric Effluent Deposition Influenced by Buildings of Nuclear Power Plant under Normal Operation <i>Authors: Bo Wang, Qiong Zhang, Ruiping Guo</i>	1597
Radon and Energy Efficient Buildings <i>Authors: Constantin Cosma, Alexandra Cucos, Tiberius Dicu</i>	1598
Assessment of Radiological Hazards from Gold Mine Tailings in Gauteng Province, South Africa <i>Authors: Caspah Kamunda, Manny Mathuthu, Morgan Morgan</i>	1599

Sensitivity Study of Inhalation Dose by Airborne Particulate Properties <i>Authors: Cheol Kyu Choi, Yong Gun Kim, Jaekook Lee, Kwang Pyo Kim</i>	1600
The ICRP System for Radiation Protection of the Environment <i>Authors: Carl-Magnus Larsson, Kathryn Higley, Almudena Real, David Copplestone, Jacqueline Garnier-Laplace, Jianguo Li, Kazuo Sakai, Per Strand, Alexander Ulanovsky, Jordi Vives i Batlle</i>	1601
Spatial Distribution of Background Radiation in Kuwait Using Different Car Borne Gamma Probes <i>Author: Darwish Al-Azmi</i>	1602
Verification of Skin-Point-Source Method to Assess Annual Effective Dose by Usage of TENORM Added Consumer Products <i>Authors: Do Hyeon Yoo, Wook-Geun Shin, Jae Kook Lee, Yeon Soo Yeom, Chan Hyeong Kim, Chul Hee Min</i>	1603
A Dynamic Model to Assess Radiation Dose Rate of Biota in Freshwater Lake <i>Authors: Dong-Kwon Keum, In Jun, Kwang-Muk Lim, Byeong-Ho Kim, Yong-Ho Choi</i>	1604
Radioecological Assessments of Natural Occurring Radioactive Materials and Dose Estimation of The Public Residing Around Mt. Homa, Homabay County, Kenya <i>Authors: David Otwoma, Simon Bartilol, Jayant Patel</i>	1605
Novel Method to make a Calibrated Thoron Source <i>Authors: Elmughera Elhag, Robert Lindsay, Joash Ongori</i>	1606
Radon Gas and Other NORM Testing of Building Materials in Israel for Public Health and Safety (Category 3F) <i>Author: Ehud Ne'eman</i>	1607
Cost-Benefit Analysis Approach to Risk Assessment of Natural Radioactivity in Powdered and Liquid Milk Products Consumed in Nigeria <i>Authors: Ezekiel O. Agbalagba, Gregory O. Avwiri</i>	1608
Comparison of Efficiency of Techniques Radon Measurement (^{222}Rn) in Air and Water with Active Detectors and Passive Detectors <i>Authors: Evaldo Paulo de Oliveira, Paulo Roberto Rocha Ferreira, Mariza Ramalho Franklin</i>	1609
Organization, Some Results and Perspectives of Protection from Radon in Italy in the European Context <i>Authors: Francesco Bochicchio, Sara Antignani, Carmela Carpentieri, Gennaro Venoso</i>	1610
 The IUR FORUM : Worldwide harmonization of networks to support integration of scientific knowledge and consensus development in radioecology <i>Authors: François Bréchnignac, Rudolf Alexakhin, Andréas Bollhöfer, Kristin E. Frogg, Frank Hardeman, Kathy Higley, Thomas G. Hinton, Lawrence A. Kapustka, Wendy Kuhne, Kins Leonard, Olivier Masson, Kenji Nanba, Graham Smith, Karen Smith, Per Strand, Hildegard Vandenhove, Tamara Yankovich, Satoshi Yoshida</i>	1611
Thoron: Radon's Lesser-Known Sister – Results from a National Survey in the Netherlands <i>Authors: Fieke Dekkers, Roelf Blaauboer, Martijn vd Schaaf, Harry Slaper, Ronald Smetsers</i>	1613
^{40}K, ^{226}Ra And ^{228}Ra in Soils of Rio de Janeiro State, Brazil: A Preliminary Study <i>Authors: Fernando Ribeiro, Dejanira Lauria, Jose Ivan Silva, Fernanda Cunha</i>	1614
Gamma in Situ Survey in an Experimental Research Area <i>Authors: Fernando Ribeiro, Rocio Reis, Monique Gabriel</i>	1615
Measurement of ^{137}Cs and ^{40}K in Wild Mushrooms and their Transfer Factors <i>Authors: Fei Tuo, Qiang Zhou, Jing Zhang, Wenhong Li, Qing Zhang</i>	1616
Assessment of Natural Radioactivity and its Radiological Impact in Ortum Region in Kenya <i>Author: Felix Wanjala</i>	1617
Radiation from Building Materials in South Africa including Granite Samples with High Concentrations of Radium <i>Authors: Farrel Wentzel, Robert Lindsay</i>	1618
Ionising Radiation from the Zanzibar Coastline: Exposure to Residents and Tourists Visiting Zanzibar <i>Authors: Gharib Mohamed, Robert Lindsay, Peane Maleka, Joash Ongori</i>	1619

Results from Interlaboratory Comparison on Gross Alpha/Beta Activity Measurement in Waters <i>Authors: Gordana Pantelic, Marija Jankovic, Natasa Sarap, Dragana Todorovic</i>	1620
Source Identification of Iodine-131 in Environmental Samples around the HANARO <i>Authors: Geun-Sik Choi, Jong-Myoung Lim, Young-Gun Ko, Mee Jang, Won-Young Kim, Wannoo Lee, Young-Yong Ji, Hyuncheol Kim, Chang-Jong Kim, Young-Hyun Cho, Chung-Sup Lim, Kun-Ho Chung</i>	1621
Natural Radioactivity Systematics in a Complex Hydrothermic Environment <i>Authors: Hudson Angeyo Kalambuka, Paul Tambo, Jayanti Patel, Michael Mangala</i>	1622
Measurements of Radon Concentrations in Drinking Water in Cities, China <i>Authors: Hongxing Cui, Yunyun Wu, Bing Shang, Jianxiang Liu</i>	1623
¹⁴C Activity in Atmospheric CO₂ and Biological Samples Around the Nuclear Power Plant Krško, Slovenia <i>Authors: Ines Krajcar Bronić, Bogomil Obelić, Jadranka Barešić, Nada Horvatinčić, Borut Breznik, Aleš Volčanšek, Andreja Sironić, Damir Borković</i>	1624
Control of Emissions from a Gold and Uranium-mining Polluted Catchment in a Semi-arid Region of South Africa: The Varkenslaagte Stream <i>Authors: Isabel Weiersbye, Peter Dye, Hlanganani Tutu, Ewa Cukrowska, Christopher Curtis, Julien Lusilao, Elisee Bakatula, Bruce McLeroth, Jozua Ellis, Etienne Grond, Maxine Joubert, Salome Mthombeni, Ike Rampedi, Christopher Davies, Patricia Omo-Okoro, Henk Nel, Joel Malan, Herman Coetzee</i>	1625
The Potential for Phytoremediation of Uranium Contaminated Substrata on the Witwatersrand Basin of South Africa: Extraction and Harvesting Versus in Situ Sequestration <i>Authors: Isabel Weiersbye, Ewa Cukrowska, Jozua Ellis, Peter Dye, Bruce McLeroth, Hlanganani Tutu, Luke Chimuka, Nosipho Mntungwa, Maxine Joubert, Shakera Arendse</i>	1626
Uranium in Phosphate mining <i>Author: Jacques Bezuidenhout</i>	1627
Uranium in Wild and Cultivated Leafy Vegetables and Consumption Patterns: A Risk Assessment <i>Authors: Jenny Botha, Isabel Weiersbye, Jozua Ellis, Hlanganani Tutu</i>	1628
Ⓡ Calculation of Lifetime Lung Cancer Risks Associated with Indoor Radon Exposure Based on Various Radon Risk Models <i>Author: Jing Chen</i>	1629
Measurement Results of Background Radiation Levels in Seals <i>Authors: Jing Chen, Weihua Zhang, Baki Sadi, Xiaowa Wang, Derek Muir</i>	1630
The Current Status and Plans for Safety Management of NORMs in South Korea <i>Authors: Jaekook Lee, Jaewoo Park, Zu Hee Woo, Boncheol Koo, Ki Hoon Yoon, Chang-Su Park, Byung-Uck Chang</i>	1631
Pre-assessment of Dose Rates for Marine Biota from Discharge of Nuclear Power Plants <i>Authors: Jingjing Li, Senlin Liu, Yongxing Zhang, Ling Chen, Yuan Yan, Weiya Cheng, Hailin Lou, Yongbao Zhang</i>	1632
Radon Profiles in Soil on Mine Dump <i>Authors: Joash Ongori, Robert Lindsay</i>	1633
Internal Radiation Exposure Dose From Some Commonly Consumed Food Stuff in Lagos A Commercial City in Nigeria <i>Authors: Kayode I. Ogungbemi, Moses A. Aweda, Olusola O. Oyebola, Margarent A. Adedokun, Chima E. Ireogbu</i>	1634
Seasonal and Diurnal Variation of Outdoor Radon Concentrations in Urban and Rural Area of Morocco <i>Authors: Lhoucine Oufni, Rabi Rabi</i>	1635
Ⓡ Study on a step-advanced filter monitor for continuous radon progeny measurement <i>Authors: Lei Zhang, Jinming Yang, Qiuju Guo</i>	1636
Survey of the Radon Environment within Lagos State Nigeria: A Preliminary Report <i>Authors: Margret Akinloye, Oluwasayo Abodunrin</i>	1637

The Importance of Understanding Basic Concepts in Radiological Environmental Impact Assessment <i>Authors: Moon Hee Han, Hae Sun Jeong, Hyo Joon Jeong, A Reum Kil, Eun Han Kim, Won Tae Hwang</i>	1638
High Precision Gamma Dose Rate Measurements using a Spectroscopic Pager <i>Authors: Michael Iwatschenko-Borho, Erich Leder, Ralf Pijahn, Norbert Trost</i>	1639
Tritium Content in the Velika Morava River Basin: Evaluation Effective Ecological Half-Life <i>Authors: Marija Jankovic, Natasa Sarap, Gordana Pantelic, Dragana Todorovic</i>	1640
Assessing the Northern Benguela Upwelling System for Radioactivity Levels: A Baseline Study <i>Authors: Martina Rozmaric, Deon Charles Louw, Isabelle Levy, Oxana Blinova, Mai Khanh Pham, Jean Bartocci, Iolanda Osvath, David Osborn, Samorna Brian Mudumbi, Tuuovauri Kauroua Sharon Kahunda, Elena Chamizo, Ljudmila Benedik</i>	1641
Comprehensive radionuclide analysis and dose assessment of thermal and mineral waters in Croatia <i>Authors: Krmpotić Matea, Rožmarić Martina, Petrincec Branko, Bituh Tomislav, Benedik Ljudmila, Fiket Željka</i>	1642
Radioactivity values for soil replaced at some building at Tikrit University <i>Author: Mohanad Salih</i>	1643
Development of a Measurement Procedure for Radon in Waterworks <i>Author: Michael Stietka, Andreas Baumgartner, Franz Kabrt, Franz Josef Maringer</i>	1644
Natural Radionuclides in River Sediments of Poços de Caldas Plateau - Brazil: Geogenic or Anthropogenic Contribution? <i>Authors: Nivaldo Da Silva, Heber Alberti, Marcos Roberto Nascimento, Rodrigo Bonifácio, Heliana Azevedo, Raul Villegas</i>	1645
Pubic Exposure due to Indoor Radon in Three Municipalities of Poços de Caldas Plateau - Brazil <i>Authors: Nivaldo Da Silva, Berenice Navarro, Ubirani Otero, Tarcisio Cunha</i>	1646
Estimation of Terrestrial Air-Absorbed Dose Rate from the Data of Regional Geochemistry Database <i>Authors: Nan Gan, Kuang Cen, Rong Ye</i>	1647
The Study of Environmental Contamination and Public Health in the Vicinity of the Uranium Legacy Sites in the Tajik Republic <i>Authors: Natalya Shandala, Vladimir Seregin, Aleksandr Tukov, Sergey Kiselev, Vladimir Shlygin, Aleksandr Pozhidaev, Mirzoshokir Hojion</i>	1648
The Study of Environmental Contamination and the Public Health in the Vicinity of Uranium Legacy Sites in the Kyrgyz Republic <i>Authors: Natalia Shandala, Vladimir Seregin, Aleksandr Tukov, Sergey Kiselev, Aleksey Titov, Sergey Akhromeev, Aleksandr Pozhidaev, Gulnura Abasova, Aleksander Samoylov</i>	1649
Estimation of Natural Ionizing Radiation Levels Based on the Data of Gamma- Ray Spectrometry and Regional Geochemical Data in Zhuhai City Urban, China <i>Authors: Nanping Wang, Ling Zheng, Xingming Chu, Ting Li, Hongtao Liu, Xiaohong Meng</i>	1650
Evaluation of Radioactivity Concentrations in Some Bottled Drinking Water Produced in Nigeria and Associated Radiological Risk to Consumers <i>Authors: Oladele Ajayi, Ademola Abokede</i>	1651
Radiological Hazard Assessment of Natural Radionuclides in Soils of Some Oil-Producing Areas in Imo State, Nigeria <i>Authors: Oladele Ajayi, Chidiebere Dike</i>	1652
Radionuclide Concentrations in Edible Mushrooms Consumed in South- Western Nigeria and Radiation Dose Due to their Consumption <i>Authors: Oladele Ajayi, Olusola Omotoso</i>	1653
Vertical Migration of Some Natural Radionuclides in Soils of Some Oil- Producing Areas in Imo State, Nigeria <i>Authors: Oladele Ajayi, Chidiebere Dike</i>	1654
Assessment of Radionuclide Concentrations in Some Cereals and Tea Products Available in Nigeria <i>Authors: Olufunmilayo Alatise, Irete Okeyode, Christianah Adebessin</i>	1655

Radioactivity Levels in Samples of Detergent Powder available in Local Markets of South-western Nigeria <i>Authors: Olufunmilayo Alatise, Thomas Olaniyan</i>	1656
Polonium-210 Concentration in Cuban Tobacco Products and their Contribution to the Annual Effective Dose by Inhalation of Cigarette Smoke <i>Authors: Osvaldo Brígido-Flores, Orlando Fabelo-Bonet, Adelmo Montalván-Estrada</i>	1657
Cancer Risk from Radon in Drinking Water in South-western Nigeria <i>Authors: Olatunde Michael Oni, Adetola Olive-Adelodun, Emmanuel Abiodun Oni</i>	1658
Radiological Impact Assessment within the Context of the Environmental Impact Assessment Process Associated with the Proposed South African Nuclear Power Programme; Challenges Associated with a Multiagency and Regulatory Overlap Environment <i>Authors: Paul Fitzsimons, Elisabeth Nortje</i>	1659
Integrating the Radiation Protection System for Human and Non-Human Biota: How to do it in Practice <i>Authors: Diego Telleria, Peter Johnston</i>	1660
A Map of Moscow Geogenic Radon Potential <i>Authors: Peter Miklyaev, Tatyana Petrova, Albert Marennyy, Andrey Tsapalov, Sergey Kiselev</i>	1661
Outdoor Radon Levels in China <i>Authors: Qifan WU, Ziqiang Pan, Senlin Liu</i>	1662
A Platform for Assessment of Doses to the Public from Routine Discharges of Radionuclides to the Environment from Nuclear Installations <i>Authors: Rodolfo Avila, Robert Broed, Erik Johansson, Vladimir Maderich, Roman Bezhenar</i>	1663
Radon In-Air Assessments within Selected Wine Cellars in the Western Cape (South Africa) and its Associated Effective Radiation Exposure Dose <i>Authors: Ryno Botha, Robert Lindsay, Richard Newman, Peane Maleka</i>	1664
Environmental Thoron: Monitoring, Techniques and Dose Conversion <i>Author: Rakesh Chand Ramola</i>	1665
Influence of Release Height on Radioactive Gas Effluent in Short-term for Nuclear Power Plant in China <i>Authors: Ruiping Guo, Chunlin Yang, Chunming Zhang</i>	1666
Synergistic Effect of Caffeine and Melatonin against Radiation Induced Damage in C57BL/6 Mice at Sub Lethal Radiation Dose <i>Authors: Ritu Kushwaha, Dhruv K Nishad, Aseem Bhatnagar</i>	1667
Radiation Protection Calculations for both ingestion of ²²⁶Ra and ²²⁸Ra in Reservoir and Spring Water from Central Region of Cameroon <i>Authors: Rose Lydie Marie, Oum Keltoum Hakam, Abdel Majid Choukri</i>	1668
Gamma-emitting Radionuclides Analysis in Water Samples from Two Mines in South Africa <i>Author: Raymond Njinga</i>	1669
Setting Up a Continuous Monitor for Controls the Temporal Variability of ²²²Rn in the Atmosphere and Groundwater of the Tadla Basin, Morocco <i>Authors: Radouan Saadi, Hamid Marah, Oum Keltoum Hakam</i>	1670
Radon-thoron Discriminative Measurements and Corresponding Dosimetry in the Thorium Bearing Region of Lolodorf, Cameroon <i>Authors: Saidou, Shinji Tokonami, Miroslaw Janik</i>	1671
A New Facility for Assuring the Measurements Traceability in the Environment Dosimetry <i>Authors: Sorin Bercea, Aurelia Celarel, Constantin Cenusă, Elena Iliescu, Ioan Cenusă</i>	1672
Bioaccumulation Factor of the Heavy Metal in Marine Organism from the Korean Coast <i>Authors: Seokwon Choi, Heungjun Cho, Daeji Kim, Jungseok Chae</i>	1673
In-situ Measurements of Radon Levels in Water, Soil and Exhalation Rate using Continuous Active Radon Detector <i>Author: Sanjeev Kumar</i>	1674

Exposure to External Gamma Radiation Emitted from Soil of the High Background Radiation Areas of Ramsar Reduces Bacterial Susceptibility to Antibiotics <i>Authors: SMJ Mortazavi, Samira Zerei, Mohammad Taheri, Saeed Tajbakhsh, S Ranjbar, F Momeni, Samaneh Masoumi, Leila Ansari, SAR Mortazavi, Masoud Haghani, S Taeb</i>	1675
Discharge of Gaseous Radioactive Waste in FDG Synthesis: Clearance Levels and Licensing in Italy <i>Authors: Sandro Sandri, Maurizio Guarracino, Ruggero Cifani</i>	1676
External Evaluation of the Amounts of Exposures and Intern to the Telluric Radiations Gamma, in the South-East of Gabon <i>Authors: Sylvere Yannick Loemba Mouandza, Alain-Brice Moubissi, Germain Hubert Ben-Bolie, Patrice Ele Abiama, Bouchra Ramzi, Mohammed Zaryah</i>	1677
Challenges in Managing Exposures due to Natural Radiation Sources <i>Authors: Tony Colgan, Trevor Boal</i>	1678
Radioactivity in Some Leafy Vegetables in Roodepoort South Africa <i>Authors: Thulani Dlamini, Victor Tshivhase, Manny Mathuthu</i>	1679
Determination of Natural Radioactivity in the North East Beach Sands of Madagascar <i>Author: Tiana Harimalala Randriamora</i>	1680
Availability and Reliability of Meteorological Data for Atmospheric Dispersion Models <i>Authors: Tamas Pázmándi, Sándor Deme, Lilla Hoffmann, Péter Szántó</i>	1681
A Study on Adsorption of the Radioactive Noble Gases in the Atmosphere by a Portable Sampling System <i>Authors: Wannoo Lee, Young-Yong Ji, Young-Hyun Cho, Sando Choi, Jiyoung Park, Geen-sik Choi, Hyuncheol Kim, Jong-Myong Lim</i>	1682
Animal-to-water Concentration Ratios of Various Elements in Marine Ecosystems around two Korean Nuclear Sites <i>Authors: Yong-Ho Choi, Kwang-Muk Lim, In Jun, Byung-Ho Kim, Dong-Kwon Keum</i>	1683
Review of Approaches based on ²¹⁰Po and other Daughters of ²²²Rn for Retrospective Estimate of Radon Concentration <i>Authors: Yazdan Salimi, Mohammad Reza Kardan, Mohammad Reza Deevband, Dariush Askari, Jalal Ordoni, Mohammad Hossein Jamshidi, Hamed Dehghani, Fatemeh Ramrodi, Hamid Behrozi</i>	1684
A Simple Method for Measurement of Radon in Groundwater <i>Authors: Yunyun Wu, Hongxing Cui, Bing Shang, Jianxiang Liu</i>	1685
Application of Non-equilibrium Adsorption Model in the Migration of Radionuclides <i>Author: Zhu Jun</i>	1686
Environmental Impact Assessment of the NPP Krško for Period of 5 years <i>Authors: Zeljka Knezevic, Zeljko Grahek, Borut Breznik</i>	1687
Area 8: Transport / Sealed Source Management	1688
Validation Testing of Canberra-Obayashi Mobile type TruckScan Pre- production Unit <i>Authors: Atsuo Suzuki, Frazier L. Bronson, Masaru Noda, Naoya Takada, Keizo Yamasaki</i>	1689
Regulatory actions in the case of a radioactive source stuck in an oil well <i>Authors: Marcela G. Ermacora, Claudia Chiliutti, Valeria Amado, Horacio Lee Gonzáles, Hugo Vicens</i>	1700
Safety and security of sealed sources during transportation to remote area in Egypt <i>Author: M A M Gomaa</i>	1707
Orphan sources search and secure in Republic of Serbia – planning, implementation and current status <i>Authors: Milan Vujovic, Maja Eremic-Savkovic, Ivana Avramovic, Vedrana Vuletic, Slađan Velinov</i>	1710
The worldwide problem of Disused Sealed Radioactive Sources (DSRS) and what should be done to alleviate the situation. <i>Author: Robin George Heard</i>	1718

Assessment of the radiological consequences of accidents in vehicle transportation of radioactive material in the area of Bologna <i>Authors: Sara Vichi, Sara Baldazzi, Angelo Infantino, Gianfranco Cicoria, Giulia Lucconi, Domiziano Mostacci, Mario Marengo</i>	1725
Actions for Spent Radioactive Sources Removal <i>Authors: Teresa Ortiz, Elena Alcaide</i>	1732
Y Leak Radiation Assessment of Scanner HCV-Mobile, THSCAN Scanner And Scanner HCP-Portal <i>Authors: Tahiry Razakarimanana, H.A. Razafindramandra, Raelina Andriambololona, J.L.R. Zafimanjato, R.D. Randriantsizafy</i>	1738
Occupational exposure in the transport of radioactive materials in Cuba <i>Authors: Zayda Haydeé Amador Balbona, Miguel Antonio Soria Guevara</i>	1743
Safety Assessment for Incident-Free Pilot Transportation of Decontamination Radioactive Waste Resulting from the Fukushima Nuclear Power Plant Accident <i>Authors: Min Jun Kim, A Ra Go, Kwang Pyo Kim</i>	1750
Operation of Radiation Source Location Tracking System <i>Authors: BokHyoung Lee, CheolHong Um, KiWon Jang, DaeHyung Cho</i>	1758
Designing a Physical Protection System for the 444 TBq Co-60 Irradiation Facility at the Centre for Applied Radiation Science and Technology, Mafikeng, South Africa <i>Authors: Cyrus Cyril Arwui, Victor Tshivhase</i>	1759
IAEA Approach to Cradle to Grave Control and Management of Disused Sealed Radioactive Sources <i>Authors: Monika Kinker, Gerard Bruno, Hilaré Mansoux</i>	1760
Safety Case of The Libyan Central Radioactive Waste Storage Facility <i>Authors: Husam Shames, Usama Elghawi</i>	1761
Safety and Radiation Protection Requirements for Cargo and Containers Inspection Services in Brazil <i>Authors: Josilto Aquino, Alfredo Ferreira Filho, Marcello Nicola</i>	1762
Radiation Protection in Radioactive Material Transport <i>Authors: Li Guoqiang, Zhuang Dajie, Wang Xuexin, Sun Hongchao, Wang Renze, Zhang Jianguang</i>	1763
Practical Application Illustrating Excellence in the Safety and Security of Industrial Radiography Sources Employed at the Eskom, Generation Power Stations <i>Author: Marc Maree</i>	1764
Safe Transport of Radioactive Material in Argentina <i>Authors: María Soledad Rodríguez Roldán, Alejandro Fernández, Emiliano Juanena, Christian Elechosa</i>	1765
Spent fuel elements transfer between the Units I and II of the Atucha Nuclear Power Plant in Argentina <i>Authors: María Soledad Rodríguez Roldán, Alejandro Fernández, Emiliano Juanena, Christian Elechosa</i>	1766
Challenges in Managing Radiation Safety Program at a Biotech Facility <i>Author: Rao Goriparthi</i>	1767
Intermediate Nuclear Waste Return December 2015 <i>Author: Steven Dimitrovski</i>	1768
Strategies to Improve the Safety Culture in the Field of Industrial Radiography in Peru <i>Author: Susana Gonzales</i>	1769
Detection of Orphan Industrial Neutron and Americium Sources in Metal Scrap Cargo <i>Author: Michael Iwatschenko-Borho</i>	1770
Area 9: Non-Ionising Radiation	1771
Evaluation of bone density importance in pediatric MR only treatment planning <i>Authors: Banafsheh Zeinali-Rafsanjani, Reza Faghihi, Mahdi Saeedi-Moghadam, Reza Jalli</i>	1772

Simulation of heat distribution in a phantom for a Philips Sonalleve MRgHIFU unit <i>Authors: Barbara Caccia, Silvia Pozzi, David Bianchini, Francesco Marcocci, Enrico Menghi, Marcello Benassi</i>	1776
R Extrapolation techniques for evaluation of 24 hours average electromagnetic field emitted by Radio Base Station installations: spectrum analyzer measurements of LTE and UMTS signals <i>Authors: Elisa Nava, Stefano Mossetti, Daniela de Bartolo, Ivan Veronese, Marie Claire Cantone, Cristina Cosenza</i>	1777
Managing Non-Ionizing Radiation through International Basic Safety Standards <i>Authors: Jacques Abramowicz, Efthymios Karabetzos, Sigurdur Magnusson, Rudiger Matthes, Mirjana Moser, Shengli Niu, John O'hagan, Rick Tinker, Emilie Van Deventer</i>	1778
Designing a Laser Lab, Errors and Solutions <i>Author: Ken Barat</i>	1779
Threshold Dose Estimation for Short Delay Onset of Cataract after In Vivo exposure to Ultraviolet Radiation, a General Strategy for Threshold Estimation for Continuous Dose Response Functions <i>Authors: Per Söderberg, Konstantin Galichanin, Nooshin Talebizadeh, Zhaohua Yu</i>	1780
Effects of Early Life Exposure to RF Fields <i>Authors: Kerry Broom, Jutta Jarvinen, Darren Addison, Zenon Sienkiewicz</i>	1781
JC@ A9)	
Area 10: Emergency Preparedness and Management	1782
Study on the Protection Planning Actions and Response to Nuclear or Radiological Emergency <i>Authors: Perez, Clarice F.A., Sahyun, Adelia, Freitas, Kenia A.M.</i>	1783
The reality of the low radiation dose on population in Fukushima Daiichi 20km zone <i>Author: Jun Takada</i>	1788
Y Application of virtual reality technology to minimize the dose to the example of staff emergency training at the center for radioactive waste management <i>Authors: K. Chizhov, I. Kudrin, I Mazur, A. Tsovyanov, L. Bogdanova, M. Grachev, I. Tesnov, N.-K. Mark, I. Szöke, V. Kryuchkov</i>	1796
Emergency Preparedness – a continuously improving Process <i>Author: Marcel Lips</i>	1804
Medium and Long-Term Inhalation Dose Following a Major Radioactive Deposition Event <i>Author: Mauro Magnoni</i>	1812
Development and Current Status of a Carborne gamma-ray Survey System, KURAMA-II <i>Authors: Minoru Tanigaki, Ryo Okumura, Koichi Takamiya, Nobuhiro Sato, Yasuhiro Kobayashi, Hirofumi Yoshino, Hisao Yoshinaga, Akihiro Uehara</i>	1818
Socially - psychophysiological Adaptation of the Patient, who has Suffered at Failure the Chernobyl Nuclear Power Station, transferred Acute Radiation Sickness of IV Heaviest Degree and Local Radiation Injuries I-IV of Severity Level. <i>Author: N.A. Metlyaeva</i>	1826
Early measurements of members of the public after the Fukushima Daiichi NPP accident: Data made available to the EURADOS WG7 Survey <i>Authors: P. Fojtík, M.A. Lopez, D. Franck, J. Oško, U. Gerstmann, C. Scholl, A.L. Lebacqz, B. Breustedt, L. del Risco Norrild</i>	1836
Large scale monitoring of radioiodine in thyroid: equipment and preparedness in the Czech Republic <i>Authors: P. Fojtík, S. Kavan, L. Novotná, T. Svobodová, E. Čermáková, J. Baloun, J. Helebrant</i>	1845
Investigation of the radiological performances of commercial Active Personal Dosimeters for the use of the PSI fire brigade radiation protection squad <i>Authors: R. Philipp, B. Hofstetter-Boillat, E. Hohmann, S. Mayer</i>	1848
The Analytical Platform of the PREPARE project <i>Authors: W. Raskob, S. Möhrle, S. Bai, T. Müller</i>	1851

Determination of Radionuclides Surface Concentration and Radiation Level In Fukushima Prefecture, Japan: November 2014 <i>Authors: Godwin Ekong, Isa Sambo, Saiyadi Sulaiman</i>	1857
Selective Bone Marrow Shielding as an Approach to Protecting Emergency Personnel <i>Authors: Oren Milstein, Gideon Waterman, Kenneth Kase, Itzhak Orion</i>	1864
RENEB – The European Network for Emergency Preparedness and Scientific Research <i>Authors: Ulrike Kulka, Elisabeth Ainsbury, Leonard Barrios, Octavia Gil, Eric Gregoire, Alicja Jaworska, Simone Mörtl, Ursula Oestreicher, Gabriel Pantelias, Laurence Roy, Laure Sabatier, Sylwester Sommer, Georgia Terzoudi, Francois Trompier, Pedro Vaz, Anne Vral, Clemens Woda, Andrzej Wojcik</i>	1872
Absorbed Dose Measurements using Ordinary Salt on Anthropomorphic Phantoms – Novel Conversion Coefficients to Effective Dose for Various Exposure Geometries <i>Authors: Christian Bernhardsson, Therese Geber-Bergstrand, Jonas Jarneborn, Maria Christiansson</i>	1873
Monitoring and Dose Assessment for Children for Internal Radiation Contamination Following a Radiological or Nuclear Emergency <i>Authors: Chunsheng Li, Florence Ménétrier, Armin Ansari, George Etherington, Wi-Ho Ha, Jean- Rene Jourdain, Boris Kukhta, Osamu Kurihara, Maria Lopez, Arlene Alves dos Reis, Ana Rojo, Stephen Solomon, Jianfeng Zhang, Zhanat Carr</i>	1874
The Radiation Situation in the Area of Radioactive Trace Resulted From the Accident in a Nuclear Submarine at the Chazhma Bay <i>Authors: Dmitry Isaev, Alexey Titov, Sergey Kiselev, Vladimir Shlygin, Natalia Novikova, Renata Starinskaya</i>	1875
 Mass media communication of emergency issues and countermeasures in a nuclear accident. Fukushima reporting in European newspapers <i>Authors: Eduardo Gallego, Marie Claire Cantone, Deborah. H. Oughton, Tanja Perko, Iztok Prezelj, Yevgeniya Tomkiv</i>	1876
The Development of Concept of “Virtual Cytogenetic Biodosimetry Laboratory” for Radiation Emergencies in Occupational Field <i>Authors: Franz Fehring, N. Maznyk, Chr. Johannes, T. Sipko, N. Pshenichna</i>	1877
Radiological Situation at the Chernobyl Shelter Site Thirty Years after the Accident <i>Authors: Gunter Pretzsch, Viktor Krasnov</i>	1878
Assessment of Measurement Capabilities in Nuclear Accident <i>Author: Helena Janzekovic</i>	1879
Study on the Derived Response Level in Case of a Radiological Accident <i>Authors: Hyeong-Ki Shin, Juyoul Park</i>	1880
Training of RPEs for Emergency Response <i>Authors: Heleen van Elsäcker-Degenaar, Folkert Draaisma</i>	1881
Research Priorities in Emergency and Recovery Preparedness and Response: the NERIS Strategic Research Agenda <i>Authors: Johan Camps, Thierry Schneider, Wolfgang Raskob</i>	1882
Mapping of Radiation Fields in Areas with Complex 3D Source Geometries Using a Shielded Two-Detector Configuration and Data Processing <i>Authors: Jonas Jarneborn, Marcus Persson, Christopher Rääf, Robert Finck</i>	1883
Dose Re-estimation Method in Emergency Radiation Exposure Situation <i>Authors: Jungil Lee, Insu Chang, Jang Lyul Kim, Kisoo Chung</i>	1884
Introduction of Uncertainty of Atmospheric Dispersion Calculation and Improvements of Urban Countermeasure Modelling in an Operational Decision Support System <i>Authors: Steen Hoe, Kasper Andersson, Jens Havskov Sørensen, Carsten Israelson</i>	1885
Protection Actions Decision Making Support during Nuclear Emergency in China <i>Authors: Jiangang Zhang, Yapeng Yang, Zongyang Feng, Linsheng Jia, Shutang Sun</i>	1886

Capabilities of the New Mobile Laboratory of the Nuclear Forensic Laboratory <i>Author: Károly Bodor</i>	1887
Ongoing Work to Enhance Post-accident Radiation Protection at Swedish Nuclear Power Plants <i>Authors: Karin Fritioff, Staffan Hennigor, Marie Carlsson, Michael Pettersson, Ingela Svensson</i>	1888
A Spectrometry Acquisition System for UAS based on Raspberry Pi <i>Authors: Magnus Gårdestig, August Ernstsson, Håkan Pettersson</i>	1889
Comprehensive Approach to Assess Radiation Induced Individual Health Injuries and Prognostic Clinical Evaluation using Integrative "Dosimetry" Strategies <i>Authors: Matthias Port, Christina Beinke, Michael Abend</i>	1890
NEA Framework for the Post-Accident Management of Contaminated Food <i>Authors: Michael Siemann, Matt Cooper, Ted Lazo</i>	1891
Industrial Radiography Accident at the Rio Turbio Power Plant: Causes of the Event <i>Authors: Maria Teresa Alonso Jimenez, Irene Raquel Pagni, Eleazar Martin Ameal</i>	1892
 Off-site Emergency Planning at UK Nuclear Licensed Sites <i>Authors: Paul Leonard, Gareth Thomas</i>	1893
Preliminarily Integrated Simulation for Severe Accident of CLEAR-I based on Virtual Reactor Virtual4DS <i>Authors: Tao He, Jinbo Zhao, Zihui Yang, Pengcheng Long, Liqin Hu, Team FDS</i>	1894
Review on Spraying Water Soluble Resin to fix the Radioactive Material after Fukushima Accident <i>Authors: Qiong Zhang, Bo Wang, Ruiping Guo</i>	1895
Training Emergency Plan in a Nuclear Installation <i>Authors: Ruy Ferraz, Ricardo Bitelli</i>	1896
 Suitability of portable radionuclide identifiers for emergency incorporation monitoring <i>Authors: Roman Galeev, Gernot Butterweck, Markus Boschung, Bénédicte Hofstetter-Boillat, Eike Hohmann, Sabine Mayer</i>	1897
Nuclear and radiological emergencies - making early health protection decisions under uncertainty <i>Authors: Stephanie Haywood, Simon French, Matthew Hort</i>	1898
Development of Prediction Models for Ambient Dose Equivalent Rates in Inhabited Areas after the Fukushima Daiichi Nuclear Power Plant Accident <i>Authors: Sakae Kinase, Tomoyuki Takahashi, Hideaki Yamamoto, Kimiaki Saito</i>	1899
²¹⁰Po Version of the Yasser Arafat's Death. Results of the Russian investigations: Part 2. Medical research <i>Authors: Yulia Kvacheva, Vladimir Uiba, Leonid Ilyin, Alexandr Samoilov, Yuriy Abramov, Irina Galstyan, Boris Kukhta, Natalia Nadezhina, Vladimir Stebelkov, Alexandr Tsovyanov, Sergey Shinkarev, Vladimir Yatsenko</i>	1900
²¹⁰Po Version of the Yasser Arafat's death. Results of the Russian Investigations: Part 1. Physical Research <i>Authors: Sergey Shinkarev, Vladimir Uyba, Alexander Samoylov, Leonid Ilyin, Yulia Kvacheva, Yury Abramov, Irina Galstyan, Angelina Guskova, Boris Kukhta, Natalia Nadezhina, Vladimir Stebelkov, Alexander Tsovyanov, Vladimir Iatsenko</i>	1901
Health Risk Assessment of Emergency Personnel Regarding Radiation Exposures during the Aftermath of the Crash of Malaysia Airlines flight MH-17 <i>Author: Tjerk Kuipers</i>	1902
Surveillance of Radioactivity in the Atmosphere by the Deutscher Wetterdienst (DWD) – Monitoring and Prognosis <i>Authors: Thomas Steinkopff, Joachim Barth, Axel Dalheimer, Jochen Förstner, Hubert Glaab, Michael Mirsch</i>	1903
 'SUDOQU': A New Methodology for Deriving Criteria for Radiological Surface Contamination <i>Author: Teun van Dillen</i>	1904
Post-Fukushima Dai-ichi Review of Radioactive Materials Users and Panoramic Irradiators <i>Author: Vincent Holahan, William Lee, Gordon Bjorkman</i>	1905


Possible Mechanism of Realization of High Doses from Beta-Particles Exposures to the Atomic-Bomb Survivors in the Area of Wet Fallout <i>Author: Victor Kryuchkov, Sergey Shinkarev, Boris Kukhta, Evgeniya Granovskaya, Konstantin Chizhov, Masaharu Hoshi</i>	1906
Regulatory Emergency Control Centre Improvement Initiatives <i>Author: Vanessa Maree</i>	1907
Application of Backpack Radiation Detection Systems for Evaluation of External Exposure after the Chernobyl Accident <i>Authors: Valery Ramzaev, Anatoly Barkovsky, Ivan Romanovich, Jonas Jarneborn, Sören Mattsson, Christian Bernhardsson</i>	1908
R Nuclear and radiological preparedness: The achievements of the European Research Project PREPARE <i>Authors: Wolfgang Raskob, Thierry Schneider, Florian Gering, Sylvie Charron, Mark Zhelezniak, Spyros Andronopoulos, Gilles Heriard-Dubreuil, Johan Camps</i>	1909
UAV Carried Emergency Radiation Detection System for Severe Nuclear Accident <i>Authors: Yang Liu, Zhiping Luo, Luzhen Guo, Guowen Zheng, Hongchao Pang, Qin Chen</i>	1910
Area 11: Decommissioning, Waste Management and Remediation	1911
Y Analysis of radioactive inventory for radionuclide contained in liquid effluents, resulting from the decommissioning of a nuclear research reactor <i>Authors: Carmen Tuca, Ana Stochioiu, Mitica Dragusin, Daniela Gurau and Felicia Mihai</i>	1912
Discussion on practical application of radiation protection system for radioactive waste management in existing exposure situations <i>Authors: Daisuke Sugiyama, Takatoshi Hattori</i>	1918
The Role of Radiation Protection Considerations in Decommissioning <i>A brief look at safety culture in Iraq and Ukraine</i> <i>Authors: Eric K. Howell, Rodolfo Avila, John Rowat, David Kenagy, Ronald Chesser</i>	1924
Calculation of Dose Rates at the Surface of Storage Containers for High- Level Radioactive Waste <i>Authors: Erik Poenitz, Clemens Walther, Thomas Hassel</i>	1932
Radiological Assessment Approach for Decisions on Mining-Related Remediation Projects <i>Author: Gert de Beer</i>	1939
Application of an Artificial Neural Network for Evaluation of Activity Concentration Exemption Limits in NORM Industry by Gamma-ray Spectrometry <i>Authors: Hannah Wiedner, Virginia Peyrés, Teresa Crespo, Marcos Mejuto, Eduardo García-Toraño, Franz Josef Maringer</i>	1948
No Nuclear Power - No Disposal Facility? <i>Author: J. Feinhals</i>	1957
Radiation Protection In The Dismantling Of Nuclear Power Plants <i>Authors: Oscar González, José Campos, Teresa Ortiz</i>	1964
German Guidelines put into Practise: Inhalation or Ingestion? <i>A study of a specific case of incorporation in an incident at a facility for dismantling nuclear installations</i> <i>Authors: Peter Hill, Martina Froning, Burkhard Heuel-Fabianek</i>	1972
Investigation into the Pu uptake pathway in Corn (Zea mays) <i>Authors: Stephanie Hoelbling, Fred Molz, Brian Powell, Nishanth Tharayil, Nicole Martinez</i>	1978
Application of USNRC Regulatory Guide 4.21 for Decommissioning Feasibility and Life-Cycle Planning <i>KHNP APR1400 Design Certification Project</i> <i>Authors: Seunggi Lee, Sangho Kang, Irving Tsang, Sara Amitrani</i>	1986
The Post Fukushima Events Development and Severe Accidents Overview: Activities to Enhance Safety and Radiation Protection Regarding Academy Perspective <i>Author: Tadashi Narabayashi</i>	1994

Radioactive waste management in case of incidental melting of a Co-60 source <i>Authors: Teresa Ortiz Ramis, Elena Alcaide Trenas, Pablo Belinchon</i>	2004
Comparative Study of Radioactive Waste Management Standards in Brazil <i>Authors: Ana Cristina Lourenço, Wagner de Souza Pereira</i>	2011
Radioecological Monitoring at the Areas of the Former Military Technical Bases at the Russian Far East <i>Authors: Akhromeev Sergey, Kiselev Sergey, Titov Alexey, Isaev Dmitry, Seregin Vladimir, Gimadova Tamara</i>	2012
The Radiological Risk Assessment for Workers Involved in Liquid Waste Transfer Operations <i>Authors: Ana Stochioiu, Carmen Tuca, Mitica Dragusin, Daniela Gurau, Felicia Mihai</i>	2013
R Slaying the Dragon – The story of one FPSO, twenty odd Vietnamese and 3 concrete mixers. Decontamination and disposal of NORM <i>Authors: Annelize van Rooyen, Anthony O'Brien</i>	2014
Issues Related to Regulation, Control, and Waste Management of Natural Radioactive Scales with Low Specific Activity in Oil Producing Establishments in Libya <i>Author: Bulgasem El-Fawaris</i>	2015
R A comparison of remediation after the Chernobyl and Fukushima Daiichi accidents <i>Authors: Brenda J Howard, Sergey Fesenko, Mikhail Balonov, Gerhard Pröhl, Shinichi Nakayama</i>	2016
Radioactive Waste Management without Adherence to Standards at the Laguna Verde Nuclear Power Plant, Mexico <i>Author: Bernardo Salas</i>	2017
Statistical Learning Approaches Applied to the Calculation of Scaling Factors for Radioactive Waste Characterization <i>Authors: Biagio Zaffora, Matteo Magistris, Francesco Paolo La Torre, Gilbert Saporta, Catherine Luccioni, Jean-Pierre Chevalier</i>	2018
R The Swiss approach to deal with radium legacies from the watch industry The Radium action plan (2016-2019) <i>Authors: Christophe Murith, Sybille Estier, Martha Palacios, Sebastien Baechler</i>	2019
Post closure safety of the SFR repository for short-lived low- and intermediate level waste <i>Authors: Eva Andersson, Fredrik Vahlund, Klas Källström, Ulrik Kautsky</i>	2020
Development of a Standardised Screening Procedure for the Evaluation of Sites Potentially Contaminated with NORM in Austria <i>Authors: Eva Maria Lindner, Claudia Landstetter, Michael Tatzber, Fabian Rechberger, Michael Dauke, Christian Katzlberger</i>	2021
Critical Factors for Radiological Closure Criteria for Uranium Mine Remediation <i>Author: Frank Harris</i>	2022
The International Standards for the Safety of Radioactive Waste Management <i>Author: Gerard Bruno</i>	2023
Talking to the Future: Sustainable Solutions for Radioactive Waste <i>Author: Gordana Lastovicka-Medin</i>	2024
The Dose Calculation on Graphite Waste Samples of the Decommissioned KRR-2 <i>Authors: Heereyoung Kim, Deokjung Lee</i>	2025
Characterization of Concrete Structures to Determine the Strategy for the Decommissioning of the 250 MeV CGR Cyclotron of the Ghent University in Belgium <i>Authors: Isabelle Meirlaen, Myriam Monsieurs, Hubert Thierens, Luc Ooms, Sven Boden, Luc Noynaert</i>	2026
Waste Management at the Decommissioning of the Ghent University Research Reactor Thetis in Belgium <i>Authors: Isabelle Meirlaen, Myriam Monsieurs, Hubert Thierens, Patrick Maris, Luc Noynaert, Luc Ooms</i>	2027

R Decontamination and Recovery of a Nuclear Facility to allow Continued Operation <i>Author: Josh Cavaghan</i>	2028
General Principles for the Short and Long Term Management of Former Uranium Mining Sites in France <i>Authors: Jérôme Guillevic, Marie Odile Gallerand, Gwenaëlle Lorient, Christophe Serres</i>	2029
Safety Standards for the Management and Disposal of Radioactive Waste from Uranium Mining in France <i>Authors: Jérôme Guillevic, Marie-Odile Gallerand, Gwenaëlle Lorient, Christophe Serres</i>	2030
Enhancing Regulatory Oversight of Radioactive Sources through International Cooperation <i>Author: Jack Ramsey</i>	2031
New Measurement Systems for Clearance of Radioactive Materials from Nuclear Facilities Decommissioning <i>Authors: Jiri Suran, Jana Smoldasova, Petr Kovar, Lukas Skala, Bent Pedersen, Dirk Arnold, Daniel Zapata, Pierino de Felice, Doru Stanga, Simon Jerome</i>	2032
Development of Postulated Initiating Event's Scenarios for the Decommissioning of Korean 1400 MWe PWR <i>Authors: Kyomin Lee, Sangho Kang, Keunsung Lee</i>	2033
Impact Assessment on Rn-222 in a Radioactive Waste Disposal Facility <i>Authors: Luis Fuentes, José-Luis Pinilla, Teresa Ortiz</i>	2034
The Process of Industrialization of the Management of Radioactive Waste: The Example of High Energy Accelerators Waste at CERN <i>Authors: Luisa Ulrici, Yvon Algoet, Luca Bruno, Doris Forkel-Wirth, Francesco Paolo La Torre, Matteo Magistris, Christian Theis, Ralf Trant, Helmut Vincke, Nick Walter</i>	2035
NORM Waste in Oil & Gas Industry (Challenges & Solutions) <i>Author: Mohammad Aref</i>	2036
Disposal of Norm Waste from Oil and Gas Industry by Underground Injection (Case Study) <i>Authors: Michael Cowie, Roman Bilak, Steve Wasson, Kelly Hatch</i>	2037
Waste Management Protocols for Iridium-192 Sources Production Laboratory Used in Cancer Treatment <i>Authors: Maria Elisa C. M. Rostelato, Carla Daruich de Souza, Daiane C. Barbosa de Souza, Carlos A. Zeituni, Rodrigo Tiezzi, Osvaldo L. da Costa, Bruna Teiga Rodrigues, João A. Moura, Anselmo Feher, Anderson Sorgatti, Eduardo Santana de Moura, José Ronaldo de Oliveira Marques, Rafael Melo dos Santos, Dib Karam Jr.</i>	2038
Clearance and Declassification of Research Reactor Thetis at Ghent University, a Prime for Belgium <i>Authors: Myriam Monsieus, Isabelle Meirlaen, Hubert Thierens, Karel Strijckmans, Geert Cortenbosch, Luc Noynaert, Luc Ooms, Sven Boden</i>	2039
Methods used for Clearance of the Rooms of Former Research Reactor Thetis at Ghent University, Belgium <i>Authors: Myriam Monsieus, Isabelle Meirlaen, Hubert Thierens, Geert Cortenbosch, Luc Ooms, Sven Boden</i>	2040
Removal of Radiocesium Aqueous Solution using Activated Carbon Modified with Anionic Surfactant <i>Authors: Michael Olatunji, Mayeen Khandaker, Yusoff Amin, Ekramul Mahmud</i>	2041
R Norwegian-Russian Cooperation in Nuclear Legacy Regulation: Continuing Experience and Lessons <i>Authors: Malgorzata K. Sneve, Natalya Shandala, Alexey Titov, Vladimir Seregin, Sergey Kiselev</i>	2042
Rationale for a Comprehensive Assessment of Radio-Ecological Safety of Near Surface Radioactive Waste Storage Facilities <i>Authors: Alexander Samoylov, Nataliya Shandala, Igor Korenkov, Tatyana Lashchenova, Vladimir Romanov</i>	2043
Assessing the Environmental Impact of Man-made Radioactive Contamination at the Andreeva Bay Site for Temporary Storage of Spent Nuclear Fuel and Radioactive Waste <i>Authors: Natalia Shandala, Vladimir Seregin, Anna Filonova, Aleksey Titov, Vladimir Shlygin, Malgozhata Sneve, Graham Smyth</i>	2044

Radiation Situation around the Shipyards Involved in Decommissioning/Dismantlement of Nuclear Submarines	
<i>Authors: Nataliya Shandala, Alexey Titov, Maria Semenova, Vladimir Seregin, Anna Filonova</i>	2045
The study of the Ground Water Contamination. The Study of the Environmental Conditions of the Region during Remediation of the Andreeva Bay STS	
<i>Authors: Natalya Shandala, Vladimir Seregin, Sergey Kiselev, Stanislav Geras`kin, Malgorzhata Sneve, Graham Smith</i>	2046
The Status of Occupational Exposure Source Term Measurement with In-situ Gamma-ray Spectrometry for NPPs in China	
<i>Authors: Qinjian Cao, Xueqi Chang, Liye Liu, Wanchun Xiong, Yunshi Xiao, Sanqiang Xia</i>	2047
Study on spraying water soluble resin for Fukushima Dai-ichi nuclear power plant accident	
<i>Authors: Qiong Zhang, Ruiping Guo, Bo Wang, Liang Wang, Fudong Liu, Xiaoqiu Chen</i>	2048
Achievements by the NORM and Legacy Sites Working Group of the IAEA MODARIA Project	
<i>Author: Rodolfo Avila</i>	2049
NORMALYSA – A Tool for Risk Assessment to Support Remediation of Legacy Sites Contaminated with NORM and Artificial Radionuclides	
<i>Author: Rodolfo Avila</i>	2050
 Information Management System Supporting a Multiple Property Survey Program with Legacy Radioactive Contamination	
<i>Authors: Ron Stager, Douglas Chambers, Gerd Wiatzka, Monica Dupre, Micah Callough, John Benson, Erwin Santiago, Walter van Veen</i>	2051
Uranyl Ions Adsorption to Na-GMZ and Interactions with FA Adsorption: experiments and modelling	
<i>Authors: Yuanlv Ye, Liang Wang, Fudong Liu, Yahua Qiao</i>	2052
Occupational Dose Evaluation during Decommissioning of a Radiological Facility	
<i>Authors: Zamazizi Dlamini, Frik Beeslaar</i>	2053
Area 12: Societies	2054
Argentine Radiation Protection Society (SAR): 50 years Straightening Radiation Protection	
<i>Author: Ana María Bomben</i>	2055
The History of the South African Radiation Protection Society	
<i>Author: Christoph Trauernicht</i>	2056
Belgian Society for Radiation Protection	
<i>Authors: Tom Clarijs, Patrick Smeesters, Claire Stievenart, Andrzej Polak, Pascal Froment</i>	2057

Note:

Submissions marked with  represent entries published in a Special IRPA 14 issue of *Radiation Protection Dosimetry*.

Submissions marked with  represent entries by contestants for the Young Scientists and Professionals Award.

**The Proceedings of the 14th International Congress of the International Radiation
Protection Association
Volume 2 of 5**

Area 3: Medical

Pediatric Head CT examination doses in two university teaching Hospitals in Tunisia

Bouaoun Abir^{a,b*}, Latifa Ben Omrane^b, Azza Hammou^a

^aUniversité Tunis El Manar, Institut supérieur des technologies médicales, LR13ES07
Laboratoire de Recherches Biophysique et Technologies Médicales (ISTMT)

^bCentre National de Radioprotection (CNRP)

Abstract. Radiation protection in pediatrics radiology particularly in CT deserves unique considerations in children due to their high radio sensitivity and longer life expectancy than adults. As head CT is the most frequent pediatric CT examination, the purpose of this study was to assess and analyze the radiation doses during head pediatric CT in two different CT units (Siemens emotion 6 and General Electric Brightspeed 16) in Children hospital and National Hospital for Neurology of Tunisia, respectively, to optimize the dose given and minimize the radiology risk to this category of patients. Patient data and exposure parameters were collected as a mean value of 10 patients on each CT unit for four age groups (<1year, 1-5years, 5-10years and 10-15years) from head CT examinations. Doses were collected in terms of CTDI_{vol} and DLP values. Effective doses and Organ doses were calculated using the Monte Carlo simulation software Impact CT Dose. CTDI_{vol} values demonstrated a wide variation between the two CT units and between the axial and helical scan techniques in the same unit (from 6,74 mGy to 35 mGy) on Siemens scanner (Children Hospital) and (from 23 mGy to 84,65 mGy) on Ge BrightSpeed scanner (Hospital of Neurology). A wide variation was also observed for DLP (from 100 mGy.cm to 864 mGy.cm) and (from 331mGy.cm to 1640 mGy.cm) for Children Hospital and Hospital of Neurology, respectively. In term of effective doses, the values vary from 0,3 mSv to 3,7 mSv for the total sample. Organ equivalent doses were estimated for specific radiosensitive organs such as Lens, Brain, Thyroid. Dose values and variations were comparable with those reported in the literature and the results are useful for dose optimization and derivation of national diagnostic reference levels.

KEYWORDS: *computed tomography; pediatrics; optimization; head CT; CT doses; radiation protection; diagnostic reference level.*

1. INTRODUCTION

The use of CT has increased rapidly as a result of recent advances, particularly multidetector technology. Radiation protection in pediatric radiology particularly in CT deserves unique considerations in children since they are considerably more sensitive to radiation than adults and have a longer life expectancy. The risk of radiation-induced cancer development should be a concern in pediatric patients because it can develop after a long-latency period [1,2]. Therefore, it is important to evaluate radiation exposure in children in order to ensure that pediatric doses are kept to a minimum whilst maintaining the clinical effectiveness in order to improve the optimization of this high-dose imaging modality for this especially vulnerable section of the population.

As head CT is the most frequent pediatric CT examination, detailed dosimetric data as presented in the current study are important for providing patient exposure data for optimization. Organ and effective doses presented highlight the magnitude of risk in CT examination of children [3,4].

The aim of this study is to assess and analyze the radiation doses during head pediatric CT in two different CT units and to estimate effective doses and Organ doses for specific radiosensitive organs.

*Presenting author, e-mail: bouaounabir@yahoo.fr

2. MATERIALS AND METHODS

Data were collected on in two different CT units (Siemens emotion 6 and General Electric Brightspeed 16) in Children hospital (site 1) and National Hospital for Neurology of Tunisia (Site 2), respectively.

Patient data and exposure parameters were collected for a total of 290 patients as a mean value of 10 patients on each CT unit for four age groups (<1year, 1-5years, 5-10years and 10-15years) from head CT examinations. Doses were collected in terms of Volumetric Computed Tomography Dose Index (CTDI_{vol}), dose-length product (DLP) values. CT organ doses and effective doses were calculated for each patient from the Monte Carlo simulation "ImpACT CTdosimetry" software package ver.1.0.4 (27/05/2011) [5] using the tissue weighting factors, W_T of the ICRP60 and the ICRP103.

Dose measurements for the determination of CTDI_{vol} were performed using a CT reference PMMA 16 cm diameter phantom representing the head of a child placed at the isocentre of the CT scanner together with a calibrated pencil-type ionization chamber Model RaySafe Xi with 10 cm sensitive length.

3. RESULT

For the two audited CT installations, The CTDI_{vol} measurement results demonstrate a good agreement between the displayed and the measured dosimetric quantities.

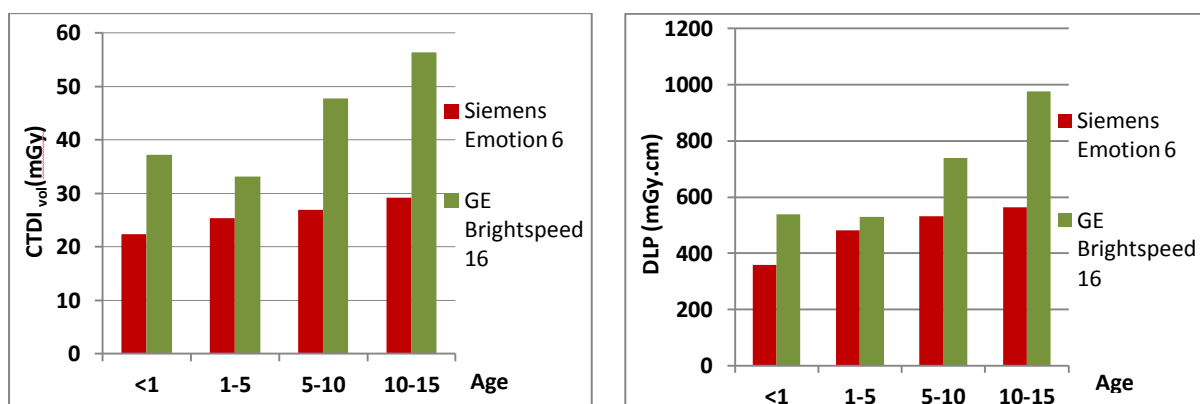
Table 1 shows the different acquisition parameters used for paediatric head CT examinations in both site 1 and 2.

Table 1: Summary of acquisition parameters for paediatric head CT examinations

		kV	Mean mAs*/mA**	Pitch	Slice Width (mm)	Rotation time (s)
Siemens Emotion 6 Unit* (site 1)	Helical	110	136	0.8	3	0.6
BrightSpeed 16 Unit** (site 2)	helical Axial	120	175	0.562 -----	1.25 5	1

Figure 1 provides details of the descriptive statistics of mean doses (CTDI_{vol}, DLP) from head examinations for children arranged in four age groups: <1 y, 1-5 y, 5-10 y, 10-15y

Figure 1: CTD_{vol} (mGy), DLP (mGy.cm) as Local DRLs for the 2 sites



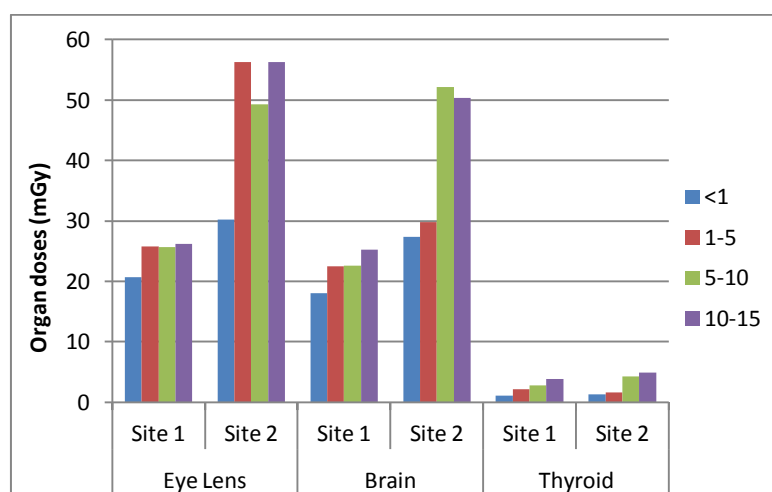
The Effective doses per hospital and per age group estimated using the Impact CT software with the ICRP60 and ICRP103 definition are displayed in Table 2

Table 2: Mean values of patient Effective dose (mSv) for different pediatric age groups with using the ICRP60 (E_{60}) and ICRP103 (E_{103}) definitions of Effective dose

Patient Age	Siemens Emotion6 (site 1)		GE BrightSpeed16 (Site 2)	
	E_{60}	E_{103}	E_{60}	E_{103}
<1	0,83	0,91	1,09	1,22
1-5	1,07	1,16	1,15	1,27
5-10	1,2	1,29	1,83	1,98
10-15	1,3	1,4	2,09	2,28

Figure 2 presents the estimated organ doses for selected organs as eye lens, brain and thyroid in terms of mean values per age groups for the two participating hospitals.

Figure 2: Organ doses (mGy) per hospital for each patient age group



4. DISCUSSION

Radiation dose from CT mostly depends on the CT acquisition parameters, including tube potential (kVp), tube current (mAs), pitch, slice width... This study revealed a significant variation in acquisition parameters among the radiology departments of each site, as displayed in Table 1. The lowest technical parameters were found in the site 1. In fact, these low values can be attributed to the fact that this radiology department belongs to a Children Hospital so that all practices and examinations are dedicated to pediatric patients who need special care and attention.

As an overall trend, dose indicators present a broad range between the two sites. The variations between hospitals were largely contributed by inherent differences in the equipment and different scanning protocols used among hospitals. In fact, both axial and helical scan mode are used in hospital 2 and it was effectively observed in figure 1 that it had the highest mean CTDI and DLP values reaching 56,4 mGy and 977 mGy.cm, respectively. An increase of CTDI with patient age is noted, this is due to the occasional slight increase in kV and mAs values with children age for both sites.

The results of effective dose estimations (E) in Table 2 show that the mean values per age group do not vary widely between hospitals with a slight increase in site 2 due to the high DLP values since

there is a strong correlation between the effective dose and DLP which takes into account CT scanning parameters.

It is evident from figure 2 that large variations of organ dose (eye, brain and thyroid) exist within and among hospitals with outstanding values in hospital 2. The eye lens and the brain are usually included either totally or partially in the irradiation field in brain CT examination and as known organs within the scan volume receive higher absorbed doses than those outside the scan volume with a high mean value reaching 56 mGy for the eye lens in hospital 2.

As it is shown, thyroid receives a dose. This is mainly due to the large scan length used in some units sometimes for clinical needs UH1 and to the over ranging which contributed to the increase in doses to organs and tissues positioned at the boundaries of the scan length [6]

Detailed dosimetry data as presented in the current study are important for providing patient exposure data for optimization, and for adoption, adaptation and application of clinical guidelines.

5. CONCLUSION

In this study, pediatric radiation dose was investigated for head CT procedures in two university hospitals in Tunisia. Our work takes a picture of the local practice in pediatric CT examination, demonstrates the necessity of the optimization of the CT procedure especially for site 2 and are useful as a base for the future optimization studies, dose optimization and derivation of national diagnostic reference levels.

6. ACKNOWLEDGEMENTS

The work was supported by the IAEA through the TC project number RAF/9/053 “Strengthening Technical Capabilities for Patient and Occupational Radiation Protection in Member States”. Authors are grateful to the participating hospitals for their time and cooperation during the data collection and dosimetric measurements.

7. REFERENCES

- [1] BRENNER DJ, HALL EJ. Computed tomography—an increasing source of radiation exposure. *N Engl J Med.* 2007;357:2277–2284.
- [2] STRAUSS KJ, GOSKE MJ, KASTE SC, et al. Image gently: ten steps you can take to optimize image quality and lower CT dose for pediatric patients. *AJR Am J Roentgenol.* 2010;194:868–873.
- [3] INTERNATIONAL COMMISSION ON RADIOLOGICAL PROTECTION (ICRP) (2007) The 2007 recommendations of the international commission on radiological protection, ICRP Publication 103. *Ann ICRP* 37(2–4):1–332
- [4] INTERNATIONAL COMMISSION ON RADIOLOGICAL PROTECTION (ICRP) (2007) Radiological protection in medicine, ICRP Publication 105. *Ann ICRP* 37(6):1–6
- [5] ImPACT CTDOSIMETRY CALCULATOR, Version 1.0.4. St. George's Healthcare NHS Trust, London, UK, 27 May 2011
- [6] K Fujii, T Aoyama, C Yamauchi-Kawaura, S Koyama, M Yamauchi, S Ko, K Akahane, and K Nishizawa, Radiation dose evaluation in 64-slice CT examinations with adult and paediatric anthropomorphic phantoms. *Radiat Prot Dosimetry.* Jun;140(1), 2010

Spanish Radiation Protection Association (SEPR) Working Groups in Radiation Protection in Medicine

Gil-Agudo, Antonio*; **Ruiz-Cruces, Rafael**; **Almansa-López, Julio**; **Torres-Cabrera, Ricardo**; **Martí-Climent, Josep María**; **Sanjuanbenito-Ruiz de Alda, Waldo**; **Prieto-Martín, Carlos**; **Macías-Dominguez, Maria Teresa**

Spanish Radiation Protection Association (SEPR).

Abstract. The SEPR has promoted the creation and monitoring of Working Groups (WG) on several topics of interest in the field of Radiological Protection in Medicine. Very often these working groups are joint- tasks with members from other professional societies and organizations, in particular with the Spanish Society of Medical Physics. Some of the recent and more Active working groups are presented below. In compliance with the requirement of the European Directive 43/1997/Euratom about having to determine the distribution of estimation of individual doses from medical exposures for the population, two WG's were created: "DOMNES" and "Registration of Dose in Radiology". DOMNES project dealt about dose to patients from Nuclear Medicine studies in Spain. On the requirement of the Directive 59/2013 about including a study of the risk of accidental or unintended exposure in Oncology Radiotherapy Departments, another WG was created in cooperation with Nuclear Safety Council: "Matrix Risk Analysis in Radiotherapy". Regarding the establishment of quality control programs for medical equipment in order to fulfil the Spanish legislation requirements, we have promoted three other WGs: "Quality Control in Diagnostic Radiology", "Quality Control in Nuclear Medicine" and "Dose estimation in patients in nuclear medicine studies". Related to his topic, a joint WG with the Federation of Manufacturers of Medical Equipment in Spain was also created "Acceptance test in diagnostic imaging equipments". Another WG about the implications of the new European Directive 59/2013/Euratom has been formed. We aim to put together all professional societies involved in the practical implementation of the Directive in order to identify the major points of interest for the professionals, prior to the transposition of the Directive into the Spanish law. Finally, we also participate and promote the Health Forum of Radiological Protection with the participation of the Nuclear Safety Council (authority responsible for nuclear safety in Spain).

1 OBJECTIVE

Medical procedures using ionizing radiation are the biggest source of man-made radiation to which people are exposed. For this reason, the SEPR has promoted the creation and monitoring of Working Groups (WGs) on several topics of interest in the field of Radiological Protection in Medicine. Very often these working groups involve members from other professional associations and organizations, in particular the Spanish Medical Physics Association. Some of the recent and most Active working groups are presented below.

2 MOTIVATION

In compliance with the requirement of the European Directive 43/1997/Euratom to determine the distribution of estimated individual doses from medical exposure in the population, in 2011 two WGs were created: "DOMNES" and "Registration of Dose in Diagnostic Radiology". The DOMNES project focused on doses to patients from Nuclear Medicine studies in Spain. Its work was completed in December 2015. The WG "Registration of Dose in Diagnostic Radiology" remains Active.

On the requirement of the Directive 59/2013 to include a study of the risk of accidental or unintended exposure in Oncology Radiotherapy Departments, another WG was created in cooperation with the

* Correspondent author: agilagudo@gmail.com

Spanish Nuclear Safety Council (CSN, the authority responsible for nuclear safety in Spain): “Matrix Risk Analysis in Radiotherapy”, still Active.

Regarding the establishment of quality control programmes for medical equipment in compliance with Spanish legislation, we have promoted three other WGs: “Quality Control in Diagnostic Radiology”, “Quality Control in Nuclear Medicine” and “Estimated dose to patients in Nuclear Medicine”. In relation to this topic, in 2013 a joint WG with the Federation of Manufacturers of Medical Equipment in Spain was also created: “Acceptance testing in diagnostic imaging equipment”. In this case, the group has focused on the publication of recommendations for the standardization of tests and criteria for the acceptance of equipment when first installed.

3 RESULTS

3.1. WG’S created and main objectives

In the next table, there are a description of the WG created, the main associations and organizations involved and the objectives of each one

Table 1:

WG name	Main organization participants	Creation date (year)	Objectives
Estimated dose to patients in Nuclear Medicine	SEFM, SEPR	2000	Develop protocols to estimate radiation doses received by target and critical organs in patients undergoing therapeutic procedures
Forum on Radiation Protection in hospitals	CSN, SEPR, SEFM	2001	Forum with CSN and scientific associations (SEFM, SEPR ...) to promote implementation of Radiation Protection in various health fields, by creating working groups, preparation of documents
Human and material resources in Radiological Protection Departments (RPD)	CSN, SEPR	2009	Preparation of document to provide guidance on resources in RPD
DOMNES	CSN	2011	Determine frequencies, dose contribution and DRL to compare with EU values
Analysis of implications of Directive 59/2013 EURATOM	SEPR, SEFM	2015	Analysis or review of existing legislation that could be affected by transposition of new Directive

Registration of dose in Diagnostic Radiology	SEPR, SEFM	2013	Establish simple methodology for conducting periodical "surveys" in Spain on dose levels in diagnostic radiology scans
Acceptance testing agreement	FENIN, SEFM, SEPR	2013	Develop consensus documents in all modes of imaging, both diagnostic radiology and nuclear medicine
Risk matrix approach in Radiotherapy	CSN, SEFM, SEPR, SEOR	2005	Development of a software tool and a methodological guide that facilitates the implementation of the risk matrices in radiotherapy
Quality control in Nuclear Medicine equipment	SEFM, SEPR, SEMNiM	2011	Update protocol of quality control in Nuclear Medicine published in 1999
Quality control in Diagnostic Radiology equipment	SEFM, SEPR, SERAM	2011	Update protocol of quality control in Diagnostic Radiology published in 2002

3.2. Main Actions and Final Documents elaborated by the WG

In the table below, we exposed the main actions and principal documents elaborated by each WG, as well as the current situation of the WG (ended or Active)

Table 2:

WG name	Creation date-end date(-)	Main actions and published documents
Estimated dose to patients in Nuclear Medicine	(2000-2015)	Document on estimation of dose to patients after administration of I-131 on thyroid carcinoma (2005) and on hypertyroidism (2015)
Forum on Radiation Protection in hospitals	(2001-Active)	Radiation Protection General Manual (2002) Needs of calibration in Spanish Hospitals in the different areas of application (2002) Radiation Protection of pregnant workers exposed to radiation in Hospitals (2002) RadioActive waste procedure (2009) Discharge of in-patients criteria in Metabolic Therapy. (2011) Protocol for monitoring by area dosimetry of workers exposed classified B in the health sector (2009)

Human and material resources in Radiological Protection Departments (RPD)	(2009 – Active)	Simulator for calculating minimum human and material resources required in Hospital RPD (2014)
DOMNES	(2011-2014)	Document with results (2014)
Analysis of implications of Directive 59/2013 EURATOM	(Active)	In progress
Registration of dose in Diagnostic Radiology	(2013 – Active)	Survey on dose levels in Diagnostic Radiology (2015)
Acceptance testing agreement	(2013 – Active)	Acceptance testing in Diagnostic imaging (X-Ray) (2014) and in Fluoroscopy (pending edition)
Risk matrix approach in Radiotherapy	(2005- Active)	Development of software of SEVRRRA (Ibero-American Forum of Radiological and Nuclear Regulatory Agencies, that include the CSN) 2005-2010 Testing of the software by a group of 10 Spanish hospitals (2013-2014)
Quality control in Nuclear Medicine equipment	(2011-2015)	New edition of document: Quality control in Nuclear Medicine equipment (2015)
Quality control in Diagnostic Radiology equipment	(2011-2013)	New edition of document: Diagnostic Radiology equipment (2011)

4 CONCLUSIONS

One of the missions of our Spanish Radiation Protection Association (SEPR) is the promotion and development of documents of interest to its affiliated members in the areas of interest. One of the most relevant areas is the radiation protection in medicine.

Promotion and monitoring working groups in this area by our Association in partnership with other companies or organizations has demonstrated a very efficient tool for the development of consensus documents on topics of great interest among professional.

5 ACKNOWLEDGMENTS

This paper is based on the work done by the members of each working group, therefore this paper is of them.

Regulatory T cells (Tregs) as a possible prognostic marker in radiation skin injury

Ana Julia Molinari^{a*}, Mercedes Portas^b, Andrés Rossini^a, Severino Michelin^a, Diana Dubner^a

^aAutoridad Regulatoria Nuclear, Pbro. Juan Gonzalez y Aragon 15 (B1802AYA) Ezeiza, Argentina.

^bHospital de Quemados, Av. Pedro Goyena 369 (C1424BSD) Ciudad Autónoma de Buenos Aires, Argentina.

Abstract. Radiation skin injury (RSI) has been reported in patients that underwent fluoroscopically guided procedures. RSI ranges in severity from mild erythema to moist desquamation and ulceration. Radiation induced skin injury can be divided into acute and chronic. Acute injury occurs in hours to weeks after irradiation exposure, whereas chronic includes ulcers and fibrosis that persist weeks to years after radiation exposure. Chronic inflammation has been associated to RSI. Human survival from injury and wound healing require an appropriate inflammatory and immune response. Regulatory T cells (Tregs) belong to a unique subpopulation of CD4⁺ lymphocytes. It has been demonstrated that CD127 expression is an excellent biomarker of human Tregs, especially when combined with CD25, in this CD4⁺ lymphocytes. Tregs represent 5-10% of peripheral CD4⁺ cells in normal condition in humans and have an important role in mediating immune homeostasis, as well as maintaining self-tolerance. Several studies about Treg cell radiosensitivity indicated that Tregs were more radioresistant than other T or B lymphocyte subpopulation. Repeated low dose irradiation has been shown to suppress inflammation in different autoimmune and allergic conditions in part to upregulation of Tregs. Tregs could accumulate at inflammatory sites induced by ionizing radiation and could influence the level of DNA damage and repair through TGF β production in responder cells. Within this context, the aim of the present study was to evaluate the percentage of Tregs by flow cytometry in patients exposed to fluoroscopy. We particularly analyzed the frequency of CD4⁺ CD25⁺ CD127⁻. Changes in the level of circulating Tregs in the peripheral blood, in combination with other inflammatory parameters, might be very important for RSI prognosis. Additionally, Tregs could be used as a potential follow up biomarker of the radio induced inflammation process in a radiological accidental scenario and could contribute to efficiently guide a personalized therapeutic treatment.

KEYWORDS: *Regulatory T cells; radiation skin injury; flow cytometry.*

1 INTRODUCTION

With the use of X-rays for medical imaging has come the well-known complication of damage to the skin. Radiation-induced injury to skin (RSI) is an infrequent but potentially serious complication to complex fluoroscopically-guided interventional procedures. Due to a lack of experience with such injuries, the medical community has found fluoroscopically-induced injuries difficult to diagnose [1]. This kind of injuries have occurred globally in many countries and hundreds of them have been reported worldwide. Although, since 1992, the U.S. Food and Drug Administration (FDA) has received reports of radiation-induced injuries to the skin in patients who had undergone fluoroscopically guided interventional procedures, treatment of such injuries remain difficult [2]. Skin lesions include a wide spectrum such as erythema, telangiectasias, atrophy, hyperpigmentation and hypopigmentation, necrosis, chronic ulceration, and squamous cell carcinoma [3]. Sometimes, these RSI involve deeper tissues to the level of bone and spine.

Radiation skin injury can be categorized as acute or late (i.e., chronic) injuries. Acute effects occur in hours to weeks after radiation exposure, and involve cellular alterations and inflammation in the epidermis and the dermis. Chronic RSI includes delayed ulcers, fibrosis, and telangiectasias that present weeks to years after radiation exposure [4, 5].

* Presenting author, e-mail: amolinari@arn.gob.ar

In fluoroscopically-guided interventional procedures, serious injuries most frequently occur on the patient's back due to the conventional orientation of the fluoroscope. X-ray beam is delivered from under the table on which the patient lies during the procedure [6]. But have also diagnosed on the axillary regions and arms.

Ionizing radiation during interventional procedures is often underestimated. The risk of developing this reaction is directly related to the radiation dose, which depends on the type of procedure, technique, time of exposure, and the patient's body constitution. The period between radiation exposure and manifestation of RSI varies from 15 days to month or years [3].

There are marked differences between radiation and thermal burns in terms of physio-pathological mechanisms, clinical aspects and evolution. The main feature of severe radiation burns is the occurrence of unpredictable successive inflammatory waves leading to the extension, in surface and in depth, of the necrotic process [7]. RSI involves immediate damage to basal keratinocytes and hair follicle stem cells, followed by a burst of free radicals, DNA damage and inflammation. The mechanism about the cascade of inflammatory mediators and continued activation of immune cells is not well understood. The ionization caused by the radiation is thought to lead to an activation of histamine-like substances, resulting in a dilation of capillaries [1]. Induction of vascular hyperpermeability is one of the early vascular responses to radiation exposure and is considered to contribute to subsequent fibrosis and tissue injuries. Skin ulcer can be triggered and worsening by minor trauma caused by scratching, applying topical agents or hot packing employed by patients to relieve the associated pruritus and pain [8].

The medical treatment sometimes involves surgical grafting that results in permanent disfigurement and compromised mobility. In case of severe RSI, surgeons may face technical difficulty in treatment due to the occurrence of successive and unpredictable inflammatory waves with progressive extension of necrosis in both superficial and deep layers. Moreover, such successive and unpredictable inflammatory waves are associated with uncontrollable pain and often resistance to analgesics [9].

Regulatory T cells (Tregs) are critical regulators of immune tolerance. Numerous studies have demonstrated the potent influence of Treg cells in suppressing pathologic immune responses in different disease. Tregs belong to a unique subpopulation of CD4⁺ cells constitutionally expressing the Foxp3 transcription factor and having high levels of CD25 on their surface. However, these markers have proven problematic for uniquely defining this specialized T cell subset in humans. Liu and colleagues have shown that CD127 can be used to quantitate Tregs and its expression inversely correlates with Foxp3 [10]. Tregs represent 5-10% of peripheral CD4⁺ T cells in normal condition in humans and have an important role in mediating immune homeostasis, as well as maintaining self-tolerance [11].

Several studies regarding Tregs cell radiosensitivity have indicated that Tregs are more radioresistant than other T or B lymphocyte subpopulations, due to reduced apoptosis and increased proliferation, which leads to their systemic enrichment. It is known that ionizing radiation producing functional alteration of the immune system and breaking self-tolerance could cause autoimmune diseases [12].

It has been suggested that Tregs circulate between blood, skin, and lymphoid tissues to regulate peripheral immune responses [13]. Zhou and colleagues have identified a role for radiation-induced alterations in skin regulatory T cells and its effects on immune homeostasis. They have demonstrated an increase in regulatory T cells in systemic lymphoid organs that is associated with a depletion of regulatory T cells from the skin [14].

Although most data agree on the fact that radiation altered Treg suppressor capacity, the different papers show relatively pronounced variations in the level of Treg damage even after comparable radiation doses [11]. Repeated low dose irradiation has been shown to suppress inflammation in different autoimmune and allergic conditions due in part to upregulation of Tregs.

Within this context, the aim of the present study was to evaluate the percentage of Tregs by flow cytometry in patients exposed to fluoroscopy in order to determine differences between them and not exposed persons and its possible correlation with patient evolution.

2 MATERIALS AND METHODS

2.1 Patients

Since 1997 patients were referred to the Radiopathology Committee of Hospital de Quemados del Gobierno de la Ciudad de Buenos Aires (HQGCBA) for the diagnosis and therapy of RSI. There is an agreement between the HQGCBA and the Autoridad Regulatoria Nuclear (ARN) with this purpose.

For this study, we include 4 patients that had been exposed to X-ray during fluoroscopically-guided interventional procedures, and 6 healthy adults as controls.

The study was approved by the Research and Ethics Committee of the HQGCBA and informed consent was obtained from all patients.

2.2 Sample collection

A total of 3 ml of blood was collected into EDTA venous blood collection tubes (Vacutainer, BD) and maintained at room temperature until processed.

2.3 Flow cytometry

All samples were analysed the same day of the blood collection.

The assessment of Tregs (CD4+, CD25+, CD127-) was performed by staining 50 µl of whole blood with anti CD4 FITC, anti CD25 PE-Cy5 and anti CD127 PE (all provided by BD).

Samples were lysed with FACS Lysing Solution (BD) and samples were analysed in a flow cytometer (BD FACSCalibur) using CellQuest Pro Software.

2.4 Statistical analysis

The statistical significance of the percentage of Tregs values were evaluated by Student's t test. Statistical significance was set at $p = 0.05$.

3 RESULTS

In order to identify the exposed patients, all samples were named as PQ followed by a number and for data analysed in this study patients were evaluated between August 2015 and March 2016.

In our study Tregs represented 9.87 ± 1.50 % of peripheral CD4+ T cells in normal condition (Control donors).

PQ20 was a female patient with heart disease, heavy smoker, who was exposed to X rays for 6 hours, during an interventional procedure(stent) in September 2005.

Early manifestations were blisters, which were diagnosed by a dermatologist as Herpes Zoster infection. Few months later, in the same localization, a deep ulcer with severe pain appeared. (Fig. 1 A). Treg were 12.08 ± 0.34 % of peripheral CD4+ T cells. This percentage was not statistically significant respect to the control value ($p=0.0674$).

PQ85 was a male with multiple fluoroscopically-guided interventional procedures. The last one was in November 2013 and it took several hours. He presented a chronic ulcer in the arm and lesions in the back. Treg were 19.30 ± 0.85 % of peripheral CD4+ T cells. This percentage of Treg was greater than the control one and this difference was statistically significant ($p=0.0001$).

PQ89 was a male with multiple fluoroscopically-guided interventional procedures. Between 20 and 30 days after the last procedure the patient started with pruritus and desquamation (Fig 1 B). We took 2 samples from this patient, the first one in November 2015 and the second one in March 2016. He referred pain and presented a crust when the first sample was taken. Treg were 12.91 ± 0.52 % of peripheral CD4+ T cells in November 2015. Compared with control value, this difference is considered to be statistically significant ($p=0.0174$). In March 2016, the lesion was bigger, presented erythema and the pain was higher. At that moment the difference between this value and control value was considered to be not quite statistically significant ($p= 0.0609$).

PQ93 was a male with 25 years' experience as interventional cardiologist. He presented some lesion on his hands. Treg were $12.33 \pm 0.56\%$ of peripheral CD4+ T cells, and the difference was statistically significant versus control value ($p= 0.0457$). All Treg values are graphed in figure 2.

Figure 1: Radiation injury following interventional cardiology procedure. A) PQ20 B) PQ89

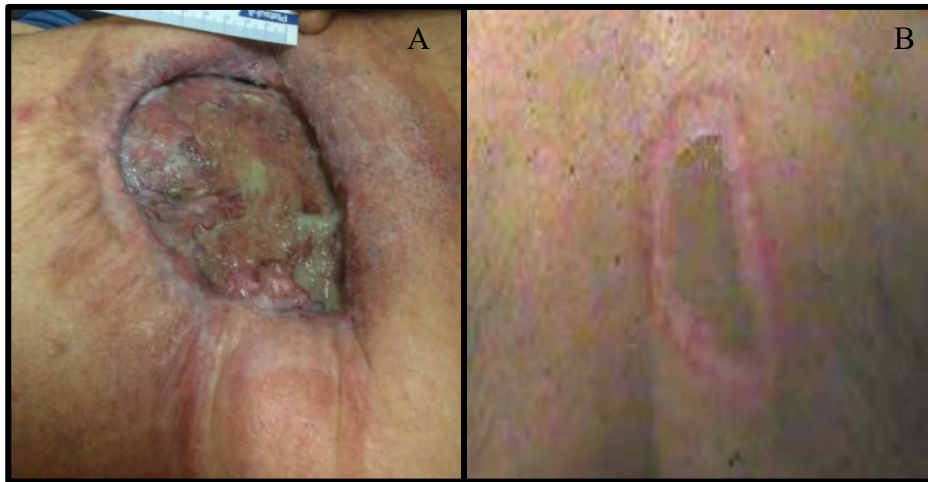
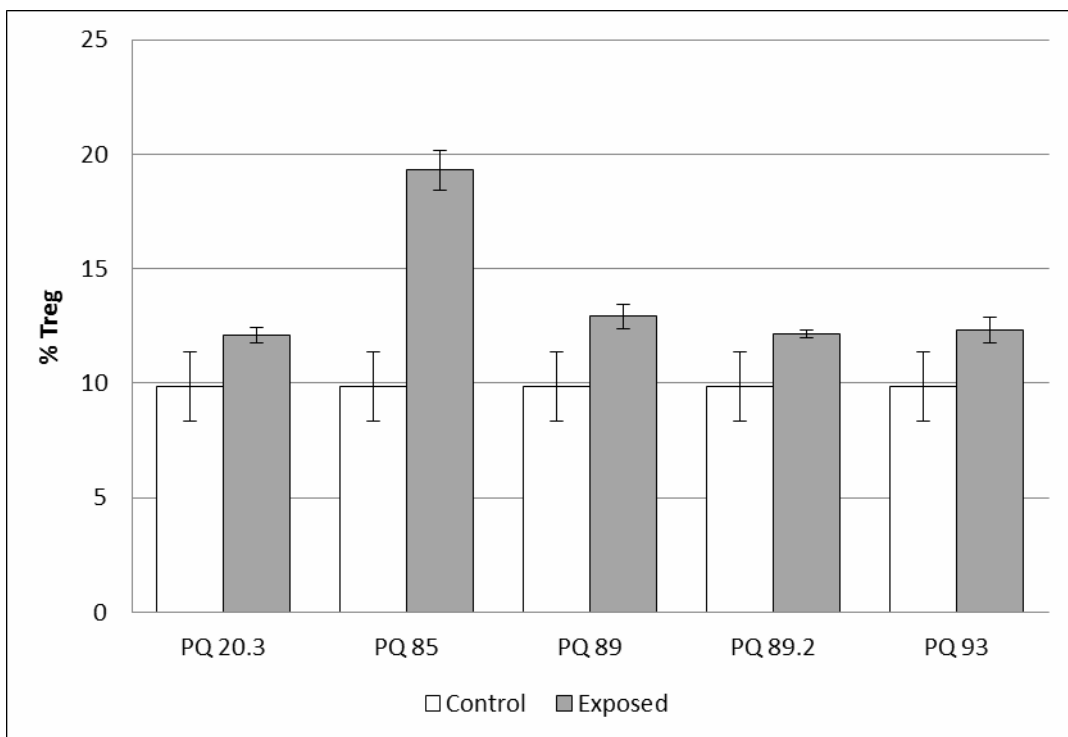


Figure 2: Percentage of Treg from control and exposed patients.



4 CONCLUSION

Up to now there is increasing published evidence about the presence of Regulatory T cells in tumor environment and tumor response but not regarding its role in irradiated healthy tissue.

The present study unequivocally demonstrated some differences in the percentage of circulatory Treg between patients that were exposed to fluoroscopy and controls. Three of the exposed patients presented differences statistically significant when contrasted with control value. PQ85 showed the highest level of Treg. In this patient, RSIs started two years before we took the sample. At the moment of the Treg measurement, the patient presented a deep chronic ulcer on his arm and other lesion on his back. RSIs have specific characteristics of the post-irradiation delay in the onset of clinical changes and the successive and unpredictable inflammatory burst [9]. An emerging concept is that Tregs not only control immune responses, but also promote tissue homeostasis by suppressing inflammation and aiding in tissue repair [15]. Related to PQ85, we hypothesised that the high level of Treg could be a positive prognosis sign because it could eventually control the inflammation process. Of course that we have no evidence of that, but in order to prove that it would be necessary analyse consecutive blood samples and correlate the level of Treg with the clinical sings of the lesion.

On the other side, we determine the level of Tregs in PQ89 in two different moments. In this case, we found that the percentage of Tregs was significantly greater than control value of the first sample, but it did not reach statistical significance in the second sample. This discovery was very interesting because the RSI worsened from the first to the second time. It has been shown that the depletion or functional alteration of the Tregs leads to the development of autoimmune diseases [16]. It could be possible that in this case we started to measure Treg level at the same time that a new inflammatory wave was ongoing. After an initial period marked by a clinical picture limited to a rash and itching, subsequent ulceration and necrosis develop, which may extend to the deep dermal and underlying muscle structures. The uncontrolled extension of the radiation necrotic process is associated to these inflammatory waves [7].

We propose that changes in the level of circulating Tregs in the peripheral blood might be very important for patient prognosis and predicting therapy response. Additionally, Tregs could be used as a potential follow up biomarker of the radio induced inflammation process in a radiological accidental scenario. This must be continued by the follow up of higher number of patients.

5 REFERENCES

- [1] Wagner L., 2007. Radiation injury is a potentially serious complication to fluoroscopically-guided complex interventions. *Biomed Imaging Interv J.* 3(2):e22. doi: 10.2349/biiij.3.2.e22.
- [2] Shope T.B., 1996. Radiation-induced skin injuries from fluoroscopy. *Radiographics* 16(5):1195-9.
- [3] Herz-Ruelas M.E., Gómez-Flores M., Moxica-Del Angel J., et al., 2014. Ulcerated radiodermatitis induced after fluoroscopically guided stent implantation angioplasty. *Case Rep Dermatol Med.* 2014:768624. doi: 10.1155/2014/768624.
- [4] Ryan J.L., 2012. Ionizing radiation: the good, the bad, and the ugly. *J Invest Dermatol.* 132(3 Pt 2):985-93. doi: 10.1038/jid.2011.411. Review.
- [5] Mendelsohn FA, Divino CM, Reis ED., et al., 2002. Wound care after radiation therapy. *Adv Skin Wound Care* 15(5):216-24. Review.
- [6] Hashimoto I., Sedo H., Inatsugi K., et al., 2008. Severe radiation-induced injury after cardiac catheter ablation: a case requiring free anterolateral thigh flap and vastus lateralis muscle flap reconstruction on the upper arm. *J Plast Reconstr Aesthet Surg.* 61(6):704-8. doi: 10.1016/j.bjps.2007.01.003.
- [7] Lataillade J.J., Doucet C., Bey E., et al., 2007. New approach to radiation burn treatment by dosimetry-guided surgery combined with autologous mesenchymal stem cell therapy. *Regen Med.* 2(5):785-94.
- [8] Wei K.C., Yang K.C., Mar G.Y., et al., 2015. STROBE—Radiation Ulcer: An Overlooked Complication of Fluoroscopic Intervention: A Cross-Sectional Study. *Medicine (Baltimore).* 94(48):e2178. doi: 10.1097/MD.0000000000002178.

- [9] Jang W.H., Shim S., Wang T., et al., 2016. In vivo characterization of early-stage radiation skin injury in a mouse model by two-photon microscopy. *Sci Rep.* 6:19216. doi: 10.1038/srep19216.
- [10] Liu W., Putnam A.L., Xu-Yu Z., et al., 2006. CD127 expression inversely correlates with FoxP3 and suppressive function of human CD4+ T reg cells. *J Exp Med.* 203(7):1701-11.
- [11] Persa E., Balogh A., Sáfrány G., et al., 2015. The effect of ionizing radiation on regulatory T cells in health and disease. *Cancer Lett.* 368(2):252-61. doi: 10.1016/j.canlet.2015.03.003.
- [12] Gyuleva I.M., Penkova K.I., Rupova I.T., et al., 2015. Assessment of Some Immune Parameters in Occupationally Exposed Nuclear Power Plant Workers: Flow Cytometry Measurements of T Lymphocyte Subpopulations and Immunoglobulin Determination. *Dose Response.* 13(4):1559325815611901. doi: 10.1177/1559325815611901.
- [13] Tomura M., Honda T., Tanizaki H., et al., 2010. Activated regulatory T cells are the major T cell type emigrating from the skin during a cutaneous immune response in mice. *J Clin Invest.* 120(3):883-93. doi: 10.1172/JCI40926.
- [14] Zhou Y., Ni H., Balint K., et al., 2014. Ionizing radiation selectively reduces skin regulatory T cells and alters immune function. *PLoS One.* 9(6):e100800. doi: 10.1371/journal.pone.0100800. eCollection 2014.
- [15] Spence A., Klementowicz J.E., Bluestone J.A., et al., 2015. Targeting Treg signaling for the treatment of autoimmune diseases. *Curr Opin Immunol.* 37:11-20. doi: 10.1016/j.coi.2015.09.002. Review.
- [16] Sakaguchi S., 2004. Naturally arising CD4+ regulatory t cells for immunologic self-tolerance and negative control of immune responses. *Annu Rev Immunol.* 22:531-62. Review.

Head and Neck Immobilization Masks: Increase in Dose Surface evaluated by EBT3, TLD-100 and PBC Method

Arnie Verde Nolasco^{a*}, Luiz Oliveira Faria^b

^a Depto. de Eng. Nuclear, UFMG, C.P. 702, 31270-970 Belo Horizonte, MG, Brazil

^b Centro de Desenvolvimento da Tecnologia Nuclear, Av. Antonio Carlos 6627, C.P. 941, 30161-970 Belo Horizonte, MG, Brazil.

Abstract. Positioning and immobilization tools are considered essential in order to guarantee that the planned dose distribution could be efficiently reached in radiotherapeutic treatments. However, the benefits brought by its use are confronted by the apparent increase in the patient skin entrance dose. In this work we have studied the dose surface effects of immobilization thermoplastic masks for head and neck radiotherapy treatments, performed in a 6 MV linear accelerator beam. The study was conducted using an anthropomorphic head-neck phantom and three different dosimetric techniques: thermoluminescent dosimetry, radiochromic film dosimetry and computational simulation using the Pencil Beam Convolution (PBC) method. After irradiation with 180 cGy, TLD chips positioned in the surface of the SCF (supraclavicular fossa) anatomic region of an anthropomorphic phantom have detected an increase in the entrance skin dose around 33%. The EBT3 small 2.0 cm² strips data, averaged among all strips used, have encountered a medium increase of 70%. Although they have discrepant results, both dosimetric systems have measured very similar doses with the presence of immobilization masks. Doses evaluated by the PBC method in electronic disequilibrium regions, unlike TLD and EBT3 dose evaluation, were inaccurate.

KEYWORDS: *surface dose; thermoplastic masks; skin sparing; radiotherapy masks, EBT films; thermoluminescent dosimetry.*

1 INTRODUCTION

An immediate benefit attained when using high energy clinical beams, for malign diseases treatments, consists simply in the low radiation dose distribution along the patient skin surface. In fact, in the dose distribution versus tissue depth curves, there is an electronic disequilibrium region usually larger than the skin thickness average, resulting in an advantageous preservation of this sensitive tissue. This effect is commonly reported in literature as Skin Sparing [1 - 3].

Regardless of this benefit, the employment of immobilization tools such as thermoplastic masks and molds, both used for patient positioning and immobilization, has competed for the disappearance of the Skin Sparing effect in radiotherapy procedures. For instances, [4] measured an average 18% increase in surface dose caused by thermoplastic masks used for intensity-modulated radiotherapy treatments. [5] measured the increase in surface dose caused by carbon fiber tables to be as much as 400%. Thus, as a consequence of this increase in surface dose, the correct evaluation of the dose superficialization effect becomes very important [2]. In clinical practice, the effect of dose superficialization in radiotherapeutic treatments confronts the benefits brought by the use of immobilization materials. In spite of this problem, the immobilization tools are considered essential in order to guarantee the reproducibility of the patient positioning and immobilization, during the entire period of treatment, ensuring that the planned dose distribution could be efficiently reached in the last section of the radiotherapy treatment. In this context, it is very important to evaluate how significant is the utilization of these immobilization devices, considering the damages provoked by the radiation dose increase in the shallow skin regions. In this work we studied the dose surface effects provoked by the use of immobilization thermoplastic masks for head and neck radiotherapy treatments, performed in a 6 MV linear accelerator beam. In this context, using mega-voltage X-ray beams, [6] tested a mask with larger holes for head and neck immobilization on the surface of a solid water phantom. They measured an increase in surface dose by a factor of at least 50% in the best conditions. On the other hand, using a 6 MV linear accelerator beam, [7] studied these effects using Gafchromic EBT films over a flat surface phantom. In addition, [8], also using EBT film, measured these effects over a rigid anthropomorphic breast phantom. Both studies have confirmed the increase in the surface dose. In our study, in order to accurately measure the delivered

* Presenting author, e-mail: arnienolasco@hotmail.com

dose to the head and neck skin during a typical radiotherapeutic treatment, we have employed an Alderson Rando anthropomorphic head-neck phantom and three dosimetric techniques: thermoluminescent dosimetry (TLD-100), radiochromic film dosimetry (EBT3) and computational simulation using the Pencil Beam Convolution (PBC) method. This methodology allows taking into account the dose variation in non-flat surfaces and the dose comparison among three different dosimetric systems, providing a more realistic dose surface evaluation.

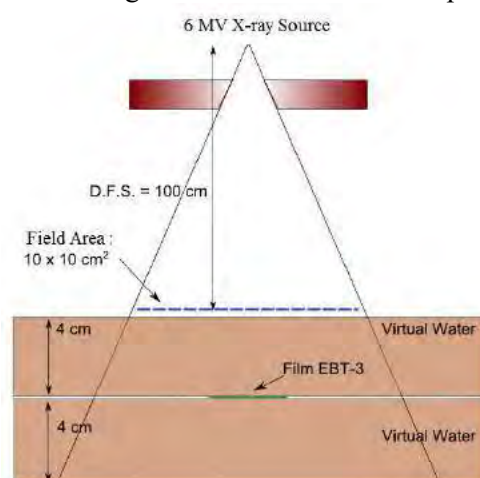
2 METHODOLOGY

2.1 Size and Page Configuration

Alderson Rando anthropomorphic phantom was used in order to reproduce radiotherapeutic treatments in the head and neck regions. The phantom was submitted to a rigorous 3D radiotherapeutic planning. The daily dose delivering parameters were obtained through computational calculations. CT scanning was employed for planning and also for spatial point localization. These spatial coordinates were used to feed the PBC algorithm simulation. The points were carefully selected in order to provide a correct evaluation of the dose superficialization effect in various cervico-facial tissue regions. For better visual identification purposes, milimetric acrylic spheres were positioned at the mapped points over the phantom skin, before the CT scanning. A fictitious injure occurring next to the base of the tongue has been considered, in order to justify the adoption of a radiotherapeutic treatment that uses the application of three daily fields. The treatment was calculated using a 3D conformational method. The thermoplastic mask and the head support, appropriated for the simulator anatomic dimensions, were prepared in accordance with therapeutic international protocols.

For calibration purposes, EBT-3 radiochromic films were cut into nine small 2.0 cm² identified pieces. They were placed between two virtual solid water plates and exposed to absorbed doses ranging from 25 to 200 cGy. A schematic diagram of the calibration arrangement is shown in Fig. 1. Exposures were performed using the 6.0 MeV beam emitted by the Clinac Linear Accelerator, model 2100 C, in accordance with the calibration protocols reported by [9,10]. Films were scanned using the MICROTEK ScanMaker 9800XL scanner at 600 dpi resolution, in RGB image mode, with no corrections or digital filtering. Image files were saved in the Tagged Image File Format (TIFF). The color intensity analysis was performed with the ImageJ® application program (<http://rsbweb.nih.gov/ij/>). Statistical tools were used in order to reduce the measurements standard deviation, following the methodology suggested by [11].

Figure 1: Schematic diagram showing the EBT3 calibration setup using virtual solid water.



EBT3 film pieces with variable forms were disposed over the skin's anthropomorphic phantom, covering all mapped points of interest. A thin adhesive tape was used to fix the film pieces on the surface as seen in Fig. 2. A set of TLD-100 chips, previously calibrated at same condition as EBT3 film, i.e. under virtual solid water plates, were placed between the adhesive tape and the radiochromic film, exactly above the previously mapped points. This methodology was employed to perform the

phantom irradiation with and without the thermoplastic mask. The PBC dose evaluation was also performed under these two conditions.

Figure 2: EBT3 radiochromic films and TLD-100 chips disposed over the skin's anthropomorphic phantom, covering all mapped points of interest in an Alderson Rando anthropomorphic phantom. This setup is covered by a thermoplastic mask.



A group of 170 commercial LiF:Mg,Ti (TLD-100) chips were preselected from a larger group by exposing the examined samples to 100 mGy of gamma rays with photon energies of 662 keV, from a ^{137}Cs gamma sources at room temperature (RT). This process was repeated three times and the chips with TL response higher than 4.0 % were discarded. The measurements of TL glow curves were performed in a Harshaw-Bicron 3500 TLD reader, operating under a linear temperature profile over the range of 50–300°C, in the resistive mode, by using a heating rate of 10°C/s and reading cycles of 35s. Annealing was performed at 400°C (1 h) and 100°C (2 hs) before irradiation. Pre-reading annealing was done by heating at 100°C during 15 min. In the generation of the TLD calibration curve, the top 4.0cm virtual solid water on Fig. 1 was changed to another one with 1.0cm, in order to compensate the 0.4mm of acrylic placed in each side of the TLD holder.

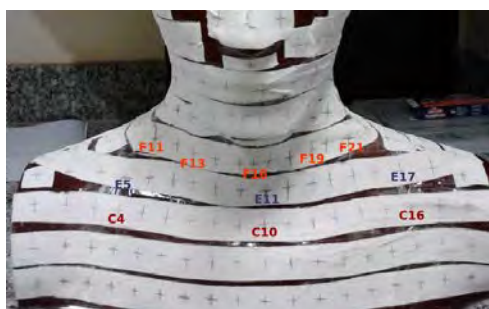
The pencil beam convolution (PBC) algorithm used in this work is a dose calculation analytical method employed by the Varian Medial Systems (Cadplan) for radiotherapy planning. According to Flosi (2011), PBC is divided in two main procedures: beam reconstruction modeling and patient modeling. For details see Ref.: [12].

3 RESULTS AND DISCUSSION

3.1 Dose Evaluation using TLD chips

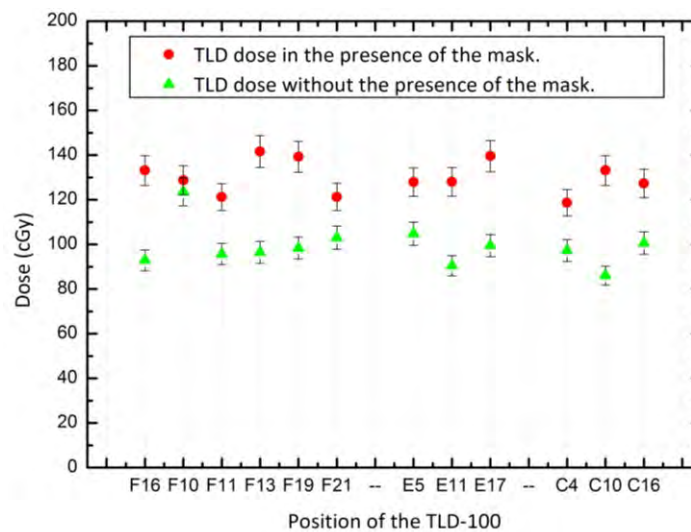
Twelve TLD chips were positioned in the surface of the SCF (supraclavicular fossa) anatomic region, as seen in Fig. 3, in order to measure the skin dose variation in radiotherapy procedures performed with and without the use of thermoplastic mask. The setups were submitted to an anterior/posterior irradiation procedure (AP), in agreement with the approved radiotherapeutic planning for head and neck radiotherapy treatments.

Figure 3: Experimental setup showing the positioning of the TLD chips over the supraclavicular fossa surface. This setup was used to estimate the entrance skin dose after the irradiation procedure, with and without the use of thermoplastic mask.



The measured skin doses after the irradiation procedure, for each chip position in the anthropomorphic phantom, are shown in Fig. 4. The planned delivered doses were 180 cGy for both procedures. As one can see in this graphic, the doses recorded by the TLD-100 chips reveal a higher superficial dose deposition for the treatment performed with the use of the thermoplastic immobilizer, because every measuring point over the slices F, E and C recorded increased doses. The average increase in each of those slices was 30.1%, 34.6% and 34.5%, respectively, resulting in a dose increase of 33% averaged over the SCF region. We remark that [6] tested an immobilization mask with small and larger holes, for head and neck irradiation procedures, on the surface of a solid water phantom in a LINAC EX21. The surface dose was estimated to change from 16% of the delivered dose (with no mask) to 31% and 35% (with mask extended 300%) for small and larger holes, respectively, exposed to 6 MV photo beams. Thus, we think that the increase in dose surface values registered using TLD-100 over the anthropomorphic phantom, i.e. 32.3% averaged over the SCF region, are in good agreement with data reported by these authors.

Figure 4: Superficial dose deposition in the supraclavicular fossa anatomic region measured by TLD-100 dosimeters, after being exposure to 180 cGy, with and without thermoplastic immobilizer. The F, E and C letters refer to the slices over the phantom, each of them containing TLD chips positioned as shown in Fig. 3.



3.2 Dose Evaluation using Radiochromic Films

The main goal of this work is to provide a more realistic dose surface evaluation, using a methodology that allows taking into account the dose variation in non-flat surfaces, based on dose comparisons among three different dosimetric systems. In this context, nowadays, radiochromic films have been extensively used for dosimetry in radiation medicine [13,14]. They have several advantages when compared to other alternative dosimeters for dosimetry of gamma and X-rays fields. Its high spatial resolution is far superior to that of ionization chambers and TLDs, offering greater X-ray sensitivity when using XR-QA series, and the ability to be used in water without waterproof encapsulation [15]. Besides, as reported by the manufacturers, the EBT series has no energy dependence when irradiated with 30 kVp, 100 kVp, 150 kVp (all with 2mm Al) and Co-60 photon fields for doses ranging from 1 to 300 cGy. Particularly, the spatial resolution of EBT radiochromic film series, commonly used for gamma fields, provides a more detailed dose mapping when compared with TLD-100 dosimeters, in spite of its lower sensitivity.

In order to compare the two dosimetric systems responses, we placed small 2.0 cm² identified EBT-3 film pieces in the same measuring points used to perform TLD-100 measurements, i.e. over the slices E and C in the SCF region, as seen in Fig. 5 and Fig.6. The results for the irradiation performed without the presence of the immobilization mask are shown in the left side of this Figure while the corresponding results related to the irradiation performed with the presence of the mask are shown in the right side. Taking into account the previous information recorded by TLD-100 shown in Fig.4, it is possible to observe an overall agreement between the two dosimetric systems. An increase in the dose

surface from 90-110 cGy range to 130-150 cGy range is observed by the EBT-3 film against 90-100 cGy to 120-140 cGy evaluated by TLD-100. The well known high spatial EBT-3 film resolution provides additional information concerning to the limit between the high dose region (above 90 cGy) and the low dose region (20 cGy), which is attributed to the secondary collimator in the linear accelerator head. Also, the EBT-3 films reveal an unexpected increase in the surface dose in the right upper side (around 150 cGy) when compared to the right side (around 120-140 cGy), provoked by the presence of the thermoplastic mask.

Figure 5: Photograph of the small 2.0 cm² identified EBT3 film pieces placed over the SCF region of the anthropomorphic phantom, after irradiation with 180 cGy in the Clinac Linear Accelerator model 2100 C at 6 MV. Films irradiated without mask are shown in the left side and films irradiated with the presence of the immobilization mask are shown in the right side. The relationship between skin dose and color scale is shown in the rightmost side (upper). Corresponding evaluated dose values by the EBT3 film pieces in slices E and C (bottom).

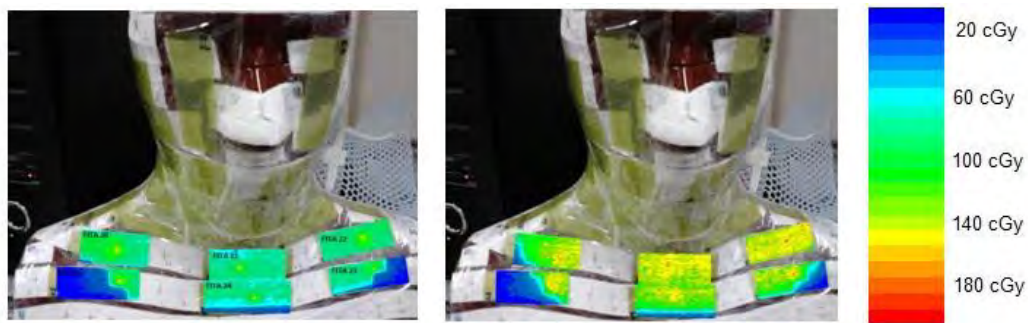
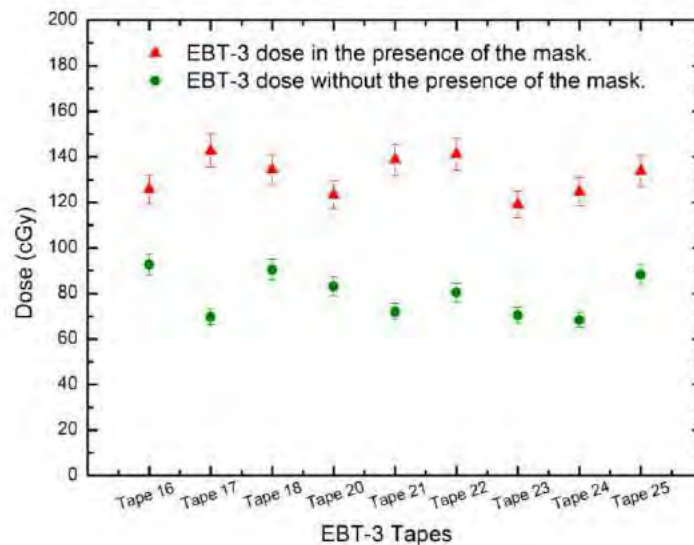


Figure 6: Superficial dose deposition in the supraclavicular fossa anatomic region measured by EBT-3 dosimeters, after being exposure to 180 cGy, with and without thermoplastic immobilizer. The tapes indicated in the graph correspond to slices E and C.



According to the data provided by both TLD and EBT3 dosimetric systems, shown in Fig. 4 and Fig. 5, respectively, it was possible to verify an increase in the entrance skin dose due to the use of the immobilization mask. Particularly, all FSC regions covered by the EBT3 film strips have registered an expressive dose increase on the superficial layers, as it can be seen in Table 1. The greatest increase was observed at the strip number 21 that measured a median increase of 66.77 cGy, i.e. an additional superficial dose of 93%. Taking into account that the medical prescription dose was 180 cGy, the EBT3 data averaged among all strips give a medium increase of 70%, originated by the presence of the immobilization mask during the treatment.

Table 1: Median dose and associated error measured by EBT3 film strips numbers 20, 21, 22, 23, 24 and 25 positioned over the supraclavicular fossa. The medical prescription dose was 180 cGy.

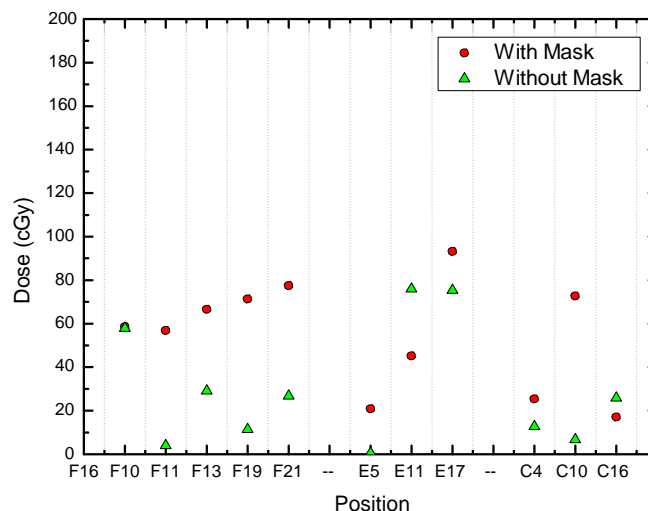
Treatment performed		Strip 16	Strip 17	Strip 18	Strip 20	Strip 21	Strip 22	Strip 23	Strip 24	Strip 25
with Thermoplastic Mask	Median									
	Dose (cGy)	125,77	142,61	134,4	123.35	138.79	141.19	119.07	124.80	133.85
	Error (cGy)	6,3	7,1	6,7	6.17	6.94	7.06	5.95	6.24	6.70
without Thermoplastic Mask	Median									
	Dose (cGy)	92,69	69,71	90,46	83.11	72.02	80.49	70.35	68.43	88.27
	Error (cGy)	4,63	3,49	4,52	4.16	3.60	4.02	3.52	3.42	4.41

3.3 Dose Evaluation using Pencil Beam Convolution (PBC)

The dose calculation algorithm used elsewhere for radiotherapeutic procedures, known as PBC (Pencil Beam Convolution), is an important Monte Carlo code based analytical method [16]. In this work we have performed computational evaluation of the dose delivered to the anthropomorphic phantom surface, in an attempt to check its accuracy when compared to two other dosimetric systems. In fact, the PBC accuracy, although largely cited in literature, may present significant failures, mainly for dose evaluation performed in small field treatments [16] as well as for distribution dose evaluation in electronic disequilibrium regions [17]. The dosimetric uncertainties observed in these regions, as for instances in the interface between tissues of different densities, seems somehow to be accepted by the international organisms that publish radiotherapeutic protocols. An example is the Task Group 53 AAPM (The American Association of Physicists in Medicine) recommendation that establishes as 40% the uncertainty limit in the build-up regions [7,18]. Nevertheless, hospitals and clinics all around the world make use of softwares that provide treatment planning systems based on the PBC method.

In Figure 6 we present the results of the PBC dose calculation analytical method dose evaluation, simulating an exposure of 180 cGy, with and without thermoplastic immobilizer. The results point to an important increase in the superficial dose when using immobilization masks, for most of the measured points. Although these results are in agreement with the previous results obtained using TLD chips and EBT3 film dosimeters, we remark the doses measured in electronic disequilibrium regions, unlike TLD and EBT3 dose evaluation, are inaccurate. Therefore we conclude that PBC dose calculation method could be of no reliability in radiotherapeutic procedures that make use of thermoplastic immobilizers.

Figure 7: Superficial dose deposition in the supraclavicular fossa anatomic region measured by PBC evaluations, after being exposure to 180 cGy, with and without thermoplastic immobilizer. The F, E and C letters refer to the slices over the phantom, each of them containing TLD chips positioned as shown in Fig. 3.



4 DISCUSSION

Thermoplastic masks used for patient positioning and immobilization have competed for the disappearance of the Skin Sparing effect in radiotherapy procedures, although they contribute decisively to a notable increase in the skin dose [4]. The magnitude of this phenomenon and its consequent clinical influence will clearly depend on some characteristics of the immobilizer material, such as thickness, and also on the characteristics of the incident beam, such as energy spectrum and obliquity. The dose surface effects measured in this work, provoked by the use of immobilization thermoplastic masks for head and neck radiotherapy treatments, also point out to an incontestable increase in the skin dose. This increase was detected by all three dosimetric systems utilized, i.e. TL dosimeters, EBT3 radiochromic films and Pencil Beam Convolution (PBC), although the PBC system has evaluated it with small differences related to the other two systems. TLD-100 and EBT3 films have found discrepant increasing doses, 33% and 70%, respectively, but both dosimetric systems have measured very similar doses with the presence of immobilization masks.

Finally, although this work has discussed about the skin dose increase arising by the use of thermoplastic immobilizers, it is fair to consider that the immobilization instrument is an essential tool for the radiotherapeutic treatments success, ensuring the reproducibility of the patient positioning. Without the immobilizer, the damages to the skin would be clearly greater than the dose superficialization effect. Thus, it is reasonable to think that the developing of new immobilization devices, which can maintain the benefits of the immobilization and simultaneously barely contribute to the dose superficialization in the patient, should be encouraged.

5 CONCLUSION

Thermoluminescent dosimeters (TLD-100), radiochromic films (EBT3) and the Pencil Beam Convolution method (PBC) have been used to evaluate the increase of dose surface provoked by immobilization masks in head and neck radiotherapy procedures. After irradiation with 180 cGy in the Clinac Linear Accelerator model 2100 C at 6 MV, TLD chips positioned in the surface of the SCF (supraclavicular fossa) anatomic region of an anthropomorphic phantom have detected an increase in the entrance skin dose around 33%. The EBT3 small 2.0 cm² strips data, averaged among all strips used, have encountered a medium increase of 70%. Although they have discrepant results, both dosimetric systems have measured very similar doses with the presence of immobilization masks. The well-known high spatial EBT-3 film resolution has provided additional information concerning to the limit between the high dose region (above 90 cGy) and the low dose region (20 cGy), which is attributed to the secondary collimator in the linear accelerator head. The PBC method has evaluated an important increase in the superficial dose when using immobilization masks, for most of the measured points. However, the entrance skin dose evaluated with the presence of immobilization masks were 50% smaller than that measured by TLD-100 and EBT3 dosimeters. Doses evaluated by the PBC method in electronic disequilibrium regions, unlike TLD and EBT3 dose evaluation, were inaccurate. Therefore we conclude that PBC dose calculation method could be of no reliability in radiotherapeutic procedures that make use of thermoplastic immobilizers.

6 ACKNOWLEDGEMENTS

We appreciate the Santa Casa de Misericórdia de Belo Horizonte for their support in this work. We appreciate Capes and CNPQ due to investment in the acquisition of some of the equipment used in this research.

7 REFERENCES

- [1] Chiu-Tsao, S.-T., & Chan, M. F. (2010). Evaluation of two-dimensional bolus effect of immobilization/support devices on skin doses: A radiochromic EBT film dosimetry study in phantom. *Medical Physics*, 37(7), 3611. <http://doi.org/10.1118/1.3439586>.
- [2] Carl, J., & Vestergaard, A. (2000). Skin damage probabilities using fixation materials in high-energy photon beams, 55.

- [3] Devic, S., Seuntjens, J., Abdel-Rahman, W., Evans, M., Olivares, M., Podgorsak, E. B., ... Soares, C. G. (2006). Accurate skin dose measurements using radiochromic film in clinical applications. *Medical Physics*, 33(4), 1116. <http://doi.org/10.1118/1.2179169>.
- [4] Lee N, Chuang C, Quivey JM, et al. Skin toxicity due to intensity-modulated radiotherapy for head-and-neck carcinoma. *Int J Radiat Oncol Biol Phys*. 2002;53(3):630–637.
- [5] Higgins DM, Whitehurst P, Morgan AM. The effect of carbon fiber couch inserts on surface dose with beam size variation. *Med Dosim*. 2001; 26(3):251–254..
- [6] Scott W. Hadley, Robin Kelly, and Kwok Lam. Effects of immobilization mask material on surface dose. *J. Appl. Clin. Medical Phys.*, V 6, No 1, winter 2005.
- [7] Ali I, Matthiesen C, Algan O, Thompson S, Bogardus C, Herman T, Ahmad S. Quantitative evaluation of increase in surface dose by immobilization thermoplastic masks and superficial dosimetry using Gafchromic EBT film and Monte Carlo calculations. *J Xray Sci Technol*. 2010;18(3):319-26. doi: 10.3233/XST-2010-0263.
- [8] Kelly, A. et al. Surface dosimetry for breast radiotherapy in the presence of immobilization cast material. *Physics in Medicine and Biology*, v. 56, n. 4, p. 1001–1013, 21 fev. 2011.
- [9] Almond, P. R. et al. AAPM ' s TG-51 protocol for clinical reference dosimetry of high-energy photon and electron beams. n. September, p. 1847–1870, 1999.
- [10] IAEA. TRS-398: Absorbed Dose Determination in External Beam Radiotherapy: An International Code of Practice for Dosimetry based on Standards of Absorbed Dose to Water. Vienna, Austria: [s.n.].
- [11] Baptista Neto, A.T. ; Meira-belo, L.C. ; Faria, L.O. . Improving analysis of radiochromic films. *Radiation Physics and Chemistry* v. 86, p. 136-139, 2013.
- [12] Storchi P, Woudstra E. Calculation of the absorbed dose distribution due to irregularly shaped photon beams using pencil beam kernels derived from basic beam data. *Phys Med Biol*. 1996;41(4):637-656.
- [13] Butson MJ, Cheung T, Yu PK. Radiochromic film: the new x-ray dosimetry and imaging tool. *Australas Phys Eng Sci Med*. 2004;27(4):230.
- [14] Soares CG. New developments in radiochromic film dosimetry. *Radiat Prot Dosimetry*. 2006;120(1-4):100–106.
- [15] Muench PJ, Meigooni AS, Nath R, McLaughlin WL. Photon energy dependence of the sensitivity of radiochromic film and comparison with silver halide film and LiF TLDs used for brachytherapy dosimetry. *Med Phys*. 1991;18(4):769–75.
- [16] Knöös, T., Ahnesjö, a, Nilsson, P., & Weber, L. (1995). Limitations of a pencil beam approach to photon dose calculations in lung tissue. *Physics in Medicine and Biology*, 40(9), 1411–20. <http://doi.org/10.1088/0031-9155/40/9/002>.
- [17] Krieger, T., & Sauer, O. a. (2005). Monte Carlo- versus pencil-beam-/collapsed-cone-dose calculation in a heterogeneous multi-layer phantom. *Physics in Medicine and Biology*, 50(5), 859–868. <http://doi.org/10.1088/0031-9155/50/5/010>.
- [18] Fraass, B., Doppke, K., Hunt, M., Kutcher, G., Starkschall, G., Stern, R., & Van Dyke, J. (1998). American Association of Physicists in Medicine Radiation Therapy Committee Task Group 53: quality assurance for clinical radiotherapy treatment planning. *Medical Physics*, 25(10), 1773–1829. <http://doi.org/10.1118/1.598373>.

MCNPX versus DOSXYZnrc in patient specific voxel-based phantom calculations

Banafsheh Zeinali-Rafsanjani^{a,b*}, Kamal Hadad^c, Mahdi Saeedi-Moghadam^a, Reza Jalli^a

^aMedical imaging research center, Shiraz University of medical sciences, Shiraz, Iran

^bNuclear medicine and molecular imaging research center, Shiraz university of medical sciences, Shiraz, Iran

^cNuclear engineering department, school of mechanical engineering, Shiraz University, Shiraz, Iran

Abstract. In this study a comparison between MCNPX and DOSXYZnrc dose calculation was performed. Unlike most of the previous studies which were used simple inhomogeneous and heterogeneous phantoms to compare different Monte Carlo photon/electron transport codes, in this study a patient specific voxel phantom was used, since voxel base phantom dosimetry have become more popular and important these days. A series of chest CT images contains of 100 frames of chest region of a male patient was used to make a voxel phantom in both codes. There was a $2.5 \times 2.4 \times 2.4$ cm³ tumor in middle lobe of right lung exposed to 6MV parallel beam. The CT images converted to a patient specific voxel phantom in MCNPX and DOSXYZnrc codes using our in-home developed voxel phantom generator and EGSnrc/CT Create respectively. In order to compare these Monte Carlo codes with together gross tumor volume (GTV) and organ at risks (OAR) doses and dose volume histograms (DVH) were calculated. Due to the differences between DOSXYZnrc and MCNPX in physical interaction data and differences in their computation of electron interactions, some discrepancies were observed. There was a dose overestimation by DOSXYZnrc. Moreover it was revealed that MCNPX isodoses can better follow the patient's anatomy in comparison to DOSXYZnrc. It was concluded that MCNPX has some advantages in comparison to DOSXYZnrc, but it is important to consider that for equal precision in voxel dosimetry calculation, DOSXYZnrc runs faster than MCNPX and it is a great advantage.

KEYWORDS: *simulation; voxel based phantom; MCNPX; DOSXYZnrc.*

1 INTRODUCTION

For many years different Monte Carlo codes have been used for medical modeling. The accuracy of calculation methods in different codes can determine the accuracy of modeling. Some studies compared these codes in order to find more accurate codes for special applications [1-7].

Unlike most of the previous studies which were used simple inhomogeneous and heterogeneous phantoms to compare different Monte Carlo photon/electron transport codes, in this study a patient specific voxel phantom was used, since voxel base phantom dosimetry have become more popular and important these days.

2 MATERIALS AND METHODS

A series of chest CT images contains of 100 frames of chest region of a male patient was used to make a voxel phantom in both codes. There was a $2.5 \times 2.4 \times 2.4$ cm³ tumor in middle lobe of right lung exposed to 6MV parallel beam. The CT images converted to a patient specific voxel phantom in MCNPX and DOSXYZnrc codes using our in-home developed voxel phantom generator and EGSnrc/CT Create respectively. In order to compare these Monte Carlo codes with together gross tumor volume (GTV) and organ at risks (OAR) doses and dose volume histograms (DVH) were calculated.

3 RESULTS

* Presenting author, e-mail: b.zeinali.r@gmail.com

Results of DOSXYZnrc and MCNPX were processed. Average dose of target, heart and spinal cord are illustrated in table 1.

Table 1: Average dose of target, heart and spinal cord. Doses are normalized to 50 Gy.

Anatomy	DOSXYZ Dose (Gy)	MCNPX Dose (Gy)
Target	57.055	54.048
Heart	0.147	0.144
Spinal cord	0.067	0.075

DVH of target and organ at risks are shown in figure 1 and 2.

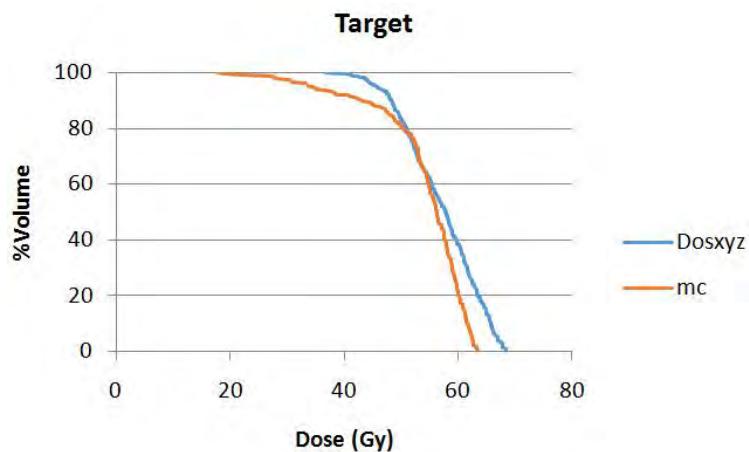


Figure 1: Dose volume histograms of target results from MCNPX and DOSXYZnrc.

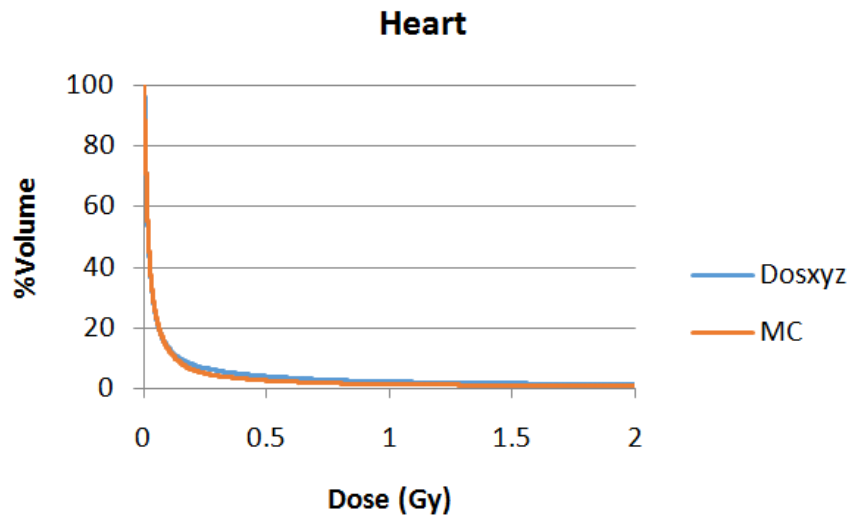


Figure 2: Dose volume histograms of heart results from MCNPX and DOSXYZnrc.

4 DISCUSSION AND CONCLUSION

Due to the differences between DOSXYZnrc and MCNPX in physical interaction data and differences in their computation of electron interactions, some discrepancies were observed (table 1 and figure 1 and 2). There was a dose overestimation by DOSXYZnrc (figure 1 and 2). It is concluded that for

problems that need more accurate calculations MCNPX is a better choice and for the problems that speed of calculation is more important than accuracy DOSXYZnrc is the better option.

5 REFERENCES

- [1] Chiavassa S., Lemosquet A., Aubineau-Laniece I., de Carlan L., Clairand I., Ferrer L., *et al.*, "Dosimetric comparison of Monte Carlo codes (EGS4, MCNP, MCNPX) considering external and internal exposures of the Zubal phantom to electron and photon sources," *Radiation Protection Dosimetry*, vol. 116, pp. 631–635, 2005.
- [2] O. Chibania and X. Allen Li, "Monte Carlo dose calculations in homogeneous media and at interfaces: A comparison between GEPTS, EGSnrc, MCNP, and measurements," *Medical Physics*, vol. 29, pp. 835-847, 2002.
- [3] R. Jeraj, P. J. Keall, and P. M. Ostwald, "Comparisons between MCNP, EGS4 and experiment for clinical electron beams," *Phys. Med. Biol.*, vol. 44, pp. 705–717, 1999.
- [4] E. Steinfelds, "Comparison of predictions by MCNP and EGSnrc of radiation dose imparted to various material targets by beams and small volumetric sources," in *Computational Medical Physics Working Group Workshop II*, University of Florida (UF), Gainesville, Florida USA on CD-ROM, American Nuclear Society, LaGrange Park, 2007.
- [5] M. Miften, M. Wiesmeyer, A. Kapur, and C. M. C. Ma, "Comparison of RTP dose distributions in heterogeneous phantoms with the BEAM Monte Carlo simulation system," *Journal of Applied Clinical Medical Physics*, vol. 2, pp. 21-31, 2001.
- [6] Li J. S., Pawlicki T., Deng J., Jiang S. B., Mok E., and Ma C. M., "Validation of a Monte Carlo dose calculation tool for radiotherapy treatment planning," *Phys. Med. Biol.*, vol. 45, pp. 2969–2985, 2000.
- [7] E. Steinfelds, "Comparison of predictions by MCNP and EGSnrc of radiation dose imparted to various material targets by beams and small volumetric sources," in *University of Florida (UF), Gainesville, American Nuclear Society*, 2007.

Justification of CT examinations *National surveys in Sweden*

Carl Bladh^{*}, Torsten Cederlund, Sven Richter

Swedish Radiation Safety Authority, SE-171 16 Stockholm, Sweden

Abstract. The Swedish Radiation Safety Authority (SSM) has run two projects to investigate the degree to which CT examinations in Sweden are justified. Referrals for all CT examinations of adult and paediatric patients performed in Sweden during one day and two weeks, respectively, were collected and evaluated retrospectively by a group of experienced physicians. Both of the studies indicated a high number of unjustified CT examinations, which suggests that clinical guidelines either are not used, or are suboptimal, or have not yet reached common acceptance and or knowledge.

KEYWORDS: *Justification, appropriate imaging, referral guidelines, paediatric examinations, CT.*

1 INTRODUCTION

Medical exposures account for the largest contribution to the dose to the population from man-made sources and are in a position to exceed exposures from natural sources. The main reason for this is that the number of CT examinations has increased in past decades.

In Sweden, CT examinations now account for 12% of all diagnostic examinations using X-rays and contribute up to 70% of the collective dose to the population from medical exposures [1]. If all examinations were justified, this would not be a problem. However, although justification is one of the basic principles of radiation protection, the extent to which X-ray examinations are justified is largely unknown. For this reason, the Swedish Radiation Safety Authority (SSM) has run two projects to investigate the degree to which CT examinations are justified.

2 MATERIAL AND METHOD

The main object of the studies was to investigate the degree of justification for CT examinations. In the first study [2], referrals for all CT examinations performed during one day, 2,435 in total, were collected and evaluated retrospectively by a group of experienced physicians (both radiologists and clinicians). The evaluation included referral quality and the degree of justification. The second study [3] comprised all referrals (CT, MRI, US), 3,149 in total (of which 628 were for CT), from paediatric examinations of children aged 0-15 performed over the course of two weeks. These referral were evaluated by a group of experienced paediatric radiologists.

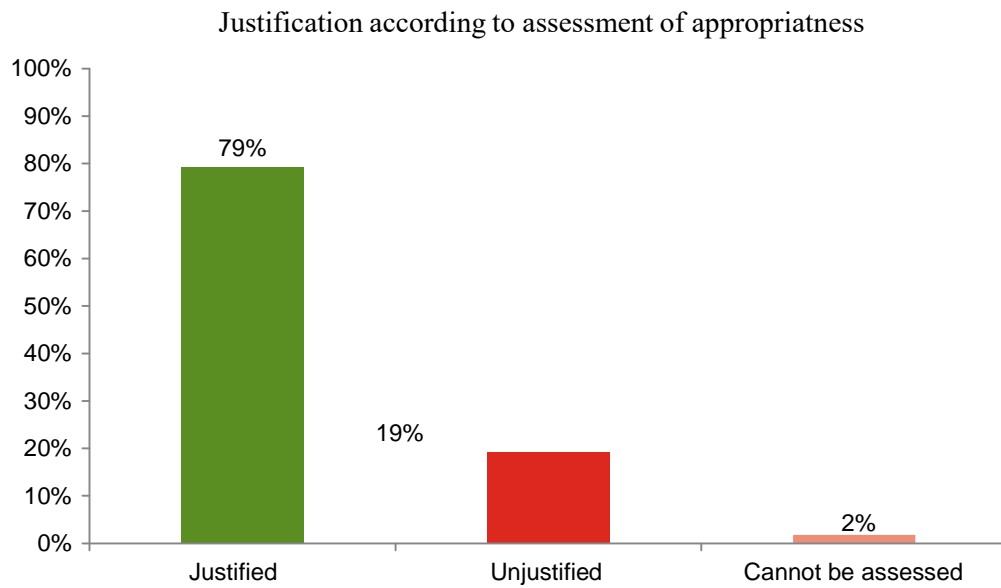
3 RESULTS

3.1 THE FIRST STUDY

The first study showed that about 93% of the referrals contained adequate or relatively adequate information. Of the examinations, 79% were considered justified, 19% unjustified and for 2% of the examinations, it was not possible to judge if the examination was justified or unjustified (Fig. 1). The degree of justification varied strongly between the organs examined, varied moderately by prescriber affiliation, and varied slightly between geographical regions. The study also indicated a lower degree of justification for younger patients.

* Presenting author, e-mail: carl.bladh@ssm.se

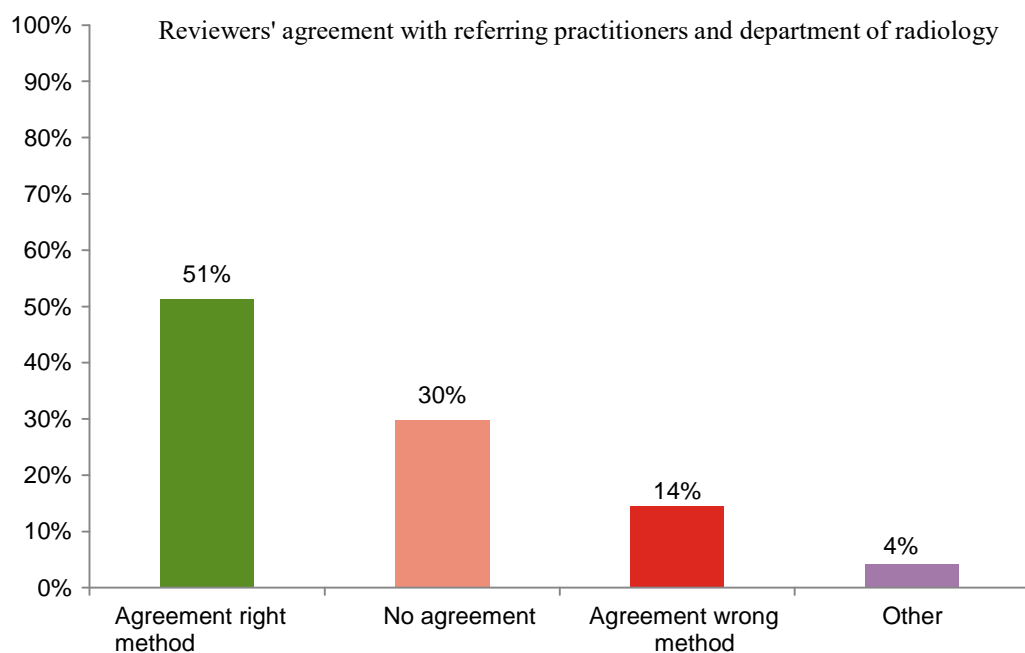
Figure 1: Justification according to assessment of appropriateness in per cent of the total number of evaluations.



3.2 THE SECOND STUDY

The second study drew the conclusion that the information in 96% of the referrals was judged to be adequate or relatively adequate. Radiological examinations were judged as justified or probably justified for 96% of all examinations, and as probably unjustified for 4% of the examinations. The observers agreed on the choice of examination method, between the observers as well as with the requested and performed method, in 51% of the requested CT examinations (Fig. 2). The observers agreed among themselves on preferring another examination method than the one requested, and other than the performed method, in 14% of the CT examinations. The observers disagreed among themselves and at least one observer agreed on the requested choice of method in 30% of the CT examinations.

Figure 2: The reviewers' agreement with referring practitioners and radiologists as regards choice of the method option CT



4 DISCUSSION

Both studies indicate a high level of unjustified CT examinations. The fact that the reviewers do not agree on justification for 21% (study 1) and 49% (study 2) of the examinations indicates that clinical guidelines either are not used, or are suboptimal, or have not yet reached common acceptance. SSM has promoted use of the translated version of the European referral guidelines for imaging (RP 118) [4] since 2001. However, the guidelines have not been updated since 2003 and are now considered to be outdated. SSM has, on the basis of inspections and cooperation with the profession, concluded that it is difficult to produce paper copies of the guidelines, available to the referring practitioners for use on a daily basis. As a result, the guidelines have not become the useful tool for imaging referral they were intended to be. Both of the present studies support the need for a new approach for ensuring that only justified examinations are prescribed and performed.

If unjustified examinations could be avoided the population dose from medical exposure in Sweden would decrease by approximately 800 manSv, which is equivalent to 14% of the total population dose from medical exposure. This would also shorten waiting times for examinations as well as lower the cost of diagnostic imaging.

5 CHALLENGES

It is of substantial importance to establish consensus on the most appropriate imaging investigation for a given diagnostic or imaging issue and to ensure that referral guidelines for medical imaging are available to referring practitioners. For this reason, SSM launched a project in 2016 to establish a clinical decision support (CDS) system to improve the degree of justification. The CDS system will be integrated in electronic medical journals and electronic referral systems as a tool to guide referring physicians in selecting correct examinations for their patients.

6 ACKNOWLEDGEMENTS

Both studies were financed through SSM's research funding. SSM expresses its gratitude to Bengt Isberg, Håkan Jorulf and Ulla Svahn for designing and performing the studies, and thanks all participating radiologists and clinicians for their efforts.

7 REFERENCES

- [1] European Commission, 2014. Radiation Protection N° 180. Medical Radiation Exposure of the European Population. Part 1/2. Contract ENER/2010/NUCL/SI2.581237. European Union, Luxembourg.
- [2] Almén A., Leitz W., Richter S., 2009. National survey on justification of CT-examinations in Sweden. Swedish Radiation Safety Authority, Stockholm.
- [3] Jorulf, H., Isberg, B., Svahn, U., 2016, Radiological examinations of children: a study of method options. Swedish Radiation Safety Authority, Stockholm
- [4] European Commission, 2001. Radiation Protection 118. Referral guidelines for imaging. European Union, Luxembourg.

The transposition and the practical implementation of the Council Directive 2013/59/Euratom in the medical field in Romania

Constantin Milu

Expert Pro-Rad srl, Bucharest, Romania

Abstract. In the Official Journal of the European Union from 17 January 2014 it was published the Council Directive 2013/59/Euratom of 5 December 2013 laying down basic safety standards for protection against the dangers arising from exposure to ionizing radiation, and repealing Directive 89/618/Euratom, 90/641/Euratom, 96/43/Euratom and 2003/122/Euratom, according to the Recommendations of the International Commission on Radiological Protection (ICRP), published in 2007 as ICRP Report No.103. As a full member of the European Union and with a support from the International Atomic Energy Agency (IAEA), Romania already started in 2015 several activities related to the transposition and the practical implementation in the country of the new international standards and recommendations. Some preliminary results in the medical field are presented.

1 INTRODUCTION

In the Official Journal of the European Union from 17 January 2014 it was published the *Council Directive 2013/59/Euratom of 5 December 2013 laying down basic safety standards for protection against the dangers arising from exposure to ionizing radiation, and repealing Directives 89/618/Euratom, 90/641/Euratom, 97/43/Euratom and 2003/122/Euratom* (1). Also in 2014 has been published by International Atomic Energy Agency (IAEA) the safety report on the *International basic safety standards (International BSSs)* (Ref.2). Both the revised Euratom Basic Safety Standards Directive as well as the International BSSs are based on the Recommendations of the International Commission on Radiological Protection (ICRP), published in 2007 as ICRP Report No.103 (Ref.3).

As a full member of the European Union, Romania already started in 2015 the activities related to the transposition and the practical implementation of the new international standards and recommendations, with a support from IAEA.

2 METHOD

During the early phase, an important task for the Romanian Nuclear Regulatory Authority (CNCAN) was the establishment of the national approach for the transposition process of the Revised European Basic Standards.

Regarding the development of radiological safety and of the radiation protection regulations in medicine, two important CNCAN decisions should be mentioned:

- to repeal the different old regulations and to elaborate a new single document (The new Fundamental Norms for Radiological Safety – “new NFSR”), representing the transposition of the Directive 2013/59/Euratom and including several main and new safety requirements in medicine;
- to keep three of old specific “Norms”, which may be very useful in the near future as parts of the implementation process, but only after their strong modification, regarding title, purpose, definitions, content, formulations, requirements, etc, in agreement with the new international documents and the new planned NFSR.

* constantinmilu@upcmail.ro

The three old specific regulations are:

- NSR - 11 – Radiological Safety Norms in Diagnostic and Interventional Radiology Practices;
- NSR – 12 – Radiological Safety Norms in Radiotherapy Practice, and
- NSR – 14 – Radiological Safety Norms in Nuclear Medicine Practice.

The elaboration of the new radiation safety regulation in medicine in Romania was preceded by a large action, including several technical meetings and discussions for:

- identification of the new provisions in the revised Euratom Directive;
- identification of principal gaps in the current Romanian regulation;
- identification of responsibilities for different Romanian competent authorities which should be involved and identification of practical regulatory problems;
- detection of main issues in medicine and identification of good practices;
- identification of topical issues which may further require a detailed attention, action and/or activities in the near future.

According to 2015 CNCAN report, the situation of the number of radiological installations used in medicine in Romania is given in Table 1.

Table 1: Number of installations/laboratories in diagnostic and interventional radiology, dental radiography, nuclear medicine and radiotherapy in Romania (according to 2015 Report CNCAN).

DIAGNOSTIC AND INTERVENTIONAL RADIOLOGY	No.	DENTAL RADIOGRAPHY	No.	NUCLEAR MEDICINE	No.	RADIOTHERAPY	No.
- CT	369	- Intraoral	1835	- In-vivo diagnostic labs	31	- Orthovoltage installations	37
- Mammography	264	- Panoramic	681	- Gamma cameras	37	- LINACs	25
- Bone densitometry	208			- PET/CT units	10	- Co-60 units	10
- Mobile	733			- SPECT/CT	3	- Gamma Knife	1
- Angiography	95			- Scintigraphy	4	- Brachytherapy labs	13
- Conventional fluoroscopy and radiography	1642			- Iod capture	4		
				- In-vitro diagnostic labs	?		
				- Therapy	?		
TOTAL	3311	TOTAL	2516	TOTAL	89+	TOTAL	86

3 RESULTS

3.1. Identification of the new provisions in the revised Directive

In 2014, the Members of the Group of Experts referred to in Article 31 of the Euratom Treaty and of the

Working Party MEDMED have identified a useful list of new provisions in the Directive 2013/59/Euratom, regarding radiological safety in medicine:

- New set of definitions and concepts.
- Increased role of justification principle and consideration of occupational doses in justification and optimization.
- New requirements in relation to exposure of asymptomatic individuals exposed as part of an approved health screening program.
- Use of diagnostic reference levels (including interventional) and regular review.
- Interventional radiology new defined, reflecting the importance of this modality in relation to staff and patient doses.

- Recognition and involvement of the Medical Physics Expert (MPE) and his new role in the modern imaging.
- Definition and recognition of the Radiation Protection Expert (RPE) and of the Radiation Protection Officer (RPO).
- Dosimetric information in all diagnostic system and transfer to the patient report.
- Dosimetric information mandatory for all interventional and CT procedures.
- Prevention, registry and analysis of all accidental or unintended exposures of patients.
- Population dose evaluation taking into account the age distribution and the gender.
- New dose limit for lens of the eyes.
- Old medico-legal exposures removed from medical chapter and a new set of requirements developed for non-medical imaging exposures.
- New criteria of acceptability for equipment.
- Enlarged practical use of the dose constraint concept.
- Education and training dealt with as part of more general requirements in medicine.

3.2 The identification of principal gaps in the current radiation safety regulation in medicine in Romania

1. All above presented new provisions in medicine, according to the Directive 2013/59/Euratom should be included and met in the new Romanian regulation in medicine.
2. The “Titles” of the new Romanian regulation should take into consideration the use of the new term “Planned Exposure situation”, which has to replace the old term “Practice” .
Consequently, the new titles of the three above mentioned regulations should be:
 - GSR - 11 – Radiological Safety Guidelines in Diagnostic and Interventional Radiology Planned Exposure Situation;
 - GSR – 12 – Radiological Safety Guidelines in Radiotherapy Planned Exposure Situation, and
 - GSR – 14 – Radiological Safety Guidelines in Nuclear Medicine Planned Exposure Situation.
3. The term “Guidelines” (or “Regulation”) was recommended, instead of “Norms”, to avoid confusion with the “Fundamental Norms”, which remain the basic national safety standards for protection against the dangers arising from exposure to ionizing radiation.
4. The term “SHALL” shall be used in all formulations of all requirements, showing a stronger (mandatory) requirement.
5. The new definitions shall be used uniform, in all documents, special attention regarding to the following definitions:

Table 2:

NEW DEFINITIONS	Current use in Romanian regulation
- “Planned exposure situation”	- “Practice”
- “Emergency exposure situation”	- “Radiological accident”
- “Exposed worker”	- “Occupational exposed worker”, “Radiation worker”
- “Referrer”, which replaced “prescriber”	- “Ordering”, “Ordonateur”
- “Practitioner”	- “Medical practitioner”
- “Medical radiological installation”	- “Radiological laboratory”
- “Carers and comforters”	- “Helper”
- “Radiation Protection Expert”, which replaced “Qualified expert”	- “Qualified Expert in Radiological Protection”
- “Radiation Protection Officer”	- “Responsible for radiological protection”, “Radiation safety responsible”
- “Medical Physics Expert”	- “Medical physicist”, “Expert in radiation physics”
- “Sealed source”	- “Closed source”
- “Licence”	- “Authorization”
- “undertaking”	- “authorization holder”, “legal person”
- “unintended exposure”	- “incident”
- “non-medical imaging exposure”	- A NEW DEFINITION
- “occupational health service”	- A NEW DEFINITION

3.3. Specific topics

3.3.1 Licence

The licence in medicine is now a complicated procedure. A new guidelines on authorization procedures need be elaborated soon, applying the graded approach to regulatory control (notification, registration, licence) and deciding some exception from authorization (ex., for possession or for renting a radiological equipment, the present Authorization Safety Authorization – ASR, for European products, a.s.o.).

These new guidelines on authorization shall be used during the final elaboration of new specific regulations GSR-11, GSR-12 and GSR-14.

3.3.2 Medical Physics Expert

The reference in NSR-11, NSR-12 and NSR-14 on the Medical Physics Expert is based on an old specific CNCAN norm regarding the medical physics expert (published in 2006).

In 2014, the European Commission published as Radiation Protection No.174 the “European Guidelines on Medical Physics Expert” (Ref.4), including a clear and enhanced role of the medical physics expert (MPE) in medicine, qualification and curriculum frameworks for the MPE, the recognition of the MPE and the MPE staffing levels in Europe.

Due to mobility of the MPE throughout the Europe, shall be important to adopt this guidelines in Romania too. In such case, several statements regarding the MPE in the current legislation shall be reformulated accordingly, in the final phase of its elaboration.

3.3.3 *Careers and comforters*

In NSR-11, NSR-12 and NSR-14 there are given some general requirements regarding individuals knowingly and willingly incurring an exposure to ionizing radiation by helping, other than as part of their occupation, in the support and comfort of individuals undergoing or having undergone medical exposure. The new regulation GSR-11, GSR-12 and GSR-14 have to use the new definitions from Directive and to clarify the procedures regarding :

- “selection” of carers and comforters (exposed workers and pregnant women are not accepted !);
- protection of carers and comforters using appropriate facilities, special provided by undertaking;
- dose evaluation of carers and comforters (using electronic and direct reading detectors, special provided for carers and comforters !);
- dose constraints applied (usually, 5mSv/duration of the procedure);
- registration of the received exposure by carers and comforters involved as their medical exposure.

The “dose constraint”, here or in any other requirement, shall not be considered as a “dose limit”. It is only a tool in the optimization of the radiation protection.

3.3.4 *Acceptability of medical radiological equipment*

The Council Directive 2013/59/Euratom prescribes a number of measures to ensure that medical exposures are delivered under appropriate conditions. It required, among other things:

- acceptance testing of new equipment,
- identification of criteria of acceptability for equipment safety and performance throughout its life, and
- establishment of quality assurance programmes.

In Radiation Protection No.162 (2012), the European Commission established new “Criteria for acceptability of medical radiological equipment used in diagnostic radiology, nuclear medicine and radiotherapy” (Ref.5) , which addresses the second of these (criteria of acceptability). New definitions and concepts are included . The criteria for acceptability (for clinical use!) are applied and they are divided into two categories “qualitative criteria” and “quantitative” criteria, also known as “suspension levels” (for clinical use!).

The qualitative criteria derive from legislation or widely accepted norms for good practice. The suspension levels, on the other hand, rely on measurements. They provide numerical limits for acceptable performance in respect of the parameters identified for each of the equipment types (diagnostic radiology, nuclear medicine and radiotherapy).

The report has a general part and three separated technical sections, including suspension levels for three categories of equipment:

- Section 2 – Diagnostic Radiology;
- Section 3 – Nuclear Medicine;
- Section 3 – Radiotherapy.

In conclusion, the report may be split in three individual parts and each of them added to the relevant “Norm” (NSR-11, NSR-12 and NSR-14) or adopted as a single document, within the implementation plan of the Directive.

3.3.5 Diagnostic Reference Levels

Diagnostic Reference Levels (DRLs) means dose levels in medical radiodiagnostic or interventional radiology practice, or, in the case of radio-pharmaceuticals, level of activity, for typical examination for group of standard-sized patients or standard phantoms for broadly defined types of equipment.

In the new “Norms” (GSR-11 and GSR-12) the new definition mentioned above has to be used, plus:
- some more and clear technical recommendations for the implementation of the DRLs concept;
- new values, particularly for interventional radiology and for different age groups for children.

For this purpose, some recent documents issued by European Commission may be useful (Ref.6 and the final report of the EC Project PiDRL – Diagnostic Reference Levels for Paediatric Imaging).

Of course, the Regulatory Authority (CNCAN) has to encourage the Ministry of Health and the Romanian Professional Associations in Radiology and in Nuclear Medicine in the developing of National Diagnostic Reference Levels (NDRLs) and for their implication in the implementation of the new NDRLs.

3.3.6 Accidental and unintended medical exposure

The accidental and unintended medical exposure are a source of continuing concern. Apart the need to use the new definitions (instead of “accidents and incidents”!), the new Romanian regulation on radiological safety in medicine has to increase the role of the competent authority in radiation protection (CNCAN) to address the *prevention* of accidental and unintended medical exposure and the follow-up in case of their occurrence. The role of quality assurance management, as part of a Radiation Protection Programme (RPP), including a study of risks in radiotherapy, to avoid such incidents should be emphasized, and recording, reporting, analysis and corrective action be required in such cases.

A very recent (2015) EC- Guidelines on risk management in external beam radiotherapy (Ref. 8) is very useful for this purpose.

3.3.7 Other competent authorities

According to the Directive 2013/59/Euratom “competent authority” means an authority or system of authorities designated by Member States as having legal authority for the purpose of this Directive. CNCAN is the competent authority for radiation protection in Romania.

Other identified competent authorities regarding radiological safety in medicine are: MS – Ministry of Health

ANM – National Agency for Pharmaceuticals

MAI – Ministry for Internal Affairs

MT – Ministry for Transportation

ME - Ministry of Education

In the new regulation, the role and specific responsibilities of other competent authorities shall be better clarified, and the ensuring that the technical and practical aspects of radiation safety in medicine are managed with a high level of competence need to be enhanced.

Radiation protection education and training shall start at the entry level to the medical, dental and other healthcare professional schools. The Euratom BSS Directive states that “Member State shall encourage the introduction of a course on radiation protection in the *basic curriculum* of medical and dental schools”. Radiation protection courses should, however, have a different orientation and content for medical and dental students. Radiation protection courses for medical students should include knowledge needed by a referring physician. The Ministry of Education has here an important role.

The Romanian National Agency for Pharmaceuticals (ANM) has to have an increased role in the new regulation in radiological safety in medicine, particularly regarding the recognition of a radiological equipment as a “Medical Device” (according to the EC Directive on Medical Devices) and on authorization of the new radiopharmaceuticals.

4 CONCLUSIONS

After a good start, many problems still have to be solved in Romania for transposition and implementation of the Council Directive 2013/59/Euratom in the medical field.

According to Chapter X - final provisions and Article 106(1) - transposition "*Member State shall bring into force the laws, regulations and administrative provisions necessary to comply with this Directive by 6 February 2018*".

5 REFERENCES

- [1] The Council Directive 2013/59/Euratom of 5 December 2013 laying down basic safety standards for protection against the dangers arising from exposure to ionizing radiation, and repealing Directives 89/618/Euratom, 90/641/Euratom, 96/43/Euratom and 2003/122/Euratom, The Official Journal of the European Union, 17 January 2014.
- [2] Radiation protection and safety of radiation sources: International basic safety standards, General Safety Requirements Part 3, No. GSR Part 3, STI/PUB/1578, Vienna – International Atomic Energy Agency, 2014.
- [3] The International Commission on Radiological Protection (ICRP), International Recommendations of the ICRP, ICRP Report No.103, 2007.
- [4] European Guidelines on Medical Physics Expert, European Commission, Radiation Protection No.174, 2014.
- [5] Criteria for acceptability of medical radiological equipment used in diagnostic radiology, nuclear medicine and radiotherapy, European Commission, Radiation Protection No.162, 2012.
- [6] Referral Guidelines for Medical Imaging Availability and Use in the European Union, European Commission, Radiation Protection No.178, 2014.
- [7] Guidelines on Radiation Protection Education and Training of Medical Professionals in the European Union, European Commission, Radiation Protection No.175, 2014.
- [8] General guidelines on risk management in external beam radiotherapy, European Commission, Radiation Protection No.181, 2015.

Level 2 justification is now part of the national system for introduction of new health technologies within the specialist health service in Norway

Eva G. Friberg*, Reidun Silkoset, Ingrid E. Heikkilä, Jan F. Unhjem

Norwegian Radiation Protection Authority, P.O. Box 55, N-1332 Østerås, Norway.

Abstract. *Introduction:* Level 2 justification must be ensured before new methods and practices in medical exposure are introduced in general clinical practice by weighting radiation detriments against clinical benefit, according to the national radiation protection regulations. It is most efficient that the process of justification is an integrated part of the total risk-benefit evaluation, and therefor implemented in already established systems for health technology assessments (HTAs). When the Ministry of Health (MoH) introduced a national system for introduction of new health technologies based on HTAs in 2013, the Norwegian Radiation Protection Authority (NRPA) identified the possibility to implement level 2 justification in this system. NRPA became a member of the national system in 2014. *National System for introduction of new health technologies:* The national system for introduction of new health technologies is based on four components: Alerts, evaluation, decision and implementation. The evaluation is based on international principles of HTAs where safety and clinical effect, cost-effectiveness, ethical, organizational, social and juridical aspects are topics under consideration. There are three categories of HTA: Full-HTA and Rapid-HTA performed at a national level and Mini-HTA performed at a local level. The national system constitute a standardized and transparent process for the introduction of new methods and ensure for a national coordination of all the four components and all the involved stakeholders. *Conclusion:* Integration of radiation detriment in total risk-benefit evaluation of HTAs is an efficient way to ensure level 2 justification in medical exposure. A national coordinated system for introduction of new health technologies ensures that NRPA is properly involved in all processes of the system and all categories of HTAs. Cooperation between radiation protection authorities and HTA competent authorities, both at national and European level, may contribute to strengthen the awareness on level 2 justification among multiple stakeholders.

KEYWORDS: *level 2 justification, generic justification, health technology assessment, risk-benefit evaluation, radiation detriment, clinical effect.*

1 INTRODUCTION

Justification is one of the core principles in the international framework for radiation protection provided by the International Commission on Radiological Protection (ICRP) and is done by weighting the radiation detriments against clinical benefit [1, 2]. The overall aim of medical exposure is to do more good than harm to the patient and the principle of justification applies at three levels: 1) general, 2) generic for particular techniques and 3) for individual patients undergoing a particular examination. Level 1 justification is no longer being evaluated within medical exposure, since the net benefit is identified to outweigh the radiation detriment in general. However, level 2 and 3 of the justification process is crucial within medical exposure and has been part of the European and international radiation protection regulatory framework for many years [3, 4]. The three levels of justification were introduced in the national radiation protection regulations in 2004 [5]. In spite of this, many countries including Norway, has not succeeded to properly implement level 2 justification at a national coordinated manner. The importance of a proper implementation of level 2 justification has been further strengthened in the newly revised European and international Basic Safety Standards (BSS) [6, 7] and the European Commission has identified the need for increased awareness of the challenges of generic justification and suggests that Member State cooperate on this issue [8].

Medical exposure is facing a rapid technological development and new radiopharmaceuticals, equipment, methods and practices involving radiation are constantly introduced to the market. Before they can be introduced into general clinical practice, their generic justification must be ensured. To be most efficient, the radiation detriment should not be handled separately, but be integrated in the total risk-benefit evaluation of the method already done in HTAs. When the Ministry of Health (MoH) introduced a national system for introduction of new health technologies within the specialist health service based on HTAs in 2013 [9], the Norwegian Radiation Protection Authority (NRPA) identified

* Presenting author, e-mail: eva.friberg@nrpa.no

the possibilities to implement the process of level 2 justification in this system. After approaching the secretariat of the national system, presenting our needs and possible solutions, the MoH acknowledged the need for integrating level 2 justification and NRPA became a member of the national system in 2014.

2 NATIONAL SYSTEM FOR INTRODUCTION OF NEW HEALTH TECHNOLOGIES

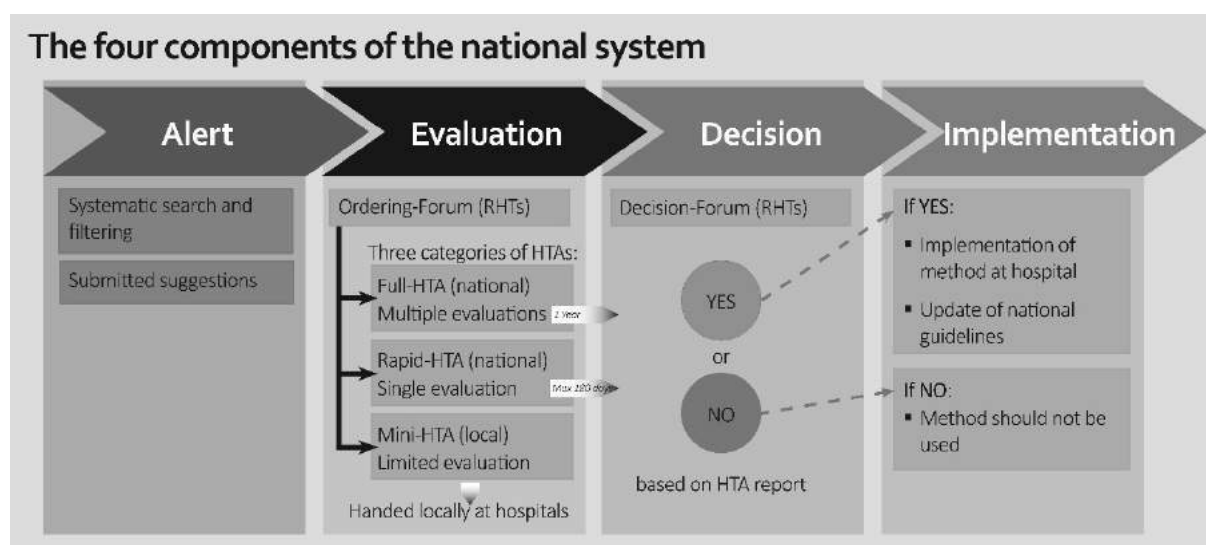
2.1 Background and purpose

Varying practice for evaluation of new health technologies and different processes for decision-making among the health regions in Norway raised the need for a national coordinated, standardized and transparent process for evaluation and decision before new methods were introduced or phased-out of clinical practice. The main purpose with the new national system is to ensure that patients get fast and equal access to new health technologies showing a safe, cost-effective and evidence based clinical effect and to avoid the introduction of unsafe and non-effective methods.

2.2 Structure and members

The national system for introduction of new health technologies (Nye Metoder) is based on four successive processes: Alerts of new methods, evaluation of methods, decision-making and in the end the implementation phase. All four processes and involved stakeholders are coordinated at a national level. The definition of new health technologies or methods within this system is broad and cover all actions to prevent, diagnose and treat diseases. In addition, actions related to rehabilitation and organizing of health services are included. The system is owned by the MoH and administrated by the secretariat, which is placed at the Norwegian Directorate of Health (NDH). Operational members of the system is the Norwegian Medicine Agency (NMA), The Norwegian Institute of Public Health (NIPH), the Norwegian Radiation Protection Authority (NRPA) and the four Regional Hospital Trusts (RHTs) in Norway. The national system has its own web-page (www.nyemetoder.no) where all method evaluations and decisions are published. A flow chart of the national system illustrating the four different processes is given in Figure 1. The secretariat is now working with the development of a monitoring function to be able to evaluation if new methods are implemented according to the decisions made within the system.

Figure 1: A flow chart of the four processes in the national system for introduction of new health technologies.



Alerts of new methods

The purpose of the alert function of the national system is a systematic search for new methods (horizon scanning) and subsequent filtering to identify and prioritize those new methods that is suitable for method evaluation in Norway. All method alerts are published in a database (www.mednytt.no) and is publicly available. In addition, all stakeholders' can submit suggestions for new methods to be evaluated in the system.

2.2.1 Evaluation of methods

Evaluation of methods is a systematic evaluation of available research on safety and clinical effect of the method. The evaluation also identifies the consequences associated with the decision to implement the method by evaluation of cost-effectiveness, ethical, social, organizational and juridical aspects and is based on international principles of HTAs. The PICO framework is central to form the clinical or health care related questions to be answered by the HTA. The PICO acronyms stand for: P – population, I – intervention, C – comparator, O – outcome. There are three categories of HTAs in the system: Mini-HTA, Rapid-HTA and Full-HTA. A Mini-HTA is a limited evaluation carried out locally at the hospitals prior to implementation of new health technologies. The evaluation is performed by filling out a form, and all Mini-HTAs are published in a database (www.nyemetoder.no) and are in this way made easily available for other hospitals to reduce duplication of work. A Rapid-HTA is a single evaluation of a method performed at a national level. In a Rapid-HTA, the manufacturers that provide the new method, are responsible for delivering a documentation package covering the aspects of an HTA, which at the end is evaluated by a competent authority. Rapid-HTAs of new pharmaceuticals and medical devices are performed by the NMA and the NIPH, respectively. A Rapid-HTA has to be finalized within 180 days after the documentation package has been received and found completed by the competent authority. If there is more than one manufacturer providing the new method under consideration, each manufacturer has to provide a documentation package to be allowed to introduce their product in Norway. A Full-HTA is a comprehensive national evaluation of new methods and is often used to compare alternative methods against each other within a treatment area (so called comparative effectiveness). A full-HTA is always performed by the NIPH, who collects all necessary documentation. The time frame of a Full-HTA is one year. NRPA assist both the NMA and the NIPH in national evaluations (Rapid- and Full-HTAs) of radiopharmaceuticals and medical devices, methods and practices involving radiation. It is the Ordering-Forum, constituted by representatives from all the four RHTs, who order evaluation of methods based on method alerts or received suggestions for method evaluations. Their decision is seen in relation to the actually need in the national health care system. New methods that are under evaluation cannot be used by the hospitals. An overview of the three categories of HTAs is given in Figure 2.

Figure 2: Overview of the three categories of HTAs that are included in the national system for introduction of new health technologies in Norway.

<p>Mini-HTA (1-3 weeks)</p>	<ul style="list-style-type: none"> • Local, limited evaluation of a method • Carried out by experts in the hospitals (filling out a form) • Decisions for implementation is taken locally by the hospitals
<p>Rapid-HTA (180 days)</p>	<ul style="list-style-type: none"> • National, single evaluation of a method • Manufacturers provide necessary documentation (according to template) • Carried out by NMA for pharmaceuticals and by NIPH for medical devices • NRPA assist when methods involv radiation • Decisions for implementation is taken nationally by the Decision-Forum
<p>Full-HTA (1 year)</p>	<ul style="list-style-type: none"> • National, comprehensive evaluation of methods, often comparative effectiveness of methods within a treatment area • Carried out by NIPH, who provide all necessary documentation • NRPA assist when methods involv radiation • Decisions for implementation is taken nationally by the Decision-Forum

2.2.2 *The decision-making process*

It is the Decision-Forum, constituted of the general directors of the four RHTs, who take the final consensus based decision to implement or phase-out a method based on the results and conclusions given in the performed HTA report seen in relation to overall national criteria for prioritizing within health care. After the competent body has finalized the HTA report, it is evaluated and approved by the Ordering-Forum to ensure its quality and completeness before it is submitted to the Decision-Forum as a basis for final decision. Decisions on implementation of new methods based on Mini-HTA are taken locally by the hospital trusts (HTs). It is the responsibility for the RHTs to ensure that the HTs has sufficient competence in carrying out Mini-HTA evaluations. However, some regional and national help functions to assist the HTs in HTAs are under development.

2.2.3 *The implementation process*

When a new pharmaceutical, new medical device, method or practice is decided to be implemented or phased-out within the specialist health service, national guidelines will be updated if necessary. This process is coordinated by the secretariat of the national system. On the other hand, if the Decision-Forum conclude not to implement the new method, it cannot be taken into clinical use by the hospitals. However, the method can be used in clinical studies to obtain stronger evidence based knowledge if relevant and appropriate.

3 DISCUSSION

3.1 Level 2 justification and HTAs at a national level

The implementation of level 2 justification in existing systems and processes for HTAs can be challenging and is not always straightforward. Justification of new methods and practices is ensured if the evaluation based on weighting the radiation detriment (to both patient and staff) against clinical benefit demonstrate a net benefit to the patient and society. However, radiation detriment should be an integrated part of the total risk-benefit evaluation of a method, since it is inappropriate to be treated in a separate evaluation. The rationale behind this statement is to include all the relevant factors that may influence the final decision whether to implement a new method or not in one process. To ensure a proper evaluation of the radiation detriment, as part of the total risk evaluation, it is important to include experts with sufficient competence in radiation protection in the evaluation process in all three categories of HTAs. Medical physics experts and radiation protection experts are identified as suitable experts with competence in radiation protection in a clinical setting and a board of national experts may be established to support national HTAs. The national radiation protection authority should be responsible for, or at least involved, in the establishment of such a national expert group.

One of the most important, but also challenging tasks in setting up a national HTA system is to establish precise criteria for when there is a need to perform an HTA on a new method or practice and at what level it should be performed (Mini-, Rapid- or Full-HTA). This is particularly challenging for the introduction of new medical devices and even more complicated for the introduction of new practises using equipment already available in the hospitals. Criteria to distinguish between a new method and a modification of a method not considered as a new method has to be developed. Inclusion criteria for new methods to enter the system can be based on the importance of the method, the risk associated with the method (risk classification systems) and the level of available evidence based consensus. However, it is important to find the right balance between when a HTA is appropriate and necessary and when it will not gain any valuable input to the final decision-making process. It is important also to ensure that the national HTA system is not being an obstacle to innovation and fast access to new methods. In the latter, available resources and timeframes for HTAs is key factors. From a radiation protection point of view, it is anticipated that Mini-HTAs will be sufficient in most cases to demonstrate and document level 2 justification. However, the need for a cost-effectiveness evaluation performed at a national level can result in the ordering of a Rapid- or Full-HTA of the method. Examples of methods that have been ordered for national evaluations is: renal nerve ablation for

resistant hypertension, tomosynthesis in mammography (screening and clinical), use of mobile CT in ambulance for early diagnostic and treatment of stroke.

Further, it is important to stress the need for separate conclusions on the risk-benefit evaluation and the cost-effectiveness evaluation in the HTA reports. In this way the HTA-report support the decision-making processes taken by different competent authorities and stakeholders. From a radiation protection point of view, the conclusion on risk-benefit is the most important input for the level 2 justification, while from a health economical point of view, the conclusion on cost-effectiveness will be of highest interest. Another aspect to keep in mind is that the documentation available on risk assessment and clinical evaluation provided by the manufacturer to declare conformity with the European Medical Device Directive [10] to obtain CE-marking is not necessary sufficient to demonstrate level 2 justification. Radiation detriment is closely related to the use of medical equipment and the competence and training of the staff operating the equipment. Such factors may result in the need for further risk evaluations to identify the actual radiation detriment associated with the intended use of the equipment.

Implementation of level 2 justification is not always sufficient to ensure proper justification of new methods alone. However, an established link between HTAs and level 2 justification and the responsible authorities (HTA competent authorities and radiation protection authorities) is a good platform for further development of the concept of level 2 justification at a national level. The national system for introduction of new health technologies in Norway is not a complete solution for national coverage of level 2 justification, since the system only cover new methods to be introduced in the public specialist health services. New methods to be introduced in primary health services are not yet implemented and other solutions need to be developed. When it comes to level 2 justification of screening programs, individual health assessments of asymptomatic individuals outside screening programs and non-medical exposure of individuals (like for insurance purposes etc.), these practises need special attention and may not fit into ordinary HTA-systems.

3.2 Level 2 justification and HTAs at an European level

The need to ensure level 2 justification is strengthened in the revised European BSS directive and need to be implemented in national legislations within 6th of February 2018 [7] and, as mentioned earlier, the European Commission suggest that Member States cooperate on this issue [8]. The European cooperation between the Heads of the European Radiological Protection Competent Authorities (HERCA) [11], have launched a working package (WP) on generic justification within their Working Group on Medical Applications (WGMA). The mandate to this WP is to identify a common understanding of the requirements regarding level 2 justification in the European BSS Directive and to assist Member States in their work with the transposition of the directive into national legislation. The outcome of the WP will be a position paper on generic justification and contain different approaches on how to implement level 2 justification at a national level. One of the approaches that HERCA is looking into is the possibilities to combine the process of level 2 justification with already established processes of HTAs.

A European HTA Network (HTAN) were established by the European Commission in 2013 [12]. The legislative framework for HTAN is the European Directive 2011/24 on the application of patients' rights in cross-border healthcare, and its structure is described in the Commission Implementing Decision [13, 14]. According to the implementation decisions, the HTAN shall be supported by a scientific and technical cooperation mechanism, which today is the European EUnetHTA platform [15]. This platform is responsible for European cooperation on HTA performance and they have developed different tools for HTAs, including a core model for HTAs. They are also the platform used to conduct European Joint Actions on HTAs, founded by the EC, like EUnetHTA Joint Action 1, 2 and 3 [16, 17, 18].

It is worth exploring the possibilities to integrate level 2 justification in HTAs at an European level, by initiate a cooperation between HERCA and HTAN. This can contribute to raise the awareness on generic justification outside the radiation protection competent authorities and foster good cooperation between national HTA competent bodies and radiation protection authorities.

4 CONCLUSION

Integration of radiation detriment in total risk-benefit evaluation of HTAs is an efficient way to ensure level 2 justification in medical exposure. A national coordinated system for introduction of new health technologies ensures that NRPA is properly involved in all processes of the system and all categories of HTAs. Such a system foster a close cooperation between NRPA and all relevant stakeholders to increase the awareness on radiation protection and the process on justification. Cooperation between radiation protection authorities and HTA competent authorities at a European level may contribute to strengthen the awareness on level 2 justification among multiple stakeholders and should be encouraged.

5 REFERENCES

- [1] ICRP, 2007. The 2007 recommendations of the International Commission on Radiological Protection. ICRP publication 103. Annals of the ICRP 2007; 37(2–4).
- [2] ICRP, 2007. Radiological protection in medicine. ICRP publication 105. Annals of the ICRP 2005; 37(6).
- [3] European Commission, 1997. Council Directive 97/43/Euratom of 30 June 1997 on health protection of individuals against the dangers of ionizing radiation in relation to medical exposure, and repealing Directive 84/466/Euratom. Official Journal L 180, 09.07.1997: 0022 – 0027.
- [4] IAEA, 1996. International basic safety standards for protection against ionizing radiation and the safety of radiation sources. IAEA safety series 155. Vienna: International Atomic Energy Agency, 1996.
- [5] Regulations on radiation protection and use of radiation (Radiation protection regulations). <http://www.nrpa.no/dav/a3e3933033.pdf> (09.05.2016).
- [6] IAEA, FAO, ILO, et al., 2014. Radiation protection and safety of radiation sources: international basic safety standards. IAEA safety standards series, GSR part 3. Vienna: International Atomic Energy Agency, 2014.
- [7] European Commission, 2014. Council Directive 2013/59/Euratom of 5 December 2013 laying down basic safety standards for protection against the dangers arising from exposure to ionizing radiation, and repealing Directives 89/618/Euratom, 90/641/Euratom, 96/29/Euratom, 97/43/Euratom and 2003/122/Euratom. Official Journal of the European Union L 13, 17.1.2014.
- [8] European Commission, 2015. Council conclusions on Justification of medical imaging involving exposure to ionizing radiation. Brussels, 3 December 2015. Council of the European Union 14617/15. <http://www.sante.public.lu/fr/politique-sante/presidence-2015/radioprotection/CCS-medical-imaging-EN.pdf> (09.05.2016).
- [9] National system for introduction of new health technologies within the specialist health service (Nye Metoder), <https://nyemetoder.no/> (09.05.2016).
- [10] European Commission, 1993. Council Directive 93/42/EEC of 14 June 1993 concerning medical devices. Official Journal L 169, 12.7.1993: 0001-0043.
- [11] Heads of European Radiological Protection Competent Authorities, <http://www.herca.org/> (09.05.2016).
- [12] Health Technology Assessment Network. http://ec.europa.eu/health/technology_assessment/policy/network/index_en.htm (09.05.2016)
- [13] European Commission, 2011. Directive 2011/24/EU of the European Parliament and of the Council of 9 March 2011 on the application of patients' rights in cross-border healthcare. Official Journal L 88, 4.4.2011: 45-65.

- [14] European Commission, 2013. Commission implementing decision of 26 June 2013 providing the rules for the establishment, management and transparent functioning of the Network of national authorities or bodies responsible for health technology assessment. 2013/329/EU. Official Journal L 175, 27.6.2013: 71-72.
- [15] European Network for Health Technology Assessment. <http://www.eunethta.eu/> (09.05.2016).
- [16] EUnetHTA Joint Action 1. <http://www.eunethta.eu/activities/eunethta-joint-action-2010-12/eunethta-joint-action-2010-12> (09.05.2016).
- [17] EUnetHTA Joint Action
2. [http://www.eunethta.eu/activities/EUnetHTA%20Joint%20Action%2020\(2012-15\)/eunethta-joint-action-2-2012-2015](http://www.eunethta.eu/activities/EUnetHTA%20Joint%20Action%2020(2012-15)/eunethta-joint-action-2-2012-2015) (09.05.2016).
- [18] EUnetHTA Joint Action 3. <http://www.eunethta.eu/news/eunethta-joint-action-3-formal-preparatory-work-starting> (09.05.2016).

Proposed diagnostic reference levels for coronary angiography, left ventriculography and pacemaker placement in South Africa: 3-year improvement from 2012 - 2015

Hendrik Johannes de Vos^{a*}, Christoph Jan Trauernicht^b

^aNetcare Medical Physics CoE, Netcare Ltd., 76 Maude Street, Sandton 2196, Republic of South Africa

^bDepartment of Medical Physics, University of Cape Town, Groote Schuur Hospital, Anzio Road, Observatory 7925, Republic of South Africa

Abstract. Introduction Interventional theatre procedures using fluoroscopy guidance are becoming increasingly more complex in many specialities as the types and uses of catheters' become more advanced. Long fluoroscopic procedures have the potential to cause severe skin reactions in patients and can increase the risk of developing stochastic radiation effects. The International Commission of Radiological Protection (ICRP) advises that in principle Diagnostic Reference Levels (DRL) could be used in fluoroscopically guided interventional procedures to avoid unnecessary stochastic radiation risk. In this study, we aim to investigate and propose national DRLs for common interventional procedures specific to the South African population in the private healthcare sector. Materials and methods: Standard procedures performed in 30 private hospitals' vascular, cardiac and electrophysiology interventional theatres were identified and included in this dataset. Each entry in the database includes a procedure description, the Dose Area Product (DAP), the screening time, patient length and weight. The 3rd quartile of the observed distribution was used to calculate DRLs. The regulated quality assurance on the equipment and specifically the DAP meter calibration was performed prior to the start of data collection and routinely thereafter. Results: Dose and exposure data was recorded for more than 40000 procedures performed. DRLs were calculated for selected procedures with high case numbers including Coronary Angiograms (57 Gy.cm²), Left Ventriculography (63 Gy.cm²) and Pacemaker placements (35 Gy.cm²). The DRL improved with between 15 -17 % from the baseline DRLs calculated in 2013. Conclusion: We propose, based on the number of cases recorded and the national spread of hospitals, that the DRLs calculated could be considered as national guidance to interventionists attempting to optimize their techniques using DRLs in South Africa.

KEYWORDS: *diagnostic reference level (DRL); dose area product (DAP); interventional radiology; interventional cardiology; interventional theatre.*

1 INTRODUCTION

The International Commission of Radiological Protection (ICRP) advises that in principle Diagnostic Reference Levels (DRL) could be used in fluoroscopically guided diagnostic & interventional procedures to avoid unnecessary stochastic radiation risk. [1] This is cautiously said as the ICRP observed that the distribution of doses in interventional radiology is very wide, which may be attributed to the complexity of individual clinical cases.[1] When radiation is used in medicine the benefit of the modality needs to be weighed against the possible risk. A well-known term in radiology is "As Low As Reasonably Achievable" (ALARA) which describes the process of justification and optimization for the responsible use of x-rays. Ionising radiation produced by interventional radiology has the ability to penetrate tissue and deposit energy in cells. These effects are damaging to the biological components within cells and can lead to different types of cellular response. [2, 3] A further danger of radiation is that the damage caused by x-rays does not stimulate the human sensory system nor does it cause noticeable heat sensation to the patient being imaged. [2]

*Presenting author, e-mail: hendrik.devos@netcare.co.za

Radiation effects are broadly classified into deterministic and stochastic effects. Deterministic tissue effects materialize when threshold doses are exceeded and some examples thereof for the skin are erythema, dermal atrophy and necrosis. [4] X-ray units in interventional radiology typically have an energy range of between 40 kV – 150 kV. At this x-ray energy skin reactions are the most prevalent deterministic effect because this is the organ that receives the most radiation dose during a fluoroscopic procedure. In megavoltage radiotherapy where higher energy photons deposit their peak dose to deeper tissue, skin sparing is possible. Even so, skin reactions are common in radiotherapy treatments because of the high dose ranges required to treat tumours. Management of these reactions is possible to lessen the extent of injury during the course of treatment. [5, 6] Interventional procedures done using fluoroscopy guidance do not commonly exceed deterministic threshold doses for routine procedures, but it is possible for long complex cases or when poor radiographic technique is used. [2, 3, 7, 8] The classification of stochastic effects or random radiation effects has no threshold dose and some examples are radiation induced malignancies or cancer, infertility and birth defects. [9]. Stochastic effects are not as easily measurable as compared with deterministic effects because there is no threshold dose indicating possible effect and no assurance, especially at low doses, that an effect is related to the exposure received. [9,10]

Interventional cardiologists have a high usage of interventional x-ray machines. Unfortunately, their training does not include as much radiation physics or radiation safety as that of radiologists. [11] One result of the lack of training may be that interventionists are unaware of the amount of radiation dose to the skin, even today on modern technology.[2] Interventional procedures are becoming increasingly more complex in many specialities, as the types and uses of catheters become more advanced [12]. The increase in complexity of interventional procedures combined with a lack of specialist training on radiation techniques poses a significant risk to patients.

These risks have not gone unnoticed by government authorities worldwide and in 2015 the South African Department of Health: Directorate Radiation Control issued requirements to license holders of interventional fluoroscopy units, requiring the use of a medical physicist to optimize their radiation usage using DRLs.[13] Currently, in the South African environment, there are limited publications referring to DRLs with none addressing interventional cardiology. This emphasized the need for this study. The Dose Area Product (DAP) quantity measured for each patient represents a dosimetry index, the value of which should be optimized against the DRL, this varies for each procedure and can be used as a tool to comply with the ALARA principle.[14] In this study, we aim to investigate and propose national DRLs for common interventional procedures specific to the South African population in the private healthcare sector.

2 MATERIALS AND METHODS

2.1 Data Selection and Collection

Interventional radiology procedures across most disciplines can be broadly classified into diagnostic studies and interventions. Typically diagnostic studies are for the purpose of diagnosing a problem or the extent thereof. Interventions normally follow after a diagnostic procedure, aiming to repair or improve the problem or function. The diagnostic procedure would normally be simpler and quicker than the intervention, which should result in diagnostic procedures having lower radiation dose.

Through discussion with the clinical stakeholders the most common procedures or procedure combinations were identified to form part of the study. In total 24 procedures were identified for investigation and each procedure was assigned a name and detailed description. Although some interventional radiology procedures were included, this study focused on cardiac diagnostic imaging and interventions, because that is the focus of most of the catheterization theatres included in this work. The literature review indicated that in South Africa there is a lack of fluoroscopy DRLs for both diagnostic and interventional procedures; thus the procedure list aimed to include both classifications. The following three procedures from the dataset were investigated because of their high incidence:

1. Coronary Angiography (CA) described as a diagnostic test to determine if there is any narrowing or blockage of the coronary arteries.
2. Coronary Angiography & Left Ventriculography (CA + LV) described as a diagnostic test to determine a patient's cardiac function in the left ventricle which normally includes stroke volume, ejection fraction and cardiac output. This procedure includes CA, but excludes Right Ventriculography (RV) studies.
3. Permanent Pacemaker (PPM) described as the insertion of a medical device that uses electrical impulses, delivered by electrodes on the heart muscles, to regulate the heart rhythm.

CA and CA+LV were split up intentionally, because not all CA have an LV function test. However, the LV test requires at least one extra radiographic run, which will lead to a higher dose. [15]

In total, 30 interventional radiology theatres were identified to participate in this study. The X-ray machines were all fixed fluoroscopy units used in cardiology, hybrid or vascular theatres and included imaging equipment built by different Original Equipment Manufacturers (OEM). The data collection was done using an online system to input procedure information for each clinical case. Each participating theatre had two persons responsible for data capturing and timeous submission. Each entry in the database includes a procedure name, the DAP reading, screening time, patient length and weight.

The selection of these 30 interventional theatres housed equipment from various OEMs which expressed DAP in different units of measure; this was corrected for in the collection sheet where all doses were converted to $\text{Gy}\cdot\text{cm}^2$. Training was given to unit managers and/or radiographers to ensure accurate data capturing. All procedures that didn't fit the procedure descriptions exactly and paediatric patients were excluded for this study.

2.2 Dose Area Product Meter Calibration

The International Atomic Energy Agency (IAEA) Technical Report Series number 457 (TRS457) recognises that there is an increased need for patient dosimetry measurements in diagnostic and interventional radiology and that it is important to have traceability of these measurements. [16] The accuracy of a DAP meter, as with any ionisation chamber, may drift over time and routine cross-calibration is necessary. The Institute of Physics and Engineering in Medicine Report Number 91 (IPEM 91) recommends calibration annually as per manufacturer specification. [17] The South African x-ray licensing requirements specify that DAP meter cross-calibration should be confirmed on acceptance to be within the manufacturer specification and at least annually thereafter. [13]

A DAP meter is normally installed in the collimator assembly underneath the field shaping device of the fluoroscopy unit. The DAP meters used for this study all measure dose per area, but are displayed in different units of $\text{Gy}\cdot\text{cm}^2$, $\text{mGy}\cdot\text{cm}^2$ or $\mu\text{Gy}\cdot\text{cm}^2$. The DAP meters were all calibrated before the start of the study and periodic cross-calibration was performed as required during its course. In cases where calibration was not possible, a correction factor was used to correct the measured value. A cross-calibration or verification of a DAP meter requires the accurate field size and a dose measurement at the same Source to Surface Distance (SSD).

Dose measurements were done using the Raysafe Unfors Xi range of measuring devices designed to perform measurements in diagnostic beam qualities. These dose meters were all calibrated with traceable calibration certificates from laboratories with ISO/IEC 17025 accreditation [18]. The cross-calibration method utilised is based on the methods of cross calibration for DAP/ Kerma-Air Product (KAP) meters explained in the TRS 457 (pg. 336-340).[16]

2.3 Diagnostic Reference Level Analysis

The exposure data received presented best when using a histogram curve which clearly shows the population frequency in different DAP ($\text{Gy}\cdot\text{cm}^2$) bins. There are different ways to define reference levels; in this study the 3rd quartile of the distribution was calculated for each type of procedure and this was set as the DRL. The 3rd quartile DRL simplifies comparisons with work published from other countries [19]. Further statistical analysis of the DAP distribution included calculation of the 1st quartile, interquartile range and the standard deviation for each procedure.

2.4 Optimization System

Throughout the period of data collection, feedback to interventional theatres was done in the form of a newsletter. The information shared with theatres included their average DAP values for common cases and comparisons to their neighbouring hospitals as well as comparisons to published international DRL references. The aim of this communication was to educate, encourage and enable interventional theatres to track their performance and possible optimization or lack thereof. Where high doses frequently occurred the focus was to distribute the IAEA radiation protection posters [20] and provide radiation protection training to staff.

It is noteworthy to mention that during this period of DRL data collection and optimization; improvements were made to the incident management system to define and quantify possible occurrences of radiation incidents. Fluoroscopic patient doses exceeding $300 \text{ Gy}\cdot\text{cm}^2$ were required to be reported for handling by the responsible medical physicist. The incidents were graded depending on possible severity of the resulting skin reaction and were handled either by electronic correspondence or site visits. The incident grading was further used to guide the responsible physicist in management and peak skin dose estimation. These incident reporting requirements reinforced the same radiation protection principals as the radiation dose optimization system.

3 RESULTS

Dose and exposure data was recorded for 41250 procedures performed from July 2012 to August 2015. This included 7126 data points for CA, 11080 for CA+LV and 2047 for PPM. The 2012 DAP values were used as a baseline for this study and the DAP values recorded in 2014-15 as current results. Figures 1-3 show the distribution of the baseline and current DAP values for the three procedures evaluated. Table 1 lists the calculated 1st & 3rd quartiles, interquartile range and standard deviation for the distribution of data received.

Figure 1: Distribution of CA DAP readings recorded for (a) 678 procedures performed during 2012 with a 3rd quartile of 65.9 Gy.cm² and (b) 3528 procedures performed during 2014-15 with a 3rd quartile of 56.0 Gy.cm².

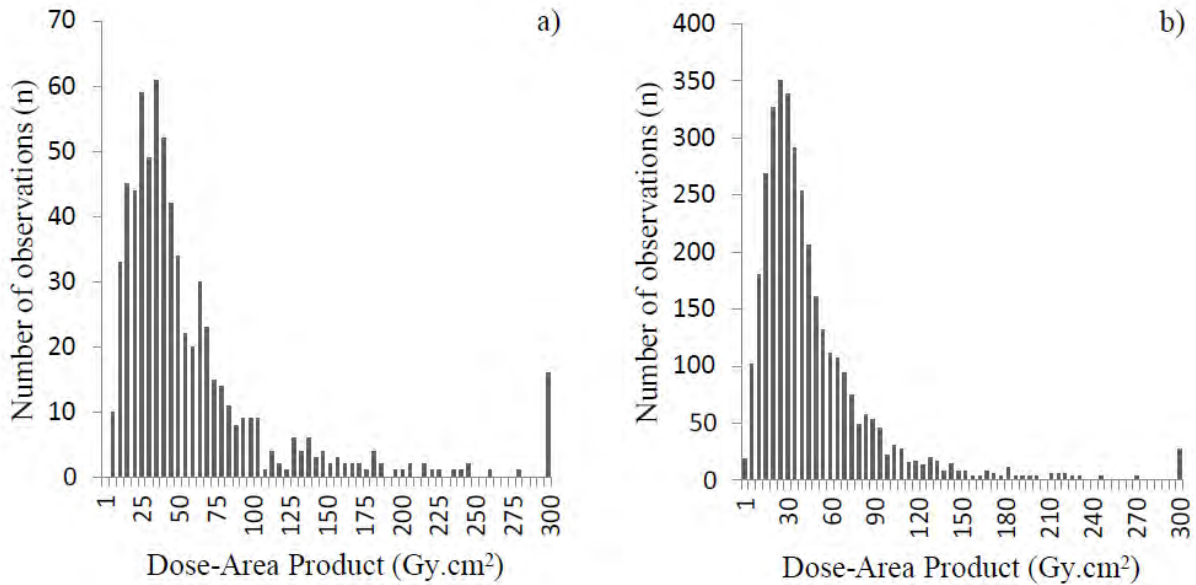


Figure 2: Distribution of CA+LV DAP readings recorded for (a) 1548 procedures performed during 2012 with a 3rd quartile of 76.8 Gy.cm² and (b) 3533 procedures performed during 2014-15 with a 3rd quartile of 63.5 Gy.cm².

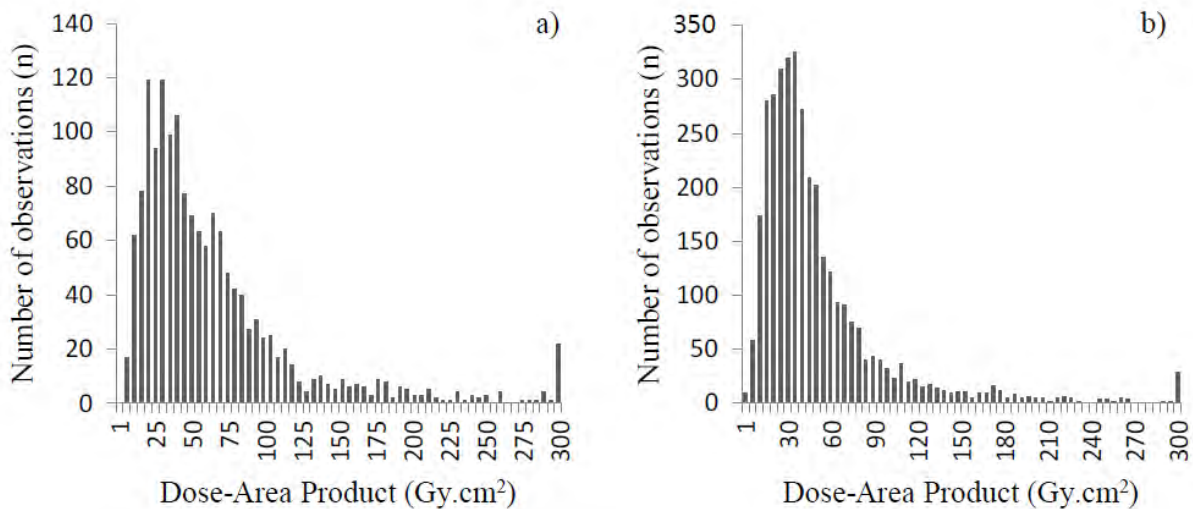


Figure 3: Distribution of PPM DAP readings recorded for (a) 466 procedures performed during 2012 with a 3rd quartile of 42.8 Gy.cm² and (b) 874 procedures performed during 2014-15 with a 3rd quartile of 36.2 Gy.cm².

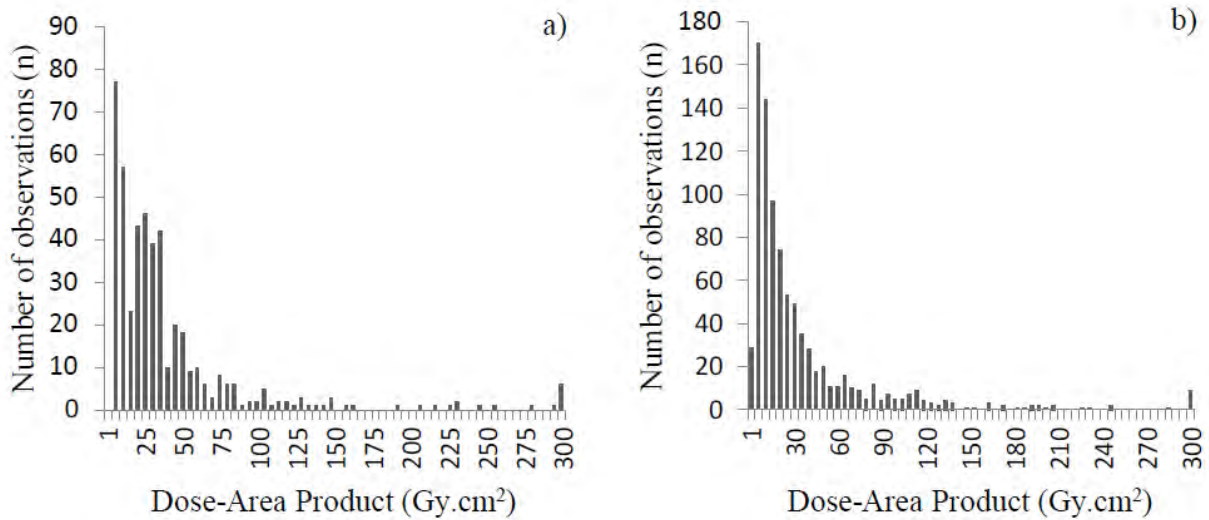


Table 1: Procedure amounts, 1st & 3rd quartiles and standard deviation values for the three procedures evaluated. Statistics include DAP data from 30 participating theatres calculated for the baseline and current time periods.

Procedure	CA		CA + LV		PPM	
	2012	2015	2012	2015	2012	2015
Record year	2012	2015	2012	2015	2012	2015
<i>n</i>	678	3528	1625	3533	466	874
1 st Quartile (Gy.cm ²)	23.1	19.7	25.4	22.8	7.9	5.6
3 rd Quartile (Gy.cm ²)	65.9	56.0	76.8	63.5	42.8	36.2
Interquartile range	42.8	36.3	51.3	40.7	34.9	30.6
Standard deviation	75.8	57.5	70.2	59.6	76.2	63.0

4 DISCUSSION

Initially the wider spread of the DAP baseline histogram is apparent in Figure 1a, 2a and 3a. The distribution became narrower with less frequency in high dose components as displayed in Figure 1b, 2b and 3b. The doses exceeding 300 Gy.cm², which is the incident dose level used by the incident management system, have also decreased in frequency from the recorded baselines. The standard deviation became smaller from baseline for CA (75.8 to 58.5), CA+LV (70.2 to 59.6) and PPM (76.2 to 63.0); this is shown in table 1 which supports the distribution changes in figure 1-3. The reduction in standard deviation shows that the amount of variation in the dataset decreased during the period of data collection and dose optimization. Further to the improvement of the standard deviation, the interquartile range decreased for CA (42.8 to 36.3), CA+LV (51.3 to 40.7) and PPM (34.9 to 30.6).

Table 2 lists the proposed DRL and quantifies the amount of optimization of DRL in the three years as and percentage change from baseline. The baseline DAP reading for CA established in 2012 was 65.9 Gy.cm² and a total of 678 procedures were used for the initial establishment of the DRL. This value has reduced to 56.0 Gy.cm² in 2015 and 3528 cases were used in the establishment of the updated DRL. The baseline for CA+LV was 76.8 Gy.cm², calculated using 1625 procedures. This improved to 63.5 Gy.cm², calculated using 3533 procedures. PPM cases showed a similar trend and improved from 42.8 Gy.cm² determined from 466 cases to 36.2 Gy.cm² for 874 procedures. These reductions in DRL translate to a 15% improvement for CA, 17% for CA+LV and 16% for PPM.

Table 2 further compares the proposed DRL with other 3rd quartile DRLs published in other countries. The proposed DRLs compares well with the listed published data; the DRL for CA is lower than data published in the United States of America (USA) and Belgium.[21, 22] Authors from Europe, Ireland and Croatia published DRLs lower than our proposed level for CA.[23-25]/

Table 2: Proposed reference levels for the private healthcare sector in South Africa; includes baseline DRLs, amount of optimization and comparison to publications from other countries. The amount of procedures evaluated for each review period (*n*) is indicated below the displayed DRL value.

	Baseline DRL (Gy.cm ²)	Proposed DRL (Gy.cm ²)	% Change	International Publications (Gy.cm ²)
CA	66 (<i>n</i> = 678)	56 (<i>n</i> = 3528)	▼15	83 (USA – Miller <i>et al</i> 2012) [21]
				71 (Belgium – Bogaert <i>et al</i> 2008) [22]
				45 (EU – Padovani <i>et al</i> 2008) [23]
				42 (Ireland – D’Helft <i>et al</i> 2009) [24]
				32 (Croatia – Brnic <i>et al</i> 2010) [25]
CA+LV	77 (<i>n</i> = 1548)	63 (<i>n</i> = 3533)	▼17	70 (EU – Padovani <i>et al</i> 1998) [26]
PPM	43 (<i>n</i> = 466)	36 (<i>n</i> = 874)	▼16	38 (Swiss – Aroua <i>et al</i> 2004) [27] 21 (Ireland - D’Helft <i>et al</i> 2009) [24]

The literature review found very few articles differentiating between CA with and without the inclusion of LV. The reference level calculated for both baseline and current data suggests that the addition of LV function increases the dose needed compared to a normal CA. Padovani *et al.* [26] published a CA reference level with LV function included of 70 Gy.cm². This is marginally higher than our proposed DRL for CA+LV of 63 Gy.cm². Clark *et al.* [15] indicated that the inclusion of LV function together with a CA procedure significantly increases the dose to the patient with 6.0 Gy.cm². The data in this study shows an increase of 7.5 Gy.cm² when LV function is done as part of CA. The proposed DRL for PPM was similar to data published in Switzerland [27] and higher than that of Ireland. [24] This is consistent with the CA comparison with Ireland which was also higher.

The optimization of radiation dose usage and 3 year improvement in DRLs may be attributed to various factors. This program, to the involved theatres, managed to increase their awareness and understanding of the DAP delivered to a patient. The availability of a local DRL metric, indicating a dose level that should not routinely be exceeded, helped the responsible medical physicist to

identify, investigate and optimize imaging techniques. The newsletters that were sent out explicitly mentioned the hospitals' names, which resulted in a degree of competition between hospitals. The data helped the responsible physicist to engage with theaters that had the same equipment, but higher doses, to determine where optimization could happen. The improvements made to the incident management system included the definition, quantification or grading and guided management of incidents. This enforced the same radiation protection principals and helped to achieve responsible radiation usage.

The system made outlier identification possible and theatres continually exceeding the DRL could be investigated and a lack of improvement could be questioned. The availability of a locally derived DRL and comparisons with achievements of other centers aided administrators to motivate, where needed, for the upgrading of equipment. During the course of this work some imaging equipment was replaced or upgraded with newer technology which also positively impacted the DRL.

5 CONCLUSION

For the majority of the 30 interventional theatres included in this study, the baseline data in 2012 was their first attempt at dose optimization and the procedures evaluated showed an improvement of 15 - 17%. A total number of 41250 procedures were recorded and DRLs were calculated for the three most common procedures evaluated. These three procedures account for 49.1% of the total data points. A total of 24 procedures were identified initially, including complex interventions and additional DRLs can be expected from this dataset. We attribute the improvement seen to various factors, including increased awareness created, changes in imaging techniques, new and upgraded imaging equipment and the improvement of incident management.

We propose, based on the number of cases recorded and the national spread of Netcare Ltd., that these DRLs could be considered guidance to interventionists attempting to optimize their techniques using DRLs for the South African population.

6 ACKNOWLEDGEMENTS

The input and participation of the nursing, radiography and medical physics staff working in the catheterization theatres at Netcare Ltd. was invaluable and we acknowledge this. Their commitment and strive towards patient safety during the project is commendable and these optimization results are an accomplishment to be proud of.

7 REFERENCES

- [1] ICRP. Diagnostic reference levels in medical imaging: Review and additional advice. International Commission on Radiological Protection. http://www.icrp.org/docs/DRL_for_web.pdf.
- [2] Koenig TR, Wolff D, Mettler FA, et al. Skin injuries from fluoroscopically guided procedures: part 1, characteristics of radiation injury. *American Journal of Roentgenology*. 2001;177:3-11.
- [3] Koenig TR, Mettler FA, Wagner LK. Skin injuries from fluoroscopically guided procedures: part 2, review of 73 cases and recommendations for minimizing dose delivered to patient. *American Journal of Roentgenology*. 2001;177:13-20.
- [4] Balter S, Hopewell JW, Miller DL, et al. Fluoroscopically Guided Interventional Procedures: A Review of Radiation Effects on Patients' Skin and Hair 1. *Radiology*. 2010;254:326-41.
- [5] Naylor W, Mallett J. Management of acute radiotherapy induced skin reactions: a literature review. *European Journal of Oncology Nursing*. 2001;5:221-33.
- [6] Bolderston A, Lloyd NS, Wong RK, et al. The prevention and management of acute skin reactions related to radiation therapy: a systematic review and practice guideline. *Supportive Care in Cancer*. 2006;14:802-17.

- [7] Hart D, Hillier MC, Wall BF. National reference doses for common radiographic, fluoroscopic and dental X-ray examinations in the UK. *The British Journal of Radiology*. 2009;82:1-12.
- [8] Karambatsakidou A, Tornvall P, Saleh N, et al. Skin dose alarm levels in cardiac angiography procedures: is a single DAP value sufficient? *The British Journal of Radiology*. 2005;78:803-9.
- [9] Ron E. Cancer risks from medical radiation. *Health Physics*. 2003;85:47-59.
- [10] Nayar AK, White BM, Stone KE, et al. Radiation exposure and associated cancer risk with cardiac diagnostic imaging. *Journal of the American Osteopathic College of Radiology*. 2013;2:14-20.
- [11] Vlietstra R, Wagner L, Koenig T, et al. Radiation burns as a severe complication of fluoroscopically guided cardiological interventions. *Journal of Interventional Cardiology*. 2004;17:131-42.
- [12] Vano E, Gonzalez L, Ten J, et al. Skin dose and dose–area product values for interventional cardiology procedures. *The British Journal of Radiology*. 2001;74:48-55.
- [13] DoH:DRC. Requirements for license holders with respect to quality control tests for diagnostic X-ray imaging systems. Department of Health: Directorate Radiation Control. South Africa; 2015. <https://sites.google.com/site/radiationcontroldoh/>.
- [14] Picano E, Vañó E, Rehani MM, et al. The appropriate and justified use of medical radiation in cardiovascular imaging: a position document of the ESC Associations of Cardiovascular Imaging, Percutaneous Cardiovascular Interventions and Electrophysiology. *European Heart Journal*. 2014;35:665-72.
- [15] Clark AL, Brennan AG, Robertson LJ, et al. Factors affecting patient radiation exposure during routine coronary angiography in a tertiary referral centre. *The British Journal of Radiology*. 2000;73:184-9.
- [16] IAEA. Dosimetry in Diagnostic Radiology: An international Code of Practice Report Number
Technical Report Series number 457. Vienna: International Atomic Energy Agency; 2007.
- [17] IPEM. Recommended Standards for the Routine Performance Testing of Diagnostic X-ray Imaging Systems. Report No 91. IPEM91. York: Institute of Physics and Engineering in Medicine; 2005.
- [18] ISO. General requirements for the competence of testing and calibration laboratories. ISO/IEC 17025. Geneva, Switzerland: International Organization for Standardization; 2005.
- [19] Aroua A, Rickli H, Stauffer J-C, et al. How to set up and apply reference levels in fluoroscopy at a national level. *Eur Radiol*. 2007;17:1621-33.
- [20] IAEA. 10 Pearls: Radiation protection of patients in fluoroscopy. International Atomic Energy Agency.
- [21] Miller DL, Hilohi CM, Spelic DC. Patient radiation doses in interventional cardiology in the US: advisory data sets and possible initial values for US reference levels. *Medical Physics*. 2012;39:6276-86.
- [22] Bogaert E, Bacher K, Thierens H. A large-scale multicentre study in Belgium of dose area product values and effective doses in interventional cardiology using contemporary X-ray equipment. *Radiation Protection Dosimetry*. 2008;128:312-23.
- [23] Padovani R, Vano E, Trianni A, et al. Reference levels at European level for cardiac interventional procedures. *Radiation protection dosimetry*. 2008;129:104-7.
- [24] D'Helft CJ, Brennan PC, Mcgee AM, et al. Potential Irish dose reference levels for cardiac interventional examinations. *The British Journal of Radiology*. 2009;82:296-302.
- [25] Brnić Z, Krpan T, Faj D, et al. Patient radiation doses in the most common interventional cardiology procedures in Croatia: first results. *Radiation Protection Dosimetry*. 2010;138:180-6.
- [26] Padovani R, Novario R, Bernardi G. Optimisation in coronary angiography and percutaneous transluminal coronary angioplasty. *Radiation Protection Dosimetry*. 1998;80:303-6.
- [27] Aroua A, Besançon A, Buchillier-Decka I, et al. Adult reference levels in diagnostic and interventional radiology for temporary use in Switzerland. *Radiation Protection Dosimetry*. 2004;111:289-95.

Procedure for measurement of Intrinsic efficiency of a High Energy collimator Gamma camera

Hugo Pérez-García*, Raquel Barquero, Monica Gómez-Incio

Hugo Pérez García, HCUV, c/Ramón y Cajal 3, 47005-Valladolid, Spain.

Abstract. *PURPOSE:* Image quantification for therapy radionuclides with I-131 is difficult because of cameras are optimised for diagnostic imaging with Tc-99m. In order to know the sensitivity of camera with High Energy (HE) collimator, both intrinsic efficiency (η_0) and geometry efficiency G are needed. η_0 is defined as the quotient between photon/s arriving the Region Of Interest (ROI) and counts/s in that ROI within the crystal detector. η_0 must be estimated in a calibration measurement with a reference ^{131}I source in air [3]. Here, a procedure to perform this calibration measurement is described. *MATERIAL AND METHOD:* First, a source with ^{131}I inside a 150 mm diameter cuvette (Petri dish) filled with radioactive water in which 111-185 MBq (3-5 mCi) ^{131}I activity (A_{ref}) is diluted. This activity of the ^{131}I in the reference source must be certified as traceable to national or international standards. Second, this standard reference phantom is centred with respect the crystal of a Siemens e.cam gamma camera, at a defined distance (10 cm) from the HE collimator face. Third, an acquisition with a 15% energy window centred on the 364 keV and with a sufficiently long acquisition time t (600 s) is performed. Fourth, The 2D DICOM image obtained is then analyzed and processed with ImageJ: Defining on the image a 15 cm diameter circle (a surface ROI $S_{\text{ROI}}=179 \text{ cm}^2$), the number of counts in full-energy peak (gross counts) n_g inside it is measured. From apart, the corresponding geometry efficiency G_{ref} for the geometry and the camera used in the measurement is determinate with MCNPX code. Finally the intrinsic efficiency η_0 is calculated according to the following formulae: $\eta_0 = \frac{(n_g/t)/S_{\text{ROI}}}{G_k \cdot A_{\text{ref}}}$. *RESULTS AND DISCUSSION:* The result for η_0 is $5.22 \cdot 10^{-2}$. Theoretical value for η_0 , is τ/μ (photo/total attenuation in sodium iodide) $1.3 \cdot 10^{-1}$ (40%). *CONCLUSION:* The procedure developed allows know experimentally the intrinsic efficiency of a HE gamma camera for I-131 imaging.

1 INTRODUCTION

In developed countries, the medical use of radiation is widespread and is the main source of radiation exposure of general public. It includes diagnostic radiology, radiotherapy, nuclear medicine and interventional radiology. Nuclear medicine procedures can be either diagnostic (90%) or therapeutic (10%). Therapeutic procedures consist primarily of thyroidal pathologies including cancer (27%) and hyperthyroidism (69%) [1].

In thyroidal metabolic treatments in Nuclear Medicine a therapeutic activity of I-131 is administered to patients. Following the 59/2013 Directive from EURATOM [2] the radiation absorbed doses in lesion and critical organs should be estimated. The most accurate procedure to estimate these doses should consider the temporal evolution of activity uptake in each from these organs [3]. The planar image which was obtained by a gamma camera (GC) have been used by many authors to determine the activity uptake in each instant [4-6] In this work, the general procedure used in spectrometric counters to obtain activity is applied [7-13]. A new point of view is developed to aboard the sensitivity of planar GC in conjunction with Monte Carlo methods in order to obtain the activity uptaken for each patient who has been treated with ^{131}I . The new procedure estimates the activity from a GC planar image acquired with a 15% energy window centred on the 364 keV by using this expression:

$$A_0 = \frac{n_n / t / S_{\text{ROI}}}{G} = \frac{n_n / t}{S} \quad (1)$$

n_n is the net counts obtained as the difference of the total gross counts and the background counts measured in the region of interest (ROI) defined in the image and in the vicinity respectively. t is the

* Presenting author, e-mail: phihugo@gmail.com

measuring time in the GC acquisition. S_{ROI} is the area in the ROI where total counts are evaluated. Geometric factor G is the mean fluence of photons of 364 keV which arrive to the crystal at the projection in the crystal-collimator surface of the ROI, and the volume defined in the crystal by this ROI. This value is obtained by using Monte Carlo methods. The term η_0 is the intrinsic efficiency that characterizes the specific response of the crystal of the GC (counts/photons), and S is the sensitivity of the GC usually in units of (cps/MBq). η_0 must be estimated in a calibration measurement with a reference ^{131}I source. The advantage of this method is that it is only needed to calibrate the GC once, and then, by using Monte Carlo code, the sensitivity S can be obtained for any geometric arrangement. In this paper, a procedure to perform this calibration measurement is described.

2 MATERIAL AND METHOD

2.1 Source preparation

A reference source containing ^{131}I may be used for this purpose. The activity or emission rate of the ^{131}I in the reference source must be certificated as traceable to national or international standards. The reference source is prepared by dilution from a standardized solution purchased to the supplier. 111-148 MBq (4 mCi) of ^{131}I in standardized solution is introduced in a 1-5 cm^3 syringe and it is accurately measured by using a dose calibrator (Capintec 15R dose calibrator (DC)). The solution is poured out a larger flat plastic dish (150 mm x 15 mm nominal size standard Petri dish of Fig. 1 recommended in NEMA test 3.3 [14] which is used in order to reduce the volatility of ^{131}I . The Petri dish should be filled previously with clean water at least 60% volume, and then, when the solution is inside, the phanton must be completely refilled. The residual activity remaining in the syringe, A_{Res} shall be promptly measured in the dose calibrator and the reading subtracted from the original reading to obtain the amount of activity in the phantom, $A_k = A_{SR} - A_{Res}$, at the time of preparation.

2.2 Image adquisition

A Siemens E-CAM system with two heads is used for experimental measurement. Only a head will be considered for calibration purpose hereafter in this paper because the intrinsic efficiency of the other head would be calculated in the same way. The detector is a 40x50 cm^2 area and 3/8"(0.9525 cm) thickness NaI (Tl) scintillation crystal. The high energy (HE) collimator is hexagonal hole shaped with a hole diameter of 3.4 mm, a length of 50.8 mm and the septa is lead with a thickness of 2 mm. The Petri dish is positioned 10 cm bellow the collimator and is centered at the field-of-view and parallel to the plane of the detector system (composed by crystal and collimator). The acquisition time with the imaging system is 600 s, an energy window centered in 364 keV and a width of 15%. The acquisition matrix was 256 pixels x 256 pixels, with a pixel size of 2.398 mm^2 .

Figure 1: Petri dish of 7 cm radius filled with ^{131}I solution of water



2.3 Processing the DICOM images

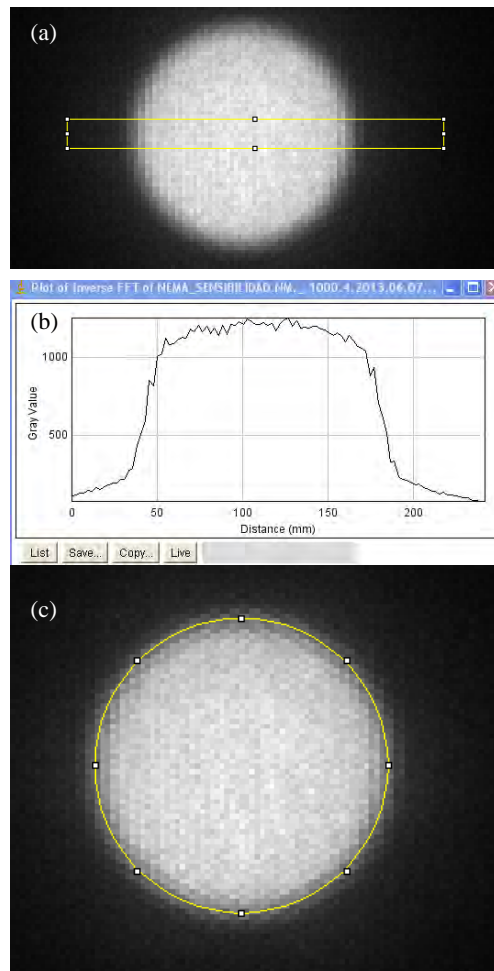
As a result of the acquisition, an image was obtained in DICOM format. The DICOM image are analyzed and processed with IMAGEJ [15]. Firstly an imaging filter is applied to the image to remove the collimator artifacts. This filter is called HURRA [16] and is a high-pass filter which eliminates the undesirable frequencies that the collimator creates. ImageJ is used to define a rectangular selection to obtain central profile. In Fig. 2 (a) these selections are included in yellow color.

Secondly, the plot is analyzed. A spreadsheet is used to obtain the corresponding full width at half maximum (FWHM) in Fig. 2 (b). An oval selection ROI is defined with a diameter of the FWHM previously measured. Fig. 2(c) show the circular ROI defined in the image. Thirdly, the circular ROI is measured to obtain the gross counts n_g inside the ROI.

2.4 Obtaining factor G_k

The geometrical factor in the calibration conditions G_k is obtained by using Monte Carlo Code. The experimental measurement is simulated using the Monte Carlo N-Particle Transport Code MCNPX. MCNPX is a general purpose Monte Carlo radiation transport that allows the user to simulate the transport of individual particles (photons in this case). The Petri dish is cylindrical in shape with a radius of 7 cm and a height of 0.3 cm, and it is simulated as water (H 67% and O 33%) with density of 1 g cm^{-3} . The source emits photons of 364 keV (81.7%), 637 keV(7.17%) and 723 keV(1.77%) from the surface on the Petri dish (a plane). The position of the source is sampled uniformly in this surface.

Figure 2: (a) Filtered image with a rectangular selections to obtain the central profiles. (b) Plots of the rectangular selection. (c) The circular ROI with a diameter as the FWHM is shown in yellow.



The collimator is simulated with the repeated structure capability of MCNPX using the FILL, U and LAT cards. The model is illustrated in Figure 2: A hexagonal lattice of apothem 0.27 cm is contained within a $40 \times 50 \times 5.08 \text{ cm}^3$ lead (Pb 100% with density 11.35 g cm^{-3}) plate. Within that hexagon lattice other hexagon lattice of apothem 0.17 filled by void cell is defined. The crystal is modeled as other plate of $40 \times 50 \times 0.95 \text{ cm}^3$ of INa (I 50% and Na 50%) with density 3.67 g cm^{-3} . The photon fluence per source particle is determined using $F4$ tally with a circular flat cell in the crystal with the same size as circular ROI in section 2.3.

2.5 Intrinsic efficiency definition

At this point, every element to calculate the intrinsic efficiency is known, so there is only one thing left to do, and it is to obtain it according the following formula:

$$\eta_0 = \frac{(n_g / t) / S_{ROI}}{A_k \cdot G_k} \quad (2)$$

The standard uncertainty $u(\eta_0)$ of a is as follow:

$$u(\eta_0) = \eta_0 \cdot \left(\frac{u(A_k)}{A_k} + \frac{u(G_k)}{G_k} \right) \quad (3)$$

3 RESULTS AND DISCUSSION

The nominal activity obtained after preparing the source was $A_{cal} = 147778000$ Bq (3.994 mCi). Originally there was 4 mCi in the syringe, with a residual activity of 0.006 mCi.

The FWHM in the image is 13.93 cm which matches the size of the source (14 cm). The ROI area S_{ROI} is 151.99 cm². The total number of counts n_g is 2849886 measured in $t = 600$ s. The mean photon fluence per disintegration calculated with MCNPX in the 15% window adding left window ($4.22 \cdot 10^{-6}$) and right window ($1.35 \cdot 10^{-7}$) results $4.35 \cdot 10^{-6}$ photon/cm² dis. The relative error with 10^{10} particles is 1%. By using equation 2 and 3, the intrinsic efficiency $\eta_0 = 5,3 \pm 0,63$ cm⁻² is obtained.

4 CONCLUSIONS

A new method to quantify the uptake activity in a tumor from a planar image acquired by a GC and ¹³¹I has been used, consisting in the calibration of the Gamma camera system with two factors calculated separately, the intrinsic efficiency η_0 and the geometry factor G . In this paper, the procedure to obtain the intrinsic efficiency is defined: An experimental measurement of a calibrated flat source in air is used to obtain the intrinsic efficiency of a E-cam gamma camera system.

This method improves the accuracy of the traditional calibration measurements based on an only one planar sensitivity measurement in each equipment relayed on the sensitivity NEMA test.

5 ACKNOWLEDGEMENTS

Funded by Gerencia Regional de Salud de Castilla y Leon. SPAIN. Project **GRS 1080/A/15 (2015)**.

6 REFERENCES

- [1] Flux, G., Bardies, M., Monsieurs, M., et al., 2006. The Impact of PET and SPECT on Dosimetry for Targeted Radionuclide Therapy, *Z. Med. Phys.* 16, pp. 47–59
- [2] EURATOM 2013/59 council directive of 5 December 2013 laying down basic safety standards for protection against the dangers arising from exposure to ionising radiation, and repealing Directives 89/618/Euratom, 90/641/Euratom, 96/29/Euratom, 97/43/Euratom and 2003/122/Euratom
- [3] MIRD Pamphlet No. 16, 1999. Techniques for Quantitative Radiopharmaceutical Biodistribution Data Acquisition and Analysis for Use in Human Radiation Dose Estimates, *J. Nucl. Med.* 4037S-61
- [4] Pollard, K.R., Bice, A.N., Eary, J.F., et al., 1992. A method of imaging therapeutic doses of iodine-131 with a clinical gamma camera, *J. Nucl. Med.*, 33, pp. 771–776.
- [5] Zasadny, K.R., Gates, V.L., Francis, I., et al., 1997. Normal organ and tumor dosimetry of I-131-anti-B1 (anti CD-20) radioimmunotherapy at non-marrow ablative doses, *J. Nucl. Med.*, 38(suppl), 230P

- [6] Early, J.F., Appelbaum, F.L., Durack, L., et al., 1989. Preliminary validation of the opposing view method for quantitative gamma camera imaging, *Med. Phys.*, 16, pp.382–387
- [7] Thomas, S.R., Maxon, H.R., Keriakes, J.G., 1976. In vivo quantitation of lesion radioactivity using external counting methods., *Med. Phys.*, pp. 3253-255
- [8] Shulkin, B.L., Sisson, J.C., Koral, K.F., et al., 1988. Conjugate View Gamma Camera Method for Estimating Tumor Uptake of Iodine-131 Metaiodobenzylguanidine”, *J. Nucl. Med.*, 29, pp. 542-548
- [9] Kobe, C., Eschner, W., Sudbrock, F., et al., 2008. Graves' disease and radioiodine therapy Is success of ablation dependent on the achieved dose above 200 Gy?, *Nuklearmedizin*, 47: doi: 10.3413/nukmed-0087
- [10] Osko, J., Golnik N., Pliszczynski, T., 2007. Uncertainties in determination of 131-I activity in thyroid gland, *Radiation Protection Dosimetry*, 1 of 4, doi:10.1093/rpd/ncm158
- [11] Zuckier, L.S., Dohan, O., Li, Y., et al., 2004. Kinetics of Perrhenate Uptake and Comparative Biodistribution of Perrhenate, Pertechnetate, and Iodide by NaI Symporter–Expressing Tisúes In Vivo, *J. Nucl. Med.*, 45: 3, pp. 500-507
- [12] Bolch, W.E., Bouchet, L.G., Robertson, J.S., et al., 1999. Bolch MIRD Pamphlet No. 17: The Dosimetry of Nonuniform Activity Distributions Radionuclide S Values at the Voxel Level, *J. Nuc. Med.*, 40:118-368
- [13] Dorn, R., Kopp, J., Vogt, H., et al., 2003. Dosimetry-Guided Radioactive Iodine Treatment in Patients with Metastatic Differentiated Thyroid Cancer: Largest Safe Dose Using a Risk-Adapted Approach, *J. Nucl. Med.*, 44:, pp. 451–456
- [14] NEMA Standards Publication, UN 1-2007. Performance Measurements of Gamma Cameras
- [15] IMAGEJ: Image processing and analysis in Java. <http://imagej.nih.gov/ij/> (Rev. Feb. 2016)
- [16] Perez-Garcia, H., Barquero, R., Cardenas, A. 2015. Filtro HURRA: un método sencillo para eliminar artefactos del colimador en imagen planar con I-131, 4º Congreso Conjunto Sociedad Española de Física Médica (SEFM) y la Sociedad Española de Protección Radiológica (SEPR). Retrived 31-1-2016 from: <http://www.sefmseprvalencia2015.es/images/comunicaciones/MNU-04.pdf>

Simulation of a High Energy collimator Gamma camera with MCNPX

Hugo Pérez-García*, Raquel Barquero, Monica Gómez-Incio

Hugo Pérez García, HCUV, c/Ramón y Cajal 3, 47005-Valladolid, Spain.

Abstract. PURPOSE: In 2D dosimetry ^{131}I therapy, quantification of patient activity in planar images acquired with a gamma camera (GC), requires the determination of the sensitivity of detector system constituted by the Gamma camera INA(Tl) crystal and the High Energy (HE) collimator. In this study, we pretend estimate the photon fluence (Φ) arriving to the Region Of Interest (ROI) in the crystal detector using Monte Carlo simulation with MCNPX code. MCNPX code can be ideal to simulate the HE hexagonal lead and air net. Different Φ values as a function of the uptake/source radius (r) at different distances (d) of the HE collimator are investigated.

MATERIAL AND METHOD: Two GC system are simulated: A Siemens E.CAM and a Philips SKYLIGHT. The crystal is modelled as a parallelepiped plate with INa. The HE collimator is simulated with the repeated structure capability of MCNP using the FILL, U and LAT cards: A hexagonal net of lead and air with HE specifications is introduced in the MCNPX input. As sources cylindrical in shape reference ^{131}I with different radius (r) range from 1 to 7 cm, made of diluted water solution (Petri dish phantom) are simulated.

RESULTS AND DISCUSSION: The range of all results obtained for the two systems E-CAM and SKYLIGHT goes from $3.56 \cdot 10^{-6} (\pm 5.17\%) \text{ photon} \cdot \text{cm}^{-2} \cdot \text{dis}^{-1}$ for $r=7$ cm and $d=5$ cm, to $3.03 \cdot 10^{-5} (\pm 11\%) \text{ photon} \cdot \text{cm}^{-2} \cdot \text{dis}^{-1}$ for $r=1$ cm and $d=40$ cm. As can be seen G dependence with size r and distance d are significant.

CONCLUSION: The simulations conducted with MCNPX allow the accurate characterization of a HE gamma camera for ^{131}I imaging. The geometric factors for any lesion size r and any distance lesion collimator can be estimated with MCNPX.

1 INTRODUCTION

Medical use of radiation is a large and continuously increasing source of radiation dose to the general public in developed countries. It includes diagnostic radiology, radiotherapy, nuclear medicine and interventional radiology. In nuclear medicine have procedures therapeutic (10%) which consist primarily of thyroidal pathologies including cancer (27%) and hyperthyroidism (69%). In thyroidal metabolic treatments therapeutic activity of I-131 is administered to patients where the radiation absorbed doses in lesion and critical organs should be estimated.

Here a new procedure to estimate the activity A from a Gamma Camera planar image acquired with a 15% energy window centred on the 364 keV has been developed. A can be known using this expression:

$$A = \frac{n_n / t / S_{ROI}}{G} \cdot \frac{n_n / t}{S}$$

n_n is the net counts obtained as the difference of the total gross counts and the background counts measured in the region of interest (ROI) defined in the image and in the vicinity respectively. t is the measuring time in the GC acquisition. S_{ROI} is the area in the ROI where total counts are evaluated. Geometric factor G is the ratio between the total fluence of 364 keV photons which arrive to the crystal at the projection in the crystal- collimator surface of the ROI, and the disintegrations in the volume or source region with activity uptake. This value is obtained by using Monte Carlo methods. The term η_0 is the intrinsic efficiency that characterizes the specific response of the crystal of the GC (counts/photons). η_0 (see poster 452) must be estimated in a calibration measurement with a reference ^{131}I source.

* Presenting author, e-mail: phihugo@gmail.com

Geometric factor G is the mean fluence of photons of 364 keV which arrive to the crystal at the projection in the crystal-collimator surface of the ROI, and the volume defined in the crystal by this ROI. This paper describes the procedure followed by Monte Carlo code for obtaining G .

2 MATERIAL AND METHOD

Computer: PC Pentium i7 frequency 2.5GHz and 4GB RAM with an output time is ~15 min.

Program code: Monte Carlo (MC) method with MCNPX code to simulate the source acquisition with a entire GC detector, i.e. the crystal and the HE hexagonal net. The acquisition energy window is 15% and the number of particles transported in each simulation is 1×10^8

Source: The cylindrical in shape with a radius r is included in the input. It is simulated as water (H 67% and O 33%) with density 1 g cm^{-3} . The source emits photons of 364 keV (81.7%), 637 keV (7.17%) and 723 keV (1.77%) from the surface on the Petri dish (a plane). The distance of the phantom-to-collimator d is included also in the input. The position of the source is sampled uniformly in this surface.

Collimator: The collimator is simulated with the repeated structure capability of MCNP using the FILL, U and LAT cards. The model is illustrated in Figure 1: A hexagonal lattice of apothem 0.27 cm is contained within a lead (Pb 100% with density 11.35 g cm^{-3}) plate of $40 \times 50 \times 5.08 \text{ cm}^3$. Within that hexagon lattice other hexagon lattice of apothem 0.17 filled by void cell is defined.

Figure 1: Representation of the collimator hexagons simulated with MCNPX

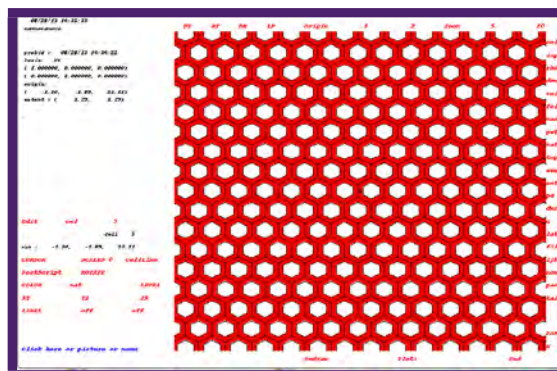
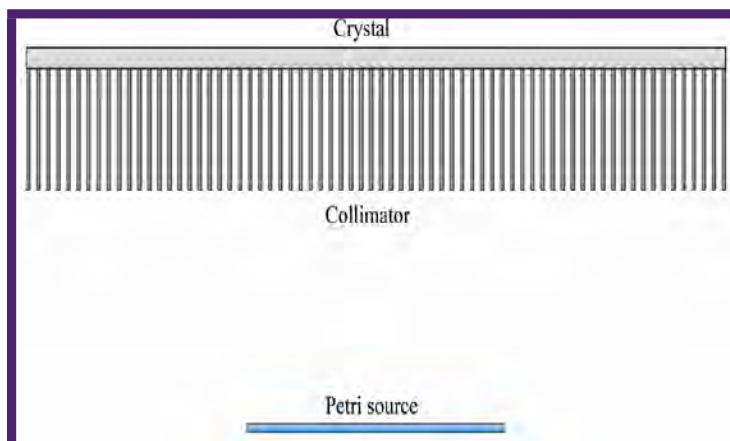


Figure 1:

Crystal detector: The crystal is modeled as other plate of $40 \times 25 \times 0.95 \text{ cm}^3$ of INa (I 50% and Na 50%) with density 3.67 g cm^{-3} .

Figure 2: Cross sectional view of the Petri phantom, the collimator and the INa crystal



2.1 Tally

The mean photon fluence per source particle is determined using *F4* tally (mean track length) in a cell defined in the crystal which volume is the surface of the ROI (SROI) by the crystal thickness (C_{th}). The window used in the experimental measurement 15%, is simulated with 4 energy bins, $[0-10^{-06}]$, $[10^{-06}-0.337]$, $[0.337-0.364]$, $[0.364-0.391]$, and $[0.391-0.8]$ MeV

2.2 Simulation

The MCNP general purpose is to simulate the transport of individual particles (photons in this case) by using a Monte Carlo radiation transport code. The user creates an input file which contains information about the problem to be simulated including geometry, material data and cross section libraries, the location and characteristics of the particle source and the type of quantities or tallies that are to be calculated by the code. The Petri dish phantom, the collimator and the scintillation crystal are modeled to be the same dimensions and materials, as realistic as possible using supplier specifications. In order to simplify the model, some components of the GC as the light guide and photomultipliers isn't included. The backscatter component from FM can be considered negligible. The different parameters that vary from one simulation to another are the distance and the real radius and the variation of ROI size with lesion size and lesion collimator distance.

3 RESULTS AND DISCUSSION

Simulation for obtain geometry factors *G* is repeated changing in the input the variables to each case studied. All vales are represented along with their errors in different diagrams, which depend on the Gamma Camera used. We show the graphs for both systems simulated.

Figure 3: Geometry factors for Skylight system as a function of the activity radius *r* and distance activity HE collimator surface *d*. The bar error are the MCNPX error with 10^9 particles simulated for all sizes

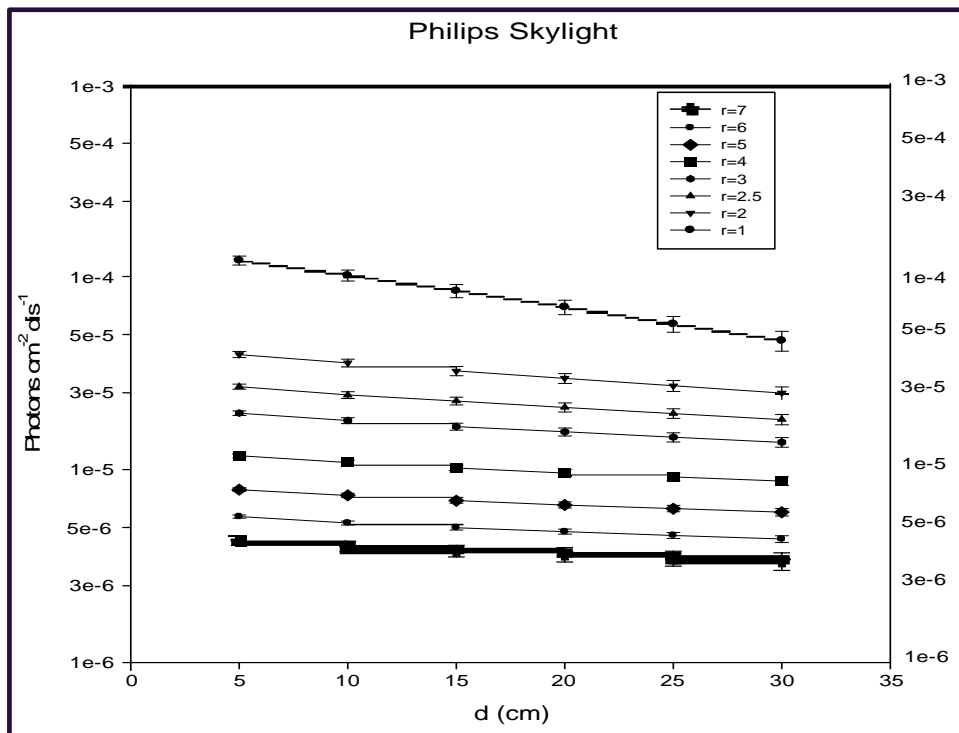
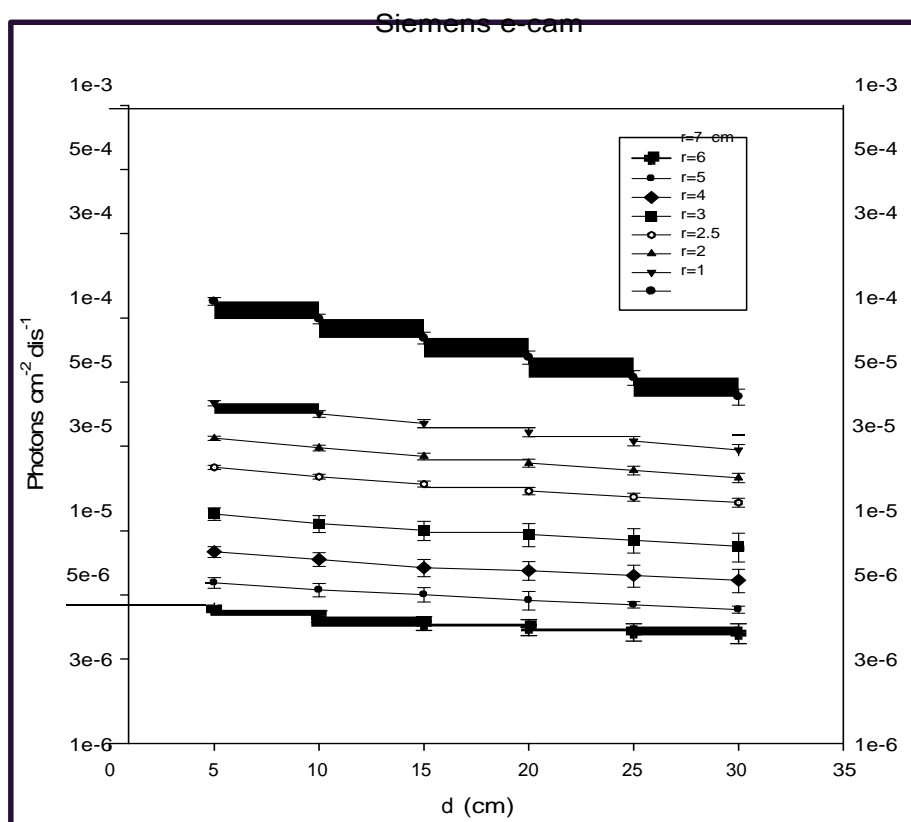


Figure 4: Geometry factors for Siemens e-cam system as a function of the activity radius r and distance activity HE collimator surface d . The bar error are the MCNPX error with 1.5 10⁹ particles simulated for radius 1, 2, 3 cm and 109 for 4, 5, 6 and 7 cm



The range of all results obtained goes from $3.56 \cdot 10^{-6}$ ($\pm 5.17\%$) $\text{photon} \cdot \text{cm}^{-2} \cdot \text{dis}^{-1}$ for $r = 7$ cm and $d = 5$ cm, to $3.03 \cdot 10^{-5}$ ($\pm 11\%$) $\text{photon} \cdot \text{cm}^{-2} \cdot \text{dis}^{-1}$ for $r = 1$ cm and $d = 40$ cm. As can be seen G dependence with d is significant it cannot be ignored in any way.

4. CONCLUSIONS

A new method to quantify the uptake activity in a tumor from a planar image acquired by a GC and ^{131}I has been developed consisting in the calibration of the Gamma camera system with two factors calculated separately, the intrinsic efficiency η_0 and the geometry factor G . In this paper, the procedure to obtain G is defined by Monte Carlo simulations which conducted with MCNPX code allow the accurate characterization of a HE gamma camera for ^{131}I imaging.

5. ACKNOWLEDGEMENTS

Funded by Gerencia Regional de Salud de Castilla y Leon. SPAIN. Project **GRS 1080/A/15 (2015)**

6. REFERENCES

- [1] Peña Sánchez de Rivera, Daniel (2001). "Deducción de distribuciones: el método de Monte Carlo" en Fundamentos de Estadística. Madrid: Alianza Editorial. ISBN 84-206-8696-4.
- [2] MA Ruiz, N Ferrer, D Córdoba, L Alonso, JM Sastre, L Arranz. "Dosimetría de pacientes con cáncer diferenciado de tiroides en tratamiento de terapia metabólica con I-131 a partir de medidas de tasa de dosis externa". Revista de Física Médica.

- [3] EURATOM 2013/59 council directive of 5 December 2013 laying down basic safety standards for protection against the dangers arising from exposure to ionising radiation, and repealing Directives 89/618/Euratom, 90/641/Euratom, 96/29/Euratom, 97/43/Euratom and 2003/122/Euratom.
- [4] Pollard, K.R., Bice, A.N., Eary, J.F., et al., 1992. A method of imaging therapeutic doses of iodine-131 with a clinical gamma camera, *J. Nucl. Med.*, 33, pp. 771–776.
- [5] Shulkin, B.L., Sisson, J.C., Koral, K.F., et al., 1988. Conjugate View Gamma Camera Method for Estimating Tumor Uptake of Iodine-131 Metaiodobenzylguanidine”, *J. Nucl. Med.*, 29, pp. 542-548.
- [6] Dorn, R., Kopp, J., Vogt, H., et al., 2003. Dosimetry-Guided Radioactive Iodine Treatment in Patients with Metastatic Differentiated Thyroid Cancer: Largest Safe Dose Using a Risk-Adapted Approach, *J. Nucl. Med.*, 44:, pp. 451–456.
- [7] NEMA Standards Publication, UN 1-2007. Performance Measurements of Gamma Cameras.

Local Computed Tomography Dose Index and Dose Length Product Values Agree with Published European DRLs

I. Garba^{a*}, A.M. Tabari^b, A. Dare^a, M. Yahuza^b, M. Barde^a, M. Abba^a

^aDepartment of Medical Radiography Bayero University Kano, Kano State, Nigeria

^bDepartment of Radiology Bayero University Kano, Kano State, Nigeria

Abstract. Aim: the study aimed to determine the CTDI and DLP values following head CT with a view of proposing DRLs. Background: modern CT scanners now offer a lot of clinical opportunity. These clinical capabilities have not been without a price, namely a major source of radiation exposure. Dose optimization strategies have been developed. One of such strategies is the use of Diagnostic Reference Levels (DRLs) which serves as a platform upon which radiation workers operate and manage radiation dose to the patient. Methods: this prospective study was conducted in a densely populated centre located in Northern Nigeria. Data was collected from consented patients that presented for a routine head CT. The scans were done on a 4-slice GE Brightspeed scanner. The data was classified based on patient's age. The measured radiation doses in the present study were compared with reported data from the international communities where there are established DRLs. The data was analysed using SPSS version (16) to determine the mean and third quartile values at the 95% confidence interval. Results: The 3rd quartile values of CTDI and DLP for head CT obtained were for: <1 year (27 mGy and 345 mGy*cm), 1-5yrs (48 mGy and 699 mGy*cm), 6-10 yrs (61 mGy and 1011 mGy*cm), 11-15 yrs (65 mGy and 1085 mGy*cm) and >16 yrs (51 mGy and 805 mGy*cm). The values compared well with data reported in the UK, Germany, and Belgium. Conclusion: The study has established radiation dose values for head CT that compared well with reported data in the literature which could be used to propose DRLs for Nigerian population.

KEYWORDS: head CT; DRLs; Northern Nigeria.

1 INTRODUCTION

Since the introduction of computed tomography into clinical practice in 1973, the modality has witnessed dramatic improvement, and the technique continues to increase and expand. The modern CT scanners now offer a lot of clinical opportunity. However, these clinical capabilities have not been without a price, namely a major source of medical diagnostic radiation exposure.¹

Therefore, to allow CT investigation to continue without unnecessary exposing patients to ionizing radiation, dose optimization strategies have been developed which ensure that doses delivered to patients are kept as low as reasonable achievable.² One of such strategies is the use of Diagnostic Reference Levels (DRLs) for different CT examinations, which serves as a platform upon which radiation workers operate and manage radiation dose to the patient.³

DRL is an investigation level used to identify situation where there is unusual high radiation doses for common radiological procedures.^{4,5}

The concept of DRL was first mentioned in the year 1990, in publication 60 of the International Commission on Radiological Protection (ICRP 60). In the year 1996, DRL was recommended in greater detail in publication 73 of the (ICRP 73).⁵

*Corresponding Author; Email Address: igarba.radg@buk.edu.ng
Phone Number: +2348034532750

DRLs allow the identification of abnormally high dose levels by setting an upper threshold at the level of third quartile value. Standard dose levels should not exceed these values when good practice is applied. Excessive radiation doses in CT are not as readily identified through image quality as in standard film-based radiography. This is because CT is a dose dependent modality (i.e. the higher you give the better the image quality and vice versa). Thus, an awareness of typical dose levels allows CT users to quickly identify and address any protocol.³

Therefore, it was recommended that every country investigates the radiation dose values for medical examinations, and establish DRLs. The DRL should be used by regional, national and local authorized bodies. The numerical values of DRL should be advisory, and the concept requires implementation by authorized body.⁵

In line with this, the study aimed to determine the CTDI & DLP with view of proposing DRLs for head CT.

2 METHODOLOGY

This was a prospective study conducted in a tertiary institution located in Northern Nigeria from May, 2013 to April, 2014. Only patients that came for routine brain CT, and consented to participate were taken for the study. Ethical clearance was sought from the research ethical committee. All the scans were done on axial mode. This is because, only axial scan is considered to be ideal for a routine brain CT. All the scans were done on a 4-slice GE Brightspeed scanner. The scanner is equipped with dose description parameters namely the CTDI and DLP. Also, the scanner is calibrated by a medical physicist, and has duly signed acceptance certificates. The information collected from the patients included: age, gender, and weight. Information collected from the CT was: kV, mAs, slice thickness, number of slices, scan time, scan mode (axial), CTDI_w and DLP.

2.1 Protocol for routine adult head CT at the study site

The protocol for routine head CT is design to be in sequential (Axial) mode. The slice group is usually in two batches, namely, batch A for the posterior fossa, and batch B for the cerebrum. In most cases automatic mA is prescribe due to its dose saving effect. The slice thickness is either 1.25, 2.5mm or 3.75mm for the posterior fossa, and 5mm for the cerebrum. A single value for the DLP is obtained by simple adding up the two DLP values displayed on the CT console for the two sections, however this does not apply to CTDI_w. The CTDI_w was obtained using the formula adopted from⁶

$$CTDI_w(average) = \frac{[CTDI_w(1) \times length(1)] \oplus [CTDI_w(2) \times length(2)]}{length(1) \oplus length(2)}$$

CTDI_w (1) = Is the displayed CTDI_w for the posterior fossa

CTDI_w (2) = Is the displayed CTDI_w for the cerebrum

Length (1) = Is the scan length for the posterior fossa

Length (2) = Is the scan length for the cerebrum

The collected data was classified based on patient age. The measured doses in the present study were compared with reported data from the international communities where there are established DRLs. The data was analysed using SPSS version (16) statistical software to determine the mean and third quartile values at the 95% confidence interval.

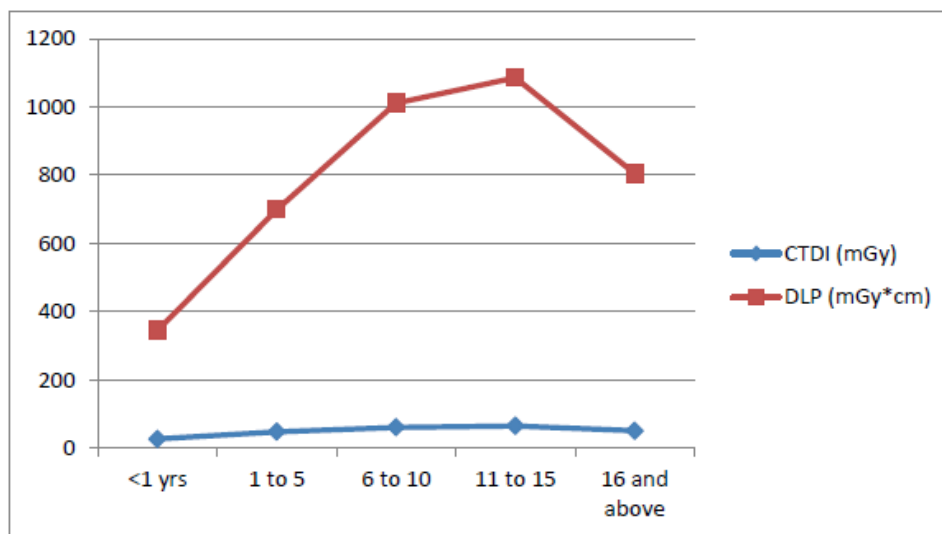
3 DATA ANALYSIS

A total of 37 patients that came for routine brain CT were included in the study. The participants were classified based on age. The 3rd quartile values of the CTDI and DLP were recorded (Table 1 & Figure 1).

Table 1: CTDI & DLP for head CT

Age Group	Dose Parameters	3 rd Quartile Values
<1 yrs	CTDI (mGy)	27
	DLP (mGy*cm)	345
1-5	CTDI (mGy)	48
	DLP (mGy*cm)	699
6-10	CTDI (mGy)	61
	DLP (mGy*cm)	1011
11-15	CTDI (mGy)	65
	DLP (mGy*cm)	1085
16 and above	CTDI (mGy)	51
	DLP (mGy*cm)	805

Figure 1: Obtained 3rd quartile CTDI & DLP data in function of age group (years)



The details of the scan parameters for all the age groups are displayed in Table 2.

Table 2: scan parameters used in the present study

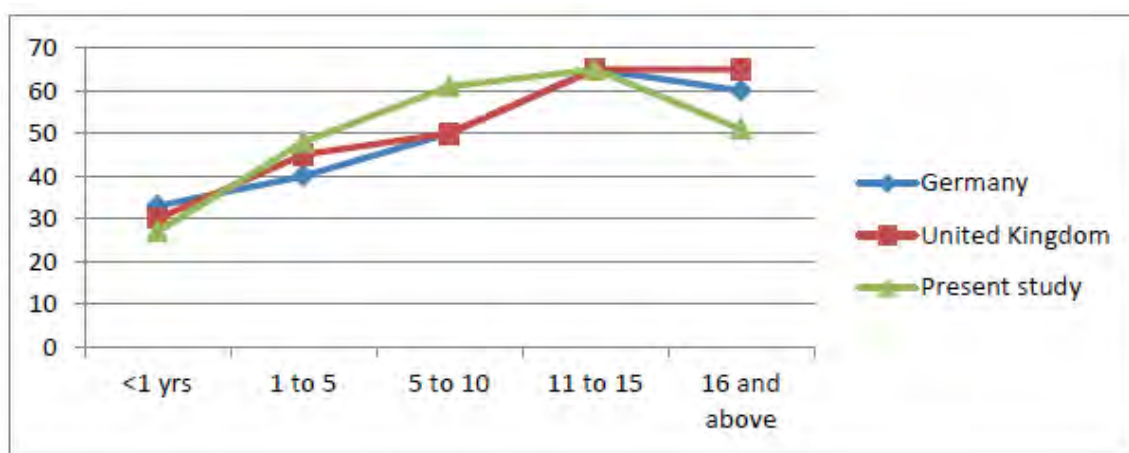
Age Groups	Scan Length (mm) Range (mean)	Number of slices Range (mean)	Slice Thickness (mm)
<1 yrs	110-130 (120)	22-50 (36)	2.5, 5
1-5	125-180 (148)	40-104 (57)	1.25, 2.5, 3.75
6-10	140-165 (155)	48-132 (72)	1.25, 2.5, 3.75
11-15	150-175 (164)	45-64 (55)	2.5, 3.75, 5
16 and above	140-175 (157)	37-55 (42)	2.5, 5
Age Groups	kV Range (mean)	Ma Range (mean)	Weight (kg) Range (mean)
<1 yrs	100-120 (115)	120-200 (161)	4-8 (6)
1-5	100-120 (115)	102-300 (196)	5-15 (10)
6-10	120	230-250 (234)	18-39 (26)
11-15	120	230-300 (250)	21-35 (27)
16 and above	120	200-301 (233)	41-88 (61)

Table 3 & Figure 2 show the characteristics of the CTDI in this study compared with the recent data established in the literature. The results compared well with values published in the literature.

Table 3: Obtained 3rd quartile CTDI (mGy) data in function of age group (years) compared with data reported from other countries.

Age Groups	Present study	Belgium	Germany	United Kingdom
<1 yrs	27	35	33	30
1-5	48	43	40	45
6-10	61	49	50	50
11-15	65	50	65	65
16 and above	51	NA	60	65

NA: Not available

Figure 2: Obtained 3rd quartile CTDI (mGy) data in function of age group (years) compared with data reported from other countries.

4 DISCUSSION

The study determined the CTDI_w and DLP to patients undergoing routine head CT scans in a tertiary centre located in Northern Nigeria. Potential Local Diagnostic Reference Levels were established.

Publications 60 & 73 of the International Commission on Radiological Protection (ICRP) and European Union Directives 93/43 adopted a concept known as Diagnostic Reference Level (DRL) in order to investigate incidences where patient dose during a radiological investigation is unusually high and in urgent need of reduction.⁷ The DRLs help to avoid excessive radiation doses to patients and population and that does not contribute to the clinical purpose of a medical imaging task. As such, in recent years it has become an important entity in the management of radiation doses delivered to the patients in diagnostic and interventional radiology. International, regional and national bodies have shown a keen interest in establishing DRLs.⁷

The radiation dose values obtained in the present study, compared well with values reported in the literature. For the age group <1 year, the study shows slightly lower value. Meanwhile, for age groups 1-5, & 6-10 years the radiation dose values are comparably higher than the values reported (table 3). However, for 11-15 years, the radiation dose value is the same for Germany and UK but higher than that of Belgium.⁸

From the data obtained it has shown that, the CT users adhere to preset protocols in the machine (table 1). This is because the scan parameters and radiation dose values increase with patient's age.

The kV appears to be fixed for <5 years, likewise for those that are >6 years. This indicates, in CT, tube voltage reduction is less straightforward than tube current reduction. Typically, adult CT scans are performed with a tube voltage of 120 kV, and less frequently at 140 kV as shown in the present

study. Meanwhile, the use of reduced tube voltage is frequently advocated for children. Of concern, is the number of slices acquired which is not consistent with the age of the patients scanned. This is likely related to the clinical task at hand, like hydrocephalus being the common indication for pediatrics.

Image quality appears to be acceptable for all the age groups. Even though, the mA value for those that are >16 year is comparably lower than those that are 11-15 years this could be as a results of manual selection of the mA value which may differ between CT users. More so, the number of slices acquired in that age group is comparably lower than other age groups which may be related to the clinical indication, and this could be explained why the radiation dose value is also lower in that age group.

5 CONCLUSION

The study has established dose values of CTDI_w and DLP for head CT using 4-slice GE CT scanner. The values obtained compared well with data reported in the literature which indicate the CT users adhere very well to the preset scan parameters.

6 REFERENCES

- [1] Meeson S., Shrimpton P.C., Hillier M.C., MacLachlan S.A. & Golding S.J. The third UK national CT dose survey, 2010-2011.
- [2] Seeram, C. *Physical Principles, Clinical Applications, and Quality Control*. 3rd Ed. Westline Industrial Drive St. Louis, Missouri: Sounders Elsevier, 2009.
- [3] Foley, S.J., MCentee, M.F. & Rainford, L.A. Establishment of CT diagnostic reference levels in Ireland. *The British Institute of Radiology*, 2012; Vol.85:1390-1397.
- [4] ACR-AAPM. ACR–AAPM Practice Guideline For diagnostic Reference levels And Achievable Doses In Medical X-Ray Imaging, 2013. Available at: www.acr.org/.../Standards-Guidelines/...Guidelines.../guidelines/Reference. [20th April, 2014]
- [5] Cody, D. & McCollough (2011). AAPM summit on CT Dose. Available at: https://www.aapm.org/meetings/.../Cody_DoseNotificationsandDRLS. [20th April, 2014)
- [6] Zarb, F., McEntee, M. & Rainford, L. Maltese CT Doses for Commonly Performed Examinations Demonstrate Alignment with Published DRLs Across Europe. *Radiation Protection Dosimetry*, 2012;150(2):198-206
- [7] Drouet François. *The Diagnostic Reference Levels (DRLs) in Europe*, 2007.
- [8] Bulis, N., Bosmans, H., Mommaert, C., Malchair, F., Clapuyt, P., Everarts, P. CT paediatric doses in Belgium: a multi-centre study, 2010

A Review of Occupational Radiation Exposure among Medical Professionals in Canada (1985 – 2006)

Jing Chen*

Radiation Protection Bureau, Health Canada, 775 Brookfield Road, Ottawa, Ontario, Canada.

Abstract. With increased use of advanced radiation technologies in medicine and a remarkable increase in radiation doses to patients and members of the public in recent decades, it is of special interest in occupational radiation protection to review the trend of radiation exposure among medical professionals. Using the annual reports of the National Dose Registry from 1985-2008, a review of occupational radiation exposure was conducted for six medical job categories: Medical Physicist, Medical Radiation Technologist, Nuclear Medicine Technologist, Radiation Therapist, Radiologist (Diagnostic) and Radiologist (Therapeutic). In the period from 1985 to 1995, annual average doses decreased significantly in all of these categories. In the subsequent 10 year period, annual average doses for nuclear medicine technologists showed a steady increase while the annual average doses for the other five job categories remained practically unchanged. For individuals, most workers received zero dose in a calendar year. The percentages of workers who received positive doses are small in all job categories except for nuclear medicine technologists, where approximately 70% of workers received positive doses. Averaged over 14 years (1993 – 2006), the annual average of positive doses received by nuclear medicine technologists was around 2 mSv while the annual averages of positive doses were below 1 mSv for all other medical professions. Even though annual averages of positive doses among medical professionals are low, individual cases exceeding the occupational annual dose limit did happen occasionally.

KEYWORDS: *occupational exposure; diagnostic radiologist; radiation protection.*

1 INTRODUCTION

Technological advances and innovations in medicine have produced significant benefits to our society. The proliferation of advanced technologies has also led to an increased perception of the need for these technologies for many routine diagnostic procedures, and therefore a remarkable increase in their utilization. As indicated in the United Nations Scientific Committee on the Effects of Atomic Radiation (UNSCEAR) 2008 Report [1], medical radiation constitutes the largest artificial source of exposure to the public, and medical exposure worldwide is increasing quickly. In a recent report, the US National Council on Radiation Protection and Measurements (NCRP) showed a significant increase in average medical radiation doses received by members of the public in the past few decades [2]. The large increase in medical exposure is attributed to the increase in the use of radiological imaging procedures. Two types of medical imaging, computed tomography (CT) and cardiac nuclear medicine examinations, appear to contribute most to this increased exposure. Similar increases in medical use of radiation and associated doses to the patients are also reported in Canada [3, 4]. From 2003 to 2007, the number of CT scanners installed in Canada increased significantly while the numbers of other imaging technologies remained almost constant [3]. In 1991, there were 199 CT scanners installed in Canada. More than fifteen years later, the number of CT scanners had doubled to 419 [2]. Due to the increased availability of CT examination services and an increased use of this imaging modality, the per capita annual effective dose from CT examinations in Canada increased by a factor of about 4 from 0.19mSv in 1991 to 0.74mSv in 2006 [4].

With increased use of advanced radiation technologies in medicine and a remarkable increase in per capita population effective dose in recent decades, it is of special interest in occupational radiation protection to monitor radiation exposure among medical professionals, especially diagnostic radiological technologists [5]. Using annual reports from the National Dose Registry (NDR) [6], average annual effective doses for selected job classes of medical professionals were assessed for roughly the same time period as assessed for the patients in a previous publication [4].

* Presenting author, e-mail: jing.chen@hc-sc.gc.ca

2 SOURCES OF DATA

The NDR has a long and successful history as Canada's repository for occupational dose records. The NDR started collecting data in 1951 and now has records for over half a million workers. Annual reports on occupational radiation exposures in Canada are available on the Health Canada website [6]. These reports provide statistics on occupational radiation exposures of monitored workers in Canada. The statistics are intended to assist regulatory authorities, organizations, and private individuals in comparing incurred occupational radiation exposures with national or provincial/territorial averages and trends in various occupations. This study was prepared using data from a total of 14 reports from 1994 to 2008 [7-20]. In the 1994 Report published in 1995 [7], detailed analyses were given for the year 1994 with comparisons to the data of 1993. Histograms of average annual doses were provided for the period 1985 – 1994, however, without numerical values. The final analysis for 1994 was given in the 1996 Report [8] where numerical values of average annual dose over ten-year periods were given. Starting with the 1996 Report, annual reports provide data on the two consecutive years prior to the year in which the data are extracted from the database. An annual report therefore contains preliminary data analysis on the second year (i.e. more recent year), and more complete data as final analysis on the first year (i.e. the year before the previous year). In this review article only data from final analyses were considered. Final analysis data are available for the period 1985 – 2006.

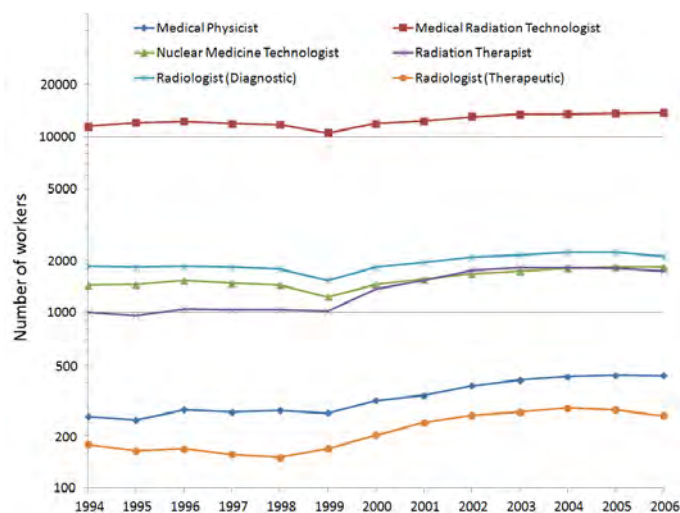
Job category designations are based on a standard list provided by the Registry. For individual workers, the job category is selected by the organization/employer from the standard list. The NDR keeps the most recent job category that an organization submits for a worker in a given year. For the job sector of medicine, this review article considered following 6 job categories: Medical Physicist, Medical Radiation Technologist, Nuclear Medicine Technologist, Radiation Therapist, Radiologist (Diagnostic) and Radiologist (Therapeutic).

For each job category in a calendar year, the total number of workers (N_T) and number of workers with zero doses (N_0) were reported. In addition, an annual collective dose (D_c) was given for each job class. For a job category, the annual average dose (A_D) in the unit of mSv was calculated as D_c/N_T ; the annual average of positive doses (A_{D+}) in the unit of mSv was calculated as $D_c/(N_T-N_0)$.

3 RESULTS AND DISCUSSION

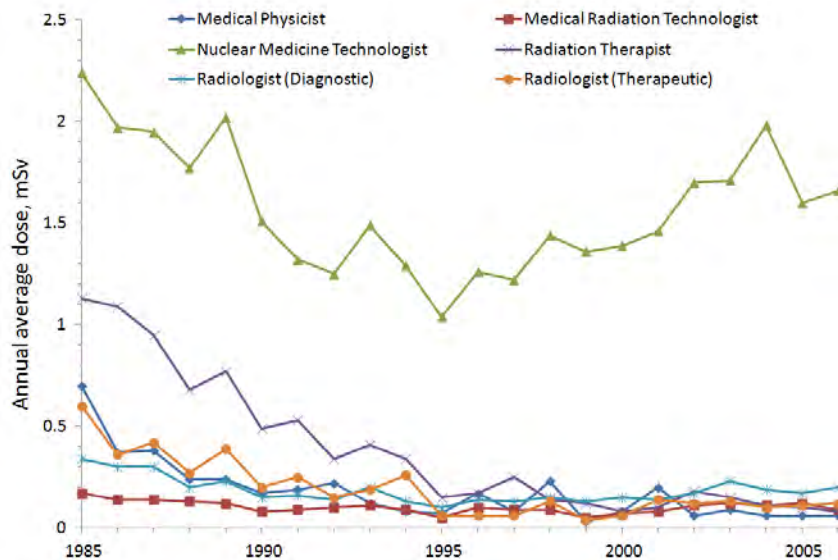
The number of workers in each of the medical job categories considered here is available for the period 1994 – 2006. Results are shown in Fig. 1. Generally speaking, numbers of workers have increased in the recent decade for all six job categories with the most significant increase for therapeutic radiologists, followed by medical physicists.

Figure 1: The number of workers in the six medical job categories from 1994 to 2006.



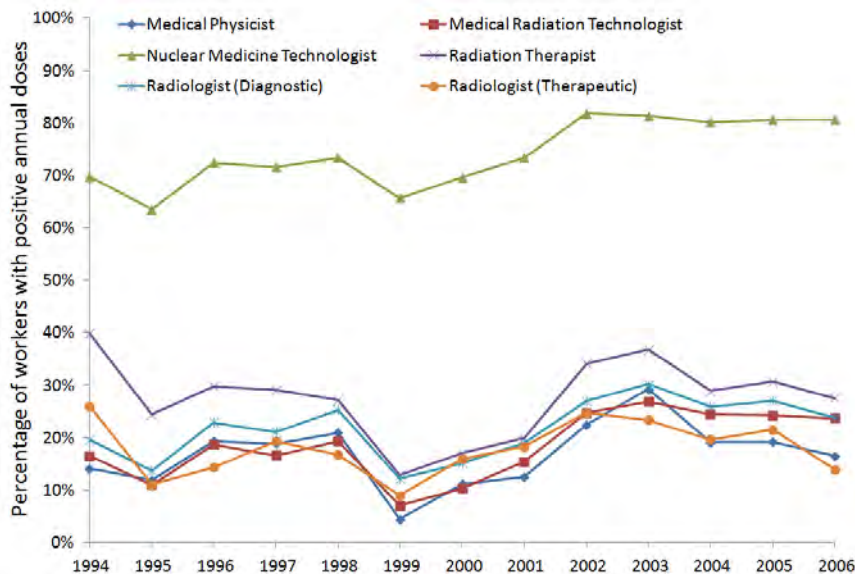
The annual average doses (mSv) are available for the period 1985 - 2006. Results are summarized in Fig.2. Generally speaking, annual average doses decreased over the past 22 years in all medical professions except for nuclear medicine technologists. Nuclear medicine technologists also consistently had the highest annual average dose among the six medical professionals studied here. Of note, in the period from 1985 to 1995, annual average doses decreased significantly among all medical professionals; however, in the subsequent 10-year period, annual average doses for nuclear medicine technologists started to increase significantly while the annual average doses for all other job categories remained practically unchanged.

Figure 2: The annual average doses for six medical job categories from 1985 to 2006.



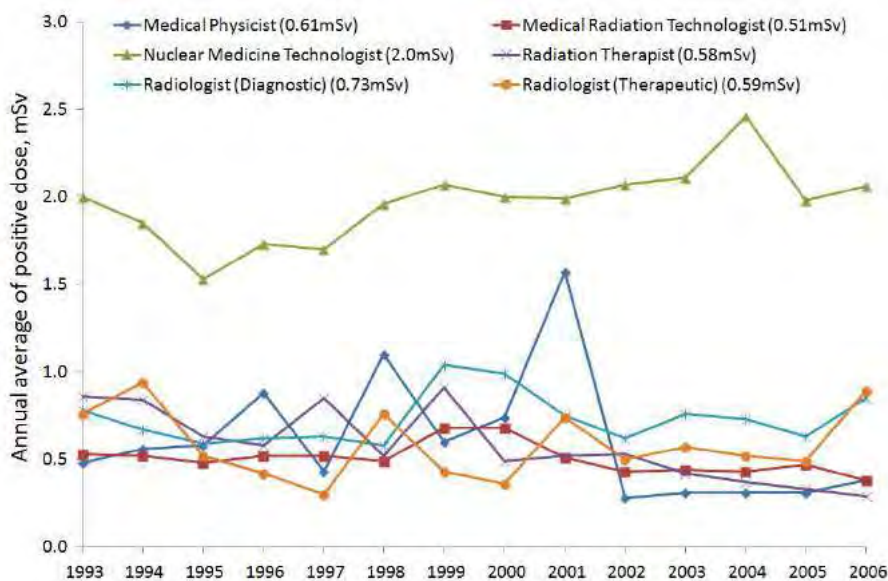
The average annual dose for a job category is the annual dose averaged over the total number of workers employed in that job category in a given year. As can be seen in Fig. 3, most workers received zero dose (doses below detection limit) in a calendar year. The percentages of workers who received positive doses are small in all job categories except for nuclear medicine technologists.

Figure 3: Percentage of workers with positive annual doses for six medical job categories (1994 - 2006).



In radiological protection, what really matters are the annual effective doses received by individual workers. This is especially true for those workers who received positive doses in a calendar year. The annual average of positive doses is calculated using the annual dose, averaged over the number of workers who received positive doses in a calendar year. Figure 4 summarizes the annual averages of positive doses for the six medical job categories from 1993 to 2006. Averaged over 14 years (1993 – 2006), the annual average of positive dose was below 1 mSv for all medical professions except for nuclear medicine technologists. In nuclear medicine, the number of workers receiving positive doses has increased slightly over the past decade (see Fig. 3), and so has the annual average of positive doses for nuclear medicine technologists (see Fig. 4).

Figure 4: Annual average of positive doses for six medical job categories (1993 - 2006). Averages over the 14 years are given in brackets.



For nuclear medicine technologists, the highest annual average of positive doses was 2.5 mSv in 2004 [18]. In that year, there were a total of 1780 nuclear medicine technologists registered in the NDR. Among them, 1427 workers (80%) received positive doses, 615 workers (35%) received positive doses more than the professional group's annual average of 2 mSv, and 5 individuals received doses of more than 50 mSv. Of note, individual doses in excess of 20 mSv/y were rare between 1994 and 2006, (information at this level of detail is not available in annual reports from before 1994). During this time period, the number of nuclear medicine technologists who received doses in the range of 20 - 50 mSv was 1 in 2001 and 2003, respectively. Except for the 5 individuals in 2004, no nuclear medicine technologists received annual doses exceeding 50 mSv.

For the job category of medical physicists, there were significant increases in annual averages of positive doses in 1996, 1998 and 2001. All of these increases were due to one single case exceeding the occupational dose limit; one individual received an annual dose of more than 50 mSv in 1996, one individual received a dose in the range of 20 - 50 mSv in 1998, and one individual received a total dose exceeding 50 mSv in 2001. It can be seen that even though annual averages of positive doses among medical professionals are low, individual cases exceeding occupational annual dose limit did happen occasionally. Occupational radiological protection is still a challenge in some clinical practices.

As mentioned above, the large increase in medical exposure to members of the public is attributed to the increase in the use of radiological imaging procedures. In 1990–1991, there were 199 CT scanners installed in Canada. More than fifteen years later, the number of CT scanners had doubled to 419. It was estimated that there were about 3.4 million CT exams in Canada in 2006 [3]. In comparison to only 37 CT examinations per 1000 Canadians in 1991, this number had increased to 103 in 2006 [3,

4]. While the availability and the use of medical imaging have increased significantly in the recent decades, the total number of medical radiation technologists and diagnostic radiologists registered in the NDR was 15775 in 2006, up only 18% from 13295 in 1994 (see Fig. 1). The per capita population effective dose resulted from CT exams has been found to have increased from 0.19 mSv in 1991 to 0.74 mSv in 2006 for Canada [4]. While the population dose from CT scan alone has increased by a factor of 4 in 15 years, the annual average doses have remained practically steady at 0.09 mSv for medical radiation technologists and 0.16 mSv for diagnostic radiologists during the same period from 1991 to 2006 (see Fig. 2). This is also true for annual averages of positive doses in the period of 1993 – 2006; 0.51 mSv for medical radiation technologists and 0.73 mSv for diagnostic radiologists, as can be seen in Fig. 4.

4 CONCLUSIONS

Generally speaking, annual average doses decreased over the past 22 years (1985 – 2006) in all medical professions except for nuclear medicine technologists. In the period from 1985 to 1995, annual average doses decreased significantly among all medical professionals. In the subsequent 10-year period, annual average doses for nuclear medicine technologists showed a steady increase while the annual average doses for other job categories remain practically unchanged.

The analysis showed that while the population dose from CT scan has increased by a factor of 4 in 15 years, the annual average doses have remained practically steady at 0.09 mSv for medical radiation technologists and 0.16 mSv for diagnostic radiologists during the same period from 1991 to 2006. The International Commission on Radiological Protection (ICRP) is considering protection of patients and staff in most of its recent documents dealing with radiation protection in imaging [21-28]. Led by the ICRP, a global approach to optimise strategies in both kinds of exposures (patients and medical professionals) has been considered in medical practices.

This study showed that most workers received zero dose (doses below detection limit) in a calendar year. The exceptions were often nuclear medicine technologists, about 70% of whom received positive doses. Averaged over 14 years (1993 – 2006), the annual average of positive doses received by nuclear medicine technologists was around 2 mSv while the annual averages of positive doses were below 1 mSv for all other medical professionals reviewed here. Even though annual averages of positive doses among medical professionals are low (well below occupational annual dose limit), individual cases exceeding occupational annual dose limit did happen occasionally. Occupational radiological protection is still a challenge in some clinical practices and more support on occupational issues in the medical field is expected from radiation protection experts in the coming years.

5 REFERENCES

- [1] United Nations Scientific Committee on the Effects of Atomic Radiation, 2010. UNSCEAR 2008 Report to the General Assembly with Scientific Annexes. Annex A – Medical radiation exposures. New York.
- [2] National Council on Radiation Protection and Measurements. 2009. Ionizing radiation exposure of the population of the United States. NCRP Report 160. Bethesda.
- [3] Canadian Institute for Health Information 2008. Medical Imaging in Canada 2007. Available at: https://secure.cihi.ca/free_products/MIT_2007_e.pdf.
- [4] Chen, J., Moir, D., 2010. An estimation of the annual effective dose to the Canadian population from medical CT examinations. *J Radiol Prot* 30, 131-137.
- [5] Vano, E. 2015. Occupational radiation protection of health workers in imaging. *Radiat. Prot. Dodim.* 164, 126-129.
- [6] Health Canada, 2016 Annual reports on occupational radiation exposure in Canada. Available at: <http://www.hc-sc.gc.ca/ewh-semt/pubs/occup-travail/index-eng.php#expose>.
- [7] Health Canada, 1995. Occupational radiation exposures in Canada – 1994. Ottawa
- [8] Health Canada, 1997. 1996 Report on Occupational Radiation Exposures in Canada. Ottawa
- [9] Health Canada, 1998. 1997 Report on Occupational Radiation Exposure in Canada. Ottawa
- [10] Health Canada, 1999. 1998 Report on Occupational Radiation Exposure in Canada. Ottawa

- [11] Health Canada, 2000. 1999 Report on Occupational Radiation Exposure in Canada. Ottawa
- [12] Health Canada, 2001. 2000 Report on Occupational Radiation Exposure in Canada. Ottawa
- [13] Health Canada, 2002. 2001 Report on Occupational Radiation Exposure in Canada. Ottawa
- [14] Health Canada, 2003. 2002 Report on Occupational Radiation Exposure in Canada. Ottawa
- [15] Health Canada, 2004. 2003 Report on Occupational Radiation Exposure in Canada. Ottawa
- [16] Health Canada, 2005. 2004 Report on Occupational Radiation Exposure in Canada. Ottawa
- [17] Health Canada, 2006. 2005 Report on Occupational Radiation Exposure in Canada. Ottawa
- [18] Health Canada, 2007. 2006 Report on Occupational Radiation Exposure in Canada. Ottawa
- [19] Health Canada, 2008. 2007 Report on Occupational Radiation Exposure in Canada. Ottawa
- [20] Health Canada, 2009. 2008 Report on Occupational Radiation Exposure in Canada. Ottawa
- [21] International Commission on Radiological Protection, 2000. Avoidance of radiation injuries from medical interventional procedures. ICRP Publication 85. Ann ICRP 30, 7-67.
- [22] International Commission on Radiological Protection. 2004. Managing patient dose in digital radiology. ICRP Publication 93. Ann. ICRP 34(1).
- [23] International Commission on Radiological Protection. 2007. Managing patient dose in multi-detector computed tomography (MDCT). ICRP Publication 102, Ann. ICRP 37(1).
- [24] International Commission on Radiological Protection. 2007. Radiological protection in medicine. ICRP Publication 105, Ann. ICRP 37(6).
- [25] International Commission on Radiological Protection. 2009. Education and training in radiological protection for diagnostic and interventional procedures. ICRP Publication 113. Ann. ICRP 39(5).
- [26] International Commission on Radiological Protection. 2010. Radiological protection in fluoroscopically guided procedures performed outside the imaging department. ICRP Publication 117. Ann. ICRP 40(6).
- [27] International Commission on Radiological Protection. 2013. Radiological protection in cardiology. ICRP Publication 120. Ann. ICRP 42(1).
- [28] International Commission on Radiological Protection. 2013. Radiological protection in paediatric diagnostic and interventional radiology. ICRP Publication 121. Ann. ICRP 42(2).

The use of the Monte Carlo simulation method for assessing the radiation burden of the hands of workers during some risky manipulations with radiopharmaceuticals

Jana Hudzietzová^a, Marko Fülöp^b, Pavol Ragan^c, Jozef Sabol^d, Povinec, P.^e

^aFaculty of Biomedical Engineering, CTU, Prague, Czech Republic.

^bFaculty of Public Health, SMU, Bratislava, Slovakia.

^cABRS, Ltd., Bratislava, Slovakia.

^dCrisis Management Department, PACR, Prague, Czech Republic.

^eBratislava Ion Technologies, Bratislava, Slovakia.

Abstract. When manipulating radiopharmaceuticals, workers are engaged in some operations which may result in excessive radiation exposure to the skin of their hands. The aim of the paper is related to the Monte Carlo simulation of specific handling operations with radioactive material at nuclear medicine departments and assessing the associated exposure, which is then compared with experimentally obtained data. This approach allows evaluation of the exposure of the entire hand with all necessary details. Such comprehensive information can be obtained neither from the reading of official finger thermoluminescent dosimeters (TLDs), usually worn at the base of one of the fingers, nor from any other special measurements relying on the use of a rather limited number of dosimeters. The problem of the regulatory control of the skin exposure is mainly associated with the unrepresentative readings of the current extremity dosimeters which in most cases considerably underestimate the real skin equivalent dose.

KEYWORDS: nuclear medicine; radiopharmaceuticals; exposure of workers; skin dose; Monte Carlo method; TLD.

1 INTRODUCTION

In order to determine the personal dose equivalent $H_p(0.07)$, which, as an operational quantity, is used to approximate the equivalent dose to the skin, at selected positions, two kinds of phantoms have been used. The measurements were carried out using physical phantoms of the hand, on the surface of thermoluminescent dosimeters (TLDs) were fixed. The geometry of the phantoms corresponded to selected risky operations which most probably would result in higher exposure to the skin. Other phantoms were voxel phantoms, which were created to approximate all relevant properties of the physical phantoms. Using these phantoms, Monte Carlo simulations made it possible to determine the values of $H_p(0.07)$ in the same locations as the positions of TLDs on the physical phantoms. The values of the local exposure obtained from these experiments and simulations were compared with the exposure at the location where the finger dosimeter was placed.

The handling of radiopharmaceuticals by workers at nuclear medicine departments always leads to inhomogeneous exposure of their hands. This exposure can be evaluated by mapping of the dose to the exposed skin on the surface of the hands, and this mapping is carried out by several TLDs fixed at various positions on the hand. Such a process is quite laborious and, to certain extent, it imposes some limitations on the work of the staff. The studies performed under the ORAMED project [1] have proven the usefulness of introducing physical phantoms representing the hands in order to measure the distribution of doses to the hands during the selected risky (characterized by higher exposure) working operations.

Later on, these phantoms were used as models for voxel phantoms intended for the assessment of the hand exposure based on the Monte Carlo method. Altogether, four voxel phantoms under the ORAMED study were created: two of these phantoms simulated various means of administering radiopharmaceuticals by shielded syringes; the third phantom was simulating the administration of radiopharmaceuticals by a worker assisting the patient to drink them from a glass and the last phantom was used to simulate the manipulation with such tools as tweezers, forceps, infusion tube etc. These

four voxel phantoms were also useful for simulating sequences of some more risky operations, including the administration of radiopharmaceuticals to patients.

The use of Monte Carlo simulation, compared to the experimental method, presents some obvious advantages, namely the process is much less time-consuming, the simulation provides complex dose distribution over the surface as well as inside the hand and, at the same time, no radiation exposure of personnel is involved.

In this study, the addition of some specific procedures to two voxel phantoms so that the simulation will include operational procedures associated with the application of radiopharmaceuticals using unshielded syringes has been suggested. Such procedures could be carried out at nuclear medicine departments where the overall patient conditions require application with unshielded syringes. In comparison to the operations with shielded syringes, the exposure of hands with unshielded syringes can result in much higher doses, and these doses have to be quantified in order to introduce relevant radiation protection measures aimed at the reduction of the radiation burden of workers [2].

2 METHODS AND MATERIALS

The analysis of video recordings of a chain of operations involving the administration of radiopharmaceuticals to a patient using unshielded syringes identified some risky operations which are characterized by dominant local exposure received by the personnel. Fig. 1 shows two frequently applied techniques of the administration using an unshielded syringe. For the indirect measurement aimed at skin dose mapping over the hands of workers, physical phantoms made of tissue equivalent material that are adjustable for modelling various ways of handling radiopharmaceuticals were used [3-5]. In the present study, selected simple phantoms simulating fairly accurately the individual investigating operations were applied. They are satisfactory for ensuring a good reproducibility of the measurement and are suitable for the construction of voxel phantoms appropriate for Monte Carlo simulation.

Figure 1: The physical phantom modelling of an unshielded syringe held between the index finger and the middle finger (a) and between the thumb and the index finger (b). The phantoms were made of epoxy resin of mass density of 1.15 g.cm^{-3} corresponding to a mixture of soft and bone tissue of the hands.



In the process of mapping of radiation doses on hands at selected locations there is no guarantee that the maximum exposure of the skin corresponds to the locations where the dose is actually measured. This disadvantage can be overcome by the use of Monte Carlo simulations relying on voxel phantoms which were based on CT images of physical phantoms. Another advantage of Monte Carlo simulations using voxel phantoms is in promptly obtaining the dose distribution on the hands for different geometries and radiopharmaceuticals without being in contact with the source of ionizing radiation. The validation of Monte Carlo simulations was performed using MCNPX code [6] by the comparison with the measurements with physical phantoms (shown in Fig. 1a and 1b) at the positions from C up to K (Fig. 2) injecting ^{18}F FDG.

3 RESULTS

For the purpose of this study, the measurements were carried out at 9 positions on the hands, marked C to K (Fig. 2), where TLDs of the type MCP-Ns were fixed in order to assess $H_p(0.07)$. The Monte Carlo simulation referred to the same positions so that the results could be compared.

Figure 2: The distribution of the TLDs on the surface of the hands (the positions from C up to K were used in this study).



The results given in Table 1 correspond to the administration of FDG using unshielded of 10 ml syringe (Fig. 1a).

Table 1: The comparison of results obtained from the measurement and Monte Carlo simulation.

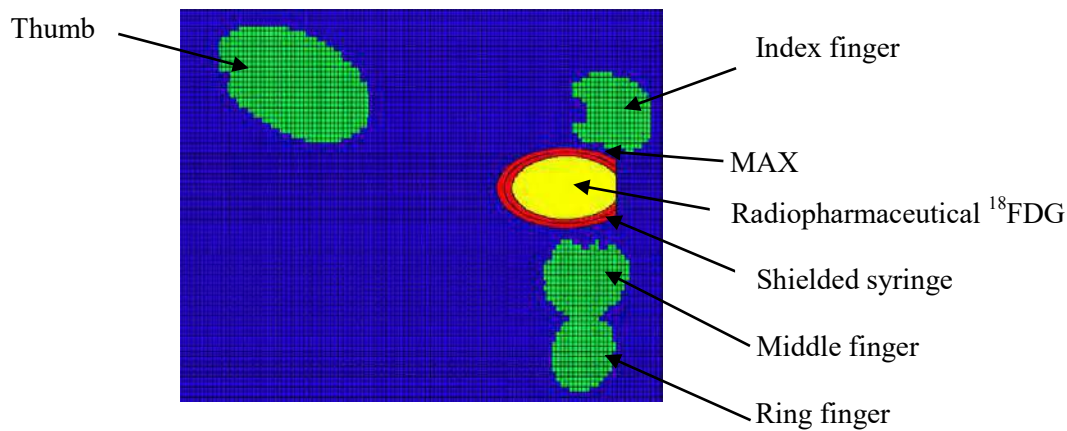
	Position of TLDs	MCP-Ns [mSv]	MCNPX [mSv]	MCP-Ns/ MCNPX
C	Index finger pad	2.27	2.14	1.19
D	Pad of middle finger	2.56	2.20	1.17
E	Pad of ring finger	1.47	1.55	0.96
F	Index finger tip*	4.84	4.79	0.95
G	Middle finger tip*	3.57	4.57	1.01
H	Ring finger tip*	1.93	2.16	1.07
I	Index finger tip **	3.48	2.71	0.84
J	Middle finger tip **	2.94	3.67	0.78
K	Ring finger tip**	1.63	158	1.04

*PS – palm side, **NS – nail side

It can be seen from Table 1 that the relative deviation of the ratio of results obtained from the reading of MCP-Ns and calculated by MCNPX is about 13.8 %. This deviation is within experimental uncertainties reflecting the accuracy of positioning of the dosimeters in locations from C up to K. Their readings are affected by inhomogeneity of the photon and positron fields. Similar results have been obtained from the simulation using the voxel phantom in the geometry shown in Fig.1b.

The use of twin TLDs with different sensitivity for the detection of positrons and photons has shown in [7] that during the administration of FDG by means of an unshielded syringe, some positrons penetrate through the wall of the syringe, the thickness of which is 1 mm. The Monte Carlo simulation enables calculation of the contribution to the dose from those penetrating positrons by comparison the magnitudes of equivalent doses due to local skin exposure at position I (the tip of the index finger on the nail side of the hand) and in the position of the expected maximum exposure (position MAX on the hand holding the unshielded syringe and syringe shielded with a 1 mm layer of polyethylene, Fig. 3).

Figure 3: The cross-section through the fingers of the voxel phantom simulating physical phantom from Fig. 1a where the hand is holding the syringe with additional 1 mm polyethylene shielding. On the cross-section of the forefinger the position of MAX is identified; this position corresponds to the location where the maximum skin exposure occurs.



The ratio of the doses using the unshielded and shielded syringes filled with FDG at locations F (index finger tip, palm side of the hand), I (index finger tip, nail side) and MAX at index finger (Fig. 2 and 3) assessed by MCNPX are shown in Table 2.

Table 2: Simulated source ^{18}F FDG - syringe unshielded/shielded.

Position on index finger	Type of radiation	
	Photons 511keV	Positrons from ^{18}F FDG
MAX	1.09	1.24
F	1.09	1.01
I	0.96	0.99

The positrons penetrating through the wall of a syringe resulted in an increase in the exposure to the skin of the index finger of approximately 15 % (1.24 -1.09) in position MAX. The MCNPX simulations revealed that the value of the equivalent dose $H_p(0.07)$ to the skin at the point MAX is 4.7 times higher than at the point F and about 5.8 times higher than at the point I.

The preliminary results have shown a sufficient agreement between the personal dose equivalent $H_p(0.07)$ obtained by experiments and simulations taking into account the shielding and the geometry of potentially risky operations.

4 CONCLUSION

It has been pointed out on various occasions (e.g., [8]) that there are some problems and inconsistencies associated with the strict use of radiation protection quantities in accordance with the ICRP definitions. This also applies to the quantification of the skin exposure to the hands (in terms of the equivalent dose to the skin) where the relevant dose limit set for regulatory control of exposure of workers is related to the most exposed position on the surface of the hand. This is obviously not known in advance and thus readings obtained from TLDs worn on the index or ring finger are only mere approximations.

Moreover, the finger TLD reading is usually calibrated using the operational quantity of the personal dose equivalent $H_p(0.07)$. In order for this reading to conform to the pertinent dose limit, the monitoring results are supposed to be averaged over 1 cm^2 (in the USA, the relevant area is 10 cm^2 [5]).

In personal monitoring, it would virtually be impossible to comply with this very specific requirement. In addition, another problem may arise due to the unclear definition of the skin dose as an average dose to the skin, which has not been defined as an organ.

Nevertheless, the use of the Monte Carlo simulation presented here can be helpful in assessing how far we are from the ICRP recommendations in practice by relying on finger dosimeters. The simulation of radiation exposure of hands using voxel phantoms allows us to map very accurately skin doses on the hands of a worker handling radiopharmaceuticals. The method does not require using TLDs on the hands or any manipulation of workers with radiopharmaceuticals. In addition, this approach provides detailed information regarding the place on the hands where the exposure reaches its maximum.

The method presented is applicable not only to the departments of nuclear medicine but it can also contribute to determining the exposure to personnel engaged in interventional radiology, where the phantom of a hand can be easily attached to whole-body voxel phantoms. Furthermore, the voxel phantoms described here can simulate various working operations by the hands and can be useful in some research or facilities where the personnel is handling radioactive material, e.g., radiochemistry laboratories, decontamination facilities, radioactive waste treatment plants, etc.

5 ACKNOWLEDGMENT

The study has been prepared with some support provided under the projects SGS15/114/OHK4/1T/17 and APVV-0241-011.

6 REFERENCES

- [1] ORAMED. Optimization of radiation protection of medical staff: Extremity dosimetry in nuclear medicine. EURODAS Report 2012-2. Braunschweig , 2012, pp. 133-177. ISBN 978-3-943701-01-2.
- [2] Ferrari, P. et al.: Main results of the Monte Carlo studies carried out for nuclear medicine practices within the ORAMED Project. *Radiat. Measurements*, vol. 46, 2011, pp. 1287-1290.
- [3] Becker, F., Blunk Ch.: Investigation of radiation exposure of medical staff: measurements supported by simulations with an articulated hand phantom. *Radiation Measurements*, vol. 46, 2011, pp. 1299-1302.
- [4] Blunk, Ch. et al.: Simulation of beta radiator handling procedures in nuclear medicine by means of a moveable hand phantom. *Radiation Protection Dosimetry*, vol. 44 (1-4), 2011, pp. 497-500.
- [5] Ilas, D., Eckerman, K.: Monte Carlo assessments of absorbed doses to the hands of radiopharmaceutical workers due to photon emitters. *Nuclear Technology*, vol. 168, 2009, pp. 164-168.
- [6] Pellowitz, D. B. MCNP User's Manual, Version 2.6.0 - No. LA CP 02 408. Los Alamos , 2007. Online (2016-02-05). Accessible from: http://www.mcnp.ir/admin/imgs/1354176297.2.6.0_Users_Manual.pdf.
- [7] Fülöp, M., Hudzietzová, J., Sabol, J. et al.: A method for the identification of hand exposure by annihilation photons and positrons during the handling of ^{18}F radiopharmaceuticals. *European Journal of Nuclear Medicine and Molecular Imaging*. 2013, vol. 40 (2), p. S236. ISSN 1619-7070.
- [8] Sabol, J. et al.: Letter to the Editor. *Radiation Protection Dosimetry*, vol. 163(2), 2015, p. 267.

Radiation dose optimization in paediatric conventional imaging using automatic dose data management software

Luis Alejo*, Eva Corredoira, Zulima Aza, Rodrigo Plaza-Núñez, Antonio Serrada

Medical Physics Department, La Paz University Hospital, Madrid, Spain

Abstract. The new 2013/59 Euratom directive (ED) requires the registration of individual radiation doses received by patients in paediatric diagnostic imaging; therefore, automatic dose data management software is needed, for which local diagnostic reference levels (DRLs) can easily be obtained. For 10 months of 2014, 11,495 imaging studies were performed using Definium 8000 (General Electric) conventional radiology digital equipment. For application of the ED, all dosimetric and demographic data were registered by the dose management software DoseWatch® (General Electric). The studies were classified according to the various age ranges commonly used in paediatrics. Local DRLs were obtained for the most common exams using the 75th percentile of the population data, and compared with the DRLs proposed by the European Commission (EC). For the age range [0, 1) year and Chest PA/AP exploration, the local DRL exceeded that proposed by the EC by 113%. To perform the consequent dose optimization, an analysis of the causes of the high doses observed was performed using DoseWatch®. The action in room was performed by activating the automatic exposure control and decreasing the predefined kVp. The postprocessing of the images was also adjusted to compensate for the expected image quality decrease. To study this effect, an analysis of the physical image quality in terms of signal-to-noise ratio and high-contrast resolution was performed before and after the action in room. A figure of merit (FOM) was also obtained to study the relationship between dose and image quality. After the optimization process, poorer physical image quality was found, although the FOM was improved. Furthermore, three paediatric radiologists performed a blind test to evaluate possible changes in clinical image quality. No significant differences were found. In conclusion, the dosimetric optimization procedure performed reduced the patient doses below the EC's DRLs in Chest PA/AP exams without significant detriment to clinical imaging quality.

KEYWORDS: *diagnostic reference levels; dose optimization procedure; automatic dose management software; physical image quality; clinical image quality.*

1 INTRODUCTION

Plain film radiography is the most common examination in radiology, representing 74% of all examinations performed in the USA [1]; for example, 129 million chest radiographs were performed in the USA in 2006 [2]. On average, diagnostic radiological examinations carry a higher cancer risk per unit of radiation dose in infants and children compared with adults [3]. The average risk is also higher in infants and young children compared with older children [4]. Following the IAEA and WHO 2012 Bonn call for action recommendations [5], it is therefore imperative that all radiological examinations be justified and optimized with regard to radiological protection for every paediatric patient. To perform dose optimization, the use of diagnostic reference levels (DRLs) is necessary [6]. The Spanish regulation on radiation protection currently in force, the Real Decreto 1976/1999 (RD) [7], requires a minimum of 10 estimates of patient dose to achieve a dose level that can be compared with DRLs. The 2013/59 Euratom Directive (ED) [8], however, requires the registration of all individual radiation doses received by patients in paediatric diagnostic imaging. Therefore, automatic dose data management software is needed, for which local DRLs can easily be obtained. In the application of ED, we used the dose management software DoseWatch® (General Electric) and we obtained local DRLs for the most common examinations performed for various age ranges in a paediatric conventional radiology room in our hospital. These values were compared with the levels of dose obtained applying RD 1976/1999. Because in some cases the local DRLs exceeded that proposed by the European Commission (EC) [9], a dosimetric optimization procedure was performed to reduce patient doses, attempting to not compromise the diagnostic ability of the clinical images. To assess the possible decrease in image quality, both physical and clinical image quality tests were performed.

* Presenting author, e-mail: luis.alejo@salud.madrid.org

2 MATERIALS AND METHODS

2.1 Application of Spanish legislation RD 1976/1999

According to RD 1976/1999, information from 10 standard patients (including age, weight and thickness) was collected during one week in 2014 for the most common examinations performed in a paediatric conventional radiology room of our hospital (Abdomen, Chest PA/AP and AP Pelvis). The equipment used was a conventional dual-panel digital radiography system, Definium 8000 (General Electric). All the patient doses, in terms of entrance surface air kerma ($K_{a,e}$), were obtained through measurements of equipment output performed with an Unfors RaySafe Xi beam analyser (<http://www.raysafe.com>), duly calibrated. A general factor of 1.35 due to the patient's radiation backscatter was applied. The average, median and third quartile $K_{a,e}$ were obtained for all the exams considered, and were compared with the EC DRLs.

2.2 Application of Euratom directive ED 2013/59

According to ED 2013/59, dosimetric and demographic data of 11,495 studies of [0, 16) year-old children, performed during 10 months of 2014, were registered by DoseWatch®. The studies were classified according to the age ranges commonly used in paediatrics. For children under 1 year of age, data were obtained for 3 additional age ranges: [0, 3), [3, 6) and [6, 12) months. The dosimetric information provided by the equipment, in terms of $K_{a,e}$, was verified on a PMMA phantom with a Radcal 10x5-60 (<http://www.radcal.com>) flat ionisation chamber, building thicknesses of 4, 8, 12, 16 and 20 cm (simulating the full range of equivalent paediatric patients). The slab was placed on the table at 100 cm focus-flat panel distance, applying a beam field of 20 cm x 20 cm. The protocol used in the measurements was Chest PA/AP, and automatic exposure control (AEC) was applied. The energy dependence of the resulting correction factor for a constant thickness of 12 cm and beams ranging from 60 to 120 kVp was also evaluated. No anti-scatter grid was used in the measurements. After the dosimetric verification, local DRLs were obtained for Abdomen (317 exams), Chest PA/AP (2213 exams) and AP Pelvis (148 exams) in the age ranges mentioned above, using the 75th percentile of the population data. The local DRLs obtained were compared with the DRLs proposed by the EC. The values of the percentiles and their uncertainties were obtained through a bootstrap algorithm [10], for a confidence interval higher than 95%.

2.3 Optimization procedure

Because the local DRL for children below 1 year of age for Chest PA/AP exceeds that proposed by the EC (see 3.2 Results section), a dosimetric optimization procedure was performed. The optimization process consisted of a step-by-step procedure that started with an establishment of the initial reference state (related to patient dose and physical image quality), continued with the action in room and the establishment of the new reference state (comparing its results with the previous one), and concluded with an analysis of the evolution of the clinical image quality.

2.3.1 Reference state establishment: patient dose and physical image quality

The Chest PA/AP $K_{a,e}$ -corrected values for children younger than 5 years of age, which were obtained in the ED application, were considered the initial dose reference state. The initial reference state of the physical image quality was obtained using the agreed protocols of the DIMOND and SENTINEL European programmes [11], and adapted, in our case, to conventional paediatric radiological procedures. Therefore, a TOR CDR Leeds phantom (<http://www.leedstestobjects.com/>) was placed in the middle of the PMMA thickness during all the measurements (again, building thicknesses of 4, 8, 12, 16 and 20 cm), placing the slab on the table at a constant 100 cm focus-flat panel distance. This setup provides optimal geometry to simulate real clinical conditions. Three acquisitions per slab thickness were performed, and no anti-scatter grid was applied. Automatic exposure control (AEC) mode (at predefined kVp) versus manual mode (at predefined kVp and mAs) in Chest PA/AP exam were considered. The metrics used were the signal-to-noise ratio (SNR) and the high-contrast

resolution (HCSR). A figure of merit (FOM), which indicates the necessary dose to obtain a certain image quality, was also obtained. These parameters are defined as follows:

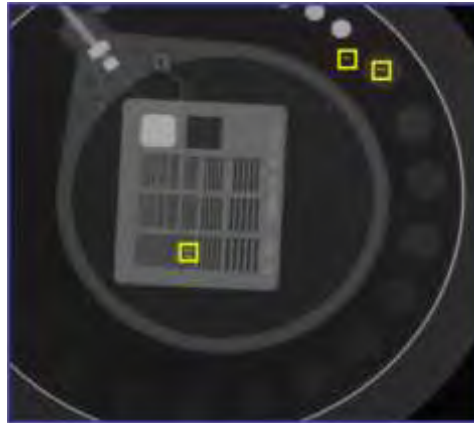
$$SNR = \frac{BG - ROI}{\sqrt{\frac{SD_{ROI}^2 + SD_{BG}^2}{2}}} \quad (1)$$

$$FOM = \frac{SNR^2}{K_{a,e}} \quad (2)$$

$$HCSR = SD_{ROI,7th} \quad (3)$$

where BG is the mean value of the pixels in the region-of-interest (ROI) in the background region (see Figure 1); ROI is the mean value of the pixels in the ROI placed in the first high-contrast circle; SD_{ROI} and SD_{BG} are the standard deviations for ROI and BG; $K_{a,e}$ is the entrance surface air kerma measured with the ionisation chamber placed on the PMMA slab; and $SD_{ROI,7th}$ is the standard deviation of the pixel values of the ROI placed in the 7th group of the bar pattern.

Figure 1: TOR CDR image used to obtain the physical image metrics for a 4-cm PMMA thickness. ROIs in the first high-contrast circle, background (BG) and 7th group bar pattern ROI (ROI 7th) are shown.



2.3.2 Action in room

Prior to performing the action in room, an analysis of the causes of the high doses observed in Chest PA/AP was performed using data provided by DoseWatch®. The consequent reduction of doses was performed, activating the AEC and decreasing the predefined kVp in Chest PA/AP protocol. The post-processing of the images was also adjusted in agreement with the radiologist and the manufacturer's engineer (varying the width and level of the grey window and enhancing the edge detection algorithm), so as not to compromise the diagnostic ability of the clinical images.

2.3.3 New reference state establishment and comparison

During a period of 6 months in 2015 (20 March to 20 September), 14,315 imaging studies of [0, 16) year-old children were performed. Local DRLs were obtained for Abdomen (230 exams), Chest PA/AP (1278 exams) and AP Pelvis (187 exams) in the same age ranges, using the 75th percentile of the population data. New local DRLs were compared with the DRLs proposed by EC and with the reference values obtained before the action in room. Metrics used to evaluate image quality were measured again and compared with the results previously obtained.

2.3.4 Clinical image quality analysis

To evaluate possible changes in clinical image quality in Chest PA/AP exams through the optimization process, 3 paediatric radiologists performed a blind test based on the clinical image quality test published in 1996 by the EC [9], adapted in-home for digital diagnostic images. Eighty Chest PA/AP images of children younger than 5 years of age were randomly selected, thus there were 40 studies before the action in room and 40 after (10 images for each age range considered). These images were anonymised and the acquisition date information was removed. The images were then sent to the PACS system in 3 groups with a different order (chosen randomly) so the paediatric radiologists could evaluate each group without mutual influence. Only the images that met all the following geometric prerequisites were evaluated: visualisation of the anterior ending of the first 5 ribs at the diaphragmatic level (inspiration prerequisite), visualisation of the bilateral ending of most ribs (rotation prerequisite) and visualisation of both lateral costophrenic angles and lung apices (field of view prerequisite). Once accepted, the analysis of the images was divided into 2 sections. The first, *Image Criteria Evaluation*, is a true/false (or seen/not seen) test of 9 anatomic items that should be observed in all the paediatric Chest PA/AP digital images: vascular pattern reproduction (in the two central thirds), trachea, main bronchi, diaphragmatic contours, costophrenic angles, spine, paraspinal lines, retrocardiac lung and mediastinum. Because this is a true/false test, wherein the variable has a low probability of being false, a Poisson model was applied in the framework of generalized linear models with the generalized estimating equations (GEE) method [12]. The model includes radiologists (R1, R2 and R3) and moment (before/after the action in room) as primary effects, as well as their interactions. The second, *General Evaluation*, is a 3-score test (optimum, 2; acceptable, 1; and unacceptable, 0) of 4 general characteristics of the clinical images: contrast, noise, edge visualisation and general diagnostic acceptability. Because all the variables had 3 possible numerical values, a multinomial model was applied, again using a GEE-based method and including radiologists and moment. In all the tests performed, a p-value less than 0.05 was considered statistically significant.

3 RESULTS AND DISCUSSION

3.1 Application of Spanish legislation RD 1976/1999

The average, median and third quartile $K_{a,e}$ of 10 patients for Abdomen, Chest PA/AP and AP Pelvis exams, obtained in application RD 1976/1999, are shown in Table 1. All the dose values obtained were below the EC DRLs; therefore, no radiation protection issue was detected.

Table 1: $K_{a,e}$ of 10 patients for Abdomen, Chest PA/AP and AP Pelvis exams, obtained in application of RD 1976/1999, and compared with EC DRLs. Age, weight and thickness means are also shown.

Type of exam	age (years)	weight (Kg)	thickness (cm)	DRL EC (mGy)		
				$K_{a,e}$ (mGy)		
				average	median	P75
Abdomen AP/PA	10.3	48.9	13.5	1		
				0.94	0.8	0.85
AP Pelvis	8.3	35.4	9.4	0.9		
				0.49	0.48	0.5
Thorax PA/AP	4.7	5.2	5.2	0.1		
				0.05	0.05	0.08

3.2 Application of Euratom directive ED 2013/59 and optimization procedure

The verification of the dosimetric information provided by the equipment, depending on PMMA thickness, is shown in Table 2. The age range equivalent to PMMA thickness is considered. Because the equipment estimates the $K_{a,e}$ for a standard patient (equivalent to 20-cm PMMA), the difference regarding the dose values obtained with the ionisation chamber increases as the PMMA thickness decreases. For paediatric patients younger than 1 year of age, a $K_{a,e}$ correction factor of 0.62 was obtained. For patients between 1 and 5 years of age, the correction factor obtained was 0.71. No significant differences were found when varying the energies from 60 to 120 kVp (CV less than 2%).

3.2.1 Patient dose reference state establishment

Table 3 shows local DRLs for Abdomen, Chest PA/AP and AP Pelvis, in the age ranges considered, obtained with DoseWatch® in application of ED 2013/59. All the dose values were compared with the DRLs proposed by EC. Children younger than 3 months of age were considered newborn. From 3 months to 5 years of age, EC DRLs corresponding to 5 years of age were applied. The local DRLs obtained were lower for all the exams and age ranges considered, except in Chest PA/AP for children younger than 1 year of age; here, the local DRLs were 60% higher. For the newborn babies, the local DRL obtained was 113% higher. This feature was not observed in the application of RD 1976/1999, probably due to the small sample used.

Table 2: Verification of the patient dose data shown by the X-ray equipment, depending on the PMMA thickness, compared with ionisation chamber dose measurements.

PMMA thickness (cm)	age range equivalent (years)	kV	mAs	$K_{a,c}$ (mGy) Definium 8000	$K_{a,c}$ (mGy) RADCAL	Δ (Definium 8000 - RADCAL) (%)
4	[0, 1)	70	0.45	0.04	0.02	62.01
8	[1, 5)	70	0.77	0.07	0.05	41.24
12	[5, 10)	80	0.97	0.12	0.09	28.81
16	[10, 16)	82	1.75	0.23	0.20	16.16
20	[16, 20)	82	3.47	0.45	0.43	3.57

Table 3: Local DRLs for Abdomen, Chest PA/AP and AP Pelvis, in terms of $K_{a,c}$, obtained applying ED 2013/53 before the optimisation process, and compared with the EC DRLs. The red box highlights values higher than the EC DRLs.

Type of exam	Age range	number of exams	$K_{a,c}$ DRL EC (mGy)*	$K_{a,c}$ Local DRL (mGy)
Abdomen	[0, 3) months	42	-	0.67 ± 0.02
	[3, 6) months	25	1.00	0.67 ± 0.60
	[6, 12) months	41	1.00	0.67 ± 0.19
	[1, 5) years	209	1.00	0.77 ± 0.01
AP Pelvis	[0, 3) months	1	0.20	not enough data
	[3, 6) months	19	0.90	0.38 ± 0.14
	[6, 12) months	18	0.90	0.38 ± 0.16
	[1, 5) years	110	0.90	0.45 ± 0.01
Chest PA/AP	[0, 3) months	122	0.08	0.17 ± 0.02
	[3, 6) months	99	0.10	0.16 ± 0.01
	[6, 12) months	328	0.10	0.16 ± 0.01
	[1, 5) years	1664	0.10	0.049 ± 0.003

* Children below 3 months of age were considered newborns. From 3 months to 5 years of age, EC DRLs corresponding to 5 years old were applied.

3.2.2 Action in room

Because the Chest PA/AP local DRLs for children younger than 1 year of age exceed that proposed by the EC, a dosimetric optimization procedure was mandatory. An analysis of the causes of the high doses observed using DoseWatch® revealed the following:

- For children who cannot stand by themselves (usually younger than 1 year of age), Chest PA/AP explorations were performed on table in manual mode.
- Predefined kV and mAs were similar to wallstand acquisitions. The acquisitions were performed at 100 cm focus-flat panel distance (table), however, instead of 180 cm (wallstand). Predefined kVp and mAs were typically not adjusted before acquisition.

As previously noted, the main action in room performed was to reduce the predefined kVp in Chest PA/AP exams and to apply the AEC for children younger than 5 years of age (thin patients). The post-processing of the images was also adjusted so as not to compromise the clinical image quality.

3.2.3 New reference state establishment and comparison

Table 4 shows the new local DRLs for Chest PA/AP exams, obtained after the action in room. Again, the dose values compared with the DRLs proposed by the EC were similar or lower for all the age ranges considered. The reduction in dose obtained for children younger than 1 year of age was approximately 60%.

Table 4: Local DRLs for Chest PA/AP, in terms of $K_{a,e}$, obtained after the action in room, compared with the EC DRLs. The blue box highlights optimised values.

Type of exam	Age range	number of exams	$K_{a,e}$ DRL EC (mGy)*	$K_{a,e}$ Local DRL (mGy)
Chest AP/PA	[0, 3) months	80	0.08	0.08 ± 0.04
	[3, 6) months	66	0.10	0.06 ± 0.04
	[6, 12) months	205	0.10	0.07 ± 0.04
	[1, 5) years	927	0.10	0.06 ± 0.02

* Children below 3 months of age were considered newborns. From 3 months to 5 years of age, EC DRLs corresponding to 5 years old were applied.

The $K_{a,e}$ distributions obtained for children younger than 1 year of age before and after the action in room, compared with the DRLs proposed by the EC, are shown in Figure 2. In all the boxplots, the whiskers represent the lowest datum within the 1.5 interquartile range (IQR) of the lower quartile, and the highest datum within the 1.5 IQR of the upper quartile (Tukey boxplot). After the action in room, the reduction of the patient doses is clear: 50% of the $K_{a,e}$ values were now below the EC DRLs in all the age ranges considered. More outliers were observed before the action in room, perhaps due to unusual changes in the predefined kVp and mAs performed by the technicians in manual mode. In terms of statistical dispersion, no effect of the AEC system applied after the action in room was clearly observed for children younger than 1 year of age: in children [0, 3) months the dispersion was high, but in children [6, 12) months of age the dispersion was lower. A weight-based boxplot study could represent this effect, if any.

Figure 2: $K_{a,e}$ distributions before (red) and after (blue) the action in room for Chest PA/AP exams in the age ranges considered: a) [0, 3) months of age, b) [3, 6) months of age, c) [6, 12) months of age. The red lines represent the EC DRLs.

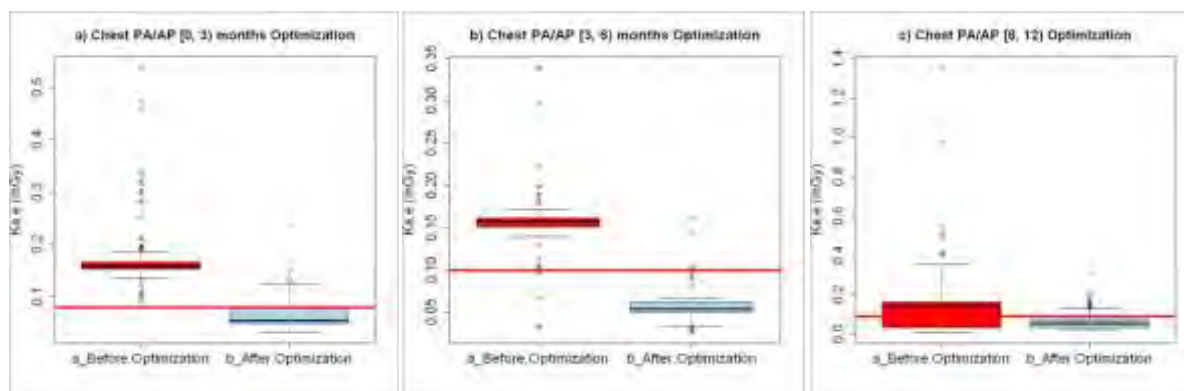


Figure 3 shows the HCSR and SNR parameters of the physical image quality depending on the slab thickness, obtained before and after the action in room. A coverage factor of $k=2$ was applied in the uncertainties estimation. Although a good correlation was observed in the exponential fit of both parameters, especially for HCSR in manual mode ($R^2 > 0.98$), a poorer correlation was observed after the action in room because the AEC system attempts to keep the image quality constant. For a 4-cm PMMA thickness, equivalent to children younger than 1 year of age, poorer image parameter values were found after the action in room. This was an expected result, because after the activation of the AEC system the patient doses involved were lower.

Figure 4 shows the relationship between physical image quality and dose to the patient, obtained in terms of FOM before and after the action in room. Again, a coverage factor of $k=2$ was applied in the uncertainties estimation. Despite the poorer image quality observed after the action in room, the FOM is higher for a 4-cm PMMA thickness because the patient doses involved were much lower. The FOM had shrunk however, from 8-cm PMMA thickness, yielding values next to zero. This feature could be due to the high noise obtained in large thicknesses because no anti-scatter grid was used in the measurements. Likewise, as focus-flat panel distance was always constant and the PMMA thickness was increasing, the TOR phantom, placed in the middle of the slab, was moving away from the image detector, causing a loss of image quality.

Figure 3: Physical image quality depending on slab thickness in terms of HCSR (left) and SNR (right), obtained before and after the action in room.

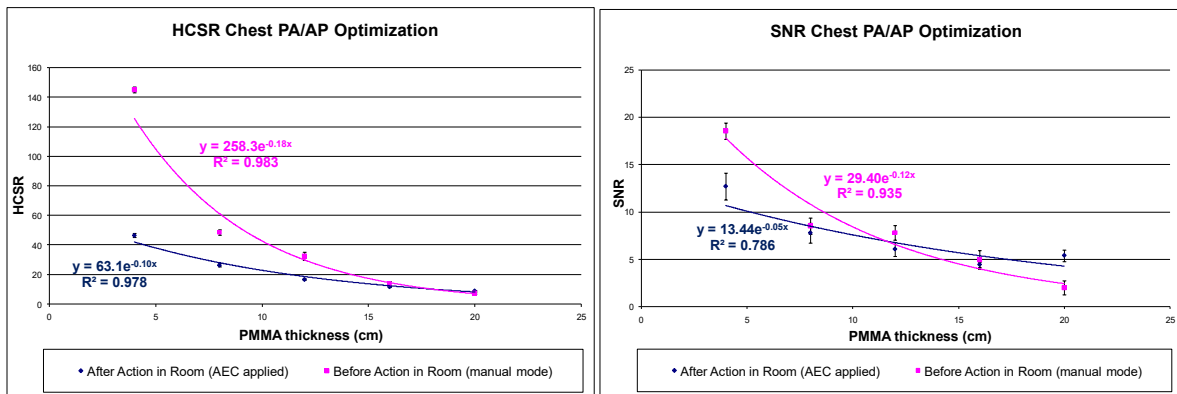
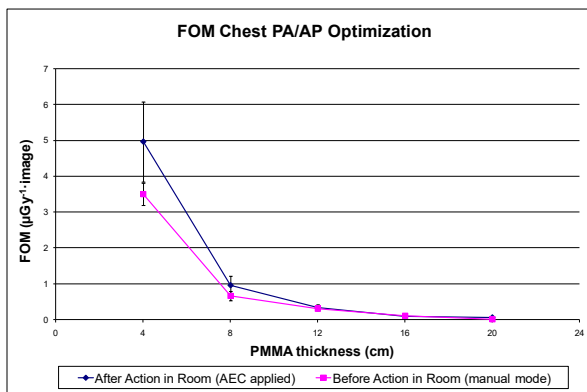


Figure 4: Relationship between physical image quality and dose to the patient, obtained in terms of FOM before and after the action in room.



3.2.4 Clinical image quality analysis

The first clinical image quality test performed, *Image Criteria Evaluation*, showed that only in the visualisation of the costophrenic angles were statistically significant differences observed before and after the action in room (contours seen in 98% of images before and 91% after, $p=.045$). This could be due to the existence of pulmonary diseases in selected images. The results of the second test performed, *General Evaluation*, were as follows: In the contrast evaluation no significant differences were found before and after the action in room (45.1% optimum contrast before and 57.9% optimum contrast after; with $p=.152$), although a different method of evaluating the contrast was observed between radiologists ($p<.001$). As with the physical image quality test, there was a statistically significant increase in the noise perception after the action in room for two radiologists (88.6% optimum noise before vs. 53.2% optimum noise after, with $p=.001$ for R1; 74.3% vs. 46.7%, $p=.021$ for R2), although R3 did not find significant differences (31.2% optimum noise before and 48% after; $p=.267$). In the edge visualization, no significant differences were found (64.7% optimum perception

of edges before the action in room vs. 75.8% after; $p=.08$), although the distribution was pointed towards better ratings. Similar to the contrast evaluation, a different method of evaluating the edges was observed between radiologists ($p<.001$). The results of the general diagnostic acceptability test depended on the radiologists: for R1 and R3 no significant differences were found (77.1% optimum acceptability before the action in room vs. 75.0% after, $p=.837$ for R1; 31.2% before vs. 54.5% after, $p=.129$ for R3); although for R2 poorer general diagnostic acceptability was found after the action in room (88.6% before and 60.0% after; $p=.01$). In summary, the clinical image quality analysis was able to detect the action in room, with a higher noise perception and a possible decrease in the general acceptability of images. However, the evaluation of the image criteria showed that the clinical image quality was not compromised in the images obtained after the action in room. To evaluate the diagnostic ability of the clinical images, further multireader and multicase receiver operating characteristic studies could be necessary to account for a binary “diseased” or “not diseased” decision.

4 CONCLUSION

Automatic dose data management software is needed to accomplish the new ED, and establishing local DRLs and performing dosimetric optimization procedures is useful. Using that software, important radiation protection problems can be detected that might otherwise go unnoticed. An ionisation chamber verification of the dosimetric information provided by the equipment and shown by the software is necessary because significant variations in the dose can be observed. To ensure that the optimization process has not compromised the diagnostic quality of the images, it is advisable to perform at least a physical and clinical analysis of the image quality.

5 ACKNOWLEDGEMENTS

We would like to thank Drs. Consuelo Prieto, Montserrat Bret and Manuel Parrón, of the Paediatric Radiology Department, as well as Rosario Madero, of the Biostatistics Department, of La Paz University Hospital. Likewise, we would like to acknowledge to General Electric’s technical support for the DoseWatch® and Definium 8000. This study was funded by the Spanish Nuclear Safety Council.

6 REFERENCES

- [1] NCRP National Council on Radiation Protection and Measurements, NCRP Report 160 (2009) Ionizing Radiation Exposure of the Population of the United States. NCRP Publications, Bethesda, MD.
- [2] Don, S. et al., 2011. Image Gently pediatric digital radiography summit: executive summary. *Pediatr. Radiol.* (2011) 41:562-565. DOI 10.1007/s00247-010-1966-2.
- [3] ICRP, 2013. Radiological protection in paediatric diagnostic and interventional radiology. ICRP Publication 121. *Ann. ICRP* 42(2).
- [4] Preston, D. L., Ron, E., Tokuoka, S., et al., 2007. Solid cancer incidence in atomic bomb survivors: 1958-1998. *Radiat. Res.* 168, 1-64.
- [5] Bonn 2012 call for action. International Atomic Energy Agency (IAEA) and World Health Organization (WHO). “International Conference on Radiation Protection in Medicine: Setting the Scene for the Next Decade”, Bonn, Germany, December 2012. https://rpop.iaea.org/RPOP/RPoP/Content/AdditionalResources/Bonn_Call_for_Action_Platform/index.htm
- [6] European Community (EC). Guidance on diagnostic reference levels (DRLs) for medical exposure. Radiation Protection n°109. Luxemburg: European Commission. Directorate General Environment, Nuclear Safety and Civil Protection. Radiation Protection. 1999.
- [7] Real Decreto 1976/1999, de 23 de diciembre, por el que se establecen los criterios de calidad en radiodiagnóstico. BOE n° 311 de 29/12/1999.
- [8] Directive of 5 December 2013 (2013/59/Euratom) laying down basic safety standards for protection against the dangers arising from exposure to ionising radiation. Official Journal of the European Union, 2013/59/Euratom, 17.01.2014.

- [9] European Commission Directorate-General XII-Science. Research and Development. "European Guidelines on Quality Criteria for Diagnostic Radiographic Images in Paediatrics". Office for Official Publications of the European Communities, 1996.
- [10] Efron, B. Bootstrap methods: Another look at the jackknife (1079). *The Annals of Statistics* 7 (1): 1–26. doi:10.1214/aos/1176344552.
- [11] Vano, E., Ubeda, C., Leyton, F., Miranda, P. Radiation dose and image quality for paediatric interventional cardiology. *Phys. Med. Biol.* 53 (2008) 4049–4062. doi:10.1088/0031-9155/53/15/003.
- [12] Hanley, J.A. et al. Statistical analysis of correlated data using generalized estimating equations: an orientation. *Am J Epidemiol.* 2003 Feb 15;157(4):364-75.

Practical Lessons for a Dosimetry Program

Michelle Baca*, Chad Hopponen

Mirion Technologies, 2652 McGaw Ave, Irvine, CA, USA.

Abstract. This paper intends to facilitate dosimetry familiarization for users of passive dosimetry with several lessons learned and associated practical applications, as identified by a high volume commercial dosimetry processor. Key considerations, discussions, and examples are included in the paper to facilitate a foundational understanding include:

- Impact of assumptions on final dose (by customer and vendor)
- Incorrect field characterization or incorrect dosimeter selection (selecting the wrong “tool” for the job)
- Background and control badge variances
- Challenges with take-home and on-site storage of Dosimetry
- Abnormal readings due to incorrect placement of dosimeters
- Record of Dose control
- Regulatory changes

As with any relationship involving a customer and a vendor, the key to success is communication. Almost all instances of dose reporting errors could be traced back to a failure to communicate; either by the customer or the vendor. There are many elements to a successful dosimetry program, and in many cases, the vendor is willing to work with the customer to ensure those programmatic elements are in place. Routine validation of assumptions by both the customer and the vendor is paramount for a quality program and the assessment and assignment of an accurate dose.

KEYWORDS: *Dosimetry program development; dosimeter care; dosimeter considerations.*

1 INTRODUCTION

Mirion, as a dosimetry provider issuing over 2 million dosimeters annually, encounters a variety of issues common to many dosimetry programs. These issues are typically addressed on an individual customer level basis, a more pragmatic approach would be to supply these lessons learned on a larger scale. Sharing this information can better equip users of dosimetry to understand practical applications and, in some cases, the physical limitations of their chosen dosimetry system. This paper will discuss some issues customers may experience within their program; utilizing test data to show the potential impact of these issues on dose results, as well as highlight some possible solutions or preventative measures.

2 GENERAL

2.1 Impact of assumptions on final dose assigned (by customer and vendor)

Account set-up is an important factor for final dose assessment. At the initiation of the account, the vendor and the customer should have a discussion regarding the needs of the customer. Many of the mistakes in account set up stem from inappropriate assumptions; therefore, it is prudent for a customer to periodically verify that assumptions (examples listed below) are still appropriate and meet the customer’s needs.

2.1.1 Expected source(s)

Most vendors will have a default source to which all their dosimeters are calibrated to, typically cesium-137 (Cs-137) or cobalt-60 (Co-60). If the expected source of exposure is significantly different in radiation type or energy, the final dose assessment could similarly be different than that which is

* Presenting author, e-mail: mbaca@mirion.com

expected. Figure 1 shows the relative photon energy response for two types of lithium-fluoride (LiF) substrate compared to Cs-137, and Table 1 shows the potential impact of incident radiation energy response on the final dose assessment. In this particular example, both types of LiF have an over-response for lower energy photons (x-rays); some method of energy correction is necessary to properly assess the dose. If the correct source, or appropriate correction factor, is not properly referenced, the reported dose assessment could be as much as 50% higher than the true dose.

Figure 1: Photon energy response relative to Cs-137 for two types of LiF substrate (LiF: Mg,Ti,P and LiF:Cu,Mg)

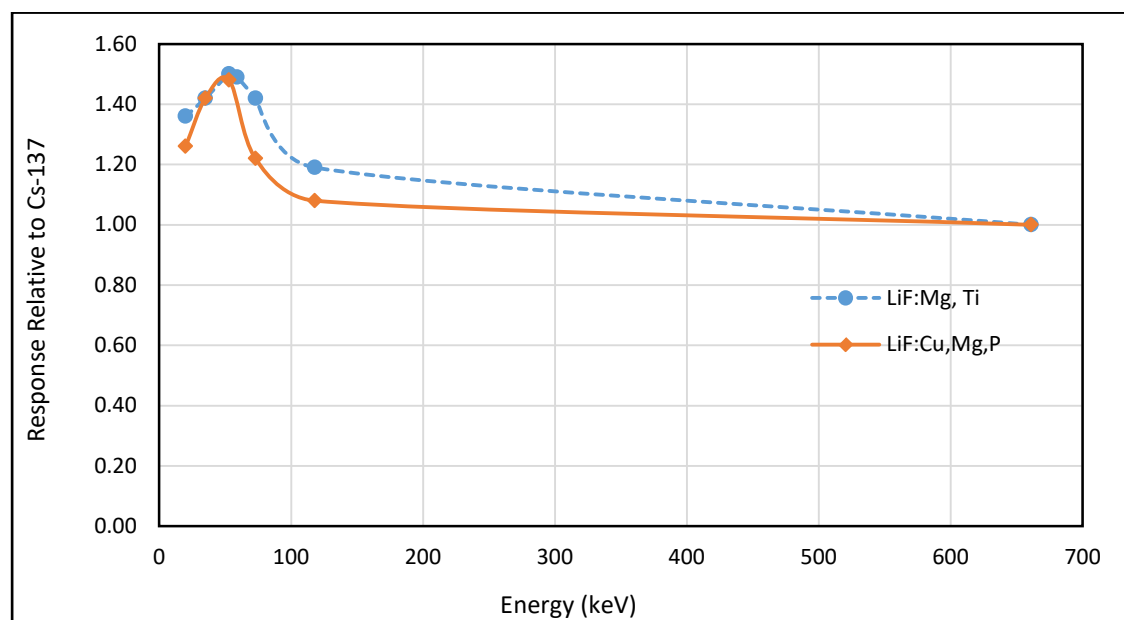


Table 1: Approximate dose impacts using Cs-137 as the radiation source incorrectly

Energy of Incident Photon (keV)	Dose with Proper Energy Correction	Dose without Proper Energy Correction	Difference in Reported Dose and True Dose
20	1.00	1.36	+36%
35	1.00	1.42	+42%
53	1.00	1.50	+50%
59	1.00	1.49	+49%
73	1.00	1.42	+42%
118	1.00	1.19	+19%
661	1.00	1.00	0

2.1.2 Dose calculation methods

Vendors provide a multitude of dosimeter options for monitoring organ specific, extremity specific, single whole body, and multiple whole body dosimeters. The use of multiple dosimeters to determine an Effective Dose Equivalent (EDE) requires a full and clear understanding of instructions by the vendor for the customer regarding how, when, and where each dosimeter is to be worn. Typical instructions to determine EDE for medical staff include wearing an unshielded dosimeter, often on the outside of a thyroid shield (collar), and a shielded dosimeter, normally under a leaded apron (whole body); both dosimeters *must* be worn together, in the correct orientation and location, returned at the same time, and ultimately processed with a common control dosimeter for the calculation to be accurate. One example of an EDE calculation is the Webster calculation, which calculates H_E and

assumes H_1 is the whole body (WB) dosimeter worn under an apron and H_2 is a collar (CL) dosimeter worn over the thyroid shield [1]:

$$H_E \cong 1.5H_1 + 0.04H_2 \quad (1)$$

Some regulators do not recognize practices such as EDE; in such instances, the customer should work with the vendor at account set-up to confirm regulatory requirements regarding what body regions require monitoring and what dose limits are applicable. Table 2 provides an example of a customer that did not return the two dosimeters (collar and whole body) at the same time resulting in an erroneous dose. If the dosimeters been returned at the same time, a single report would have been issued, using the Webster calculation (typical EDE calculation) in the final dose assessment. However, in this particular case, two reports were issued, with one report showing a final dose assessment which exceeded regulatory limits.

Table 2: Dose discrepancy due to customer return error

	Initial CL (Uncorrected)	Report Dose WB (Uncorrected)	Report Dose (Combined Reports)	Total Dose EDE Webster (Corrected)	using
Deep Dose (mSv)	54.21	3.05	57.26	6.74	
Shallow Dose (mSv)	61.30	3.42	64.72		

2.2 Incorrect field characterization or dosimeter selection

2.2.1 Dosimeter selection considerations

As stated in section 2.1, the reference source can have a profound influence on the final dose assessment. Familiarity with the dosimeter capabilities, in conjunction with a well-defined source term, will assist greatly in choosing a dosimeter that will provide the best possible results. Table 3 provides some common dosimeter technologies and their detection capabilities by radiation type.

Table 3: Dosimeter capabilities listed by dosimeter type

Dosimeter Type	Detection Capability							
	Low- Energy Photon (<20 keV)	Low- Energy Beta (<20 keV)	Medium Energy Photon (<100 keV)	Medium Energy Beta (<100 keV)	High Energy Photon (>100 keV)	High Energy Beta (>100 keV)	Thermal Neutron s (eV)	Fast Neutrons (>200 keV)
LiF-Nat	x	(a)	x	x	x	x	x	-
LiF: Mg,Cu,P	x	(a)	x	x	x	x	(b)	-
LiF:Mg,Ti	x	(a)	x	x	x	x	(b)	-
CaSO ₄	x	(a)	x	x	x	x		-
LiBO	x	(a)	x	x	x	x	(b)	-
CR-39		-	-	-	-	-	-	x
OSL (BeO)	x	(a)	x	x	x	x	-	-
OSL (Al ₂ O ₃)	x	(a)	x	x	x	x	-	-

^(a) Is capable of detection; requires additional considerations for monitoring

^(b) Requires appropriate species of lithium

Many dosimeters have noted poor performance for low and medium energy betas. For those customers routinely exposed to isotopes similar to promethium-147 (Pm-147) with an average beta energy of 62

keV and krypton-85 (Kr-85) with an average beta energy of 252 keV, monitoring methods must be considered during account set-up for the adequacy of the dosimeter chosen.

The lower limits of detection (LLD) for the dosimeter must also be taken into consideration. The LLD for a dosimeter is often vendor, dosimeter, and wear-period specific. For example, CR-39/Track etch dosimeters typically cannot discern any dose less than 0.2 mSv, thermal-luminescent (TL) dosimeters have a typical LLD of 0.1 mSv. Reporting of doses below the LLD is not considered an accurate measurement due to statistical uncertainties. Individuals should guard against using a dosimeter with an LLD that is greater than the desired or required limits for reporting (in all cases, minimum reporting level should be greater or equal to the LLD).

2.2.2 *Field characterization considerations*

Errors in dose assignment will presumably be introduced when incorrectly or incompletely characterizing the source term. As illustrated in Table 3, an individual working in a wide spectrum neutron field should not use CR-39 as a sole means for monitoring; contrariwise, an individual working with x-ray equipment producing a near mono-energetic photon field could easily use a single dosimeter technology for monitoring. Of note, there are often specific definitions to types of dosimeters and consideration for the intended method of monitoring is important. As outlined in the example below, environmental dosimeters are used to monitor environmental or background radiation. These dosimeters are inappropriate choices if using them to assess dose for monitored individuals; these dosimeters do not have standards that allow for such an assessment. Area monitoring dosimeters are dosimeters that are accredited to be used to assess dose to individuals working in an area (should other methods of monitoring fail or are unavailable).

Customers should make every effort to properly and fully characterize the radiation source term to which their personnel will be exposed; the customer should make this information available to the vendor during the account set-up process. The dosimetry vendor can, and should, provide recommendations based on experience; nevertheless, the responsibility for proper and complete characterization ultimately rests with the customer. For example, a customer required dosimetry to monitor the environmental/background radiation (environmental dosimetry); during account set-up, the customer did not identify that the environment to be monitored was an Independent Spent Fuel Storage Installation (ISFSI) boundary, an environment in which a neutron flux should be expected. The provided environmental dosimetry was a 'photon only' dosimeter, not designed for use in the presence of a neutron flux. The customer did not monitor for the neutrons, but was comfortable with the conclusion that no neutron flux was present (based on the survey results when little or no spent fuel was actually in the ISFSI). The customer did not consider the impact of not measuring for neutron flux on the actual radiation field present at the ISFSI boundary. This is a clear example of poor source term characterization; the radiation field characterization was incomplete. The customer changed dosimeters to one that was designed for use in a neutron flux and questioned the results when the response confirmed the presence neutron radiation. The investigation revealed the presence of a steady neutron flux (as would be expected for a spent fuel storage installation), a source term component that had been unidentified until the neutron sensitive dosimeters were placed in service.

2.3 Background and control badge variances

2.3.1 Method for background subtraction

Selection of the background subtraction method can have a statistical impact on the final dose assessment. Vendors often employ a default subtraction method based on the physical location of the processor if no specific background rate is supplied by the customer or control dosimeters are not used. In most circumstances, dose results for a passive dosimeter will not differentiate between natural radiation and occupational radiation; consequently, the customer has the responsibility of ensuring that the assumptions made for the chosen background subtraction method are valid and appropriate for the customer's specific needs.

Some vendors and customers prefer that control dosimeters be used; when selecting the storage location for control dosimeters, the customer should consider an area that is representative of the background radiation level *without* occupational exposures. Typically the control dosimeter storage area should be one of a low natural radiation area that is free of environmental extremes (heat, cold, humidity, etc.); a location with high background radiation will result in a non-representative high control subtraction, resulting in a lower final dose assessment than the true occupational dose, and a location with low background radiation will result in non-representative low control subtraction, resulting in a higher final dose assessment than the true occupational dose. Additionally, failure to return the control dosimeters with the monitoring dosimeters could result in the vendor using an assumed exposure rate; such assumptions can introduce greater uncertainties into the final dose assessment.

The use of control dosimeters adds the additional protection of monitoring for non-occupational in-transit exposures. If control dosimeters are not used, in-transit exposures cannot be differentiated from occupational exposures; this could result in the inclusion of non-occupational exposures in the individual's final dose assessment. Although in-transit exposures are rare, customers have had as much as 2.0 mSv added to an individual's final dose assessment that was ultimately attributed to an in-transit exposure following a lengthy investigation. For individuals typically at or below the Minimum Reportable Dose (MRD) (no dose assigned), a final dose assessment of 2.0 mSv can have a significant psychological impact, even though such a dose is not physiologically significant.

An alternative background subtraction method is to use a specified background dose rate; this rate may be customer specific or the default rate implemented by the vendor. Use of a specified dose rate reduces the number of dosimeters to be sent from and received by the vendor; dose rate calculations simplify the assumption of appropriate background subtraction (typically a dose rate/day multiplied by the number of days the dosimeter was in the field). Determination of a customer specific rate should be the result of planned, detailed, studies of the natural radiation. The customer could choose to simply give the vendor a rate to use; however, this could introduce greater uncertainties into the final dose assessment. However, use of the vendor's default dose rate may not be representative of the customer's physical location; this would be another potential source for introduction of uncertainties into the final dose assessment.

2.3.2 Challenges associated with take-home and on-site storage of dosimetry

For customers, control of the dosimeters during off-hours should obligate some attention. As the dosimeters are passive, they continuously register any exposure – to include natural sources of background radiation. Typically, the customers are primarily concerned with the exposure to the individual due to occupational sources, not only are the discussions of section 2.3.1 important for the subtraction of non-occupational exposures, but dosimeter storage locations in off-hours will have an impact on the magnitude of non-occupational exposure which must be subtracted for the final dose assessment.

On-site storage of dosimeters should maintain dosimeters in close proximity to their respective control dosimeters (if used), which allows for a more consistent subtraction of background dose. On-site storage does require a physical storage space at the work location and a method for distributing the dosimeters at the beginning of the work day and collecting dosimeters at the end of the work day. Another possibility is to allow workers to retain their dosimeters at all times; however, this could introduce considerable variability between final dose assessments regarding the amount of non-occupational background or natural radiation to be subtracted. If the individual's background radiation is significantly different than the control dosimeter background radiation, the final dose assessment can be significantly different than the true occupational dose. Table 4 shows a summary of advantages and disadvantage of take-home and on-site dosimetry storage.

Table 4: Advantages and disadvantages of dosimetry storage methods

Take-Home Storage		On-Site Storage	
Advantages	Disadvantages	Advantages	Disadvantages
Less space required on site	Variance in background based on personnel locations	Controls more effective due to less background variation	Need space to store all dosimeters (problematic for large user populations)
No need to issue/collect daily	Increased number of lost and damaged dosimeters	Infrequent issues with lost and damaged dosimeters	More personnel needed to manage dosimetry program
Less personnel needed to manage dosimetry program	Controls less effective due to background variance	Dosimeters on site at all times – effective control of program	Need to have system for issuing and collecting daily
	Less control over program		

2.4 Abnormal readings resulted from incorrect placement of dosimeters

Any method employed to determine dose received requires proper placement of dosimeters. Section 2.1.2 discussed a common method for calculating EDE when wearing two sufficiently different shielded dosimeters (Webster method); one on the collar over the apron, and one on the torso under the apron. In many cases, discrepancies in final dose assessment occur because a dosimeter is not worn properly: worn away from the body during exposure (e.g., the dosimeter is on a lanyard that swings into the radiation field), or oriented incorrectly during exposure (e.g., a finger ring dosimeter is worn like a normal ring, with the finger shielding the dosimeter from the source).

In the examples provided, the final dose assessment would not be representative of true occupational dose. In the case of the lanyard swinging the dosimeter into the radiation field, the final dose assessment would be greater than the true occupational dose actually received by the individual (since the individual's body likely did not enter the plane of the radiation field, caused by sources such as x-ray or PET machines). In the case of the finger ring, the final dose assessment would be less than the true occupational dose (extremity) received, as the finger was providing shielding (and receiving dose) for the dosimeter.

Lax program requirements often mean additional work for the dosimetry personnel at the site, as well. This is most often seen in lost, unreturned or damaged badges. While most vendors will charge for a lost/unreturned/damaged badge, the vendor will also be unable to provide a final dose assessment. This typically means that the site must perform an investigation to calculate the occupational dose of the individual.

A medical facility provided an example of an abnormal reading. An individual had a designated collar dosimeter (CL). After the dosimeter was processed, the element readings were indicative of a neutron component in the exposure; this caused the dose algorithm to include a neutron dose in the final dose assessment as follows:

Hp(10) – 8.7 mSv
 Hp(0.07) – 8.7 mSv
 Hp(3) – 8.7 mSv
 Hp(10) neutron – 8.2 mSv

If it was certain that the individual was *not* exposed to a neutron flux (e.g., the individual only works with technicium-99 (Tc-99m)), the final assigned dose can be amended by disregarding the apparent indications of neutron response and assessing the dosimeter response with an algorithm other than the default. In this particular case, the facility was unable to provide, with sufficient certainty, confirmation that the exposure was absent a neutron flux; thus, the final dose assessment stood as originally reported. Had the facility provided amplifying information during the course of the investigation it may have been prudent to assign a lower dose, such as: the individual was working with a linear accelerator, the dosimeter was known or likely to have been partially shielded, etc.

This particular example demonstrates the need to have detailed knowledge of the work environment to provide guidance and support for adjustments in the final dose assessment; without such guidance and support, the vendor cannot typically discern if the final dose assessment requires adjustment, particularly with the use of a single dosimeter. In the scenarios when multiple dosimeters are used, the vendor and the customer will have greater measurement data for use in determining the appropriate final dose assessment.

3 REGULATORY CONSIDERATIONS

3.1.1 Radiation protection program and monitoring requirements

Depending on the regulatory body enforcing the rules of personal monitoring, the orientation and location of the dosimeters determined at account set up can have a significant impact on the final dose assessment. Each regulatory body has established limits for when monitoring is required; typically the regulatory body has guidelines or laws in place that mimic or use international standards and recommendations. For instance, in the United Kingdom, only Classified Workers (CW) are required to be monitored. A CW is defined as an individual that is likely to receive an effective dose in excess of 6 mSv per year or an equivalent dose in excess of 3/10ths of any relevant dose limit. The employer is required to make the determination if monitoring an individual as a CW is appropriate; once so designated, these individuals are monitored (medical surveillance) and their doses are required to be assessed, recorded, and reported to the UK government at regular intervals [2].

Depending on the regulatory framework for the customer, occupational exposure monitoring with passive dosimetry can be a small component of the radiation protection program; however, it is frequently a cornerstone of actual radiation protection. In many cases, lenient radiation protection programs can be identified by a regulator through discrepancies and abnormalities identified within the dosimetry program records. Failure to review final dose assessments in a timely manner, or failure to identify discrepancies in those assessments (e.g., an individual received three times their normal dose while the individual was on vacation) can provide to a regulator indications that the radiation protection program is not being well supported or managed.

3.1.2 Accreditations

Understanding the assumptions the vendor makes during the assessment of final dose is beneficial when interacting with the various regulatory bodies. For example, a customer stated that the vendor made a particular assumption regarding the operating condition of a power plant prior to dose

assessment. The customer concluded that the dosimeter chosen was being used in a manner inconsistent with the methods described by the vendor. In reality, the statements the customer made were incorrect; the vendor should not attempt to change the specific correction factors applied during processing of the dosimeters without specific and direct input from the customer because the vendor does not typically have sufficient information from the dosimeter response alone to accurately make said changes. The customer incorrectly concluded, based on a misunderstanding of the accreditation scope (and requirements) of the chosen dosimeter, that the vendor could determine the operational status of a nuclear power plant and was applying an appropriate correction factor based on that determination.

3.1.3 Reporting dose and records retention

Many regulatory bodies require that the vendor retain dose records and provide the data for any national reporting requirements. In all cases, the customer and the vendor have equal responsibility for providing accurate information to ensure regulatory compliance. Both the vendor and the customer should be cognizant of the specific regulatory reporting requirements. Failure to adhere to said requirements could result in suspension or revocation of the customer license, the vendor's accreditation, and monetary fines being levied on one or both parties, or perhaps all of the above.

Most national registries for exposed workers (Classified Workers, Nuclear Energy Workers, Radiation Workers, etc.) require an accredited "record keeper," often not the individual worker's employer, to submit the official final dose assessment. This is important to keep in mind when considering any investigations, and the associated outcome, into the validity of a final dose assessment to an individual.

4 CONCLUSION

As with any relationship, but particularly one involving a customer and a vendor, the key to success is communication. As outlined in the examples above, almost all instances of dose reporting errors could be traced back to a failure to communicate; either by the customer or the vendor. There are many elements to a successful dosimetry program, and in many cases, the vendor is willing to work with the customer to ensure those programmatic elements are in place.

Understanding the exposure source term that a customer works in and conveying that information to the dosimetry vendor will establish a foundation for a successful monitoring program. There are many elements to a successful dosimetry program, and in many cases, the vendor is willing to work with the customer to ensure those programmatic elements are in place. Routine validation of assumptions by both the customer and the vendor is paramount for a quality program and the assessment and assignment of an accurate dose.

5 REFERENCES

- [1] Webster, E.W., April 1989. EDE for Exposure with Protective Aprons. *Health Physics Journal*, 568-569.
- [2] Health and Safety Executive (HSE). Appropriate designation of classified persons. <http://www.hse.gov.uk/radiation/ionising/doses/designation.htm>
- [3] Health and Safety Executive (HSE). 1999. Work with ionising radiation, Ionising Radiation Regulations 1999, Approved Cod of Practice and guidance, 87.

Large scale multi-national studies on radiation protection of children in CT

Madan M. Rehani*

Massachusetts General Hospital, Harvard Medical School, Boston and Duke University
Radiology and Medical Physics, USA

Abstract. Findings from large part of the world on radiation doses to children including as well multi-national studies conducted through International Atomic Energy in 52 low-resource countries are reviewed. It is apparent that pediatric CT usage in Asian and African facilities is almost double that those in Eastern Europe. The ratio of maximum to minimum CT dose index (CTDI) values were between 15 to 100 in few situations. Scattered findings included CTDI values for pediatric patients higher than those for adults. Use of adult protocols for children was associated with CTDI_w or CTDI_{vol} values in children that were double those of adults. Patient dose records were kept in nearly half of the facilities, with the highest frequency in Europe (55% of participating facilities), and in 49% of Asian, 36% of Latin American and 14% of African facilities. The important outcome is capability building in patient dose assessment and dose management.

KEYWORDS: *international organization's role; pediatric CT in developing countries; pediatric CT; radiation protection in pediatric CT; multi-national study of pediatric CT.*

1 INTRODUCTION

It has been estimated by the United Nations Scientific Committee on Effects of Atomic Radiation (UNSCEAR) that annually about 3.6 billion diagnostic x-ray examinations are performed globally, of which about 180 million examinations are performed on children⁽¹⁾. Further, typically about 10% of these examinations are CT studies, and that translates to 18 million CT examinations on children⁽²⁾. Even if 1/3rd or 1/4th of these examinations are performed in professionally less resourced countries that amounts to 4.5 to 6 million. Are children undergoing these examinations getting the right amount of radiation dose or an order of magnitude more? Are they getting the CT examination for the right reason or the CT examination is not the most appropriate in that particular situation? Thus, looking back in early 2000's we realized that there is lack of information from most professionally less resourced countries and most information was available from developed countries^(3,4). The ground reality was that most professionally less resourced countries had reached the level of testing x-ray machines through the quality control kits supplied by International Atomic Energy Agency (IAEA). With lack of professional competence (diagnostic medical physicists with patient dosimetry skills) in these countries, there is important role for international organizations whose support and direction is pursued by these countries. Realizing this, we in IAEA initiated projects on assessing patient doses and managing patient doses. But the question was who will assess patient doses? In near absence of diagnostic medical physicists in most of these countries, the option was to look towards regulators, medical physicist working in hospitals in radiotherapy, other physicists in university settings, research staff in radiation protection and radiobiology institutes, radiographers and radiologist. It is much more convenient for regulators and radiation protection experts to test machines whereas any work pertaining to patients requires coordination with hospital staff, needs periodic and continued actions unlike one time testing of machines, poses difficulty in getting data at multiple level and understanding intricacies of exposure parameters and their impact on patient doses. But once a person crosses threshold of coordination and cooperation is established, the work appears much more exciting than machine testing. While working at the IAEA, this was the first important issue I had to deal with. For regulators, this resulted in change of working style from enforcement to cooperation. The

* Presenting author, e-mail: madan.rehani@gmail.com

next was to train these people with diverse background in patient dosimetry. Thus the normal training programs were transformed into hands on sessions at an institution in a developed country for specific training targeted at patient dose assessment and dose management skill development. The conventional system of choosing participants was changed to choosing only those who have done preliminary work in the project of IAEA and have provided results for phase 1. The phase 1 consisted of collecting data on frequency of different CT examinations in children with respect to adults with different age and in different body parts. That essentially provided training in cooperation building and handling patient data. Another important aspect was preparing all Forms for data collection so as to have uniform data collection system. The training included meaningful data collection and providing information as per format. This created a pool of professionals who were oriented to the task. As a result we were able to have useful information about status of practice as summarized below.

2 COUNTRIES FROM WHICH DATA IS AVAILABLE IN MULTI-NATIONAL STUDY COORDINATED BY THE IAEA AND OTHER STUDIES

The countries from which data was available were: Algeria, Argentina, Armenia, Belarus, Bosnia & Herzegovina, Brazil, Bulgaria, Chile, China, Costa Rica, Croatia, Cuba, Czech Republic, Democratic republic of Congo, Ecuador, Estonia, Ghana, Indonesia, Iran, Israel, Kuwait, Lebanon, Lithuania, Madagascar, Malaysia, Malta, Mexico, Montenegro, Moldova, Myanmar, Nicaragua, Oman, Pakistan, Paraguay, Peru, Poland, Qatar, Saudi Arabia, Serbia, Singapore, Slovakia, Slovenia, Sri Lanka, Sudan, Syria, Tanzania, Thailand, The Former Yugoslavia Republic (FYR) of Macedonia, Uruguay, United Arab Emirates (UAE) and Zimbabwe. In addition, data was also available from Japan on same format as used for other countries and thus it provided some reference for comparison. The detailed results of these studies are available in papers already published⁽⁵⁻⁹⁾

3 SNAPSHOT OF FINDINGS

At the outset it was evident that modern technology of multi detector CT is available in major centers in almost all countries mentioned above⁽²⁾. Of the 146 CT facilities, 23% were single detector CT (SDCT) and 77% were MDCT. Automatic exposure control (AEC) was reported to be available in 84%. Dose display in CT dose index (CTDI_w or CTDI_{vol}) and dose length product (DLP) was available in 79% of facilities. There was a trend of increasing CT exams in lower-resource countries during the period of the surveys (2007-2009). Despite some CT facilities showing a decrease, there was an overall increase in the number of pediatric examinations of 6.8%, compared with an increase of 19.8% for adults. The availability of dose displays in CT equipment was reported to be among 75% participants in the survey. However, dose information was collected by only 70%. Nearly 1/5th had dose display as CTDI_w others as CTDI_{vol}.

The ratio of max/min CTDI_{vol} values varied among examinations and age groups, from 15 for abdomen CT in the age group 5–10 years to up to 100 for chest CT in the age group <1 year. Variation between maximum and minimum was up to a factor of 49 among protocols from the 19 facilities with CTDI_w display. There were instances of CTDI values for paediatric patients being higher than for adults in 8% for at least one age group and for one type of examination. For example, at one facility using 64-detector CT, the CTDI_{vol} for the head was between 31.3 mGy and 59.4 mGy for children of different ages, against a very low value for the adults of 12.3 mGy. At this facility 120 kVp was used for all ages and tube current was between 140 mA and 380 mA for children of different age groups, versus 170 mA for adults. In one of the SDCT systems, adult protocols were used for children. With CTDI_w display, the values for children were double those of adults for head examination (64 mGy versus 34 mGy), and for chest examination (16.4 mGy versus 7.8 mGy). Patient dose records were kept at 49% of facilities, with the highest frequency in Europe (55% of participating facilities), and in 49% of Asian, 36% of Latin American and 14% of African facilities. Seven percent of respondents were not aware whether such records were available. When records were kept, in 82% it was in the patient electronic file and in 18% it was

recorded manually in a physical file.

How far appropriateness criteria are used was tested in 7 clinical conditions namely: i) an infant with hydrocephalus, ii) infant with congenital torticollis, iii) a child with a clinical suspicion of appendicitis (or acute abdominal pain), iv) a child with indication for pleural effusion, v) a child with persistent headache, vi) a child with possible ventriculo-peritoneal shunt malfunction, and vii) a small child (< 5 years old) with acute sinusitis. The results showed that while practice was mostly in accordance with guidelines for situations i), iii) and v) (hydrocephalus, appendicitis and persistent headache), this was not as consistent for situations ii), iv), vi) and vii) (congenital torticollis, pleural effusion, ventriculo-peritoneal shunt and acute sinusitis).

There has been lot of impact of the IAEA work ⁽¹⁰⁾ in large part of the world, but important in this respect is the momentum in Africa. A study from Sudan ⁽¹¹⁾ investigated a total of 296 pediatric patients (aged 6-10 y) in 8 hospitals equipped with 64-, 16- and dual-slice CT machines. The mean dose length product values were 772, 446 and 178 mGy cm for head, abdomen and chest, respectively. Imaging protocols were not adapted to the patient's weight in certain CT machines. The authors indicate that pediatric patients are exposed to an unnecessary radiation dose. The established DRLs were higher than those available in other countries. The study showed the need for harmonization of the practice in CT departments and radiation dose optimization.

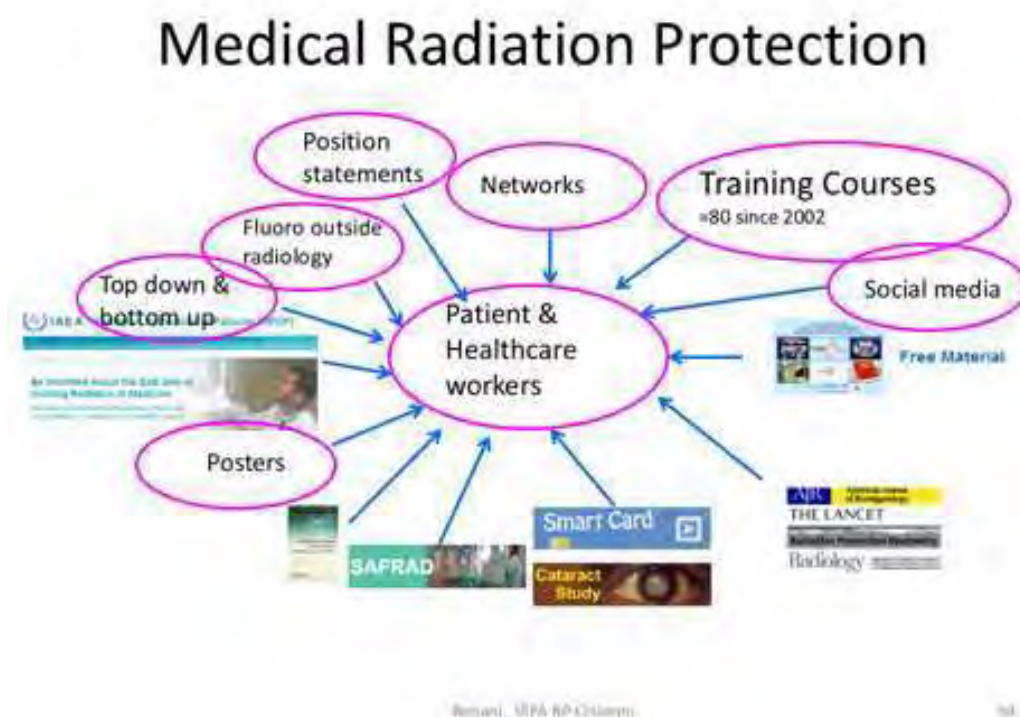
To determine the knowledge of paediatricians in Nigeria about the basic principle of radiation protection and ALARA (As Low As Reasonably Achievable) and their knowledge of the radiation doses that children receive during some common radiological procedures, a study was reported in 2014 ⁽¹²⁾. Of the 162 Paediatricians that participated, 54.9% would not recommend CXR to screen an apparently healthy child for tuberculosis and 87% believe that children are at greater risk of adverse effects of ionising radiation. For dose estimation, 51.9% and 51.2% of the paediatricians underestimated doses received during Cranial and abdominal computerized tomography respectively while 13.6% and 37% respectively erroneously believed that abdominal ultrasound and brain magnetic resonance imaging utilise ionising radiation. Only 13.6% gave the correct meaning of the Acronym ALARA.

There are a number of publications in radiography and CT adult but here only those in pediatric CT are cited.

Looking back, our studies have set the ball rolling and the impact is evident from publications in recent years. This provided bottom up approach in addition to top down approach that IAEA had been using traditionally. Since not many professionals in smaller countries are able to reach the level of making publication in indexed journals. Despite the important role of learning through doing, there is limited outreach of this approach. Since our objective was to make a difference in millions of patients undergoing x-ray procedures, we had to think of other approaches. An important advance was creation of a website on radiation protection of patients commonly known as RPOP website ^(13,14) that has vast and extensive information on patient and staff radiation protection, even though the name is patient protection. The outreach of website has been so much that it appears on first page of Google search with relevant search terms such as: radiation protection in.....pregnancy, ...mammography, ...fluoroscopy, ...CT, ...radiology, ...nuclear medicine, ..radiotherapy, ...cardiology, ...children, ...dental radiology, ...DEXA, ...PET/CT, ...interventional radiology, ...fluoroscopy, ...gastroenterology, ...urology, ...orthopedic surgery.....USA is the largest user of the website with almost 1/3rd of global visits. UK among top 5 and Canada among top 10 users. For many years there were >30% increase in number of visitors each year on RPOP website ^(14,15). Also Facebook and Twitter pages of RPOP were created. This extended the outreach to many developed countries besides less resourced countries. After utilizing training programs, making available training material on RPOP website that is available for free download, making publications in journals and making dozens of IAEA publications that are available for free download from RPOP website, providing position statements, creation of networks that included a network of health ⁽¹⁶⁾ and other networks,

reporting systems for higher exposures, another important action was development of “10 Pearls posters”. These posters are available for free download from RPOP website and in many languages⁽¹⁷⁾. The vision is that if every x-ray machine in the world has a 10 Pearl poster pasted beside the operating point, it will point quick access to vital information that can help the process of justification and optimization. These posters have been developed for CT, interventional procedures and for referring physicians. There have been thousands of downloads of these posters. Ultimately the concept of smart card for patient exposure tracking and having history of patient’s exposures shall provide opportunities for enhancing justification and optimization and meaningful information for follow up of children who undergo repeated radiological examinations⁽¹⁸⁻²¹⁾. Fig 1 consolidates all these approaches. It is anticipated that with all the above approaches the impact on millions of imaging examinations on children and billions on adults shall be possible for safer and appropriate imaging.

Figure 1: Schematics of approaches used to make advances in medical radiation protection.



4 CONCLUSIONS

A combination of training actions, engagements of health workers through projects, making available training material for free download from website, publications in indexed journals and international organization’s publications, social media actions, creation of network, patient exposure tracking, reporting systems and posters provides possibilities to make a difference in making imaging safer for children.

5 REFERENCES

- [1] United Nations Scientific Committee on the Effects of Atomic Radiation, 2010: UNSCEAR 2008 Report Vol. I. Sources of ionizing radiation. Annex A: Medical radiation exposures. New York, United Nations.
- [2] Rehani MM. 2014. CT Imaging in large part of the world: What we know and what we can learn, *Pediatric Radiology* 44 (Supplement 3), 511-514.
- [3] Rehani MM, Tsapaki V. 2011. Impact of the international atomic energy agency (IAEA) actions on radiation protection of patients in many countries. *Radiat Prot Dosimetry* 147, 34-37.
- [4] Rehani MM, Ciraj-Bjelac O, Al-Naemi HM et al.,2012. Radiation protection of patients in diagnostic and interventional radiology in Asian countries: Impact of an IAEA

- project. *Eur J Radiol.* 81, e982-989
- [5] Vassileva J, Rehani MM, Al-Dhuhli H et al.,2012. IAEA survey of pediatric CT practice in 40 countries in Asia, Europe, Latin America, and Africa: Frequency and Appropriateness *AJR Am J Roentgenol* 198, 1021-1031.
- [6] Vassileva J, Rehani MM, Applegate K et al.,2013. IAEA survey of pediatric CT practice in 40 countries in Asia, Europe, Latin America, and Africa: Procedure and protocols. *Eur Radiol*, 23, 623-631.
- [7] Vassileva J, Rehani M, Kostova-Lefterova D et al. 2015. A study to establish international diagnostic reference levels for paediatric computed tomography. *Radiat Prot Dosimetry* 165, 70-80.
- [8] Vassileva J, Rehani M. 2015. Patient grouping for dose surveys and establishment of diagnostic reference levels in paediatric computed tomography. *Radiat Prot Dosimetry.* 165. 81-85.
- [9] Muhogora WE, Ahmed NA, Alsuwaidi JS et al., 2010. Paediatric CT examinations in nineteen developing countries: frequency and radiation dose. *Rad Prot Dosimetry* 140, 49-58.
- [10] Rehani MM, Tsapaki V. 2011. Impact of the international atomic energy agency (IAEA) actions on radiation protection of patients in many countries. *Radiat Prot Dosimetry.* 147, 34-37
- [11] Sulieman A. 2015. Establishment of diagnostic reference levels in computed tomography for paediatric patients in Sudan: a pilot study. *Radiat Prot Dosimetry.*165, 91-94
- [12] Famurewa OC1, Obiajunwa PO, Elusiyan JB et al., 2014. Radiation dose and radiation protection principle awareness: a survey among Nigerian paediatricians. *Niger Postgrad Med J.*21(1), 28-33.
- [13] Radiation protection of patients website of IAEA.
<https://rpop.iaea.org/RPOP/RPOP/Content/index.htm>
- [14] Rehani MM, Holmberg O. 2015. IAEA experience in communicating radiation risks through the rpop website. *Radiat Prot Dosimetry* 165, 22-24..
- [15] Rehani MM. Radiation Protection of Patients Website of the IAE as a Major Resource for Medical Physicists. *Medical Physics International* vol.1, No.1, 2013,
<http://mpijournal.org/pdf/2013-01/MPI-2013-01-p037.pdf>
- [16] Network on radiation protection of children.
https://rpop.iaea.org/RPOP/RPOP/Content/SpecialGroups/2_Children/children-network.htm
- [17] 10 Pearls potters on radiation protection of IAEA.
<https://rpop.iaea.org/RPOP/RPOP/Content/AdditionalResources/Posters/index.htm>
- [18] Rehani MM, Frush DP. 2011. Patient exposure tracking – the IAEA smart card project. *Radiat Prot Dosimetry* 147, 314-316.
- [19] Seuri R, Rehani MM, Kortensniemi. 2013. How Tracking Patients Radiological Procedures and Dose Helps?: Experience from Finland. *AJR Am J Roentgenol.* 200(4),771-775.
- [20] Rehani MM. 2015. Tracking of examination and dose: overview. *Radiat Prot Dosimetry.*165, 50-52.
- [21] Rehani M, Frush D. 2010. Tracking radiation exposure of patients. *Lancet.* 376(9743), 754-755.

Extension of the IAEA-International Nuclear and Radiological Event Scale (INES) for Medical Events

Marc Valero^{a*}, Maria Luisa Ramirez Vera^b, Nera Belamaric^c

^aASN, Autorité Sûreté Nucléaire, Montrouge, France.

^bCSN, Consejo Seguridad Nuclear, Madrid, Spain.

^cConsultant, Zagreb, Croatia.

Abstract. The International Nuclear and Radiological Event Scale (INES) is used for communicating to the public the safety significance of events associated with the transport, storage and use of radioactive material and radiation sources. It covers a wide spectrum of practices, including the use of radiation sources in medicine. Currently the scale does not cover the actual or potential consequences for patients. The need to rate events concerning persons intentionally exposed to ionizing radiation in the context of a medical procedure is recognised and its consideration is the subject of the work done within IAEA and INES participating countries since 2007. The term medical events encompasses events that result in unexpected or unforeseeable health effects that are likely or clearly due to inappropriate doses or irradiated volumes in radiotherapy, misadministration in nuclear medicine or unintended exposures in diagnostic and interventional radiology. Medical events could be rated on INES based on impact on patients or on defence in depth. Impact on patients is defined by the occurrence or likely occurrence of a deterministic effect or an increased risk of stochastic effect. The proposed methodology addresses all situations where the ionizing radiation was not delivered as intended and is for the moment applicable to actual or potential consequences on patients for all medical practices using ionizing radiation (radiotherapy, nuclear medicine and radiology); however, with regard to the defence in depth criteria, the methodology is limited to radiotherapy only.

“The views expressed in this presentation remain the responsibility of the contributors and do not necessarily represent the views of the IAEA or its Member States”

KEYWORDS: *Patient, Unintended exposures, medical events, INES.*

1 BASIS FOR EXTENDING INES TO MEDICAL EVENTS

The International Nuclear and Radiological Event Scale (INES) was developed in 1990 to communicate in a consistent way the safety significance of events at nuclear installations. Since then, INES has been expanded to meet the growing need for communication on the safety significance of events giving rise to radiation risks. INES applies to events associated with the transport, storage and use of radioactive material and radiation sources, whether or not the event occurs at a facility. When a radiation source is used for medical purposes, the existing guidance on INES methodology [1], can be used to rate events resulting in actual exposures to workers and the public, or involving degradation of the device or deficiencies in the safety provisions. Currently the scale does not cover the events affecting patients exposed to ionizing radiation as part of a medical procedure referred to as ‘medical events’.

The term medical events encompasses events that result in unexpected or unforeseeable health effects that are likely or clearly due to inappropriate doses or irradiated volumes in radiotherapy, misadministration in nuclear medicine or unintended exposures in diagnostic and interventional radiology.

Not included are any adverse reactions, i.e. an unexpected harm resulting from a justified action where the correct process was followed for the context in which the event occurred [2], whatever their grade, which may result from an exposure incurred by a patient in accordance with a diagnostic or treatment plan chosen by the practitioner. The term medical event is consistent with the term ‘unintended and accidental medical exposures’ used in IAEA International Basic Safety Standards [3].

Medical events are not covered by the current guidance on INES methodology. There is thus a need to consider the extension of INES to medical events.

* Presenting author, e-mail: marc.valero@asn.fr

To begin with, the patient protection and medical exposures have gained increased attention in the past few years. The International Commission on Radiological Protection (ICRP) has introduced recommendations on these topics in its publications.

Moreover, medical exposure is the largest human-made source of exposure to ionizing radiation and continues to grow at a substantial rate leading to an increased total annual collective dose from all diagnostic exposures. Interventional procedures typically give the largest doses among imaging practices, and several millions of them are performed per year worldwide. The use of radiation therapy increased and, if serious events are rare, they may have serious consequences.

Finally, several hundred events related to medical overexposure have been reported in the relevant literature [4]. Such events have had an important impact on the media and the public. Therefore public communication on events associated with sources of radiation could benefit from using a single unified scale to put into perspective the safety significance of all events.

The proposed INES rating methodology for medical events should apply to exposure of individuals for therapeutic and diagnostic purposes and should be applicable to events in radiotherapy (external beam radiotherapy and brachytherapy) including over an under dosage, radiology (exposures for diagnostic and interventional procedures) and nuclear medicine (exposures for diagnostic and therapeutic procedures). As for others radiological events where INES is already applied, medical events are rated on impact on “people”, in this case patients and on defence in depth. Impact on patients is defined by the occurrence or likely occurrence of deterministic effects or an increased risk of stochastic effects. Criteria for rating events considering impact to patients are developed for all medical practices using ionizing radiation.

The defence in depth approach allows to cover those events where there are no actual consequences to the patient, but some of the safety provisions or barriers to prevent possible consequences have failed. However, with regard to the defence in depth criteria, the methodology in its current state is limited to radiotherapy only.

2 RATING OF EVENTS BASED ON THE ACTUAL OR LIKELY OCCURRENCE OF CONSEQUENCES

2.1 Common Terminology Criteria for Adverse Events (CTCAE) – adaptation to radiotherapy and interventional radiology

Originally developed by the U.S. National Cancer Institute, the Common Terminology Criteria for Adverse Events (CTCAE) [5] was further refined through an international harmonization effort for use in adverse event reporting.

The scale is:

- a reference library of definitions for grading the effects related to any medical treatment or procedure;
- designed as an instrument to document and standardize adverse events through a combination of clinical and laboratory evaluations;
- the standard for adverse event reporting in the oncology community.

CTCAE grading scale is by definition a 5-point scale generally corresponding to: mild, moderate, severe, life-threatening effects and death. Grading is based on specific clinical criteria that are provided in multiple tables and usually require evaluation by the clinician.

In order to grade the severity of the detriment, adaptations of the Common Terminology Criteria for Adverse Events (CTCAE) severity grading scale [5] for radiotherapy RTOG-EORTC [6] (Table 1) and BALTER for interventional radiology [7], are used in INES.

Table 1: CTCAE Severity Grading Scale and example of RTOG/EORTC (Radiation Therapy Oncology Group - European Organization for Research and Treatment of Cancer) scoring criteria and scheme for skin.

Grade	Description CTCAE	SKIN - RTOG/EORTC Acute (A) – Late (L) Morbidity Scoring Scheme
1	Mild: asymptomatic or mild symptoms; clinical or diagnostic observations only; intervention not indicated.	A : Follicular, faint and dull erythema; epilation; dry desquamation; decreased sweating L : Slight atrophy; Pigmentation change; Some hair loss
2	Moderate: minimal, local intervention or non invasive intervention indicated;	A : Tender or bright erythema; patchy moist desquamation ; moderate edema L : Patch atrophy; Moderate telangiectasia; Total hair loss
3	Severe or medically significant but not immediately life-threatening: hospitalization or prolongation of hospitalization indicated;	A: Confluent moist desquamation other than skin folds, pitting edema L : Marked atrophy; Gross telangiectasia
4	Life-threatening consequences; urgent intervention indicated.	A: Ulceration, haemorrhage, necrosis L : Ulceration
5	Death related to adverse event.	Death directly related to radiation late effect

2.2 Elements to be considered in evaluating the consequences

The evaluation should be conducted by a multidisciplinary team including a physician, a medical physicist and other healthcare professionals involved in the practice.

Dose should be estimated to assist in the medical evaluation or may be used in rating when there are no current deterministic effects. If there are no actual consequences at the time of the rating, the detriment of unintended delivered doses that is likely to occur should be taken into account.

Dosimetric consequences of an event shall be evaluated by a medical physicist using appropriate tools and dosimetric data available by considering mainly in

- Radiotherapy: Dose volume histogram of the resultant treatment with special focus on dose deviation on total prescribed dose to Planning Target Volume (PTV) and Organ at Risk (OAR);
- Interventional radiology: the Peak Skin Kerma/Dose and dose reconstruction to skin, organ involved;
- Diagnostic imaging (radiology and nuclear medicine): Kerma/Dose Area Product for plain radiology, Dose Length Product for computed tomography, activity and radiopharmaceutical for nuclear medicine imaging. These data allows to determine the effective dose related to the event;
- Nuclear medicine therapy: the deviation of activity of the radiopharmaceutical to be administered; administration of wrong radiopharmaceutical and/or wrong route of administration.

Elements that should be considered in the medical evaluation supported by dosimetric data are depending on the type of practice.

For radiotherapy and interventional radiology

- whether the health effects encountered are induced by ionizing radiation;
- the initial physical condition and the medical history of the patient;
- confounding factors including other medical treatments such as surgery, chemotherapy or previous radiation exposures;
- known effects related to the prescribed treatment.
- possible acute and late deterministic effects related to the event based on the CTCAE grading scale;

- radiobiological consequences of the altered treatment scheme (fractionation and/or overall treatment time);

For diagnostic imaging, the increase of stochastic risk correlated to effective dose if there are no deterministic effects.

2.3 Underdosage

Under-exposure in therapeutic procedures may result in ineffective treatment. Determining if subsequent consequences are a result of such treatment is very difficult. A clinical and dosimetric evaluation of the treatment, conducted by a radiation oncologist and a medical physicist, is needed to assess the clinical significance of the under-exposure and the possible clinical consequences for the patient or, in case of a relapse of the disease to establish if there is a link between the relapse and the underexposure.

Ford et al. [8] have considered that a proven under dose could be rated at the same level than life threatening event, i.e. grade 4 on CTCAE scale. Under-exposure considered as clinically significant which cannot be corrected, should be rated on INES as a Level 4 event.

As long as the treatment plan is achieved with correction or the under dose is not considered as clinically significant, the event should not be rated considering actual impact on the patient. Such an event could reveal defence in depth and/or safety culture issues and hence should be rated using the defence in depth approach.

For diagnostic procedures, if the dose is too low to obtain a good quality image, an additional exposure will probably be required, resulting in a higher dose then only the total dose should be considered in the rating of the event.

2.4 Stochastic effects

When there is an actual or high probability of deterministic effects, there is no need to take into account stochastic risks except for paediatric patients. However, if there are no deterministic effects, it does seem reasonable to rate events based on a significant increase in stochastic risk.

As mentioned in ICRP 103 [9]: “In the case of cancer, epidemiological and experimental studies provide evidence of radiation risk albeit with uncertainties at doses about 100 mSv”. Therefore, for INES rating, effective dose higher than 100 mSv should be considered to lead to a significant increase in stochastic risk. Children are considered approximately 2-3 times more sensitive to stochastic risk of radiation than adults.

While it is felt that medical events involving patients with a significant increase in stochastic effects risk should be rated, it is clear that quantifying ‘significant increase in stochastic risk’ needs further development in consultation with medical professionals from the applicable disciplines.

For INES rating, an effective dose higher than 100 mSv should be considered to lead to a significant increase in stochastic risk. A significant increase in stochastic risk for adult patients should be rated at Level 1, while, for paediatric patients, it should be Level 2.

2.5 Criteria for the assessment of the minimum rating for one single patient involved

Taking into account the aforementioned criteria the INES rating levels for medical events involving one single patient are defined as follows:

Level 4 is the minimum level for events that result in:

- (1) The occurrence of a lethal deterministic effect i.e. CTCAE 5
- (2) The occurrence or likely occurrence of a life-threatening deterministic effect i.e. CTCAE 4
- (3) For radiotherapy, under-exposure that is clinically significant and cannot be corrected.

Level 3 is the minimum level for events that result in the occurrence or likely occurrence of a non-lethal severe deterministic effect i.e. CTCAE 3.

Level 2 is the minimum level for events that result in:

- (1) The occurrence or likely occurrence of a moderate deterministic effect i.e. CTCAE 2
- (2) A significant increase in the stochastic risk for a paediatric patient.

Level 1 is the minimum level for events that result in:

- (1) The occurrence or likely occurrence of a mild deterministic effect i.e. CTCAE 1;
- (2) A significant increase in the stochastic risk for an adult patient

2.6 Criteria for the assessment of the rating of events involving multiple patients

Events involving multiple patients should be rated based on two factors: the degree of consequence and the number of patients involved. The event rating is the highest level obtained from the consideration of these two factors.

The rating methodology follows the criteria applied for rating on INES based on impact on people and the environment, INES User's Manual [1], and is summarized in table 2.

Table 2: Summary of rating system for medical events for actual or likely occurrence of consequences

Detriment	Minimum Rating	Numbers of Individuals	Actual Rating
The occurrence of a lethal deterministic effect or the occurrence or likely occurrence of a life-threatening deterministic effect or for radiotherapy, under-exposure that is clinically significant and cannot be corrected	4	Few tens or more Between several and a few tens Less than several	6 5 4
The occurrence or likely occurrence of a non-lethal severe deterministic effect	3	Few tens or more Between several and a few tens Less than several	5 4 3
The occurrence or likely occurrence of a moderate deterministic effect or significant increase in the stochastic risk for a paediatric patient	2	100 or more 10 or more 3 Less than 10	4 3 2
The occurrence or likely occurrence of a mild deterministic effect or significant increase in the stochastic risk for an adult patient	1	100 or more 10 or more 3 Less than 10	3 2 1

As guidance to help with a consistent approach to the application of these criteria, it may be considered that ‘several’ is more than three and ‘a few tens’ is more than 30.

3 RATING OF EVENTS BASED ON THE ASSESSMENT OF THE IMPACT ON DEFENCE IN DEPTH

3.1 General approach for rating of events based on the assessment of the impact on defence in depth

In medical practice human errors or equipment failures may occur, so different safety layers are in place to prevent any harm to the patient. The prevention of accidents is part of the design of the equipment, facilities, and work procedures. As stated in ICRP 105 [10] “a key feature of accident prevention has long been the use of multiple safeguards against the consequences of failures. This approach, called ‘defence in depth’, aims to prevent equipment failures and human errors, and mitigates their consequences should they happen. Some defences are provided by the design of equipment, others by the working procedures”

Defence in depth criteria provides a means to rate the significance of failures in safety provisions. In evaluating defence in depth INES typically considers the number of safety provisions that still remained functional in an event and the potential consequences if all the safety provisions had failed. Using the defence in depth approach allows to cover those events where there are no actual consequences to the patient, but some of the safety provisions or barriers to prevent possible consequences have failed.

3.2 Methodology for rating medical events based on impact on defence in depth

3.2.1 Identify the initiating event:

An initiating event is an event identified in the risk analysis that leads to a deviation from the normal operating state. Initiating events may involve human errors or equipment failures. Examples of initiating events in the medical field are: failure to follow the correct procedure, errors in patient identification, calibration errors on medical devices, equipment failures.

3.2.2 Identify the safety layers

Table 3: Safety Layer and provisions

Safety Layer	Provision
Procedures to identify patient correctly	<ul style="list-style-type: none"> • open questions for identification • check of photo • check of identity bracelet, card with chip or barcode • check of insurance/identity card with chip • double checking by second person
Periodic examination of the patient during treatment	
Machine controls and interlocks, regular equipment performance verification	
Periodical (daily, weekly, quarterly, ...) quality checks	<ul style="list-style-type: none"> • Dosimetric • key machine parameters
Preventive maintenance	<ul style="list-style-type: none"> • post-repair/changes verification

There is a wide range of safety provisions that can be used to prevent an event with consequences previously described from happening. Some of these may be physical barriers, others may rely on interlocks, others may be active systems such as warnings that are built in into the software, and others may be based on administrative controls or actions by personnel.

The INES methodology for rating events involving such a wide range of safety provisions is to group the safety provisions into separate and independent safety layers. (Table 3).

When considering the number of safety layers, it is necessary to ensure that the effectiveness of a number of separate provisions is not reduced by a common support system or a common action by personnel.

Safety layers are specific for a practice/activity or installation and that what constitutes a safety layer for one practice /installation is not necessarily one for another activity/facility.

3.2.3 Identify the maximum potential consequences

Expert judgement and a multidisciplinary team is required to estimate the maximum potential consequences if all the identified safety provisions failed. Sometimes the maximum potential consequences should consider both, a scenario where a single patient is affected and a scenario with multiple patients. Once the maximum potential consequences are estimated, their rating should be done according to INES methodology described in chapter 2 (table 2).

3.2.4 Identify remaining safety layers

A multidisciplinary team is required to analyse the cause of the event and to identify how many safety layers were remaining when the event was discovered and which have prevented the maximum consequence from happening. Using the same methodology as in INES, maximum rating under defence in depth would be evaluated by using Table 3 accounting for maximum potential consequences and number of remaining safety layers.

Table 4: Basic rating of events using the safety layers approach

Number of remaining safety layers	Maximum potential consequences (a)		
	Levels 5 or 6	Levels 3 or 4	Levels 2 or 1
More than 3	0	0	0
3	1	0	0
2	2	1	0
1 or 0	3	2	1

(a) The maximum ratings cannot be increased due to additional factors because they are already the upper limit for defence in depth

4 THE FINAL RATING OF A MEDICAL EVENT ON INES

The final rating of an event needs to take account of all the relevant criteria described above.

The overall approach in rating is summarized below.

1. Actual or likely occurrence of consequences (deterministic effects). If yes, determine the rating of the event using multidisciplinary evaluation and table 1
2. Defence in depth: identification of the event and the safety layers, determine the maximum potential consequence and the remaining safety layers, determine basic rating from table 3 and consider safety culture issues (upgrade of rating by 1)

According to the methodology defined in INES, the highest derived rating from both areas is the one to be applied to the event [1].

5 CONCLUSION

The patient protection and medical exposures have gained increased attention in the past few years and several hundred events related to medical unintended exposure have been reported. Such events have had an important impact on the media and the public. Till now, these events are not included in the scope of INES.

The proposed extension of the INES rating methodology for medical events could be applied to exposure of patients for therapeutic and diagnostic purposes and should be applicable to events in radiotherapy including over an under dosage, radiology and nuclear medicine. Public communication on events associated with sources of radiation including patients unintended exposure could benefit from using a single unified scale to put into perspective the safety significance of all events.

Two documents related to a potential future extension of the scope of INES for rating medical events are available on the INES Collaborative Workspace and are ready to be used on a voluntary basis:

- “Rationale for the Use of INES for Medical Events” contains justification for using INES to rate medical events and explanation of rating basis and rating system as well as of defence in depth approach and safety culture and
- “Additional Guidance for Rating Medical Events on INES” contains the rating methodology and examples of events.

As stated in the INES National Officers Technical Meeting 2014 report, all Member States are invited to use this additional guidance, and to report on its use to the INES Secretariat. The Secretariat will collect and assess all reports and will brief the IAEA INES Advisory Committee and the INES National Officers Technical Meeting on the findings.

6 ACKNOWLEDGEMENTS

This work is the result of an international working group supported by INES Advisory Committee involving : Sylviane Carbonnelle - Belgium, Simon Coenen - Belgium, Margarida Eiras - Portugal, Michael Fuller - USA, Aurelie Lorin - OCDE/NEA, Stephen Mortin - United Kingdom, Barbara Ott - Switzerland, Carlos Prieto-Martin - Spain, Sven Richter - Norway, Pankaj Tandon – India, Eliseo Vano - Spain and Ola Holmberg, Debbie Gilley - IAEA.

7 REFERENCES

- [1] INTERNATIONAL ATOMIC ENERGY AGENCY, OECD NUCLEAR ENERGY AGENCY, INES: The International Nuclear and Radiological Event Scale, User's Manual, 2008 Edition, IAEA (2013).
- [2] WORLD HEALTH ORGANIZATION, Conceptual Framework for the International Classification for Patient Safety, Version 1.1. Final Technical Report - January 2009. WHO (2009)
- [3] INTERNATIONAL ATOMIC ENERGY AGENCY, Radiation Protection and Safety of Radiation Sources: International Basic Safety Standards, IAEA Safety Standards Series GSR Part 3, IAEA (2014).
- [4] WORLD HEALTH ORGANIZATION, Radiotherapy Risk Profile, Technical Manual, World Health Organization (2008).
- [5] NATIONAL CANCER INSTITUTE, Cancer Therapy Evaluation Program, Common Terminology Criteria for Adverse Events (CTCAE) Version 4.03, (2010) (http://evs.nci.nih.gov/ftp1/CTCAE/CTCAE_4.03_2010-06-14_QuickReference_8.5x11.pdf)
- [6] Cox JD., Stetz J., Pajak TF.: Toxicity criteria of the Radiation Therapy Oncology Group (RTOG) and the European Organization for Research and Treatment of Cancer (EORTC), *Int. J. Radiation Oncology Biol. Phys.*, 31(5) (1995), 1341-1346
- [7] Balter S., Hopewell J.W., Miller D.L., Wagner L.K., and Zelefsky M.J.: Fluoroscopically guided interventional Procedures: A review of radiation effects on patients' skin and hair. *Radiology* 254 (2), February 2010.3
- [8] Ford et al, AMERICAN ASSOCIATION OF PHYSICIST IN MEDICINE (AAPM): Consensus recommendations for Incident learning structure. *Medical Physics*, Vol. 39, No. 12, December 2012.
- [9] INTERNATIONAL COMMISSION ON RADIOLOGICAL PROTECTION: The 2007 Recommendations of the International Commission on Radiological Protection. ICRP Publication 103. *Ann. ICRP* 37(2-4) (2007)
- [10] INTERNATIONAL COMMISSION ON RADIOLOGICAL PROTECTION, Radiological Protection in Medicine, Publication 105, *Ann. ICRP* 37 (6), 2007 (2007).

Control of Radiation Exposure to Pediatric Patients at Conventional Radiology and Cardiac Centers at Dubai Hospital

Najlaa K. Almazrouei^{a*}, Jamila S. Alsuwaidi^b, Adel H. Hashish^c

^aDepartment of Physics, United Arab Emirates University, Al-Ain, UAE & Medical Physics Department, Dubai Hospital, Dubai Health Authority, Dubai, UAE.

^bMedical Education Department, Dubai Health Authority, Dubai, UAE.

^cDepartment of Physics, United Arab Emirates University, Al-Ain, UAE.

Abstract. Paediatric radiation safety is considered as one of the critical subjects in the modern medical imaging. Paediatric patients are at higher risk from ionizing radiation than adults if they receive same amount of dose. This project was conducted to evaluate paediatric patient radiation dose levels in digital radiology (both fixed and mobile x-ray units) and interventional cardiology at Dubai Hospital. The results of this study are expected to contribute in establishing local and national diagnostic reference levels in United Arab Emirates (UAE).

A combination of phantom studies and patient data collection were utilized in this paediatric dosimetry project. The patient data collection was obtained through both manual contributions from radiographers and data obtained from Digital Imaging and Communications in Medicine (DICOM) header. The first method was performed using Polymethyl methacrylate phantom with different thicknesses to represent different age groups of paediatrics; whereas the second method was without phantom where the exposure factors extracted from DICOM header. Then, effective dose was estimated using Monte Carlo dose calculation software.

The entrance surface air kerma was calculated from the incident air kerma and then executed with the application of appropriate backscatter factors. For the fixed x-ray machine, the radiation dose levels were lower than the recommended values and other published data while for the mobile x-ray the findings were comparable and slightly higher than other surveyors. In interventional cardiology, the radiation dose values were higher compared to other values shown in previous researches. Evidently, the values of effective doses showed that the radiation risk is higher with small ages.

In UAE, this study is considered as one of the first structured studies performed on paediatric dosimetry. Further researches are needed to include image quality assessment to stress on obtaining optimum image quality with lower radiation dose.

KEYWORDS: *ionizing radiation; patient dosimetry; paediatric radiation safety; radiation protection; diagnostic radiology, x-ray; effective dose; DRLs.*

1 INTRODUCTION

Exposure to ionizing radiation in childhood should be highly monitored as this group has a higher readiness to develop cancer than adults when receiving the same dose and longer life expectancy which allows more time for any harmful effects of radiation to arise [1]. Therefore, special attention for paediatric patients of different age groups has been given by various international organizations such as the World Health Organization (WHO), the United Nations Scientific Committee on the Effects of Atomic Radiation (UNSCEAR), the International Committee of Radiological Protection (ICRP) and the International Atomic Energy Agency (IAEA). These international organizations have recommended the implementation of a set of best practice procedures which are documented in the Basics Safety Standards (BSS) guidelines. All diagnostic exposures to ionizing radiation shall follow the main radiation protection principles of justification and optimization, particularly in paediatric care. For instance, the ICRP provides guiding principles of radiological protection for referring clinicians and clinical staff performing diagnostic imaging and interventional procedures specifically focuses on paediatric patients [1]. Quantification of radiation exposures for the paediatric patients in the diagnostic radiology reflects one of the main goals to optimize the patient's protection. Also, it may expect to reduce the stochastic effects without compromising the quality of the diagnostic image [2, 3].

* Najlaa Almazrouei, e-mail: nkalmazrouei@dha.gov.ae; nkalmazrouei12@gmail.com

In Dubai hospital, the radiological procedures of paediatric patient are performed in a mixed environment with the adult's patients. This project aims at evaluating the radiation safety practices, the radiation exposure level for this group of patients and to estimate the radiation risk associated with the different diagnostic procedures. Moreover, endorse the paediatric Diagnostic Reference Levels (DRLs), and to provide new data on patient doses for optimization purposes in diagnostic radiology. The diagnostic modalities which were evaluated in this thesis includes: conventional radiology (fixed x-ray unit and the mobile x-ray unit which dedicated to the premature and newborn patients in the neonatal intensive care unit (NICU)) and the interventional cardiology (IC) the catheterization laboratory (**Cath lab**).

2 METHODOLOGY

The methodologies used in this study are based on the IAEA code of practice published at their Technical Report Series No. 457 (TRS 457) [2] and the IAEA series no. 24 [3]. It is stated that the dose measurement is made wherever possible both with phantoms and collected patient dosimetry data. Specifically, the report illustrates the code to measure the incident air kerma, K_i , in conventional x-ray and incident air kerma rate in IC.

The dosimetry measurements rely on the use of polymethyl methacrylate (PMMA) slab phantom to represent the different thicknesses of paediatric patients. Furthermore, collection of relevant patient imaging data and exposure parameter were obtained from the Digital Imaging and Communications in Medicine (DICOM) system in the period from 2012 to 2014 associated with clinical procedures to determine radiation dose quantities. The exposure parameter collected were the peak tube voltage (kVp), exposure current time product (mAs), Field size (cm) and the KAP. These measurements may allow for evaluation of radiation risk assessment through Monte Carlo program **PCXMC 2.0**, aimed to estimate patient organ doses and the **Effective dose (E)** in medical x-ray examinations.

2.1 Dose Measurement Methods in Conventional Radiography and mobile x-ray unit

The measurements were made for two x-ray machines: the first one was the fixed digital x-ray machine (Philips, Digital Diagnostic while the second was the mobile digital x-ray (SHIMADZU, MobileDaRt Evolution) at Dubai hospital. For the fixed digital x-ray machine, five common radiological examinations were chosen for different paediatric age groups, where the age groups were classified as follow: newborn (0- 1 m), >1m – 1y, >1 -5y, >5 -10y and >10 -15y. For the first two age groups the selected common examinations were: Chest, Abdomen, combined Chest-Abdomen, Pelvis and Extremities while for the rest of the groups the following examinations were selected: Chest, Abdomen, Lat. Skull (post nasal space), Pelvis and Extremities. The premature babies (neonates) commonly need to be treated for respiratory or digestive diseases in NICU. For this study, combined chest-abdomen examination was selected.

In diagnostic radiology energy ranges the entrance skin dose (**ESD**) and the entrance surface air kerma (**ESAK**) are equivalent. Hence, patient doses were estimated in terms of **ESD or ESAK** defined as the air kerma measured on the X-ray beam axis at the point where the X-ray beam enters the patient or a phantom, including the contribution of the backscatter (B) [3]. To simulate the clinical practice situation, the exposure parameters collected from the DICOM system were averaged and used for both the phantom and free in air measurements. Phantom K_i were used to compare with the air kerma displayed by the imaging system (indicated) and to reduce then patient dose by repeating the experiment with lower exposure parameters.

2.1.1 Calculation of entrance surface air kerma (ESAK)

Calibrated semiconductor dosimeter (Unfors Xi meter and RF detector) was used to measure the air kerma $K(d)$, then these measurements were used later to estimate patient doses through a three-step protocol [1], that include x-ray output Y (d) measurements, K_i calculation and ESAK estimates, K_e . The x-ray tube output measurements calculated by $Y(d) = K(d) / P_{It}$ (1)
Where $K(d)$ is the air kerma at the measurement point (dosimeter level (d)) and P_{It} is the tube loading during the exposure. The values of the x-ray tube output Y (d) were plotted against the tube potential and the resulting curve was fitted using a power function. Then the K_i were calculated and corrected by

the inverse square law as shown on following $K_i = Y(d) P_{it} (d / d_{FTD} - t_p)^{-2}$ (2)

, where d_{FTD} is the distance from the tube focal spot to the table and t_p is the patient thickness. The ESD or ESAK were calculated by multiplying the K_i by the backscatter factor (B) [1],

$$K_e = K_i * B \quad (3)$$

The B is depending on the kVp, field size, HVL, thickness and composition of the patient or the phantom.

Moreover, ESAK can be derived from the displayed KAP value indirectly. To obtain the patient doses (ESAK) from the KAP value, the following steps are considered:

- a) Calibration of KAP meter.
- b) Dividing the KAP value by the selected field size and then multiplied by an appropriate backscatter value.

2.2 Clinical Dose Measurement Methods in Interventional Cardiology

The IC procedures were performed using a Biplane system (Philips Allura Xper FD 10/10) equipped with flat panel detector. The machine has three fluoroscopy mode (low, normal and high) and three fields of view (25, 20 and 15) cm. The inherent filtration in this system is 2.5 mm Al/75 and additional filtration of (1mm Al + 0.1 mm Cu) for defaulted protocol for Adult while (1mm Al + 0.4 mm Cu) for paediatric protocol. The pulse rate frequently used at pulsed fluoroscopy mode was 15 pulses/s and for cine mode was 30pulses/s. Focal spot to isocentre distance was 76.5 cm. The primary dosimetry quantities in the interventional cardiology are the entrance surface air Kerma rate, \dot{K}_e and the KAP.

The ESAK rate was measured with phantoms slabs of different thickness (4.8, 7.4, 9.5, 12, 14.5 and 16.8 cm), while for patient dosimetry vales of the KAP was collected from calibrated KAP meter fitted within the x-ray tube. According to the clinical practices at Dubai hospital Cath lab, the adult default protocol was used for all paediatric patients. However, for newborn patients a paediatric protocol was used. The measurements were taken using normal fluoro mode and 25cm x-ray field size. This mode is used for the majority of acquisition runs during a coronary angiography procedure.

2.2.1 Calculation of entrance surface air kerma rate

The mean dosimeter reading \bar{M} was calculated. Then the entrance surface air kerma rate, \dot{K}_e , calculated as follows

$$\dot{K}_e = \bar{M} N_{K,Q0} k_Q k_{TP} \left(\frac{B_w}{B_{PMMA}} \right) \quad (4)$$

Where B_w and B_{PMMA} are the B for water and PMMA, respectively.

2.2.2 Verification of patient dose indicators

Kerma area product (KAP) and skin dose indicators (cumulative air kerma (CAK)) are the main parameter to assess the patient dose value in the IC. Accordingly, the meter should be calibrated correctly and verified.

2.3 Effective Dose and Risk Assessment

Effective dose (E) is the main parameter used to predict stochastic effects and assess the radiation risk. In this study the E were estimated for paediatric patient in both conventional radiology and interventional cardiology. The software PCXMC 2.0 was used to calculate the E and estimate the radiation risk.

2.3.1 Paediatric E in fixed and mobile x-ray

In this study, the patient age and exposure parameter were collected from the DICOM header in the period from 2012 to 2014. The exposure parameters collected were the peak tube voltage (kVp), exposure current time product (mAs), Field size (cm) and the KAP values. Patient demographic information (weight and height) were not available in the DICOM header, therefore, the PCXMC 2.0 software settings for weight and height was used. The dose unit of KAP reading was $\mu\text{Gy.m}^2$ and it was converted into mGy.cm^2 then entered into PCXMC 2.0 program.

2.3.2 Paediatric E in interventional cardiology

For this part of study, the patient demographic information and dosimetric parameter were collected manually because the interventional cardiology system was not integrated with the DICOM system. Since the x-ray tube is under the couch; the projection angle selected in the PCXMC program was Posterior Anterior with angle 90 degree. The focus to skin distance was kept as much as possible at 61 cm. The collected readings for KAP, air kerma and fluoroscopic time were derived from the sum of both planes (frontal and lateral). The collected data were missing information related to the type of the clinical procedure. Hence, the collected dosimetric values were mixture of diagnostic and therapeutic procedures. It is noticed that the majority of the cases were described as therapeutic procedures. The patient KAP readings were corrected for patient table absorption factor 0.75 and for KAP calibration factor 1.39. For CAK, the corrections for table absorption factor 0.75 and CAK calibration factor 1.07 were applied. The paediatric patient's stochastic radiation risks were estimated by the PCXMC 2.0 software for both genders.

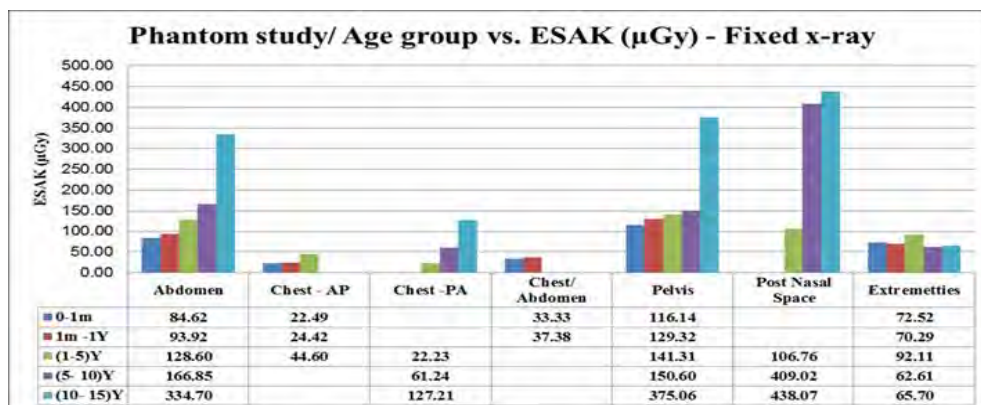
3 RESULTS AND DISCUSSION

This study was designed to reflect authentic clinical imaging situations for paediatric patients in the general x-ray and interventional cardiology practices. The outcomes of the present work based on phantom study and clinical data derived from the DICOM header for both fixed x-ray and mobile x-ray machines while for interventional cardiology procedures the patient exposure data were collected manually by the Cath lab technicians.

3.1 Digital Fixed X-ray

For the phantom study it is recognized from the below graph Fig.1 that the ESAK increases as patient age group increase except for the extremities examinations. The highest extremities value were found for the age group >1-5y; because the mAs was higher than the other age groups. Moreover, to reduce child dose in the chest examinations, especially the age group (>1-5y), vertical bucky is recommended with cooperative patients otherwise the grid should not be used for lying position.

Figure1: Phantom study- ESAK vs. Patient age groups



The patient data which was collected from the DICOM header is considered as one of the most efficient methods used recently for estimating the patient ESAK indirectly from the digital system. A number of surveyors and organizations recommended the use of this method as it is more straightforward and systematic [3-5]. The data collected for local Diagnostic Reference level (LDRL) shows that the numbers of the cases for newborn patients were 2 and 4 for the pelvis and extremities examinations, respectively. The results of this group were limited because the sample is very small. The mean ESAK values published by different surveyors were summarized in Table 1 for the five common examinations covered in this study and compared to the current study values.

Table 1: Fixed x-ray- LDRL Comparison between current study and other surveyor's

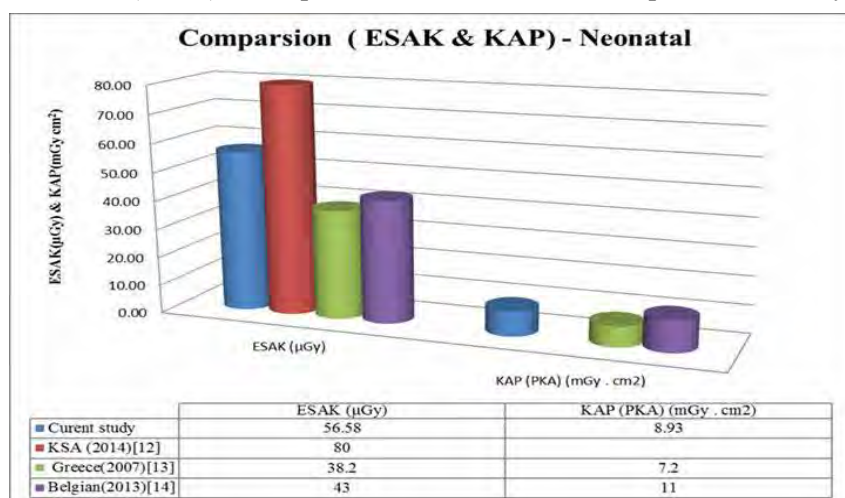
Examination	Age group	ESAK (K_e) (μGy)						
		Current study	DHA-Children and women's hospital	Austria	UNSCARE	Italy	Ireland	UK
Chest	Newborn	37.53	54.69	55	60	80	-	50
	>0-1y	37.36	68.87	69	80	-	57	50
	>1-5 y	41	45.84	82	110	100	53	70
	>5 - 10 y	62.33	64.3	108	70	-	66	120
	>10 - 15 y	61.78	136.44	112	110	-	88	-
Abdomen	Newborn	62.18	56.4	100	110	-	-	-
	>0-1y	117.1	65.3	172	340	-	330	400
	>1-5 y	107.49	94.88	511	590	1000	752	500
	>5 - 10 y	207.35	284.95	966	860	-	-	800
	>10 - 15 y	396.31	-	-	2010	-	-	1200
Pelvis	Newborn	69.44	-	-	170	200	-	-
	>0-1y	162.29	-	-	350	-	265	500
	>1-5 y	165.06	-	-	510	900	475	600
	>5 - 10 y	231.45	-	-	650	-	807	700
	>10 - 15 y	450.01	-	-	1300	-	892	2000
Lat. Skull (Post Nasal Space)	Newborn	-	-	294	-	-	-	-
	>0-1y	-	-	700	340	-	-	500
	>1-5 y	131.92	-	506	580	1000	-	800
	>5 - 10 y	508.81	-	557	-	-	-	800
	>10 - 15 y	506.74	-	676	-	-	-	800

The dose levels for *chest examinations* of the first two age groups (newborn and > 0-1y) were almost identical. This is because AEC was switched off for these two age groups. This dose level similarity also observed for the last two age groups (> 5-10 y and >10 – 15 y). That is due to the automatic selection of same exposure parameters. The *abdomen examinations* have shown an increasing trend with the increase of the patient age except for the group (> 0-1y). The ESAK value for the group (> 0-1y) was 117.1 μGy which is higher than the group (>1-5y) where the value was 107.49 μGy . There was no clear reason except that there is a variation between the patient sizes within the same age group. Similar findings were observed by Matthews K. et al., (2013) [5], where he stated that the reason for the variation in the KAP values was not related to the radiographer technique; it was due to the variation in the patient size within the same age category. Moreover, the ICRP and IAEA mentioned this issue in their publications [1-3]. Similar dose levels were observed for the *skull examinations* of the last two age groups; the ESAK values for the (>5-10 y) was 508.81 μGy while for the (>10-15y) was 506.74 μGy . However, the dose difference between these two groups was not significant. It is expected that the reason behind this situation is that the exposure parameters were similar. The *pelvis examinations* demonstrated smooth linear relationship with the increasing of the patient age. For the extremities, the mean ESAK values were fluctuating between the patient age groups; the main reason was the limited number of the patients in the first two age groups and the collimation selected by the radiographer. In general, the trend is that the patient radiation dose is increasing with the increasing of the age group which has been also stated in Linet et al., (2009) survey [6]. It is clearly shown that our ESAK values were the lowest among the other published data. Also, it is noticed that there is no data by the other surveyors on the radiation dose for the combined chest-abdomen and extremities examinations.

3.2 Digital Mobile X-ray (Neonatal Intensive Care Unit)

The highest percentage of the examinations performed was for the paediatric patients of age group (0-1) y. Hence, 41 patients were selected from the DICOM system at Dubai hospital NICU to investigate the radiation dose level delivered to them during their hospitalization. The mean value for the exposure parameters that used for the neonates in this study were 53 kVp and 1.98 mAs, were less than those recommended by the Commission of the European Communities (CEC) (CEC, 1996) [7], where the voltage of kVp ranged from 60 to 65 for screen film system. From Fig. 2, it is noticed that the mean ESAK values for the combined chest –abdomen examination for this work was higher than the data published for Greece and Belgium [8, 9] and lower than those for Kingdom of Saudi Arabia (KSA) [10]. The KAP readings in this study were lower than the readings from Belgium [8] and comparable to those from Greece [9]. The main reasons for this variation in the ESAK doses among the surveyors are mainly due to the use of different exposure factors, type of the x-ray machines used (digital, computed tomography or screen film), tube filtration and collimation.

Figure 2: Neonatal (NICU) - Comparison the LDRL with other published surveys



3.3 Interventional Cardiology

Interventional cardiology is considered as the x-ray modality that delivers the highest radiation dose to the patients compared to the fixed and mobile x-ray units. As a first step, the performance of this imaging system was assessed. The ESAK values for the different six phantom thicknesses used under pre-set clinical conditions shows that for both Fluoro mode and image acquisition (cine mode) have a linear relationship between the phantom thicknesses and the ESAK values. This relationship has strong correlation; it was $R^2 = 0.93$. The same trend observed for the exposure parameters (kVp and mAs).

The total number of paediatric patients collected with sufficient information was 88 patients where the mean weight were 3.36, 7.14, 12.16, 18.34 and 52.33 kg and mean ages were 5.8 day, 7 month, 2.9 year, 6.58 year and 12.3 year for the five age groups, respectively. The highest number of cases of paediatric patients were for the two age groups (>0-1y and >1-5y) while the lowest number of cases was for the newborn. For the dosimetric values, the data collections were total KAP, Air kerma value and Fluoro Time (FT). The mean KAP values were 2.258 ± 0.82 , 10.682 ± 9.26 , 20.454 ± 31.96 , 19.09 ± 14.23 and 53.622 ± 63.52 Gy.cm² for the newborn, >0-1y, >1-5y, >5-10y and >10-15y, respectively. It is noticed that the KAP value of age group (>1-5 y) is slightly higher than the second one (>5-10), this is possibly due to the limited number of the collected cases in the second group and the heterogeneous of the patient in the same age group. The mean value for the skin dose (Air kerma) were 26.76 ± 8.59 , 10.68 ± 9.26 , 217.19 ± 282.71 , 175.57 ± 139.64 and 538.2 ± 492.1 mGy for the newborn, >0-1y, >1-5y, >5-10y and >10-15y, respectively. The mean FT were 7.03 ± 1.4 , 17.5 ± 5.69 , 14.4 ± 11.9 , 10.6 ± 6.8 and 30.3 ± 34.6 minutes (min) for the five age groups, respectively. This large variation in the range of the paediatric dosimetric values (KAP, Air Kerma and FT) in the interventional cardiology also observed and stated by several researchers [11-14].

3.4 Effective dose (E) and Risk Assessment

Table 2 illustrates the value of E for each age group at the fixed x-ray and it is noticed that the E of the (chest, abdomen and combined chest-abdomen) examinations show how much the paediatric groups are sensitive to radiation, where the sensitivity increases as the age decrease.

Table 2: Fixed x-ray Effective dose for paediatric patient and the stochastic radiation risk for both genders

Age Group	Newborn		>0 - 1 y		>1 - 5y		>5 - 10 y		>10 - 15 y	
	KAP $\mu\text{Gy.m}^2$	E μSv	KAP $\mu\text{Gy.m}^2$	E μSv	KAP $\mu\text{Gy.m}^2$	E μSv	KAP $\mu\text{Gy.m}^2$	E μSv	KAP $\mu\text{Gy.m}^2$	E μSv
Chest	0.48	15.8	0.73	12.9	1.24	12.6	2.81	22.1	4.27	22.7
Abdomen	1.4	35.1	4.05	37.0	5.57	36.8	16.78	80.7	39.97	103
Chest/ Abdomen	0.9	28.5	1.99	28.3	-	-	-	-	-	-
Lat. Skull	-	-	-	-	3.1	4.16	13.12	10.8	15.78	9.72
Pelvis	1.7	9.02	3.3	30.8	5.54	29.6	13.53	41.8	33.3	68.6
Extremities Hand	0.8	0.84	0.89	0.37	1.37	0.25	1.45	0.09	2.06	0.05

For the neonatal patients in the NICU, the values of the E show that the combined chest-abdomen was (**23.03 μSv**) which is comparable to that for the newborn patient (28.5 μSv) in the fixed x-ray. The exposure parameters used with neonatal patient were (kVp=53 and mAs=1.98) lower than those used for the newborn in fixed x-ray (kVp =60.8 and mAs=2.17) as extracted from the DICOM header. It has to be kept in mind that the risk of ionizing radiations is strongly dependent on the child's age and the time of exposure as revealed by IAEA and ICRP [3, 1].

For the IC, it is clearly shown in Table 3 that the E and the radiation risk from this type of ionizing procedure are higher than what is demonstrated earlier. The IC effective dose is given in mSv while in general x-ray was given in μSv . In terms of gender sensitivity in IC, the similarity was observed as in general x-ray. That is the female is more sensitive than male by a factor of around 1.7.

Table 3: IC (Cath-lab) -Effective dose and stochastic radiation risk

Interventional Cardiology			Male -Stochastic radiation risk		Female -Stochastic radiation risk	
Age group	Total KAP Gy.cm^2	Effective dose E mSv	Risk of Exposure - Induced cancer death %	Loss of life expectancy	Risk of Exposure - Induced cancer death %	Loss of life expectancy
Newborn	2.26	2.44	3.01E-02	3.4 days	5.10E-02	6.5 days
> 0 - 1 y	10.68	6.35	9.23E-02	11.6 days	1.42E-01	18.3 days
>1 - 5y	20.45	12.24	1.39E-01	14.4 days	2.49E-01	23.5 days
>5 - 10 y	19.09	9.78	9.74E-02	9.2 days	1.66E-01	15.7 days
>10 -15 y	53.62	14.04	1.22E-01	11.2 days	2.08E-01	20.2 days

4 CONCLUSION

- The indirect measurements of the ESAK in digital fixed x-ray examinations were not exceeding the recommended values reported by international organizations and they were lower than other published data. DICOM system was a very useful tool to extract the patient demographic and dosimetric information. Moreover, the tube output measurements also are considered a very good

alternative method for indirect measurement of the ESAK in case of KAP damage or DICOM system corrupted.

- Although the E value for the chest examination is the lowest in x-ray imaging. Nevertheless, it has to be borne in mind that the frequent request of this type of examinations result in relatively high cumulative radiation doses.
- The patient collected data shown that our KAP readings were higher than some of other published data and comparable to one of them. A wide variety found between the patient KAP values, even with same age group, may be due to the complexity of some of IC procedures and different patient sizes.
- Patient effective doses were easy to be estimated by using the Monte Carlo software PCXMC 2.0.
- In order to manage the establishment of DRLs (local and national), it is important to collect more patient dosimetry data and cover more x-ray systems.
- Further researches are needed to include image quality assessment to stress on obtaining optimum image quality with lower radiation dose.

5 ACKNOWLEDGEMENTS

The authors would like to thank Dubai Hospital (Administration, Medical Physics section, Radiology department and Cardiac centre). Moreover, DHA higher authority and Ethics committee. Colleagues from Zayed military and Alain hospitals and Philips Company for purchasing Monte Carlo software PCXMC 2.0. Moreover, all Physics department member at UAEU and thesis committee (Dr. Renato Padovani and Dr. Bashar Issa).

6 REFERENCES

- [1] Khong PL, Ringertz H, Donoghue V, et al., 2013. ICRP publication 121: radiological protection in paediatric diagnostic and interventional radiology. *Annals of the ICRP*. 42(2):1–63.
- [2] Pernička F, McLean ID, International Atomic Energy Agency, 2007. *Dosimetry in diagnostic radiology: an international code of practice TRS No. 457*. Vienna: International Atomic Energy Agency.
- [3] Delis H, Mclean ID, Van W, 2013. *Dosimetry in diagnostic radiology for paediatric patients*. IAEA human Health Series No.24. Vienna.
- [4] Smans K, Vano E, Sanchez R, et al., 2008. Results of a European survey on patient doses in paediatric radiology. *Radiation Protection Dosimetry*. 129(1-3):204–10.
- [5] Matthews K, Patrick C, Brennan, McEntee MF, 2014. An evaluation of paediatric projection radiography in Ireland. *Radiography*. 20: 189-194.
- [6] Linet MS, pyo Kim K, Rajaraman P, 2009. Children's exposure to diagnostic medical radiation and cancer risk: epidemiologic and dosimetric considerations. *Pediatric radiology*.39(1):4–26.
- [7] Kohn MM, Moores BM, Schibilla H, et al., 1996. *European guidelines on quality criteria for diagnostic radiographic images in paediatrics*. Luxembourg: Office for Official Publications of the European Communities.
- [8] Dabin J, Struelens L, Vanhavere F, 2014. Radiation dose to premature new-borns in the Belgian neonatal intensive care units. *Radiation Protection Dosimetry*.158(1):28–35.
- [9] Dougeni ED, Delis HB, Karatza AA, et al., 2007. Dose and image quality optimization in neonatal radiography. *BJR*. 80(958):807–15.
- [10] Alzimami K, Sulieman A, Yousif A, et al., 2014. Evaluation of radiation dose to neonates in a special care baby unit. *Radiation Physics and Chemistry*. 104:150–3.
- [11] McFadden S, Hughes C, D'Helft CI, et al., 2013. The establishment of local diagnostic reference levels for paediatric interventional cardiology. *Radiography*. 19(4):295–301.
- [12] Tsapaki V, Kottou S, Korniotis S, et al., 2008. Radiation doses in paediatric interventional cardiology procedures. *RadiatProt Dosimetry*. 132(4):390–4.
- [13] Bacher K, Bogaert E, Lapere R, et al., 2005. Patient-Specific Dose and Radiation Risk Estimation in Pediatric Cardiac Catheterization. *Circulation*. 111(1):83–9.
- [14] Barnaoui S, Rehel JL, Baysson H, et al., 2014. Local Reference Levels and Organ Doses from Pediatric Cardiac Interventional Procedures. *PediatrCardiol*. 35(6):1037–45.

Radioprotection in Radiosynovectomy Concerning Accompanying Persons and the Public

Susie Medeiros Oliveira Ramos^{a*}, Sylvia Thomas^b, Mônica Araújo Pinheiro^{b,c}, Mirta Bárbara Torres Berdeguez^d, Lidia Vasconcellos de Sá^c, Sergio Augusto Lopes de Souza^a

^aDepartamento de Radiologia. Universidade Federal do Rio de Janeiro – Rio de Janeiro – Brasil

^bServiço de Medicina Nuclear. Hospital Universitário Clementino Fraga Filho. Universidade Federal do Rio de Janeiro – Rio de Janeiro – Brasil

^cDivisão de Física Médica. Instituto de Radioproteção e Dosimetria - IRD. Comissão Nacional de Energia Nuclear - CNEN. Rio de Janeiro – Brasil

^dPrograma de Engenharia Nuclear / COPPE. Departamento de Engenharia Nuclear / Escola Politécnica. Universidade Federal do Rio de Janeiro - Rio de Janeiro - Brasil

Abstract. Radiosynovectomy (RS) is a procedure used for chronic synovitis, consisting on synovial ablation by injection of radiopharmaceuticals. It has been used for treatment of patients with haemophilic arthropathy. However, individuals comforting patients are also exposed to radiation. The present study analyzed the radiological safety of caregivers and family members of patients undergoing radiosynovectomy with 90 Y-Hidroxiapatite. Methods: For this study it was included 51 patients and their caregivers. The injected activities were between 37 and 407 MBq. Dose rates in $\mu\text{Sv}/\text{hour}$ were measured 0.1 to 2.0 meters from the joint. A survey was carried with questions to analyze the profile of the caregivers and discuss about risk groups. Dose rates were far below the one established by Brazilian regulations. About 69% of the patients attended the hospital with their mothers and 20.83% of patients shared bedrooms with younger siblings. There were direct contact with pregnant women in 16.67% of the cases. The majority of patients went home by taxi or private vehicle (92%). Although dose rates were in accordance with national regulations, some doses were relatively high at 0.1 and 0.5 m from the patient, showing that protective measures are important in order to reduce doses from internal and external exposure. Physicians should recommend precautions including limiting time around risk groups, and taking preferences with private transport. It is important to emphasize that the external exposure of members of the public to patients that underwent radiosynovectomy with 90 Y-Hidroxiapatite does not require special restrictions.

KEYWORDS: *radiosynovectomy; haemophilic arthropathy; family members; caregivers; radiological safety; 90Y-Hidroxiapatite.*

1 INTRODUCTION

Radiosynovectomy (RS) is an outpatient procedure frequently used for chronic synovitis. This technique consists on synovial ablation by injection of beta-emitting radionuclides, such as Yttrium-90, and has been widely used to treat patients with haemophilic arthropathy [1-5].

It is well established that after every medical procedure there is a need to educate patients, family members and other caregivers to ensure that the needs of the patients are met, as described in the comprehensive care program by the World Federation of Hemophilia's Guidelines [6].

However, according to the International Commission on Radiological Protection (ICRP), Publication 103, individuals caring for and comforting patients are also exposed to radiation [7].

These individuals include family and close friends who hold children during procedures and may come close to patients following radiopharmaceutical administration. It is also very important to avoid

*Susie M. O. Ramos, e-mail: medeiros.susie@gmail.com

internal and external exposure of children and pregnant women belonging to the same family due to their higher sensitivity to radiation [7,8].

The International Atomic Energy Agency (IAEA) published in their Safety Reports Series No. 63 (2009) recommendations for dose constraints per episode for different categories of caregivers after therapy with radioiodine, which was adapted from ICRP 94 and based on a rationale developed in the European Union [8-10]. These recommendations have been interpreted differently in various countries. Brazilian regulations have determined that the release of patients can only occur if dose rates are below 30 $\mu\text{Sv/h}$ at 2.0 m from the patient and establish a dose constraint of 5 mSv for caregivers per episode [11].

According to IAEA, patients do not need to be hospitalized automatically after all radionuclide therapies. Instead, the relevant national dose limits and dose constraints should be observed. This should be followed by optimization [9]. For ICRP 94, the decision to hospitalize or release a patient should be determined on an individual basis, and should consider factors such as the residual activity in the patients, their wishes, occupational and public exposures, family considerations, cost, and environmental aspects [8].

When the patient is released from the hospital, exposure to members of the general public also occurs, but this exposure is almost always very small. The unintentional exposure of members of the public on public transport usually is not high enough to require special restrictions on nuclear medicine patients, except for those being treated with radioiodine, according to ICRP [8,12].

Yttrium-90 is considered one of the beta-emitters less harmful for comforters and carers after the patient is released [8]. ICRP 94 states that if a patient is treated with up to 200 MBq, there is no need for further precautions when it comes to public exposure [8]. In IAEA Safety Reports Series n° 63 it is shown some national maximum activities of ^{90}Y for patient release [9]; no values were given by the USA due to minimal exposures of the public. However, Sweden and Japan recommend a maximum of 1200 MBq, and Australia, 4000 MBq [9].

The present study aimed to analyze and discuss the radiological safety of caregivers and family members of patients undergoing radiosynovectomy with ^{90}Y -Hydroxiapatite for the ablation of the inflamed synovium tissue in a Brazilian cohort.

2 MATERIALS AND METHODS

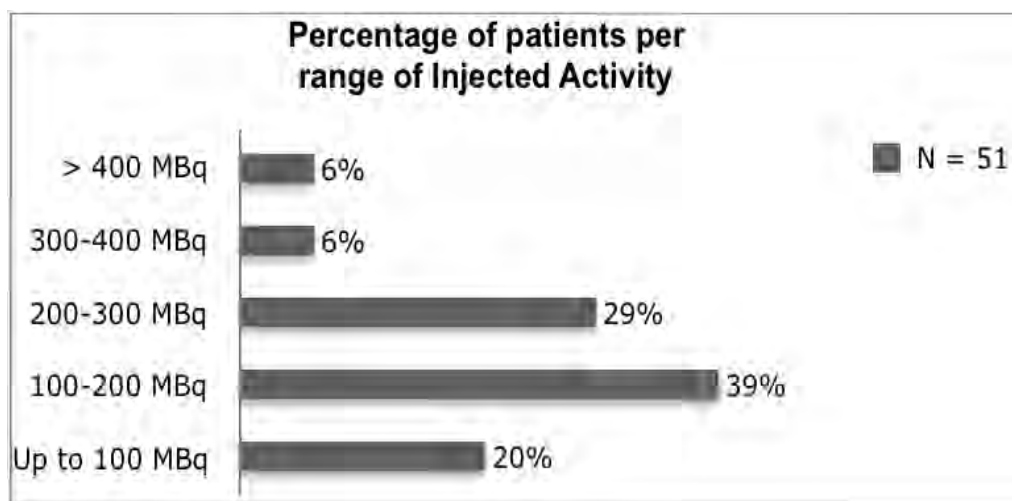
This is a preliminary study that belongs to a research project concerning all radiological safety aspects of radiosynovectomy with ^{90}Y -Hydroxiapatite in male patients with haemophilic arthropathy, which is being carried out in a Brazilian University Hospital.

For this study it was included a total of 51 (fifty-one) patients with mean age of 15.09 (range 3- 31, SD 6.13) and their caregivers with mean age of 37.35 (range 25-52, SD 8.55). The injected activities were between 37 and 407 MBq, according to the medical condition of the patient, with 88% of patients receiving below 300 MBq (Fig. 1).

Dose rates in $\mu\text{Sv/hour}$ (minus the background radiation) were measured 0.1 to 2.0 meters from the treated joint of the patient with a calibrated Eberline E600 Survey Meter from Thermo Electron Corporation about ten minutes after injections, with the purpose to evaluate the dose rates received by the caregivers, comforters and family members who remained by these distances from the patients.

Furthermore, a survey was carried with questions to analyze the age groups, degree of kinship, means of transportation, presence of individuals from risk groups, such as infants, children or pregnant women, close to the patient and the time they spent next to these individuals.

Figure 1: Percentage of patients per range of injected activity. The majority of patients (88%) received less than 300 MBq of ^{90}Y -Hydroxiapatite.



3 RESULTS

Preliminary results concerning caregivers and family members of a Brazilian research project concerning all radiological safety aspects of radiosynovectomy with ^{90}Y -Hydroxiapatite in patients with haemophilic arthropathy are shown in this study.

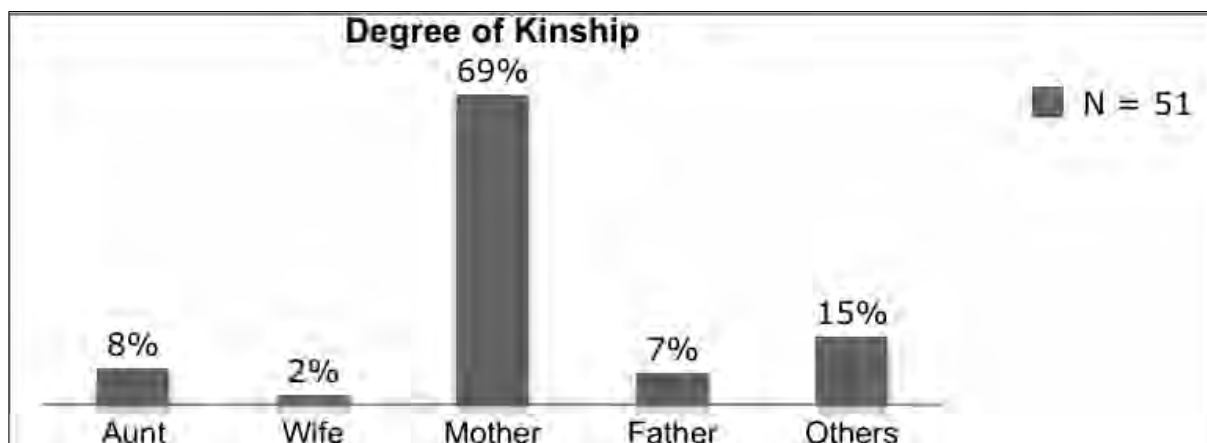
The mean dose rates ($\mu\text{Sv/h}$) minus the background radiation measured from 0.1 to 2.0 meters from the treated joints of the patients with an Eberline E600 are shown in Table 1. Background radiation (Bg) was between 0.2 and 0.5 $\mu\text{Sv/h}$.

Table 1: Mean dose rates ($\mu\text{Sv/h}$) from 0.1 to 2.0 m from the patients.

Distance from the patient in meters	Mean dose rates in $\mu\text{Sv/h}$ minus background radiation (range)
0.1	20.50 (2.00 - 55.00)
0.5	5.67 (1.30 - 32.00)
1.0	1.01 (0 - 2.00)
2.0	0.21 (0 - 1.50)

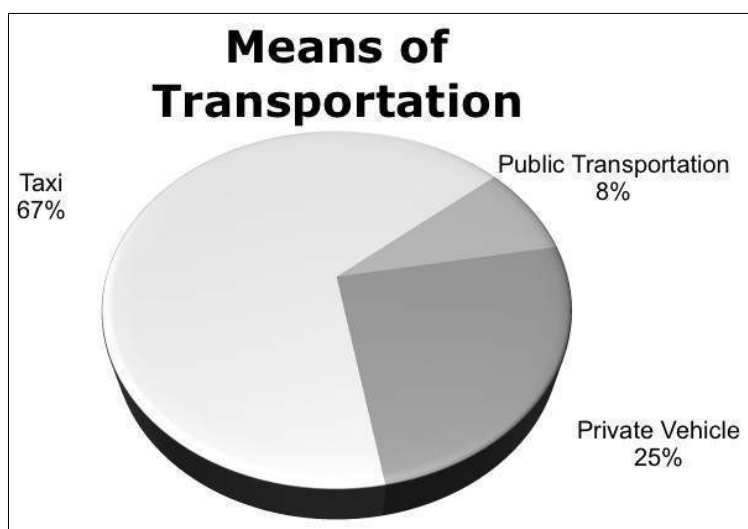
Considering that most patients (72%, n=51) were under 18 years old, some were being accompanied by young mothers and younger siblings. For that reason, 69% of the patients attended the hospital with their mothers, whom some were still young (mean age 37, range 27-52, SD 8.62), and 20.83% of the patients shared bedrooms with younger siblings (youngest was 8 months old). The degree of kinship from family members who were making accompany is available in the chart of Fig.2. There were direct contacts with pregnant women in 16.67% of the cases.

Figure 2: Degree of kinship from family members making accompany to RS patients. “Others” include: close friends, grandmothers, cousins and in-laws.



When it comes to means of transportation used after the release of patients, only 8% of them went home by public transportation, as shown in Fig.3. The majority went home by taxi or private vehicle.

Figure 3: Means of transportation used by the patients after hospital release (N=51).



4 DISCUSSION

Although some patient were treated with up to 407 MBq of ⁹⁰Y-Hydroxiapatite, the activities injected were 1/3 of the maximum recommended for the release of patients treated with Yttrium-90 by the Swedish and Japanese governments, and 1/10 of the Australian recommendations.

Dose rates were far below the one established by Brazilian regulations of 30 μSv/h at 2.0 m from all patients. The maximum dose rates counted in this study or analysis were 1.5 μSv/h at this distance.

In spite of the fact that the dose rates were in accordance with national regulations, some doses were relatively high at 0.1 and 0.5 m from the patient, therefore it is important to take protective measures in order to reduce doses from external exposure. Shortening the time of exposure, increasing distance from the radiation source (joint of the patient with the radiopharmaceutical) and shielding are the basic

countermeasures, also known as General Principles of Radiation Protection. The professionals involved in this procedure should always be trained in the principles of radiological protection, including the basic principles of physics and biology [7].

Patients travelling after radiosynovectomy rarely present a hazard to other passengers in public means of transportation if travel times are limited to a few hours, but it could be recommended preference for taking private transport when leaving the hospital. Notwithstanding, it is also very important to avoid contamination of pregnant women, infants and young children, owing to their sensitivity to biological radiation effects [9].

Due to the fact that the majority of individuals making accompany were young women of childbearing age – mothers, aunts and wives, some also with younger siblings – it could be recommended grandparents, who are much less sensitive to radiation, to make accompany during this procedure and/or a suitable distance of 1.0 meter from the patient, when feasible.

5 CONCLUSION

Physicians should recommend some precautions including limiting time around infants, children, young or pregnant women, and taking preferences with private means of transportation, since contamination should always be a concern. Nevertheless, it is important to emphasize that the external exposure of members of the public to patients that underwent radiosynovectomy with 90 Y-Hidroxiapatite is not high enough to require special restrictions.

6 ACKNOWLEDGEMENTS

The authors acknowledge the professionals from the 23 Brazilian hemophilia treatment centres who referred their patients to this study, and the multidisciplinary team from the Nuclear Medicine Service of the University Hospital Clementino Fraga Filho, RJ - Brazil and Coordenação de Aperfeiçoamento de Pessoal de Nível Superior (CAPES) - Brazil for a scholarship.

7 REFERENCES

- [1] Llinas A. The role of synovectomy in the management of a target joint. *Haemophilia* 2008;14(Suppl.3): 177-180.
- [2] Rodriguez-Merchan EC. Hemophilic synovitis of the knee: radiosynovectomy or arthroscopic synovectomy. *Expert Review of Hematology* 2014; 7(4): 507-511.
- [3] Thomas S, Gabriel MB, Assi PE, *et al.* Radioactive synovectomy with Yttrium90 citrate in haemophilic synovitis: Brazilian experience. *Haemophilia* 2011; 17: e211-e216.
- [4] Rodriguez-Merchan EC, Valentino LA. Safety of radiation exposure after radiosynovectomy in paediatric patients with haemophilia. *Haemophilia* 2015; 1-8.
- [5] Thomas S, Gabriel MC, Souza SAL, *et al.* 90Yttrium-hydroxyapatite: a new therapeutic option for radioactive synovectomy in haemophilic synovitis. *Haemophilia* 2011; 17: 985–989.
- [6] Srivastava A, Brewer AK, Mauser-Bunschoten EP, *et al.* Guidelines for the management of hemophilia. *WFH Guidelines*. *Haemophilia* 2013; 19 (Issue 1): e1–e47.
- [7] ICRP. The 2007 Recommendations of the International Commission on Radiological Protection. *ICRP Publication 103 2007; Ann. ICRP 37 (2-4).*
- [8] ICRP. Release of patients after therapy with unsealed sources. *ICRP Publication 94 2004b; Ann. ICRP 34(2).*
- [9] IAEA Safety Reports Series No. 63: Release of patients after radionuclide therapy, with contributions from the International Commission on Radiological Protection (ICRP). *STI/PUB/1417 (89 pp.;2009) ISBN 978–92–0–108909–0*

- [10] EUROPEAN COMMISSION, Radiation Protection Following Iodine-131 Therapy (Exposures due to Out-patients or Discharged In-patients), Radiation Protection 97, European Commission, Luxembourg (1998).
- [11] Comissão Nacional de Energia Nuclear, Norma NN 3.05. Requisitos de Segurança e Proteção Radiológica para Serviços de Medicina Nuclear. Resolução CNEN 159/13, Dezembro. CNEN NN 3.05 2013, p.16.
- [12] ICRP. Radiological protection in medicine. ICRP Publication 73. Ann. ICRP 26 1996a.

Physicians' Knowledge about patient Radiation Exposure from CT Examinations: Case of Hassan II Hospital Agadir-Morocco

Slimane Semghouli^{a*}, Bouchra Amaoui^b, Abdelmajid Choukri^c, Oum Keltoum Hakam^c

^aHigher Institute of Nursing Professions and Health Techniques Agadir-Morocco

^bRegional Center of Oncology, Agadir-Morocco

^cNuclear Physics and Techniques Team, University of Ibn Tofail, Kenitra- Morocco.

Abstract. The purpose of this study was to assess physicians' knowledge of radiation doses and potential health risks of radiation exposure from CT. A standardized questionnaire was distributed to physicians. The questionnaire covered the demographic data of the prescriber, the frequency of referrals for CT scan examinations, the physicians' knowledge of radiation doses, the potential health risks of radiation exposure from CT scan and training on patients' radiation protection. A total of 72 physicians (55%) completed the questionnaire. 99% of the practitioners' prescribe CT examinations for patients during their exercises but only 10% of physicians use the guideline during CT prescriptions. 38% of prescribers took into account the ratio benefit/risk related to x-rays during radiological exam prescription. While 4% of prescribers' explained the risk related to x-rays to the patients during radiological exam prescription, 14% of physicians have correctly estimated the effective dose received during an abdomen pelvic scan compared to the dose of a standard chest x-ray radiograph in an adult. 54% of doctors underestimated the lifetime risk of fatal cancer attributable to a single computed tomography scan of the abdomen pelvic and 8% of practitioners have received formal training on risks to patients from radiation exposure. Recurrent training in advanced radiation protection of patients could lead to significant improvements in knowledge and practice of CT prescribers.

KEYWORDS: *CT scans; physicians' knowledge; patient' radiation exposure.*

1 INTRODUCTION

Every day in each hospital, Physicians use various X-rays technologies to screen diagnose, stage and treat cancers with the aim of saving thousands of lives. The use of CT in medical diagnosis delivers radiation doses to patients which are higher than those from other radiological procedures.

The biological effects of low doses received during medical diagnostic imaging can cause harm. The cancer radiogenic is well documented [1,2], indeed the lifetime attribute to the risk of cancer is 1 for every 82 in high-use groups [3] and 1 in every 1000 CT abdomen pelvic examination [4]. For example, in the United Kingdom, it has been estimated that 100 to 250 death cases occur each year because of the radiological exposures [5,6].

In any diagnostic procedure the dose of radiation delivered should be [7, 8] enough to answer the relevant clinical question. Moreover, it should be and as low as reasonably achievable to minimise the risk to the patient.

It is very important that physicians who prescribe radiological imaging should be well trained in deciding whether diagnostic imaging is necessary and have an accurate knowledge of the associated risks.

The absence of studies on doctors' knowledge in Moroccan Hospitals and the lack of knowledge on the medical exposure per inhabitant in Morocco [9] initiated us to undertake the current study.

The aim of this study is to assess knowledge of patient radiation exposure from CT examinations prescribed in Hassan II Hospital.

*Corresponding author email address: ssemghouli@gmail.com

2 MATERIALS AND METHODS

We carried a survey between November 2014 and March 2015. The study was conducted in Southern Morocco in Agadir Ida Outannane city which has 421 844 urban inhabitants [10].

The concerned population included the prescribers of CT scans in Hassan II hospital. In total, the entire population studied comprised 130 practitioners [11]. The participants in this study have received a standardized questionnaire.

The 16 sections of the questionnaire were designed to evaluate the current practice regarding the prescriptions of CT examinations. The questionnaire covered five main areas:

The first requested demographic data of prescriber (department, gender, qualification, years of experiences).

The second part included questions and aimed at:

- Prescription frequency of CT scans,
- The use of medical imaging examinations guide before prescription.
- Knowledge of benefit /risk ratio of the use of x-rays,
- Routine patient's information about possible health risks.

The third tackled doctors' knowledge on radiation doses which can be assessed into two approaches:

- Compare the average of effective dose received during Abdomen pelvic CT scan ($D_{AP}^{CT} \sim 11$ mSv) and Radiography Skull ($D_{SC}^R = 0,07$ mSv) examinations [4].
- Evaluate the effective dose received during Abdomen pelvic CT scan examination.

The fourth dealt with prescribers' knowledge of the risk of cancer induction after one CT scan Abdomen pelvic examination.

Finally, we asked doctors if they had already received training with regards to radiation protection.

3 RESULTS

3.1. The study population

Out of the 130 physicians' practitioners in our hospital, 72 participated in the questionnaire giving a response rate of 55%. There were 42 men (sex ratio 1.4). The study group contained the General practitioners, Interns, Surgeons and Medical specialists. The percentage of each specialty was respectively 10%, 19%, 36% and 37%. The average professional experience for all participants was $10,29 \pm 6,83$ years with 58% of them having more than 10 years of experience.

3.2. Current Prescribers Practice Regarding CT Examinations

99% of respondents to the survey were prescribers' of CT examinations. The physicians' non prescribers were Medical specialists in dermatology.

Only 8% of our study group used a guideline for prescribing the less irradiating exam. It was constituted by 33% of Interns and 20% of General practitioners.

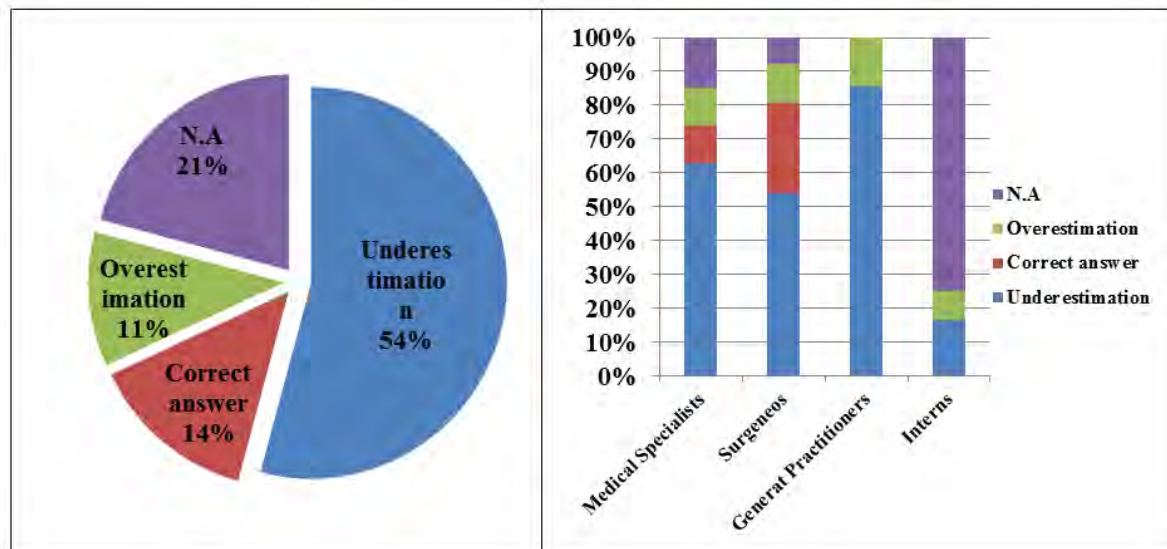
38% of them said that they always take into account the benefit /risk ratio of X-rays when prescribing a scanner, while 54% sometimes use it and 8% never. The benefit/risk of X-rays is still considered by 42% of senior doctors and only 17% of juniors.

Only 4% of practitioners have always informed patients about the probable risks due to their exposure to X-radiation, while 68% did so occasionally and 28% never. Thus only 5% of Physicians seniors have always passed such information to the patient, while Interns represent 0%.

3.3. Knowledge of Doses and Health Risks Related to Radiations by Doctors

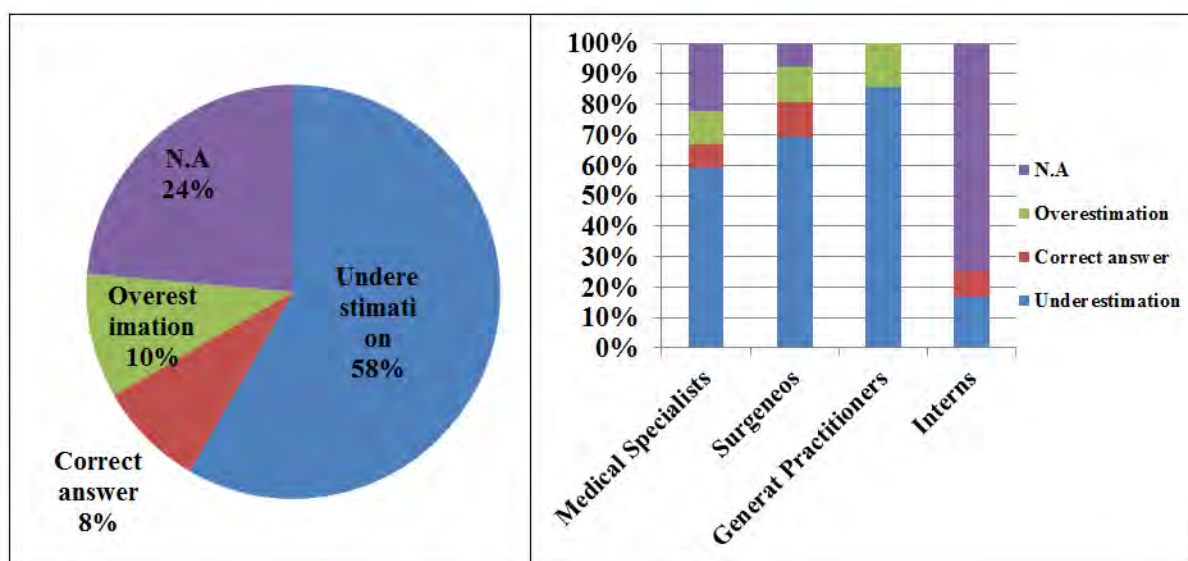
On the assessment of the effective dose received during an abdomen-pelvic CT compared to chest X-ray front, 14% of our practitioners had correctly assessed that dose. 11% had overestimated it while 54% of practitioners had underestimated it and 21% have no answers, regardless of the different specialties (Figure N°1).

Figure 1: Assessment of knowledge of the effective dose received during an abdomen-pelvic CT comparatively to an adult chest radiography by physicians per speciality.



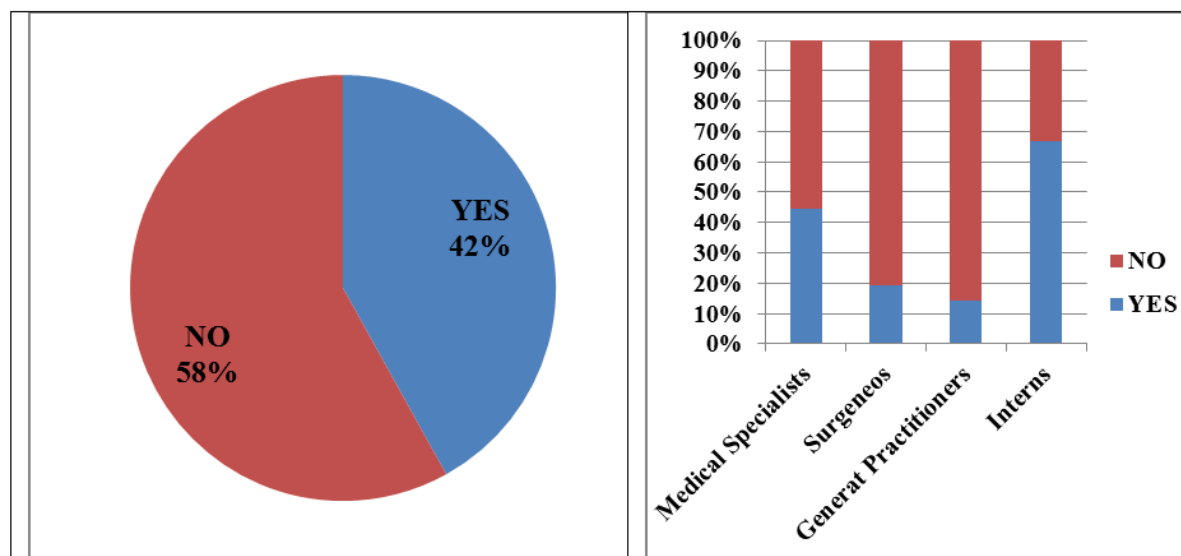
During the absolute evaluation of the dose delivered during a standard abdomen-pelvic CT, with reference to natural radiation in Morocco estimated to average 2.5 mSv per year, 8% of practitioners had correctly assessed the dose. 10% of prescribers had overestimated it, 58% underestimated it while 21% had expressed no opinion (Figure N°2).

Figure 2: Assessment of the knowledge of effective dose received during an abdomen-pelvic CT comparatively to annual background exposure in Morocco by physicians per speciality.



Estimations of doses delivered were misjudged, and the risk of radiation-induced cancer were greatly underestimated since a large majority of practitioners (58%) had replied that there was no risk of radiation-induced cancer due to the realization of one abdomen-pelvic CT (Figure N°3).

Figure 3: Assessment of knowledge on radiation-induced cancer after one abdomen-pelvic CT by physicians per speciality.



3.4. Further Education and Training:

Only 8% of clinicians had already benefited from training in radiation protection of patients. The more detailed analysis showed that neither Intern, General Doctor nor Surgeon had received training of this type while only 20% of Medical Specialists have received such training.

4 DISCUSSION

Our study group showed that Physician' knowledge of radiation exposure from medical imaging is insufficient, and that is due to the fact that they don't inform their patients of the risks of radiation exposure, and they underestimate radiation exposure of frequently used diagnostic imaging and the associated risks.

- Only 8% of physicians of this study used a guideline during prescriptions of CT exam. Yet the European directive on the radiation protection for medical purposes requires justification of the radiological procedure which is one of the necessary steps to obtain the radiation protection of patients as part of a quality assurance process [12]. The lack of use of referral guidelines could be explained by the Moroccan radiologists by the absence of national protocols [13].
- 38% of prescribers in our study group took into account the ratio benefit/ risk. This result is much lower than 70% reported by Gervaise et al. in a similar study for a population of French hospital doctors [4].
- Only 4 % of our physicians group have explained the x ray risk to the patients during prescription. This result is much lower than 22% reported by Lee et al. in a similar study for a population of emergency physicians in USA [14] and then 25% reported by Gervaise et al. in a similar study for a population of French hospital doctors [4].
- The knowledge on radiation doses in our study group is limited. In detail, we asked to compare the average effective dose received during an abdomen pelvic CT scan in adults to a standard chest radiograph. Only 14 % of the study participants answered correctly. This result is lower than 30% reported by Lee et al. in a similar study for a population of emergency physicians in USA [14]. And it is also less than 32,5 % obtained by Merzenich et al. in a

similar study in Germany [15]. It is more than 13 % reported by Gervaise et al. in a similar study for a population of French hospital doctors [4].

- The physicians' knowledge on the lifetime risk for the development of cancer after one abdomen pelvic CT examination was answered correctly by only 42% (approx. 1 cancer death per 1,000 deaths) of responds in our study group [16,17]. This result is higher than 12,5 % reported by Jacob et al. for a population of hospital doctors [18]. It is approximately the same as the 31% obtained by Rice et al. for a population of paediatrics surgeons [19]. It is higher than 39% reported by Gervaise et al. in a similar study for a population of French hospital doctors [4].
- The poor knowledge results achieved in this study could be explained by many factors: About 92% of the questioned doctors reported that they have never undergone formal training on patients' radioprotection. This reflects a poor knowledge of the principles of radiation protection by our clinicians. This result is higher than 75 % reported by Gerben et al. for a physician population of the Australian emergency departments [20], and higher than 34% reported by Gervaise et al. in a similar study for a population of French hospital doctors [4].

5 CONCLUSION

The objective of this study was to explore the physicians' knowledge on patients' radiation protection during their prescriptions of CT scan examinations. The obtained results showed that the physicians' knowledge on patient's radioprotection is characterized by:

- 8 % of physicians used a guideline during prescriptions of CT exam.
- 38% of prescribers took into account the benefit/risk ratio.
- Only 4 % of our doctors have been explained the x ray risk to the patients during prescriptions.
- 14 % of the physicians have correctly approximated the radiation doses received during an abdomen pelvic CT scan.
- 42% of physicians' have estimated the lifetime risk for the development of cancer after one abdomen pelvic CT examination in a correct way.
- 92% of doctors have never undergone formal training on patients' radioprotection.

We recommend training during the university curriculum of interns and also the periodic ongoing training of all doctors from all specialties with the aim of improving their understanding of medical radiation exposure.

6 REFERENCES

- [1] Ron E. Cancer risks from medical radiation. *Health Phys* 2003; 85: 47-59.
- [2] Mather R. The physics of CT dose. Toshiba America Medical Systems Inc.
- [3] Griffey RT, Sodickson A. Cumulative radiation exposure and cancer risk estimates in emergency department patients undergoing repeat or multiple CT. *AJR Am J Roentgenol* 2009; 192: 887-892.
- [4] Gervaise. A, Esparbe-Vigneau. E, Pernin. M, Naulet. T, Porton. Y, Lampierre-Combe. M: Evaluation of knowledge prescribing CT examinations on the radiation protection of patients. Elsevier Masson. *Radiology Journal* (2011), 92, 671-678.
- [5] Einstein AJ, Henzlova MJ, Rajagopalan S. Estimated risk of cancer with radiation exposure from 64-slice computed tomography coronary angiography. *JAMA* 2007; 298: 317-323.
- [6] Shiralkar S, Rennie A, Snow M, et al. Doctors' knowledge of radiation exposure: questionnaire study. *BMJ* 2003; 327: 371-372.
- [7] Health Physics Society. ALARA. <http://www.hps.org/public/information/radterms/radfact1.html> (accessed Mar 2009).
- [8] Cember H. Introduction to health physics. 3rd edition. McGraw-Hill, 1996.

- [9] Semghouli S, Amaoui. B, Maamri: Estimated radiation exposure from medical imaging for patients of radiology service of Al Faraby Hospital, Oujda Morocco. *International Journal of Cancer Therapy and Oncology*.2015; 3(3):3325
- [10] Authenticating the numbers laying the legal population of the Kingdom, " Official Gazette of the Kingdom of Morocco, Decree No. 2-15-234 of 28 Jumada I 1436 (19 March 2015), p. 2952 (ISSN 0851-1217) No. 6358, May 7, 2015.
- [11] Publications, Studies Survey: Health in numbers 2013. Edition 2014, Ministry of Health, Kingdom of Morocco.
- [12] Council Directive 97/43/EURATOM/ of 30 June 1997 on Health protection of individuals against the dangers of ionizing radiation in relation to medical exposure and repealing Directive 84/466/Euratom. (OJ L-180 of 9 July 1997).
- [13] Semghouli. S, Amaoui. B, El Fahssi. M, Choukri A., Hakam O. K:Practitioners' Knowledge on Patients' Radioprotection in Emergency and Radiology Services of Hassan II Hospital Agadir Morocco. *International Journal of Modern Physics and Applications* ISSN: 2381-6945 Vol. 1, No. 5, (2015), pp. 205-209.
- [14] Lee CI, Haims AH, Monico EP, Brink JA, Forman HP: Diagnostic CT scans: assessment of patient, physician, and radiologist awareness of radiation dose and possible risks. *Radiology*. 2004 May;231(2):393-8.
- [15] Merzenich., H, Krille. L, Hammer. G, Kaiser. M, Yamashita. S, Zeeb. H: Paediatric CT scan usage and referrals of children to computed tomography in Germany-a cross-sectional survey of medical practice and awareness of radiation related health risks among physicians. *BMC Health Services Research* 2012, 12:47.
- [16] Board on Radiation Effects Research Division on Earth and Life Studies, Committee to Assess Health Risks from Exposure to Low Levels of Ionizing Radiation. *Health Risks From Exposure To Low Levels Of Ionizing Radiation Beir Vii Phase 2*. National Research Council Of The National Academies The National Academies Press Washington, D.C. 2006.
- [17] BrennerDJ , Doll R, Goodhead DT, salle EJ, Terre CE, Little JB, Lubin JH, Preston DL, Preston RJ, Puskin J, Ron E, Sachs RK, Samet JM, Setlow RB, Zaider M. Cancer risks attributable to low doses of ionizing radiation: assessing what we really know. *Proc Natl Acad Sci USA*. November 2003 25; 100 (24): 13761-6. [18] Jacob K, Vivian G, Stell JR. X ray dose training: are we exposed to enough? *Clin Radiol*.2004;59:928–934.
- [19] Rice H E, Frush D. P, Harker M J, Farmer D, Waldhausen J H , Peer assessment of pediatric surgeons for potential risks of radiation exposure from computed tomography scans. *Journal of Paediatric Surgeons* Volume 42, Issue 7, Page 1157-1164.
- [20] Gerben B Keijzers and Charles J Britton: Doctors' knowledge of patient radiation exposure from diagnostic imaging requested in the emergency department. *MJA*• Volume 183 N.

Changes in patients' radiation doses during CT exams in Japan (1997-2014)

Shoichi Suzuki^{a*}, Yuuta Matsunaga^{b,e}, Ai Kawaguchi^{c,e}, Kazuyuki Minami^a, Masanao Kobayashi^a, Yasutaka Takei^{d,f}, Yasuki Asada^a

^aFujita Health University, Toyoake, Aichi, Japan.

^bNagoya Kyoritsu Hospital, Nagoya, AICHI, Japan.

^cToyota Memorial Hospital, Toyota, Aichi, Japan.

^dHamamatsu University Hospital, Hamamatu, Shizuoka, Japan.

^eTohoku University, Sendai, Miyagi, Japan.

^fKanazawa University, Kanazawa, Ishikawa, Japan.

Abstract. Five nationwide surveys on the radiation doses received by patients during CT exams were conducted in Japan from 1997 to 2014. The subject areas were the head, chest, and abdomen of adults, and the head chest, and abdomen of children (5 years old). CTDI was used to evaluate CT doses. In this study, we mainly compared the 2014 data to data from past surveys. The results showed that doses in cranial exams increased from 55.3 mGy in 1997 to 77.4 mGy in 2014. In the 2014 data, doses for single detector CT (SDCT) and multi detector CT (MDCT) were 81.4 mGy and 73.4 mGy, respectively, indicating lower doses with MDCT. Doses in abdominal exams declined slightly from 1997 to 2014 (18.8 mGy to 17.7 mGy) but major changes were not evident. Doses for children were about 50% of adult doses. Except for cranial CT exams, the 2014 data resembled international data. Improvements in equipment and algorithms have increased the number of facilities that can perform exams at 1/10 the dose of past exams, but these institutions are not common in Japan. Dose discrepancies between institutions for the same test are decidedly not rare. The increasing diversity of CT equipment has made lower radiation doses possible, but has not necessarily lowered doses overall. We described the changes in radiation doses from CT exams in Japan over 18 years.

KEYWORDS: *computed tomography; patient exposure; computed tomography dose index (CTDI); survey.*

1 INTRODUCTION

It was shown in reports from the United Nations Scientific Committee that the radiation dose received by patients in radiological scanning in Japan is the highest in the world. However, the details were unclear. Based on the latest results from studies carried out by Japanese academic bodies, diagnostic reference levels were determined for Japanese for X-ray and radioisotope scans, and were announced in June 2015. A part of the data used was our data. Independently, we have been investigating the dose received by patients during X-ray scans in Japan since 1974. Based on independent studies since 1997, we have also been estimating the dose based on imaging conditions in X-ray CT scans. Focusing on data from 2014, we have analyzed the radiation dose received by patients during X-ray CT scans in Japan, compared to past data.

Table 1: Japan DRLs for Adult Computed Tomography [1]

	CTDI _{vol} (mGy)	DLP (mGy·cm)
Routine brain	85	1350
Routine chest	15	550
Chest to pelvis	18	1300
Abdomen to pelvis CT	20	1000
Liver, multi-phase	15	1800
Coronary CTA	90	1400

1) Standard patient weight: 50–60 kg or 50–70 kg for coronary CTA.

2) Liver, multiphase does not include the chest region or pelvis.

*Presenting author, E-mail: ssuzuki@fujita-hu.ac.jp

Table 2: Japan DRLs for Paediatric Computed Tomography [1]

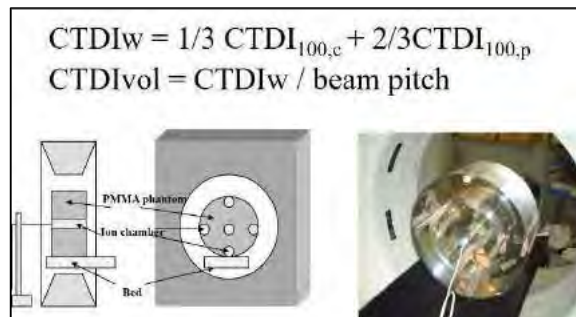
	Younger than 1 year		1–5 years		6–10 years	
	CTDI _{vol} (mGy)	DLP (mGy·cm)	CTDI _{vol} (mGy)	DLP (mGy·cm)	CTDI _{vol} (mGy)	DLP (mGy·cm)
Head CT	38	500	47	660	60	850
Chest CT	11 (5.5)	210 (105)	14 (7)	300 (150)	15 (7.5)	410 (205)
Abdomen CT	11 (5.5)	220 (110)	16 (8)	400 (200)	17 (8.5)	530 (265)

1) Values for a 16-cm diameter phantom along with values for a 32-cm diameter phantom in parentheses.

2 METHODS

We investigated CT scan imaging conditions at 3000 leading facilities in Japan. Five studies were carried out. The first was in 1997, followed by studies in 2005, 2007, 2011, and 2014. The number of valid responses varied from year to year, but was between 20-25%. The studies looked at simple head, chest, and abdominal X-ray CT scans of adults and children (5 years old[A1]). We evaluated our dose value in the standard CTDI_{vol}, as stipulated by the ICRP, IEC, etc. We compared the data we gathered to those publicly released by other countries and institutions. Adult head scans were performed using a 16 cm diameter PMMA, and adult chest and abdominal scans were performed using a 32 cm diameter PMMA.

The child scans were all evaluated using a 16 cm diameter PMMA. We investigated the detector number and image reconstruction at the same time. We calculated CTDI_{vol} dose values based on the imaging conditions at each facility using the dose calculation program ImPACT. The accuracy of the dose calculation program was checked beforehand by comparing the calculated CTDI_{vol} to that obtained by real data.

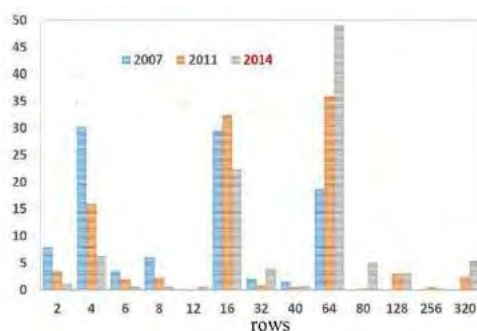
Figure 1: CT dose evaluation: CTDI_{vol}

3 RESULTS

3.1. Changes in the number of detector rows

Here we present our results from the three studies that took place in 2007, 2011, and 2014. In the 2007 study, the percentage of equipment with 4 detector rows was 30% and with 16 detector rows was 29.6%. However, in the 2011 study, the number of detector rows in the equipment had increased such that 32.5% had 16 rows and 35.9% had 64 rows. With the introduction of equipment with 320 detector rows [A2][A3], which had not existed during the 2007 study, it could be seen that in 7 years the change to multi-rows had greatly progressed [A4].

Figure 2: CT rows



3.2. Adult and child doses

In the 2014 study, the child (5 years old [A5]) dose compared to the adult dose was 55%, 73%, and 64% for head, chest, and abdominal scans, respectively. The average dose for each of these scans was 77.4 mGy, 13.0 mGy, and 17.7 mGy for adult head, chest, and abdominal scans, respectively. For abdominal scans, the difference in the results between facilities was larger for children than for adults. It became clear that there was a large difference between child scans at different facilities. There was a significant difference between the image reconstruction methods of the filtered back projection (FBP) and iterative reconstruction (IP), with lower results using the latter method. According to the 2014 data, the use of the IP method was approximately 15% for both adult and child head scans. For adult and child chest and abdominal scans, its use was 35%.

Table 3: Mean CTDIvol for adult and child

	Adult	Child	Child/Adult
Head	77.4	42.7	0.55
Chest	13.0	9.5	0.73
Abdomen	17.7	11.3	0.64

[mGy]

Table 4: Comparison of the distributions of CTDIvol using reconstruction algorithms [2]

Anatomical regions	Reconstructi on algorithm	CTDIvol (mGy)				P-Value	
		n	Mean	Median	CV (%)		
Head (Non-helical)	Adults	IR	66	72.2	69.0	36	<0.05 ^a
		FBP	415	82.1	76.0	34	
	Children (5y)	IR	44	41.6	38.3	42	0.4 ^b
		FBP	254	44.2	41.1	43	
Head (Helical)	Adults	IR	77	66.7	64.0	40	<0.05 ^a
		FBP	362	75.2	72.2	32	
	Children (5y)	IR	47	38.4	31.6	41	0.13 ^a
		FBP	207	43.3	40.0	43	
Chest	Adults	IR	183	10.4	10.0	42	<0.05 ^b
		FBP	359	14.4	12.9	69	
	Children (5y)	IR	92	8.2	6.0	112	0.12 ^a
		FBP	169	10.0	7.1	86	
Abdomen	Adults	IR	184	15.8	14.8	49	<0.05 ^b
		FBP	344	18.7	17.2	46	
	Children (5y)	IR	95	9.2	7.6	92	<0.05 ^a
		FBP	161	12.2	9.9	76	

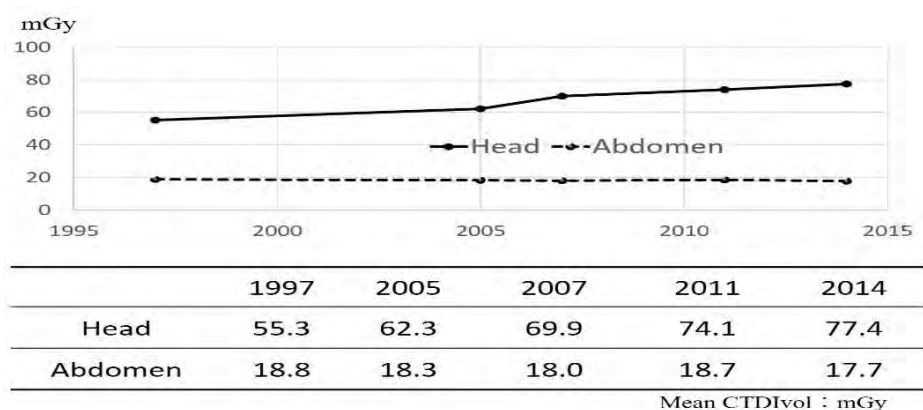
^a indicates that statistical analyses were performed using Student's t-test.

^b indicates that statistical analyses were performed using Welch's t test.

3.3. Dose changes

No significant difference was found between the 2011 and 2014 study of adult and child head scans. A significant difference was found for chest and abdominal scans. For children, the dose had increased slightly since 2011. Based on the results of the 5 studies carried out between 1997 and 2014, the dose increased by 40%, with an average CTDIvol of 55.3 mGy in 1997 and 77.4 mGy in 2014. We found that the dose for head scans has tended to increase in Japan. For abdominal scans, the dose decreased by approximately 6%, from 18.8 mGy in 1997 to 17.7 mGy in 2014. The abdominal dose did not greatly change over 17 years, although it did decrease slightly.

Figure 3: Mean CTDIvol for adult patients (1997–2014)



3.4. Comparison of our data to those of other institutions

The effective doses calculated by multiplying the CTDIvol by the ICRP effective dose conversion factor (k-factor) were found to be larger than the ICRP data for head, chest, and abdomen. In the 2014 study, values of 3.2 mSv, 9.5 mSv, and 16.0 for head, chest, and abdomen, respectively, were found. Further, through a comparison with international data for a 75% dose, it was found that the adult head data were higher. Adult chest and abdomen, and child data were slightly higher, but at the same level as other institutions.

Table 5: Effective dose (75% values: mSv)

	ICRP 87	ICRP 102	Our data
Head	2	2.8	3.2
Chest	8	5.7*	9.5
Abdomen	10-20	14.4	16.0

*MDCT

Table 6: The 75th percentile of CTDIvol for each anatomical region compared with the 75th percentile of CTDIvols reported in other countries [2].

Anatomical regions		UK	Switzerland	Ireland	Thailand	Italy	Portugal	Korea	This study
		2003	2008/2010	2010	2010	2011	2012	2013	2014
Head	Adults	100	65	66	-	69	75	53	92
	Children (5y)	50	40	-	40	-	49.95	-	50
Chest	Adults	13	10	9	-	15	14	13	16
	Children (5y)	13	10	-	10	-	5.6	-	12
Abdomen	Adults	14	15	12	-	18	18	13	22
	Children (5y)	-	13	-	14	-	-	-	14

(mGy)

4 DISCUSSION

It was clear that the detector number of the CT devices is moving towards multi-row devices. As the number of detector rows increases, a decrease in dose is possible, but such a decrease did not necessarily occur. The dose received by patients in CT scans in Japan did not change greatly over 18 years. The head was the body part that received the highest dose. The dose received by a child was 60% that of an adult. Comparing the data from 2014 with international data, the dose received was at the same level except in the case of CT head scans. Through improvements in equipment and algorithms, equipment capable of scanning with less than 1/10 of the conventional dose has been developed, but has not spread to general facilities. The IP method, a calculation algorithm that takes into account image quality and dose, is being introduced in an increasing number of facilities, but looking at Japan as a whole, the proportional use was approximately 15% for head, and 35% for chest and abdominal scans. The difference in dose between facilities for the same procedure is certainly not small. We need to aim for optimum image quality and dose, and to reduce unnecessary doses as much as possible.

5 CONCLUSION

According to our study, the dose for adult head CT scans increased 40% over 18 years. When compared to data from other countries, the adult head scan data from 2014 showed that the dose was larger than that in other countries. The adult abdominal CT scan dose had decreased by 5% over 18 years. When compared to international data, the 2014 abdominal scan data were approximately equal. The data were also approximately the same for children when compared to other countries. We were able to clarify the changes in radiation doses in CT scans in Japan over an 18 year period.

6 REFERENCES

- [1] Diagnostic reference levels based latest surveys in Japan-Japan DRLs 2015-.J-RIME 2015: (<http://www.radher.jp/J-RIME/report/DRLhoukokusyoEng.pdf>).
- [2] Matsunaga Y, Kawaguchi A, Kobayashi K, Kinomura Y, Kobayashi M, Asada Y, Minami K, Suzuki S, Chida K. Survey of volume CT dose index in Japan in 2014. *Br J Radiol* 2015; 88.
- [3] International Commission of Radiological Protection. The 2007 recommendations of the International Commission on Radiological Protection. ICRP publication 103. ICRP; 2007.
- [4] International Commission of Radiological Protection. Managing Patient Dose in Multi-Detector Computed Tomography (MDCT). ICRP publication 102. ICRP; 2007.

Estimation of response characteristics for radiophotoluminescent glass dosimeters in X-ray diagnosis by using Monte Carlo simulation method

Toshioh Fujibuchi^a, Emi Ishibashi^b

^aDepartment of Health Sciences, Faculty of Medical Sciences, Kyushu University, Fukuoka, Japan

^bDepartment of Health Sciences, School of Medical Sciences, Kyushu University, Fukuoka, Japan

Abstract. For radiological diagnosis, patient dose management is important. Especially fluoroscopy-guided procedures such as interventional radiology can be exposed to high dose. Recently, radiophotoluminescent glass dosimeters (RPLDs) are often used for estimation in X-ray diagnosis because RPLDs are very small and able to be place anywhere. To estimate not only entrance surface doses, but also organ doses are important. The actual measured results of RPLDs need to be energy calibrated because RPLDs have the energy dependence especially low energy region. We compared air kerma with absorbed dose of RPLDs by using Monte Carlo simulation code. We used one types of RPLD (GD-302M, Chiyoda Technol Co., Japan). We adopted PHITS as Monte Carlo simulation code. To estimate the energy dependence of RPLDs, the sensitivity of the detector was assessed in photon energy ranging from 20 keV to 100 keV with 20 keV steps and 662 keV. Furthermore, we compared the results with measured data from literature. The relative absorbed dose ratio glass to air in more than 100 keV almost equal the reference value. However the relative absorbed dose ratio in low energy regions are from 1 to 4 times as large as the 662 keV. We confirmed that this low energy dependence of calculated data by using PHITS were identical with measured data.

KEYWORDS: *radiophotoluminescent glass dosimeters; energy dependence; Monte Carlo simulation.*

1 INTRODUCTION

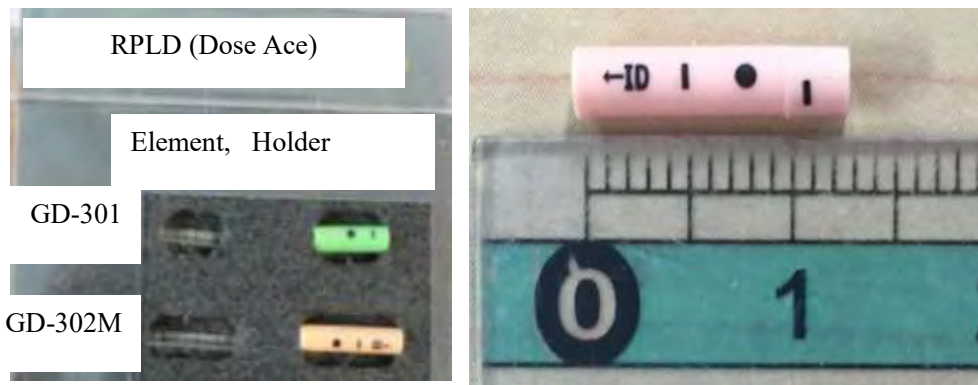
For radiological diagnosis, patient dose management is important. Especially fluoroscopy-guided procedures such as interventional radiology can be exposed to high dose. Recently, radiophotoluminescent glass dosimeters (RPLDs) are often used for estimation in X-ray diagnosis because RPLDs are very small and able to be place anywhere [1, 2]. To estimate not only entrance surface doses, but also organ doses are important for estimation of effective dose at medical exposure. The actual measured results of RPLDs need to be energy calibrated because RPLDs have the energy dependence especially low energy region. We compared air kerma with absorbed dose of RPLDs by using Monte Carlo simulation code.

2 MATERIALS AND METHODS

2.1 Radiophotoluminescent glass dosimeters

We used one types of RPLD (GD-302M, Chiyoda Technol Co., Japan). GD-302M is silver-activated phosphate glass. Its weight composition is as follows: 11.0% Na, 31.55% P, 51.16% O, 6.12% Al and 0.17% Ag [3]. We shows the photograph of RPLDs in Fig 1. The size of glass elements is 12 mm in length and 1.5 mm in diameter. The holder of RPLD is 13 mm in length and 2.0 mm in diameter.

Figure 1: The photograph RPLDs and GD-302M holder.



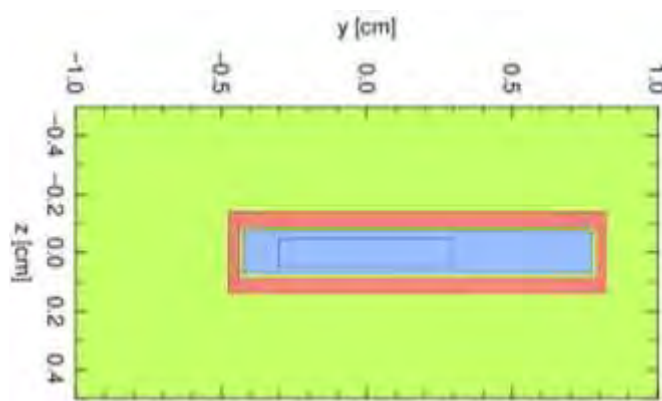
2.2 Monte Carlo simulation code

We adopted Particle and Heavy Ion Transport Code System (PHITS) version 2.80 (Japan Atomic Energy Agency, Japan) as Monte Carlo simulation code [4]. It can deal with the transport of all particles over wide energy ranges, using several nuclear reaction models and nuclear data libraries. We are able to deduce physical quantities such as flux and heat and depict the 2D or 3D geometry in certain area. PHITS is able to chain EGS code system [5]. We used EGS function with PHITS.

To calculate, we used the command named “Tally”. To estimate heat and deposition energy, we used [T-deposit]: Calculating ionization energy losses by charged particles. To estimate the energy dependence of RPLDs, the sensitivity of the detector was assessed in the photon energy ranging from 20 kV to 100 kV with 20 keV steps and 662 keV. About the geometry of calculation, source to glass element distance was 200 cm and 300 cm. At 662 keV, 2 mm thickness of PMMA set in front of glass element to occur electron equilibration. The reconstructed geometry of GD-302M in Monte Carlo simulation is shown in Fig. 2.

To confirm whether behavior of glass dosimeters in Monte Carlo Simulation equal to that of actual, we compared actual measurement reference data of Asahi Glass Co., Ltd. data with calculation data in PHITS, and we made the graph of absorbed dose ratio of glass dosimeter to air. [1].

Figure 2: The reconstructed geometry of GD-302M in Monte Carlo simulation. The components are followings; green; air, pink; Acrylonitril Butadiene Styrene holder, and blue; glass element.

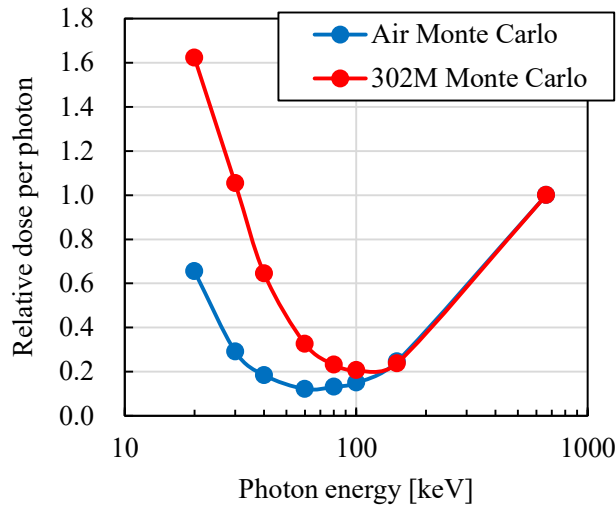


3 RESULTS

3.1 Relative dose per photon

Simulated relative dose per photon of Air, GD-302M are shown in Fig. 3. The reference value is the relative absorbed dose of water to RPLDs with 662 keV. The difference of relative dose to photon were large at low energy.

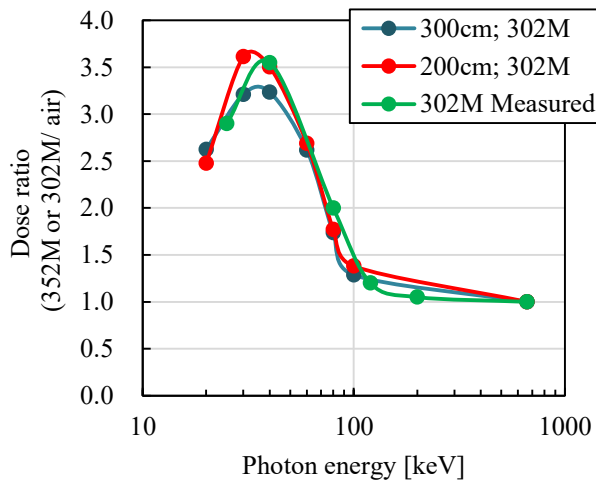
Figure 3: Simulated relative dose per photon of Air, GD-302M. Doses were normalized to 662 keV.



3.2 The energy characteristics of RPLD

The Comparison of the energy characteristics of RPLDs using Monte carlo simulation are shown in Fig. 4. Dose ratio means absorbed dose of glass divided absorbed dose of air at the same point. Additionally, we compared the results with the measured value. The relative absorbed dose in more than 100 keV almost equal the reference value. However the relative absorbed values in low energy regions are from 1 to 4 times as large as the reference value at no filter type. We confirmed that this low energy dependence of calculated data by using PHITS were identical with measured data.

Figure 4. The Comparison of the energy characteristics of RPLD using Monte Carlo simulation and measured data. Doses ratio were normalized to 662 keV.



4 CONCLUSION

The relative absorbed values in more than 100 keV almost equal the reference value. However the relative absorbed values in low energy regions are from 1 to 4 times as large as the reference value at no filter type. We confirmed that this low energy dependence of calculated data by using PHITS were identical with measured data.

5 REFERENCES

- [1] Asahi Glass Co., Ltd. : Fluoro glass dosimeters mall element systems, Dose Ace basic characteristic document, 5/2013
- [2] H. Mizuno, et al. Feasibility study of glass dosimeter postal dosimetry audit of high-energy radiotherapy photon beams, *Radiotherapy and Oncology*. 86:2, 258-263 (2008).
- [3] M. Tsuda. A few remarks on photoluminescence dosimetry with high energy X-rays. *Jpn J Med* 2000;20:131-9.
- [4] T. Sato, et al. Particle and Heavy Ion Transport Code System PHITS, Version 2.52, *J. Nucl. Sci. Technol.* 50:9, 913-923 (2013)
- [5] NEA(Nuclear Energy Agency): CCC-0331 EGS4, Electron Photon Shower Simulation by Monte-Carlo

Small size OSL dosimeter to measure patient exposure dose in X-ray diagnosis - Evaluation of invisibility

Tohru Okazaki^{a*}, Hiroaki Hayashi^b, Kazuki Takegami^b, Yoshiki Mihara^b,
Natsumi Kimoto^b, Yuki Kanazawa^b, Takuya Hashizume^a, Ikuo Kobayashi^a

^a Nagase Landauer, Ltd., Tsukuba, Japan.

^b Tokushima University, Tokushima, Japan.

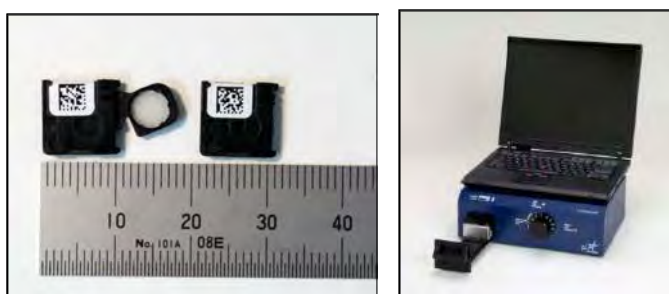
Abstract. The small size OSL dosimeter (nanoDot OSL dosimeter), commercialized by Landauer, Inc., has relatively small angular and energy dependences in the diagnostic X-ray, therefore it was considered to be applied to direct measurement of patient exposure dose. For the direct measurement of the patient dose, the influence of the dosimeter to the medical X-ray image should be studied. The aim of this study is to evaluate the irradiation condition in which nanoDot OSL dosimeter cannot be identified in the X-ray images.

KEYWORDS: OSL dosimeter; x-ray diagnosis; patient exposure dose.

1 INTRODUCTION

Advance in X-ray diagnostics establishes various examines for finding abnormalities of human body. At the same time, the patient dose evaluation is studied based on an ALARA principle. An X-ray irradiation of each examination is performed based on the generalized condition, but in fact a patient exposure dose depends strongly on the physical constitution of the patient. In addition, recent diagnosis system is operated with an automatic exposure control system, so we do not know the actual exposure doses in many cases. Therefore we proposed to perform the direct measurement of patient exposure dose by using a small size OSL dosimeter (nanoDot OSL dosimeter). **Fig. 1** shows photographs of the nanoDot OSL dosimeter (**left**) and its reader (**right**) named “microStar”. The outer size of the dosimeter is 10 x 10 x 2 mm so that it is easy to wear during the X-ray examinations. The microStar reader is a compact system, which can derive the exposure dose with several seconds measurement.

Figure 1: nanoDot OSL dosimeter and microStar reader.



In the past, we studied the characteristics of nanoDot OSL dosimeters for the application to the direct measurement of patient exposure dose in X-ray diagnosis. The dose is mainly constructed by the primary incident X-rays (~70%) and back scattered X-rays (~30%) [1-2]. The energy of scattered X-rays varies with the primary X-ray energies and the scattering angles. These conditions are complicated with the sites of X-ray photographs, the irradiation conditions, and physical constitution of the patient. As a result, the scattered X-rays generated in various locations are incident on the nanoDot OSL dosimeter.

* Presenting author, e-mail: okazaki@nagase-landauer.co.jp

Thus, we evaluated the energy and angular dependences of nanoDot OSL dosimeter with the diagnostic X-ray [3-6], and we expect that the nanoDot OSL dosimeter can be used for direct measurement of patient exposure dose. However it is unclear whether the dosimeter disturbs medical X-ray images or not.

The aim of this study is to evaluate the irradiation condition in which nanoDot OSL dosimeter cannot be identified in the X-ray images.

2 MATERIALS AND METHODS

First of all we explain the concept of our experiments. In this study, we assumed that the response of the one pixel of the two-dimensional X-ray detector can be estimated by the measured spectrum of the X-rays which were through the small-size collimator. **Figure 2** shows schematic drawings of our experiments. In the setup (a), the X-ray spectrum penetrating the phantom with nanoDot OSL dosimeter is measured. In the setup (b), the X-ray spectrum penetrating the phantom without nanoDot OSL dosimeter is measured. We considered that the nanoDot OSL dosimeter can be identified in the X-ray image when we can distinguish these two X-ray spectra. The X-ray spectrum is formed by the Poisson distribution. Accordingly, these two X-ray spectra cannot be clearly separated with consideration of the statistical uncertainties when they have low statistics (with large statistical uncertainties). Namely, the nanoDot OSL dosimeter may not be identified when these two X-ray spectra have low statistics.

Figure 2: Schematic drawing of the experiments. (a) and (b) show irradiation conditions for phantom with nanoDot OSL dosimeter and phantom only, respectively.

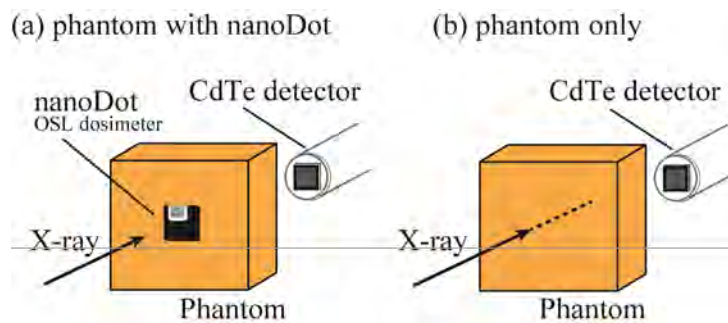
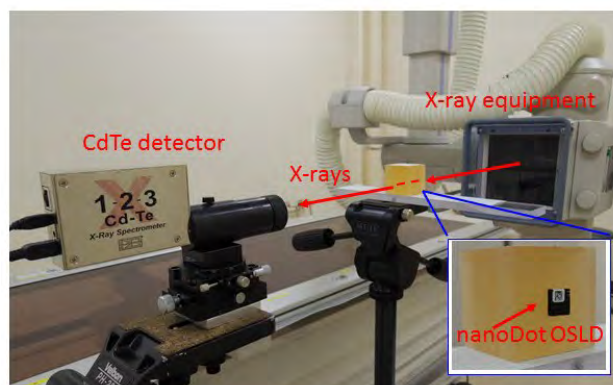


Figure 3 shows a photograph of the experimental setup. 40, 60, 80 and 120 kV of X-rays were generated by the medically-used X-ray apparatus at the 100 cm distance from the CdTe detector. In front of the CdTe detector, there is a multiple-stage collimator having 0.2 mm in diameter; the actual fluence in the 0.2 mm diameter is equivalent to the square (pixel) having 0.18 mm in side. The tube current-time products are 0.5 to 1000 mAs. Between the CdTe detector and the X-ray source, a soft-tissue equivalent phantom of 1, 5, 10, and 20 cm was set.

Figure 3: Photograph of experiment. The inset shows a front view of the soft-tissue equivalent phantom; we can see the nanoDot OSL dosimeter in the center of the phantom.



The X-ray spectra measured with the CdTe detector were corrected by the response functions derived by the Monte-Carlo simulation code (electron gamma shower ver. 5: EGS5) [7, 8]. From the corrected spectra, energy fluence “ Ψ ” and the fluctuation of the energy fluence “ σ ” were calculated as the equation (1), (2) based on the fluence “ Φ ” and the energy “ E ” of the X-ray.

$$\Psi = \int \Phi(E) \times E dE \quad (1)$$

$$\sigma = \sqrt{\int (E \times (\sqrt{\Phi(E)}))^2 dE} \quad (2)$$

Based on the explanations described above (see **Fig. 2**), we evaluated the $\Psi \pm \sigma$ of two experimental conditions: $(\Psi \pm \sigma)_{\text{phantom+OSL}}$ was determined by the experiment in **Fig. 2 (a)**, and $(\Psi \pm \sigma)_{\text{phantom}}$ was determined by the experiment in **Fig. 2 (b)**. We are concerned with the difference between $(\Psi \pm \sigma)_{\text{phantom+OSL}}$ and $(\Psi \pm \sigma)_{\text{phantom}}$, and the dependence of it on the tube voltage and the phantom thickness. Basically speaking, the $(\Psi \pm \sigma)_{\text{phantom+OSL}}$ should be smaller value than $(\Psi \pm \sigma)_{\text{phantom}}$ because the nanoDot makes an additional X-ray attenuation. Thus, we compare the magnitude relation between the maximum value of $(\Psi \pm \sigma)_{\text{phantom+OSL}}$ “ $(\Psi + \sigma)_{\text{phantom+OSL}}$ ” and the minimum value of $(\Psi \pm \sigma)_{\text{phantom}}$ “ $(\Psi - \sigma)_{\text{phantom+OSL}}$ ” as,

$$(\Psi - \sigma)_{\text{phantom}} < (\Psi + \sigma)_{\text{phantom+OSL}} \quad (3)$$

$$(\Psi - \sigma)_{\text{phantom}} > (\Psi + \sigma)_{\text{phantom+OSL}} \quad (4)$$

$$(\Psi - \sigma)_{\text{phantom}} = (\Psi + \sigma)_{\text{phantom+OSL}} \quad (5)$$

In equation (3), the nanoDot OSL dosimeter cannot be identified in the medical X-ray image, because $(\Psi \pm \sigma)_{\text{phantom}}$ cannot be distinguished from $(\Psi \pm \sigma)_{\text{phantom+OSL}}$. On the other hand, equation (4) indicates the situation in which the influence of nanoDot OSL dosimeter appears larger, and the nanoDot OSL dosimeter can be identified. Then we determine the boundary condition of invisibility using equation (5). As the exposure dose (tube-current time products (mAs) value) increases, the values of Ψ and σ become large and the ratio of σ/Ψ becomes small. As the results, the relationship between “ $(\Psi - \sigma)_{\text{phantom}}$ ” and “ $(\Psi + \sigma)_{\text{phantom+OSL}}$ ” varies from equation (3) to (4) via equation (5) when the exposure dose increases. Based on the measured X-ray spectra of each irradiation condition, we determined the unobservable condition (equation (5)).

3 RESULTS AND DISCUSSION

Figure 4 shows a relationship between irradiation dose and energy fluence of a typical irradiation condition in 60 kV X-rays and phantom thickness of 15 cm. The results concerning experiments **(a)** and **(b)** in **Fig. 2** represent blue and red data, respectively. As shown in the insets, these two data cannot be distinguished in 5 mAs exposure, and they can be distinguished in 100 mAs exposure. In this case, we can determine the boundary condition as 15 mAs.

Figure 4: Relationship between irradiated dose and energy fluence. In this case, we cannot identify the nanoDot OSL dosimeter with the irradiation conditions under 15 mAs.

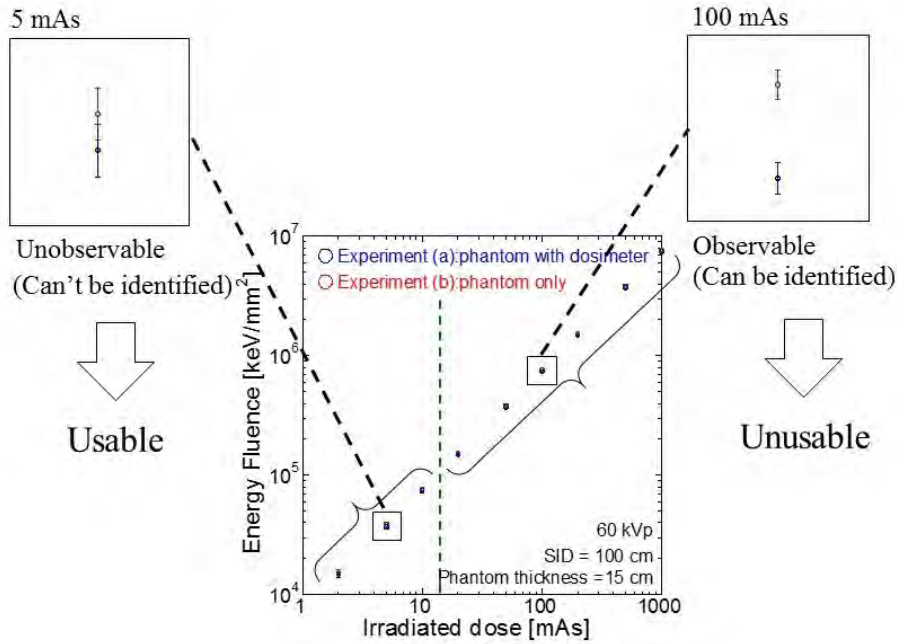


Figure 5: Estimation of the usable irradiation conditions. Figures of (a), (b), (c) and (d) show the results in the 40, 60, 80 and 120 kV X-rays irradiation, respectively. The large blue circles show typical irradiation conditions, which were adopted at the clinics in Japan.

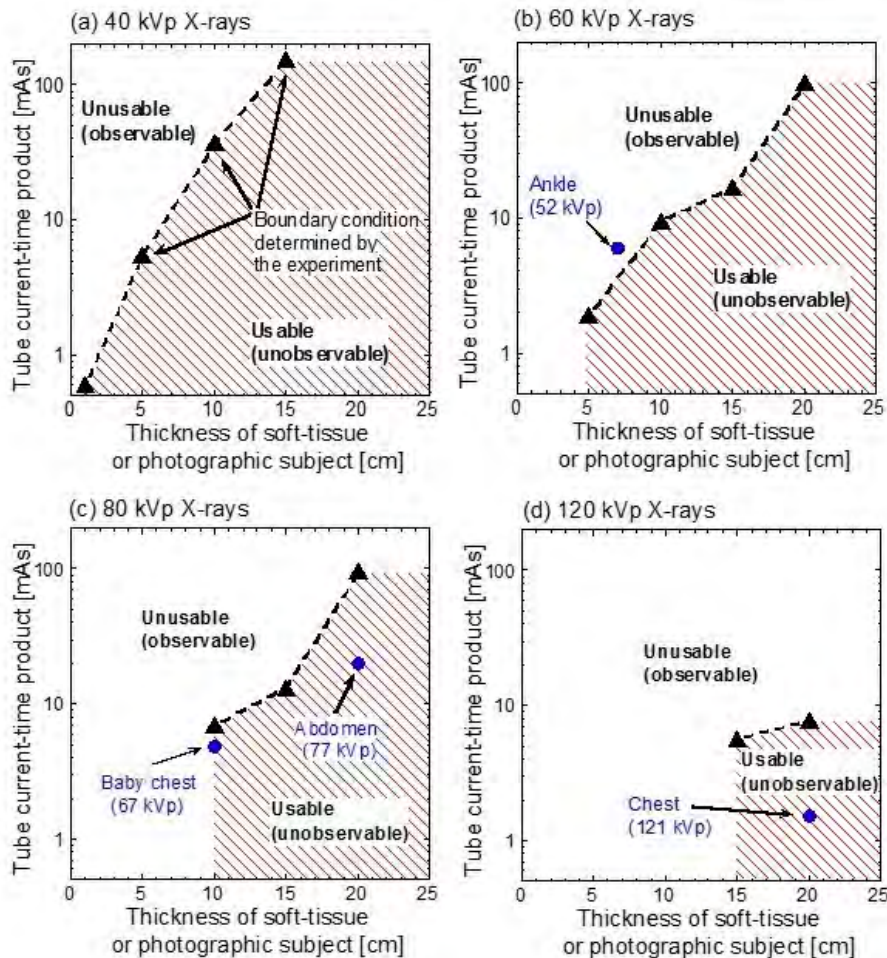
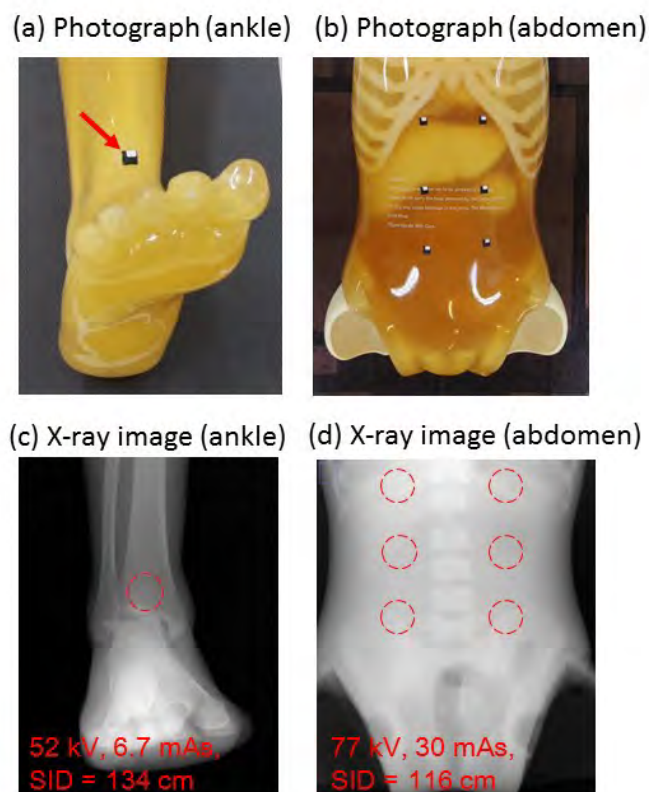


Figure 5 shows the results; the closed triangles and dashed lines represent experimentally determined boundary conditions, and the shaded portions show the conditions where the nanoDot OSL dosimeter can be used. **Fig. 5 (a), (b), (c), and (d)** are the results of the 40 kV, 60 kV, 80 kV, and 120 kV X-rays irradiation, respectively. The boundary conditions were determined on 5, 10, 15, and 20 cm phantom. In generally, the nanoDot OSL dosimeter is usable under the following conditions; the mAs value is smaller, the phantom is thicker, and/or the tube voltage is smaller than the boundary conditions. As described above, the influence of the nanoDot OSL dosimeter cannot be identified in the medical X-ray image when we used the dosimeter in the conditions of shaded portions. These results were compared with the general irradiation conditions which are derived by questionnaire investigation carried out in hospitals and clinics in Japan [9]. They are plotted by large blue circles. The irradiation condition of baby chest, abdomen, and chest are in inside of the usable area. The irradiation condition of the ankle (tube voltage = 52 kV) is slightly-deflected from the usable area of 60 kV, but the condition is included in the usable area of 40 kV. From the present experiment, we cannot declare that the nanoDot OSL dosimeter can be applied to the ankle radiography without disturbing the medical X-ray image.

Finally, we demonstrate the invisibility of the nanoDot OSL dosimeter using the phantom experiments. The X-ray examinations of the body phantom (Kyoto Kagaku Co., Ltd., Kyoto, Japan) with the nanoDot OSL dosimeter were performed in general irradiation conditions [9]. **Figure 6 (a)** and **(b)** show the photographs of the examination of ankle and abdomen, respectively. The X-ray images corresponding to them are represented by **(c)** and **(d)**; the radiography images are obtained by the computed radiography system (RP-4S, Konica Minolta Healthcare Ltd., Tokyo, Japan). The attached nanoDots were not identified on medical X-ray images in the abdomen image. Moreover, we cannot identify the dosimeter in the ankle radiography. In our experiment based on the X-ray spectra, a soft-tissue equivalent material was used (see **Fig. 5 (b)**). On the other hand, the nanoDot OSL dosimeter was placed on the tibia at the X-ray examination of ankle phantom. Then higher X-ray attenuations were occurred compared with the soft-tissue, and it led to lower energy fluence with a larger uncertainty. Therefore the nanoDot OSL dosimeter becomes unobservable.

Figure 6: Demonstration of the invisibility of the nanoDot in X-ray images.



4 CONCLUSION

To evaluate the patient exposure dose in X-ray diagnosis, we proposed to apply nanoDot OSL dosimeters. This small size dosimeter has less energy and angular dependences in diagnostic X-rays, so it is applicable for the dose evaluation of back scattered X-ray as well as primary incident X-rays. In the present study, we evaluated the invisibility of the nanoDot OSL dosimeter on the medical X-ray image by a quantitative identification method. As the results, we determined the boundary conditions of invisibility at the various irradiation conditions used in the clinical X-ray examination. Additionally, we demonstrated that the nanoDot cannot be identified on the medical X-ray image under the general irradiation conditions used in clinical situations in Japan. The nanoDot OSL dosimeter is further expected to be a convenient dosimeter to manage the patient exposure dose based on our previous and present research.

5 REFERENCES

- [1] Grosswendt B. Backscatter factors for x-rays generated at voltages between 10 and 100 keV *Physics in Medical and Biology*. 1954;29(5):579-591.
- [2] Klevenhagen SC. Experimentally determined backscatter factors for x-rays generated at voltages between 16 and 140 kV. *Physics in Medical and Biology*. 1989;34(12):1871-1882.
- [3] Takegami K, Hayashi H, Okino H, et al. Energy dependence measurement of small-type optically stimulated luminescence (OSL) dosimeter by means of characteristic X-rays induced with general diagnostic X-ray equipment. *Radiological Physics and Technology*. 2016; 9(1): 99-108.
- [4] Okazaki T, Hashizume T, Hayashi H, et al. Evaluation of energy dependence of nanoDot optically stimulated luminescence (OSL) dosimeter using characteristic X-ray induced by medical X-ray equipment. *European Congress of Radiology (EPOS)*. 2016; DOI: 10.1594/ecr2016/C-0338.
- [5] Hayashi H, Takegami K, Okino H, et al. Procedure to measure angular dependences of personal dosimeters by means of diagnostic X-ray equipment. *Medical Imaging and Information Sciences*. 2015;32(1):8-14.
- [6] Okazaki T, Hayashi H, Takegami K, et al. Evaluation of angular dependence of nanoDot OSL dosimeters toward direct measurement of entrance skin dose. *European Congress of Radiology (EPOS)*. 2015; DOI: 10.1594/ecr2015/C-0721.
- [7] Hirayama H, Namito Y, Bielajew AF, et al. The EGS5 code system, SLAC Report number: SLAC-R-730, KEK Report number: 2005-8.
- [8] Okino H, Hayashi H, Nakagawa K, et al. Measurement of Response Function of CdTe Detector Using Diagnostic X-ray Equipment and Evaluation of Monte Carlo Simulation Code. *Japanese Journal of Radiological Technology*. 2014; 70(12):1381-1391(in Japanese).
- [9] Asada Y, Syoichi S, Kenichi K, et al. Summary of Results of the Patient Exposures in Diagnostic Radiography in 2011 Questionnaire-Focus on Radiographic Conditions-. *Japanese Journal of Radiological Technology*. 2012; 68(9):1261-1268(in Japanese).

Analysis of reasons for the multiple scans of paediatric CT examinations: Finding whether there is possible confounding by indication.

Takayasu Yoshitake^a, Koji Ono^b, Tsuneo Ishiguchi^c, Michiaki Kai^d

^aShinbeppu Hospital, 3898 Tsurumi, Beppu, Oita, Japan.

^bMinistry of Health, Labour and Welfare, 1-2-2 Kasumigaseki, Chiyoda, Tokyo, Japan.

^cAichi Medical University Hospital, 1-1 Yazakokarimata, Nagakute, Aichi, Japan.

^dOita University of Nursing and Health Sciences, 2944-9 Megusuno, Oita, Oita, Japan.

Abstract. Recent epidemiological studies suggested paediatric CT examinations can increase the cancer risk in children[1]. Current radiological protection assumes the linear-non-threshold dose-response models based on epidemiological studies of the atomic bomb survivors. However, there has been little direct evidence on the cancer risk increase of low-dose exposure. Of importance is to determine whether multiple CT examination can increase cancer risk in children[2, 3]. The recent record linkage studies between doses and cancer incidence lack the analysis of reasons for the multiple scans of paediatric CT examinations. The aim of this study was to analyze the reasons in order to find whether there is possible confounding by indication. A retrospective study of two hospitals was conducted during six months from Jun 1 2012 to Dec 31 2012. We obtained the data from the radiologic examination report systems, such as date of birth, sex, age, department of diagnosis and treatment, scan part, scan date, and the reason of scan indication. We analyzed the scan reasons to find the association among scans. CT examinations more than three times were focused on. The scan reasons of multiple CT examinations were classified into trauma, tumor, inflammation, and symptom. In each patient, we found strong association among the scan reasons that indicated follow-up examinations. This association was likely to be related with ages and hospitals. Patient with multiple CT examination more than three times in children were limited, while the number of CT examination was increasing due to the need of imaging diagnosis. A question remains whether the scan reasons that indicated follow-up examinations would be related with predisposing cancer risk factors.

KEYWORDS: *CT; cancer risk; paediatric; multiple scans; examination reason.*

1 INTRODUCTION

Recent epidemiological studies suggested paediatric CT examinations can increase the cancer risk in children. The recent record linkage studies between doses and cancer incidence lack the analysis of reasons for the multiple scans. The aim of this study was to analyze the reasons in order to find whether there is possible confounding by indication.

2 METHODS AND MATERIALS

A retrospective survey was conducted among children under 16 years of age in hospital A from April 1, 2002 to December 31, 2014. We obtained the data using the radiological reporting system, patient ID, age, sex, date of birth, diagnostic treatments of departments, examination date, scan parts, and order comments. The reasons of examination were estimated based on order comments. The examination reason was classified into trauma, tumor, inflammation and others.

2.1 Comparison between the hospital A and B for six months

We compared the number of examination, gender ratio, the frequency of the scan parts, histogram of the number of examinations. The association among the examination reasons for each child was investigated. We also examined the frequency distribution of the examination reason for each age.

2.2 Analysis of the data for 12.75y in hospital A

We analyzed the number of examination, gender ratio, frequency of the scan parts, histogram of number of examinations and frequency of disease in hospital A. The age at first time CT scan was considered to be oldest date by each patient ID. Analysis of examination intervals was done by the number of examinations.

3 RESULTS

3.1 Comparison between the hospital B and A for six months

Comparison between hospital A and B indicated a similar trend on the number of examinations, gender ratio, frequency of the scan parts and histogram of the number of examinations. Frequency distribution of disease in hospital A was 24% for trauma, 52% for tumor, 16% for inflammation and hospital B was 60% for trauma, 28% for tumor, 7% for inflammation. There was no statistically significant association between examination reasons and ages.

3.2 Analysis of the data for 12.75y in hospital A

Analysis of the data for 12.75y in hospital A was indicated a similar trend on the gender ratio, frequency of the scan parts of the hospital A for six months. Frequency distribution of disease was 29% for trauma, 25% for tumor and 10% for inflammation. The ages for the first time CT scan were most frequent under 1y. The average examination interval in trauma was smaller than in tumor whereas the examination intervals were widely distributed.

4 CONCLUSIONS

The examination reasons of multiple CT scans was strongly inter-associated, although endogenous and exogenous reasons was found. The CT use for follow-up appeared justified. It would be necessary to verify the association of exogenous reasons with cancer risk in order to avoid possible confounding on exogenous reasons.

5 REFERENCES

- [1] UNSCEAR, 2000. United Nations Scientific Committee on the Effects of Atomic Radiation 2000 Report to the General Assembly, Annex D:Medical Radiation Exposures.
- [2] Pearce MS, Salotti JA, Little MP, et al., 2012. Radiation exposure from CT scans in childhood and subsequent risk of leukaemia and brain tumours: a retrospective cohort study. *Lancet* 380, 499–505.
- [3] Mathews JD, Forsythe AV, Brady Z, et al., 2013. Cancer risk in 680,000 people exposed to computed tomography scans in childhood or adolescence: data linkage study of 11 million Australians. *BMJ* 346, f2360.

Note: Detailed results were not described since this paper is under preparation for submission to a international journal.

A Multi-Center Study on Eye Lens Radiation Doses for Medical Staff Performing Non-Vascular Interventional Procedures in Japan

Kosuke Matsubara^a, Yasutaka Takei^{b,a}, Ikuo Kobayashi^c, Hiroshige Mori^d,
Kimiya Noto^e, Shoichi Suzuki^f, Takayuki Igarashi^g, Keiichi Akahane^h

^aKanazawa University, Kanazawa, Japan

^bHamamatsu University Hospital, Hamamatsu, Japan

^cNagase Landauer, Tsukuba, Japan

^dJCHO Hokkaido Hospital, Sapporo, Japan

^eKanazawa University Hospital, Kanazawa, Japan

^fFujita Health University, Toyoake, Japan

^gAsahi General Hospital, Asahi, Japan

^hNational Institute of Radiological Sciences, Chiba, Japan

Abstract. Purpose: The International Commission on Radiological Protection (ICRP) reviewed recent epidemiological evidence and set the threshold for absorbed dose in the eye lens as 0.5 Gy; it recommended an equivalent annual dose limit for the eye lens at 20 mSv, which is the average over defined periods of 5 years, with the dose not exceeding 50 mSv in any year. This study aimed to determine the actual state of the eye lens dosage for doctors and nurses who engaged in non-vascular endoscopic interventional procedures in Japan. Material and Methods: From October 2014 to September 2015, 25 doctors and 17 nurses engaged in non-vascular endoscopic interventional procedures at 11 Japanese medical facilities wore for 1 month radio-protective lead glasses, equipped inside and outside with small optically stimulated luminescence dosimeters (nanoDot; Nagase Landauer, Tsukuba, Japan), and personal dosimeters (Quixel Badge; Nagase Landauer) at the neck. Their equivalent doses for the eye lenses were obtained from the dosimeters after the experimental period. The eye lens doses were evaluated by converting the monthly absorbed doses into annual equivalent doses [Hp(3)]. The type and number of examinations, fluoroscopy time, and role during each examination were also recorded for each doctor and nurse. Results: The monthly average number of examinations were 13 ± 6 (range 4–24) for the doctors and 10 ± 9 (range 3–42) for the nurses. Endovascular retrograde cholangiopancreatography and its related examinations were the most frequent examinations performed. Among doctors, the estimated annual equivalent doses for the eye lens were 27.5 ± 44.4 mSv (range 0.4–166.8) for the left lens and 9.6 ± 18.8 mSv (range 0.3–82.4) for the right; those for the nurses were 3.1 ± 2.4 mSv (range 0.4–7.9) and 2.8 ± 2.7 mSv (range 0.5–11.5), respectively. Conclusion: The eye lens dosage for doctors and nurses who engaged in non-vascular endoscopic interventional procedures depended on the medical facilities. Some doctors exceeded the annual equivalent dose limit for eye lens that was recommended by the ICRP.

FTS (Fused Toes Homolog) can be a Target to Modulate Radiosensitivity in Uterine Cervix Cancer Cells and Normal Cells

Arunkumar Anandharaj^a, Senthilkumar Cinghu^a, Won-Dong Kim^a, Jae-Ran Yu^b, Woo-Yoon Park^a

^aChungbuk National University, Cheongju, Chungbuk, Republic of Korea

^bKonkuk University, Chungju, Chungbuk, Republic of Korea

Abstract. Radiation therapy (RT) is the major treatment modality for uterine cervix cancer. Some of the patients receive RT will suffer from recurrence and/or normal tissue complications in bladder and/or bowels. To improve RT effect, defining the molecular events that contribute to radiosensitivity in not only cancer cells but also normal cells is of critical importance. FTS (Fused Toes Homolog) gene was initially identified as one of six genes deleted in a mouse mutant called Fused Toes, due to defects in limb development, and referred as FT1/FTS. However, the function of FTS has not been elucidated well in human. Here, we evaluated the role of FTS (Fused Toes Homolog) in radiation sensitivity of cervix cancer cells and normal cells. Immunostaining of cervix cancer cells and tissues revealed that nuclear localization of FTS was increased after irradiation. Targeted stable knockdown of FTS in HeLa cells led to the growth inhibition after irradiation. Radiation-induced AKT mediated cytoprotective effect was countered by FTS knockdown, which leads to PARP cleavage and caspase-3 activation leading to cell death. Also, FTS knockdown promoted radiation-induced cell cycle arrest at G0/G1 and apoptosis of HeLa cells with concurrent alterations in the display of cell cycle regulatory proteins. Overexpression of FTS in normal HEK293 cells which lack endogenous FTS protein increased the surviving fraction. Taken together, targeted inhibition of FTS can lead to increased radiosensitivity in cervix cancer cells and overexpression of FTS can lead to radioprotection of normal cells.

Standardized and Automated Risk Assessment Forms for a Dutch Radiation Organization

Arjanka Bandstra, Marcel Wiegman

University Medical Center St. Radboud, Nijmegen, The Netherlands

Abstract. Background: In our organization (University Medical Center and University) the decentralized radiation experts are responsible for doing risk assessments and the centralized radiation protection experts are responsible for undependable assessments of the risk assessments. However in practice, most of the risk assessments were carried out and assessed by the same centralized radiation protection experts. So there was no question of independent assessment. In addition our organization did not meet the requirements of risk analysis as set by Dutch legislation. Goal: Regain the independent role of the centralized radiation protection experts and meet the latest risk analysis requirements of the Dutch legislation. Method: In cooperation with the decentralized radiation experts and medical physicists of our organization new standardized calculation methods were agreed. Result: New standardized and automated risk assessment forms were created. The forms meet the latest risk analysis calculation methods and Dutch legal requirements and can be used for approximately 95% of all applications. The decentralized radiation experts only need to collect and fill in the correct data at the forms. They no longer have to determine the appropriate method of calculation and the centralized radiation protection experts no longer be asked to help or in other words to do the risk calculations. The centralized radiation protection experts have regained their independent role and in most cases only have to assess the output parameters. The output parameters are a fixed set of dose rates and annual doses that are automatically calculated and verified against the Dutch law. Conclusion: The most important conclusion of this project is that the division of responsibilities are back where they should be and that we meet again with all Dutch laws and regulations. In addition it has also provided less quality differences in risk analyses between different departments of our organization and time gains for both parties.

Bonn Conference 2012 - Implementation of Results

Axel Böttger

Federal Ministry for the Environment, Bonn, Germany

Abstract. Before ionizing radiation and radioactive material is used in medicine each application should be considered carefully. Benefit and risk have to be evaluated and balanced before application. Radiation protection has to involve patients as well as personal and carers. In 2012 the International Conference on Radiation Protection in Medicine - Setting the Scene for the Next Decade –took place in Bonn, Germany. Participants from 77 countries and 16 organizations followed the invitation of IAEA and WHO. Medical application of ionizing radiation and radionuclides in diagnostic, intervention and therapy have a valuable benefit for patients all over the world. The application of radiation may enhance the health and welfare but is also combined with risks related to ionizing radiation exposure so every use has to balance risk and benefit. The specific outcome is the Bonn Call-for-Action highlighted by the following actions: 1. Enhance the implementation of the principle of justification, 2. Improve implementation of the principle of optimization, 3. Task manufacturers to contribute to the overall safety regime, 4. Enforce evaluation of compliance with the safety regulations, 5. Shape and promote a strategic research agenda, 6. Provide information on medical exposures – worldwide, 7. Prevent radiation incidents and accidents, 8. Strengthen radiation protection culture in health care, 9. Foster radiation benefit-risk-dialogue, 10. Enforce/Support the implementation of safety requirements. Implementation of the actions will be led by partnership of national governments, civil society, international agencies, researchers, educators and professional associations dedicated to identifying, implementing and advocating solutions as well as leadership, harmonization and co-ordination of activities and procedures at international level. There is a need for a holistic approach which includes partnership of national governments, civil society, international agencies, researchers, educators, institutions and professional associations aiming at identifying, advocating and implementing solutions to address existing and emerging challenges as well as leadership, harmonization and co-ordination of activities and procedures at an international level.

Radiological Zoning and Radiation Exposure Assessment of External Staff in the CHU-Ibn Rochd-Casablanca Nuclear Medicine Service

Abdelmajid Choukri^a, Said Ouzouh^a, Oum Keltoum Hakam^a, Rachida El Gamoussi^b, Amal Guensi^c

^aUniversity of Ibn Tofail, Kenitra, Morocco

^bNational Centre of Radiation Protection, Sale, Morocco

^cCHU-Ibn Rochd, Casablanca, Morocco

Abstract. In Morocco, nuclear medicine discipline emerged there thirty years at the Avicenne hospital in Rabat which houses a nuclear medicine department. But now several centers of private and public nuclear medicine have been installed in several cities in Morocco. The majority of nuclear medicine services has sophisticated devices such as PET-SCAN and conventional gamma camera. The use or handling of radioactive sources (radiopharmaceuticals, radioactive calibration sources, ...) within the nuclear medicine services, can be a real hazard (exposure and contamination) for staff if the radiation protection standards have not been respected when handling. Hence the importance to evaluate the individual exposure which is one of the main elements of radiation protection of workers exposed to ionizing radiation and which aims to provide an estimate of doses received at the whole organism and to implement the principle of optimization that exposures should be kept as low as reasonably achievable. On the other side, it is important to protect and educate staff against radiological risks in the workplace by mapping the radiation risks (radiological zoning) within this service. To meet the radiation protection standards established by national legislation and which will protect personnel against possible exposure, we have investigated in collaboration with the National Centre for Radiation Protection (CNRP), in the framework of the Master Radiation Protection and Nuclear Techniques (TNRP) a study on radiological zoning and assessment of external exposure of personnel in main premises of CHU-Ibn Rochd-Casablanca nuclear medicine center. The obtained results showed that the all measured dose levels remain low and well below regulatory limits.

Multistep Optimization Approach in Medical Radiology - The Patient Imperative

Andrejs Dreimanis

Radiation Safety Centre of the State Environment Service, Riga, Latvia

Abstract. In view of increasing amount of medical radiological procedures and relatively high patient doses received in computer tomography and nuclear medicine, a whole optimisation of medical radiology management shall include not only all existing aspects of optimization considering patient doses as the optimization targets, but also aware participation of patients as essential stakeholders in the process of implementation of ALARA principles. There is proposed an interdisciplinary approach to optimization of the tripartite educator- medical personnel-patient interaction. All forms of patient involvement, their education and mutual patient-medical personnel interactions can be regarded as optimization tools. There is revealed an essential role of the patients risk awareness and his general radiation protection knowledge in decision making on accomplishment of the recommended radiological procedure. In line of advanced international (EU, IAEA, WHO) projects on radiological personnel education, as the most efficient routes of education of public - or potential patents - are considered the following ones: 1) basic knowledge on radiation applications and protection to be received in secondary school, 2) life-long public educating – via printed and electronic (internet) publications and lectures issued by teaching institutions, regulatory authorities and professional bodies; 3) direct goal-oriented knowledge acquisition from the involved medical personnel about particular radiation risk/benefit issues of the certain radiological procedure.

Advanced aspects of radiation protection in the use of particle accelerators in the medical field

Angelo Infantino^a, Gianfranco Cicoria^b, Giulia Lucconi^b, Davide Pancaldi^b, Sara Vichi^a, Federico Zagni^b, Domiziano Mostacci^a, Mario Marengo^b.

^aDepartment of Industrial Engineering, Laboratory of Montecuccolino, University of Bologna, Via dei Colli 16, 40136, Bologna, Italy.

^bMedical Physics Department, University Hospital “S. Orsola-Malpighi”, Via Massarenti 9, 40138, Bologna, Italy.

Abstract. Radiation protection (RP) in the use of medical cyclotrons involves many aspects both in the routine use and for the decommissioning of a site. Guidelines for site planning and installation, as well as for RP assessment, are given in international documents, which however typically offer analytic methods of calculation of shielding and materials activation, in approximate or idealized geometry set ups. The availability of Monte Carlo (MC) codes with accurate up-to-date libraries for transport and interaction of neutrons and charged particles at energies below 250 MeV, together with the continuously increasing power of nowadays computers, makes the systematic use of simulations with realistic geometries possible, yielding equipment and site specific evaluation of the source terms, shielding requirements and all quantities relevant to RP at the same time. In this work, the well-known MC FLUKA code was used to simulate different aspects of RP in the use of biomedical accelerators, particularly for the production of medical radioisotopes. In the context of the Young Professionals Award, held at the IRPA 14 conference, only a part of the complete work is presented. In particular, the simulation of the GE PETrace cyclotron (16.5 MeV) installed at “S. Orsola-Malpighi” University Hospital evaluated the effective dose distribution around the equipment; the effective number of neutrons produced per incident proton and their spectral distribution; the activation of the structure of the cyclotron and the vault walls; the activation of the ambient air, in particular the production of ^{41}Ar . The simulations were validated, in terms of physical and transport parameters to be used at the energy range of interest, through an extensive measurement campaign of the neutron environmental dose equivalent using a rem-counter and TLD dosimeters. The validated model was then used in the design and the licensing request of a new PET facility.

KEYWORDS: *FLUKA; Monte Carlo; medical cyclotron; radiation protection, shielding.*

Radiation Protection Dosimetry (2017), Vol. 173, No. 1-3, pp. 185–191

doi:10.1093/rpd/ncw302

French Recommendations on the Conditions of Implementation of “New Techniques and Practices” in Radiotherapy

Aurelie Isambert^a, Eric Lartigau^b, Albert Lisbona^c, Philippe Cadot^c, Sylvie Derreumaux^d, Olivier Dupuis^e, Jean-Pierre Gérard^f, Dominique Ledu^g, Marc-André Mahé^c, Vincent Marchesi^h, Jocelyne Mazurierⁱ, Aurelien De Oliveira^j, Olivier Pharé^k, Marc Valero^a, Bernard Aubert^l

^aFrench Nuclear Safety Authority, Montrouge, France

^bOscar Lambret Centre, Lille, France

^cInstitute of Cancer Research in Western France, Saint Herblain, France

^dRadiation protection and nuclear safety Institute, Fontenay-aux-Roses, France

^eJean Bernard Centre, Le Mans, France

^fAntoine Lacassagne Centre, Nice, France

^gGeorges Pompidou Hospital, Paris, France

^hInstitute of Cancer Research in Lorraine, Vandoeuvre les Nancy, France

ⁱOncorad Garonne group, Toulouse, France

^jCurie Institute, Orsay, France

^kTivoli and Bordeaux North clinics, Bordeaux, France

^lPresident of the ASN WG on medical applications, Montrouge, France

Abstract. In 2013, the French Nuclear Safety Authority asked its group of experts in radiation protection for medical applications of ionizing radiation to issue recommendations concerning the conditions of implementation of new techniques in radiotherapy and the associated practices, focusing in particular on the techniques of intensity-modulated radiotherapy and stereotactic irradiation, and on new treatment devices, knowing that they are developing with insufficient recommendations and with no specific supervision in the current French licensing systems. A set of 12 recommendations were developed and issued in 2015, including: organise clinical audits by peers, verify the prerequisites of a centre before starting to implement the new technique or practice, ensure rigorous and robust project management, including the medical-economic aspect, adapt the human resources when setting up and using innovative or special techniques, integrate the changes in techniques and practices into the initial and continuous training as soon as they arise and reinforce the role of the manufacturer, improve the testing of the technical and dosimetric performance of new equipment or techniques at acceptance testing, and periodically thereafter (quality control), supervise external services in medical physics, develop the prospective collection and analysis of data concerning radiotherapy patients for the new techniques, enhance the informing and involvement of patients, and improve the dissemination of information relative to medical devices vigilance and experience feedback. These recommendations were sent to the French Ministry of Health and will be studied at the occasion of the next meeting of a committee set up to follow the implementation of measures regarding radiotherapy in the framework of the French Cancer plan. They were also sent to IAEA, WHO, and the European Commission (DG ENER).

A Cross-sectional Study of Nuclear Cardiology Practices and Radiation Exposure in Africa: Results from the IAEA Nuclear Cardiology Protocols study (INCAPS)

Andrew J. Einstein^a, Salah Bouyoucef^b, Thomas Pascual^c, Mathew Mercuri^a, Mboyo D.T.W. Vangu^d, Adel Allam^e, Madan Rehani^{c,f}, Ravi Kashyap^c, Maurizio Dondi^c, Diana Paez^c

^aColumbia University, New York, NY, USA

^bCentre Hospitalo-Universitaire de Bab El Ouéd, Alger, Algeria

^cInternational Atomic Energy Agency, Vienna, Austria

^dJohannesburg Academic Hospital, University of the Witwatersrand, Johannesburg, South Africa

^eAl Azhar University, Cairo, Egypt

^fMassachusetts General Hospital, Boston, MA, USA

Abstract. Background: Radiation exposure from nuclear myocardial perfusion imaging (MPI) raises concerns regarding harmful radiation induced health effects in patients. There exist numerous best practices for reducing radiation exposure from MPI. The recent International Atomic Energy Agency (IAEA) Nuclear Cardiology Protocols (INCAPS) study suggests worldwide variations in MPI patient radiation doses and adherence to best practices. However, little is known regarding MPI practice and radiation dose among nuclear cardiology laboratories in Africa. Objectives: We sought to characterize the MPI practice and patient dose among African nuclear cardiology laboratories, and examine it relative to practice among laboratories worldwide. Methods: This study utilized data from INCAPS. Demographics and clinical characteristics were collected for a consecutive sample of 7911 patients undergoing an MPI procedure in one of 308 laboratories in 65 countries (including 348 patients from 12 laboratories in 6 African countries) over a one-week period between March 18 and April 22, 2013. Radiation effective dose (ED) was estimated for each patient using updated International Commission on Radiological Protection methodology, and a quality index score enumerating the adherence to eight best practices was identified a priori by an IAEA expert panel was calculated for each laboratory. Results: Mean patient ED in Africa was similar to the rest of the world (9.7 ± 5.5 mSv vs. 10.0 ± 4.5 mSv, $p=0.33$), although a larger proportion of African patients received an ED ≤ 9 mSv (49.7% vs. 38.2%, $p<0.001$), a goal established in nuclear cardiology guidelines. Adherence to best practices was higher among African laboratories compared to the rest of the world (QI score: 6.3 ± 1.2 vs. 5.4 ± 1.3 , $p=0.013$). However, ED varied significantly among African laboratories (Mean ED range: 3.5 to 15.2 mSv, $p<0.0001$; Median ED range: 2 to 16.3 mSv, $p<0.0001$), and QI score ranged from 4 to 8. Conclusions: While radiation dose from MPI in Africa was similar to that in the rest of the world, and adherence to best practices was relatively high in African laboratories, incomplete adherence to best practices indicates opportunity to further reduce radiation exposure from MPI in Africa, often with no extra cost to care.

Quality Control of Radiography X-ray Generators in Kerman Province, South-Eastern Iran

Ali Jomehzadeh^a, Zahra Jomehzadeh^a, Mohammadbagher Tavakoli^b

^aMedical Physics Dept, Medical School, Kerman University of Medical Sciences, Kerman, Iran

^bMedical Physics Dept, Medical School, Isfahan University of Medical Sciences, Isfahan, Iran

Abstract. The main objective of this study was to evaluate the QC tests on radiography X-ray generator equipment installed in Kerman province hospitals. In this study, the QC tests such as Kvp and timer accuracy/reproducibility, exposure reproducibility, mA and timer linearity and H.V.L values were performed on 28 conventional radiography X-ray units based on the criteria recommended by the Atomic Energy Organization of Iran (AEOI) using a calibrated Gammex QC kit. Among 28 X-ray units, 25%, 4%, 29%, 18%, 11%, 12% and 7% was out of acceptable limits for KvP accuracy, KvP reproducibility, timer accuracy, timer reproducibility, exposure reproducibility, mA/timer linearity and H.V.L values, respectively. Conclusion: As radiography X-ray equipment in Kerman province are relatively old with high workload; it recommends that AEOI change the frequency of implantation QC tests at least as annually instead of the current policy.

Occupational Dose Profiles of Radiation Workers in Oman Hospitals: A 5 year Dose Analysis

Arun Kumar.L.S., Jamal Al-Shanfari, Saeed Al-Kalbani

Medical Physics and Radiation Protection Service, DGPEA, Ministry of Health, Oman, Muscat, Oman

Abstract. In Ministry of Health (MOH), Oman, ionizing radiation is widely used in many areas such as for diagnosis, radiation therapy, bio-medical research and for blood irradiation etc. In 1970 there were only 2 hospitals in Oman where as in 2014 the number is 49 with 203 health centres. One of the balancing consequences of increased x-ray use in Oman is the increased radiation dose to the population. During 2014, a total of 1,426,789 radiological procedures were performed in Ministry of Health (MOH) institutions. The corresponding number in 2000 was 799,452. This shows that there is about 80% increase in radiological examinations for the last 15 year period. This indicates that the population dose is on the rise as the radiological facilities are increasing in Oman which in turn increases the occupational dose of radiation workers. The occupational exposure of radiation workers of MOH hospitals were monitored by Thermo Luminescent Dosimeters (TLD's) which are dispatched to each location by post. We have developed an in-house national dose registry - Centralised Dose Recording System (CDRS) - for the management of dose of MOH radiation workers which manage the issue of TLD, collection from respective hospitals/ institutions after wear period, dose assessment & monitoring, and finally dispatching the dose reports to MOH hospitals/ health centres / institutions. Also, the dose registry will handle the individual dose(s) of each worker(s) and their dose history. Every month we are dispatching more than 1500 plus badges to 160 hospitals/ institutions of MOH throughout the Sultanate of Oman. Some of the hospitals are very remote (few thousand kilometers away from the capital city- Muscat). In this study, we have analysed the dose pattern of radiation workers in the Ministry of Health hospitals for the five year period 2010-2014. Of the 2366 radiation workers monitored in 160 hospitals/institutions, 54% reported less than 0.1 mSv, only 8% workers reported doses above 1 mSv with none exceeding the permissible dose limits. It has been observed that workers in cardiology receives the highest effective doses from among all the radiation workers where as those workers in radiation oncology receive the lowest as expected. Further details will be discussed during presentation.

Investigation of Potential Use of ^{124}Xe -incorporated Amorphous Si Films in Brachytherapy

Alexandre Leal^a, Telma Fonseca^a, Lucas Reis^b

^aCenter for Development of Nuclear Technology (CDTN), Belo Horizonte, Minas Gerais, Brazil

^bFederal University of Minas Gerais (UFMG), Belo Horizonte, Minas Gerais, Brazil

Abstract. An important and promising application of xenon-incorporated amorphous silicon (Xe@a-Si) films (or matrices) lies on the field of medicine. As already known stable ^{124}Xe atoms can be converted into ^{125}Xe , according to the atomic reaction $^{124}\text{Xe}(n, \gamma) ^{125}\text{Xe}$, that, in turn, decays to the radioisotope ^{125}I widely employed in brachytherapy, an invasive anticancer radiotherapy technique applied in some types of cancer, e.g., prostate tumors. The radiation from the radioisotope-incorporated matrix must be effective enough to kill the cancerous cells and simultaneously preserve the integrity of the adjacent healthy tissues. These matrices are in general covered by a titanium (Ti) capsule, a bio-inert material and also transparent to the desired radiation. The complete set, matrix and cover, are named as brachytherapy seed. ^{125}I is an appropriate isotope to be employed in brachytherapy due to its nuclear properties such as low X-ray energies (27.2 – 31.9 keV), low gamma energy (35.5 keV), and half-life of 59.4 days. The proposed seed is composed of a cylindrical $^{124}\text{Xe@a-Si}$ matrix of 5 mm length and of 0.8 mm of diameter covered by a Ti capsule of 0.7 mm thick. In a previous work, it has been shown that an activity up to 1 mCi can be achieved under standard radiation conditions such as the ones mostly used at the nuclear reactors worldwide. In this work, a set of simulations has been run, using MCNP5, in order to obtain the dosimetric parameters of the proposed seed. These parameters shall be used to know the potentialities and difficulties to make a $^{124}\text{Xe@a-Si}$ matrix based brachytherapeutic seed which presents potential clinical applications.

Evaluation of Patient Dose in Interventional Cardiology

Ayoub Momivand^a, Reza Zohdiaghdam^b, Zhaleh Behrouzki^a, Ebrahim Khayati Shal^c

^aMedical Physics Department, Urmia University of Medical Sciences, Urmia, West Azerbaijan, Iran

^bImaging Department, Urmia University of Medical Sciences, Urmia, West Azerbaijan, Iran

^cCardiology Department, Seyyed-Al-Shohada Hospital, Urmia University of Medical Sciences, Urmia, West Azerbaijan, Iran

Abstract. Background: In diagnosis and treatment of coronary artery diseases performed with x-ray, numerous images have to be taken from this area of the body which causes an increase in patient's radiation dose. Objectives: The objectives of this study are the measurement of Dose Area Product (DAP) and fluoroscopy time. Furthermore it evaluates the correlation between DAP and fluoroscopy time, DAP and Body Mass Index (BMI), and fluoroscopy time and BMI. Patients and Methods: In this study, 119 patients were investigated during a six-month period. Among these patients, 43 patients underwent Percutaneous Transluminal Coronary Angioplasty (PTCA) and 76 patients underwent Coronary Angiography (CA). Similar angiography system was used in all of the patients. Results: The mean values of DAP for CA and PTCA were respectively 17.99 and 55.49 Gy.cm² in women and 18.87 and 51.74 Gy.cm² in men. Strong correlation for CA ($p < 0.001$) and PTCA ($p < 0.02$) between DAP and fluoroscopy time was observed. Correlation between DAP and fluoroscopy time with BMI was investigated but significant relationship was not found between them. Conclusions: By comparing the mean values of DAP and the fluoroscopy time obtained in this study with other studies carried out in the field, it is revealed that these values are lower than the outcomes of previous studies. This difference was due to the high knowledge and experience of the cardiologist and the suitable pulse rate (15 frames per second) which was used in this study.

Review of Radiation Safety in Medical Diagnosis in Kenya

Arthur Omondi Koteng

Radiation Protection Board, Nairobi, Kenya

Abstract. Medical X-Ray machines have been used for more than a century for non-invasive diagnosis of patients for the benefit of mankind. The safety of operators and patients during such practice has improved with time, but, still cases of detrimental effects to Radiation Workers in Kenya including cancer related deaths have been reported in the recent past. An ongoing study is reviewing the safety status of the worker and patients during medical and dental exposures. The study was initiated following complaint of recurrent headaches by a radiographer working in a busy Kenyan hospital. The current study is being conducted using a hand-held survey meter for measurement of scatter radiation at points of interest within (the head position, to the left and to the right of the radiographer at their control positions), and, in the immediate vicinity of x-ray facilities (behind entry doors and walls). Exposures are undertaken at given parameters using a water phantom to generate scatter radiation, and readings are recorded at each point. This exercise is done to both new and existing facilities. Comparison is made to monthly dose readings from various service providers using the TLD or Film Badge system of personal dosimetry. The most commonly used medical x-ray unit is the radiographic x-ray machine with a control panel inside the x-ray room and, behind a radiographer's shield. Initial results indicate that the radiographer operating in such a situation absorbs radiation several times of what is recorded on their dosimeters. This is because while the front of the radiographer where the dosimeter is worn is shielded, his/her head, back, left and right hand side is not and therefore open to scatter radiation. Interim calculations indicate that some radiographers may be receiving doses above the maximum dose limit of 20 millisieverts per year for a radiation worker. The study is raising a lot of debate among medical radiation workers in Kenya and x-ray manufacturers regarding the current shielding arrangements in medical x-ray diagnosis.

Study on Incidence of Radiation Induced Cataract among Radiographers in Interventional Fluoroscopy

Aruna Pallewatte, Suvini Karunaratne, MPN Piyasena

National Hospital of Sri Lanka, Colombo 10, Sri Lanka

Abstract. Introduction: The human eye is vulnerable to radiation damage leading to posterior subcapsular cataract which is a known occupational hazard among radiation workers. The currently accepted maximum permissible occupational doses to eye is 20 mSv/Year. Radiation cataract has distinctively different features compared to other types of cataracts. Objectives: The aim was to determine incidence of radiation induced cataract among radiographers in interventional fluoroscopy in the largest tertiary hospital in Sri Lanka, in relation to the duration of radiation exposure, co-morbidities and use of protective eye shielding. This was compared with incidences of other common types of cataracts occurring in the same age group. Methodology: This research was a prospective, cross sectional analysis with ethical approval. Study included radiographers in Interventional Radiology and Cardiology with over 5 years active service. They were assessed by ophthalmologist with slit lamp examination and fundoscopy. Lens opacities were documented using "Lens Opacity Classification System 111". Data on their co-morbidities, working practice and awareness on eye protection were recorded. Analysis was done with chi-square test. Results: A total of 34 staff radiographers (68 eyes) were surveyed. Ages varied between 36 to 60 years while 53% were female. 69 % had over 15 year exposure to radiation. Only 12 had access to eye shielding regularly. However all were aware about value of eye shielding and lead goggles. Number of Radiographers using personal dose monitors were 31. No separate eye dose monitors were available. There were no cases of posterior sub-capsular cataract in the study group. 14 eyes with nuclear sclerosis related to age were identified though none had undergone surgery. Conclusion: There were no cases of posterior sub-capsular cataract in this study population. Further long term follow up is needed to detect delayed development of radiation induced cataract.

The Impact of Fluoroscopic Technique on Incidence of Radiation Injuries in Neurointervention

Aruna Pallewatte

National Hospital of Sri Lanka, Colombo 10, Sri Lanka

Abstract. Objective: The objective of this study was to review radiation injuries in relation to the practice of fluoroscopy in neurointerventional radiology and to determine the causative factors related to the clinician, patient and equipment. Technique-Patients who exceeded predetermined trigger factors i.e. total fluoroscopy time >30 min or number of angiographic study series >20 or already detected injuries or repeat procedures within one month, were included in the study. During the two year study period there were 26 cases exceeding one or more of these factors. They were followed up for six months after the last procedure for appearance of radiation injuries. Equipment used was GE Advantx (2001) digital subtraction Angiography unit. Technical factors such as use of magnification, source-object distance, kV, mA, etc. were recorded. Results: 3 out of 26 patients were detected to have scalp radiation injuries out of whom 2 were after AVM embolization and 1 after aneurysm coiling. All 3 patients had epilation in fluoroscopy field in the head appearing within 2 weeks of procedure. They had a complete recovery after 6-12 weeks. Conclusion and discussion: Radiation injuries in neurointervention were rare and usually self-limiting. Main contributory factors were use of magnification, shorter source-object distance, higher acquisition runs and higher fluoroscopy times. Therefore the severity and incidence of radiation injuries can be minimized by improving interventionist alertness on these factors and better fluoroscopy equipment. Most important practical way of minimizing the incidence of radiation injuries in patients is by educating the interventionist about optimum use of fluoroscopy time, magnification and number of acquisition runs.

Tandem KAP Meters Calibration Parameters by Monte Carlo Simulation using Reference RQR Radiation Qualities

Ademar Potiens Jr., Nathalia Costa, Eduardo Correa, Lucas Santos, Vitor Vivolo, Marie Da Penha Potiens

Nuclear Energy Research Institute - National Nuclear Energy Commission (IPEN/CNEN-SP), São Paulo, Brazil

Abstract. The Kerma-area product quantity can be obtained by measurements carried out with a kerma-area product meter (KAP) with a plane-parallel transmission ionization chamber mounted on the X ray system. It is the integral of the air kerma over the area of the X ray beam in a plane perpendicular to the beam axis. This quantity has been important to establish the diagnostic reference levels (DRLs) all over the world. In this work the MCNP5 code was used to calculate the imparted energy in the air cavity of KAP meter and the spatial distribution of the air collision kerma in entrance plan of the KAP meter. From these data, the air kerma-area product (KAP) and the calibration coefficient for the KAP meter were calculated and compared with those obtained experimentally. The X-ray tube was easily modelled as well the complete tandem calibration set up was possible. The spectra of the diagnostic radiology RQR reference qualities measured were used as a source definition in the input card for the Monte Carlo simulation. The clinical KAP meter calibration coefficients were obtained experimentally and by Monte Carlo simulation. The differences between those values were about 2%, except for RQR 10 (5.45%). The uncertainties in Monte Carlo simulation were less than 0.5% in all cases and the FOM (Figure of Merit) was constant for a number of histories of 1 million.

The IAEA Latin American Working Group on Internal Dosimetry of Radionuclides in Human Body

Ana Rojo^a, Nancy Puerta^a, Bernardo Dantas^b, Arlene Reis^b, Mariella Teran^c, Rodolfo Cruz Suarez^d

^aAutoridad Regulatoria Nuclear, Buenos Aires, Argentina

^bInstituto de Radioproteção e Dosimetria, Rio de Janeiro, Brazil

^cFacultad de Química, Montevideo, Uruguay

^dInternational Atomic Energy Agency (IAEA), Viena, Austria

Abstract. The internal exposure due to manipulation of radiopharmaceuticals in nuclear medicine centres (NMC) represents a potential intake by workers, mainly in the routinely manage of ¹³¹I volatile solutions for therapy of thyroid diseases. According with the criteria recommended by IAEA, ISO and ICRP, an internal monitoring should be carried out whenever the potential internal exposure leads to a value of annual committed effective dose above 1 mSv. Nowadays, the international Standardization Organization is developing a new Standard focusing this topic: ISO 16637 “Radiological protection -- Monitoring and internal dosimetry for staff exposed to medical radionuclides as unsealed sources”. In the framework of the IAEA Latin American Project RLA 9/075, it was identified that the surveillance of workers exposed to ¹³¹I in NMC is a subject of common interest and it should be advisable to perform a routine “in situ” thyroid measurements. With the main objective of strengthening technical capabilities and harmonizing towards the implementation of “in situ” routine monitoring programmes in NMC, the Latin American’s task group on internal dosimetry (GT DILA) was constituted. The impact of IAEA Projects on Occupational Radiation Protection implemented over more than 10 years in Latin America enables the group to count with specialized human resources on internal dosimetry. The core group of internal dosimetry experts is leading this initiative contacting the potential regional members to propose them an action plan. The main future activities will be to develop a harmonized “in situ” monitoring program using the detection systems available in NMC. Also, it a proposed the conformation of data base, including contacts from Radiation Protection Societies, Medical Physicist and Biology and Nuclear Medicine Societies, the organization of training courses and internal dosimetry intercomparisons. All the information will be shared in REPROLAM web site. The GT DILA has invited experts from 18 regional countries to join the task group with the compromise of carrying out the action plan for strengthening radiation protection of workers in the NMC.

The Effect of Single Catheter on Patient and Operator Radiation Dose during Trans-radial Coronary Angiography

Ali Tarighatnia^{a,b}, Amirhossein Mohammadalian^c, Alireza Farajollahi^{e,b}, Morteza Ghojzade^d

^aImmunology Research Center, Tabriz University of Medical Sciences, Tabriz, Iran

^bDepartment of Medical Physics, Tabriz University of Medical Sciences, Tabriz, Iran

^cInterventional Cardiology Unit, Aalinasab Hospital, Tabriz, Iran

^dLiver and Gastrointestinal Disease Research Center, Tabriz University of Medical Sciences, Tabriz, Iran

^eMedical Education Research Centre, Tabriz, Iran

Abstract. Introduction: One of the important factors in reducing radiation dose in coronary angiography is fluoroscopy time (FT). It is believed that using single catheter could lead to reduced fluoroscopy time and consequently decreased patient' & operator' radiation dose may cause to reduce radiation time and radiation exposure. The aim of this study is to assess the radiation doses result from CA procedures during TRA access using two types of single and double catheters. Method and Materials: 37 out of 74 cases of trans-radial angiography were carried out using single catheter and the rest carried out using double catheter (Judkin' catheters). The allocation of the cases for each group was random. The patient & operator radiation doses associated with each catheter group was then measured and compared with each other. Results: The Mean FT and DAP of patient in single catheter group were 2.9 min & 1736.31 μ Gym², and were 3.77min and 1728.8 μ Gym² in Judkin' s group. (P>0.05). Mean Operator dose were 34.83 μ sv in single catheter and 31.85 μ sv in double (Judkin' s catheters). (P=0.72) Conclusion: Although single catheter could slightly reduce fluoroscopy time, but Patient and operator dose in Coronary Angiography with single catheter are the same as using double catheters.

The Impact of Both Radial & Pelvic Lead Shields on Operator Radiation Exposure during Trans-radial Coronary Procedures

Ali Tarighatnia^{a,b}, Aida Khaleghifard^b, Amirhossein Mohammadalian^c, Alireza Farajollahi^{e,b}, Morteza Ghojzade^d

^aImmunology Research Center, Tabriz University of Medical Sciences, Tabriz, Iran

^bDepartment of Medical Physics, Tabriz University of Medical Sciences, Tabriz, Iran

^cInterventional Cardiology Unit, Aalinasab Hospital, Tabriz, Iran

^dLiver and Gastrointestinal Disease Research Center, Tabriz University of Medical Sciences, Tabriz, Iran

^eMedical Education Research Centre, Tabriz, Iran

Abstract. Objectives: The aim of this study was to determine the impact on radial and pelvic lead shields on reduction of operator radiation dose during Trans-radial (TRA) coronary procedures. Background: Trans-radial approach is known to have many clinical advantages over the trans-femoral, but with expense of increased operator 's radiation dose. Therefore the operator 's radiation dose was evaluated for shield and non-shield procedure for the effect of radial& pelvic shield in reducing operator dose. Methods: from 160 patients undergoing radial coronary procedures, 80 were carried out using radial& pelvic shields and routinely other 80 procedures were performed by the same operator without any additional shields. Operator radiation doses were measured by electronic dosimeter (Smart Rad) that was attached to outside the lead apron on the left upper thoracic region. Results: operator radiation dose was significantly decreased in group of patients with radial & pelvic shields from 57.83 μ Sv to 42.34 μ Sv ($P < 0.05$). Conclusion: The result of the study has been proved that the operator radiation dose can be reduced by using radial& pelvic shield during coronary procedures.

Establishing Diagnostic Reference Levels for Conventional X-ray Procedures in the Russian Federation

Aleksandr Vodovatov

St-Petersburg Institute of Radiation Hygiene after P.V.Ramzaev, St-Petersburg, Russia

Abstract. Diagnostic reference levels (DRLs) are an efficient tool for optimizing the patient protection from medical exposure. Establishing DRLs in a big country is complicated due to the variety of X-ray equipment and differences in radiological practice between different regions. In 2009, a program was started in the Russian Federation to introduce DRLs into clinical practice. One of the main objectives of the program was to evaluate the possibility to establish the first DRLs on a country level, as this was more feasible than to perform dose surveys in all Russian regions simultaneously. In 2009-2014, a dose survey was performed in seven Russian regions, selected as representative for the metropolis, industrial and rural regions. The survey was focused on the conventional X-ray examinations of the skull, chest, cervical, thoracic and lumbar spine, abdomen and pelvis. The survey included collecting the X-ray equipment data, parameters of the X-ray examinations and doses of the standard patients. Patient doses were assessed in terms of Dose-Area Product and effective dose. More than 80 hospitals and 250 X-ray units were included in the survey. The results of the survey indicated that mean doses and 75%-percentiles of the dose distributions were comparable between the regions. Less than 50 percent differences were observed for the majority of the conventional X-ray examinations, although the X-ray equipment and the local radiological practice varied much between the hospitals. Based on the results of the survey, preliminary DRLs for conventional X-ray examinations were established on a country level. Additionally, the local authorities were granted a possibility to establish their regional DRLs if the local 75%-percentiles of the dose distributions significantly differed from the proposed DRLs of the country.

Radiation Protection Dosimetry (2017), Vol. 173, No. 1-3, pp. 223–232

doi:10.1093/rpd/ncw341

Computing Calibration Factor with Visual Monte Carlo - VMC simulations of an Accident Contamination with ^{99m}Tc

Bruno Mendes^a, Fernanda Paiva^a, Marco Aurelio Lacerda^a, John Hunt^b, Telma Fonseca^a

^aCentro de Desenvolvimento da Tecnologia Nuclear - CDTN/CNEN, Belo Horizonte, MG, Brazil

^bInstituto de Radioproteção e Dosimetria - IRD/CNEN, Rio de Janeiro, RJ, Brazil

Abstract. The Laboratory of Internal Dosimetry of the Center for Development of Nuclear Technology – LDI/CDTN in BH/MG Brazil is responsible for routine monitoring of internal contamination of the Individuals Occupationally Exposed (IOEs). In routine measurement of ^{18}F in the skull of IOEs whose are working (or producing) ^{18}F -FDG, (it) was found an internal contamination of ^{99m}Tc . The challenging of this work was to assess the activity incorporated through inhalation, of an unknown amount of ^{99m}Tc -DTPA type of aerosol used for therapy purpose in nuclear medicine. The project was divided in two tasks, (1) the validation of the Visual Monte Carlo – VMC model with the experimental calibration and (2) the calibration factor (CF) calculation of the ^{99m}Tc . For the validation, the VMC model say, the phantom and the 3"x3" NaI(Tl) detector was modelled and the calibration factor was calculated for the ^{18}F in the skull. The result was compared to the CF calculated in the experimental process. As soon as, the ratio between the simulated and experimental calculation was within 5 to 10% deviation, the same model was used to calculate the CF for the ^{99m}Tc . The calibration factor calculated was then, used to estimate the incorporated activity of the ^{99m}Tc for two extremes and possible scenarios based on the distribution of this radionuclide in the body. First case, the contamination of the IOE happened early in the morning and second case, the incorporation of ^{99m}Tc happened later in the same morning. The methodology used to calculate the calibration factors using VMC code, the estimation of the activity incorporate and distribution of ^{99m}Tc in different organs in the body are discussed here.

Establishing the Quality Management Baseline in the use of Computed Tomography Machines in Kenya

Bernard Ochieng^a, Geoffrey Korir^b, Jeska Wambani^c

^aTexas Cancer Centre, Nairobi, Kenya

^bUniversity Of Massachusettes, Lowell,Boston, USA

^cKenyatta National Hospital, Nairobi, Kenya

Abstract. The objective of this study was to assess the level of compliance to quality assurance and image quality standards in Computed Tomography (CT) in Kenyan hospitals. A quality assurance inspection and physical image quality assessment in eighteen representative CT facilities were done. A quantitative method was developed and used to score the results obtained from the physical image quality measurements using the American Association of Physicists in Medicine (AAPM) water phantom. Inspection was done in order to establish the level of compliance with internationally recognized standards such as those stipulated in European Guidelines on Quality Criteria for Computed Tomography and the International Basic Safety Standards for Protection against Ionizing Radiation. The overall findings placed the national quality management performance at $50 \pm 3\%$, while image quality and quality assurance performance were $61 \pm 3\%$ and $37 \pm 3\%$ respectively. The quality assurance assessment benchmarked the country's quality management system compliance in diagnostic radiology. During accreditation appraisal, the scrutiny of scores from each stage in the medical imaging chain per facility will encourage continual implementation of the quality improvement process.

Radiation Exposure in Interventional Procedures

Bernard Ochieng^a, Geoffrey Korir^b, Jeska Wambani^c

^aTexas Cancer Centre, Nairobi, Kenya

^bUniversity Of Massasuchettes, Lowell,Boston, USA

^cKenyatta National Hospital, Nairobi, Kenya

Abstract. The aim of this study was to estimate radiation doses patients and staff is exposed to during interventional procedures (IPs), compare them with the international diagnostic reference levels and to develop initial national Diagnostic Reference Levels (DRLs). The IP survey was undertaken as the initial task of which, retrospective data were collected from four hospitals carrying out interventional radiology and cardiology procedures at the time of the study. Real-time measurement of radiation dose to patients and staff during these procedures was done. To the patients, kerma-air product (KAP) and fluoroscopic time measurements were done using an in-built KAP meter, while Peak Skin Dose (PSD) was measured slow Extended Dose Rate (EDR2®) radiographic films. The staff occupational doses were measured using individual thermoluminescent dosimeters (TLDs). The maximum and minimum KAP values were found to be 137.1 and 4.2 Gy.cm², while the PSD values were 740 and 52 mGy respectively. The fluoroscopic time range was between 3.3 to 70 min. The staff doses per procedure ranged between 0.005 and 1.41 mSv for physicians, 0.03 and 1.16 mSv for nurses, 0.04 and 0.78 mSv for radiographers; and 0.04 and 0.88 mSv for the non-clinical staff such as porters normally present during the procedure. The measured PSD was within the threshold limit for skin injuries. However, with the few IP specialists, an annual increase in workload as determined in the study will possibly result in the International Commission on Radiation Protection (ICRP) annual eye lens dose being exceeded by 10%. A concerted effort is required to contain these dose levels through the use of protective gear, optimization of practice and justification.

Study on the Effects of Gorkha Earthquake in Radiological Facilities (Nepal)

Buddha Ram Shah^a, Shanta Lal Shrestha^b, Kanchan Prasad Adhikary^c

^aNepal Academy of Science and Technology, Khumaltar, Lalitpur, Nepal

^bTribhuvan University Teaching Hospital, Maharajganj, Kathmandu, Nepal

^cNational Academy of Medical Sciences, Kathmandu, Nepal

Abstract. In the wake of April 25, 2015 destructive Gorkha earthquake in Nepal, an attempt for radiation monitoring has been made in public and private hospitals and nursing homes across Kathmandu, Bhaktapur and Lalitpur districts to assess the damage, if any, in the radiological facilities of some hospitals. With the prevailing fact, exposure to radiation can be dangerous at any level and has cumulative effect with time, it is important to know the radiation levels to which personnel are being exposed. Radiological facilities of altogether 18 public and private hospitals were monitored for the radiation level at specified locations. The radiation monitoring was performed by Radalert 100 Nuclear Radiation Monitor, International Medcom, USA. Radiation dose rates were recorded from a maximum of around 933 $\mu\text{Sv/hr}$ to a minimum of around 0.30 $\mu\text{Sv/hr}$. The patient waiting room and even the control console area of some of the hospitals demonstrated a significant dose rate which over a long term exposure could prove detrimental to radiation workers as well as patients and the public. Based on the conclusions, recommendations have also been made considering them to be helpful in ensuring compliance of radiation protection with regulatory standards as set up by International Commission on Radiological Protection (ICRP).

Evaluation of Important Physical Parameters in Micro Beam Radiotherapy of Lung Tumors

Banafsheh Zeinali-Rafsanjani^{a,b}, Mohammad-Amin Mosleh-Shirazi^b, Mahdi Haghigatafshar^a, Mahdi Saeedi-Moghadam^b

^aNuclear medicine and molecular imaging research center, Shiraz university of medical sciences, Shiraz, Iran

^bMedical imaging research center, Shiraz University of medical sciences, Shiraz, Iran

Abstract. In the history of radiation therapy since the first years a good treatment plan was a plan which can differentially destroy the tumor cells and secure normal tissues. Lots of methods have been developed so far to reach to this goal, one of which is micro beam therapy (MRT). In MRT radiation field divides in to several separate fields with the thickness of 10-100 μm and 100-400 μm spacing. In this treatment normal tissue can tolerate high doses that are delivered to the small volumes of it. MRT is mostly used for brain tumors to spare central nervous system (CNS). It may also possible to use it in chest tumors placed near the surface to protect heart and lung. MCNPX 2.4 was used to assess the possibility of using MRT for chest tumors by calculating dose distribution of MRT in lung tumor in a simulated Rando phantom. A lung tumor defined as target in order to check the dose distribution of MRT in this region. A spherical tumor with the radius of 1 cm was modeled in the right lung in the close vicinity of ribs and heart. The center of tumor was located at the depth of 3 cm from the surface of the phantom. Two energies were used for x-ray beams 150 and 600 kVp in order to be able to make a comparison between medium and highest energy beam which use for this treatment. The thickness of pencil beams were 0.63 mm with the same spacing. 0.5 cm-margin considered around the tumor. Two orthogonal interlaced beams were simulated which each of them contained 24 planar beams and the results of single and two fields were compared. Dose volume histogram (DVH) and beam profile of tumor and organ at risks was assessed and the dose uniformity in tumor region was evaluated by using homogeneity and conformity indexes. A comparison has done between the dose distribution in tumor region of inhomogeneous and homogenous phantom with the same contour. To check the effect of using contrast media in this region on uniformity of treatment, Iodine was used as contrast agent in tumor and the results of the treatment with and without contrast were compared. The results revealed that MRT can be adapted for treatment of shallow chest tumors. The inhomogeneity of this region does not interfere significantly in treatment. The usage of contrast media or increase the number of beams can improve the homogeneity of treatment and decrease the dose of surrounding tissues.

Dicentric Assay in DTC Patients with High Dose Radioiodine Therapy

Chung Mei-Ling^{a,c}, Huang Ying-Fong^{a,b}, Chen Yu-Wen^b, Jong Shiang-Bin^b, Lai Yung-Chang^{b,c}

^aRadiation Accident Management Center in Southern Taiwan, Kaohsiung, Taiwan

^bDepartment of Nuclear Medicine, Kaohsiung Medical University Hospital, Kaohsiung, Taiwan

^cDepartment of Public Health, Kaohsiung Medical University, Kaohsiung, Taiwan

Abstract. In the past, nuclear emergency event has shown that environmental radioiodine release is always a major issue. It is well-known that I-131 would uptake by human body through food consumption or by inhalation that would cause body radiation burden. Epidemiology studies based on Chernobyl accident had proved that I-131 exposure was a main cause to thyroid carcinoma. The absorbed dose severity due to I-131 exposure could be easily evaluated by internal dosimetry. In past four years, we have accumulated more than 350 DTC therapy patients' data for blood toxicity evaluation based on radiation dose rate measurements at one meter fixed distance that has been published elsewhere. Several cases have calculated values of more than two Gray that is set as limit from I-131 therapy guideline. The dicentric scorings method would provide a gold standard for validating estimated blood doses by other means. In this bio-dosimetry study, we plan to use dicentric scorings method in blood samples on DTC patients under I-131 therapy. The patients selected for this dicentric scorings study would be administered dose of 150mCi or higher. The methodology in use was based on EPR Biodosimetry 2011 (IAEA). There are two purposes in this study: one is for quick radiation-related triage of mass population during a nuclear emergency; the other is for blood toxicity evaluations of the DTC patients under relative high dose therapy in our hospital.

Animal Sporting Events and Radioprotection Management

Roy Catherine^{a,b}, Audigie Fabrice^c, Coudry Virginie^c, Malet Christophe^d, Sgro Geraldine^d

^aSFRP, Paris, France

^bCommission De Radioprotection Veterinaire, Paris, France

^cCentre for Imaging and Research in Equine Locomotor Disorders (CIRALE), Env Alfort, Goustranville, France

^dGrande Odyssee, Paris, France

Abstract. During sporting events, animals are subjected to considerable physical effort; they are trained for months or years and their physical and mental capabilities represent a significant human and financial investment. These animals may however be injured, either during the trip to join the site of the competition or at sporting events. The challenge is to diagnose as soon as possible injuries including bone lesions whether the animal can return to competition after a rest period or whether it should abandon the trials. Early diagnosis can process as soon possible bone lesions while sparing the animal welfare. That is why, during two international events, a mobile X-ray equipment, licensed by the Nuclear Safety Authority, was available for the veterinary team directly on the site of trials: World Equestrian Games ALLTECH Caen in 2014; La Grande Odyssee Savoie Montblanc, dog sled race during 2015 and 2016. The "outside" veterinary radiology practice is an activity with risk of professionals and public exposure because it is performed in conditions of "yard" in mobile clinics under tents. Decline the implementation of this activity following quality and safety management allow to integrate principles of radiation protection (justification, optimization and limitation) at all stages: Policy, Human and material resources management, Processes, Check and evaluation with projected and proven dosimetry issues. The organization of these activities could so be developed in accordance with the principles of radiation protection as defined by the International Commission for Radiological Protection (ICRP) and incorporated in the Basic Safety Standards 2011 the International Agency for Atomic Energy (IAEA) and the new Directive EURATOM of 5 December 2013.

Occupational Exposure Observations at Groote Schuur Hospital

Christoph Trauernicht^{a,b}, Tobie Kotzé^{a,b}

^aGroote Schuur Hospital, Cape Town, South Africa,

^bUniversity of Cape Town, Cape Town, South Africa.

Abstract. *Aim:* The aim of this study is to look at the occupational exposure histories of all radiation workers at Groote Schuur Hospital since November 2011, when active tracking of the monthly exposure records began.

Method and Materials: The monthly TLD exposure records of 732 individuals at Groote Schuur Hospital have actively been tracked since November 2011, with almost 20.000 individual dose records in the database.

The histories were divided into the various areas in the hospital and higher-risk areas were identified. Active tracking of the exposure records also allows for identifying individuals who consistently pick up non-zero exposures and may point to working practices that do not conform to the ALARA principle.

Results: In 93 % of cases a zero dose was recorded, which enables low-risk groups to be identified. 3 higher-risk areas were identified, which accounted for 84 % of alleged overexposures: the catheterization labs, the vascular labs and the GIT units, all of which have fluoroscopic screening units. Doses above 4 mSv / month are queried by the regulator, but any dose less than that is automatically allocated. If a TLD badge is worn outside a rubber apron and the recorded dose is less than 10 mSv, the regulator allocates a 0 mSv dose, while a 2 mSv dose is allocated for readings above 10 mSv. *Conclusion:* Active tracking of exposure histories has allowed the identification of higher-risk areas in the hospital. It also points to areas in the hospital in need of increased radiation protection awareness and training.

Comparison of Primary Doses Obtained in Three 6 MV Photon Beams Using a Small Attenuator

C Trauernicht

Division of Medical Physics, Groote Schuur Hospital and University of Cape Town-LC32, Private Bag, 7935 Observatory, South Africa

Abstract. It is a common technique in radiotherapy treatment planning systems to simplify the calculations by splitting the radiation beam into two components: namely the primary and scattered components. The contributions of the two components are evaluated separately and then summed to give the dose at the point of interest. Usually, the primary dose is obtained experimentally by extrapolating the ionization measured within the medium to zero-field size (Godden, Gamma radiation from cobalt 60 teletherapy units. Br. J. Radiol. Suppl. , 45(1983)). This approach offers the opportunity to obtain the primary component of dose without the need for an uncertain non-linear extrapolation. The primary dose can be obtained from two measurements of ionization in a large beam in a water phantom, as well as four measurements of ionization in a narrow beam geometry. The measurements were done over a range of different depths and thus the primary linear attenuation coefficient was also obtained. The calibrated output of a linear accelerator is usually 1.00 Gy per 100 monitor units (MU) at the depth of maximum dose (d_{max}) in water for a $10\text{ cm} \times 10\text{ cm}$ field. The values for the primary dose components at d_{max} in a $10\text{ cm} \times 10\text{ cm}$ field obtained in three different 6 MV beams using this method are $D_P(d_{max}, 10\text{ cm} \times 10\text{ cm}) = 0.925\text{-}0.943\text{ Gy}/100\text{ MU}$. The obtained values of the primary dose components compare well with measurements in the same beams extrapolated to zero-field size and also to literature. One can thus conclude that this method has the potential to provide an independent measurable verification of calculations of primary dose.

Radiation Protection Dosimetry (2017), Vol. 173, No. 1-3, pp. 198–202

doi:10.1093/rpd/ncw332

Detector Dependence of the Measured Spectra of the OncoSeed IMC6711 Iodine-125 Seed

Christoph Trauernicht^a, Paul Papka^b, Peane Maleka^b, Egbert Hering^a, Freek Du Plessis^c

^aUniversity of Cape Town, Cape Town, South Africa.

^biThemba LABS, Cape Town, South Africa.

^cUniversity of the Free State, Bloemfontein, South Africa.

Abstract. *Aim:* I-125 seeds are used routinely for low-doserate brachytherapy of the eye at Groote Schuur Hospital. A project is underway to calculate the dose distribution of a particular eye applicator, as well as the dose to critical surrounding structures, with the DOSXYZnrc Monte Carlo code. The code requires the I-125 energy spectrum as one of the input parameters. *Method and Materials:* The spectrum of the I-125 seed was measured with various detectors: A thin-window NaI detector, a HPGe detector, a silicon drift detector (SDD) and the lowenergy photon spectrometer (LEPS) at iThemba LABS. *Results:* The energy resolution of the NaI detector is very poor and all the energy peaks are averaged into one large peak. The HPGe has a better energy resolution (stated as 2.0 keV at 1332 keV) and the LEPS has an energy resolution of about 0.8 keV at 40 keV and a number of peaks can be seen. The energy resolution of the LEPS is slightly superior to the hpGe detector. The SDD has the best energy resolution of the detectors used (about 0.3 keV at 40 keV). A number of peaks, including the silver and titanium characteristic x-rays, can clearly be seen. When the gold backing is added, additional gold characteristic x-rays can be seen as well. The detector is only about 10 % efficient at the I-125 photopeak of 35.5 keV, but more efficient at lower energies. *Conclusion:* The SDD has the best energy resolution of the detectors used. An efficiency correction needs to be applied to the measured data to get a corrected spectrum. The spectra that were obtained with the SDD will be used to create the input spectrum for the Monte Carlo code. The simulations will be able to accurately account for the dose anisotropy of the seeds and as such determine the dose to critical surrounding structures more accurately.

Measured Anisotropy of the OncoSeed IMC 6711 Iodine-125 Seed

Christoph Trauernicht^a, Paul Papka^b, Egbert Hering^a, Freek Du Plessis^c

^aUniversity of Cape Town, Cape Town, South Africa.

^biThemba LABS, Cape Town, South Africa.

^cUniversity of the Free State, Bloemfontein, South Africa.

Abstract. *Aim:* Groote Schuur Hospital uses the OncoSeed 6711 I-125 seeds for LDR brachytherapy in and around the eye. Currently dose calculations are done by approximating each source as a point source with an isotropic emission of radiation. In order to do more accurate dose calculations and Monte Carlo simulations it is important to know the actual dose distribution around these seeds. *Method and Materials:* The anisotropy was measured in air using a Silicon Drift Detector, coupled to a 4096 channel MCA. The SDD is thermoelectrically cooled and does not operate at liquid nitrogen temperatures. The entrance Be-window of the detector is specified as 12.5 μm thick and the detector has a surface area of 7 mm². A special measurement jig was constructed for the anisotropy measurements. *Results:* Spectra of three I-125 seeds were measured in air at various distances to the detector in 5° intervals and averaged for display purposes. The dead time of the detector at 6 kHz was 0.24% and at 15.5 kHz it was 1.15%. A region of interest was drawn to include all counts in the energy range from 21.07 keV – 36.85 keV, including all the main peaks except the Titanium characteristic X-rays at about 5 keV. Spectra were counted for 30 s each, giving count uncertainties of less than 1 % over the ROI in most cases. Anisotropy results are shown for the performed measurements at 5 mm, 10 mm and 30 mm from the detector face. The results are compared to published data. *Conclusion:* Spectral changes are visible as the angle of the seed is changed, because less radiation is emitted through the ends of the seeds compared to the sides of the seeds. There are thus worse count statistics when counting through the seed ends. There is reasonable correspondence when comparing measured to published anisotropy values at 5 mm and 10 mm, but for 30 mm the deviations become larger. This may be because the measurements were done in air and not in water and additional scatter is not accounted for. A measurement set-up in water may have to be investigated. Improved dose calculations in and around the eye applicators should become possible if the dose anisotropy is taken into account.

The Monte Carlo Simulation Study of Secondary Neutron Dose for Proton Therapy at Samsung Medical Center using FLUKA

Chae Young Lee^{a,e}, Jin Sung Kim^c, Yong Hyun Chung^{a,e}, Sungkoo Cho^c, Dae-Hyun Kim^c, Youngyih Han^c, Jongho Kim^d, Yunho Kim^d, Sangmin Lee^b, Chan Woo Park^a

^aDepartment of Radiation Convergence Engineering, Yonsei University, Won-ju, Republic of Korea

^bProgram in Biomedical Radiation Sciences, Department of Transdisciplinary Studies, Graduate School of Convergence Science and Technology, Seoul, Republic of Korea

^cDepartment of Radiation Oncology, Samsung Medical Center, Sungkyunkwan University School of Medicine, Seoul, Republic of Korea

^dKorea Research Institute of Standards and Science, Daejeon, Republic of Korea

^eDepartment of Radiological Science, Yonsei University, Won-ju, Republic of Korea

Abstract. Purpose: Proton therapy is a rapidly expanding in cancer treatment field. From all over the world, proton therapy facilities are being commissioned or under construction. To validate the commissioning process of the proton therapy at Samsung Medical Center(SMC), we have designed a proton therapy facility (nozzles) by using FLUKA Monte Carlo simulation toolkit. The purpose of this study is to measure and evaluate secondary neutron dose from proton therapy beam according to various combination of elements of proton therapy facility parts at SMC using FLUKA. Materials and methods: In this study, we have designed proton treatment nozzles using the FULKA simulation toolkit. FLUKA simulation was performed to beam properties, like percent depth dose curve, spread-out Bragg peak (SOBP) and verified against measured beam data. Also, we have measured secondary neutron dose from each parts of nozzle (Ridge filter, MLC, Block, Compensator etc.), respectively. Using these data, we can analyse and evaluate secondary neutron dose. Results: Results of our secondary neutron dose contributions, spectrums from each part in nozzle are different. We have calculated secondary neutron dose at several different points in nozzles. Especially, the neutron sources in wobbling mode are bigger than scanning mode. In scanning mode, the main neutron sources are only profile monitor and dose monitor in the beam nozzle. Conclusions: We have designed and simulated the two proton therapy nozzles at SMC by using FLUKA simulation. Each nozzle elements has been designed in detail, we have studied by examining dosimetric properties. We have evaluated results and proposed the secondary neutron generation amount per substance of nozzle parts. Furthermore, Using these data, we will prepare the groundwork for radiation safety regulation technology in medical particle accelerator.

KEYWORDS: *secondary neutron; FLUKA; Monte Carlo simulation; proton therapy; neutron ambient dose equivalent.*

Biological Effects of Radioactive Hot Particles on the Human Lung. Assessment of the Cancer Risk

Diana Apostolova^a, Zdravko Paskalev^b

^aMedical University, Clinic of Occupational Diseases, Sofia, Bulgaria

^bNational Center of Radiobiology and Radiation Protection, Sofia, Bulgaria

Abstract. Introduction Exposure of the lung to beta irradiation from discrete highly radioactive particles (called “hot particles”) represents a difficult problem for assessment the radiation risk and radiological protection. After the Chernobyl accident fallout contained extensive amount of pulverized nuclear fuel composed of uranium and its decays products. The effects of these highly radioactive particles on human are not well known due to lack of reliable data on the extent of the exposure. The aim of this investigation is to undertake studies of human cadaver lungs in an effort to detect presence of hot particles and concurrently define the isotope composition of particulate contained in these lungs after the Chernobyl accident. Lungs were from cadavers of previously healthy Sofia residents having led an active life and died in tragic circumstances. We have provided the epidemiological study for determining the rate of lung cancer among Bulgarian population in the latest period after the Chernobyl accident. The rate of lung cancer among Bulgarian population was determining for the period 1992- 2003. Results Our measurements have shown activities of lung of identified hot particles to range from several tens to several hundreds Bq per particle. Total beta-gamma measurement showed 10-fold differences between whole lungs, with values varying from 2-3 Bq to 20-30 Bq. For some lungs from the early post accident period, was indicated presence of Ce-144 (2-3 Bq), Ru-103 (3-4 Bq), Cs-134 (10-13 Bq), Cs-137 (11-15 Bq). At later time in the lungs presence the elements Cs-134 (5-7 Bq), Cs-137 (12-15 Bq), Ru-103 (4-5Bq), Ce-144 (0.5 Bq). In this manner, total gamma activity of the lung calculated on the basis of gamma- spectrometric analysis was found to amount up to 35 Bq per one lung. After the Chernobyl accident we can expect the lung cancer incidents may increase from 1996. The epidemiological results among Bulgarian populations show that the increasing of lung cancer incidents varying in the range of spontaneous frequency.

Mathematical Modeling of Dose Profile of a Dental Facilities

Deise Diana Lava, Diogo da Silva Borges, Maria de Lourdes Moreira, Antonio Cesar Ferreira Guimarães

Instituto de Engenharia Nuclear, Rio de Janeiro, Rj, Cidade Universitária, Brazil

Abstract. The determination of the dose profile is important to classify the level of danger which the individuals are exposed (considering their positioning) for the predicted workload for building of the installation. From this, this paper aims to present a methodology capable of mapping the dose within dental rooms. The methodology used for dose mapping in conjunction with techniques for calculating shielding for dental facilities, provided by the National Council on Radiation Protection & Measurements (NCRP), make a complete system able to generate meaningful data on the safety of occupationally Exposed Individuals (IOEs) and of the public. The model of room to be presented, as a case of illustration of the methodology, was arbitrarily constructed to generate better understanding of the problem. Its inclusion in the calculus was made through discretizations performed with the aid of high-performance computers. This discretizations allowed to associate deferent points of the room volume with the isocenter of the source. This mode of mapping of the dental room allows to take measurements of the dose for an infinitesimal distance after the point where the initial dose was defined.

In Young Women: Justification of Breast Ultrasound Rather than Combined Breast Ultrasound and Mammography. Radiation Protection Perspective

Dina Salama, Hanan Gewfel

Egyptian Atomic Energy Authority, Cairo, Egypt

Abstract. Background: Diagnosis of breast cancer in young women poses a real challenge to radiologists because their breast tissue is often denser than the breast tissue of older women. There is a significant level of consistent and inappropriate use of mammography in young women and thereby many examinations are not justified in terms of radiation exposure. The objective of this study was to compare the accuracy of combined breast ultrasound and mammography (ionizing radiation) versus breast ultrasound alone (non-ionizing radiation) in diagnosing breast cancer in young women. Methodology: We retrospectively analysed all electronic breast ultrasound and mammographic reports of young women from May 2011 to January 2014. Records were reviewed and divided into two groups: The first group were those who underwent both breast ultrasound and mammography and the second group were those who underwent breast ultrasound alone. Breast Imaging and Reporting Data System (BIRADS), breast density and histopathology were assessed in both groups. Examinations rated as BIRADS categories; 1, 2, and 3 were considered negative for malignancy, while 4 and 5 were considered positive. Results: A total of 256 patients were included in the study. 158 patients (61.7%) were evaluated using both breast ultrasound and mammography, while 98 patients (38.3%) were evaluated using breast ultrasound alone. Palpable mass was the presenting symptom in 111(43.4 %) of the cases. Biopsies were performed for 36 (14.1%) patients, while follow up for one year or more was done in 220 (85.9%) patients. 22 patients were malignant (8.6%) while 234 (91.4%) were benign cases. For the 158 cases who were evaluated with breast ultrasound and mammography (the first group), the sensitivity, specificity, positive predictive value, negative predictive value and over-all accuracy were 92.9% , 98.6% , 86.7% , 99.3% and 98.1 %respectively; while for the 98 cases who were evaluated with breast ultrasound only (the second group), the results were 87.5%, 100%,100 % 98.9% and 89.8% respectively. Conclusion: In young women, breast ultrasound alone can accurately and independently reveal malignant cases; however performing combined breast ultrasound and mammography could be restricted to suspicious cases only. This is ethically required for the justification of radiation exposure.

Cone Beam CT Patient Dose in Paediatric Cardiac Catheterization Procedures

Eva Corredoira Silva^a, Luis Alejo Luque^a, Eliseo Vañó Carruana^b, Cristina Koren^a, Rodrigo Plaza^a, Antonio Serrada^a, Carlos Huerga Cabrerizo^a

^aHospital Universitario la Paz, Madrid, Spain

^bHospital Clínico san Carlos, Madrid, Spain

Abstract. Cone Beam CT (CBCT) uses a flat panel detector to acquire X-ray projection images around the patient and get a volumetric reconstruction. In paediatric cardiology offers the ability to acquire high contrast spatial resolution 3D images of vascular volumes with the option of visualising complex spatial relationships from any angle. This option can have clinical benefits in planning and guiding surgical and non-surgical interventions. Although there have been several recent evaluations of patient radiation doses in paediatric interventional cardiology, no particular studies of patient doses in CBCT exist in this context. Paediatric cardiologists need to know the impact of CBCT in patient doses to ensure that use of this new imaging modality is justified and to optimise protocols. The purpose of the present study was to establish local diagnostic reference levels (DRLs) in paediatric diagnostic cardiac catheterization procedures using CBCT acquisitions. Between November 2009 and December 2014 radiation data were collected for paediatric diagnostic cardiac catheterisations: $n = 68$ and therapeutic cardiac catheterisations: $n = 102$, with CBCT acquisition. Air Kerma-area product (P_{ka}) and reference air kerma at the patient entrance reference point ($K_{a,r}$), and fluoroscopy time were recorded. DRLs for cardiac catheterisation were obtained for five age categories and five weight categories. The third quartile values for P_{ka} due to CBCT acquisitions for diagnostic and therapeutic procedures respectively by age category, were: <1 year: $0,6 \text{ Gy.cm}^2$ and $0,8 \text{ Gy.cm}^2$; 1-5 years: $1,2 \text{ Gy.cm}^2$ and $1,1 \text{ Gy.cm}^2$; 5-10 years: $3,0 \text{ Gy.cm}^2$ and $1,8 \text{ Gy.cm}^2$; 10-16 years: $4,8 \text{ Gy.cm}^2$ and $3,6 \text{ Gy.cm}^2$; ≥ 16 years: $5,1 \text{ Gy.cm}^2$ and $13,9 \text{ Gy.cm}^2$. The corresponding values by weight category were: <5 kg: $0,8 \text{ Gy.cm}^2$ for diagnostic procedures; 5-10 kg: $0,8 \text{ Gy.cm}^2$ and $1,0 \text{ Gy.cm}^2$ for diagnostic and therapeutic procedures respectively; 10-22 kg: $1,2 \text{ Gy.cm}^2$ and $1,3 \text{ Gy.cm}^2$; 22-40 kg: $3,8 \text{ Gy.cm}^2$ and $2,3 \text{ Gy.cm}^2$; ≥ 40 kg: $5,0 \text{ Gy.cm}^2$ and $6,4 \text{ Gy.cm}^2$. Proposed local DRLs for cardiac procedures with CBCT acquisitions are provided to help the optimization when using this new imaging modality and to contribute to the refinement of national and European DRLs for paediatric cardiology.

Proposal of a spreadsheet to monitor units verification for intracranial radiosurgery treatments

Erick Hernandez, Ricardo Contreras, Miguel Ortega

San Carlos University, Guatemala, Guatemala

Abstract. Verification requirements of monitor units calculated doses prescribed for patients are recommended on several protocols of quality assurance in radiotherapy. It is recommended that this check is done by a second person with an independent method of initial calculation. In stereotactic radiosurgery, levels of action required must take into account the limitations of the method of calculation of monitor units, including difficulties associated with dosimetry of small fields and the requirements of the particular treatment. A spreadsheet monitor units was designed to calculate MU for intracranial radiosurgery treatment with a single arc. This spreadsheet was tested for 40 different cases; the comparison between the MU generated by this method, and the MU generated by TPS used (MNPS) was in the interval (1.5% to 3.5 %).

Establishment of National Dose Reference Levels (DRLs) for Digital Mammography Practices at the UAE

Fatima Al Kaabi^a, Najla Al Mazrouei^b, Jamila AlSuwaidi^c, Jacek Janaczek^d, Alfani Al Ameri^e, Sara Booz^e, Wadha AlShamsi^f

^aMedical Physics Department, Tawam Hospital, Abu Dhabi Health Services (SEHA), Al Ain, Abu Dhabi, United Arab Emirates

^bMedical Physics Department, Dubai Hospital, Dubai Health Authority (DHA), Dubai, United Arab Emirates

^cDepartment of Medical Education, Dubai Health Authority (DHA), Dubai, United Arab Emirates

^dGulf Medical University, Ajman, United Arab Emirates

^eClinical Imaging Department, Mafraq Hospital, Abu Dhabi Health Services (SEHA), Abu Dhabi, United Arab Emirates

^fRadiology Department, Al Ain Hospital, Abu Dhabi Health Services (SEHA), Al Ain, Abu Dhabi, United Arab Emirates

Abstract. Mammography is the best technique for early detecting breast cancer and it is considered to be an effective method to meet this objective. The aim of this study is to establish national Diagnostic Reference Levels (DRLs) of mammography in UAE. DRLs is a practical tool to optimize patient radiation protection and to manage the patient radiation dose so that the dose is appropriate with the clinical purpose. In this survey only digital mammography units were involved. The main dosimetry parameters evaluated in this study were Mean glandular dose (MGD) and entrance to skin dose (ESAK). A standard PMMA phantom of 45 mm thicknesses was used to accomplish the measurements in the clinical setting. Variation of glandular doses for a range of typical breast thicknesses was determined also for some mammography units at main hospitals within UAE according to European Guidelines method. Consideration must be drawn to the risk of radiation exposure against the clinical benefit of an optimal image quality. Patient doses acquired in the mammography practices at UAE are comparable to the accepted dose level recommended by the European guidelines. This is an effective assessment of the existing mammography protocols.

KEYWORDS: *DRLs; patient dose; digital mammography; MGD; dosimetry.*

Risk of a Second Kidney Carcinoma Following Childhood Cancer: Role of Chemotherapy and Radiation Dose to Kidneys

Florent de Vathaire^{a,c}, Boris Schwartz^{a,c}, Chiraz El-Fayech^{a,c}, Rodrigue Allodji^{a,c}, Bernard Escudier^b, Mike Hawkins^d, Ibrahima Diallo^{a,c}, Nadia Haddy^{a,c}

^aInstitut national de la santé et de la recherche médicale (INSERM) U1018, Villejuif, France

^bGustave Roussy, Villejuif, France

^cUniversité Paris XI, Villejuif, France

^dCentre for Childhood Cancer Survivor Studies, Department of Public Health & Epidemiology, Birmigham, UK

Abstract. Purpose: Kidney carcinoma is a rare second malignancy following childhood cancer. Materials and Methods: We sought to quantify risk and assess risk factors for kidney carcinoma following treatment for childhood cancer. We evaluated a cohort of 4,350 patients who were 5-year cancer survivors and had been treated for cancer as children in France and the United Kingdom. Patients were treated between 1943 and 1985, and were followed for an average of 27 years. Radiation dose to the kidneys during treatment was estimated with dedicated software, regardless of the site of childhood cancer. Results: Kidney carcinoma developed in 13 patients. The cumulative incidence of kidney carcinoma was 0.62% (95% CI 0.27%-1.45%) at 40 years after diagnosis, which was 13.3- fold higher (95% CI 7.1-22.3) than in the general population. The absolute excess risk strongly increased with longer duration of follow-up ($p < 0.0001$). Compared to the general population, the incidence of kidney carcinoma was 5.7- fold higher (95% CI 1.4-14.7) if radiotherapy was not performed or less than 1 Gy had been absorbed by the kidney but 66.3- fold higher (95% CI 23.8-142.5) if the radiation dose to the kidneys was 10 to 19 Gy and 14.5- fold higher (95% CI 0.8-63.9) for larger radiation doses to the kidney. Treatment with chemotherapy increased the risk of kidney carcinoma (RR 5.1, 95% CI 1.1-22.7) but we were unable to identify a specific drug or drug category responsible for this effect. Conclusions: Moderate radiation dose to the kidneys during childhood cancer treatment increases the risk of a second kidney carcinoma. This incidence will be further increased when childhood cancer survivors reach old age.

Developing Light Nano-Composites with Improved Mechanical Properties for Neutron Shielding

Fatemeh Jamali^a, SMJ Mortazavi^a, MR Kardan^b, Sedigheh Sina^c, MA Mosleh-Shirazi^a, Jila Rahpeyma^a

^aShiraz University of Medical Sciences, Shiraz, Iran

^bRadiation Application School, Nuclear Science And Technology Institute, Tehran, Iran

^cRadiation Research Center, School Of Mechanical Engineering, Shiraz University, Shiraz, Iran

Abstract. Although radiation exposures in manned space missions are normally below the limits recommended to NASA by NCRP, in long-duration deep space exploratory missions astronauts may receive relatively high doses of ionizing radiation. Novel light polyethylene-based composites can be considered as effective radiation shields in space explorations. However, normally these composites cannot provide desired mechanical properties. Over the past several years our laboratories have focused on developing efficient methods for both physical and biological protection of the crew in long term space missions. In this study carbon nanotubes and either nano-sized or micro-sized boron carbide (B₄C) fillers were incorporated into the continuous phase of low density polyethylene (LDPE). In the next phase, the mechanical characteristics of the composites as well as their neutron attenuation properties were studied. Findings of this study indicated enhanced mechanical properties accompanied by an enhanced shielding efficiency for neutrons at some specific weight fraction of the fillers.

Evaluation of the Scattered Radiation Field in an Interventional Radiology Room

Francesca Mariotti^a, Paolo Ferrari^a, Lorenzo Campani^a, Elena Fantuzzi^a, Luisa Pierotti^b, Pier Luca Rossi^c

^aENEA, Bologna, Italy

^bPoliclinico S.Orsola-Malpighi, Bologna, Italy

^cUniversità degli Studi di Bologna, Bologna, Italy

Abstract. The medical radiation exposure represent the major artificial contribution to the population annual dose. For that reason the medical and scientific community has been made aware of the necessity to promote the optimization of radiation protection. Particularly important are the interventional cardiology and radiology practice that, notwithstanding yield a lower contribution to the collective dose with respect diagnostic X-ray and CT procedures, on the other hand, are characterized by higher doses both for the patient and the medical staff. At the present time a major concern in this field comes from the recently published report by ICRP on tissue radiosensitivity that lowered the threshold dose for the cataract and opacity effect in the eye lens. In that framework a collaboration has been established between ENEA-Radiation Protection Institute and S.Orsola-Malpighi Bologna Hospital to perform a survey on the medical staff working in interventional radiology. That survey demonstrated the necessity to optimize the radiation protection of the staff that can receive doses to the eye lens that can easily reach the annual limit of 20 mSv recommended by ICRP. These results suggested to investigate better the X-ray scattering field, in which the head of the physician is irradiated, in order to provide recommendations on the better use and positioning of the shielding and anti-X goggles. The project will be carried on through in field measurements and simulation, with phantoms, ionization chambers and dosimetric systems in order to better characterize the scattered X-ray field. The present paper reports on the main results of the performed in-field survey and the aim and methodology of the project.

In Vivo Dosimetry for the Measurement of Doses to Breast Cancer Patients During External Beam Radiotherapy Treatment, using the Optically Stimulated Luminescence (OSL) Dosimeters at the Douala General Hospital, Cameroon

Fokou Mvoufo^a, Samba Richard^b

^aNational Radiation Protection Agency (ANRP), Yaounde, Centre, Cameroon

^bUniversity of Ghana, School of Nuclear and Allied Sciences (SNAS)- GAEC, Accra,, Ghana

Abstract. October is National Breast Cancer Awareness month! Every year, millions of people die from either one or many forms of cancer. Cancer is a malignant tumor or growth caused when cells multiply uncontrollably destroying healthy tissues. The different forms of cancer include; Leukemia, Carcinomas, Lymphomas and Sarcomas. Most of those tumors arise for women between 45 – 65 years, with some at younger age. Breast cancer is most common in women. From the ‘USA breast cancer statistics’ in April 2011, 12% of women in USA will develop breast cancer over the course of their lifetime. The World Health Organization reports that 60% of all cancer patients require radiotherapy at one point of their treatment, and 40% of cancer cure result from radiotherapy. In Cameroon, breast cancer is the leading cause of cancer-related morbidity and mortality. Preventive actions against breast cancer are less visible. Effective strategies to control this form of cancer need to be informed with accurate data on incidence. For breast cancer cases in 2011, 91.944% of women were 30 years old or more. Cervical cancer was more frequent than breast cancer from 2004 to 2007 then, the later became more frequent. The constant rise in incidence of breast cancer may be due the lack of an effective national prevention policy against it. Given the weakness of the national health information, we carried out this study in view of determining trends in incidences of breast cancer in radiotherapy Center of the Cameroon Douala General Hospital, using the Optically Stimulated Luminescence (OSL) Dosimeters.

UNSCEAR's Assessment of Medical Exposure

Ferid Shannoun

United Nations Scientific Committee on the Effects of Atomic Radiation, 1400 Vienna, Austria

Abstract. Today, it is known that medical radiation exposure is by far the largest artificial source of radiological exposure in many countries and it continues to increase considerably. The United Nations has established the Scientific Committee on the Effects of Atomic Radiation (UNSCEAR) to assess and report levels, effects and risks of exposure to ionizing radiation from all sources, including those used in medicine. Over the past 30 years, UNSCEAR has regularly assessed the levels and trends of medical exposures globally and has carried out surveys to collect the required information from UN Member States. Its recent Global Medical Exposure Survey was launched in 2014 with the support of the World Health Organization (WHO) by inviting UN Member States to submit data on medical radiological exposure from diagnostic and interventional radiology, nuclear medicine and radiation therapy via UNSCEAR's online platform (www.survey.unscear.org). UNSCEAR has developed an improvement strategy to address some existing deficiencies in data quality and collection of former surveys, including the update of its extrapolation methodology for global estimates of exposures and related uncertainties. This paper will present the main elements and the progress achieved.

Radiation Dose in Childhood Cancer Management: Challenges and Recommendations for Dose Reduction

Hamid Abdollahi

Department of Medical Physics, School of Medicine, Iran University of Medical Sciences, Tehran, Iran

Abstract. Cancer is the second leading cause of death in children. According to American Cancer Society, about 15,780 new cases of cancer have been diagnosed and 1960 deaths from cancer have been occurred among children aged birth to 19 years in 2014 in United States. Early diagnosis and treatment of cancer is of importance in children. Medical imaging and radiation therapy played a vital role in cancer management. Imaging modalities such as radiology, CT scan, SPECT and PET/CT use ionization radiation and may induce cancer risk particularly in children. In this era, PET as a molecular imaging approach, is a feasible diagnostic issue in early detection, prognosis and therapy assessment, but deliver a high radiation dose. In another section, CT is a gold standard of cancer imaging and treatment planning, but is the most abundant source of radiation exposure. In the other hand, radiotherapy uses ionization radiation and hence, is a main source of secondary cancer induction. In addition, due to high children radiosensitivity, any error in therapy chain including target delineation, treatment planning and dose delivery may induce complicated health consequences such as second malignancies. Radiation dose assessment from diagnosis to end of therapy should be taken into account in all children. In this condition, clinicians are the first experts who can reduce radiation exposure. Justification of medical imaging using a high precision order of radiological examinations is best strategy for dose reduction. Also, a highly knowledge based treatment planning based on individualizing therapy can be most effective remedial approach in children radiotherapy with as low as possible normal tissue complications. Therapy assessment using image guidance technologies during and after treatment should be done with a justified and optimized manner. Dose reduction methods, are of importance in all cancer management road. Radiation protective devices should be present in all departments.

Review and Evaluation of Imaging Methods and Analysis of Images Obtained by Magnetic Resonance Imaging to Determine the Absorbed Dose in the Phantom by Polymer Gel Dosimetry

Hamed Deghani^a, Amin Farzadnia^b, Saeed Shanehsazzadeh^f, Yazdan Salimi^d, Jalal Ordoni^c, Dariush Askari^c, Mohammad Hossein Jamshidi^e

^aDepartment of Biomedical Engineering and Physics, Faculty of Medicine, Tehran, Iran

^bSchool of Paramedical Science, Student's Research Committee, Shahid beheshti University of Medical Science, Tehran, Iran

^cDepartment of Radiology, Faculty Paramedical Sciences, Shahid Beheshti University of Medical Sciences, Tehran, Iran

^dDepartment of Physics & Medical Engineering, Faculty of Medicine, Shahid Beheshti University of Medical Sciences, Tehran, Iran

^eDepartment of Medical Physics, Faculty of Medicine, Jundishapur University of Medical Sciences, Ahvaz, Iran

^fAssistant Professor of Medical Physics, Nuclear Science and Technology Research Institute (NSTRI), Tehran, Iran

Abstract. Magnetic resonance imaging (MRI) is a method based on magnetization of hydrogen atoms in the water molecules with high spatial resolution and in three dimensions, which combined with the dosimetry methods makes it as optimal tool for assessing the accuracy of radiation therapy. Unlike conventional methods of dosimetry that have limited resolution and measuring only one or a few specific points, the polymer gel with tissue equivalent structure is capable of measuring complex three-dimensional dose distribution with high accuracy and spatial resolution. By exposure to a polymer gel phantom, polymerization reaction of free radicals leads to a change in clusters or chains of polymers in the gelatin matrix. Magnetic resonance imaging contrast mechanisms, directly or indirectly, reveals the polymer changes. The unique characteristics of this method is measuring the changes in viscosity, its relationship to the absorbed dose and display the dose distribution in three dimensions. Treatment planning should be implemented according to the reference image data that obtained from the irradiated calibration vials in the gel dosimetry phantom. In this paper, by review and analysis of articles about polymer gel dosimetry and also imaging methods based on magnetic resonance imaging physics, the optimal quantitative parameters of the imaging sequences are provided to obtain R1 ($1 / T1$) and R2 ($1 / T2$) imaging and magnetization transfer ratio (MTR), with good signal to noise ratio and lowest distortion artifacts. Also image analysis methods will be checked to achieve parametric maps and dose volume histograms (DVHs).

KEYWORDS: *polymer gel dosimetry; pulse sequence; relaxation time; dose distribution; dose volume histograms.*

Standard Calibration of Ionization Chambers Used in Radiation Therapy Dosimetry and Evaluation of Uncertainties

HyoJin Kim, Sung Jin Noh, Hyun Kim, Sang koo Kang, Manwoo Lee, Dong Hyeok Jeong, Kwangmo Yang, Yeong-Rok Kang

Dongnam Institute of Radiological & Medical Sciences, Busan, Republic of Korea

Abstract. To achieve a good clinical outcome in radiotherapy treatment, a certain accuracy in the dose delivered to the patient is required. Absolute dosimetry of external beam radiotherapy is carried out by the use of ionization chambers. These chambers must be calibrated at a standard dosimetry laboratory before any use in clinical dosimetry. The present work has described traceability of SSDL radiation measurement standards to relevant international standards, and calibration of therapy level ionization chambers in terms of air kerma and absorbed-dose-to-water against ^{60}Co gamma radiation, as well as uncertainty evaluation of calibration coefficients. The Second Standard Dosimetry Laboratory (SSDL) is part of an international network of dosimetry laboratories established by the International Atomic Energy Agency (IAEA) and the World Health Organization (WHO). The network provides a framework of international comparisons of the absorbed dose measurements that help to maintain consistency and accuracy particularly amongst the radiotherapy community. The SSDLs are designated by national laboratories (such as Primary Standard Dosimetry Laboratories, PSDLs) to provide national and international radiation dosimetry traceability for users in that country. Korea's national primary standard is the responsibility of the Korea Research Institute of Standards and Science (KRISS). The Dongnam Institute of Radiological & Medical Sciences (DIRAMS) SSDL has measurement traceability to KRISS. As the results, the expanded uncertainties in the determination of air kerma and absorbed-dose-to-water are estimated to be 1.1% and 1.2% at approximately 95% confidence level, respectively.

Radiological Risk Assessment in Tunisian University Hospital

Hager Kamoun, Samar Kallela, Mohamed Faouzi Ben Slimane

Centre National de Radioprotection, Tunis, Tunisia

Abstract. Introduction: Ionizing radiation in the medical field is used in both the conventional and interventional radiology. Radioprotection follows rules which help reduce occupational exposure. The aim of this study was to assess the management of the radioprotection of workers in the Rabta university hospital, to recommend corrective actions. Methods : First, we conducted a descriptive study during June 2015 on the management of radioprotection of workers. We used a pre-established check-list. Then we calculated a score of risk in each department. Second, we calculated the annual passive exposure dose in 2013. Results : Some insufficiencies were found at several levels such as the workspace design non authorized by the CNRP, radiation protection tools and the lack of staff training. For the annual dosimetry, the lowest value was recorded in cardiology (0.57mSv/year) and the highest was recorded in visceral surgery (1.12 mSv/year). These values were below the annual limits. A significant correlation between the annual dosimetry averages and the score of the risk related to the management of radioprotection was proven. Conclusion : While these dosimetry values were below the annual limits, a continuous vigilance in the field of the radioprotection of the workers remain essential. The synergistic collaboration between the various participants will lead to a better management of the radioprotection of the staff.

KEYWORDS: *x-rays; occupational exposure; radiation protection; radiation dose.*

An Automated Mechanical Quality Assurance System for Medical Accelerators using a Smartphone

Hwiyoung Kim^a, Il Han Kim^b, Hyunseok Lee^{c,d}, Sangmin Lee^{b,c}, Sung-Joon Ye^{b,c}

^aInterdisciplinary Program in Radiation applied Life Science, Seoul National University College of Medicine, Seoul, Republic of Korea

^bDepartment of Radiation Oncology, Seoul National University Hospital, Seoul, Republic of Korea

^cProgram in Biomedical Radiation Sciences, Department of Transdisciplinary Studies, Graduate School of Convergence Science and Technology, Seoul National University, Seoul, Republic of Korea

^dDepartment of Radiological Emergency Preparedness, Korea Institute of Nuclear Safety, Daejeon, Republic of Korea

Abstract. Purpose: The mechanical quality assurance (QA) of medical accelerators consists of time-consuming and error-prone procedures. To avoid this inconvenience, we developed an automated mechanical QA system using a smartphone. Materials and methods: For the assessments of gantry and collimator angle indications, motion sensors (gyroscope, accelerometer, and magnetic field sensor) embedded in the smartphone were used. A combination use of several different sensors enhanced the accuracy of determining the orientation of the smartphone with respect to the gravity. For the assessments of jaw position indicator, cross-hair centering, and optical distance indicator (ODI), an optical-image processing module using a picture taken by the high-resolution camera embedded in the smartphone was implemented. The preparation for the automated process was done by attaching a smartphone to the gantry facing upward. The application was developed with the Android software development kit (SDK) and OpenCV library. Results: The system accuracies in terms of angle detection error and length detection error were less than 0.1° and 0.1 cm, respectively. The mean absolute errors for gantry and collimator rotation angles were 0.03° and 0.04° , respectively. The mean absolute error for the measured light field size was 0.07 cm. The developed system has precisions of 0.063° and 0.023 cm for angle and length measurements, respectively. Conclusions: The automated system we developed can be used for the mechanical QA of medical accelerators with proven accuracy.

Patient Doses in a Hybrid Operating Room

Hugo Perez-Garcia, Carlos Andrés Rodríguez, Manuel Agulla Otero, Ricardo Torres Cabrera, Raquel Barquero Sanz

Hospital Clínico Universitario de Valladolid, Valladolid, Spain

Abstract. Purpose: This work aims to evaluate the dosimetric parameters associated with doses to patients from a vascular hybrid room during the first six months of use. Material & Methods: The vascular hybrid room is equipped with a multi-axis robotic imaging system Siemens Artis Zeego. Intervention's parameters were obtained by means of a software from the manufacturer, called CARE Analytics. 124 interventions that required the use of X-rays in the hybrid room were analyzed according to the following parameters: radiation time, skin dose, interventional reference point dose and dose-area product. Average and the maximum values of each data series were obtained. Results & Discussion: On average, each intervention lasted 19:47 minutes (3:44 minutes 95%CI), with a maximum value of 2:22:33 hours. Patient skin dose were, on average, 0.23 Gy (0.13 Gy 95%CI) while interventional reference point dose reached 0.51 Gy (0.21 Gy 95%CI) with maximum values of 1.81 Gy and 9.3 Gy respectively. The average dose-area product was 0.009 Gy² (0.004 Gy² 95%CI) with a maximum of 0.21 Gy². Fluoroscopic irradiation mode accounts for 93.9% of the irradiation time (1.0% CI) while the acquisition irradiation mode accounts only for 6.1%. Nevertheless, the acquisition irradiation mode accounts for 68.7% of total interventional reference point dose, while the fluoroscopy accounts only for 31.3% (3.9 CI). Conclusions: Patient doses in a vascular hybrid room are evaluated. The heterogeneity of the interventions that are performed in the vascular hybrid room leads to a large variability in the dosimetric results obtained. Approximately two-thirds of the patient dose was due to the acquisition mode, despite it represents less than 10% of the total irradiation time in the vascular hybrid room. A few interventions have long values of irradiation time, so care must be taken to prevent the possibility of deterministic effects in patient's skin Acknowledgements: To the Vascular Surgery and Radiology Services from Hospital Clínico Universitario de Valladolid.

Comparison of Patients CTDI from Two Different "Make" 16-SLICE CT Scanners in Maiduguri North Eastern Nigeria

Idris Garba^a, Aisha Abba Kato^b, Auwal Abubakar^b, Chogozie Nwobi^b, Mansur Yahuza^c, Nasiru Isha Fagge^a

^aBayero University Kano, Kano, Nigeria

^bUniversity Of Maiduguri, Borno, Nigeria

^cAminu Kano Teaching Hospital, Kano, Nigeria

Abstract. Aim: the study aimed to investigate the patients CTDI from two different make CT scanners for head CT. Background: modern CT scanners now offer a lot of clinical opportunity. However, these clinical capabilities have not been without a price, which is a major source of radiation exposure. Therefore, use of appropriate scan parameters is highly recommended as tools for radiation dose optimisation. Methods: This was a retrospective study involving two CT centres in Nigeria. Scan and radiation dose data of head CT from GE and Philips 16-slice were obtained. CTDI and DLP were compared between centres. The data was analysed using SPSS Version 16 statistical software. Results: The CTDI and DLP for head CT obtained were: (63 mGy & 1193 mGy.cm) for centre (A) and (48 mGy & 340 mGy.cm) for centre (B). The difference in absorbed dose in both CTDI & DLP between centers was found to be statistically significant ($p=0.0001$ and $p=0.0001$) respectively. Conclusion: The study has established radiation dose values from two CT centres. Centre (A) has higher values in terms of CTDI and DLP partly due to the use of higher mAs value and in some cases taken too many slices.

KEYWORDS: *head CT; CTDI; 16-slice CT.*

Hearing Radiation and its Application to in Vivo Radiation Dosimetry during Radiation Treatment

I.J. Kim^a, J.H. Kim^a, C.Y. Yi^a, C.H. Kim^b, J.S. Kim^b, E.Y. Park^b, Y.H. Jung^b

^aKorea Research Institute of Standards and Science, Daejeon, Republic of Korea

^bPohang University of Science and Technology, Pohang, Republic of Korea

Abstract. It is well known that ionization radiations cannot be seen, heard, tasted, smelled or felt, directly. But sensitive acoustic sensors make it possible to hear the sound caused by ionizing radiations and also to get their spatial information. So, now, it can be said that ionizing radiations can be heard and be seen using the acoustic devices. Furthermore, this kind of technique is non-destructive and it gives prompt response to the ionizing radiations. Thus, we authors expect that it will be applicable to in-vivo radiation dosimetry during radiation treatment or therapy using various kinds of radiation beams, in near future. In this study, a measurement system was built to realize hearing high energy X-rays, and preliminary studies were performed to figure it out the feasibility of the technique for dosimetric applications. The measurement system was built with a focused ultrasound transducer (focal length: 1.25 inch, center frequency: 500 kHz). Signals from the transducer were acquired with a fast digital oscilloscope and the acquired data were processed on Matlab® platform to get images. Targets were irradiated by 6, 10, 18 MV X-rays with an Elekta synergy platform linear accelerator at KRISS (Korea Research Institute of Standards and Science). During irradiation, pulse forming network signals of the linear accelerator was fed to the measurement system in order to give start signals of the sounds. Sounds from small lead block was heard at various X-ray energies, dose rates or water depths, etc. Sounds from other kinds of materials were also heard. The results will be presented and discussed.

Effectiveness of Dose Modulation Technique of CT scan on Organ Dose

Il Park, Seung Cheol Oh, Kwang Pyo Kim

Kyung Hee University, Yongin-Si, Gyeonggi-Do, Republic of Korea

Abstract. Computed tomography (CT) is the largest contributor to collective effective dose to patients in medical radiology. CT scanner manufacturers have developed and applied the dose modulation technique to appropriately manage or reduce radiation dose to patient from CT scan. The purpose of this study was to estimate the effectiveness of dose modulation technique on organ doses for abdomen and pelvis CT scan. Radiation doses were calculated using MCNPX simulation for organs positioned in abdomen and pelvis regions. Six different CT scanner models from 4 different manufacturers were used for the dose calculation. To analyze the effectiveness, organ doses with or without dose modulation technique were calculated and compared. For all CT scanners, when dose modulation technique was applied, radiation doses to organs in abdomen region were lower compared with organ doses without the dose modulation technique while radiation doses to organs in pelvis region were higher. However, the dose change in abdomen and pelvis regions varied depending on CT scanner models. The CT scanner model with the biggest dose change showed about 7-14% decreased organ doses in abdomen region and about 18-20% increased organ doses in pelvis region. The CT scanner model with the smallest dose change showed about 5-10% decreased organ doses in abdomen region and about 6-9% increased organ doses in pelvis region. In this study, organ doses were calculated with and without applying dose modulation technique. Organ doses varied with scanning position of patients. Improved accuracy of radiation dose calculation method given in this study will be able to be applied for optimization of radiation protection. This research was supported by a grant of the Korea Health Technology R&D Project through the Korea Health Industry Development Institute (KHIDI), funded by the Ministry of Health & Welfare, Republic of Korea (grant number : HI13C0004).

Application of Prospective Approaches in Preventing Accidental Exposure in Radiotherapy: A Review of Italian Experiences

Ivan Veronese^a, Marie Claire Cantone^a, Luisa Begnozzi^b

^aUniversità degli Studi di Milano, Dipartimento di Fisica, Milan, Italy

^bOspedale Ca' Foncello, UOC Fisica Sanitaria, Treviso, Italy

Abstract. The interest in the definition and maintenance of a radiation protection culture in medicine is gaining importance and new initiatives are accordingly being launched by national and international organizations. In this context, studies and activities aimed to reduce the risk of accidental exposure to patients undergoing modern radiation therapy (RT) treatments are encouraged. In fact, the high level of complexity of the new RT methodologies places demands of innovative approaches to patient safety. Proactive methods of risk analysis fit for the purpose to anticipate the potential hazards that may occur during these RT treatments. This work aims to review the recent scientific studies carried out by multidisciplinary working groups of the Italian Association for Medical Physics and dealing with the application of the failure mode and effects analysis (FMEA) approach to various modern RT processes, generally characterized by the delivery of high radiation doses with short fractionation schemes and high dose conformity. In particular, risk analysis related to intraoperative radiation therapy, tomotherapy, proton-therapy and stereotactic body radiation therapy by means of CyberKnife units are considered. The experience gained during these studies enabled to come to light the strengths and weakness of the FMEA approach in RT. Advantages, limits and challenges of the use of this methodology for an effective improvement of the patient safety in the modern RT are here presented. Furthermore, the contribution given by these studies for the enhancement of a radiation protection culture in medicine is discussed.

Survey of Radiation Protection in Patients Undergoing X-ray Medical Examination

Justina Achuka, Mojisola Usikalu

Covenant University, Ota, Ogun State, Nigeria

Abstract. The aim of the work is to create awareness on the need for proper protection of patient going for radio diagnostics examination. Seven (7) radio-diagnostic centres in Ota, Ogun State were used for the study. The outcome of the research revealed that 100 % of the centres do not observe radiation protection safety rules. We found that an average of thirty three (33) patients underwent radio-diagnostic examination in a day and only 50 % of the radiographers adhered to optimization of procedures. This is an indication that at least 50 % of these patients would have been over exposed to ionizing radiation. Therefore, there is need to increase the awareness of harm from over-exposure of patients and proper optimization for radiation protection of patients undergoing radio diagnostic procedures which is the potent dose reduction strategy.

Long Half-Life Isotopes Europium-152 and Europium-154 Found in Hospital Waste

Janneke Ansems, Bunna Damink, Jelle van Riet, Corinne Valk, Ruud Hack

Bravis Hospital, Roosendaal, NB, The Netherlands

Abstract. Purpose: The Dutch public service for the treatment of waste rejected waste from Bravis Hospital, Roosendaal, The Netherlands, due to radioactivity. The Dutch Inspection of Environment and Transport detected Europium-152 (Eu-152, half-life 13 years) and Europium-154 (Eu-154, half-life 8 years) with a dose rate of 0,8 $\mu\text{Gy/h}$ (at the surface of the waste container). The radiation protection expert (RPE) of the Hospital was asked to investigate and apply methods to prevent recurrence. Materials and Methods: Literature on Europium and its decay scheme was reviewed, the procedure for waste disposal at the Nuclear Medicine department was investigated and dose calculations were performed. Results: Eur-152 en Eur-154 are impurities of Samarium-153 (Sm-153, half-life 2 days), which is used at the Nuclear Medicine department as a palliative treatment for bone metastases. The RPE was unaware of impurities of Eur-152 and Eur-154 in Sm-153. Waste of Sm-153 treatment, i.e. vials, needles and gauzes, are put in waste containers. After three months these are measured to be below background and then discarded as normal waste. Dose calculations showed that the amount of radioactivity found at the waste treatment service could have been caused by one vial used for Sm-153 treatment. However, dose calculations also showed that the activity and activity concentrations of Eu-152 and Eu-154 disposed by the Hospital were well below legal limits and therefore no sanctions were imposed by the Dutch Inspection. Conclusion: Eu-152 and Eu-154 are impurities of Sm-153. Although the found activities and activity concentrations of Eu-152 and Eu-154 are below Dutch legal limits, vials and needles from Sm-153 treatment will be disposed as radioactive waste to protect the environment from long life isotopes and to prevent rejection by the public waste treatment service.

Prospective Risk Assessment of the Use of Radioactive Iodine-125 Seeds for the Localisation of Impalpable Breast Lesions

Janneke Ansems, Bunna Damink, Jelle van Riet, Pieter Buijs, Els Vanaert

Bravis Hospital, Roosendaal, NB, The Netherlands

Abstract. Purpose: Impalpable breast lesions require pre-operative image-guided localisation. In Bravis Hospital, Roosendaal, The Netherlands, low radioactive iodine seeds (I-125, half-life 60 days) are used to localise impalpable breast lesions. The seeds are very small (1 by 4 mm) and have an activity of 7 MBq (0,2 mCi). A radiologist places the seed in the lesion under ultrasound or x-ray guidance. During the resection operation, the surgeon uses a probe to find the radioactive seeds and excises the lesion with seeds. The resected lesion with seed is transported to Pathology, where the seed is retrieved and returned to the Nuclear Medicine department for disposal. Many employees are involved in this procedure and have to work together to adequately manage radiation protection issues. Before localisation with radioactive iodine seeds was commenced, a prospective risk assessment was performed. Materials and Methods: A multidisciplinary Health Failure Mode and Effect Analysis (HFMEA) was performed with a selection of people from all the departments involved. All the steps of the procedure were listed and for each step the possible failure modes, (radiation) effects, risks and possible control measures were determined. Results: The most important failure mode was loss of a radioactive I-125 seed. Additional checks were added to the procedure to confirm location of the seed after localisation and resection. The received dose by employees due the radioactive seeds is very minimal due to its low energy (30 keV). Conclusion: The prospective risk assessment was essential to safely implement the use of radioactive iodine seeds for localisation of impalpable breast lesions. Furthermore, awareness of proper handling of the I-125 seed, mainly after resection, is very important in order to prevent loss of I-125 seeds.

Global Developments in DRLs and Assessment of Medical Exposures

John Damilakis

University of Crete, Heraklion, Greece

Abstract. The term ‘Diagnostic Reference Levels’ (DRLs) was introduced by the International Commission on Radiological Protection (ICRP) in 1996. In 1999 the European Commission (EC) issued Radiation Protection 109 (RP 109) publication on "Guidance on diagnostic reference levels DRLs for medical exposure". DRLs have proven to be an effective tool for optimisation of protection in medical exposures of patients. The newly published ‘Euratom Basic Safety Standards’ states that ‘Member States shall ensure the establishment, regular review and use of diagnostic reference levels for radiodiagnostic examinations, having regard to the recommended European diagnostic reference levels where available, and when appropriate, for interventional radiology procedures, and the availability of guidance for this purpose’. The ‘European DRLs for Paediatric Imaging’ project (abbreviation: PiDRL) is an EC project aimed to a) develop a methodology for establishing and using DRLs for paediatric medical imaging and b) update and extend the European DRLs to cover as many as possible procedures. The PiDRL project has very recently drafted European Guidelines on how to establish and how to use paediatric DRLs. A list of the most important procedures and/or clinical indications for which paediatric DRLs should be defined is included in the PiDRL guidelines. For body examinations, weight should be used as a parameter for patient grouping. For head examinations, age is recommended as the grouping parameter. Dose management solutions can play a very important role in the establishment and use of DRLs. ICRP has finalized a document on “Diagnostic Reference Levels (DRLs) in Medical Imaging”. The draft report was available for public consultation until April 15, 2016. This report provides information and guidance on issues related to the determination of the values for DRLs, the appropriate interval for reviewing and updating DRLs, appropriate use of DRLs in clinical practice, methods for practical application of this tool and application of the DRL concept to newer imaging technologies.

Persistence of Dicentric Chromosomes associated with Telomere Dysfunction: A Biomarker of Prognosis in Patients Undergoing Total Body Irradiation

Julien Dossou^{a,b}, Theodore Girinsky^c, Dominique Violot^a, Jean-Henri Bourhis^d, Eric Lartigaux^e, Luc Morat^f, Claude Parmentier^a, Radhia M'kacher^{f,g}

^aMolecular Radiotherapy, RAMO, INSERM 1030, Gustave Roussy Institut, Villejuif, France

^bEcole Polytechnique/Université d'Abomey, Cotonou, Benin

^cRadiation therapy department, Gustave Roussy Institut, Villejuif, France

^dHematology Department, Gustave Roussy Institut, Villejuif, France

^eRadiation Therapy Department, Lille, France

^fLaboratoire de Radiobiologie et Oncologie, CEA, Fontenay aux Roses, France

^gCell & Environment, Paris, France

Abstract. Background: Total body irradiation (TBI) based preparative regimens are considered to be standard conditioning therapy for allogeneic and autologous cell transplantation in patients with hematologic malignancies. Dicentric chromosomes are not only the most specific chromosomal aberration to irradiation, but also the formation of dicentric chromosomes containing two functional centromeres can lead to chromosomal instability. This study examines the prognostic impact of the persistence of dicentric chromosome and telomere dysfunction after allogeneic and autologous cell transplantation on relapse free survival (RFS) and overall survival (OS) in patients. Patients and methods: 40 patients with hematologic malignancies (Chronic myeloid leukemia, myeloma, acute lymphoblastic leukemia and acute myeloid leukemia) undergoing TBI were included in the study. Blood samples were obtained from patients before TBI irradiation, after the first and second fraction of 1.8 Gy and for 6 months after transplantation. Dicentric chromosomes were scored using telomere and centromere staining and telomere length and telomere aberrations were assessed using the Q-FISH technique. Results: Median follow-up for surviving patients was 30 months. Patients with a higher frequency of dicentric chromosomes after transplantation had significantly shorter RFS ($p=0.03$) and OS ($p<0.01$) compared to patients with normal cytogenetic profiles. Among the patients with a persistently of high frequency of dicentric chromosomes, telomere dysfunction was observed. This dysfunction was related to changes in telomere length, the presence of cells with very long telomeres and a high frequency of telomere aberrations (loss and doublets). Of note, the presence of cells with greater telomere length in patients with poor clinical outcome appears from the first fraction of TBI and increased after transplantation. Conclusion: This first study demonstrates the impact of the persistence of dicentric chromosomes and telomere dysfunction in poor clinical outcomes of patients treated with TBI. The persistence of dicentric chromosomes and change in telomere length over time after transplantation could be a biomarker of prognosis. Research on determinants of telomere length and change is needed.

Dosimetric Analysis with the Specifically Selected Low-Dose Threshold on Gamma Evaluation for VMAT QA

Ji-Hye Song^a, Min-Joo Kim^a, So-Hyun Park^{a,b}, Seu-Ran Lee^a, Min-Young Lee^a, Dong Soo Lee^b, Tae Suk Suh^a

^aDepartment of Biomedical Engineering and Research Institute of Biomedical Engineering, College of Medicine, The Catholic University of Korea, Seoul 137-701, Korea, Seoul, Republic of Korea

^bDepartment of Radiation Oncology, Uijeongbu St. Mary's Hospital, Uijeongbu 480-717, Korea, Uijeongbu, Republic of Korea

Abstract. Purpose: The AAPM TG-119 instructed institutions to use a low-dose threshold of 10% or a ROI determined by the jaw when they collected gamma analysis QA data of planar dose distribution. Also, based on a survey by Nelms and Simon, more than 70% of institutions use a low-dose threshold between 0% and 10% for gamma analysis. However, there are no clinical data to quantitatively demonstrate the impact of the low-dose threshold on the gamma index. Therefore, we performed a gamma analysis with low-dose thresholds of 0%, 5%, 10%, and 15% according to both global and local normalization and different acceptance criteria: 3%/3 mm, 2%/2 mm, and 1%/1 mm. Methods: A total of 30 treatment plans—10 head and neck, 10 brain, and 10 prostate cancer cases—were randomly selected from the Varian Eclipse TPS, retrospectively. For the gamma analysis, a predicted portal image was acquired through a portal dose calculation algorithm in the Eclipse TPS, and a measured portal image was obtained using a Varian Clinac iX and an electronic portal imaging device. Then, the gamma analysis was performed using the Portal Dosimetry software. Result: For the global normalization, the gamma passing rate (%GP) decreased as the low-dose threshold increased, and all cases of low-dose thresholds exhibited a %GP above 95% for both the 3%/3 mm and 2%/2 mm criteria. However, for local normalization, the %GP increased as the low-dose threshold increased. The gamma passing rate with the low-dose threshold of 10% increased by 7.47%, 10.23% and 6.71% compared with the 0% in the case of the head and neck, brain and prostate for 3%/3 mm criteria, respectively. Conclusion: Applying low-dose threshold in the global normalization does not have critical effect to judge patient-specific QA results. However, low-dose threshold for the local normalization should be carefully selected because applying low-dose threshold could affect the average of the %GP to increase rapidly.

The Influence of the Dose Calculation Resolution of VMAT Plans on the Calculated Dose for Eye Lens and Optic Apparatus

Jong Min Park^a, So-Yeon Park^a, Jung-in Kim^a, Hong-Gyun Wu^b, Jin Ho Kim^a

^aDepartment of Radiation Oncology, Seoul National University Hospital, Seoul, Republic of Korea

^bDepartment of Radiation Oncology, Seoul National University College of Medicine, Seoul, Republic of Korea

Abstract. The effect of dose calculation grid size on the accuracy of calculated doses in the treatment planning system (TPS) for each eye lens and optic apparatus was investigated. A total of 20 patients who received volumetric modulated arc therapy (VMAT) for head and neck (H&N) cancer located at nasal cavity were selected retrospectively for this study. All patients were treated with VMAT technique and the treatment plans were generated with the Eclipse system using 6 MV photon beams. For dose calculation, the sizes of calculation grids were varied from 1 mm to 5 mm at intervals of 1 mm. After that, dose calculations with various calculation resolution were performed maintaining same number of monitor units (MUs). The planning risk volume (PRV) for each eye lens, each optic nerve and optic chiasm were defined with a 2 mm margin from each structure. The calculated maximum dose delivered to left and right eye lens increased from $14.9 \text{ Gy} \pm 19.1 \text{ Gy}$ to $16.6 \text{ Gy} \pm 17.8 \text{ Gy}$ and from $7.5 \text{ Gy} \pm 3.1 \text{ Gy}$ to $9.8 \text{ Gy} \pm 3.9 \text{ Gy}$, respectively, as increasing the size of dose calculation grid from 1 mm to 5 mm. Those values for PRV of each lens also increased from $17.1 \text{ Gy} \pm 19.6 \text{ Gy}$ to $19.9 \text{ Gy} \pm 18.1 \text{ Gy}$ and $9.7 \text{ Gy} \pm 3.8 \text{ Gy}$ to $13.2 \text{ Gy} \pm 4.8 \text{ Gy}$, respectively. For left and right optic nerves, the calculated maximum delivered doses increased from $47.5 \text{ Gy} \pm 15.1 \text{ Gy}$ to $48.6 \text{ Gy} \pm 15.0 \text{ Gy}$ and from $47.7 \text{ Gy} \pm 11.8 \text{ Gy}$ to $48.9 \text{ Gy} \pm 11.5 \text{ Gy}$, respectively. Those values for PRV of each optic nerve increased from $51.7 \text{ Gy} \pm 13.3 \text{ Gy}$ to $52.0 \text{ Gy} \pm 13.9 \text{ Gy}$ and from $51.8 \text{ Gy} \pm 10.0 \text{ Gy}$ to $52.4 \text{ Gy} \pm 10.9 \text{ Gy}$, respectively. In the case of optic chiasm and its PRV, those values increased from $44.0 \text{ Gy} \pm 12.6 \text{ Gy}$ to $45.0 \text{ Gy} \pm 12.8 \text{ Gy}$ and from $49.6 \text{ Gy} \pm 11.4 \text{ Gy}$ to $49.7 \text{ Gy} \pm 12.0 \text{ Gy}$, respectively. For eye lens, differences in the maximum dose delivered to left and right eye lens were 11.6% and 31.4%, respectively, as increasing the size of dose calculation grid from 1 mm to 5 mm. To evaluate exact delivered dose to eye lenses as well as optic apparatus, of which volumes are small, the size of dose calculation grid should be small when calculating dose distributions with patient CT images.

Monte Carlo Estimation of Effective Dose to Patients Undergoing Contrast Based X-Ray Fluoroscopy Procedures

J. E Ngaile^a, P. Msaki^a, R. Kazema^b

^aDepartment of Physics, University of Dar es Salaam, P O Box 35063, Dar es Salaam, Tanzania

^bDepartment of Radiology, Muhimbili University of Health and Allied Sciences, P O Box 65001, Dar es Salaam, Tanzania.

Abstract. The aim of this study was to assess the radiation burden imparted to patients undergoing contrast based fluoroscopy procedures in Tanzania. The air kerma area product (KAP), effective doses to patient from five contrast based X-ray fluoroscopy procedures were obtained from four consultant hospitals. The KAP was determined using a flat transmission ionization chamber, while effective doses was estimated using the knowledge of the patient characteristics, patient related exposure parameters, geometry of examination, KAP and Monte Carlo based software. The mean values of effective dose for the BS, BM, BE, HSG and RUG were 0.82 ± 0.85 mSv, 2.42 ± 2.39 mSv, 3.03 ± 1.44 mSv, 0.78 ± 0.64 mSv, and 1.02 ± 1.35 mSv, respectively. The overall differences between individual effective doses across the four hospitals varied by up to a factor of 53, 58.9 and 11.4 for the BS, BM, and BE, respectively, while for the HSG and RUG differed by up to a factor of 22 and 40.7, respectively. The mean values of KAP and effective doses in the present study were mostly lower than reported values from Spain, UK, Ghana, and Greece, while slightly higher than those reported from India. The observed significant variation of mean values of KAP and effective dose for similar fluoroscopy procedure within and across hospitals was largely influenced by the complexity of the procedure, dynamic nature of the procedures, patient characteristics, skills and experience of personnel, and different protocols employed among hospitals. In light of the observed causes of variation of patient doses, it was concluded that further studies are needed to investigate methods that can reduce dose to patients without impairing image quality.

KEYWORDS: *kerma-area product; effective dose; contrast based fluoroscopy procedures; Monte Carlo simulation.*

Radiation Protection Dosimetry (2017), Vol. 173, No. 1-3, pp. 203–211

doi:10.1093/rpd/ncw338

An Assessment of Radiographers' Technical and Protective Performance in Hospitals Affiliated to Birjand University of Medical Sciences in 2012

Jalal Ordoni^a, Saeid Ghasemi^b, Dariush Askari^a, Yazdan Salimi^c, Fatemeh Ramrodi^d, Mohammad Hossein Jamshidi^e, Hamed Dehghani^f

^aDepartment of Radiology, Faculty Paramedical Sciences, Shahid Beheshti University of Medical Sciences, Tehran, Iran

^bDepartment of Radiology, Faculty Paramedical Sciences, Birjand University of Medical Sciences, Birjand, Iran

^cDepartment of Physics & Medical Engineering, Faculty of Medicine, Shahid Beheshti University of Medical Sciences, Tehran, Iran

^dDepartment of Radiology, Faculty Paramedical Sciences, Zahedan University of Medical Sciences, Zahedan, Iran

^eDepartment of Medical Physics, Faculty of Medicine, Jundishapur University of Medical Sciences, Ahvaz, Iran

^fDepartment of Biomedical Engineering and Physics, Faculty of Medicine, Tehran, Iran

Abstract. Introduction: Notwithstanding the benefits of radiography, the staff of radiography wards must take necessary care to minimize their own and patients' exposure to harmful rays. Therefore, the present paper aimed at assessing the radiographers' awareness and performance concerning technical and protective principles. Materials and Methods: In this descriptive-analytical study, all the 26 radiographers working in the radiology wards of Vali-asr and Imam Reza hospitals of Birjand participated. In order to collect data about their performance, a checklist whose reliability and validity had been approved was provided. For the radiography staff 17 technical and 12 protective items during three work shifts were checked and recorded. In order to measure their awareness of technical and protective principles, a 12-item questionnaire was completed by each of them. The obtained data was statistically analysed by means of SPSS software using X2. Results: Mean Performance score in the technical area in the three work shifts was 15 ± 1.60 , and that of the protective area was 10.9 ± 1.1 both of which were at an average level. Around 46.5% of the subjects gave correct answers to protective and 37.2% of them to the technical questions. The comparison of technical and protective performance scores showed no significant difference in terms of work shifts, education, gender, and type of employment ($P > 0.05$). Conclusion: The radiographers' awareness of technical and protective principles was at a very low level. Therefore, both quality academic training and in-service education seem necessary.

Patient Radiation Safety Control in Nuclear Medicine Practices in View of the New Basic Safety Standards (BSS)

Jamila S AlSuwaidi, Priyank Gupta, Shabna Miyanath

Dubai Health Authority, Dubai, United Arab Emirates

Abstract. In cooperation with international and professional organizations, the International Atomic Energy Agency (IAEA) published, in 2014, the new Radiation Protection and Safety of Radiation Sources: International Basic Safety Standards (BSS). Justification of practice and optimization of protection are the main radiation protection principles applied to patients. Justification of practice is categorized in the new BSS as of three levels; the third level concerns with the justification of individual patient. Implementation of radiological referral guidelines is considered as an effective approach to achieve patient radiation safety. This paper discuss the Dubai Health Authority (DHA) survey and program carried out to involve radiological professional teams and referring physicians in the UAE national project for patient radiation safety and dosimetry. The DHA ultimate aim is to improve the quality and the outcome of patient care. The optimization principle in relation to patient protection comprises subjects related to the management of radiopharmaceutical laboratory and the NM imaging procedures. This paper is concisely discussing the general daily operational safety procedures in radio-pharmacy practices and in nuclear medicine (NM) imaging facility at the DHA in view of recent introduction of the BSS. The DHA efforts in establishing the UAE National Diagnostic Reference Levels (NDRLs) for NM examinations for adult and paediatric patients are presented in this paper. Our radiation safety survey results demonstrated that 80% respondents admitted that patients get increased radiation exposure in absence of clear referral guidelines. This underpinning the challenge of over-prescription & overutilization of services. 63% believed that in presence of clear referral guidelines the number of ordered investigations will definitely decrease. 80% of respondents believed that their referral practice will improve in presence of clear referral guidelines. The UAE adult NDRLs results, in terms of average administered activity (in MBq), were compared to the Australian and European Commission (EC) findings. In general, the results were shown within acceptable values. The UAE NDRLs for bone and thyroid examinations were slightly higher than those published by the EC while the cardiac values were to some extent higher compared to the Australian adult DRLs. Establishing UAE NDRLs for paediatric NM examinations is in the process.

New X-ray Technology Results in 70% Dose Reduction in Pacemaker and Implantable Cardioverter Defibrillator (ICD) Implantations

Joris van Dijk^{a,b}, Jan Paul Ottervanger^a, Peter Paul Delnoy^a, Martine Lagerweij^a, Siert Knollema^a, Cornelis Slump^a, Piet Jager^a

^aIsala Hospital, Zwolle, The Netherlands

^bMIRA: Institute for Biomedical Technology and Technical Medicine, University of Twente, Enschede, The Netherlands

Abstract. Background: Implantation of pacemakers and implantable cardioverter defibrillators (ICD) are commonly performed and are exposing both patients and staff to relatively high doses of radiation. The aim was to quantify the reduction in radiation exposure during pacemaker and ICD placements by using a new X-ray technology. Materials and methods: In this retrospective study, 1185 consecutive patients who underwent the novo pacemaker or ICD placement during a two year period were included. All implantations in the first year were performed using the reference technology (Alura Xper), whereas in the second year the new X-ray technology (Allura Clarity) was used. Radiation exposure, expressed as the dose-area-product (DAP), was compared between both periods to determine the reduction. The number of leads, procedure duration and contrast volume were used as measure of complexity and image quality. Multivariable analyses were performed to adjust for differences in baseline variables. Results: The study population consisted of 591 patients with implantations with the reference technique, and 594 patients with the new X-ray technology. Both groups were comparable regarding age, gender and body mass index, but the number of leads was higher in the new X-ray technology group (38%, vs 31%, $p < 0.001$). A reduction of 70% in the cumulative radiation exposure for pacemaker and ICD implantations was observed when using the new X-ray technology, DAP decreased from 33.6 ± 44.8 to 10.1 ± 13.5 Gy·cm² ($p < 0.001$). Procedure duration and contrast volume were not statistically different between the two groups. Conclusion: Introduction of new X-ray technology resulted in a radiation exposure reduction of 70% in pacemaker and ICD placements while image quality seemed unaffected.

The Study on the Interspace Materials of Radiographic Anti-scattering Grid with Monte Carlo Calculation

Jun Woo Bae, Hee Reyoung Kim

Ulsan National Institute of Science and Technology, Ulsan metropolitan city,
Republic of Korea

Abstract. The radiographic anti-scattering grid has been used for radiography device in order to reduce scattered photon which decreases the resolution of X-ray image and increase primary photon relative to scattered photon. There were many studies for fabrication of the grid, but few studies for optimizing the anti-scattering grid, where the optimization could lead to the reduced radiation exposure to the patient. The design optimization of radiographic anti-scattering grid was carried out using Monte Carlo Calculation of which code was MCNP with the version of MCNP6.1. The geometry for the simulation consisted of phantom, source and detector. The phantom was assumed as water chest which was expressed as a cylindroids and the grid was designed as the shape with the parallel criss-cross type. The interspace material of the grid included aluminium, copper, graphite, air and PMMA(Poly(methyl methacrylate)). The effect of the interspace material with the various density and atomic number on the performance of grid was analyzed when the shielding material of pure lead with the density of 11.34 g/cm^3 was used. Three parameters were used to compare the performance of grid: Bucky factor, CIF(Contrast Improvement Factor) and Scatter-to-Primary Ratio(SPR). The Bucky factor, CIF and SPR are defined as an inverse of transmission of total photon, the ratio of transmission of primary photon to transmission of total photon and the ratio of transmission of scattered photon to transmission of total photon, respectively. The aluminium interspace grid showed the highest performance by considering both Bucky factor (2.365) and CIF (1.561). The absolute value of CIF was the highest for copper (1.620) interspace grid but it had higher Bucky factor (2.910) than that of aluminium. The air interspace grid represented CIF value of 1.554 and Bucky factor of 2.344. For SPR, without consideration of copper interspace grid, aluminium interspace grid had the lowest value (0.496) while the values of SPR of graphite and air intermediate were 0.501 and 0.499, respectively. It was understood that aluminium interspace grid would give the best performance even though the grid with the lower density of interspace material would intuitively.

¹³¹I Activity in the Thyroid in Members of the Nuclear Medicine Medical Personnel

Kamil Brudecki^a, Aldona Kowalska^b, Pawel Zagrodzki^{a,e}, Artur Szczodry^b, Tomasz Mroz^c, Pawel Janowski^d, Jerzy Wojciech Mietelski^a

^aInstitute of Nuclear Physics, Polish Academy of Sciences, Krakow, Poland

^bDepartment of Endocrinology and Nuclear Medicine Holycross Cancer Center, Kielce, Poland

^cDepartment of Cell Biology and Genetics, The Pedagogical University of Cracow, Krakow, Poland

^dAGH University of Science and Technology, Krakow, Poland, ^eDepartment of Food Chemistry and Nutrition, Medical College Jagiellonian University, Krakow, Poland

Abstract. The first treatment using ¹³¹I was conducted in 1942 for the hyperthyroidism affliction. It was applied primarily for the diagnosis and treatment of the thyroid gland diseases, where its natural affinity for this organ is used. Nowadays, ¹³¹I is still used for the hyperthyroidism and thyroid cancer treatment, but also for kidney and bladder function tests. Main objective of present study was to estimate the occupational exposure to ¹³¹I for medical staff working at the Department of Endocrinology and Nuclear Medicine Holycross Cancer Center in Kielce. The medical staff to be investigated may have uncontrollably absorbed ¹³¹I while performing their duties, as they are exposed to radioactive iodine, which could be released in traces from pills or solutions, as well as from patients treated with this radiopharmaceutical. This part of the project was aimed specifically to measure ¹³¹I activity in the thyroid in members of the nuclear medicine medical personnel, while whole body counter (WBC) provided results more relevant for the assessment of occupational risk. WBC consists of two HPGe detectors. The spectrometer shield of 20 cm, was made of 19th century steel free from ⁶⁰Co traces, and 2 cm pure copper lining completes the design. In total we examined 30 members of the medical staff working the Department of Endocrinology and Nuclear Medicine Holycross Cancer Center in Kielce, which consist about 70% of total workers. Among them there were 3 medical doctors, 2 technicians, 19 nurses and 6 cleaners. The ¹³¹I activity in thyroid was observed in 11 persons, mainly technicians and cleaners. The maximum observed activity reached 217 ± 56 Bq. This work was supported by the National Science Center, Poland [2014/15/B/NZ7/00925].

Impact of Earthquake on Radiological Facilities in Kathmandu Valley

Kanchan P. Adhikari^a, Yaduram Panthi^b, Deepak Subedi^b

^aNational Academy of Medical Sciences, Bir Hospital, Kathmandu, Nepal

^bTribhuvan University, Kathmandu, Nepal

Abstract. Introduction: On 25th April, 2015 devastating earthquake with a magnitude of 7.8 Richter scale hit central Nepal (Epicenter: Barpak, Gorkha) which had killed more than 9000 people and injured more than 23000 people. The devastating tremor and its subsequent aftershocks had created fissures and cracks in buildings, houses, hospitals and other physical infrastructures which also could lead to the possible damage at the radiological facility as well as radiotherapy bunkers. It was therefore decided to evaluate the radiation in the occupying area that housed the radiation at diagnostic radiology, nuclear medicine and radiotherapy facility. Objective: This study was done to find out the status of radiation level, shielding structure after the earthquake. The main objective of this study is to find out the impact of an earthquake on radiological facilities in the Kathmandu Valley. Method: The study was done at twenty three different hospitals in Kathmandu Valley that had twenty one diagnostic centers, one nuclear medicine facility and two radiotherapy centers. The selection covered government hospitals, teaching hospitals, private hospitals and poly clinic with radiation facility. This study includes nineteen X-ray unit fifteen CT Scan, one gamma camera, two Cobalt-60 Tele-therapy and two HDR Brachytherapy. Onsite inspection was also done at two newly under construction radiotherapy bunkers for Linear Accelerator. Radiation Survey as well as onsite inspection of the room/bunker was made. Result: Altogether, twenty three different hospitals/institutions from Kathmandu valley were monitored, which include nineteen X-ray, fifteen CT Scan and in radiotherapy unit, two Tele-cobalt, two HDR Brachytherapy. Radiation survey result shows that most of the X-ray & CT working areas are within the safe limit. Most of the X-ray, Ct room at different hospitals had developed hairline cracks in walls because of the earthquake. Radiation level in nuclear medicine facility was found within the safe limit. Radiation dose level at two radiotherapy centers shows that all the reference points are within safe limit. We didn't find any crack in the wall of the radiotherapy bunker. Personnel monitoring for radiation workers is not happening in some of the hospitals. There is a great need for rules, regulation and radiation act in the field of radiation used in medical field. There is no quality control program in diagnostic radiology. A QC program should be performed on the X-ray equipment regularly, following international protocols.

KEYWORDS: radiation; diagnostic radiology; radiotherapy; dose limit; quality control.

Radiation Dose from Whole Body F-18 FDG PET/CT: Nationwide Survey in Korea

Keon Wook Kang^{a,b}, Hyun Woo Kwon^b, Jong Phil Kim^b, Jin Chul Paeng^b, Hong Jae Lee^b, Jae Sung Lee^{a,b}, Gi Jeong Cheon^{a,b}, Dong Soo Lee^{a,b}, June-Key Chung^{a,b}

^aSeoul National University, Seoul, Republic of Korea

^bSeoul National University Hospital, Seoul, Republic of Korea

Abstract. The purpose of this study was to estimate average radiation exposure from F-18 fluorodeoxyglucose (FDG) positron emission tomography/computed tomography (PET/CT) examinations and to analyze possible factors affecting the radiation dose. A nationwide questionnaire survey was conducted involving all institutions that operate PET/CT scanners in Korea. From the response, radiation doses from injected FDG and CT examination were calculated. A total of 105 PET/CT scanners in 73 institutions were included in the analysis (response rate of 62.4%). The average FDG injected activity was 310 ± 77 MBq and 5.11 ± 1.19 MBq/kg. The average effective dose from FDG was estimated to be 5.89 ± 1.46 mSv. The average CT dose index and dose-length product were 4.60 ± 2.47 mGy and 429.2 ± 227.6 mGy·cm, which corresponded to 6.26 ± 3.06 mSv. The radiation doses from FDG and CT were significantly lower in case of newer scanners than older ones ($P < 0.001$). Advanced PET technologies such as time-of-flight acquisition and point-spread function recovery were also related to low radiation dose ($P < 0.001$). In conclusion, the average radiation dose from FDG PET/CT is estimated to be 12.2 mSv. The radiation dose from FDG PET/CT is reduced with more recent scanners equipped with image-enhancing algorithms.

Using I-125 Seeds for Localisation; a Retrospective Overview of Radiation Safety Issues

Linda Janssen-Pinkse

Antoni van Leeuwenhoek, Amsterdam, The Netherlands

Abstract. Radioactive seed localisation (with a I-125 seed) is a method where the seed is preoperatively implanted in the centre of the lesion (tumour or lymph node) and during the operation the gamma-probe guides the local excision. With this procedure the risk factor of incomplete resection of the tumour or lymph node can be reduced. In 2007 the first I-125 seed was implanted in a breast tumour and in 2010 the localisation of the lymph node was introduced. Halfway 2015 a total of 2254 I-125 seeds were implanted and removed. 279 out of the 2254 were used for localisation of the lymph node. A challenge arrived when starting to use the seeds for the lymph node. Because of the irradiation of the lymph node, caused by the placed I-125 seed, and therefore difficulty for proper pathology, the activity must be lower than 1,7 MBq. The standard activity of 13,7 MBq must decay in a storage facility and maintain their sterility by repacking the container with the I-125 seed. In some indications, simultaneous use of an I-125 seed and Tc-99m for sentinel node is necessary. A gamma-probe with a sensitivity and distinctive capacity is needed. After removing the seed from the tissue in the department of Pathology, the seeds are all collected in a shielded waste container. There is a very small chance the seed is damaged by the sharp knife used. Therefore precaution must be taken with handling of the seeds after removing of the tissue. The seeds can contain parts of human tissue and therefore must be sterilized. With every step in the multidisciplinary procedure there is a small chance the seed is not traceable any more. Therefore every step in the procedure with a risk of losing the seed a barrier is implemented, for example extra measurements, double checks and administration. In conclusion the procedure with the I-125 seed for localisation is a proven positive technique for patients. The radiation dose for personnel is low. Extra accuracy is necessary for optimising and changing within the procedure.

Activimeter Response Behaviour Analysis Related to Well Depth

Lilian Kuahara, Eduardo Corrêa, Maria da Penha Potiens

Nuclear Energy Research Institute - National Nuclear Energy Commission (IPEN/CNEN-SP), São Paulo, Brazil

Abstract. The activimeter, instrument used to radionuclide activity measure, consist primarily of a well type ionization chamber coupled to a special electronic device. Its response, after calibration, is shown in units of the activity quantity (Becquerel or Curie). It also has a special holder designed to accommodate all kinds of syringes and vials containing the radiopharmaceuticals. Many factors influence the response of an activimeter such as the volume of the sample, its position inside the activimeter well and the geometry of the vials. The idea of this study is to find the better position inside the well to get the best activity values, positioning the holder in different profundity, simulating a clinical procedure. The reference activimeter used was the Secondary Standard NPL-CRC radionuclide calibrator, traceable to the National Physical Laboratory (NPL), England, taking as reference the depth of 400 mm. Two other activimeters were tested: Capintec, CRC-15BT model with the depth of 170 mm and one CRC-25R model with depth of 257 mm. They all belong to the Instrument Calibration Laboratory of IPEN, São Paulo, Brazil. The measurements were made using three radioactive check sources: Co-57, Ba-133 and Cs-137. Sources readings were taken at various depths inside the ionization chamber well. The results shown maximum variation of 14.28% for Co-57, 11.27% to Ba-133 and 8.8% to Cs-137. All measurements were compared with those values found for the reference depth in each activimeter. The variation found show the necessity of include this kind of determination in all quality control programs that are applied to an activimeter used by a Nuclear Medicine Service

Digital Breast Tomosynthesis: Preliminary Results of Patient Radiation Dose Survey in a Brazilian Facility

Larissa Oliveira^a, Fernando Mecca^b, Simone Renha^a

^aRadiation Protection and Dosimetry (IRD/CNEN), Rio de Janeiro, Rio de Janeiro, Brazil

^bNational Cancer Institute (INCA), Rio de Janeiro, Rio de Janeiro, Brazil

Abstract. In Brazil, the National Cancer Institute estimated for 2016 the diagnostic of 57,960 new cases of breast cancer, resulting in approximately 14,400 deaths. After non-melanoma skin cancer, breast cancer is the most frequent among women. Although breast cancer is considered a relatively good prognosis cancer when diagnosed and treated timely, breast cancer mortality rates remain high in Brazil (14 deaths per 100,000 women in 2013). In the last years, many efforts have been made to promote earlier diagnostic including the implementation of new technologies such as Digital Breast Tomosynthesis (DBT). This technology enables acquiring images of a stationary compressed breast at multiple angle during a sort scan, reduce tissue superposition, projection complementary and false-positive exams. The objective of this work was to determine the patient radiation dose undergoing DBT procedures in a private facility in Rio de Janeiro. Averaged glandular doses (AGD) provided by a Hologic Selenia Dimensions system in a DBT mode were estimated from the incident air kerma (K_i) for exposure of patients using tabulated conversion coefficients. A RadCal dosimetric system, composed by a calibrated ionization chamber (model 10X-6M) and an electrometer (model 9015), was used for K_i measurements. The image quality was evaluated using the NORMI PAS (T42028) phantom. Patient data was collected from 600 mammograms of 150 women with COMBO modalities (2D + 3D). Patients ranged in age between 33 and 83 y with a mean age of 54 y, where screening mammography and symptomatic occur concurrently in this unit. The compressed breast thickness varied between 45 and 70 mm. The mean compression force was 82.3 ± 20.6 N, which is 31% lower than the value recommended by the European Protocol. For a compressed breast thickness of 45mm, the AGD average was 1.5 mGy (ranged 0.99 mGy - 2.38 mGy), 25% lower than the reference level established by the European Protocol. The minimum physics performance requirements of image quality were not complied. Although the AGD was under the European reference levels, the image quality did not comply with international recommendations. Optimization Programs and new actions should be implemented.

Measurement of Entrance Skin Dose for Pediatric Patients during Cardiac IVR

Lue Sun^a, Yusuke Mizuno^b, Takashi Moritake^a

^aInstitute of Industrial Ecological Sciences, University of Occupational and Environmental Health, Japan, Kitakyushu, Fukuoka, Japan

^bDepartment of Anesthesiology, Yokohama City University, Yokohama, Kanagawa, Japan

Abstract. Children with complex congenital heart diseases often require repeated cardiac catheterization; however, children had higher risk of radiation-induced late effect, such as leukemia and solid cancers than adults. Therefore, radiation-induced carcinogenesis is an important consideration for children who undergo those procedures. We measured entrance skin doses (ESDs) using radio-photoluminescence dosimeter (RPLD) chips during cardiac catheterization for 15 pediatric patients with cardiac diseases. Three RPLD chips were placed on the patient's posterior chest, and one chip was placed on the patient's lateral chest. Correlations between maximum ESD and dose-area products (DAP), total number of frames, total fluoroscopic time, number of cine runs and cumulative dose at the interventional reference point (IRP) were analyzed. The maximum ESD (the largest ESD value recorded from the four RPLD chips put on the individual patient) was 80 ± 59 mGy. The maximum ESD closely correlated with both DAP ($r = 0.78$) and cumulative dose at the IRP ($r = 0.82$). The maximum ESD for coiling and ballooning tended to be higher than that for ablation, balloon atrial septostomy, and diagnostic procedures. In conclusion, we directly measured ESD using RPLD chips and found that maximum ESD could be estimated in real-time using angiographic parameters, such as DAP and cumulative dose at the IRP.

New Concept: Reduction of Dose of the Lens

Lue Sun^a, Yuji Matsumaru^b, Takashi Moritake^a

^aInstitute of Industrial Ecological Sciences, University of Occupational and Environmental Health, Japan, Kitakyushu, Fukuoka, Japan

^bDepartment of Endovascular Neurosurgery, Toranomon Hospital, Minato-ku, Tokyo, Japan

Abstract. Neurointerventional procedures provide a great benefit to a large number of patients, but they carry the risk of radiation-induced skin injury (RSI) or lens opacification. Generally, radiation exposure during therapeutic procedures is greater than that during diagnostic angiography; physicians should strive to reduce the radiation dose as large as reasonably achievable (ALARA). The International Commission on Radiological Protection (ICRP) reviewed recent epidemiological evidence and issued a statement on April 21, 2011. Based on this statement, the threshold dose to the lens is 0.5 Gy. Furthermore, for occupational exposure in planned exposure situations, the ICRP recommends an average annual equivalent dose limit of 20 mSv for the lens over a 5-year period with no single-year dose exceeding 50 mSv. In this study, we measured lens doses using radio-photoluminescence dosimeter (RPLD) chips during neurointerventional therapy for 30 patients. We found that lenses received a dose over 0.5 Gy in more than 20% of patients, and the dose received to the lens on the lateral X-ray tube side were higher than that on the contralateral side. Suggesting, X-rays from lateral projections, which directly enter the lens have highly contributed to the lens dose of patients. Thus, we have been developing a novel X-ray shielding device for reduction of the dose to the lens. The device equipped with 2 movable shielding plates is directly placed over the tube cover. Operator can control the position of the shielding plates by using a controller. Our experiments indicated that the device could reduce the lens dose by approximately 30% from the X-rays exposed from a posterior to anterior, and by 70% from the direct X-rays exposed from the lateral tube. In conclusion, this device could be useful for reducing the lens dose in neurointerventional procedures.

Development of a Specialization Program in Radiation Protection: Proposal to CPLP

Lidia V. Sá, Simone K. Renha

Institute of Radiation Protection and Dosimetry, Rio de Janeiro, RJ, Brazil

Abstract. Introduction: Educational programs have been developed by IAEA as part of the action plan for GSR – Part 3 implementation. Despite of these efforts, some Portuguese-speaking countries do not have achieved the minimum knowledge in Radiation Protection in medical field. A sustainable system can only be achieved setting an education program which provides qualified and well trained professionals. In health area, the undergraduate, graduate, postgrad and refresher courses to medical physicist, physician and technologist are insufficient or even non-existent. Objective: The proposal of this paper is to develop a radiation protection course in medicine to Portuguese-speaking countries. Material and Methods: A diagnosis of each country was carried out considering: demographic data, gross domestic product (GDP), health system level, academic indicators. Based on this information and international recommendations, a syllabus and training material was developed addressing: practical and theoretical course load, educational topics, approval criteria, outcome indicators and an effectiveness evaluation system. Results: The community comprises 9 countries, 78% are concentrated in African Continent; total population 270,195,000 and area 10,957,277km² (74% and 77% in Brazil respectively); GDP per capita from US\$ 510.4 (Guinea Bissau) up to 20,006 (Portugal), health system level I up to IV; education index from 0.294 (Guinea Equatorial) up to 0.727 (Portugal) demonstrating a wide diversity. The education program was development addressed specifically to physicians, medical physicists and technologist. It was also identified the necessity to create a technical group to translate document of mutual interest like as guidelines and technical documents. This training program will be proposed to the Community of Portuguese-speaking countries “Comunidade dos Países de Língua Portuguesa-CPLP”. Considering that this community has scientific agreements, there is an opportunity to disseminate the proposal program to the engaged countries. Conclusion: This material is an important tool to promote a better quality of health service to the population in developing countries. This education program can be a first action arising from workshop in Justification and Optimization in Medical Exposures held in Lisbon, last September. Also, it is an initiative to comply with the IAEA “Bohn call for action”.

Diagnostic Reference Levels in CT: First Experience in one Major Hospital in Algeria

Merad Ahmed^a, Khelassi-Toutaoui Nadia^a, Mansouri Boudjemaa^b

^aDépartement de physique médicale, Centre de Recherche Nucléaire d'Alger, Bd Frantz Fanon BP 399 Alger RP, Alger, Algeria

^bCentre Hospitalier Universitaire Lamine Debaghine, Boulevard Saïd Touati, Bab El Oued, Alger, Algeria

Abstract. CT is a powerful clinical tool for the diagnosis and management of patients. At the core of optimisation is the establishment of diagnostic reference levels (DRLs), first proposed by the International Commission on Radiation Protection (ICRP) in 1996. DRLs allow the identification of abnormally high dose levels by setting an upper threshold, which standard dose levels should not exceed when good practice is applied. Objective: To propose Local CT Diagnostic Reference Levels (LDRLs) by collecting radiation doses for the most commonly performed CT examinations in one site. Examination-specific DRLs for various patient groups can provide the stimulus for monitoring practice to promote improvements in patient protection. Such DRLs can be set not only at a national level (as investigation levels for unusually high typical doses), but also locally by each CT centre. Methods: In order to establish a national reference levels for CT in Algeria, a pilot study investigated the most frequent CT examinations at the National Centre on medical imaging located in the academic teaching hospital Bab-El-Oued. The survey includes the recording of CT parameters for each of 6 CT examinations. Dose data [CT volume index ($CTDI_{vol}$) and dose length product (DLP)] on a 30 average-sized patients in each category were recorded. The rounded 75th percentile was used to calculate a local DRL for the Centre. Results are compared with international DRL data. Results: Locals DRLs are proposed using $CTDI_{vol}$ (mGy) and DLP (mGy. cm) for CT head, thorax, abdomen, thorax-abdomen, abdomen-pelvis and thorax-abdomen-pelvis. Wide variations in mean doses are noted between CT scanners. These values are comparable to other international studies. Conclusion: The survey of dose estimates from CT highlights the substantial variations in practice in the same centre for similar types of examination and similar patient group. Such observations indicate the need for improvement through implementation of measures to keep all doses within acceptable ranges for the clinical purpose of each examination.

Occupational Radiation Exposure in Nuclear Medicine

Mashari Alnaaimi^a, Mohammed Alkhoryaf^b, Fareda Alkandri^a, Mousa Aldouij^a,
Mohamed Omer^a, Nawaf Abughaith^a, Talal Salhudeen^a

^aKuwait Cancer Control Center, Kuwait, Kuwait

^bDepartment of Physics, University of Surrey, Guildford, UK

Abstract. Objectives: To evaluate the occupational radiation exposure in Kuwait Cancer Control Center nuclear medicine department and to compare it to the dose limits of the International Commission of Radiological Protection (ICRP). Materials and Methods: The annual average effective whole-body dose Hp(10), extremities dose Hp(0.07), and eye lens dose Hp(3) received by the staff from 2011 till 2015 were measured. The Hp(10) was measured using the thermo luminescent dosimeters (TLD), Hp(0.07) for the extremities using rings TLD, and the Hp(3) using high-sensitive thermo-luminescence detectors MCP-N (LiF:Mg,Cu,P). Six categories of staff grouped as cyclotron staff, hot lab staff, physicians administering therapy dose, PET physicians, PET technologists, and PET nurses were included. The annual average doses were calculated for each group and comparisons were made between the groups and the years. A two-sided Mann-Whitney test was carried out, at the $p = 0.05$ level, to compare the means. The mean Hp(10), Hp(3) and Hp(0.07) were compared with the limits of the ICRP. Results: Cyclotron staff received the highest dose about 10 mSv whole body dose, 100 mSv extremities dose and 7 mSv eye lens dose. Hot lab staff received about 3 mSv, 1.5 mSv and 43 mSv for Hp(10), Hp(3) and Hp(0.07) respectively. Physicians responsible for administering therapeutic doses receive similar dose to hot lab staff. In addition, the technologist staff involved in performing PET studies received high dose to the eye. Interestingly, PET nurses received higher dose than technologists and physicians, as they are close to patients especially elderly and pediatric. The radiation dose was significantly reduced for PET physicians that are responsible for ^{18}F administration, by about 40% after 2012 due to the introduction and usage of the automatic PET injection system.

High Voltage Consideration to Determine the Dose Received by Patient in Conventional Radiology

Mbolatiana Anjaraso Luc Ralaivelo^a, **Andriambololona Raelina**^a, **Edmond Randrianarivony**^b, **Solofonirina Ravelomanantsoa**^b, **Hery Fanja Randriantseho**^a, **Ralainirina Dina Randriantsizafy**^a, **Tiana Harimalala Randriamora**^a, **Veroniaina Raharimboangy**^a, **Tahiry Razakarimanana**^a, **Hary Andrianarimanana Razafindramiandra**^a

^aInstitut National des Sciences et Techniques Nucléaires, Antananarivo, Madagascar

^bFaculté des Sciences, Université d'Antananarivo, Antananarivo, Madagascar

Abstract. The main step to optimize the delivered dose during an X-Ray diagnostic radiology is the establishment of the dose received by the patient. The dose optimization process is among the methods that improve the protection of patient against the secondary effect of ionizing radiations. A national project was carried out in Madagascar to evaluate the dose received by patient. The output of a batch of Radiology machines were measured for some regions of Madagascar with the parameters used for each type of examination (high voltage, distance, charge). Curves giving the exposition versus the high voltage were plotted and equations determined. Quality control program were performed to evaluate the accuracy of the high voltage for these machines and followed by the determination of the dose deviation.

Diagnostic Reference Levels for Fluoroscopically Guided Interventions at a Major Australian Hospital

Mohamed Badawy^{a,b}, Tegan Clark^a

^aAustin Health, Melbourne, Victoria, Australia

^bRoyal Melbourne Institute of Technology University, Melbourne, Victoria, Australia

Abstract. There has been an increase in the number of fluoroscopic guided interventions in the hospital setting as the technology has become more accessible. These interventions use ionising radiation to assist in the diagnosis or therapeutic outcomes for a patient. The amount of radiation given during the examinations are significantly greater than general X-rays and attention to radiation dose optimisation is required to decrease the risk of radiation induced injury. Establishing local and national diagnostic reference levels assists in dose optimisation. At a major teaching hospital in Victoria, Australia the patient radiation dose for multiple diagnostic and interventional procedures has been collected. The third quartile value for each procedure has been used to establish local diagnostic reference levels and presented. The values are used as an upper limit at the hospital with any procedures exceeding the DRL being investigated and used as a teaching tool to drive radiation dose optimisation. Since the establishment of the DRLs there has been a statistically significant difference between the average patient dose compared to previous years.

Image Quality and Patient Dose Assessment in Simple Radiographic Examinations in Ghana

Mary Boadu^a, Stephen Inkoom^b, Cyril Schandorf^c, Geoffrey Emi-Reynold^b, Emmanuel Akrobortu^b

^aRadiological and Medical Sciences Research Institute, Ghana Atomic Energy Commission, Kwabenya, Accra, Greater Accra, Ghana

^bRadiation Protection Institute, Ghana Atomic Energy Commission, Kwabenya, Accra, Greater Accra, Ghana

^cGraduate School of Nuclear and Allied Sciences, University of Ghana Atomic Campus, Kwabenya, Accra, Greater Accra, Ghana

Abstract. The quality of radiographic images in relation to patient doses have been carried out in some selected medical institutions in Ghana, through the implementation of the International Atomic Energy Agency's Technical Co-operation Project for the African Region on Strengthening Radiological Protection of the Patient and Medical Exposure Control, RAF/9/033. Ghana was among 13 other African countries that took part in the survey in which image quality and entrance surface air kerma (ESAK) to patients from simple radiographic examinations were conducted in order to establish a national Guidance Levels for medical exposure for their countries. Four medical institutions (total of 7 x-ray rooms) in Ghana were selected for the survey from which image qualities of simple radiographic examinations were determined using a standard procedure provided by IAEA. The survey showed that poor image quality of radiographic films could be as high as 23%. It was also observed from that majority of films with poor image qualities were due to over or under exposure factors and processing challenges. The survey has also shown significant variation in dose values for patients of similar sizes undergoing the same type of x-ray examinations. The ESAK variation ranged from a factor of 8 (chest PA) to 52 (abdomen AP). Thus, requiring the need to establish a national Guidance Levels for medical exposures.

Determination of attenuation properties of lead glasses used in the catheterization laboratory

Marcin Brodecki, Marek Zmyslony

Nofer Institute of Occupational Medicine, Lodz, Poland

Abstract. Since International Commission on Radiological Protection (ICRP) released its statement on the new threshold dose for eye lens opacities (0.5 Gy) and dose limit for the eye lens (20 mSv/year), radiological protection of sight organ has become an area of increased interest. In some medical applications, radiation doses to the lens of eye have the potential to exceed the dose limit. According to the literature, such a situation can occur to operators with high workloads, performing interventional cardiology and radiology procedures. The basic method of reducing the exposure in this case is the use of individual eye protective equipment with confirmed attenuation properties. This work presents a study performed to determine the attenuation equivalent for different types of commercially available lead glasses with a nominal lead equivalence of 0.75 mm. Measurements of lead equivalent were made following the adopted methods and measurement geometry given in recently updated standard IEC 61331-1:2014. The measurements were performed on an experimental system developed in the accredited dosimetry calibration laboratory over the range of X-ray tube voltages from 60 to 150 kV and aluminium and copper total filtration consistent with the clinical applications. To determine the lead equivalent of glasses, three different measurement conditions were used: narrow beam, broad beam and inverse broad beam. Results of the study demonstrate the effect of radiation energy and beam quality on the lead equivalent as well as a measurement geometry influence the final result. Comparison of attenuation properties for the new and previous edition of the standard was also shown.

Dose Reassessment Applied in Routine TL Dosimetry by using the PTTL method in LADIS Laboratory

Maciej Budzanowski, Renata Kopec, Anna Bieniarz-Sas

Institute of Nuclear Physics Polish Academy of Sciences, Krakow, malopolska, Poland

Abstract. Reassessment of doses in film and OSL dosimetry is well known and standard method in contrary to TL dosimetry. By using the phototransferred thermoluminescence (PTTL) method which consists of the first readout, UV exposure and second readout it is possible to reassess doses in TL dosimetry. This method was applied to reassess doses in whole body and ring dosimetry. Standard MTS-N (LiF: Mg,Ti) sintered detectors (4.5 mm diameter and 0.9 mm thickness for whole body dosimeters and 0.7 mm thickness for ring dosimeters) have been applied. Some of them were used in routine control for 12 years long. The TL detectors were read in automatic RE2000 (Rados Oy, Finland) readers. After readout the PTTL method was applied. Detectors were subjected to UV radiation (254 nm length) and read once again. The PTTL method was applied to dose reassessment in individual and ring dosimetry. Due to checking behaviour of different detectors from different batches and different dose history it is possible to observe influence of residual dose to the PTTL effect. The reassessed doses are observed to be linear over the dose range 5-100 mSv in individual and 5-500 mSv in ring dosimetry. The dose reassessment method based on PTTL phenomenon elaborated in LADIS Laboratory was applied to MTS-N detectors used in individual and ring dosimeters. Due to applying this method it is possible to reassess dose and check the measurement correctness. It is especially required in case when the dose exceeded the annual dose limit.

Occupational Doses of Medical Staff in Interventional Cardiology Procedures and Correlations with Patient Dose Levels

Maciej Budzanowski, Agnieszka Szumska, Renata Kopec

Institute of Nuclear Physics Polish Academy of Sciences, Krakow, malopolska, Poland

Abstract. Introduction: Radiation exposure in interventional cardiology procedures has recently been the subject of numerous studies. Because of the introduction of new techniques and equipment and the ever-increasing use of radiation ionizing in medicine, it is important to continue to assess the doses resulting from medical exposure to radiation. Also the attention devoted in recent years to eye lens dose assessment was increased due to evidence that cataracts can be induced by ionizing radiation at dose levels lower than previously expected. Because of the potential for doses received by interventional radiology personnel to be high, it is important that they are monitored properly and the dose to the eye lens should be evaluated more carefully. Material and methods: Data obtained during 60 Interventional coronary angiography (CA) and percutaneous coronary intervention (PCI) were collected and investigated. Patient kerma– area product PKA, cumulative kerma in the air KIRP for patient were recorded. To measure personal doses for medical staff were used whole body personal dosimeters for the personal dose equivalent quantities Hp(10) worn on the trunk, ring dosimeters worn on finger to measure the quantity Hp(0.07) and specially dedicated dosimeters EYE-D™ for the dose quantity Hp(3) are used. Correlations between patient doses and staff doses, between eye lens doses Hp(3) and other personal doses were investigated. Results: The measured occupational and patient's doses varied considerably among procedure. In general, within the medical team, operators always received the highest doses, followed by nurses and technicians. No meaningful correlation could be established between occupational doses and patient exposure, however some degree of correlation was observed between values of dose to the eye lens and whole body dose. Annual eye lens doses received by the operators in 8% cases were above recently recommended annual dose limit of 20 mSv. Conclusions: Results indicate the necessity of radiation protection measures in interventional cardiology and demonstrate that only monitoring of the eyes with specific dosimeters for yearly follow-up can provide the accurate doses.

Out-of-field Dose and Risk of Radiogenic Second Cancer for children Treated with Craniospinal 3D-Conformal RadioTherapy or TomoTherapy

Marijke De Saint-Hubert^a, Željka Knežević^b, Natalia Adamek^c, Marija Majer^b, Liliana Stolarczyk^c, Remy Savelli^a, Vedran Rajevac^c, Saveta Miljanić^b, Pawel Olko^c, Roger M. Harrison^d, Filip Vanhavere^a, Dirk Verellen^f, Lara Struelens^a

^aThe Belgian Nuclear Research Centre SCK-CEN, Mol, Belgium

^bRuder Boškovi Institute, Zagreb, Croatia

^cHenryk Niewodniczański Institute of Nuclear Physics (IFJ-PAN), Krakow, Poland

^dUniversity of Newcastle, Newcastle, UK

^eUniversity Hospital for Tumours, Zagreb, Croatia

^fUniversitair Ziekenhuis Brussel, Brussel, Belgium

Abstract. Children undergoing craniospinal irradiations (CSI) are at risk of developing side effects such as radiogenic second cancer. We measured and modelled out-of-field doses to assess this risk comparing 3D Conformal RadioTherapy (3D-CRT) and tomotherapy (TT). For both treatment approaches, standard clinical planning aims were used with no special constraints to out-of-field organs. For TT we also assessed the absorbed dose of on-board imaging (OBI). The 5 year anthropomorphic phantom (CIRS) was filled with both thermoluminescent detectors (TLD), MCP-N, and optically stimulated luminescent (OSL) detectors, Luxels, to estimate out-of-field doses in 28 organs. Besides, our experimental data were used to validate doses from the treatment planning systems (TPS) and from analytical modelling, by fitting the dose in each measurement point towards the 50 % isodose distance [Taddei, et al 2014]. Finally, dose risk models based on Biological Effects of Ionization Radiation VII (BEIR VII) report were used to estimate second cancer risk in 7 to 9 organs for boys and girls, respectively. With standard optimization constraints, the 3D-CRT results in higher doses to a limited number of organs while TT spreads the dose over more organs. For example the eye dose is 5 times higher for 3D-CRT compared to TT and thus the chance of inducing cataract is also larger. Applying BEIR VII models, the risk for thyroid cancer following 3D-CRT is 2 times higher compared to TT while TT induces 7 times more lung cancer when compared to 3D-CRT. For girls the chance of developing breast cancer over their lifetime is 5 times higher with TT than 3D-CRT. For TT, 20 sessions of OBI, result in cumulative organ doses ranging between 6 mGy for adrenals and around 430 mGy for thyroid and C-spine. The TT-TPS shows small deviation (4 %) from measurements while the analytical modelling deviates largely (49 %) from measurements reaching overestimations, up to a factor 8, for organs receiving low doses. To conclude 3D-CRT results in higher doses to fewer organs such as the eyes and thyroid while the chance of lung and breast cancer is higher for TT. The TPS, of the studied TT, can be used to assess the out-of-field dose while analytical modelling needs to be optimized mainly for low doses.

Evaluation of Thyroid Function after Radiotherapy for Patients with Breast Cancer

Masomeh Dorri Gav^a, Seyed Mahmood Reza Aghamiri^a, Mohammd Hossien Bahreini Toosi^b

^aRadiology and Radiotherapy department, school of paramedical, Shahid Beheshti University of Medical Science, Tehran, Iran, Tehran, Iran

^bMedical Physics Research Center, Faculty of Medicine, Mashhad University of Medical Sciences, Mashhad, Iran, Mashhad, Iran, Iran

Abstract. Background: The researches have widely been conducted into thyroid hormones level following radiotherapy for breast cancer. Consequently, in this study, we evaluated to relate rate of thyroid hormones level with the dose distribution within the breast cancer. Methods and Materials: Thirty patients were treated with 4-field breast cancer radiotherapy. The dose volume histograms the volume percentages of the thyroid absorbing respectively 20, 30, 40 and 50 Gy were then estimated (V20, V30, V40 and V50) together with the individual average thyroid dose over the whole gland that they were derived from their computed tomography-based treatment plans. Then, in the serum samples triiodothyronine [T3], thyroxine [T4], thyroid-stimulating hormone [TSH] of the patients were measured before and after radiotherapy. Results: There were no significant different in thyroid hormones level before and after radiotherapy for Patients with Breast Cancer (P- value >.05). Conclusions: On the balance, we understood that thyroid stimulating hormones level did not change before and after cancer breast radiotherapy.

KEYWORDS: *thyroid; breast cancer; radiotherapy.*

Preliminary Diagnostic References Levels of Audit CT at Aristide LeDantec National Hospital

Magatte Diagne, Fama Gning, Mamadou Moustapha Dieng, Latifatou Gueye

Hospital Aristide LeDantec, Dakar, Senegal

Abstract. Computed tomography (CT) scanner under operating conditions has become a major source of human exposure to diagnostic X-rays. The dose associated with CT exams is a worrying problem now a day, since this technique is the main contributor to population exposure to ionizing radiation with medical exposure. The establishing of diagnostic reference levels (DRLs) is a way to optimize the radiation arising from CT procedures to as low as reasonable (ALARA) without compromising the diagnostic quality and to ensure good practice. In this context, weighted CT dose index ($CTDI_w$), volumetric CT dose index ($CTDI_v$), and dose length product (DLP) are important parameters to assess procedures in CT imaging as surrogate dose quantities for patient dose optimization. **OBJECTIVE:** The purpose of this study is to establish Local Diagnostic Reference Levels (LDRLs) at the University Hospital of Aristide LeDantec for CT examinations and to compare these values with the international Diagnostic Reference Levels (DRLs) to benchmark the local practice. **MATERIALS/METHODS:** Data pertaining to patient and machine details were collected for 700 CT scan examinations performed on adult patients for head, chest, abdomen, pelvis, Chest Abdomen Pelvis, Abdomen pelvis and lumbar. The values of $CTDI_w$, $CTDI_v$ and DLP were calculated using ImPACT (Imaging Performance and Assessment of Computed Tomography) software for Siemens Definition AS scanner of HALD. This was done by correlating the measurements from the National Radiological Protection Board (NRPB-R250) scanners with the effective dose calculated, using the CT-EXPO software. Data was analyzed using mean, range, 3rd quartile, as well as mean. Frequency tables and histograms were used to summarize the data. **RESULTS:**

The 3rd quartile doses in this study were 48 mGy and 820 mGy.cm for head, 10 mGy and 370 mGy.cm for chest, 17 mGy and 765 mGy.cm for abdomen, 9,5 mGy and 255 mGy.cm for pelvis, 21 mGy and 1005 mGy.cm for Chest Abdomen Pelvis, 18 mGy and 792 mGy.cm for Abdomen pelvis and 18,5 mGy and 405 mGy.cm for lumbar. These values are well below European Commission Dose Reference Level (EC DRL). The present study is the first of its kind to determine the DRL for scanners operating in Dakar region. Similar studies in other regions of Senegal are necessary in order to establish a National Dose Reference Level.

KEYWORDS: *computed tomography; diagnostic reference levels; $CTDI_w$; $CTDI_v$; dose length product.*

Frequency of Overscan in Standard CT Protocols

Michael Galea^a, Mohamed Badawy^{a,b}

^aAustin Health, Melbourne, Victoria, Australia

^bRoyal Melbourne Institute of Technology, Melbourne, Victoria, Australia

Abstract. The increased number of CT studies has seen a push for radiation dose optimisation. Controlling the scan length of each study is a simple way of reducing the radiation dose significantly. A recent study shows that an extra 1 mSv could be imparted on the patient with only 6 cm of overscan. This study aims to assess that if increasing the awareness surrounding this topic will result in a reduction in both the frequency and magnitude of overscan and consequently patient radiation dose. Data was collected of the average overscan over a one-month period. Awareness was increased through teaching and data was collected in the subsequent month. The average overscan in standard protocols was calculated in pre and post awareness month. The frequency of overscan was also calculated. Results show that in the month previous to raising awareness there was a significant number of cases overscanned. This number reduced in the month following raising awareness. Furthermore, the average dose length product in the subsequent month was reduced. This study shows that raising awareness regarding strict adherence to protocolled scan length will see a significant reduction in patient radiation dose.

Overview of the Activities on Eye Lens Dosimetry within EURADOS WG 12 (Dosimetry in medical imaging)

Merce Ginjaume, Isabelle Clairand, Eleftheria Carinou, Olivera Ciraj Bjelac, Paolo Ferrari, Marta Sans-Merce, Jad Farah, Frank Becker, Vadim Chumak, Josiane Daures, Joanna Domienik, Zoran Jovanovic, Renata Kopec, Dragana Krstic, Agnieszka Szumska, Denisa Nikodemova, Pedro Teles, Sara Principi, Filip Vanhavere, Zeljka Knežević

European Radiation Dosimetry Group (EURADOS), Munich, Germany

Abstract. EURADOS is a scientific community for the promotion and co-ordination of research activities in the various fields of dosimetry. EURADOS Working Group 12 (WG12) is specialized in the field of dosimetry in medical imaging, including staff and patient dosimetry. There is an increased interest amongst the scientific community in eye lens dosimetry for occupationally exposed medical workers due to the new dose limits (ICRP 118). In spite of the new developments for eye lens dose monitoring, there are still many open questions and topics which need to be addressed. For this reason, in 2013, a sub-group of 22 scientists, from 12 countries in Europe, was formed within WG12 to participate in the following SG tasks: A literature review on eye lens dose data and on available procedures for estimate or measuring eye lens doses (2015); The distribution of a questionnaire to European hospitals to collect feedback about the current status of eye lens monitoring in hospitals (2014); The organization of an intercomparison within European individual monitoring services (IMS) which provide eye lens monitoring (2014-2015); Collection of data on eye lens doses in interventional radiology and cardiology (2014-2015); Study of the efficiency of protection means (goggles and shields), including experimental and Monte Carlo results (2014-2015); The correct and systematic use of protection means is essential for high work-load personnel. Furthermore, the appropriate use of operational quantities for eye lens monitoring is underlined. Finally the satisfactory performance level of IMS in eye lens monitoring is one of the essential results that came up from the intercomparison exercise. Main results of the tasks will be presented and discussed.

Imaging for Saving Kids - Improving Radiation Safety in Paediatric Radiology

Donald Frush^a, Lawrence Lau^b, Maria del Rosario Perez^c, Michael G Kawooya^a

^aAfrican Society of Radiology, AFROSAFE, Kampala, Uganda

^bInternational Society of Radiology, Melbourne, Australia

^cWorld Health Organization, Geneva, Switzerland

Abstract. The use of ionizing radiation procedures for children has rapidly increased globally during the past 20 years. This increase includes computed tomography (CT), a valuable tool for assessing paediatric illness and injury, as well as paediatric image-guided procedures, which may replace more risky surgical options. However, these procedures use relatively high radiation doses, and consequentially increased scrutiny, including public. To this end, this paper reviews the current challenges and opportunities to improve radiation protection (RP) in paediatric radiology, building upon the conclusions of the side event “Imaging for Saving Kids – the Inside Story about Patient Safety in Paediatric Radiology” (68th World Health Assembly, May 2015). This event gathered imaging experts, health authorities, policymakers, health care providers, professional societies, equipment manufacturers, and patient advocates to discuss quality and safety for medical imaging in children. The pivotal role of medical imaging is often juxtaposed with children’s relative increased susceptibility to radiation, including the potential for cancer from low-level exposures, necessitating policies and guidelines that place benefits and risks in an appropriate perspective. While individual radiation risks are at most quite small, RP in paediatric imaging is a public health issue due to the large population exposed and public concern. Appropriateness (justification) of procedures and optimization of protection provide opportunities for dose reduction while maintaining diagnostic benefit. Radiation safety culture (RSC) is a pillar of RP. Radiation risk communication has a key role to inform the appropriate risk-benefit dialogue between health professionals as well as with the children, their families and carers. IRPA14 will provide an exceptional opportunity to strengthen global, regional and national partnerships to improve RSC in paediatric health.

Evaluation of Survived Neuronal Tissue Area around Brain Tumor Lesions Post Radiation Therapy by Diffusion-weighted Imaging (DWI)

Mohammad Hossein Jamshidi^a, Alireza Eftekhari Moqadam^b, Jafar Fatahi^a, Hamid Behrozi^c, Yavar Shahvali^d, Jalal Ordoni^e, Yazdan Salimi^f, Dariush Askari^e, Hamed Deghani^g

^aDepartment of Medical physics, Faculty of Medicine, Jundishapur University of Medical Sciences, Ahvaz, Iran

^bDepartment of Anatomy, Faculty of Medicine, Jundishapur University of Medical Sciences, Ahvaz, Iran

^cDepartment of Radiologic Technology, Faculty of Paramedicine, Jundishapur University of Medical Sciences, Ahvaz, Iran

^dJundishapur University of Medical Sciences, Ahvaz, Iran

^eDepartment of Radiology, Faculty Paramedical Sciences, Shahid Beheshti University of Medical Sciences, Tehran, Iran

^fDepartment of Physics & Medical Engineerings, Faculty of Medicine, Shahid Beheshti University of Medical Sciences, Tehran, Iran

^gDepartment of Biomedical Engineering and Physics, Faculty of Medicine, Tehran, Iran

Abstract. Introduction: The differentiation of progressive or recurrent brain tumor from radiation injury after radiation therapy (LINAC 18 MEV) is difficult using conventional MR imaging (MRI). Accurate diagnosis of tumor recurrent or radiation injury is critical to determining therapy. A surrogate marker for treatment response that can be observed earlier than comparison of sequential magnetic resonance imaging (MRI) scans, which depends on relatively slow changes in tumor volume, may improve survival of brain tumor patients by providing more time for secondary therapeutic interventions. Diffusion-Weighted imaging (DWI), which has made it possible to obtain measurements of apparent diffusion coefficient (ADC), may be useful in differentiation of tumor recurrence within irradiated lesions and radiation necrosis. Our aims were to evaluate the DWI in the characterization of newly developed enhancing lesions within irradiated regions after the treatment of brain tumor. Methods: In 27 patients with glioma tumors, diffusion-weighted imaging within 1 week before and 1 week after radiation therapy was performed. The normalized ADC (nADC) was measured. The nADCs in the tumor and peritumoral region before radiation therapy were compared with those after radiation therapy and the change in tumor nADC compared with the change in tumor size. Results: The response to radiation therapy could be differentiated by using mean ADC values and ADC ratios. ADC ratios in the recurrence group showed significantly lower values (mean \pm SD, 1.41 \pm 0.12) than those of the nonrecurrence group (1.80 \pm 0.06, P< .001). Mean ADCs of the recurrent tumors (mean \pm SD, 1.28 \pm 0.11 \times 10⁻³ mm/s²) were significantly lower than those of the nonrecurrence group (1.43 \pm 0.16 \times 10⁻³ mm/s², P< .006). Conclusion: Assessment of ADC ratios of enhancing regions in the follow-up of treated gliomas is useful in differentiating radiation effects from tumor recurrence or progression. These results suggest that diffusion MRI will provide an early surrogate marker for quantification of treatment response in patients with brain glioma tumors.

Surveying the Relationship between Brain CT Scan Findings in Children with a Clinical Signs and Determining the Appropriate Indications for Requesting CT Scan

Mohammad Hossein Jamshidi^a, Hamid Behrozi^b, Dariush Askari^c, Jalal Ordoni^c, Yazdan Salimi^d, Hamed Dehghani^e

^aDepartment of Medical Physics, Faculty of Medicine, Jundishapur University of Medical Sciences, Ahvaz, Iran

^bDepartment of Radiologic Technology, Faculty of Paramedicine, Jundishapur University of Medical Sciences, Ahvaz, Iran

^cDepartment of Radiology, Faculty Paramedical Sciences, Shahid Beheshti University of Medical Sciences, Tehran, Iran

^dDepartment of Physics & Medical Engineerings, Faculty of Medicine, Shahid Beheshti University of Medical Sciences, Tehran, Iran

^eDepartment of Biomedical Engineering and Physics, Faculty of Medicine, Tehran, Iran

Abstract. Introduction: CT scan is a noninvasive procedure and diagnosis of many neurological disorders and injuries caused by trauma makes it easier and more accurate. Diseases and brain disorders with symptoms such as seizures, headache, loss of consciousness occurs. To review and determine the precise underlying causes that have led to these signs can paraclinic equipment used in these CT scan can be useful. CT scan in cases where the result does not help much with the diagnosis, causes unnecessary radiation received by the patient. Therefore, this study aimed to evaluate the applicability of the results of CT scans of children with clinical signs and symptoms in the CT scan was performed as a reliable indication for CT requests Child and the unnecessary exposure prevention in this age group. Methods: In this prospective study, 173 children under 4 years of age (98 male and 75 female with a mean age of 45.2 ± 3.9 months) between September 2014 and March 2014 were included. Physical examination and clinical symptoms, as well as CT findings and patients' outcome were evaluated. Results: CT brain scans of 173 children were evaluated. In 73% of cases were normal. The most common abnormalities included brain atrophy (19%) and intracranial hemorrhage (17%) and the most common cause of CT requests seizures (31%) and developmental delay (22%), respectively. CT scan of the brain in 8.23 % of cases of meningitis, 15% of patients with epilepsy and in 47% of patients with a final diagnosis of brain structural abnormalities, abnormal was reported. CT in meningitis without loss of consciousness does not help and MRI of the brain structural abnormalities in neurodevelopmental delay are more useful. Conclusion: In children under 4 years old with headache and meningitis without loss of consciousness, most CT scans are unnecessary. Considering clinical symptoms as predictors of abnormal CT scans we can reduce unnecessary ones.

Radiation Emergency Medicine Preparedness: Web-Based Reporting of News and Events from SREMC to Target Expert Groups

Marita Lagergren Lindberg^{a,c}, Karin Lindberg^{a,b}, Rolf Lewensohn^{b,c}, Giuseppe V Masucci^{b,c}, Jack Valentin^{a,c}, Leif Stenke^{a,c}

^aSwedish Radiation Emergency Medicine Centre (SREMC), Stockholm, Sweden

^bDept. of Oncology and Pathology, Karolinska Institutet, Stockholm, Sweden, ³National Board of Health and Welfare, Stockholm, Sweden

Abstract. In connection with radiological and nuclear (RN) emergencies there is a strong demand for well-founded medical information and advice to health care providers, as well as to the general public and media. This has again been highlighted in the aftermath of the Fukushima accident. Medical personnel, with special knowledge on clinical aspects of inadvertent exposure to ionizing radiation, are expected to provide advice, despite often scarce data and limited previous experience on unique emergency scenarios. The Swedish Radiation Emergency Medicine Center (SREMC) constitutes a group of trained and clinically active physicians (specialized mainly in hematology and oncology) with focused interest and expertise on the medical management of exposed individuals in the context of an RN event. The center, which is a recognized liaison WHO-REMPAN center, is under supervision of the Swedish National Board of Health and Welfare and has its academic affiliation with the medical university at Karolinska Institutet. An important task is to provide the Swedish RN- preparedness network and health care sector timely medical assessments and advice in connection to RN emergencies. The project: With the aim to expand the RN medical information provided by the SREMC, a project that assesses events relevant for radiation emergency preparedness was recently launched. A web site was initiated, aiming at providing news on radiation emergency medicine to RN preparedness networks. The ambition includes scanning of international novel scientific publications and reports on ionizing radiation and RN events and to provide readers with summaries of and comments to selected articles. The site, <http://sremc-kcrn.org/>, is directed primarily towards Swedish-speaking health care workers and experts (physicians, hospital physicists, etc), as well as governmental and other organizations involved in RN- preparedness, but is also accessible to the general public. News items on the site are mainly published in Swedish, but non-Swedish visitors may still find the website's resource links page useful, since these links generally refer to items in English. The website is managed by a group of medical and radiation physics experts, forming an editorial board, linked to the SREMC. The site is updated at monthly intervals to assure a high level of readability and topical importance. Our poster will present additional information on this website.

Evaluation of Organ Doses and Cancer Risk from Paediatric Head CT Examination – Phantom Study

Marija Majer^a, Zeljka Knezevic^a, Saveta Miljanic^a, Liu Haikuan^b, Weihai Zhuo^b

^aRudjer Boskovic Institute, Zagreb, Croatia

^bFudan University, Shanghai, China

Abstract. In addition to growing use of computed tomography (CT) for children and increasing awareness of radiation risk, interest for CT doses has increased in order to assess life-time cancer risk and also to compare and optimise CT technologies and scan protocols. In this study antropomorphic phantoms representing 5 and 10 year old child were exposed to the protocol for head CT examination. Organ doses were measured with radiophotoluminescence (RPL) detectors placed in the 28 organs and results were compared with MC calculations. Measurements were done at multi-slice CT simulator. Measured organ doses were compared with the doses measured during gamma knife (GK) treatment. Radiation risks of cancer incidence for three organs (thyroid, lung, and breast) in the form of the lifetime attributable risk (LAR) were estimated using BEIR VII model. Measured doses for organs within the scan volume were comparable for both phantoms and decreased with distance from the scan volume. Doses were on average 3.9 times higher for 5 year old phantom. Highest dose was measured for 5 year old phantom: 27.6 ± 0.2 mGy and 27 ± 1 mGy for eyes and thyroid respectively. Preliminary results of risk calculations showed that the highest risks were estimated for girls (115 and 31 thyroid cancers per 10^5 5y and 10 year old patients respectively). The highest organ risk in the case of boys was also for thyroid (21 cancers per 10^5 5 year old patients). Compared with measured doses during GK treatment, for thyroid CT dose was 6% of the GK dose for 5 year and 3% for 10 year old phantom respectively.

Radiation Protection Optimization in I-131 Therapy of Thyroid Cancer to Ablate Postthyroidectomy Remnants or Destroy Residual or Recurrent Tumour

Mario Medvedec

University Hospital Centre Zagreb, Zagreb, Croatia

Abstract. Radioiodine therapy (RIT) with I-131 has been commonly applied in case of thyroid (THY) diseases since 1940s, among which thyroid cancer (TC) is currently one with the increasing incidence and within the top fifteen primary sites in Croatia. Since there are several issues requiring further clarification, the purpose of this work was to try to optimize RIT for TC, as based on the results of comprehensive in-vivo dosimetric quantification. In 49 patients after total thyroidectomy for differentiated TC (group A) 87 ± 34 and 2582 ± 926 MBq I-131 were given for diagnostic (DG) and therapeutic (TH) purpose, respectively, and solely 900 ± 15 MBq of therapeutic I-131 in 220 patients (group B). Different serial measurements were performed in group A during the first week after each I-131 administration to determine absorbed doses (D) and dose rates (DR). Biokinetics of DG- and TH-activity of I-131 in THY remnant were different, but correlated, The ratio of normalized TH- vs. DG- cumulative activity in THY remnant per MBq was significantly lower than the ratio of applied TH- vs. DG- activity, showing non-linear effect of THY 'stunning' for $DR_{DG,THY} > 0.1$ Gy/h and $DD_{DG,THY} > 10$ Gy ($p < 0.05$). Small volumes of ellipsoidal scintigraphic appearances of THY remnants were found to be quantifiable from two orthogonal images acquired by pinhole gamma camera, delineated by using variable gray-scale threshold, and corrected for limited spatial resolution if dimensions were less than 1.5 full width at half maximum. Whole-body residence time of diagnostic I-131 was 21 ± 11 h, whereas $D_{TH,1M}$ at 1 m from patients was 0.9 ± 0.2 μ Gy/MBq, so such patients could be released from the hospital less restrictively upon receipt of any TH-activity of I-131. A success-rate of RIT was 93% and 86% in group A and B, respectively, but it was higher in case of $DR_{TH,THY} > 1.6$ Gy/h and $D_{TH,THY} > 100$ Gy ($p < 0.05$) if achieved simultaneously, instead of commonly recommended 3 Gy/h or 300 Gy, respectively. Furthermore, a necessity and common way of preparing patients for RIT by rising their thyrotropin levels was not dosimetrically justified. A high quality of life, radiation protection standards, benefit-cost ratio and success-rate of radioiodine therapy for thyroid was achieved by our new procedure and the lowest ever used activity of I-131.

Operational Radiation Safety with Y-90 Microspheres

Mark Miller, Charles Martin III

Cleveland Clinic, Cleveland, OH, USA

Abstract. Y-90 microspheres treatments are increasing in numbers in US medical centres. We will review practical operational radiation safety issues for treating patients with Y-90 microspheres. We will discuss microspheres in general from both vendors including a brief review of treatment planning and delivery. Package receipt, treatment team roles, room setup, equipment setup, and a walkthrough of treatment activities will be covered. Post treatment actions including residual dose assay, patient, personnel, and room surveys will be discussed. Finally waste handling methods and incidents as reported to regulatory authorities will be covered.

In-Vivo Tooth Dosimetry Using L Band EPR. The Research Involving Human Subjects Related to Fukushima Nuclear Power Plant Accident

Minoru Miyake^a, Ichiro Yamaguchi^b, Yasuhiro Nakai^a, Hiroshi Hirata^c, Naoki Kunugita^b, Harold Swartz^d

^aKagawa University, Kita-gun, Kagawa, Japan

^bNational Institute of Public Health, Wako, Saitama, Japan

^cHokkaido University, Sapporo, Japan

^dGeisel School of Medicine at Dartmouth, Hanover, NH, USA

Abstract. EPR tooth dosimetry using L-band (1.0-1.2GHz) has several desirable characteristics for screening and providing guidance such a triage following a mass-exposure incident because of instrumental developments of in vivo EPR has recently progressed. We carried out in vivo EPR tooth dosimetry asking volunteers who had experienced the nuclear power plant accident in Fukushima due to the Japan Great East Coast Earthquake 2011 to evaluate the willingness for acceptance of this method. All volunteers who were residents in Fukushima prefecture and had at least one complete healthy upper incisor. All residences where the volunteers lived are located at the distance of 40-80km from Fukushima Nuclear power plant. 1.2 GHz (L-band) spectrometer using an electromagnet which is originally developed by Dartmouth EPR Center. All measurements are performed using surface loop resonators that have been specifically designed for EPR measurements of the upper incisor teeth. The EPR signals from the upper incisor of volunteers were detected. These signals included not only RIS (Radiation Induced Signals) but also background signals and did not indicate any effects due to the Fukushima Power Plant Disaster. Volunteers felt little uncomfortableness and they accepted and appreciated this method partially due to the advantages of in vivo EPR tooth dosimetry such as quick sharing of measured data with each volunteer and invasiveness of test. The potential application of tooth EPR dosimetry may include estimating long-term risks/consequences of the residences after a radiation event such as the Fukushima Power Plant Disaster. We were able to successfully carry out in vivo EPR measurements from human upper incisors in volunteers from Fukushima. This study also demonstrated that the EPR tooth dosimeter is capable of being transportable to a distant site and successfully make estimates of radiation exposure.

Establishment of Local DRLs on Standard Radiographic Examinations and Estimation of Cancer Risk for Paediatric and Adult Patients at Two Tunisian Hospitals

Mohamed Mogaadi^{a,b}, Latifa Ben Omrane^a, Azza Hammou^a

^aNational Center of Radiation Protection, Tunis, Tunisia

^bSciences University of Bizerte, Bizerte, Tunisia

Abstract. Introduction: Nowadays conventional radiology represents one of the main sources of radiation exposure in medical field because is still remained as an important diagnostic tool. The establishing of Diagnostic Reference levels (DRLs) is a way to optimize radiation arising from standard radiographic examinations and to ensure good practice. And The effective dose is useful to estimate risk of carcinogenesis especially in paediatric patients. Objectives and Methodology: The aim of this study was to calculate local DRLs and to estimate the Effective doses associated with the most common standard radiographic examinations for the purpose of optimization. This was achieved by collecting patient and radiographic data for 281 for both paediatric and adult patients performing four X-rays examinations (Chest, Abdomen, Pelvis and Lumbar Spine). This data are collected at two Tunisian hospitals using two different technologies (screen-film (Regional's Hospital RH) and computed radiography (Children's Hospital CH)). The Entrance Surface Air Kerma (ESAK) was determined for each patient, using the measured X-ray tube output. Effective doses were calculated, for all the examinations by the PCXMC software. Results: The local DRLs across all paediatric age groups were 214-317 μGy (CH) and 85-162 μGy (RH) for chest AP examination; 985-2726 μGy (CH) for abdomen AP examination; and 905-1512 μGy (CH) and 136-169 (RH) μGy for pelvis AP examination. Effective dose estimates were 29-68 μSv (CH) and 15-29 μSv (RH), 304-334 μSv (CH), and 159-259 (CH) and 24-28 μSv (RH) for chest AP, abdomen AP and pelvis AP examinations, respectively. For adult patients (≥ 16 years), the data are collected only at RH, were the LDRLs proposed for chest, abdomen, pelvis, lumbar spine (LS) PA and lateral are, respectively, 0.28, 5.8, 3.7, 6.2 and 16.4 mGy. The median value of effective dose were calculated for all examinations 40, 994, 404, 478, 436 and 533 μSv for chest PA, abdomen AP, abdomen PA, pelvis AP, LS PA and LS Lateral, respectively. Conclusion: To use new technologies (computed or digital radiography) can avoid repetition of examination but allows the manipulator to give high dose to the patient, this was the case of CH where the doses are higher than RH and international values.

Audit of Clinical Image Quality in Chest Radiography using Visual Grading Analysis

Michael Sandborg, Jonas Nilsson Althen, Erik Tesselaar

Medical Radiation Physics, IMH, Linköping University, Linköping, Sweden

Abstract. Background: Clinical audit of image quality and patient dose is mandatory according to Swedish regulations and encouraged by the European Commission Medical Exposure Directive (EU 2013/59/Euratom). While data of patient exposure indicators, such as the air kerma-area product (PKA) are readily available from the Radiological Information System, measures of clinical image quality need to be compiled through careful evaluation of sets of clinical radiographs by a group of trained radiologists. Aim: The aim was to apply visual grading analysis to assess and compare the quality of two sets of chest posterior-anterior (PA) radiographs from two chest radiography systems. Method: Twenty radiographs were assessed by each of the twenty-four radiologists, ten for each imaging system. Ten adult patients (5 male), 35-75 years old, that were scheduled for chest radiography on two separate occasions on Siemens Vertex FD and Samsung GC85 imaging system, respectively were included. Radiologists with between 1-4 years of clinical experience evaluated each image using five different image criteria, including the visibility of vessels (retro-cardiac and in the pleural margin), hilar region, and carina. Radiologists were blinded with respect to the names of the imaging systems. A 5-point graded scale was used to indicate to what extent the criterion was considered to be fulfilled. For each case, the number of scores 1 to 5 was computed for each imaging system separately. By plotting the cumulative fractions of case with score = 5, score ≥ 4 , ≥ 3 , ≥ 2 and ≥ 1 , respectively for both imaging systems, and separately for each criterion, the area under the curve AVGC indicates whether any imaging system has superior performance with regards to that criterion. Results: The results showed that while the PKA was approximately 50% higher with the Samsung system, the image quality was significantly superior ($p < 0.05$) for all image criteria except the criterion regarding visibility of the hilar region. The fraction of score ≥ 4 (sure or probably sure that the criterion was fulfilled) was 74% for the Samsung and 60% for the Siemens system, respectively. The median reading time per image was < 1 minute or approximately 15 minutes in total per radiologist. The Samsung system shows superior image quality in the chest PA view, but also a 50% higher $PKA = 0.07 \pm 0.03$ $Gycm^2$. Conclusion: Visual grading analysis of image criteria is time-efficient and thereby a promising method for audits of clinical image quality and dose optimisation even in a busy radiology department.

Radiation Protection in Medical Imaging and Radiation Oncology: A Cooperative Effort between IOMP and IRPA

Magdalena Stoeva^a, Richard Vetter^b, K.Y. Cheung^c, Renate Czarwinski^d, Francesca McGowan^e

^aMedical University - Plovdiv, Plovdiv, Bulgaria

^bMayo Clinic, Rochester, MN, USA

^cInternational Organization of Medical Physics and Hong Kong Sanatorium & Hospital, Hong Kong, China

^dInternational Radiation Protection Association and German Federal Office of Radiation Protection, Berlin, Germany

^eCRC Press, Taylor & Francis Group, London, UK

Abstract. A radiation protection culture is important to enhance protection of patients, healthcare workers and the public. Hospitals, medical institutions, and national and international organizations are increasing their efforts to enhance radiation protection culture. Radiation safety and quality assurance departments in medical institutions aim to maximize benefits while reducing radiation risks. To improve protection of patients, workers and the public, a concerted effort is required by radiologists, nuclear medicine physicians, radiation oncologists, referring practitioners, physicists, technologists, professional organizations, international bodies and regulators. The International Organization for Medical Physics (IOMP) and the International Radiation Protection Association (IRPA) worked together to produce a book *Radiation Protection in Medical Imaging and Radiation Oncology*, intended for use in countries that have well developed medical and health physics disciplines and in developing countries. This book addresses professional, operational, and regulatory aspects of radiation protection covering virtually all regions of the world. Practical sections and professional discussions by leading medical physics and health physics professionals complement technical background information, which is organized into discreet chapters from basic protection to advanced imaging and treatment modalities. Contents acknowledge that medical physicists and health physicists are often challenged to maximize protection while minimizing the cost of resources necessary to keep radiation doses ALARA. A review chapter recognizes that advances in medical physics and health physics will continue to be based on evidence gathered through basic and applied research. Periodic review of the evidence will help medical health physicists focus on the issues and to advance the science. This book is a valuable source of information for the medical physicist, health physicist, and related specialties targeting a reading level of Master of Science and above.

Monte Carlo Calculation of Neutron Doses to Organs of a Female Undergoing A Pelvic 18 MV Irradiation

Mansour Zabihzadeh^{a,b}, Seyyed Rabi Mahdavi^c, Mohammad Reza Ay^d, Zahra Shakarami^a

^aDepartment of Medical Physics, School of Medicine, Ahvaz Jundishapur University of Medical Sciences, Ahvaz, Iran

^bDepartment of Radiotherapy and Radiation Oncology, Golestan Hospital, Ahvaz Jundishapur University of Medical Sciences, Ahvaz, Iran

^cDepartment of Medical Physics, School of Medicine, Iran University of Medical Sciences, Tehran, Iran

^dDepartment of Medical Physics and Biomedical Engineering, School of Medicine, Tehran University of Medical Sciences, Tehran, Iran

Abstract. Applying of high-energy photon beams beside all advantages obstructed by photoneutrons that may cause extra dose to the patient that has not been considered in routine radiotherapy. The purpose of this study is calculation of neutron and gamma doses to a female undergoing a pelvic 18 MV irradiation. A simplified Linac head model as a sphere with 10 cm radius of tungsten and with the total spectrum of an isotropic neutron distribution was located inside a typical bunker. The female anthropomorphic phantom was irradiated with equal weighted four-field pelvic box (18MV). MCNPX (2.4.0) code was used to calculate of absorbed doses. The greatest effective dose, 1.04 mSv Gy⁻¹, was calculated for the AP field while the lowest effective dose, 0.36 mSv Gy⁻¹, was obtained for the RL field. The Percent risk of fatal second malignancy of neutron contamination following a 70 Gy x-ray treatment dose (with equal weights for each field, 17.5 Gy) is 0.152 %, including 0.056 % for the AP field, 0.033 % for the PA field, 0.031 % for the RL field and 0.032 % for the LL field. If this dose delivered only with the AP field, the risk would be 0.224 %, which is 32 % higher than that is in case of 4-field irradiation. Our present analysis shows that this simplified model can be used to estimating of photoneutron doses.

Study of the Radiation Effect on the Biological Cellule DNA by Determination Bragg Peak Position of the Proton Beams

Noura Harakat^{a,b}, Jamal Inchaouh^a, Abdenbi Khouaja^a, Mohammed Benjelloun^b, Hamid Chakir^a, Said Boudhaim^a, Zouhair Housni^a, Mohamed Lhadi Bouhssa^a, Abdellatif Kartouni^a, Mohamed Reda Mesradi^c, Sara Stimade^a, Meriem Fiak^a, Mustapha Krim^a

^aHassan II University-Casablanca, Faculty of Sciences Ben M'Sik, Casablanca, Morocco

^bChouaib Doukkali University, Faculty of Sciences, El Jadida, Morocco

^cHassan I University, High Institute of Sciences and Health, Settat, Morocco

Abstract. In the last few years, much more interest has been devoted to study the interaction of charged particles with biological molecule. That will help us for deep understanding the physical and chemical stages of radiation actions on the matter. The proton collisions with the water molecules are already estimated around the Bragg peak region, taking into account ionization, excitation, charge-changing processes, and energetic secondary electron behaviour. The Bragg peak profile and position were determined by adopting a new approach involving discretization, incrementation, and dividing the target into layers. The thickness of each layer is selected randomly from a distribution weighted by the values of the total interaction cross section, from excitation up to ionization of the target, and the incident projectile charge exchange. In this work, we study, using the GEANT4 code, the influence of biological molecules during irradiation with proton, which is a major subject in irradiation science. By the knowledge of this phenomenon it will be very important to evaluate the contribution of the free radicals created from the biological molecules.

Internal dose assessment of new ^{177}Lu -radiopharmaceuticals and its role in radiation protection of patients

Nancy Puerta Yepes^a, Ana Rojo^a, Sebastián Gossio^a and José Luis Crudo^b

^aNuclear Regulatory Authority (ARN), Ciudad Autónoma de Buenos Aires (C1429BNP), República Argentina

^bNational Atomic Energy Commission (CNEA), Centro Atómico Ezeiza (B1802AYA), República Argentina

Abstract. This article reviews the internal dose assessment of new therapeutic radiopharmaceuticals, based on Lutetium-177 locally produced, made by the Internal Dosimetry Laboratory (LDI) of the Argentine Nuclear Regulatory Authority. Currently, the study of these radiopharmaceuticals has an increased interest thanks to their potential as an alternative treatment for various types of cancers. Since 2006, the Basic and Applied Radiopharmacy Division of National Atomic Energy Commission (CNEA) has been conducting studies on the production, labelling, quality control, and NIH mice biodistribution of several radiopharmaceuticals based on ^{177}Lu locally produced, which include: ^{177}Lu -EDTMP, ^{177}Lu -DOTMP, ^{177}Lu -DOTA-Substance P, ^{177}Lu -DOTA-Minigastrine and ^{177}Lu -DTPA-SCN-Rituximab. In order to contribute to ensuring the radiation protection of patients, the Internal Dosimetry Laboratory has been complementing the preclinical study of these new radiopharmaceuticals performing a dose assessment. The internal dose assessment of these radiopharmaceuticals included: the activity biodistribution analysis in NIH mice, the estimation of the absorbed dose in healthy organs of interest using MIRD methodology, the extrapolation of the results obtained in mice to humans, the identification of healthy organs with high risk and the estimation of the maximum activity that can be administered to a patient without exceeding the threshold of radiotoxicity in healthy organs. The dosimetric results discussed in this paper are the background needed to progress into the next stage of clinical trials with these radiopharmaceuticals. It can be observed that internal dosimetry assessment has an important role for ensuring radiation protection in patients, since treatment parameters can be optimized out of the estimation of the maximum activity to be administered to the patient. Better protection of healthy organs is thus achieved by avoiding exceeding the Maximum Tolerable Activity (MTA).

KEYWORDS: *internal dose assessment; ^{177}Lu ; new therapeutic radiopharmaceuticals.*

Radiation Protection Dosimetry (2017), Vol. 173, No. 1-3, pp. 192–197

doi:10.1093/rpd/ncw317

Design Shielding Assessment for a Nuclear Medicine Service

Osvaldo Brígido-Flores^a, José Hernández-García^b, Orlando Fabelo-Bonet^a, Adelmo Montalván-Estrada^a

^aEnvironmental Engineering Centre of Camagüey. Radiation Protection Unit, Camagüey, Cuba

^bOncological Hospital of Camagüey „Marie Curie”, Camagüey/Camagüey, Cuba

Abstract. It is recognised worldwide that the security of radioactive materials is very important and that the design of facilities where these sources are used and stored must cater for the implementation of good security measures, including the shielding of some treatment and diagnostic rooms. The radiation protection assessment of a nuclear medicine facility consists of the evaluation of the annual effective dose both to workers occupationally exposed and to members of the public. This assessment take into account the radionuclides involved, the facility features, the working procedures, the expected number of patients per year, the administered activity, the distribution of rooms, the thickness and physical materials of walls, floors and ceilings and so on. The assessment results were compared to the design requirements established by the Cuban regulatory body in order to determine whether or not, the nuclear medicine facility complies with those requirements, both for workers and for members of the public. The evaluation presented is useful for facility designer and for member of regulatory body.

Performance Study of Hybride Imaging SPECT/CT: Case of Nuclear Medicine Service - Ibn Sina Hospital in Rabat-Morocco

Oum Keltoum Hakam^a, Abdelmajid Choukri^a, Rajaa Sebihi^b, Youness Esserhir El Fassi^a

^aUniversity of Ibn Tofail, Kenitra, Morocco

^bNuclear Medicine, Hospital Ibn Sina, Rabat, Morocco

Abstract. The medical physicist in nuclear medicine department's mission is to ensure radiation safety of personnel and the patient by the establishment of a quality assurance program in the medical imaging service that aims quality control detection equipment such as gamma camera, the activity meters ..., and optimizing all diagnostic or therapeutic procedures. The arrival of the hybrid cameras Single Photon Emission Computed Tomography (SPECT) coupled to a scanner (CT), has greatly improved the scintigraphic imaging performance in terms of, firstly to improve the image by correcting attenuation of gamma photons into the tissue and, secondly of topographic precision. The introduction of the scanner in the scintigraphic detection system imposes severe radiation protection with a quality control implementation of the detection chain in order to ensure the quality of the scintigraphic image offered to the patient. Nuclear Medicine department Ibn Sina Rabat has established a quality assurance program in medical imaging with quality control protocols to ensure excellence in nuclear medicine. Moreover quality control can predict SPECT/CT failures and ensures both good quality images and radiation protection of the patient and staff. The objective of our work is to study the performance of the integration of SPECT and CT in a single imaging device. A set of tests were performed on a regular gamma camera coupled to the scanner to maintain it within the limits of the required quality. The main quality control SPECT / CT tests were performed: Uniformity test, Center Of Rotation COR test, the overall performance (SPECT) test, daily X-ray test, and finally X ray to Nuclear Medicine registration test. Our study was carried out to test the Center Of Rotation COR which has allowed correcting an abnormality in tomography rotations. Regularity tests will help prevent accidental shutdown that could generate repeat diagnostic and endangers the radiation protection of patients and staff.

Comprehensive quality audits in radiation oncology, diagnostic and interventional radiology

Ahmed Meghizifene, Ola Holmberg

International Atomic Energy Agency, Vienna, Austria

Abstract. As part of a comprehensive approach to quality assurance (QA) in the diagnosis and treatment of patients by radiation, an independent external audit (peer review) is important to ensure adequate quality of practice and delivery of imaging and treatment. Quality audits can be of various types and at various levels, either reviewing critical parts of the diagnosis or treatment process (partial audits) or assessing the whole process (comprehensive audits). The International Atomic Energy Agency (IAEA) has supported the implementation of comprehensive audits in radiation oncology and in X-ray diagnostic radiology for the past ten years. The support started with the publication of harmonized methodologies to be applied for comprehensive audits: Quality Assurance Team for Radiation Oncology (QUATRO) and Quality Assurance Audit for Diagnostic Radiology Improvement and Learning (QUAADRIL), were published in 2007 and 2011, respectively. The IAEA publications contain checklists that may be considered helpful audit tools to be used flexibly by auditors, depending on the local situation. They do not represent one radiology or radiation oncology standard applicable to all visited departments. The objective is to provide a general audit methodology that can be applied in a range of economic settings. The audit includes an assessment of the ability of an institution to maintain the imaging and radiation oncology technology at the level corresponding to the best clinical practice in the specific economic setting. In addition to the publication of guidelines on the implementation and reporting of comprehensive audits, the IAEA has initiated a number of train-the-auditors events and implementation of audits in the various regions with the support of the IAEA technical cooperation programme. Till the end of 2015, the IAEA has conducted QUATRO audits in 50 countries and QUAADRIL audits in 4 countries. The comprehensive audits should not be viewed as substitutes for regulatory inspections or investigations following a misadministration or accident in a radiotherapy or radiation oncology facility.

International Response to the Bonn Call for Action – from the Viewpoint of the Organizers of the Bonn Conference: the IAEA

Ola Holmberg

International Atomic Energy Agency, Vienna, Austria

Abstract. At the end of 2012, an international conference was organized to focus efforts in radiation protection in medicine for the next decade and to maximize the positive impact of future international work in this area. With the World Health Organization as co-sponsor, and the Government of Germany through the Federal Ministry for the Environment, Nature Conservation and Nuclear Safety as host, the International Atomic Energy Agency (IAEA) organized the International Conference on Radiation Protection in Medicine - Setting the Scene for the Next Decade. The conference was held in Bonn, 3-7 December 2012 and was attended by more than 500 participants and observers from 77 countries and 16 organizations. The conference resulted in Bonn Call for Action, a joint position statement between the IAEA and the WHO, which will continue to guide stakeholders over the next number of years on the efforts that are necessary to strengthen radiation protection in medicine. It is noted in the joint position statement that action by all stakeholders is encouraged, and a strong response to this call has been seen since it was issued in mid-2013. Several international organizations, professional bodies and other entities have aligned new actions, initiatives, position papers, policy statements and priorities with the Bonn Call for Action. Some of these actions will be referred to in the presentation, together with actions taken by the IAEA. The 11-15 December 2017, the next International Conference on Radiation Protection in Medicine will be organized in Vienna by the IAEA. Among the objectives of this conference, will be to look back at the implementation of Bonn Call for Action; review approach; harmonize activities, and look forward at new developments impacting radiation protection in medicine.

Assessment of the Practice of Optimizing Paediatric Doses in Conventional Radiography in Cameroon

Odette Ngano Samba^{a,b}, Jean Bernard Kamgang^b, Ariane Lynda Kengne Fonkam^a, Emmanuel Chi^a, Lukong Cornelius Fai^a, Jean Yomi^c

^aUniversity of Dschang, Dschang, West region, Cameroon

^bGeneral Hospital of Yaoundé, Yaoundé, Centre Region, Cameroon

^cUniversity of Yaoundé I, Yaoundé, Centre Region, Cameroon

^dInternational Centre for Theoretical Physics, Trieste, Italy

Abstract. This study focused on the evaluation through a questionnaire (including specificity on paediatric radiation protection) of the practices of 32 technicians in radiology working in government and private own health institutions and of 214 children between 0 and 14 years old (54% male and 46% female) who underwent Chest and abdomen conventional radiology examinations. Furthermore base on tube output of the unit and the exposure parameters used for each projection, Entrance Surface Dose (ESD) was calculated through the CALDose_X software while effective dose (E) was determined. All radiography devices are three phases machine with 2,5 inherent mm Al with and without additional filter. The Quality Assurance (QA) is not yet routinely implemented in these hospitals. The study found that for a total of 280 projections realizes there were 36 repeated (17%). 78% of paediatric X-rays examinations were performed with an anti-scatter grid and 73% without collimation of the X-ray beam while 75% of the technicians immobilise the children themselves or resort to the assistance of a relative to immobilise them. Mean, median, third quartiles and maximum to minimum ratio of ESDs are determined and variations were found in the technique used within each health institution and between the hospitals. The result showed ESD's values 1,5 to 3 times higher than the European Commission's (EC) Diagnostic Reference Levels (DRL) and the United Nations Scientific Committee on the Effects of Atomic Radiations (UNSCEAR 2000) for Chest X-rays. There is a need of QA implementation, of procurement and utilization of paediatric contentions and harmonization of the paediatric radiological techniques in radiological centres through continuous training that can be held during the annual seminars of radiographer and of radiologist. This study provides informations on practice in some paediatric radiology centre in Cameroon, paediatric 3rd quartile which future dose measurements may be evaluated and is also useful to the statutory authorities for the establishment of the National Diagnostic Reference Level (NDRL) for paediatric diagnostic radiology in Cameroon.

Can Standard CT be replaced by Contrast Enhanced Ultra-low-dose CT with Iterative Reconstruction for the Screening of Patients Admitted with Acute Abdominal Pain? A Comparative Study

Pierre-Alexandre Poletti, Minerva Becker, Thomas Perneger, Christoph D Becker, Alexandra Platon

University Hospital of Geneva, Dpt of Radiology, Geneva, Switzerland

Abstract. Purpose: to determine whether the dose of radiation delivered to patients undergoing a contrast-enhanced abdominal CT for acute abdominal pain can safely be reduced to that of an abdominal radiograph (<1.5 mSv), using a very low-dose CT protocol (LDCT) with iterative reconstruction algorithms. Material and Method: This study was approved by the IRB. 151 consecutive patients, in whom a standard contrast enhanced abdominal CT (CECT) was required for acute abdominal pain, were included. CECT series were immediately followed by an LDCT (30 mAs) while the contrast media was still in the venous compartment and reconstructed in LDCT-ASIR and LDCT-MBIR (VEO^R). LDCT-ASIR and LDCT-MBIR images were reviewed independently by 2 board certified radiologists, blinded to the results of CECT considered reference standard. Separate analyses were performed according to patients' BMI. Results: An abdominal condition was reported at CECT in 120 (79%) patients. In patients with a BMI<30, the accuracies at LDCT-ASIR and at LDCT-MBIR for rater 1 were 95% (104/109) and 99% (108/109) respectively for suggesting the correct diagnosis, when compared to CT results. They were 93% (103/109) and 100% (109/109) for rater 2 (p=0.029). In patients with BMI>30, the accuracies at LDCT-ASIR and LDCT-MBIR were 88% (37/42) and 90% (38/42) for rater 1. They were 79% (33/42) and 93% (39/42) for rater 2. Conclusion: Our data suggest that the dose of radiation delivered by CT to non-obese patients with acute abdominal pain can be safely reduced by using a LDCT-MBIR protocol. This cannot be achieved by LDCT-ASIR.

Radiological and Dosimetrical Aspects of CO₂ Peripheral DSA: Optimization of X-ray Spectrum

Pier Luca Rossi^a, David Bianchini^b, Alessandro Lombi^a, Giacomo Feliciani^b, Manami Zanzi^a, Romano Zannoli^b, Ivan Corazza^b

^aDept. of Physics and Astronomy - University of Bologna, Bologna, Italy

^bDept of Specialised, Experimental, and Diagnostic Medicine - University of Bologna, Bologna, Italy

Abstract. Peripheral digital subtraction angiography is a powerful instrument for the evaluation of vascular diseases, commonly using iodine as contrast medium to visualize vessels. However, an increasing number of patients presents high risk factors for the use of traditional iodinated contrast media, such as diabetes, renal diseases and allergies, reducing the possibilities to perform interventions. Carbon dioxide represents an interesting alternative, thanks to its lack of allergic reactions and renal toxicity. Along with a number of advantages, the usage of CO₂ gaseous contrast media entails a series of technical issues. In particular, because of its linear absorption coefficients, CO₂ provides a negative contrast than iodinated contrast media (almost 10 times lower): to compensate the lack of vessels visualization, image post-processing elaborations (such as stacking) are mandatory and higher doses than traditional DSA seems to be required. In this work we addressed the dosimetric aspects of CO₂ angiography, studying the influence of the parameters – so, the influence of the X-ray spectrum – on the image quality to dose ratio and proposing some optimizations to increase the signal-to-noise ratio. In particular, we decided to start analysing how different fluoroscopy equipment set their irradiation conditions when CO₂-DSA is performed. Due to the absorption characteristics, we expected that equipment with CO₂-specific protocols would modify parameters (not only in terms of kV and currents, but also in terms of frame rate and exposure times per frames) to increase the image contrast. Our results, however, show that the irradiation parameters were left completely unchanged between the traditional and CO₂ angiographic programs. This leads to think that these CO₂ protocols do not operate on the X-ray emission – as expected and requested to optimize image quality to dose ratio-, but at this time differ only on an image manipulation level.

Establishment of National Diagnostic Reference Levels for Nuclear Medicine in Australia

Paul Marks, Toby Beveridge, Peter Thomas, Anna Hayton, Anthony Wallace

Australian Radiation Protection And Nuclear Safety Agency, Melbourne, Victoria, Australia

Abstract. In 2011, the Australian Radiation Protection and Nuclear Safety Agency (ARPANSA) instigated a National Diagnostic Reference Level Service (NDRLS) to provide individual facilities with a tool for comparing their representative patient dose metrics with National Diagnostic Reference Levels (DRLs). The collated data from individual facilities is used to establish and maintain National DRLs for common diagnostic imaging procedures. The Service is available for Multi Detector Computed Tomography, diagnostic Nuclear Medicine, and Image-Guided Interventional Procedures (diagnostic and therapeutic). Future development has been planned for mammography and general radiography. Nuclear medicine “most common administered activities” surveys have been performed in the past. However, this one differed in a number of ways; firstly, it collected actual patient data rather than what was set out in the facilities protocols. This has been useful in providing an insight to what is really happening clinically across the nation. Secondly, information, such as DLPs and $CTDI_{vol}$, which relates to the computed tomography component of SPECT/CT and PET/CT procedures, has provided data about the overall aspect of the patient’s dosimetry. Australia has approximately 216 nuclear medicine facilities that operate both within the private and public sectors, and are regulated by individual States and Territories. Much of the preliminary work of the survey was centred on gaining access to these facilities, which resulted in being able to make personal contact with each in most cases. Facilities were required as part of the survey to record de-identified patient data, procedure information and the activities administered over a four-week period. Once facilities registered and provided their unique practice identifier, they were able access an Excel spreadsheet, which was then emailed back to ARPANSA on completion. All data collected was treated confidentially, and not shared in any identifiable manner with third parties. Upon submission, ARPANSA provided a report that allowed facilities to compare administered activities to current benchmarks. The survey was produced in conjunction with the relevant clinical bodies in Australia, these being the Australian and New Zealand Society of Nuclear Medicine and The Australasian Association of Nuclear Medicine Specialist.

Survey of Knowledge about Radiation Dose in Radiological Investigation in Kermanshah Hospitals, Iran

Rasool Azmoonfar^a, Hosein Faghirnavaz^b, Edalat Morovati^b, Hosein Younesi^b

^aMSc of Radiobiology & Radiation Protection, Radiology Department, School of Paramedical Sciences, Kermanshah University of Medical Sciences, Kermanshah, Iran

^bRadiology Department, School of Paramedical Sciences, Kermanshah University of Medical Sciences, Kermanshah, Iran

Abstract. Background: Although ionizing radiation is very important in diagnostic and treatment of many diseases but hazardous of this radiation considerable and irrefutable. One of the main stages in radiation protection is knowledge about radiation dose in radiological investigation. The aim of this study was to determine the physicians' knowledge in radiological examinations. Materials and Methods: The data collected by questionnaire was designed and the most commonly requested radiological investigations were listed. Questionnaire was circulated to 100 consultant physician. The survey was conducted of the awareness of radiation dose and risk among health professionals in Imam Reza Hospital, Kermanshah, Iran. Results: The results indicate that only 36.4% of physicians know the unit of radiation and evaluation of absorb dose in patient and many of these physicians were not aware of radiations risks and the most important aspects of radiation protection despite of pass in radiobiology and medical physics courses. Conclusion: because of radiological examinations play an indispensable role in medicine therefor knowledge about radiation doses and hazards is very important. Generally this study showed knowledge of radiation doses of investigation is inadequate among physicians.

KEYWORDS: *ionizing radiation; knowledge; radiation protection.*

Measurement of ^{131}I activity with a High Energy Gamma Camera

Raquel Barquero, Hugo Perez-Garcia, Monica Gomez-Incio

Hospital Clinico Universitario Valladolid, Valladolid, Spain

Abstract. Purpose: In order to know the activity of an uptake inside of a patient in Nuclear Medicine, a procedure must be available. Here, a procedure to perform this measurement is tested for different phantoms of known activity. Material and Method: 32 cases in two geometries are tested in this study, point source (a clinical pill of ^{131}I) and flat cylinders (Petri dish) with three different radius (r) 2.5, 4.5 and 7 cm filled with radioactive water in which different ^{131}I activity (A_{ref}) is diluted. In all cases, the pill and the phantom are centred with respect to the crystal of a Siemens e.cam gamma camera, at several distances (from 5 to 40 cm, 5 cm at a time) from the HE collimator. A Capintec 15R dose calibrator (DC), certified as traceable to international standards, is used to measure the reference activities (A_{ref})_{DC} of the pill and that diluted in the different Petri dish. To determine each activity with the Gamma camera an acquisition with a 15% energy window centred on the 364 keV and with a sufficiently long acquisition time t (600 s) is performed for each r and d values. The respective 2D DICOM image obtained is processed with ImageJ software: Defining on the image a r radius circle (a surface ROI $S_{ROI}=\pi \cdot r^2 \text{ cm}^2$), the number of counts in full-energy peak (gross counts) n_g inside it is measured. From apart, the corresponding geometry efficiency G_{ref} for each geometry used in each acquisition is determinate by using Monte Carlo method with MCNPX. The intrinsic efficiency of the Gamma camera is known from a previous calibration, $5.22 \cdot 10^{-2}$. Finally the Activity measured in the image is calculated according to the following formulae: $(A_{ref})_{image} = \frac{(n_g/t)/S_{ROI}}{G_{ref} \cdot 5.22 \cdot 10^{-2}}$. Results and Discussion: The accuracy of the procedure to estimate the activity in image is verified by the good agreement between measured activity in DC and in the image GC, estimated with the relative error $\epsilon_{rel}=[(A_{ref})_{GC}-(A_{ref})_{DC}]/(A_{ref})_{GC}$. ϵ_{rel} are less than 12% in all cases (32 values). : The procedure developed allows know experimentally the intrinsic efficiency of a HE gamma camera for I-131 imaging.

Situation of Radiation Therapy, Cancer Diagnosis and Radiation Protection of Patients in Cameroon

Richard Ndi Samba^a, Augustin Simo^a, Ernest C. Nwabueze Okonkwo^b

^aNational Radiation Protection Agency, Yaounde, Centre, Cameroon

^aOrtenau Klinikum Offenburg, Department of Radiation Oncology, Offenburg-Gengenbach, Germany

Abstract. In Cameroon, cancer cases have been estimated to rise from almost 12,000 in 2008 to more than 20,000 cases by 2030 (GLOBOCAN, 2008). Breast and cervical cancers account for more than half of cancers among women, while prostate and liver comprise more than a third of cancers for men. Cancer is of significant public health concern and its treatment poses a problem which is frequently unsuccessful. Cameroon has cancer centres in Yaoundé General Hospital and Douala General Hospital. However, at present, only Douala has a functional radiotherapy facility. Constraints in patients' access to cancer treatment (radiotherapy, chemotherapy and surgical services) present a significant challenge for Cameroon's cancer control programme. Regulatory bodies are mandated through laws and regulations to regulate all ionizing radiation sources as well as the protection of people and environment against ionizing radiation hazards. There are only three certified Medical Physicists with one working with the Regulatory Body. It is hoped that with the collaboration and help of renowned Medical Physics association, IAEA, WHO and Non-profit organisation together with the Cameroon ministry of health, cancer care and radiation protection of patients will be taken to a new improved level.

KEYWORDS: *regulatory; medical physics; radiotherapy in Cameroon; cancer burden; challenges.*

Promoting Fluoroscopic Personal Radiation Protection Equipment: Unfamiliarity, Facts, and Fears.

Stephen Balter

Columbia University Medical Center, New York, NY 10032, USA.

Abstract. Reducing any health risk usually requires the expenditure of both time and money. Basic safety measures reduce risk at reasonable cost. The reasonableness of a safety measure can be quantified in terms of the amount of money needed to avert a statistical death. Most individuals have little understanding of risk. This often causes unnecessary fear. This paper examines Personal protective equipment (PPE) offered for the prevention of brain cancer in interventional fluoroscopists and PPE offered for the prevention of brain cancer associated with cell phone use. Current publications relating to fluoroscopy staff brain cancer and its mitigation and similar papers relating to the risk of brain cancer attributable to cell-phone use were reviewed. The availability of ionizing radiation and radiofrequency safety materials was sampled in an internet search was performed February 2016 using combinations of relevant search terms. A small random number of ionizing radiation websites offering IR-PPE and similar devices for different anatomical areas were visited. RF, EMF, and Wi-Fi websites were randomly visited to find RF-PPE stylistically matching the IR-PPE. The lifetime risk of a fatal radiogenic brain cancer can be roughly estimated (order of magnitude) using different sets of dosimetry assumptions and irradiation models. The conservative cost of averting a fatal fluoroscopic brain cancer is in the range \$ 10,000,000 - \$ 100,000,000. Vendor claims seldom address the magnitude of the risk. Individuals and institutions are able to buy a wide variety of safety goods in the open market. However, budgets are finite. A gratuitous purchase of radioprotective equipment reduces the funds available to mitigate other safety risks. Unwarranted user fears derived either from vendor assertions or user hearsay should not be allowed to drive the radiation protection system to the point of decreasing overall safety.

KEYWORDS: *fluoroscopy; operator safety; risk; economics; personal protective equipment.*

Radiation Protection Dosimetry (2017), Vol. 173, No. 1-3, pp. 180–184
doi:10.1093/rpd/ncw307

Traceability of the KAP-Meters Used for Patient Dosimetry in Radiodiagnostic

Sorin Bercea, Constantin Cenusă, Ioan Cenusă, Aurelia Celarel, Elena Iliescu

“Horia Hulubei” National Institute for R&D in Physics and Nuclear Engineering (IFIN-HH), Magurele, Romania

Abstract. The traceability of the K_{air} x area product measurements is an important feature in QA for the patient protection during the radiodiagnostic procedures (using X-ray of different qualities). The correct measurement, as well as the accuracy of the measurements of the K_{air} x area product have a direct impact on the dosimetry for these radiological procedures. The paper presents the irradiation facility and the methods used for calibration the KAP- meters at different X-ray qualities. The results of the measurement of k_{air} and active area of the ionization chamber are compared with the direct measurement of the k_{air} x area product. The results of these measurements are also presented as well as an assessment of the uncertainties associated to these results.

Radiation Dose Assessment for Abdominal Computed Tomography

Seung Cheol Oh, Il Park, Kwang Pyo Kim

Kyung Hee University, Yongin-Si, Gyeonggi-Do, Republic of Korea

Abstract. Abdominal Computed Tomography is the predominant procedure for diagnosing acute appendicitis. However, radiation dose from CT has given rise to growing concerns. The objective of this study was to calculate radiation doses resulting from abdominal CT examination. Recently, a nationwide practice of CT examination was investigated in Korea. CTDIvol was measured under typical equipment settings such as kVp and mAs at each hospital. Additionally, the data for technical parameter settings and others associated with patient radiation doses were collected. The measured and collected data for abdominal CT were coupled with adult phantoms within a Monte Carlo code, MCNPX. Absorbed doses were calculated for a total of 30 organs and tissues, including active marrow. Radiation doses to the organs positioned in the abdomen region were 10.6–24.6 mGy. Organ doses were higher for colon and kidneys, followed by spleen, small intestine, stomach, liver, pancreas, gall bladder, adrenal, bladder. Effective dose based on ICRP 103 tissue weighting factors was 10.7 mSv (9.95 mSv for male and 11.42 mSv for female). Substantial difference in radiation doses was observed depending on equipment operation. The wide variation in the radiation doses and organ and effective doses calculated in this study can be applied to optimize abdominal CT protocol for the radiation protection purposes. This research was supported by a grant of the Korea Health Technology R&D Project through the Korea Health Industry Development Institute (KHIDI), funded by the Ministry of Health & Welfare, Republic of Korea (grant number : HI13C0004).

Implementation on Methodology for the Calibration of well type chambers used in ^{192}Ir -Brachytherapy Sources

Stefan Gutierrez Lores^a, Gonzalo Walwyn Salas^a, Jorge Luis Morales^b

^aCenter for Radiation Protection and Hygiene, Havana, Cuba

^bNational Institute of Oncology and Radiobiology, Havana, Cuba

Abstract. Purpose: This report presents the experiences of the Cuban's Secondary Standard Dosimetry Laboratory (SSDL) in the implementation of a methodology for the calibration of well type chambers used in ^{192}Ir -Brachytherapy sources. Methods and materials: Under International Atomic Energy Agency (IAEA) technical co-operation project CUB6017 a dosimetric system was acquired composed by a well type chamber model PTW33004 and an electrometer PTW model UNIDOS^{Webline} T10022, which was sent to the Primary Secondary Standard Laboratory (PSDL) of Germany for their calibration in terms of Reference Air Kerma Rate (RAKR). A microSelectron HDR ^{192}Ir -Brachytherapy manufactured by Nucletron was used for the determination of the calibration coefficients of the well type chambers models HDR 1000 plus and Nucletron model 077092 respectively. The methodology used follows the recommendations of the technical report IEAE-TECDOC 1274. Results: These well type chambers to the LPCD of Germany were sent for to participate in the proficiency test by inter-laboratory comparison. For checking the stability of the chamber during the transportation to LPCD of Germany were carried out measurements by using a source of ^{137}Cs model cylinder and code CDCSJ5 calibrated in terms of RAKR and a ^{60}Co Theratron-Phoenix-20 irradiator. The results were satisfactory. Those results of testing confirm that the methodology implemented has led to comparable results and the calibration procedure is ready for dissemination of the quantity to the users. Conclusions: The proficiency test constitutes a fundamental tool to evaluate the reliability of the results of a calibration laboratory. In addition in the present paper is confirmed the technical competition of the Cuban SSDL in the application of the methodology. Finally once calibrated the well type chambers used for HDR ^{192}Ir -Brachytherapy will maintain the traceability to the International System, contributing this way to elevate the quality of life of the oncology patients of our system of health.

KEYWORDS: HDR ^{192}Ir -brachytherapy sources; reference air kerma rate; calibration coefficient.

Study of the ^{131}I Thyroid Monitoring Measurements Using MCNP Simulations

Sebastián Gossio, Nancy Puerta, Ana Rojo

Nuclear Regulatory Authority, CABA, Argentina

Abstract. Internal dosimetry laboratory (LDI) has the accreditation under ISO 17025 for “in vivo” detection of ^{131}I thyroid body burden. The aim of this paper is to begin a study of the iodine detector’s response for detecting ^{131}I intakes activities including theoretical simulations. It was focused on the influence of different anatomical geometries and fluctuations of the detector position. The software MCNP6 was used to simulate our measurement system with the own IRD physical neck phantom and ICRP 110 Adult Reference Computational Phantoms. These results are the first stage of a LDI project to study all the measurement system response when varying the physical phantoms using Monte Carlo simulation.

Dosimetric Studies of Radionuclide Therapy of Neuroendocrine Tumors with ^{177}Lu -Dotatate

Santosh Kumar Gupta^a, Suhas Singla^b, Chandrasekhar Bal^b

^aNational Center for Accelerator Based Research, Guru Ghasidas University, Bilaspur, Chhatisgarh, India

^bDepartment of Nuclear Medicine, All India Institute of Medical Sciences, New Delhi, Delhi, India

Abstract. Objectives: Aims of this work was the calculation of radiation absorbed dose of Kidneys, Liver, Spleen and Neuroendocrine Tumors (NETs) of patients affected by NETs treated with ^{177}Lu -DOTATATE. Methods: We enrolled fifty seven patients (M/F: 36/21) with mean age 47.85 ± 15.30 affected by different types of NETs diagnosed with ^{68}Ga -DOTANOC PET-CT and biochemical markers. For radiation protection of kidneys, amino acid (lysine and & arginine mixture) was infused to each patient 30 minutes prior to therapeutic dose. 3.7 GBq to 7.4 GBq of ^{177}Lu -DOTATATE was infused to each patient over 30 minutes. Each patient underwent nine series of whole Body Scan with Dual Head Symbia Siemens Gamma Camera with LEAP collimator and dual energy window (108KeV and 211KeV: 15% energy window), at 30 minutes (pre-void), 4h, 8h, 12h, 24h, 48h, 96h, 144h and 168h (Post-void). The organs involved in dosimetric calculation were kidney, liver, spleen and NETs. Dosimetric calculations were done using the OLINDA/EXM 1.0 software. Renal Biological Effective Dose (BED) was calculated. Total 4- 6 cycles of therapy were given to each patients and time interval between each cycle was 10-12 weeks. Results: A physiological uptake of ^{177}Lu -DOTATATE was seen in all patients in Kidneys, liver and spleen. Mean \pm SD of radiation absorbed doses were calculated: 0.73 ± 0.17 mGy/MBq for Kidneys, 0.33 ± 0.39 mGy/MBq for liver, 1.27 ± 0.70 mGy/MBq for Spleen and 3.17 ± 1.92 mGy/MBq for NETs. Mean \pm SD of renal BED was 17.29 ± 9.12 Gy. No any renal and hematological toxicity was recorded during and after six months of completion of therapy course. Conclusions: ^{177}Lu -DOTATATE is an effective radiopharmaceutical used in the treatment of NETs especially in inoperable cases and patients with distant metastases. Maximum cumulative activity of ^{177}Lu -DOTATATE that can be safely administered to a patient without crossing permissible renal threshold is 33.74 GBq.

Managing the Gaseous Waste in Nuclear Medicine: A Novel Approach

Shahed Khan, Eleonora Santos

RCS, Twickenham, UK

Abstract. The production and administration of radiopharmaceuticals often results in the release of radionuclides into the air. To prevent the risk to the environment and population living around the plant, worldwide legislation requires the existence of air filtration systems, which must be monitored and controlled, in order to comply with the legislative requirements with respect to the dose, released into the air per year. The standard solution in dealing with these toxic radionuclides is via the use of alarms in stacks monitoring the release. These radionuclides require treatment, storage or decay facilities. Traditional methods include trapping vapours into charcoal or HEPA filters, which are stored for decay. However, this process is expensive. We present and describe a new method for the treatment of gaseous waste that is economically feasible. It focuses in diverting the toxic radionuclides into the cyclotron bunker where they are allowed to decay by electron emission. After decaying, the radionuclides can be discharged to the environment through the exhaustion system. This method complies with legislation and presents the advantage of using the already existing resources in the radiopharmaceutical production facility.

Monitoring and Evaluating the Air Concentration of Radionuclides in the Vicinity of a Nuclear Medicine Facility

Shahed Khan, Eleanora Santos

RCS, Twickenham, UK

Abstract. Council Directive 2013/59/EURATOM requires the appropriately monitoring and evaluation of radioactive airborne into the environment and to report the results to the competent authority in order to avoid accidental release of high levels of radionuclides during the production of radiopharmaceuticals. Hence, we carry out the first assessment of dose to the population living in the vicinity of a nuclear medicine facility in Portugal. We collect samples and measure radionuclide concentration in air released through the stack. The continuously collection of samples, carried out over a period of two weeks, was performed using a shielded remote controlled syringe and a shielded container. This process allowed for 1200 values of air concentration per day. A gamma detector was used to perform Gamma-ray spectrometric measurements. Concentration values were compared with results of a simulation based on a Gaussian plume air dispersion model. Findings indicate that the average values do not exceed $10 \mu\text{Sv y}_1$ for inhalation of the population. These results allow us to confirm that the air concentration of radionuclides outside the stack does not harm people and the environment.

Neutron Measurement for Proton Therapy Facility at Samsung Medical Center with Wobbling and Line Scanning Mode using WENDI-2

Sangmin Lee^a, Jin Sung Kim^b, Sungkoo Cho^b, Dae-Hyun Kim^b, Jungho Kim^c, Yunho Kim^c, Youngyih Han^b, Sung-Joon Ye^a, Chae Young Lee^d, Yong Hyun Chang^d

^aProgram in Biomedical Radiation Sciences, Department of Transdisciplinary Studies, Graduate School of Convergence Science and Technology, Seoul National University, Seoul, Republic of Korea

^bDepartment of Radiation Oncology, Samsung Medical Center, Sungkyunkwan University School of Medicine, Seoul, Republic of Korea

^cKorea Research Institute of Standards and Science, Daejeon, Republic of Korea

^dDepartment of Radiation Convergence Engineering, Yonsei University, Wonju, Republic of Korea

Abstract. Purpose: The primary objective of this study was to measure secondary neutron dose during proton therapy at Samsung Medical Center using a detector, which covers entire neutron energy range produced in proton therapy. We analyzed and compared the neutron dose during proton treatment with passively scattering and line scanning. Materials and methods: The neutron ambient dose equivalents were measured with 190-MeV wobbling and line scanning proton beam. The center of Plastic water phantom (30×30×60 cm³) was placed at isocenter. A WENDI-2 (Wide-Energy Neutron Detection Instrument, Thermo Scientific™, USA) was located 1 m from the isocenter with four different angles (0°, 45°, 90° and 135°). Both wobbling and line scanning mode with multi-purpose nozzles (Sumitomo Heavy Industries, Ltd, Japan) were used to obtain 10 cm width of SOBP (Spread Out Bragg Peak) for the measurements. Results: The H*(10) value was normalized by proton therapeutic dose at isocenter. For wobbling mode, the highest and lowest H*(10) value were 1.972 mSv/Gy at position 4 and 0.3958 mSv/Gy at position 2, respectively. With line scanning mode, the highest H*(10) value was 0.099 mSv/Gy at position 1 while the lowest value was 0.0104 mSv/Gy at position 3. Conclusions: We measured the neutron ambient dose equivalents at four positions generated by a 190-MeV proton beam using wobbling and line scanning mode with WENDI-2. These reference data could be used for neutron reduction methods and other analysis for advanced proton treatment in the near future.

KEYWORDS: *secondary neutron; neutron ambient dose equivalent; proton therapy; wobbling mode; scanning mode.*

Utilizing 3D Scanner/Printer for a Dummy Shield: Monte Carlo Dose Calculations on Artefact-free CT Images of a Metallic Shield for Electron Radiation Therapy

Jong In Park^a, Il Han Kim^{a,c}, Jaegi Lee^a, Hyeonseok Lee^a, Sung-Joon Ye^{a,b}, Sangmin Lee^a

^aProgram in Biomedical Radiation Sciences, Department of Transdisciplinary Studies, Graduate School of Convergence Science and Technology, Seoul National University, Seoul, Republic of Korea

^bInterdisciplinary Program in Radiation applied Life Science, Seoul National University College of Medicine, Seoul, Republic of Korea

^cDepartment of Radiation Oncology, Seoul National University Hospital, Seoul, Republic of Korea

Abstract. Introduction: A metallic shield has been used to protect regions of unwanted normal tissues in radiation therapy. However, patient's CT images taken with the metallic shields suffer from the metallic artefact, which causes difficulties in delineating the targets and normal tissues. Further the current TPS has a limitation on assigning the CT number and physical density to shielding materials, such as lead and tungsten. Objectives and Methodology: The purpose of this work is to accurately evaluate the effect of a metal shield on patient's dose distributions. A 3D scanner (ArtecTM) was used to extract the dimension and shape of metallic shields. Scanned data was transferred into a 3D printer (3D systemsTM, Projet 3500). For three patients who have a target located around a lip or an eye area, dummy shields were custom-printed using bio-resin (3D systemsTM, VisiJet M3 Proplast). The patient replacing the metallic shield with the dummy shield was scanned to produce artefact-free planning CT images. We used Monte Carlo (MC) simulations to obtain the doses. EGS4/BEAMnrc was commissioned from our measured electron beam data and then used to simulate the patient's treatment geometry. EGS4/DOSXYZnrc was used to calculate dose distributions on patient's CT-images. For this CT images were converted to a phantom file through the ccreate code. The phantom file had the same resolution as the planning CT images. Using MATLAB, we assigned the appropriate physical densities of the dummy shield regions. TPS-calculated doses were based on Eclipse 8.6 (Varian medical systems) that could assign the maximum CT number to only 3000 in lead or tungsten shield. In vivo measurements with radiochromic films were performed for the two lip patients. Results: For the eye patient treated by 6 MeV the TPS estimated near 50% of the prescription dose below the eye shield, while the MC did 5% of that. For the lip patients treated by 9 and 12 MeV the TPS showed dose reduction of about 20% and 15% below the lip shields, respectively. However, the MC expected dose reduction of about 80% and 70% below the shields. In vivo measurements also expected dose reduction of 83.6% and 69.6% below the shields for the lip patients treated by 9 and 12 MeV, respectively. Thus, the MC-based doses to the lens and to the gum showed an appropriate shielding effect that couldn't be accurately estimated by TPS. Conclusions: Utilizing 3D scanner/printer, the artefact-free CT images were successfully incorporated into the CT-based Monte Carlo simulations. The developed method was useful in predicting the realistic dose distributions around the organs blocked with the metallic shield.

Comparison of Cadmium Zinc Telluride (CZT) with Photomultiplier Tube (PMT) Detectors in SPECT and Bismuth Germanate (BGO) in PET

Seyed Mohsen Zahraei-Moghadam^a, Mehdi Saeedi –Moghadam^b, Banafsheh Zenali – Rafsenjani^d, Masoumeh Dorri-Gev^c, Fatemeh Shekoochi –Shooli^{b,c}

^aRadiation Medicine Engineering Dept. Shiraz University, Shiraz, Iran

^bIonizing and Non-Ionizing Radiation Protection Research Center (INIRPRC), Shiraz University of Medical Sciences, Shiraz, Iran

^cRadiology and Radiotherapy Department, School of Paramedical, Shahid Beheshti University of Medical Science, Tehran, Iran

^dMedical Imaging Research Center, Shiraz University of Medical Sciences, Shiraz, Iran

Abstract. Over the past few years, rate of cancers are widely increasing, so early diagnosis with SPECT and PET is regarded as one of the most important manners for prevention and therapy. These methods encounter to a large number of problems such as time, resolution and dose levels, which can be so controversial. In spite of these problems, SPECT with Photomultiplier Tube (PMT) Detectors and PET with Bismuth Germanate (BGO) Detectors have been using and even developing yet, but these problems are still remained. Semiconductor detectors such as Cadmium Zinc Telluride (CZT) are one of the most important alternative devices instead of scintillation detectors such as Photomultiplier Tube (PMT) and Bismuth Germanate (BGO), which can solve mentioned problems. The density of CZT is almost 5.8 g/cm³ and also it has high effective atomic number ($Z_{\text{eff}} \sim 50$) which lead to high stopping power for typical energies of interest in SPECT with a linear attenuation coefficient greater than PMT and BGO, so that CZT gives rise to higher resolution at lower dose levels and faster scan times. Consequently, we have concluded that usage of semiconductor detectors is better than scintillation detectors and consequently this method requires further study and research.

Nurses Knowledge of Ionizing Radiation and Radiation Protection during Mobile Radiodiagnostic Examinations

Samuel Opoku

University of Ghana, Accra, Ghana

Abstract. Introduction: Ionizing radiation is used extensively in the field of medicine for either diagnosis or treatment. Hence, an understanding of radiation safety principles and how to apply them in practice is critical for nursing practice. Methodology: The study was performed to assess nurses' knowledge of ionizing radiation and radiation protection during mobile radiodiagnostic examination. The study received ethical clearance from the Ethics and Protocol Review Committee, SBAS, University of Ghana. A quantitative, descriptive cross-sectional survey was employed for this study to provide better means of investigating and assessing the knowledge, misconceptions and perceptions among 43 nurses assigned to clinical rotations in selected wards of the Korle-Bu Teaching Hospital regarding ionizing radiation and its radiation protection. A purposive sampling method using self-administered questionnaires was used to obtain. Results: Out of the population of 43 nurses, 25.6% (n=11) were of the view that objects in the X-ray room emitted radiation after an x-ray exposure and the same percentage indicated that dangerous radiation is emitted from good quality microwave equipment. Also, 37.2% (n= 14) presumed that patients emitted radiation after an x-ray examination, while 60.5% (n=26) were of the opinion that magnetic resonance imaging (MRI) procedure was a source of ionizing radiation. Conclusion: The majority of nurses have inadequate knowledge and mistaken beliefs about various aspects of radiation sources and its protection. A course on radiation and radiation safety principles for nurses is thus recommended

Personal Radiation Monitoring of Occupationally Exposed Radiographers in the Biggest Tertiary Referral Hospital in Ghana

Samuel Opoku

University of Ghana, Accra, Ghana

Abstract. Background: The use of radiation in the health sector is of tremendous diagnostic and therapeutic benefit to patients. However, scatter radiation associated with its use poses detrimental risks to occupational staff and other health personnel whose activities are associated with the use of radiation. Therefore, there is a need to ensure effective monitoring of occupational exposed health personnel. Presently, the effectiveness of this programme at the biggest tertiary hospital in Ghana is however unclear. Aim: The aim of this study was to investigate if occupationally exposed radiographers in the biggest tertiary referral hospital in Ghana were monitored in compliance with international regulations. Methods: A quantitative descriptive survey design was used to obtain data on radiation monitoring in the biggest tertiary referral hospital in Ghana from February 2014 to April 2014. The study received ethical clearance from the Ethics and Protocol Review Committee, SBAS, University of Ghana. Two different tools, observation and questionnaire, were employed for data collection from 50 radiographers purposively sampled in the study. The data was analysed with Microsoft Excel 2010. Results: A 100 % response rate was obtained. All respondents were monitored by means of a TLD badge except 4(8 %) who did not have any personal radiation monitoring device. Although 86 % of respondents confirmed that their personnel dosimeters were collected for reading after 3 months of use, all the respondents however, did not receive TLD readings feedback until after 3 or more months. In particular, 38 % of diagnostic radiographers claimed they never received any feedback, while 66 % respondents indicated radiation monitoring in their various departments were unsatisfactory. Delays from the service provider (regulatory body) were identified as the causes of irregularities in supply of dosimeters and monitoring feedback. Conclusion: Radiation monitoring of occupational personnel at the biggest tertiary hospital was unsatisfactory and did not meet required standards. Hospital management and the regulatory body should ensure strict compliance with international regulations for purposes of achieving occupational radiation safety.

KEYWORDS: *radiation safety; monitoring; dosimeters; radiographer.*

Health Physicist Monitors Own Medical Dose from Radioiodine Thyroid Ablation Procedure

Sander Perle, Kip Bennett, Chad Hopponen, Michael Lantz

Mirion Technologies, Irvine, CA, USA

Abstract. The paper discusses the establishment of a Design of Experiments protocol for detecting and reporting dose from the thyroid after administration of I131 Sodium Iodide where hourly reads are performed using Instadose dosimeters and then compared to TLDs for the cumulative dose after 1 week of measurement. The dosimeters were worn on a lanyard measuring the dose from the thyroid after the ablation procedure as well as dosimeters strategically placed throughout the home in areas where the patient accesses. The paper addresses the requirements for an effective study that concludes the Instadose dosimeter is viable for use not only for an official dose of record for occupationally exposed individuals, but can also be used for patient dosimetry where real-time measurements are desired and can also be used for measuring dose for individuals who visit patients after receiving a nuclear medicine administration. The measured dose over the week identified and positively concludes that there is the Circadian Rhythms phenomenon during non-waking hours, which could also assist in lowering the dose required when administering radioactive materials during an administration. Instadose General Information: The Instadose dosimeter utilizes Direct Ion Storage Technology and is read by plugging the dosimeter into any USB port that is connected to the internet. This allows for measurements at any time interval without requiring shipping the dosimeter back to a processor for dose results. TLD General Information: The TLDs used in the comparison were 4 element Harshaw TLD (3 7LiF:Mg, Cu, P [TLD700H] and 1 6LiF:Mg, Cu, P [TLD600H]). Accreditations: The Instadose and TLD dosimeters are accredited through the U.S. Department of Commerce, National Institute of Standards and Technology, National Voluntary Laboratory Accreditation Program (NVLAP). Prior to use within the U.S. as a dosimeter of legal record it must pass the NVLAP review process, that includes blind performance testing over 3 months as well as an on-site evaluation demonstrating compliance with ISO 17025 standard. Test Data Review: The data for the test included: Instadose and TLD dosimeters on the neck to measure the dose from the I131 administration, multiple Instadose and TLD dosimeters were strategically located in the computer room, sleeping area, living room as well as on spouse, and the cumulative Instadose and TLD doses were compared for all locations to determine whether or not a real-time dosimeters such as an Instadose device is applicable for patient monitoring or to be worn by patient visitors after a nuclear medicine administration. This paper will discuss the results of each of these tests.

KEYWORDS: *Instadose; TLD; DIS; patient monitoring.*

Evaluation of Eye Lens Doses of Interventional Cardiologists

Sumi Yokoyama^a, Shoichi Suzuki^a, Hiroshi Toyama^a, Shinji Arakawa^b, Satoshi Inoue^b,
Yutaka Kinomura^b, Ikuo Kobayashi^c

^aFujita Health University, Toyoake, Aichi, 470-1192, Japan

^bFujita Health University Hospital, Toyoake, Aichi, 470-1192, Japan

^cNagase Landauer, LTD., Suwa, Tsukuba, Ibaraki, 300-2686, Japan

Abstract. The effective dose of medical staff members, especially interventional radiologists and cardiologists, is classified as a relatively high level. We measured the air kerma for interventional cardiologists by using optically stimulated luminescence dosimeters (OSLDs). However, this quantity is not the same as $H_p(3)$. In experiments, the air kerma and $H_p(3)$ at the eye-lens position of a phantom were measured using OSLD and thermoluminescent dosimeters (TLDs), respectively. A conversion factor from air kerma to $H_p(3)$ was estimated from these results. In addition, the eye doses of interventional cardiologists in clinical situations were measured, and the effect of eyewear on the eye-lens dose was discussed.

KEYWORDS: *dose of the lens of the eye; air kerma; $H_p(3)$; interventional cardiologist; OSLD; TLD.*

Radiation Protection Dosimetry (2017), Vol. 173, No. 1-3, pp. 218–222

doi:10.1093/rpd/ncw321

Development of Thermoplastic Mask set up Monitoring System using Force Sensing Resistor (FSR) Sensor

Tae Ho Kim^a, Siyong Kim^b, Min-Seok Cho^a, Seong-Hee Kang^a, Dong-Su Kim^a, Kyeong-Hyun Kim^a, Dong-Seok Shin^a, Tae-Suk Suh^a

^aDepartment of Biomedical Engineering, the Catholic University, Seoul, Republic of Korea

^bDepartment of Radiation Oncology, Virginia Commonwealth University, VA, USA

Abstract. Purpose: To improve the setup accuracy of thermoplastic mask, we developed a new monitoring method based on force sensing technology and evaluated its feasibility. Methods: The thermoplastic mask setup monitoring system consists of a force sensing resistor sensor unit, a signal transport device, a control PC and an in-house software. The system is designed to monitor pressure variation between the mask and patient in real time. It also provides a warning to the user when there is a possibility of movement. A preliminary study was performed to evaluate the reliability of the sensor unit and developed monitoring system with a head phantom. Then, a simulation study with volunteers was conducted to evaluate the feasibility of the monitoring system. Note that the sensor unit can have multiple end-sensors and every end-sensor was confirmed to be within 2% reliability in pressure reading through a screening test. Results: To evaluate the reproducibility of the proposed monitoring system in practice, we simulated a mask setup with the head phantom. FRS sensors were attached on the face of the head phantom and pressure was monitored. For 3 repeated mask setups on the phantom, the variation of the pressure was less than 3% (only 1% larger than 2% potential uncertainty confirmed in the screening test). In the volunteer study, we intended to verify that the system could detect patient movements within the mask. Thus, volunteers were asked to turn their head or lift their chin. The system was able to detect movements effectively, confirming the clinical feasibility of the monitoring system developed. Conclusion: Through the proposed setup monitoring method, it is possible to monitor patient motion inside a mask in real time, which has never been possible with most commonly used systems using non-radiographic technology such as infrared camera system and surface imaging system.

Measurements of Photon Spectra around IVR for the Evaluation of Eye-lens Dose

Tadahiro Kurosawa^a, Masahiro Kato^a, Sumi Yokoyama^b

^aNational Institute of Advanced Industrial Science and Technology, Tsukuba, Ibaraki, Japan

^bFujita Health University, Toyoake, Aichi, Japan

Abstract. Recently, the dose of eye-lens becomes important because of the new dose limit by the ICRP. One of the high dose fields for eye-lens is a treatment room for IVR. The photon spectra around IVR were measured using a CdZnTe detector. The unfolding method is applied to evaluate photon spectra from measured the pulse height spectra. And also the measurements of H*(3) were done by a thin window dosimeter. The PMMA plate of 3 mm thickness was attached in front of the dosimeter to evaluate the dose of H*(3). The measurement points are the positions of an operator and a nurse, not a direct x-ray from IVR. The phantom was used as a patient to simulate the scattered photons by a body of a patient. The spectrum information is useful for the evaluation of the shielding effect for the safety goggle and a development of a personal dosimeter for an operator.

RADIREC: System for Mapping and Collecting Entrance Skin Dose during Neurointerventional Radiology

Takashi Moritake^a, Lue Sun^a, Koichiro Futatsuya^a, Satoru Kawauchi^b, Yasuhiro Koguchi^c, Mikito Hayakawa^d, Yuji Matsumaru^b

^aUniversity of Occupational and Environmental Health, Japan, Kitakyushu, Fukuoka, Japan

^bToranomon Hospital, Minato-ku, Tokyo, Japan

^cChiyoda Technol Corporation, Oarai-machi, Ibaraki, Japan

^dNational Cerebral and Cardiovascular Center, Suita, Osaka, Japan

Abstract. Although measurement and management of entrance skin dose (ESD) during interventional radiology (IVR) are deemed extremely important, accurate determination of maximum ESD and its location during procedure is generally difficult because of the dependence on therapeutic technique and position of the dosimeter placed on a round-shaped head. We, therefore, launched the RADIREC project since 2007 to carry out the optimization of radiation protection. We first built a direct measurement system so that the ideal dosimetry for ESD during neuro-IVR can be easily determined. This system was then applied to patients to establish the efficacy of precise mapping of ESDs using a number of radiophotoluminescent glass dosimeters (RPLDs) to avoid radiation skin injury (RSI). Finally, we constructed an exposure analyzing system to help the medical staff collect patient's irradiation data with clinical information, and to make it easier to access such data through picture archiving and communication system (PACS) in a hospital. We showed here a case study of ESDs in both angiography (n = 46) and neuro-IVR (n = 47). The maximum ESD for angiography and neuro-IVR was 431 ± 136 (mean \pm SD) mGy and 1902 ± 1309 mGy, respectively. We also illustrated a case in which the ESD information could assist the physician to prevent further RSIs in subsequent procedures. In conclusion, the RADIREC system could prevent from excessive radiation, thereby reducing the risk of RSI.

Diagnostic Reference Levels (DRLs) for CT Examinations in Adults in Cameroon

Thierry Ndzana Ndah, Boniface Moifo, Mathurin Neossi Nguena

University of Ngaoundéré, Ngaoundéré, Cameroon

Abstract. CT dose index (CTDI) and dose-length product (DLP) are two dosimetric quantities used to determine the dose of patients from diagnosis reference levels (DRLs) determined by CT. DRLs are used to ensure the optimization of the patient dose in order to ensure better radiation protection. The objective was to determine the levels of DRL CT scans of adults in Cameroon. Dose measurements on 15 CT scanners. The following parameters were recorded: age, sex, acquisition mode (sequential or helical), the series (with or without injection), height acquisition, turnaround time, voltage, the load, the pitch, slice thickness reconstructed, CTDIvol and DLP. In this study, we selected 696 patients; the sex ratio was 1.26 male / female. Patients were aged between 20 and 90 years. The modal class was that of 55-60 years with a mean age of $52 \pm$. The helical acquisition was more exploited and represented 94% of acquisitions respectively. Brain CT examination was performed most (41.23%) followed by Abdominopelvic CT (26.86%). CTDIvol distribution was: 53mGy examination for brain, 25mGy for lumbar examination, 22mGy for chest examination and 14mGy for abdominopelvic examination. The 75th percentiles distribution doses are: 1150mGy.cm for "cerebral" protocol; 715mGy.cm for the "thoracic" protocol; 716mGy.cm for the "abdominal" protocol; 716mGy.cm for the "abdominopelvic Protocol" and 769 mGy.cm for the "lumbar" protocol. The dose levels will allow the user to ensure that his practice is in the middle and dosimetric will help optimize the compromise dose / image quality.

KEYWORDS: *DRL; TDM; DLP; CTDI; ADULT.*

The Dose Kernels for Pencil Beam and Differential Pencil Beam of Photons with Spectrum of Treatment Machine with ^{60}Co Source and their Analytical Approximations

Vladimir Klimanov^{a,b}, Alexey Moiseev^c, Maria Kolyvanova^a

^aFSI, SRC of Russian Federation - FMBC FMBA named AI Burnazyan, Moscow, Russia

^bNational Research Nuclear University «MEPhI», Moscow, Russia

^cTreatment - Rehabilitation Center, Moscow, Russia

Abstract. This work includes results of dose kernel Monte-Carlo calculations in EGSnrs program in terms of point spread function (differential pencil beam kernel) and pencil beam kernel in water medium for photons spectrum of ROKUS Co-60 treatment machine. Photons spectrum of ROKUS machine also was calculated with Monte-Carlo simulation. Calculated data were approximated along radial dimension separately for primary and scattered dose kernel terms with sums of exponential functions divided by radius for pencil beam and by square radius for differential pencil beam. This approximation makes possible direct implementation of Collapsed cones convolution method and Pencil beam method. Original algorithms were developed for verification of approximation formulas. Mean accuracy turned out to be better 5 %. Verification algorithms can be useful for independent checking calculations in radiation therapy.

Radiation Protection of the Public and of the Immediate Family of a Patient Following the Therapy with Iodine-131

Youssef Ech Chaykhy

University Ibn tofail, Kenitra, Morocco

Centre National de Radioprotection, Salé, Morocco

Abstract. The unsealed radionuclides are used in the diagnosis and treatment of various diseases in the form of radiopharmaceuticals provided to patients by injection, ingestion or inhalation. These radiopharmaceuticals can be localized in the body tissues so they are either reduced or removed by various means (urine, sweat...). In order to propose recommendations and durations of application restrictions for radiation protection of the public and of the immediate family of the patient then contact with a patient treated with iodine-131, as part of a thyroid cancer, simulations have been conducted in order to assess the exposure of family members and the public. Dose constraints were simulated for relatives to 3 mSv and 15 mSv (adults), 0.3 mSv (children) and 1 mSv for the public. Several contact models were tested: visits to a family member, the use of public transport, contact with a colleague, spouse and children. The durations of the recommendations were evaluated based on the residual activity (patient treatment) determined from the measurement of dose rate at 1 m. The calculation of respect for recommendations during a period of time determined after 5 days of hospitalization or after 3 days of hospitalization to calculate the durations of recommendations. The results obtained allow the professional of nuclear medicine to assess population exposure and to offer the patient and family appropriate recommendations for a rational, effective, and controlled radiation protection in order to meet the minimum irradiation compliance with relatives according to ALARA principle.

KEYWORDS: *exposure; dose rate; iodine 131; radiation protection: distance; hospitalization duration; duration of recommendation.*

A Study Evaluating the Dependence of the Patient Dose on the CT Dose Change in a SPECT/CT Scan

Young-Hwan Ryu^{b,c}, Ho-Sung Kim^a, Kyung-Rae Dong^c, Chang-Bok Kim^e, Yun-Jong Lee^d

^aDepartment of Nuclear Medicine, Asan Medical Center, Seoul, Republic of Korea

^bDepartment of Radiology, Seoul Medical Center, Seoul, Republic of Korea

^cDepartment of Nuclear Engineering, Chosun University, Gwangju, Republic of Korea

^dKorea Atomic Energy Research Institute, Jeonnam, Republic of Korea

^eDepartment of Radiological Technology, Gwangju Health College University, Gwangju, Republic of Korea

Abstract. This study assessed ways of reducing the patient dose by examining the dependence of the patient dose on the CT (computed tomography) dose in a SPECT (single-photon emission computed tomography)/CT scan. To measure the patient dose, we used Precedence 16 SPECT/CT along with a phantom for the CT dose measurement (CT dose phantom kit for adult's head and body, Model 76-414-4150), a 100-mm ionization chamber (CT Ion Chamber) and an X-ray detector (Victoreen Model 4000M+). In addition, the patient dose was evaluated under conditions similar to those for an actual examination using an ImPACT (imaging performance assessment of CT scanners) dosimetry calculator in the Monte Carlo simulation method. The experimental method involved the use of a CT dose phantom to measure the patient dose under different CT conditions (kVp and mAs) to determine the CTDI (CT dose index) under each condition. An ImPACT dosimetry calculator was also used to measure CTDI_w (CT dose indexwater), CTDI_v (CT dose indexvolume), DLP (dose-length product), and elective dose. According to the patient dose measurements using the CT dose phantom, the CTDI showed an approximately 54 fold difference between when the maximum (140 kVp and 250 mAs) and the minimum dose (90 kVp and 25 mAs) was used. The CTDI showed a 4.2 fold difference between the conditions (120 kVp and 200 mAs) used mainly in a common CT scan and the conditions (120 kVp and 50 mAs) used mainly in a SPECT/CT scan. According to the measurement results using the dosimetry calculator, the elective dose showed an approximately 35 fold difference between the conditions for the maximum and the minimum doses, as in the case with the CT dose phantom. The elective dose showed a 4.1 fold difference between the conditions used mainly in a common CT scan and those used mainly in a SPECT/CT scan. This study examined the patient dose by reducing the CT dose in a SPECT/CT scan. As various examinations can be conducted due to the development of equipment, the patient faces increasing medical exposure. At this juncture, radiation workers and equipment manufacturers are required to make efforts to obtain as much medical information as possible while using the minimum radiation dose.

KEYWORDS: PACS numbers: 87.58.-b, 87.58.Ce, 87.58.Sp, 87.5.

A Study on Quantitative Analysis of Exposure Dose Caused by Patient Depending on Time and Distance in Nuclear Medicine Examination

Young-Hwan Ryu^{b,c}, Ho-Sung Kim^a, Yun-Jong Lee^d, Kyung-Rae Dong^e, Jin-Kyu Kim^d, Chang-Bok Kim^e

^aDepartment of Nuclear Medicine, Asan Medical Center, Seoul, Republic of Korea

^bDepartment of Radiology, Seoul Medical Center, Seoul, Republic of Korea

^cDepartment of Nuclear Engineering, Chosun University, Gwangju, Republic of Korea

^dKorea Atomic Energy Research Institute, Jeonnam, Republic of Korea

^eDepartment of Radiological Technology, Gwangju Health College University, Gwangju, Republic of Korea

Abstract. This study evaluated possible actions that can help protect against and reduce radiation exposure. by measuring the exposure dose for each type of isotope that is used frequently in nuclear medicine before performing numerical analysis of the effective half-life based on the measurement results. From July to August in 2010, the study targeted ten, six and five people who underwent an ¹⁸F-FDG PET scan, ^{99m}Tc-HDP bone scan, and ²⁰¹Tl myocardial SPECT scan, respectively, in the nuclear medicine department. After injecting the required medicine into the subjects, a survey meter was used to measure the dose depending on the distance from the heart and time elapsed. For the ¹⁸F-FDG PET scan, the dose decreased by approximately 66% at 90 minutes compared to that immediately after the injection and by 78% at a distance of 1m compared to that at 0.3m. In the ^{99m}Tc-HDP bone scan, the dose decreased by approximately 71% in 200 minutes compared to that immediately after the injection and by approximately 78% at a distance of 1m compared to that at 0.3m. In the ²⁰¹Tl myocardial SPECT scan, the dose decreased by approximately 30% in 250 minutes compared to that immediately after the injection and by approximately 55% at a distance of 1m compared to that at 0.3m. In conclusion, the dose decreases by a large margin depending on the distance and time.

KEYWORDS: ¹⁸F-FDG; ^{99m}Tc-HDP; ²⁰¹Tl; dose.

Medical Personnel Radiation Safety in Autopsies for Radiation Accidents

Yulia Kvacheva

State Research Center - Burnasyan Federal Medical Biophysical Center, Moscow, Russia

Abstract. Deaths following radiation incidents are rare. To date, about 200 fatal cases were registered worldwide. Nevertheless, their possibility associated with industrial accidents or terrorist attacks (including in mass casualty scenario) has to be taken into account. In comparison with autopsies on cadavers with planned radiation exposure the necropsy on bodies exposed accidentally is quite complicated due to uncertainties in dose, duration, organs and organic systems involved and radionuclides internalized. This paper focuses especially on our own experience in prosectory examination of radiation deaths (e.g. after the Chernobyl disaster). The basic principles were postulated like the next: (i) Staff members involved in an accidental postmortem practice face risks of life threatening irradiation/radioactive contamination. (ii) The nature and the degree of these risks may not be apparent before or during the necropsy. (iii) Special precautions have to be taken in order for the autopsy to proceed safely. The strategy for reducing these risks is proposed. Thorough analysis of individual situation of the deceased with advanced pre-necropsy planning and prompt organization should be undertaken. The immediate cooperation of pathologists, health physicists and nuclear safety staff is required. Special measures to keep personnel radiation exposure within permissible limits are developed. These include documentation of both personnel radiation exposure and protection. Careful practice during the course of autopsy is recommended. The pathologists are instructed to obtain quickly the autopsy specimens with separate examination of radioactive and essentially non-radioactive organs. Time limit for working and the maximal practice distances are defined. Prevention of the autopsy room contamination is established including the controlled entrance to and exit from the autopsy room as well as controlled in- mortuary transport of radioactive bodies and decontamination procedures with residual radioactivity estimation. As a result of preventive efforts personnel radiation exposures are kept as low as reasonably achievable and within permissible limits. Thus, the risks of accidental post-irradiation autopsy could be prevented by safety police strategy and careful practice.

Evaluating Patient Dose in Conventional Radiology for Ten Routine Projections in Tehran, Iran: Recommendation for Local Diagnostic Reference Levels

Yazdan Salimi^a, Mohammad Reza Deevband^a, Dariush Askari^b, Jalal Ordoni^b,
Mohammad Hossein Jamshidi^c, Isaac Shiri^d, Hamed Dehghani^d, Hamid Behrozi^e

^aDepartment of Physics & Medical Engineering, Faculty of Medicine, Shahid Beheshti University of Medical Sciences, Tehran, Iran

^bDepartment of Radiology, Faculty Paramedical Sciences, Shahid Beheshti University of Medical Sciences, Tehran, Iran

^cDepartment of Medical Physics, Faculty of Medicine, Jundishapur University of Medical Sciences, Ahvaz, Iran

^dDepartment of Medical Physics, School of Medical Sciences, Iran University of Medical Sciences, Tehran, Iran

^eDepartment of Radiologic Technology, Faculty of Paramedicine, Jundishapur University of Medical Sciences, Ahvaz, Iran

Abstract. Introduction: ICRP didn't establish any dose limit for patient dose in diagnostic procedures. Large variations in patient doses for the same examinations were reported. In this regard, the standards require the establishment of diagnostic reference levels (DRL) or guidance levels for medical exposure. According to lack of this reference level, local DRL is recommended. In studies done in Iran the important issue of the image quality and the effect of optimization process on patient dose and image quality were ignored. We surveyed patients' dose in order to establish a local DRL for Tehran, Iran. Method and materials: Our propose in this study was indicating local DRL coordinated with IAEA protocol for Tehran province, Iran for ten routine projections; just for conventional radiography rooms; our surveyed factor was ESAK. The RTI solid state dosimeter was used to measure X-ray output. For each projection data of at least ten patients were recorded; then Radiographic images were evaluated and scored by experienced radiologist. ESAKs were plotted against the number of patients and DRL was indicated by third quartile method. Then equipment and systems in each radiography room controlled and optimization conditions applied. We offered to technicians guidelines published by European Commission for each procedure, after that patient dose and images were recorded again. Results showed that in some projections the dose to patients from a given type of examination may vary by factor 10. DRLs for chest PA, chest Lateral, cervical spine AP, cervical spine Lateral, lumbar spine lateral, skull PA, skull lateral, thoracic spine AP, thoracic spine lateral and abdomen was calculated: 0.99, 1.72, 0.71, 0.78, 2.11, 4.05, 1.58, 1.67, 1.64, 2.76, 1.76 mGy respectively. After implementing changes mean patient doses were reduced up to 60% for some projections. The low quality radiographs were decreased. Conclusion: according to results, in comparison with other studies there is considerable difference between cities in Iran. It is mainly due to absence of ineffective Quality Assurance program at hospitals and any guideline and exposure tables in radiography centers offered by legal unit. By applying simple and easy modification image quality will improve and the dose to patients will decrease. And it will lead to decrease in social costs in addition to the economic costs of health care.

Eye Lens Dosimetry: Measurement in Hospitals

Zina Cemusova^a, Daniela Ekendahl^a, Lucie Sukupova^b, Michael Zelizko^b, Martin Mates^c, Kamil Sedlacek^b, Jiri Novotny^b, Iva Krulova^c

^aNational Radiation Protection Institute, Prague 4, Nusle, Czech Republic

^bInstitute for Clinical and Experimental Medicine, Prague 4, Krc, Czech Republic

^cNa Homolce Hospital, Prague 5, Czech Republic

Abstract. As the new conclusions that the dose threshold to induce cataract in the lens of the human eye is lower than supposed, were made, the annual occupational dose limit was reduced from 150 mSv to 20 mSv averaged over five years, with a maximum of 50 mSv per year. It has a consequence in the need of proper monitoring of doses to the eye lens. In recent years, special dosimeters measuring the quantity $H_p(3)$, which serves as the estimate of the dose to the eye lens, have been produced. These dosimeters are supposed to be worn in the proximity of eyes. But there are some opinions that the use of these dosimeters is not necessary and a suitable algorithm for the quantity $H_p(0.07)$ measured with standard device provides an acceptable estimate too. These theories were successfully verified in our laboratory in conditions simulating interventional radiology exposures. Our results supported the opinion that the values measured with standard whole-body dosimeters can be employed avoiding significant inaccuracies in the eye lens exposure assessment. The next task was to investigate real conditions of interventional radiology and cardiology (IR/IC), which are workplaces with the high risk of exceeding the new dose limit. The group of physicians from several hospitals in the Czech Republic was monitored. To measure $H_p(3)$, a special dosimeter placed on the temple was utilized. Personal dosimeters measuring $H_p(0.07)$, $H_p(10)$ and $H_p(3)$ were worn on the body under and over the protective equipment. Except the fact that most of the physicians reach low doses far from the annual limits, relations between values measured with eye and whole-body dosimeters were revealed similar to the laboratory experiment results. Most of the physicians are expected to obtain the annual dose to the eye lens of several millisieverts, which is a very conservative estimate because the vast majority of physicians wear lead goggles. In this case, when the standard personal dosimeter detects low doses and the person is equipped with a protective eyewear, it seems to be enough to assess the eye lens dose with help of a dosimeter calibrated in $H_p(0.07)$ quantity, placed on the body, and a specific algorithm.

A National Audit Programme for Radiotherapy Centres

Zakithi Msimang

National Metrology Institute of South Africa, Pretoria, South Africa

Abstract. Radiation doses delivered to patients, through radiation therapy, in South Africa, are checked by teams of medical physicists, radiographers and radiation oncologists employed in the radiotherapy hospital. Medical physicists perform 'quality assurance' measurements which confirm the radiation delivered to the patient. The treatments prescribed by radiation oncologists and the treatment plans generated by radiographers require review and cross-checking and this is done within the radiation oncology department. There is a need to perform independent checks for equipment and patient doses. IAEA Safety Standards for protecting people and the environment, GSR Part 3, published in 2014, places the responsibility on the registrants and licensees to ensure that regular and independent audits are performed in accordance with the programme for quality assurance for medical exposures. The frequency of these audits should be in accordance with the complexity of the radiological procedures being performed and the associated risks. Having your own national programme, which will be easily accessible for all, will assist the hospitals to comply. The programme to establish the national audit programme in South Africa will be discussed and progress highlighted in the poster.

Calculation of Organs Doses and Secondary Cancer Risk during Mantle Field Radiotherapy for Hodgkin's Lymphoma

Zahra Shakarami^a, Mansour Zabihzadeh^{a,b}, Mohammad Javad Tahmasebi Birgani^{a,b},
MohammadAli Behrooz^a, Hojatollah Shahbazian^b

^aAhvaz Jndishapr University of Medical Sciences, AHVAZ, Iran

^bDepartment of Radiotherapy and Radiation Oncology, Golestan Hospital, Ahvaz Jundishapur University of Medical Sciences, AHVAZ, Iran

Abstract. Introduction: Occurrence of radiation-induced secondary cancer risk following mantle field radiotherapy for Hodgkin's lymphoma (HL) patients with long survival demands well established radiotherapy strategy. Organs doses and resulted secondary cancer risk due to out-of field photons were calculated during mantle field radiotherapy for HI patient. Method: The male and female mathematical phantom of the Oak Ridge National Laboratory (ORNL) and validated 6MV photon beam of a Varian 2300 C/D were modeled by MCNPX 2.4.0 MC code. Using suitable lungs and thyroid shields for AP and PA fields, the organ specific absorbed doses, effective dose, and secondary cancer risk were calculated following to mantle field radiotherapy for HL. Results: Among the out-of-field organs, the nose, eyes, head and neck's skins and sinuses have the higher received doses. The total effective doses and secondary cancer risk for a male and female were estimated to be 199, 234 mSv and 1.72%, 1.87% respectively. Conclusion: During mantle field radiotherapy for Hodgkin's lymphoma, accurately estimations of organs dose near to the field's edge and suitable shielding of critical in-field organs are crucial factor to establish an optimal treatment plan.

Organ doses and associated cancer risks for CT examinations of thorax

Marija Majer^a, Željka Knežević^a, Jelena Popić Ramač^b, Hrvoje Hršak^c, Saveta Miljanić^a

^aRuđer Bošković Institute, Bijenička cesta 54, 10000 Zagreb, Croatia

^bClinical Hospital Merkur, Zajčeva 19, 10000 Zagreb, Croatia

^cClinical Hospital Centre Zagreb, Kišpatićeva 12, 10000 Zagreb, Croatia

Abstract. The use of computed tomography (CT) is increasing rapidly and doses are not negligible especially when medical procedures require more than one CT scan. The purpose of the present study was to measure doses in/on an anthropomorphic Rando phantom during standard and low dose CT protocol of thorax and to estimate risks of radiation induced cancer for adult patients that undergo multiple CT scans of thorax. Thermoluminescent (TL) and radiophotoluminescent (RPL) dosimeters were used for dose measurements. Radiation risks of cancer incidence, in the form of lifetime attributable risk (LAR), were estimated using BEIR VII model. For five exposures with standard protocol mean organ doses were 94 mGy (breast), 85 mGy (stomach), 85 mGy (thyroid), 78 mGy (lung), 52 mGy (liver) and 16 mGy (colon). Associated LARs were found to be up to 0.401% (401 breast cancers per 100 000 exposed patients) and 0.116% (116 lung cancers per 100 000 exposed patients) for female and male, respectively. Low dose protocol reduces doses (and risks) by the average factor of 5 and therefore the use of low dose protocol is recommended whenever it is medically justified.

KEYWORDS: *organ dose; radiation cancer risk; CT of thorax; low dose protocol.*

Optimization of image quality and patient dose in radiographs of paediatric extremities using direct digital radiography

Jones A.^{a,b}, Ansell C.^c, Jerrom C.^a, Honey Id^a

^aMedical Physics Department, Guy's and St Thomas' NHS Foundation Trust, London, UK

^bMedical Physics Department, Western Sydney Local Health District, Sydney, NSW, Australia

^cRadiology Department, Evelina London Children's Hospital, Guy's and St Thomas' NHS Foundation Trust, London, UK

Abstract. *Objective:* The purpose of this study was to evaluate the effect of beam quality on the image quality (IQ) of ankle radiographs of paediatric patients in the age range of 0–1 year whilst maintaining constant effective dose (ED). *Methods:* Lateral ankle radiographs of an infant foot phantom were taken at a range of tube potentials (40.0–64.5 kVp) with and without 0.1-mm copper (Cu) filtration using a Trixell Pixium 4600 detector (Trixell, Morains, France). ED to the patient was computed for the default exposure parameters using PCXMC v. 2.0 and was fixed for other beam qualities by modulating the tube current-time product. The contrast-to-noise ratio (CNR) was measured between the tibia and adjacent soft tissue. The IQ of the phantom images was assessed by three radiologists and a reporting radiographer. Four IQ criteria were defined each with a scale of 1–3, giving a maximum score of 12. Finally, a service audit of clinical images at the default and optimum beam qualities was undertaken. *Results:* The measured CNR for the 40kVp/no Cu image was 12.0 compared with 7.6 for the default mode (55 0.1mm Cu). An improvement in the clinical IQ scores was also apparent at this lower beam quality. *Conclusion:* Lowering tube potential and removing filtration improved the clinical IQ of paediatric ankle radiographs in this age range. *Advances in knowledge:* There are currently no UK guidelines on exposure protocols for paediatric imaging using direct digital radiography. A lower beam quality will produce better IQ with no additional dose penalty for infant extremity imaging.

**The Proceedings of the 14th International Congress of the International Radiation
Protection Association
Volume 2 of 5**

Area 4: General Ionising Radiation Protection

Side by Side Monitoring Test for Radon Emissions from an Underground Uranium Mine

Douglas Chambers^a, David Frydenlund^b, Jaime Massey^b, Ron Stager^a,
Kathy Weinel^b

^aDouglas Chambers, Ron Stager SENES Consultants Limited (now Arcadis Canada Inc.),
121 Granton Drive, Suite 12, Richmond Hill, ON L4B 3N4, Canada.

^bEnergy Fuels Resources (USA) Inc.

Abstract. The USEPA requires that emissions of radon to the ambient air from an underground uranium mine shall not exceed those amounts that would cause any member of the public to receive in any year an effective dose equivalent (“dose”) of 10 millirems per year. The EPA (in 40 CFR Part 61 Subpart B) allows two methods for assessing radon emissions, namely, Method A-6 (scintillation cell monitors), and Method A-7 which relies on passive alpha track detectors “ATDs” when it has been proven to EPA’s satisfaction that the method produces data comparable to data obtained with Method A-6. To investigate this, a 12 month monitoring program was performed whereby scintillation cell monitors (EPA’s Method A-6) and ATDs (EPA’s Method A-7) were installed side by side in ventilated mine exhausts, and the results were compared to determine if ATDs can be used to accurately determine mine radon emissions. Standard Operating Procedures (“SOPs”) for the use of the two devices were developed and provide detailed descriptions of the field implementation, documentation, maintenance, and calibration procedures for operation of each device. Practical (operational) challenges that were encountered during the monitoring program are discussed, as are data management and quality assurance. Overall, Energy Fuels successfully collected comparison data using Method A-6 and Method A-7 devices at nine mine vents or portals at three different mine sites from May of 2011 through the end of September 2012. Statistical analysis of the data demonstrated that the data collected from the ATDs and the scintillation devices during the Study proved to be suitable for developing an ATD calibration factor and that ATDs could be used to reliably estimate radon emissions. Moreover, ATDs are lower cost, passive without the need for electrical power, and for this study yielded more reliable, continuous data collection than the scintillation cells.

KEYWORDS: *radon; radon monitoring; underground mines; uranium.*

1 INTRODUCTION

The uranium ore produced from the Colorado Plateau has relatively low levels of radiation and metal content compared to some of the higher-grade deposits mined in other countries. The average grade of the uranium ore is typically between 0.20 and 0.25 percent uranium. Uranium mine operators are also required to minimize exposure of the general public to radon emissions released from their uranium mine ventilation systems. Radon emissions from mine exhaust vents are monitored and controlled in accordance with standards implemented under State of Utah and EPA regulations that require that the radon dose to the nearest receptor (member of the public) be limited to 10 mrem/yr or less. These regulations require that a mine operator monitor the air flow and radon concentration levels at the mine exhaust points and use this information to derive an annual radon emission rate estimate the annualized emission rate data which is then used in models to estimate the dose from radon to compare against the 10 mrem/yr standard.

In order to address the EPA's concerns, EFRI developed a monitoring program which consisted of installing Method A-6 scintillation cell monitors and Method A-7 ATDs side by side in ventilated emissions from a number of mines in a number of different physical environments and comparing the results to determine if ATDs can be used to accurately determine mine radon emissions. Method A-6, which allows for continuous monitoring of radon gas with a scintillation cell, is the method specified for underground mine ventilation use; however, as discussed in detail in the Data Summary Report, the scintillation monitors currently available for use in underground mines have proven to be very unreliable and labour intensive. In contrast, the Method A-7 ATDs have proven to be reliable, easy to use, and relatively inexpensive.

2 OBJECTIVES FOR STUDY

In broad terms, the objectives of the radon monitoring study were to:

1. Demonstrate that Method A-7 produces data comparable to data obtained with Method A-6;
2. Compare ATDs to continuous gas (scintillation cell) monitors in different geographic settings;
3. Compare ATDs to continuous gas monitors under a number of different physical conditions; and
4. Develop an ATD calibration factor (relative to continuous gas monitors) for the mines or conditions tested.

The focus of this paper is objective 4, namely the use of method A-7 to predict equivalent radon concentration that would be measured using Method A-6. Methods. The radon monitoring program developed to support this analysis consisted of installing scintillation cell monitors and ATDs side by side in ventilated emissions from the mines and comparing the results for Method A-6 and Method A-7 to determine if ATDs can be used to accurately determine mine radon emissions.

3 METHODS

The Test Plan (EFRI 2011) was designed to achieve the objectives listed above, was developed after a review of the requirements for radon monitoring in 40 CFR 61 Appendix B Method 114 ("Method 114") which outlines the specific requirements for Method A-6 and Method A-7. EFRI's Test plan was to perform this side-by-side test at a total of nine locations over a period of approximately 12 months at each test location to represent the full range of seasonal variations in the results.

3.1 Monitoring Equipment

Method A-6, which allows for continuous monitoring of radon gas with a scintillation cell, is the method specified for underground mine ventilation. The regulations allow for use of Method A-7, which is identified as an alternate method, when it has been proven to EPA's satisfaction that it produces data comparable to data generated by Method A-6. In Method A6, radon is measured in a continuously extracted sample stream that passes through a calibrated scintillation cell using a sampler that collects a controlled volume of air at specific time intervals.

There are a limited number of manufacturers that make radon detection equipment that meets the requirements for Method A-6 and Method A-7. For Method A-6, EFRI chose two types of radon monitors manufactured by Pylon Electronics of Canada ("Pylon"). The monitors are Pylon's AB-5 Portable Radiation Monitor ("AB-5") and CRM-1 Active Radiation Monitor ("CRM-1"). Both monitors provide continuous measurement of a slipstream drawn from a mine vent or portal. (See Figure 1) The two models differ primarily in size, portability, data output, and data storage capacity. The AB-5 records hourly data for up to two weeks, and provides a data report in counts per hour. The counts per hour are then converted into pCi/L by subtracting the background of the device from the counts, and then dividing the counts by the efficiency factor of the device. The CRM-1 records hourly data for up to 30 days, and provides a data report electronically converted by the device into pCi/L.

In Method A-7, radon is measured directly in the effluent stream using ATDs (Method 114, Section for Method A-7), EFRI chose to use Radtrak® ATDs manufactured by Landauer. The ATDs are placed on a mine vent or portal for 30 days. The ATDs collect alpha particles emitted by radon, and its decay products, on a small, plastic strip located within the ATD. The ATDs are processed by Landauer; who provides EFRI with data reports in pCi/L. All data used for the comparison of Method A-6 and Method A-7 in this study were based on ATDs with thoron-proof filters.

3.2 Test Locations

Test locations were selected to represent a variety of mine operation and environmental conditions. The EPA considers that ATDs are constructed for a more stagnant airflow environment and may not accurately report radon activity when measuring radon emissions in the more dynamic flow found in a mine vent. Additionally, EPA considered that environmental conditions at exhausting mine vents would not occur in stagnant airflow conditions which could cause the ATDs to greatly overestimate or underestimate the radon emissions released from a mine vent. The study design considered this issue by placing the AB-5/CRM-1s alongside the ATDs in a number of mine vent locations with different operating characteristics and at geographically different mine sites to account for differences in temperature, humidity, and wind conditions. The Study enabled EFRI to determine if there were statistically significant differences in the data obtained using Method A-6 as compared to the data obtained using Method A-7. Overall, EFRI chose nine locations at three mine sites. Figure 1 shows a monitoring site EFRI's Beaver Mine in Utah.

Figure 1: Beaver Vent 2300 #2 at the La Sal Mines Complex



It is important to note that the availability of constant, reliable electricity was taken into account when choosing the locations for the Study. The Method A-6 monitoring devices require a continuous, uninterrupted source of electricity, as power drops typically result in the monitors resetting their monitoring parameters to inappropriate default settings and, in some cases, losing the previously stored data. Accordingly, mine sites with line power were preferentially selected for the Study to minimize power drops.

3.3 Background Test Locations

As described in the Test Plan, EFRI committed to collect data on local background levels of radon near La Sal. Using modelling tools, specifically air modelling was performed to provide information on the anticipated pattern of annual average radon concentrations the La Sal mine. Four locations considered based on air dispersion modelling reasonably to be outside of the envelope of influence of the existing sources were chosen to monitor background. The locations chosen were in the four cardinal compass directions of North, South, East, and West.

3.4 Data Collection and Management

Guidance for routine field operations included well defined SOPs and detailed quality assurance plans. EFRI field personnel were also responsible for maintenance of all devices used for the study. Prior to commencement of the Study, EFRI personnel received a significant amount of training in order to successfully collect data in the field. EFRI had been monitoring using ATDs prior to the Study, but needed specific training on operating the Method A-6 AB-5s and CRM-1s. EFRI subcontracted Pylon to provide a technician at the beginning of the Study. The Pylon technician travelled to the mine sites, and to provide training and oversight of the Method A-6 instruments deployment.

In addition to maintenance, each Method A-6 device is required to be removed from the field at least once a year for calibration. Calibration of each device must be done by Pylon or another manufacturer-approved calibration supplier. Calibration of the AB-5/CRM-1 and the Lucas cells associated with each device is required prior to initial use, after repair or service and, annually per the manufacturer's specifications. Upon completion of calibration and return of the AB-5/CRM-1 and the Lucas cells, the expired certificates of calibration were removed from use and marked with the date of expiration/replacement. The new information (sensitivity) was used for calculations from the date of the calibration forward until the next recalibration.

Each location for the study had at least one AB-5 or CRM-1 and one ATD. However, in order to achieve all of the data collection objectives outlined in the Test Plan, some locations had ATDs with and without thoron filters, and/or had a second ATD, AB-5/CRM-1 for collection of sample duplicates. EFRI field personnel also collected the radon background data, described above, with ATDs at eight background locations. With each device used in the Study having different data collection capabilities and storage limitations, the data collection/download schedule for EFRI Field Personnel was as follows:

- Method A-6 AB-5 – every two weeks;
- Method A-6 CRM-1 – every 30 days;
- Method A-7 ATDs for mine vent and portal monitoring – every 30 days;
- Method A-7 ATDs for radon background monitoring – every 90 days; and
- Method A-7 ATDs for presence of thoron monitoring – every 30 days (2 canisters each).

4 STATISTICAL ANALYSIS

4.1 Preliminary Statistical Analysis

A statistical analysis of the Study data was performed to determine whether a statistical correlation exists between paired results from Method A-6 and Method A-7, and if so, whether a regression model provides a statistically significant fit to the data. The objective was to determine whether a predictive statistical model can be used to estimate Method A-6 with a bounding condition that radon concentrations and associated doses would not be underestimated as the potential underestimation of dose is the potential error of greatest concern.

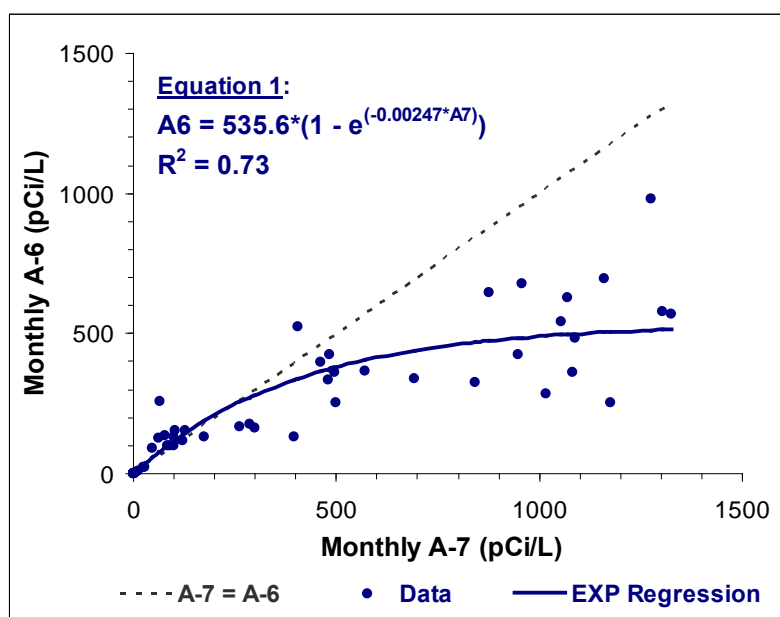
To evaluate data "comparability" between methods, it was necessary to control to the greatest extent possible potentially confounding factors that could result in non-representative data. For example, incomplete monthly Method A-6 data in a given month could skew results in an inaccurate manner relative to results from Method A-7. For this reason, only paired data with "complete" (i.e., greater than 90%) data coverage for the month were considered in the analysis. In addition, all data that were suspect due to known/identified issues with unreliable power supply or equipment malfunction were excluded from the analysis.

To help control for non-representative data that can result from factors that are not readily identified, a simple statistical test for data outliers (an interquartile range test) was performed on the ratio of Method A-7 to Method A-6 concentrations. In all, seven statistical outliers having unusually high Method A-7/Method A-6 ratios were identified in the data set with complete monthly measurements for both Method A-6 and Method A-7. These outliers were excluded from the statistical regression analysis, and this omission is conservative. Inclusion of statistical outliers with unusually high Method A-7/Method A-6 ratios would tend to result in underestimation of predicted Method A-6 equivalent values.

In all, there were 48 paired monthly Method A-6/Method A-7 results that were used for the regression analysis. No distinction was made by mine or vent. All pairs for all mines and vents were combined into one data set. The analysis involved weighted non-linear regression to account for the curvilinear nature of the relationship and the non-constant absolute variability across the data range. The weighting was based on the inverse square of the Method A-7 measurement and fitted to an exponential function as illustrated in Figure 2.

As illustrated in Figure 2, EFRI was able to successfully compare the Method A-7 ATDs to the Method A-6 AB-5/CRM-1 under a variety of physical conditions during the Study. The physical, environmental conditions at the nine monitoring locations did not appear to have an impact on the data collected using either method. However, a preliminary comparison of the two data sets illustrated in Figure 2, shows a clear difference between the data collected using each method when radon concentrations are above 200 pCi/L where the data from the Study indicates that the ATDs generally overestimate radon concentrations relative to the Method A-6 scintillometers. The reasons that the ATDs read higher than the Method A-6 monitors at high exposures is unclear. Due to the consistency of the pattern of variation between Method A-7 and Method A-6 across the various locations, the data collected using ATDs during the Study proved to be suitable for developing an ATD calibration factor. The statistical data analysis and justification for development of an ATD calibration factor are discussed below.

Figure 2: A6/A7 Exponential Regression Relationship



4.2 Final Statistical Model

The regression model (Equation 1) provides a statistical estimate of the true average relationship between Method A-6 and Method A-7 measurements and can thus be used to predict Method A-6 equivalent values based on the Method A-7 measurements. However, given the ultimate use of the data (dose estimation), and the observed amount of data scatter about the regression curve (residuals indicative of potential prediction error), it is desirable to reduce the probability that a predicted Method A-6 equivalent value could underestimate the radon concentration that might otherwise be measured with Method A-6. For these reasons, additional statistical models were investigated.

Various relationships were investigated, including the use of the 95% upper confidence limits (“UCLs”) on the slope of the regression and the use of the 95% upper prediction limits (“UPLs”). These measures were one-sided. For the UCL, this measure provides a 95% level of confidence that the true slope of the relationship does not exceed this upper limit. For the UPL, this measure is the value at which there is less than a 5% probability that an individual radon concentration as measured with the A-6 methodology would exceed this upper limit.

For individual monthly Method A-7 measurements, a conventional 95% one-sided UPL would be appropriate in terms of limiting under-prediction error rates to 5% or less. However, the prediction error of interest is that associated with the estimated annual dose based on 12 monthly radon releases. In this context, individual prediction error associated with Method A-6 equivalent values will balance out such that some actual monthly Method A-6 measurements would be lower than the predicted value and

some would be higher. In effect, we are looking for a prediction limit that accounts for the fact that 12 individual monthly measurements are used to predict estimated annual dose as the use of a conventional UPL would not account for variability in measured monthly Method A-6 values averaging out on an annual basis.

While this regression model provided a statistical estimate of the true average relationship between Method A-6 and Method A-7 measurements and could be used to predict Method A-6 equivalent values based on the Method A-7 measurements, there was considerable scatter about the regression curve and it was considered desirable to reduce the probability that a predicted Method A-6 equivalent value could underestimate the radon concentration that might otherwise be measured with Method A-6. For this reason, additional statistical measures were established for the relationship including 95% upper confidence limits ("UCLs") on the slope of the regression and 95% upper prediction limits ("UPLs") with the objective of developing a (reasonably) conservative conversion from measured Method A-7 radon concentration to Method A-6 such that the Method A-6 equivalent is highly unlikely to underestimate the annual dose received by nearby receptors. (See Figure 3.) The UPL(12) was calculated from the variance indicated by UCL and the UPL. The UPL variance includes uncertainty in the slope and individual variability. The variation due only to uncertainty in individual measurements can be determined by subtracting the uncertainty in the slope from the variance for individual samples.

Figure 3: Exponential Regression Results with 95% UP and UPL(12)

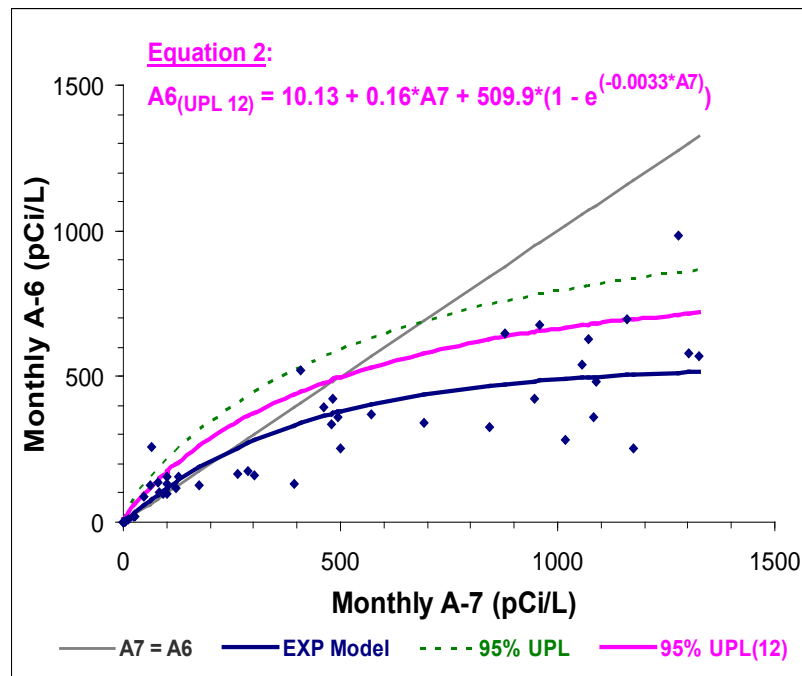


Figure 3 includes a plot of "complete" monthly study data along with the corresponding exponential regression, but also includes 95% UPL and UPL(12) curves. Application of the UPL(12) for predicting Method A6-equivalents will provide a high degree of confidence (approximately 95% probability) that average annual radon concentrations are not underestimated. The model proposed for using a UPL(12) based Method A-6 equivalent value for any given monthly Method A-7 measurement includes an intercept term and both linear and non-linear terms with an exponentially decreasing slope. The details of equation 2 shown on Figure 3 are as follows:

$$\text{Equation} \quad A6_{(\text{UPL } 12)} = m_1 + m_2 * A7 + m_3 * (1 - e^{(-m_4 * A7)}) + \varepsilon \quad (1)$$

Where:
 $A6_{(\text{UPL } 12)}$ = Predicted Method A-6 equivalent value (pCi/L) based on the UPL(12)
 $A7$ = Monthly ATD measurement (Method A-7)
 m_1 = Model parameter 1 (intercept)
 m_2 = Model parameter 2
 m_3 = Model parameter 3
 m_4 = Model parameter 4
 ε = Prediction uncertainty

Table 1 provides provides the parameter estimates for the UPL12). Use of these parameter estimates for predicting UPL(12)-based Method A-6 equivalent values based on measured Method A-7 values is appropriate given the near perfect fit.

Table 2: Parameter Estimates and Confidence Intervals

Parameter	Estimate	Approximate Standard Error	Approximate 95% Confidence Limits	
UPL(12) Fit				
m_1	10.1292	1.1702	7.7709	12.4875
m_2	0.16	0.00863	0.1426	0.1774
m_3	509.9	10.5682	488.6	531.2
m_4	0.00329	8.70E-05	0.00312	0.00347

5 CONCLUSIONS

Throughout this Study, environmental measurements were collected in accordance with established procedures to produce data that are scientifically valid and of known and acceptable quality to meet the Study's objectives. The sampling procedures were designed to accurately characterize the environmental conditions at the mine sites. These procedures addressed the purpose for sampling, selection of sampling locations, the number of samples to be collected, the ambient conditions for sample collection, the frequencies and timing for sampling, and the required sampling techniques.

EFRI successfully collected comparison data using Method A-6 and Method A-7 devices at nine mine vents or portals at three mine sites from May of 2011 through the end of September 2012. As discussed above, differing physical, environmental conditions do not appear to impact the relationship between either method. As a result, the conclusions reached in this Study should be considered to be representative of all uranium mine sites, not just the sites and vents included in the Study. The physical difference seen in the data collected from the ATDs and the scintillation devices during the Study proved to be suitable for developing a statistical ATD calibration factor. Moreover, the Study also showed the benefits of Method A-7; namely, ATDs are lower cost, passive without the need for electrical power and had 100 percent completeness throughout the Study and yielded reliable, continuous data collection. As discussed in EFRI (2014), scintillation monitors currently available for use in underground mines have proven to be very unreliable and labour intensive. In contrast, the Method A-7 ATDs have proven to be reliable, easy to use, and relatively inexpensive.

The statistical analysis of the Study data shows that for radon concentrations below about 200 pCi/L, monitoring with the Method A-7 will generally produce results that are very close to Method A-6 results. At higher concentrations, Method A-7 has a strong tendency to overestimate concentrations relative to Method A-6. Accordingly, Method A-7 results, when used for modelling, are likely to overestimate the doses received at receptor locations compared to doses determined based on results from Method A-6.

EFRI believes that the results of the Study proved to be suitable for developing an ATD calibration factor, and the use of the UPL(12) conversion equation allows for exclusive use of Method A-7 monitoring with probabilities on the order of 95% or higher that the predictive model will avoid overall underestimation of the 12 monthly concentrations that would otherwise be measured with Method A-6.

Overall, the main conclusions from this study are that:

- ATDs produce comparable, consistent, continuous, and reliable data.
- Scintillation cell monitors provide accurate and representative data, however, the devices proved to be unreliable and labour intensive in outdoor environments.
- ATDs produce data comparable to scintillation cell monitors at lower radon concentrations (<200 pCi/L).
- ATDs overestimate radon concentrations in high velocity environments which result in higher radon concentrations (>200 pCi/L).
- The results are suitable for a calibration factor to account for overestimation when determining annual NESHAPs compliance.

6 ACKNOWLEDGEMENTS

The contributions of Jaimie Massey, formerly with Energy Fuels who helped to plan and implement the study and Danny Flannery who performed much of the underlying field work is gratefully acknowledged.

7 REFERENCES

- [1] Energy Fuels Resources (USA) Inc. (Energy Fuels), 2013. Vent Shaft Gamma Survey and Sampling Report, Lakewood, CO, August.
- [2] Marcinowski, F., R.M. Lucas and W.M. Yeager, 1994. National and Regional Distributions of Airborne Radon Concentrations in U.S. Homes. *Health Phys.* 66(6): 699-706.
- [3] U.S. Environmental Protection Agency (EPA), 1985. Draft Background Information Document, Standard for Radon-222 Emissions from Underground Uranium Mines, Office of Radiation Programs, Washington D.C. February 14.
- [4] Data Summary Report Test of Method A-6 versus Method A-7 Radon Monitoring Side-by-Side Test Study EFRI 2014.
- [5] Revised Radon Monitoring Side-By-Side Test Plan at La Sal Mine Complex and Pinenut Mine EFRI February 4, 2011.

From Radiation Solutions for Engineering Problems to Engineering Solutions for Radiation Problems: the uses of industrial radiation

Edward Waller*

Edward Waller, UOIT, 2000 Simcoe St. N, Oshawa, Ontario, L1H7K4 CANADA

Abstract. The industrial benefits of ionising radiation were realised not long after the discovery of x-rays by Roentgen. Radiation has unique properties, depending upon the source, that range from shallow to highly penetrating through materials, which makes it extremely useful for industrial measurements. In addition, interaction mechanisms of radiation give it the ability to alter properties of materials with desirable endpoints. The fact that radiation cannot be detected by the human senses can be both an advantage and disadvantage when utilising radiation, and also underscores the fact that we require some sort of instrumentation for detection. The early and numerous uses of radiation also introduced potential associated hazards, ultimately yielding a new field of radiation protection and ultimately the as low as reasonably achievable (ALARA) principle. Historically, in an industrial setting, we have used radiation as a solution to engineering problems. Measurements of materials properties such as surface conditions, flaws, stress, flow, thickness, density, and composition are all possible with ionising radiation techniques. Monitoring industrial process conditions such as level and count, as well as presence of smoke or gas make radiation a very versatile technique. The uses of radiation for security issues, both in passive and active detection of contraband, are mainstream in society. Due to the potential hazards of ionising radiation, we have also needed to develop engineering solutions to potential problems associated with the use of radiation. Fission and fusion reactors are engineering marvels. Management of radioactive waste and spent nuclear fuel requires engineered storage solutions. Nuclear and radioactive materials in use or in storage require security measures in the form of physical protection systems to guard against potential theft and sabotage. Medical usage of radiation requires engineered solutions for isotope production and for shielding medical devices. Production and use of high energy radiation and radiation associated with space exploration, both near Earth and deep space, requires specialized engineering considerations. This paper considers historical, current and future industrial uses of ionising radiation and how the practise of radiation protection relates to these uses.

KEYWORDS: *Industrial, Radiation, Gauges, Safety, Monitoring, Material changes, Security, Shielding, Alternative technologies*

1 INTRODUCTION

Radiation has been used for material investigations (and the predecessor to industrial measurements) beginning shortly after Rontgen's discovery of x-rays [1]. The natural question one may ask is "*Why do we use radiation for industrial purposes?*" First and foremost, radiation interacts with basic building blocks of matter; that is, with the nucleus of an atom or the electron cloud around an atom. This allows radiation to provide information related to elemental composition and/or bulk properties. Radiation can be very penetrating, which allows investigation inside structures in which it would normally not be desirable to breach, such as pressure vessels. Radiation generally does not "touch" the material under investigation, which makes it non-intrusive/non-destructive. The application of a radiation-based technique is sturdy in harsh environments, such as those encountered in an industrial setting. Since radioisotope sources are small, the device used to make the measurement can be very portable. Finally, the technique can be used in-situ, which can be cost effective for industrial processes. It is clear that radiation can be, and has been, used to improve the quality of our lives, however the use of radiation-based techniques can also be hazardous if the radiation emitting system is not controlled properly. Therefore, as radiation protection professionals, it is in our best interests to understand the safe utilization of radiation for solving some of our most common engineering problems. Due to the possible hazards from misuse of radiation-based techniques, we need to design appropriate

* Presenting author, e-mail: ed.waller@uoit.ca

engineered systems around these sources, in the form of shielding, fail safe components and interlocks. Also, as radiation protection professionals, it should be our duty to understand the types of alternative technologies that could replace a radioisotope technology. The following sections describe some of the uses of radiation to solve industrial engineering problems, some of the engineering techniques needed to secure radiation sources, and the need to consider alternative technologies for industrial applications.

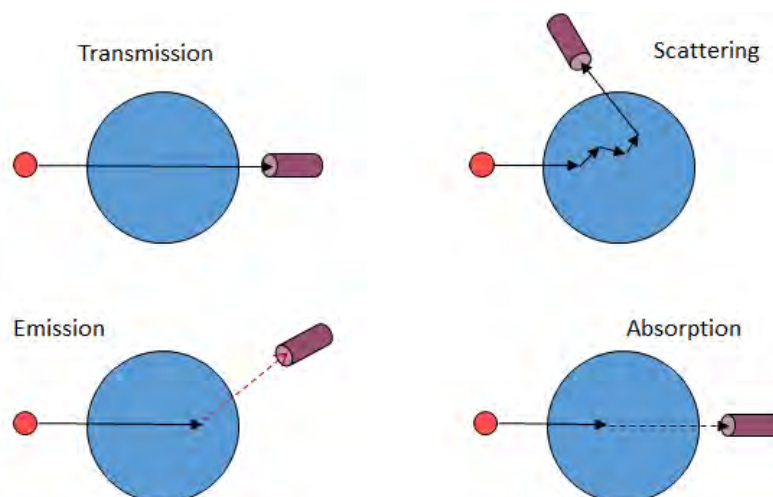
2 RADIATION FOR SOLVING ENGINEERING PROBLEMS

In the field of measurements (metrology), we use radiation for both probing and inspection of systems. We also use radiation-based techniques for industrial process monitoring, security applications and material modification. Finally, sometimes the radiation is providing a physical characteristic that we desire (such as nuclear fission energy). These concepts are discussed below.

2.1 Some Essential Physics

The types of radiation emissions that we consider for industrial applications can be broadly grouped into (i) heavy charged particles, (ii) light charged particles, and (iii) neutral particles. Which, on Earth, practically means alpha (α), beta (β), x-ray (x), gamma (γ) and neutron (n) radiations. The interactions can be quantified by range relationships, stopping powers, linear energy transfer, transmission and attenuation, scattering and capture formulae, etc. At accelerators, at high Earth altitude and extra-terrestrial environments the particle compositions and interaction mechanisms are augmented by other interactions such as spallation, intra-nuclear cascades, etc. The important point is that it is these interactions that provide information about the system under investigation, when radiation is used to interrogate a system. Broadly speaking, the four primary categories of interactions used for industrial measurements fall into either (a) transmission, (b) scattering, (c) emission and (d) absorption [2]. The categories are depicted in Figure 1.

Figure 1: Categories of radiation interactions for industrial measurements



In the transmission technique, radiation is sent into one side of a system being measured, and the radiation is measured on the other side. As such, transmission requires access to both sides of a system under investigation. The amount of radiation transmitted, either in an absolute or relative sense, can reveal information about the properties of the material under investigation, or can simply be a measurement of a bulk property (e.g. something is there or something is not there). Scattering can also yield information about the properties of a material the radiation is interacting with, or again bulk properties. The information

yielded through scattering can be more complex to analyse, however a great advantage is

only needing access to a single side of a system under investigation. Emission of secondary radiation can provide a great deal about the elemental composition of a material under investigation, and relies on the fact that some elements will emit characteristic radiation, usually at a specific energy, upon capture of the incident radiation. This technique can provide a “fingerprint” of a material. Absorption is the opposite of transmission, in so far as it is the lack of measurement of a radiation signal from incident radiation on a system under investigation, and again can provide “fingerprint” like information about the materials in the system.

Of course, any good textbook on atomic/nuclear physics, health physics, radiation protection or radiation detection and measurement can provide detailed discussions of the physics involved. For example, the seminal tome of Robley Evans [3], the health physics/radiation protection texts of Cember and Johnson [4] and Turner [5] and the radiation detection and measurement texts of Knoll [6] and Tsoufanidis and Landsberger [7] all have excellent discussions of the physics of radiation interactions.

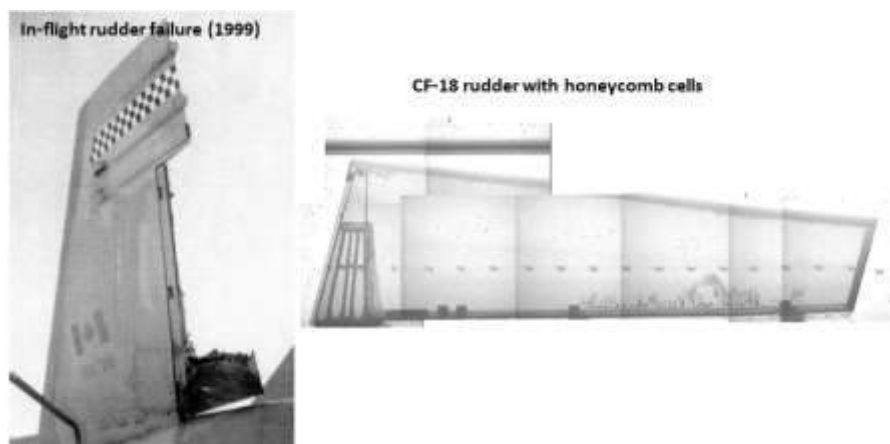
2.2 Metrology

For measuring system parameters, we can define some concepts. Probing is investigation of a particular location, inspection is an overall assessment that need not be location specific and monitoring is a passive process of probing or inspection [2]. We usually probe to look for specific characteristics in a material, process or system, and the process of inspection may include imaging.

A very commonly used type of measurement is Non-Destructive Testing (NDT). NDT is utilized worldwide to inspect pipe-welds, structures, vehicle components, etc. Radioisotopic sources, x-ray generators and even neutron sources are used in the technique. However, it is not uncommon for sources get *out of regulatory control* through bad practice and management. Indeed, numerous people have died from overexposure to radioisotope sources that become lost and are found by persons who do not know what they have found [8].

An interesting radiation based non-destructive application is neutron radiography. In Canada, early in the CF-18 fighter program, some aircraft were having in-flight control surface failures, as depicted in Figure 2. It was discovered, through the use of neutron radiography, that water ingression into the carbon-epoxy and aluminum honeycomb structure was causing delamination and control surface failure.

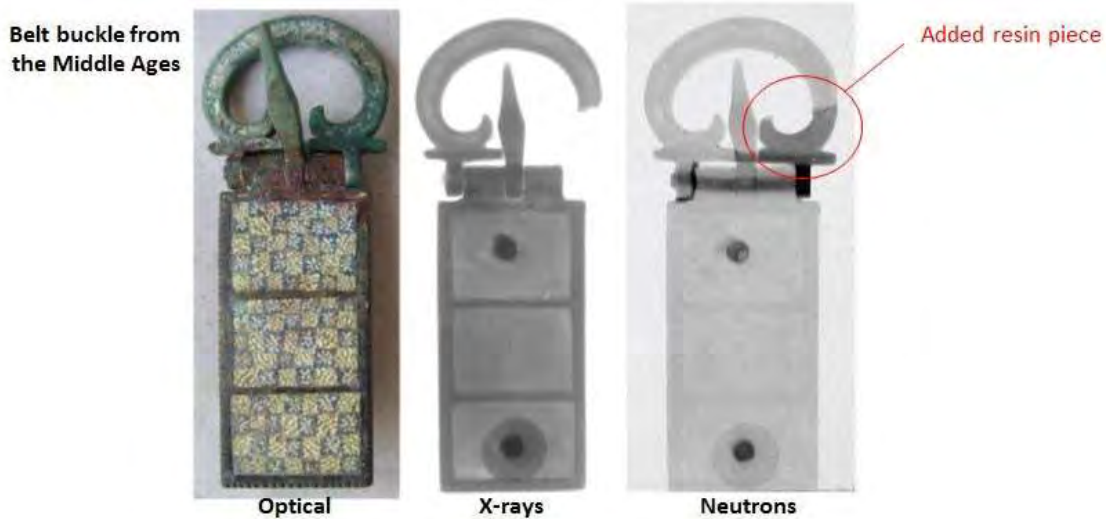
Figure 2: Neutron radiography on aircraft control surfaces [9][10]



There are a plethora of other examples of probing, inspection and monitoring possible. Another interesting example, comparing techniques, is taken from the historical sciences. In Figure 3, an x-ray and neutron radiograph are compared for a belt buckle of historical

significance. The neutron radiograph clearly shows that a light material (in this case a resin) was used to reconstruct part of the buckle. This is a clear demonstration that the appropriate radiation should be used for to obtain the greatest depth of information about the material under investigation. In addition, using multiple techniques can aid in greater understanding of the system under investigation.

Figure 3: Comparison of three non-destructive investigation techniques [11]

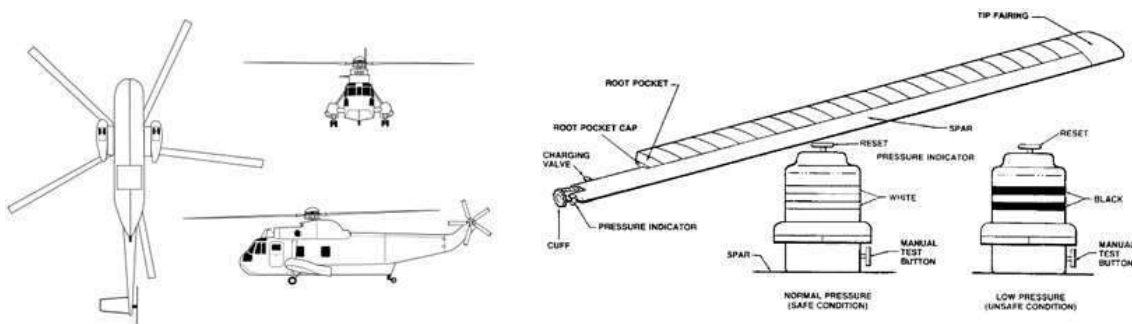


2.3 Industrial Process Monitoring

Industrial process monitoring can also be called gauging. In general we can monitor for gas and fumes (e.g. smoke detectors) and failure (e.g. stress), as well as industrial process parameters, such as flow, level, density, thickness, moisture, and voidage (porosity/permeability/firmness).

An interesting example of an on-line process monitor is an in-flight blade integrity system (IBIS). The IBIS uses a small (~3.7 MBq) ⁹⁰Sr source which is normally shielded. When pressure in the main rotor blade spar drops, the source becomes unshielded. There is a (non-radioactive) visual indication externally, and in-flight cockpit indication of blade integrity through detection of beta radiation with an ionization chamber. This system is seen in Figure 4.

Figure 4: Beta radiation low pressure indicator for helicopter rotors



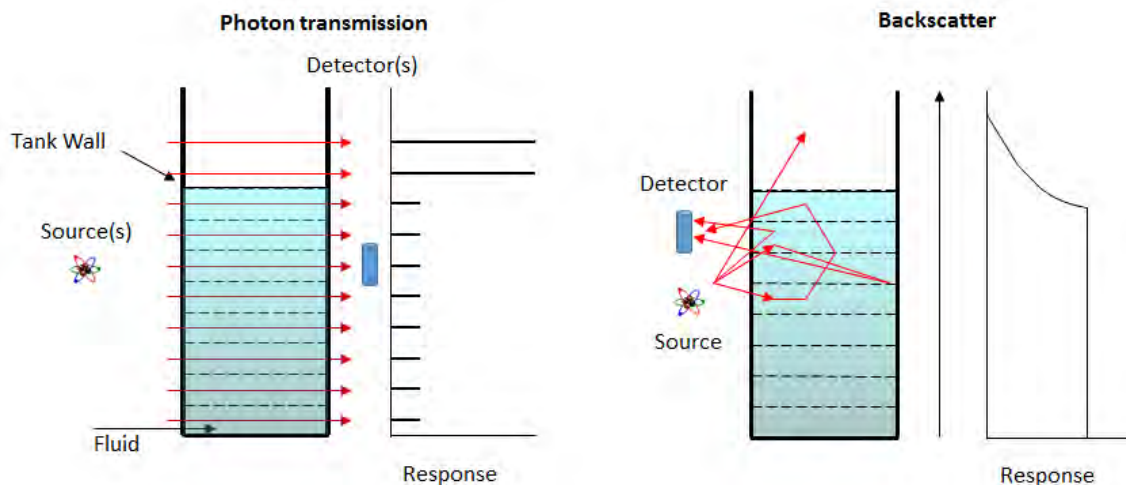
More common are process monitors that involve attachment of a radioisotope source to a vessel, tank or conveyor and placing a detector or multiple detectors to measure, typically, radiation transmission. A line source (left) and a point source (right) may be seen in Figure 5. The actual metallic sources are seen in the figure, and it is worthy to note that the line source is actually a metal (^{60}Co) wire wrapped around a metal rod (the helical wrap is depicted on the left of the figure).

Figure 5: Line (left) and point (right) source gauges for industrial measurement (photos courtesy J.A. Tompkins, IAEA)



Gauges have been used to measure paper, metal and plastic sheet thickness, cigarette rope thickness, density and moisture of soil and asphalt and fluid flow/leakage from pipes. One very common measurement is the level gauges, depicted in Figure 6. The detector response in either case is directly related to the material location in the system. In transmission, the less material between source and detector, the greater the response at the detector. Alternately, in backscatter, less material will result in a drop in detector response. In either case, the change in detector response is indicative of an interface, or in this case, the level. As was alluded to before, with vessels in which you do not want to violate the pressure boundary, this non-intrusive way to measure level is extremely desirable.

Figure 6: Transmission and backscatter level gauges



Although radioisotope gauges are capable of providing complex information about a system, the actual gauges are relatively simple in construction. A representative radioisotope gauge is

depicted in Figure 7. The gauge housing is essentially one large shield of (typically) a steel shell filled with lead. An armature rotates a drum with a hole drilled through it, which acts as a collimator. When the source is “off”, the drum is rotated so that the radiation from the source has no direct (unobstructed) pathway to the exit aperture. When the source is “on” the drum is rotated such that the radiation has a line-of-sight pathway to exit the shield. There are, of course, variations to this, depending upon the gauge manufacturer.

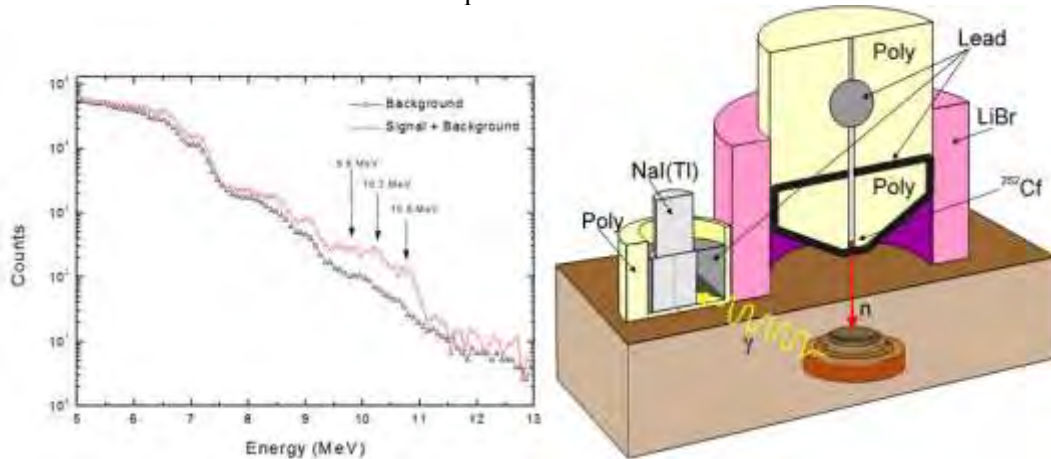
Figure 7: Typical industrial gauge being disassembled



2.4 Security Applications

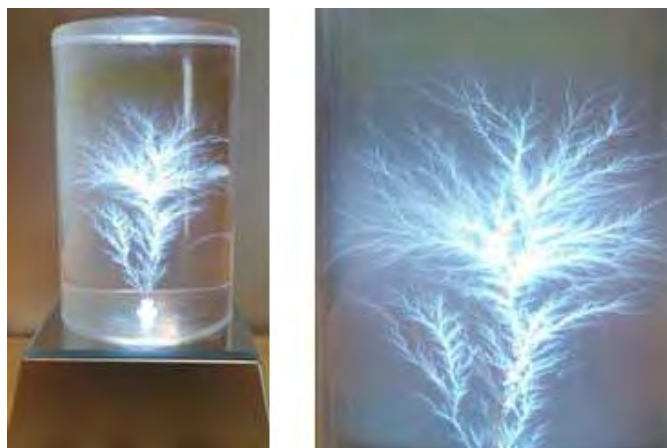
Radiation has been used in security applications for a very long time. Radiation techniques are used in illicit material detection, for example in packages or on persons, for contraband (e.g. drugs) detection, for detection of prohibited items (e.g. knives) and for items that may be used with malicious intent (e.g. explosives and firearms). In addition, radiation techniques are used in border crossing detection of the above, and also radioactive material and special nuclear material (SNM) detection at airports, land crossing and seaports.

One interesting application of a radiation based technique for security applications is that of landmine detection. One of the main problems of anti-personnel landmines is that they can be made with little to no metal content, and as such can be extremely difficult to detect using traditional means. Explosives, however, contain between 30-40% nitrogen by mass, and therefore a technique that can detect nitrogen can also detect the explosive in landmines. Neutron activation of ^{14}N yields a very specific gamma ray signature at 10.8 MeV, which is in a very useful portion of the natural background spectrum (as there are no significant natural gamma ray emitters at that energy). A system that makes use of thermal neutron activation (TNA) for landmine detection is depicted in Figure 8. On the right of the figure you can see a TNA-based system, in which fast neutrons from spontaneously fissioning ^{252}Cf enter soil and interact with ^{14}N in an explosive. Upon activation, the nitrogen de-excites through emission of a 10.8 MeV gamma ray. This gamma ray is measured by a gamma spectroscopy system (in this case, based upon sodium iodide scintillation detectors) to create the spectrum observed in the left of Figure 8 (it is noted that the single and double escape peaks are both present as well). Comparing the TNA signal with the background gives a clear indication of an explosive.

Figure 8: Thermal neutron activation for explosives detection

2.5 Material Modification

Radiation can be used to induce desirable material changes. Radiation can be used for sterilization, with respect, for example, to bulk items, food and pest control. Packages medical supplies are routinely irradiated to high absorbed dose to destroy bacteria and viruses that may have been introduced into the packaging, and that would not be desirable if introduced into a human body during a medical procedure. The mechanism of destroying a bacteria or a virus is the same mechanism as that in which radiation can harm humans. Food irradiation works the same way in so far as if bacteria and viruses are killed on food, the food does not change but with the absence of bacteria/viruses it will last longer and be safer. The sterile insect technique (SIT) works by reproductively sterilizing a pest (for example, male mosquito) and then re-introducing it back into the pest colony, which has the effect to curb reproduction. This technique is currently being used against the spread of the Zika virus in some countries. Radiation induced cross-polymerisation can be used to alter the mechanical properties of some materials. For example, wire bundles in car engines have usually been irradiated to change their properties, such that they will not crack under large changes in temperature. Radiation has been used to color certain gemstones, such as topaz (through the introduction of so-called color centres), to change them from clear to blue. And other, more esoteric, uses of radiation can include using radiation for art. An example includes production of Lichtenberg figures, as depicted in Figure 9. This item is made by directing a beam of electrons into a plastic cylinder, such that the electrons stop within the plastic. This has the net effect of charging the plastic up, like a capacitor. The end face of the plastic can then be struck with a grounded hammer, resulting in a discharge path for the electrons. The electrons generate a plasma that etches tracks in the plastic, producing the effect observed in the figure.

Figure 9: Beautiful Lichtenberg figure

2.6 Radiation as the Resource

Although we use radiation as a tool for industrial application, radiation can also be the resource. For example, in nuclear power, the radiation from fission deposits heat, in which we turn water to steam and steam to run a turbine and generator for electricity. Radiation can also be used in radioisotopic thermoelectric generators (RTG) when you need a source of electricity with no maintenance (such as remote Earth locations or space probes). Radiation sources have also been used as batteries, for example, in cardiac pacemakers. Other applications include static eliminators, electron vacuum tubes, self-luminous indicators (signs, watch hands, etc) and lightning rod conductors. In all of these cases, radiation is the solution to the engineering problem!

3 ENGINEERING FOR SOLVING RADIATION PROBLEMS

Due to the potential hazards that can be associated with radiation-based industrial applications, a great deal of engineering is required to protect workers, the public and the environment from radiation. Some examples include nuclear reactors, radioactive waste management systems, nuclear security applications, medical applications, high energy physics facilities and space applications. One common area of engineering used to protect us from radiation exposure is shielding design, which is required in reactors, medical facilities, industrial facilities, high energy accelerators and space applications. We also need engineering solutions to short and long term storage of radioactive waste. On the radioactive source safety side, we need safety engineered systems consisting of redundancy, diversity and interdependence. In short, we need to protect people from radiation sources. On the security side, we need engineered solutions for physical protection systems and nuclear material accountancy and control. In short, we need to protect the radiation sources from people!

4 CONCLUSION

It can be seen that the use of radiation to solve engineering problems and the use of engineering to solve radiation problems have complementary roles. There industrial use of radiation and radioactive sources will continue into the future and we as radiation protection professionals need to understand and manage the risks. In addition, we should be knowledgeable in alternative technologies such that we can help industries make risk-informed decisions when selecting probing, gauging and measurement tools. Radioactive source security should continue to be a priority with all people working with radioisotope sources.

5 REFERENCES

- [1] Assmus, A., 1995. Early History of X-Rays. Beam Line. Pp. 10-24. Retrieved 2016-01-18 from <http://www.slac.stanford.edu/pubs/beamline/25/2/25-2-assmus.pdf>
- [2] Hussein, E. 2007. Radiation Mechanics—Principles and Practice. Elsevier, New York, NY.
- [3] Evans, R. 1955. The Atomic Nucleus. McGraw-Hill Book Company. Toronto, ON.
- [4] Cember, H. and Johnson, T. 2009. Introduction to Health Physics, 4th ed. McGraw-Hill, Toronto, ON.
- [5] Turner, J. 1995. Atoms, Radiation, and Radiation Protection, 2nd Edition. Wiley Interscience, Toronto, ON.
- [6] Knoll, G. 2010. Radiation Detection and Measurement, 4th Edition. Wiley, New York, NY.
- [7] Tsoulfanidis, N. and Landsberger, S. 2015. Measurement and Detection of Radiation, 4th Edition. CRC Press. Boca Raton, FL.
- [8] IAEA. 1998. Lessons Learned from Accidents in Industrial Radiography. International Atomic Energy Agency. IAEA Safety Report Series No.7. Vienna, Austria.

- [9] Bennett, L., Lewis, W. and Hungler, P. 2013. The development of neutron radiography and tomography on a SLOWPOKE-2 Reactor, *Phys. Procedia*. 43:21-33.
- [10] Edwards, A. 2010. Characterization of the Effects of Water and Disbond on Ultrasonic Signals in Honeycomb Composite Structures. The 3rd International CANDU In-Service Inspection and NDT in Canada 2010 Conference. Toronto, ON.
- [11] Mannes, D., Lehmann, E., Masalles, A., Schmidt-Ott, K., Przychowski, A., Schaeppi, K., Schmid, F., Peetermans, S. and Hunger, K. 2014. The study of cultural heritage relevant objects by means of neutron imaging techniques, *Insight*. 56(3):137-141.

Patrimonial management of source term in French nuclear power plants

François Drouet^a, Serge Blond^b, Alain Rocher^c, Charlotte Dabat-Blondeau^d, François Renard^d, Samir Ider^e

^aEDF Saint-Alban NPP, Saint-Maurice l'Exil, France.

^bEDF NPP Operations, Saint-Denis, France.

^cEDF UNIE, Saint-Denis, France.

^dEDF UTO, Montevrain, France.

^eEDF CIDEN, Lyon, France.

Abstract. In the next few years, EDF which operates the 58 nuclear power plants in France, will implement an important maintenance and modification program on all the nuclear units. The objective of these activities is to maintain the safe production capacity of the French nuclear fleet. This program implies a significant increase of the work volume in radiation controlled area and will then have an influence on the total collective dose. One of the main stakes is then to identify the actions to manage the radiation exposure of workers. The source term management is one of the principal actions to optimize radiation exposure for which the operator of the unit is directly responsible for. The source term can be managed through preventive (cold shutdown management – use of materials, which cannot be activated, etc.) and curative (chemical decontamination, hot spot management, use of biological shielding) actions. To secure the implementation of curative actions during outages, a long-term program of these actions has been defined. The approach, which has been validated by the management of EDF Nuclear Power Plant Operations, aims to reduce the dose rate of circuits in the most polluted units. The objective of the presentation is to present the approach which has been implemented at the EDF corporate level to define an optimized program of the source term curative actions for the period 2015-2021 (analyze of the source term indicators, discussion with the units to identify the best outage for implementing the action, etc.). Some first feedback experience will also be discussed.

1 INTRODUCTION

In the next few years, the implementation of an important maintenance and modification program in the French nuclear power plants will have a significant impact on the dose results. The source term management has been identified by the EDF Nuclear Power Plant Operations as one of the major levels to mitigate the increase of collective dose.

In order to secure their implementation, a long-term program of the curative actions on the source term has been defined and validated both by the management of the EDF NPP Operation and the management of each NPP.

The objectives of this paper are to detail the methodology implemented to build the program and to present the very first results of the implementation of the program.

2 SOURCE TERM INDICATORS

Three main source term indicators are measured during each outage: the loop index, the reactor building index and the CZT measurements. These indicators and their evolution are used to analyze the follow-up of the radiological state of the circuits and to establish a benchmark between the different units. The following table describes the specificities of each indicator.

Table 1:

Indicator	Loop index	Reactor building index	CZT measurements
Where?	9 to 12 measurements - 3 measurement points on each loop (hot, cold and U legs)	40 to 50 measurement points on each level of the reactor building	8 measurement points : 3 on RCS, 3 on RHRS, 3 on CVCS, 1 on SIS
When?	12 to 16 hours after shut down	When downgrading red zone areas of the reactor building	Before and after RCS oxygenation
Since when?	1980	2011	2011
Why?	Knowing and comparing RCS contamination	Knowing and comparing auxiliary circuits contamination	Characterising the nature of contaminants of circuits

3 RESULTS AFTER 2014 OUTAGES

The 2 following tables present the synthesis of the indicators for respectively each 900 MWe and 1300-1450 MWe units after 2014 outages.

- The red color means that the indicator is above 25% of the average for the standardized plants,
- The green color means that the indicator is below 25% of the average for the standardized plants,
- The up arrow (↗) means that the indicator increased by more than 25% compared to the previous outage,
- The down arrow (↘) means that the indicator decreased by more than 25% compared to the previous outage,
- The smileys mean:
 - o For the dose rate column
 - 😊 more than 5 green index,
 - 😞 more than 5 red index,
 - 😐 other cases.
 - o For the dose/hr.RCA column
 - 😊 the indicator average dose received per hour spent in radiation controlled area is below 25% of the average for the standardized plants,
 - 😞 the indicator average dose received per hour spent in radiation controlled area is above 25% of the average for the standardized plants,
 - 😐 other cases.
 - o For the evolution column
 - 😊 more than 5 down arrows,
 - 😞 more than 5 up arrows,
 - 😐 other cases.

Table 2:

900 MWe	2014 outages												Synthesis		
	Dose/hr.RCA	I _{Loop}	I _{RB}	RB sub-index									Dose rate	Dose/hr.RCA	Evolution
				RHRS	CVCS	NVDS	SIS	PZR	SG	RCS	FPCS				
1		↗	↗			↗	↗		↗	↗	↗	☹	☹	☹	
2	↗											☹	☹	☹	
3	↘				↘		↘	↘	↘	↘		☹	☹	😊	
4		↗	↘	↗	↗	↘	↗				↘	☹	☹	☹	
5		↗	↗		↗	↘			↗	↗	↗	☹	☹	☹	
6	↗	↘	↗	↗	↗	↘	↗			↗	↘	😊	☹	☹	
7	↗						↗		↘		↘	😊	☹	☹	
8	↘				↘		↗	↗	↗		↘	😊	😊	☹	
9						↘	↗	↗	↘	↗	↗	😊	😊	☹	
10	↗	↗				↗	↗	↘			↘	☹	☹	☹	
11	↘		↘				↘			↘	↘	😊	😊	😊	
12	↗	↗	↗	↗		↗	↗	↘	↗	↗	↘	☹	☹	☹	
13		↗	↘	↘			↘	↘	↘	↘	↘	😊	😊	😊	
14		↗			↘	↗	↘	↗	↘	↗	↗	😊	😊	☹	
15			↘	↘		↘	↘		↘		↘	😊	☹	😊	
16			↗	↗		↗	↗	↘	↘	↗		☹	☹	☹	
17						↘	↘	↗			↘	😊	☹	☹	
18	↘	↗	↘	↘		↗					↗	☹	😊	☹	
19				↘		↗		↘			↘	😊	☹	☹	
20			↘				↘	↘	↘	↘		😊	☹	😊	
21		↘	↘	↘	↘	↘	↘			↘	↘	😊	☹	😊	
22				↘	↘	↘	↘	↗	↘	↗	↘	☹	☹	😊	
23				↗		↘		↘	↘		↘	☹	☹	☹	
24	↘		↘	↗	↘	↘	↗	↗	↘	↘	↘	☹	☹	😊	
25		↗	↘	↘	↗			↗		↘	↘	☹	☹	☹	
26							↘			↗	↘	☹	☹	☹	
27	↗	↗	↗		↗	↗	↗	↗	↗	↗	↗	☹	☹	☹	
28		↗			↗	↗					↗	☹	☹	☹	
29				↗			↗			↗	↘	☹	☹	☹	
30						↗	↘	↗			↗	☹	☹	☹	
31				↘	↗			↘	↗		↗	☹	☹	☹	
32				↘	↗	↘	↘	↘		↗	↗	☹	☹	☹	
33				↗	↘	↗	↗				↗	😊	☹	☹	
34	↗			↗			↘	↗			↘	😊	☹	☹	

Table 3:

1300 - 1450 MW	2014 outages											Synthesis		
	Dose/hr.RCA	I _{Loop}	I _{RB}	RB sub-index								Dose rate	Dose/hr.RCA	Evolution
				RHRS	CVCS	NVDS	PZR	SG	RCS	FPCCS				
1			↘	↘		↘	↘	↘			↘	☹	☹	😊
2				↗					↘		↗	☹	☹	☹
3			↗		↗	↗			↗	↗	↘	☹	☹	☹
4			↗	↗				↘	↗	↗	↘	☹	☹	☹
5										↗		😊	😊	😊
6	↘		↘	↘	↘	↗	↘		↘		↘	☹	😊	😊
7				↗		↗	↗		↗	↗	↗	😊	😊	☹
8		↗				↗	↗				↘	😊	😊	😊
9	↗				↗			↘			↘	😊	😊	😊
10					↘		↗				↗	😊	😊	😊
11	↘				↘		↗	↘				😊	😊	😊
12	↗				↗			↘			↘	😊	😊	😊
13						↘	↗		↘		↗	😊	😊	😊
14							↘				↘	😊	😊	😊
15											↗	😊	😊	😊
16			↗	↗	↗			↗	↗			😊	😊	☹
17				↗	↗			↗	↘		↘	😊	😊	😊
18	↘				↗	↗			↘			😊	😊	😊
19						↘	↗	↘			↘	😊	😊	😊
20	↗	↗		↘	↗		↗	↘			↘	😊	☹	😊
21	↗			↗	↘	↘	↘	↘			↗	😊	😊	😊
22			↗	↗	↗	↗	↗	↗	↗	↗	↗	😊	😊	☹
23			↗	↗	↗		↘	↗			↗	😊	😊	☹
24	↘			↗	↗	↗	↘	↘	↘	↗	↘	😊	😊	😊

4 PROPOSED CURATIVE ACTIONS AND DECISION MAKING PROCESS

Three different curative actions can be proposed to manage the source term:

- CADOR, which is a software developed for EDF to optimize the use of biological shielding on the RCS during outages. The software proposes the localization of biological shielding depending on the activities to be realized during the outage. In parallel with the implementation of that tool, new materials are provided and advisors are available on the field to provided case-by-case biological shielding solutions.
- Chemical decontamination of circuits using a specific process. The choice of the process depends on the major radionuclide in the contaminated circuit. The nature of the pollutant is determined with the CZT measurements. Up to now, the chemical decontamination is implemented specifically on CVCS and RHRS.
- Hot spots elimination actions. Many treatments can be implemented such as flushing, replacement of valves, etc. The EDF feedback experience is synthesize in an internal document which is used by the units.

Depending on the results of the measurements, different curative actions can be proposed. The following table describes the decision process.

Table 4:

SYSTEM	INDEX	CURATIVE ACTION
RCS	If the I_{loop} and/or RCS and/or SG index are red, this means that the primary circuit is contaminated	CADOR and/or zinc injection (not treated in this work)
RHRS/CVCS	If the RHRS and/or CVCS index are red, this means that RHRS and/or CVCS are contaminated	Chemical decontamination with the EMMAC-POA or EMMAg process
OTHER AUXILIARY SYSTEMS	If the NVDS and/or SIS and/or PZR and/or FPCCS index are red, this mean the unit is polluted with hot spots.	Hot spot treatment

5 PROGRAM PROPOSAL

Using this methodology, it appears that the source term of 43 units over the 58 of the EDF fleet could be improved by implementing one or more of the proposed solutions:

- One proposed curative action for 15 units,
- Two proposed curative actions for 14 units,
- Three proposed curative actions for 14 units.

In order to make the program realistic, the feasibility of the integration of CADOR and chemical decontamination actions in the maintenance program of each outage has been evaluated.

- CADOR: 35 implementations planned between 2015 and 2021 (3 to 8 each year),
- Chemical decontamination: 27 implementation planned between 2015 and 2021 (1 to 6 each year),
- Hot spot treatment: 28 units to be treated.

6 CONCLUSIONS

The first feedback of this work is the following:

- In 2015, the CADOR software has been implemented on 6 outages with an estimated dose benefit between 20 and 40 person.sieverts depending on the outage,
- In 2015, one chemical decontamination of CVCS has been performed with an estimated dose benefit is about 600 person.sieverts over 5 years. The cost-benefit of this activity is positive,

These first results are encouraging because the dose savings easily justify the costs of the treatment. The management at the top-level of the EDF Nuclear Power Plant Operations of these actions remains essential in order to assure that the proposed program is implemented and efficient.

7 GLOSSARY

CVCS – Chemical and Volumetric Control System

CZT – Cadmium Zinc Tellurium

EDF – Electricité de France

FPCCS – Reactor Cavity and Spent Fuel Pit Cooling and Treatment System

NPP – Nuclear power plant

NVDS – Nuclear Island Vent and Drain System

PZR – Pressurizer

RCA – Radiation Controlled Area

RCS – Reactor Cooling System

RB – Reactor Building

RHRS – Residual Heat Removal System

SIS – Safety Injection System

SG – Steam Generator

Public Dose Assessments for Atmospheric Pathways at Rössing Uranium Mine, Utilising Direct Monitoring Data

Gunhild von Oertzen^{a*}

^aRössing Uranium Limited, Private Bag 5005, Swakopmund, Namibia.

Abstract. The risks to the public from the mining operations at Rössing Uranium include those from the inhalation of radioactive dust and radon as are generated and emitted in on-site mining processes. Typically, public dose assessments involving atmospheric pathways require detailed quantification of dust and radon emissions, which then inform atmospheric dispersion models, from which resulting inhalation doses of members of selected critical groups are calculated. This process is laborious, and often the dispersion models can be inaccurate. This paper describes a process for arriving at inhalation doses for the public that is based on site specific measurements of atmospheric dust and radon, correlated with wind speed and direction. This method allows a quick assessment of dose-relevant dust and radon concentrations, and leads to a reliable risk assessment for public exposures, based on empirical air quality data rather than model predictions, as is otherwise often used in public dose assessments.

KEYWORDS: *public dose assessment; uranium mining; long-lived radioactive dust; radon; atmospheric pathway.*

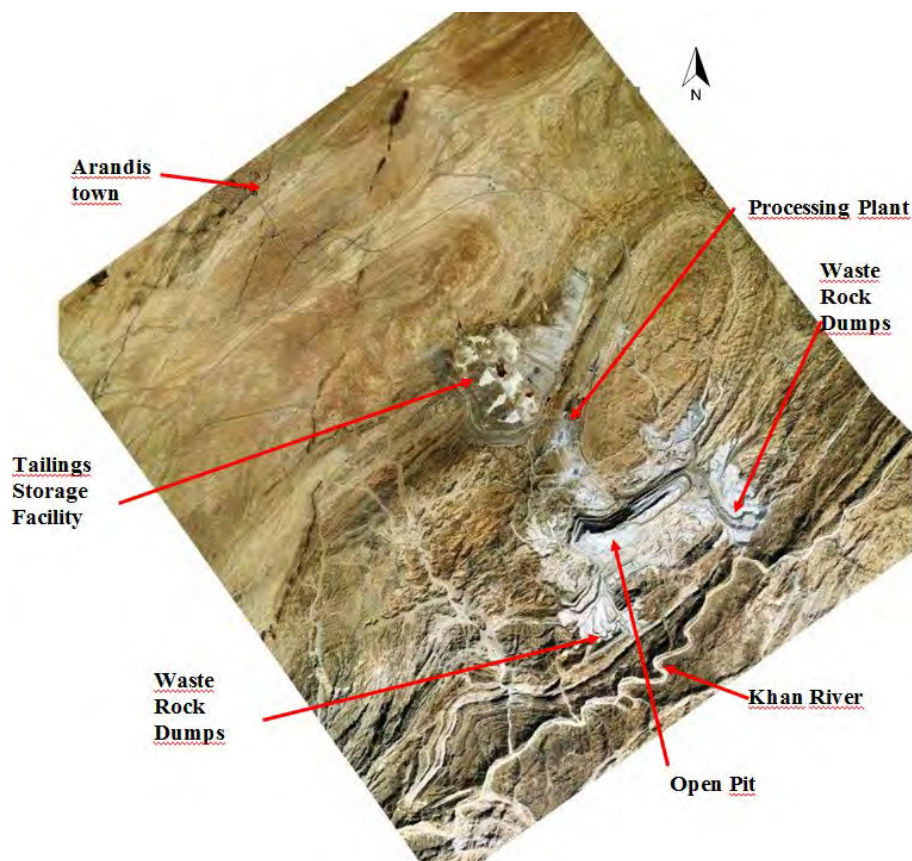
1 INTRODUCTION

Rössing Uranium Limited (Rössing Uranium) is an open pit uranium mine located in the Namib Desert in western Namibia. It is located some 60 km inland from the coastal town of Swakopmund, and about 10 km from the town of Arandis, which is home to many of Rössing Uranium's workers, both those employed there currently and those who are retired or otherwise no longer employed at the mine. The mine has a footprint of 2,500 ha, with disturbed areas including the Tailings Storage Facility (TSF) and the Waste Rock Dumps (WRD) combined covering about 1,400 ha, as well as the mining pit with a surface area of approximately 440 ha.

The mine is located in a dry desert environment, with little or no vegetation cover, and seasonal episodes of strong wind. The closest community to the mine site is that of Arandis, the population of which represents the critical group for public radiation exposures along the atmospheric pathway. The mining operation results in the emission of low-grade long-lived radioactive dust (LLRD), both from the mining operations in the pit, as well as from the exposed surfaces of the dry TSF and the WRD. In addition, these structures are also a source of radon exhalations.

The inhalation dose to the public at Arandis from the two atmospheric pathways (inhalation of LLRD and inhalation of radon progeny resulting from the mining operation) needs to be quantified so as to allow a comparison with the Namibian public dose limit which is set at 1 mSv per annum.

* Presenting author, e-mail: Gunhild.vonoertzen@riotinto.com

Figure 1: Satellite image of area surrounding Rössing Uranium mine, scale: 1:60,000

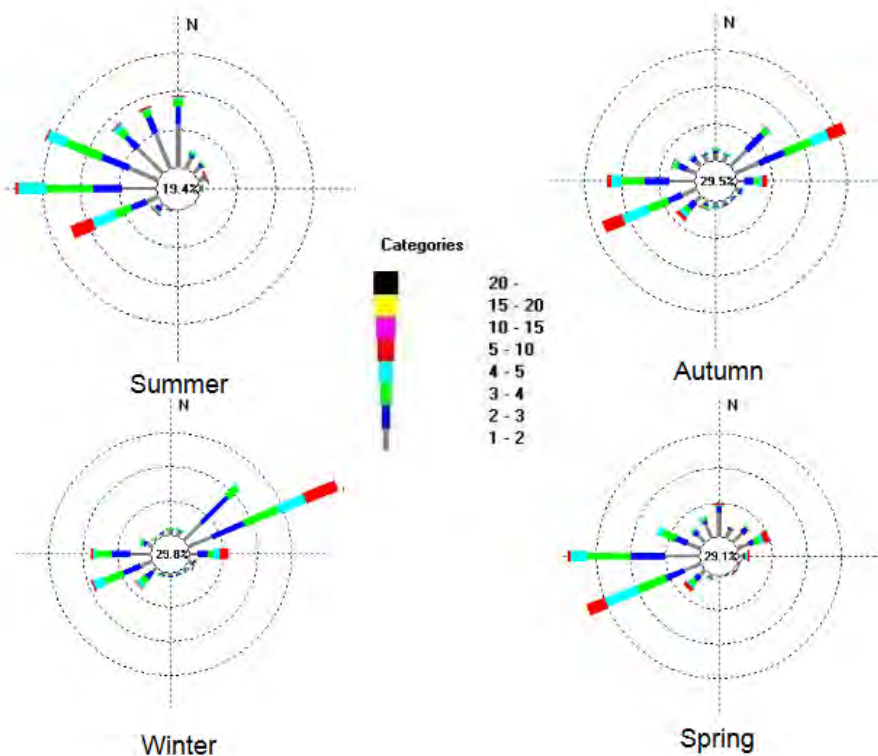
1.1 Geographical setting

The geographical location and layout of Rössing Mine is indicated in Figure 1. Mining takes place by way of blasting, loading and hauling from the main open pit, before the uranium-bearing rock is processed and uranium oxide is produced. The open pit measures 3 km by 1.5 km and is 390 m deep. Waste rock is deposited on the existing rock dumps around the pit.

Run of mine material is fed through primary and secondary crushers to the metallurgical processing plant, where uranium is leached from the ore and transferred into solution. The remaining mineral substrate is removed from the leachate and transported to the TSF by conveyor. Uranium-rich slimes are washed in a thickener circuit, after which the barren slimes are pumped to the TSF. Here, sand and slimes are recombined and deposited on the TSF in a paddock deposition system.

The mining area is characterised by three dominant wind patterns, i.e. a sea/land breeze system created by the interface between air from the cold Atlantic Ocean and the warm continent, a mountain valley system induced by the Khan and other close-by dry river systems draining from the escarpment towards the coast, and a system resulting from the altitude difference between the central highlands and the coastal plains [1]. Representative wind roses are displayed in Figure 2. The highest wind speeds are reached in autumn and winter, and result in winds in a north-east-east (NEE) direction, and a south-west-west (SWW) direction in autumn. During spring and summer, the prevailing winds are predominantly from westerly directions.

Figure 2: Prevailing wind directions at Rössing Mine, after [2]. The frequency interval between one circle and the next bigger one is 5%, and the colour codes indicate the wind speed in metres per second (m/s).



2 SAMPLING LOCATIONS

Sampling locations for air quality monitoring were selected with consideration to the geography of the area. Air samplers collecting the inhalable fraction of the air, i.e. the so-called particulate matter smaller than 10 microns, or PM10, were placed to the NEE and SWW of the mining area, thus representing the downwind directions during times where the strongest winds are expected. Another PM10 sampler is installed at the town of Arandis, although the location of this critical group is not downwind during strong wind episodes (Figure 3).

In addition to the three PM10 samplers indicated in Figure 3, one radon station is positioned directly north of the TSF, which is the principal source of radon exhalations at the mine of relevance to the critical group of members of the public residing at Arandis.

3 PUBLIC DOSE ASSESSMENT

Data from the air quality monitoring stations includes hourly readings of the PM10 dust concentration, wind direction and wind speed. In the case of the radon station, ambient atmospheric radon concentration, radon progeny concentration, wind direction and wind speed, amongst others, are available in 10-minute intervals.

This information may be correlated with the known geography of the receptor location relative to the mine. When the wind is blowing from the mine site towards the receptor, the dust and radon arriving there are likely of mining origin. If the wind is not blowing from the mine site, the concentrations measured are likely of background origin and will therefore not likely contribute to the mining-related public exposure dose.

Figure 3: Rössing mine in relation to the locations of PM10 samplers (red) and radon monitoring station (blue)

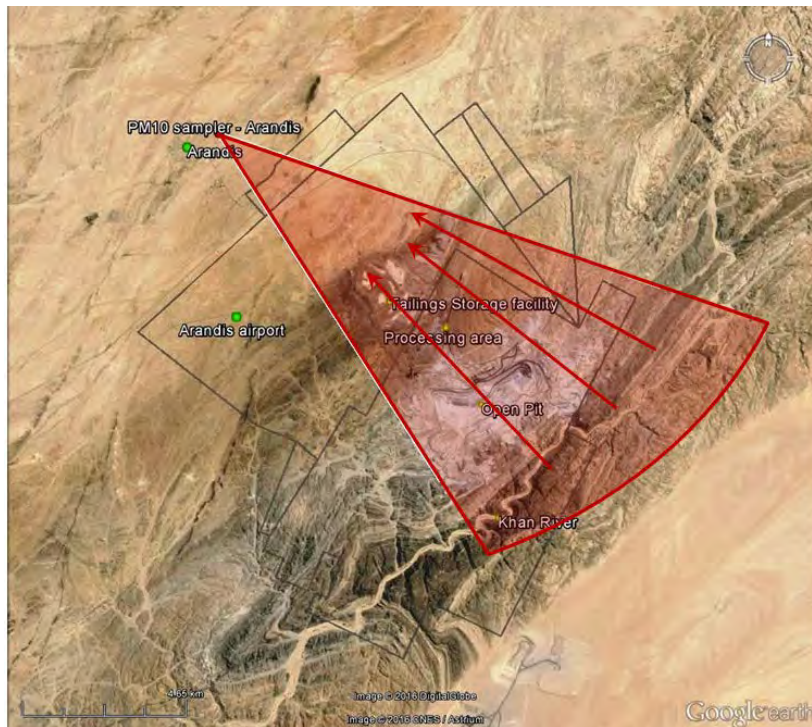


3.1 Long lived radioactive dust (LLRD)

We correlated the wind direction at each of the three PM10-samplers mentioned with the direction relative to the mine, for a full year. One of these three PM10 samplers is located at the town of Arandis, the nearest public receptor. The two other PM10 samplers are located roughly downwind of the mine during major wind events, i.e. one on the SWW boundary of the mine, and to the NEE of the mine.

For example, for the PM10 sampler at Arandis, the wind directions from the mine are between 110 and 147 degrees from true north (Figure 4), where 0 degrees represents a wind blowing directly from the north.

Figure 4: Wind directions relative to mining related contributions to the dust concentration at Arandis, indicated as a red segment superimposed on the satellite image of the area.

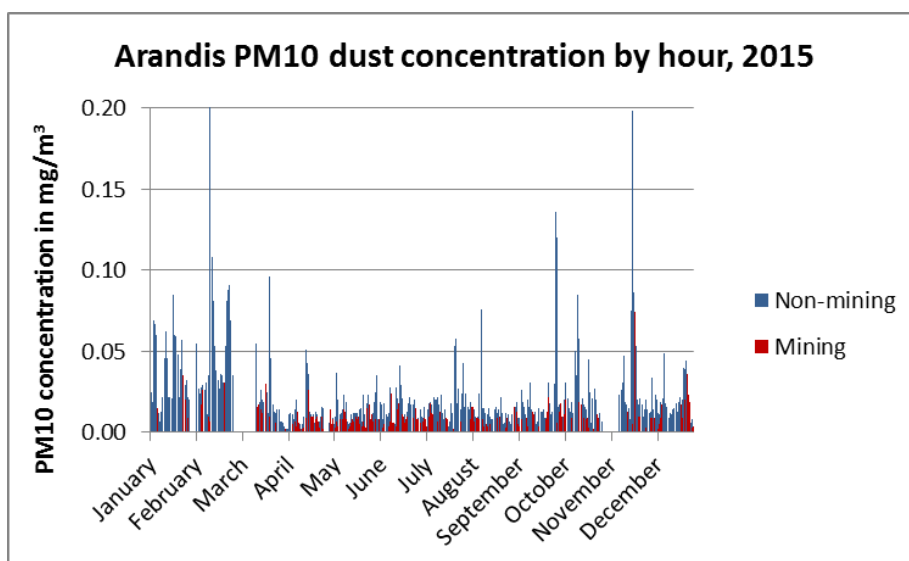


Similarly, the wind directions at the SWW mine boundary PM10 station relative to the mine are between 9 and 90 degrees.

The third PM10 monitoring station is located at to the NEE pf the mine. Here, the wind directions from the mine range between 148 and 248 degrees.

For Arandis, the measured PM10 dust concentrations are displayed in Figure 5. A major part of the ambient dust in air at the town originates from directions other than that of the mine, as can be anticipated from the wind roses representative for the area, and only some 5% of the year does the town receive winds directed from the mine.

Figure 5: Hourly PM10 concentrations measured at the town of Arandis during 2015



In order to arrive at the public dose for this location, we have performed a radionuclide analysis of the PM10-portion of typical dust as measured at Arandis. Using the dose conversion coefficients from the IAEA's Basic Safety Standards (BSS, [3]), the required dose conversion coefficients and respective public dose for the proportion of dust that is not of mining origin is determined. For the portion of the dust that arrives at the receptor location from the direction of the mine, we make the worst-case assumption, i.e. that such dust is pure ore dust originating from the mining and crushing process. On average, the uranium concentration of the ore processed at Rössing is of the order of 300 parts per million (ppm). Using this information, and based on the coefficients given in the BSS, we arrive at the required conversion coefficients for the public dose at this location.

The annual dose is then given by

$$Dose = C \cdot BR \cdot t \cdot \sum_i DCF_i \cdot A_i, \quad (1)$$

where

<i>Dose</i>	is the annual dose in micro-Sieverts per annum ($\mu\text{Sv/a}$),
<i>C</i>	is the measured PM10 dust concentration in micro-grams per cubic metre ($\mu\text{g/m}^3$),
<i>BR</i>	is the assumed breathing rate of members of the public in cubic metres per hour (m^3/h),
<i>t</i>	is the occupancy time in hours per year (h/a),
<i>DCF_i</i>	is the dose conversion coefficient from radionuclide <i>i</i> from the uranium, actinium and thorium decay chains in Sieverts per Becquerel (Sv/Bq), and
<i>A_i</i>	is the specific activity of radionuclide <i>i</i> in (Bq/g).

Table 1 summarises the relevant conversion coefficients, measured PM10 dust concentrations and resulting mining and background doses for members of the public.

Table 1: Measured PM10 dust concentrations, wind directions, dose conversion coefficients and annual dose from background and mining origin respectively, for the year 2015.

	Adult	Infant < 1 year	Proportion of year measured	Location
$\sum_i DCF_i \cdot A_i$, background origin ($\mu\text{Sv/g}$)	120	425		
$\sum_i DCF_i \cdot A_i$, mining origin ($\mu\text{Sv/g}$)	200	675		
Breathing rate (m^3/h)	0.9	0.2		
Occupancy time (h/a)	8 760			
Average PM10 concentration, related to mining ($\mu\text{g}/\text{m}^3$)	8.2		4%	Arandis
Average PM10 concentration, non-mining related ($\mu\text{g}/\text{m}^3$)	10.9		96%	Arandis
Annual dose, non-mining related, corrected for wind direction, $\mu\text{Sv/a}$	9.9	7.8		Arandis
Annual dose, mining related, corrected for wind direction, $\mu\text{Sv/a}$	0.5	0.4		Arandis
Average PM10 concentration, mining related ($\mu\text{g}/\text{m}^3$)	24.2		23%	SWW boundary
Average PM10 concentration, non-mining related ($\mu\text{g}/\text{m}^3$)	22.1		77%	SWW boundary
Annual dose, non-mining related, corrected for wind direction, $\mu\text{Sv/a}$	16.1	12.6		SWW boundary
Annual dose, mining related, corrected for wind direction, $\mu\text{Sv/a}$	9.0	6.7		SWW boundary
Average PM10 concentration, mining related ($\mu\text{g}/\text{m}^3$)	21.1		86%	NEE sampler
Average PM10 concentration, non-mining related ($\mu\text{g}/\text{m}^3$)	19.3		14%	NEE sampler
Annual dose, non-mining related, corrected for wind direction, $\mu\text{Sv/a}$	2.6	2.0		NEE sampler
Annual dose, mining related, corrected for wind direction, $\mu\text{Sv/a}$	28.6	21.4		NEE sampler

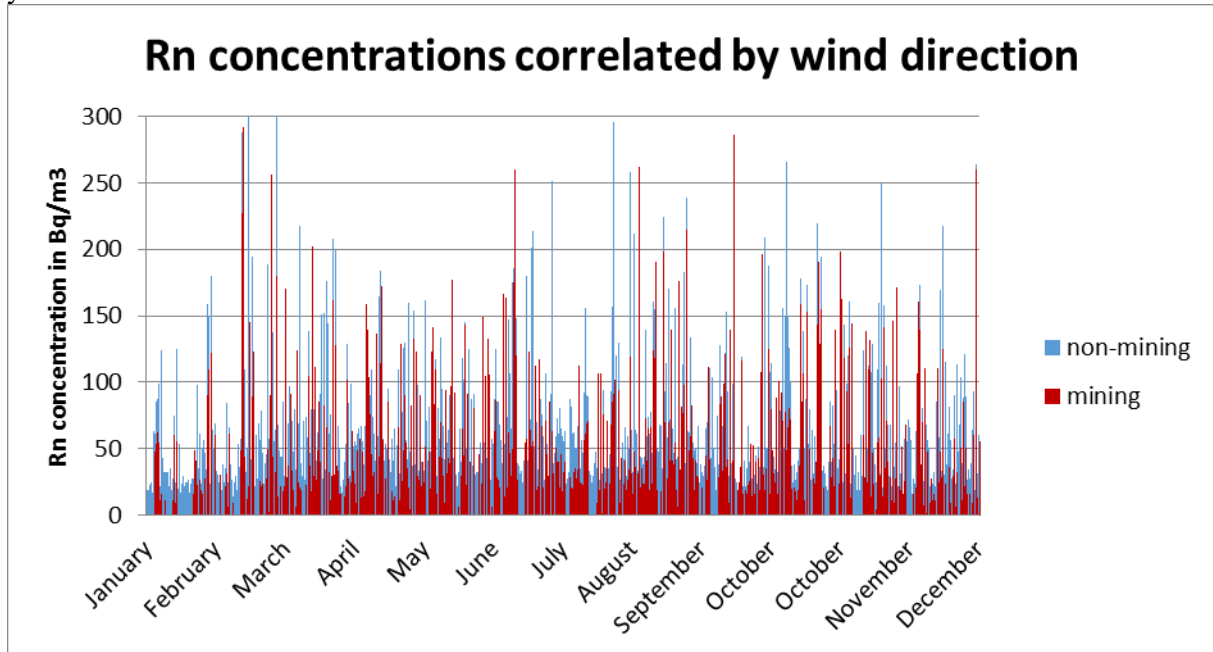
For all three sampling locations, the maximum annual dose is obtained for adults and infants of less than one year of age. Although the dose conversion coefficients for infants as considered above are the largest for any member of the public, their lower breathing rate reduces the resulting dose for this group to a value that is less than that of adults.

From Table 1, it becomes apparent that for Arandis, the inhalation dose due to LLRD of mining related origin is at most $0.5 \mu\text{Sv/a}$, or only about 5% of the dose resulting from background origin ($9.9 \mu\text{Sv/a}$). For the SWW boundary sampler, the mining related dose amounts to some $9.0 \mu\text{Sv/a}$, which is some 56% of the dose from background sources ($16.1 \mu\text{Sv/a}$), while at NEE sampler, the mining related dose is highest at $28.6 \mu\text{Sv/a}$, which is 110% higher than the background-related contribution ($2.6 \mu\text{Sv/a}$).

3.2 Radon

The method for calculating the public dose due to the inhalation of radon progeny is similar to that used for LLRD. At the radon monitoring station, the relevant wind directions from the mine range between 113 and 203 degrees. Atmospheric radon concentrations are measured in 10-minute intervals, and can be correlated with the wind direction measured at the same time and location. The measurements are summarised in Figure 6.

Figure 6: Radon concentrations at the radon monitoring station, correlated for wind direction, for the year 2013.



The resulting annual dose is given by [4]

$$Dose = C \cdot t \cdot DCF \cdot CF \cdot F, \quad (1)$$

where

- $Dose$ is the annual dose in milli-Sieverts per annum (mSv/a),
- C is the measured atmospheric radon concentration in Bequerels per cubic metre (Bq/m^3),
- CF is the conversion factor from equilibrium equivalent concentration of radon to potential alpha energy concentration, $5.56E - 6 \text{ mJ/m}^3$ per Bq/m^3
- t is the occupancy time in hours per year (8760 h/a),
- DCF is the dose conversion coefficient for members of the public (1.1 mSv per mJh/m^3), and
- F is the measured equilibrium factor between radon and progeny concentrations.

The measured concentrations and respective calculated doses are collected in Table 2.

Table 2: Measured radon concentrations correlated by wind direction, equilibrium factor and calculated annual dose from background and mining origin respectively, for the year 2013.

	Rn concentration (Bq/m ³)	Fraction of time measured	Equilibrium factor (measured)	Resulting dose (mSv/a)
Average	22			0.8
Non-mining	21	87%	0.7	0.7
Mining	32	11%	0.7	0.1

Although at the location of the radon station, there is definitely an excess radon concentration due to the nearby mining operation, wind from the mining area contributes only during 11% of the time during the year and hence reduces the mining-related dose due to the inhalation of radon progeny to 0.1 mSv/a. The resulting mining-related public exposure dose is therefore only 16% of the total radon inhalation dose at the location of the radon monitoring station, i.e. of 0.8 mSv/a.

4 CONCLUSION

The direct measurement and correlation of environmental and meteorological variables, including the inhalable dust concentration, atmospheric radon concentration and wind direction, readily enable the estimation of the worst-case public exposure dose from the inhalation pathway at specific locations, and can be used to determine the maximum dose contribution attributable to nearby mining operations.

5 REFERENCES

- [1] Ashton, P.J.; Moore, C.A. and McMillan, P.H., 1991. An Environmental Impact Statement for the Rössing uranium mine, Namibia, Rössing Uranium Limited.
- [2] Thomas, R.G., 2007. Air Quality Impact Assessment for the Proposed Expansion Project for Rössing Uranium Mine of Namibia: Phase 1, Airshed Planning Professionals.
- [3] IAEA, 2014. Radiation Protection and Safety of Radiation Sources: International Basic Safety Standards, General Safety Requirements Part 3, No. GSR Part 3, International Atomic Energy Agency, Vienna.
- [4] ICRP, 1993. Protection Against Radon-222 at Home and at Work, ICRP Publication 65, Ann. ICRP 23 (2).

Health impact assessment of recovery/disposal options of sewage sludge: methodology and critical parameters

Hélène Caplin^{a*}, Alain Thomassin^a

^aInstitute for Radiological Protection and Nuclear Safety, BP 17, 92262 FONTENAY-AUX-ROSES CEDEX, France.

Abstract. Health impact of artificial radioactive materials released in sewers is a more and more important topic for the stakeholders of sewers and/or wastewater treatment plants (WWTPs). Many models have been developed to describe the behaviour and to assess the health impact of radionuclides in sewers and in WWTPs. Some models enable also to assess health impact of land application and/or landfill disposal, and sometimes sludge incineration. But the application of these models to the French WWTPs is not straightforward because of the diversity and specificities of the recovery options encountered in France. So the aim of IRSN is to develop a comprehensive methodology to assess the health impact of each type of recovery/disposal option taking into account all potentially exposed persons (workers and public) and all exposure pathways.

KEYWORDS: *health impact; sewage sludge; recovery.*

1 CONTEXT

The need to apply innovative technologies for maximizing the efficiency of sewage treatment plants and minimizing their carbon footprint has the consequence for sewage sludge management to be now a highly sophisticated research and development sector. Sewage sludge are not to be regarded solely as 'waste'; it is also a renewable resource for energy and material production. In France, the following recovery options for sewage sludge are:

- energy recovery: incineration, gasification, pyrolysis...
- agriculture uses: farmland application, composting...
- manufacturing building materials.

In France, waste water treatment plants (WWTPs) often operate several recovery options.

Health impact of artificial radioactive materials released in sewers is a more and more important topic for the stakeholders of sewers and/or WWTPs (owners and operators, national or local authorities), mainly due to high activity released in sewers by hospitals or increasing number refusals of solid wastes in landfill following detection of radioactivity. Several models in different countries have been developed to describe the behaviour and to assess the health impact of radionuclides in sewers and in WWTPs. Some of them enable also to assess health impact of land application and/or landfill disposal, and sometimes sludge incineration. For these three recovery/disposal options however, the above models allow to assess exposure for only some potentially exposed groups.

Since 2000, the Institute for Radiological Protection and Nuclear Safety (IRSN, the French national public expert in nuclear and radiological risks) is more and more involved in studies concerning radionuclides in sewers and WWTPs. The main purpose is the radiological characterisation of wastewater and/or sludge, sometimes associated with workers exposure assessment; and for a few years now, regulators are often interested by the health impact on the population due to sludge recovery.

Lastly, to answer to some stakeholder expectations (especially hospitals, that are responsible for the main releases of radionuclides in sewers), IRSN has developed a generic method to assess radiological exposure of a sewer worker and of a WWTP worker working near sludge storage. This method

* Presenting author, e-mail: helene.caplin@irsn.fr

considers also workers involved in sewage sludge loading and transport operations or in land application. But, it doesn't allow the dose assessment for all sewage sludge recovery options and for all exposed persons, and, as any generic method, hypotheses are very – and even too – conservative.

Finally, to respond to all possible requests of any stakeholder of sewers or WWTPs and to be consistent with its mission, IRSN needs a comprehensive method to assess exposure due to radionuclides in sewage or in sludge. The present paper focuses on the health impact assessment of recovery/disposal options of sewage sludge.

2 OVERVIEW OF WORLDWIDE ASSESSMENT MODELS

Among the models mentioned above and dealing with assessment of worker exposure, some permit also to assess exposure of the population due to some sludge recovery options and are presented below.

2.1 United States of America

A limited survey of radioactivity in sewage sludge was conducted by the Interagency steering committee on radiation standards (ISCORS) across the United States. To assess the levels of the associated doses to people, ISCORS modelled the transport of the relevant radionuclides from sewage sludge into the local environment [1]. Seven general scenarios were considered to represent typical situations in which members of the public or WWTP workers may be exposed to sewage sludge:

- residents of a house built on a former agricultural field where sewage sludge was applied,
- recreational visitors to a park where sewage sludge has been used in land reclamation,
- residents of a town near a sewage sludge land-application site,
- neighbours of a landfill that contains sewage sludge or ash from sludge,
- neighbours of an operating sludge incinerator,
- workers who operate equipment to apply sewage sludge to agricultural lands,
- WWTP workers involved in sewage sludge sampling, transport or loading operations.

2.2 United-Kingdom

The study [2] aims to provide relevant information for the Environment agency to review the acceptability of releases of liquid radioactive wastes to sewer systems. Scenarios are:

- neighbours of a sludge incinerator,
- neighbours of a landfill that contains sewage sludge or ash,
- disposal of sludge off-shore,
- application of sludge to farmland.

2.3 Sweden

The Swedish study [3] assesses the doses to the public and sewage workers in order to provide supporting information to be used for regulation revision. Scenarios are:

- consumers (adults) of food produced in agricultural land where sludge has been used as fertilizer,
- consumers (adults) of food produced in a landfill where sludge has been disposed of and which has been used for agriculture after its closure.

2.4 Conclusions

These models consider all exposure pathways for their different scenarios; however, for residents and consumers, adults are the only considered age group. Furthermore, these models take into account recovery options which are in a strong accordance with their national regulations. Some of these recovery options are not allowed in France and some of the hypothesis which are retained for the recovery options do not comply with the French regulation. This is why IRSN decided to develop its own exhaustive model, taking into account all potentially exposed persons (workers and public) and all exposure pathways, to respond to all public expectations.

3 METHODOLOGY USED BY IRSN

3.1 Methodology

In France, several recovery options for sewage sludge are encountered: energy, agriculture and building materials; when sludge can't be reused, they are disposed in a landfill. Tables 1, 2 and 3 present, according to recovery option, potentially exposed persons and exposure pathways to be considered.

Table 1: Energy recovery - Potentially exposed persons and exposure pathways

Options	Persons	Pathways
Incineration in the WWTP	Patrolman	Irradiation by sludge or ashes Inhalation of resuspended dust Inadvertent ingestion of sludge or ashes
	Residents	Irradiation by plume and deposit Inhalation of the plume and resuspended dust from deposit
	Consumers	Ingestion of vegetables, meat from contaminated surfaces Inadvertent ingestion of soil
Co-incineration in a cement facility	Driver Patrolman	Irradiation by sludge or cement Inhalation of resuspended dust Inadvertent ingestion of sludge or cement
	Residents	Irradiation by plume and deposit Inhalation of the plume and resuspended dust from deposit
	Consumers	Ingestion of vegetables, meat from contaminated surfaces Inadvertent ingestion of soil
Co-incineration in a coal-fired plant or Co-incineration with household refuse	Driver Patrolman Boilermaker Electrician Heap agent	Irradiation by sludge or ashes Inhalation of resuspended dust Inadvertent ingestion of sludge or ashes
	Residents	Irradiation by plume and deposit Inhalation of the plume and resuspended dust from deposit
	Consumers	Ingestion of vegetables, meat from contaminated surfaces Inadvertent ingestion of soil
Wet air oxidation	Driver Patrolman	Irradiation by sludge or sand Inhalation of resuspended dust Inadvertent ingestion of sludge or sand
Gasification	Driver Patrolman	Irradiation by sludge or ashes Inhalation of resuspended dust Inadvertent ingestion of sludge or ashes

Residents	Irradiation by plume and deposit Inhalation of the plume and resuspended dust from deposit
Consumers	Ingestion of vegetables, meat from contaminated surfaces Inadvertent ingestion of soil

Table 2: Agricultural recovery - Potentially exposed persons and exposure pathways

Options	Persons	Pathways
Farmland application with or without a storage platform	Driver Platform agent (if storage platform) Farmer	Irradiation by sludge Inhalation of resuspended dust Inadvertent ingestion of sludge
	Residents	Irradiation by sludge Inhalation of resuspended dust
	Consumers	Ingestion of vegetables, meat from contaminated surfaces Inadvertent ingestion of soil
Composting and amendment (agriculture or garden)	Driver Platform agent Farmer (if agricultural amendment)	Irradiation by sludge Inhalation of resuspended dust Inadvertent ingestion of sludge
	Residents	Irradiation by sludge Inhalation of resuspended dust
	Consumers	Ingestion of vegetables, meat from contaminated surfaces Inadvertent ingestion of soil
Mulching	Driver Farmer	Irradiation by sludge Inhalation of resuspended dust Inadvertent ingestion of sludge
	Residents	Irradiation by sludge Inhalation of resuspended dust
	Consumers	Ingestion of vegetables, meat from contaminated surfaces Inadvertent ingestion of soil

Table 3: Building materials recovery - Potentially exposed persons and exposure pathways

Options	Persons	Pathways
Concrete	Drivers	Irradiation by sludge or building materials
	Building materials maker	Inhalation of resuspended dust Inadvertent ingestion
Bricks	Building materials user	
Ceramics	Building materials user	Irradiation by building materials
	Residents	

Table 4 presents the potentially exposed persons and the exposure pathways for disposal in a landfill.

Table 4: Disposal in a landfill - Potentially exposed persons and exposure pathways

Persons	Pathways
Driver	Irradiation by sludge
Platform agent	Inhalation of resuspended dust
	Inadvertent ingestion of sludge
Residents	Irradiation by resuspended dust
	Inhalation of resuspended dust

Some of these scenarios can be mixed; for instance a patrolman can be a resident and a consumer.

Performing so many assessments requires a lot of information on workers: different operations achieved by each worker, annual duration of exposure for each operation, workers' positions relative to each source, geometry and composition of each source, *etc.* Information can be obtained from visit of the different places (plant(s), platform(s), landfill(s)), literature and essentially workers interviews. For population, the main information to acquire are: location of the exposed persons, age groups, food consumption for each age group, weather conditions distribution in case of atmospheric releases.

The model considers the radioactive decay for long-term operations (for instance composting process) or operations taking place a long time after the sludge production (for instance agricultural activities in a field where sewage sludge was applied), the partition of the radionuclides between ashes and released plume in case of sludge incineration, the dilution of sludge or ashes by other products (for instance in the case of co-incineration in cement facility, concrete production or composting).

In case of lack of specific information (for instance partition factor of radionuclides between ashes and released plume, dimensions of the radioactive sources for some operations, weather conditions, food consumption...), the assessor will retain conservative hypothesis (investigation of literature data, regulatory recommendations in some cases...).

This methodology can appear very - even too - exhaustive but radiological impact, even for small sources and low levels of exposure, can be a huge societal issue; each potentially exposed person wishes to know her own health impact.

3.2 Critical parameters

Many parameters have influence on dose assessment. However the parameters related to the source term (activity of sludge, ash, by-products of flue gas cleaning systems, compost...) are the most critical ones because their influence is linear (partition factor for example) or exponential (duration for storage on a platform for example) on the dose assessed for some or all pathways. These parameters must be considered with great attention, especially:

- the fraction of the radionuclide that is not vented as part of the exhaust gas stream. It depends on the plant design, the element and its chemical form. It can range from 0.0 for noble gases such as radon to greater than 0.99 for metals such as uranium, thorium and plutonium;
- the dilution of sewage sludge by municipal solid waste for the incineration or by green waste for composting;
- the dilution of ashes in concrete or in building materials.

Values of these parameters are in a wide range or are not well-defined in the literature; the choice of relevant values of these parameters must be done with judgement or caution.

The operational times are also important parameters. Most of radionuclides released in sewers are short-lived radionuclides; so the radioactive decay impacts significantly the exposure.

For the exposure assessment due to atmospheric releases, the conditions - such height and surrounding buildings - and the distribution of weather conditions influence significantly the assessed doses. For external exposure assessment, the knowledge of nature, thickness and density of materials between sludge and the exposed person is essential to assess reasonably the dose.

3.2.1 As Application: the more exposed persons

In order to show the relevance to look for the more exposed persons among all potentially exposed persons taking into account all exposure pathways, and also to show the importance of one of the critical parameters listed above – radioactive half-life, an arbitrary example is presented below with iodine 131 and caesium 137 and main agricultural recovery options (farmland application and agricultural composting).

Iodine 131 is chosen because it is the most frequently measured radionuclide in the sewers, mainly due to nuclear medicine department releases or patients excreta; it is a short-lived radionuclide with a half-life of 8 days. Inversely, caesium 137 is rarely measured in sewers, but can appear in the authorized releases in sewers for some research centres; half-life of caesium 137 is 30 years, much more than iodine 131. Moreover, iodine 131 and caesium 137 are rather similar from the only radiological point of view; the dose coefficient for external exposure of caesium 137 are 50% more than those for iodine 131, and it is the inverse for internal exposure.

Sludge is considered in its dried form except for recovery options which don't accept dried sludge (wet air oxidation, co-incineration with household refuse, mulching); in these cases dewatered sludge is considered. If no information is available, dried sludge is preferred.

To compare the radiological impact of different agricultural recovery options for iodine 131 or caesium 137 contaminated sludge, basic hypothesis are the same for the two radionuclides (1 Bq.g⁻¹, sources dimensions, transport times, positions in regard to sources, time budget, ...). As for iodine 131, 1 Bq.g⁻¹ is a relatively high value of mass activity in sludge; the only radiological characterization of sludge known up to now by IRSN for a WWTP downstream nuclear medicine department showed a maximal mass activity around 0.37 Bq.g⁻¹.

Figure 1 and figure 2 present a comparison of effective doses, calculated respectively for iodine 131 and for caesium 137, for the main recovery options used in agriculture, i.e. farmland application with and without a storage platform, composting.

Figure 1: Annual effective doses (mSv.y⁻¹) due to 1 Bq.g⁻¹ of iodine 131 in sewage sludge for main agricultural recovery options

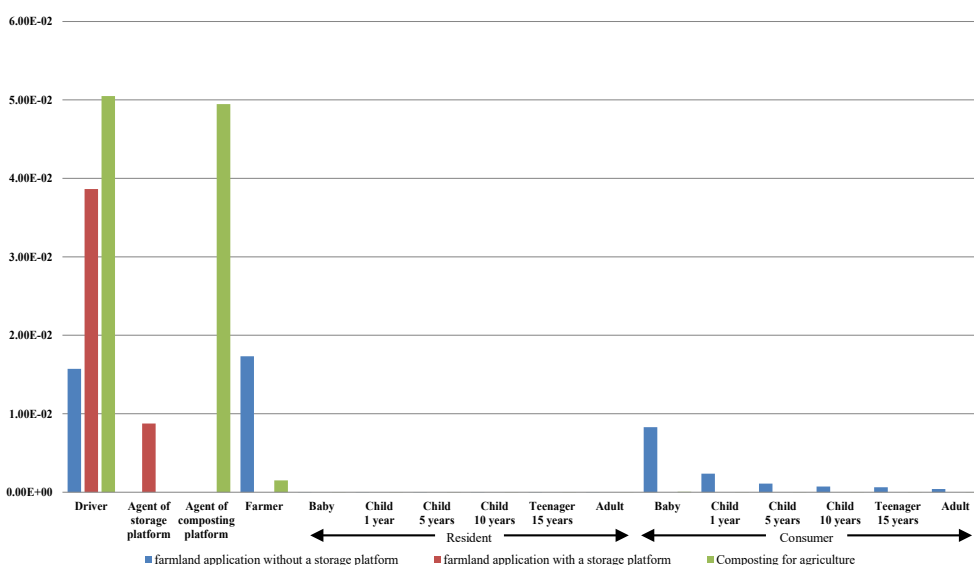
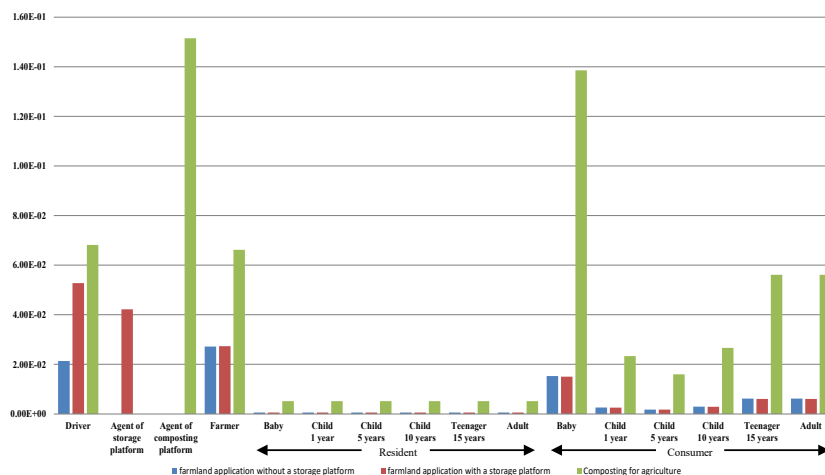


Figure 2: Annual effective doses (mSv.y⁻¹) due to 1 Bq.g⁻¹ of caesium 137 in sewage sludge for main agricultural recovery options



Beyond the observation that effective doses for caesium 137 are higher – and sometimes much more than 50% - than those for iodine 131, it is interesting to note that the most exposed persons depend on the radionuclide. In particular, residents or consumers are not systematically the most exposed persons in the case of agricultural recovery. The effect of radioactive decay is obvious: a longer half-life allows pathways concerned by longer duration (because linked to occupation or consumption) to become significant; in such cases residents and/or consumers can be the more exposed persons. Inversely, a short half-life doesn't lead these pathways to be significant, and the most exposed person can be a driver or a compost platform agent. As the most exposed persons cannot be predicted *a priori*, it is necessary to assess doses for all persons potentially exposed.

4 CONCLUSION

Exposure of persons due to radionuclides in sewage, and subsequently in WWTPs and sludge, is increasingly a subject of interest for many people (sewage network or WWTPs owners or operators, national or local authorities, residents...). IRSN is now often questioned about radiological characterization of sewage or sludge and also about health impact on workers or persons of the general population potentially exposed due to all possible fates of artificial radionuclides in sewage. In order to achieve its mission with very various requests and configurations, and because the more exposed persons cannot be identified *a priori* as demonstrated before, IRSN develops a reliable and comprehensive method to assess doses for all possible persons exposed to radionuclides present in sewage or in sludge. This detailed investigation of actual exposure conditions provides robustness and credibility of IRSN assessments for stakeholders, especially in case of societal issues. Still in development, this method will soon be used in a systematic way for any sewer or WWTP, allowing a global approach for exposure due to artificial radionuclides in sewage.

5 REFERENCES

- [1] ISCORs, 2005. ISCORs assessment of radioactivity in sewage sludge: modelling to assess radiation dose. ISCORs Technical report 2004-03. Interagency steering committee on radiation standards.
- [2] Titley, J.G., Carey, A.D., Crockett, G.M., et al., 2000. Investigation of the sources and the fate of radioactive discharges to public sewers. R&D Technical report P288. National Radiological Protection Board (NRPB).
- [3] Avila, R., de la Cruz, I., Sundell-Bergman, S, et al., 2007. Radiological consequences of radionuclide releases to sewage systems from hospitals in Sweden. SSI rapport 2007:10. Statens strålskyddsinstitut (Swedish radiation protection authority).

Criticality Safety and Control System for Nuclear Fuel Fabrication Plant

H.A. Elsayed^a, M.K. Shaat^a, M.E. Nagy^b, S.A. Agamy^b

^aReactors Department, Nuclear Research Center, Egyptian Atomic Energy Authority, 3 Ahmed El Zomor Street, Nasr City, P.O.Box 9621, Cairo 11787, Egypt

^bProfessor of Nuclear Engineering, Nuclear and Radiation Engineering Department, Faculty of Engineering, Alexandria University, Alexandria, Egypt

Abstract. The prevention of criticality accidents is of paramount importance. Nuclear Criticality Safety provides requirements for the prevention of criticality accidents in the handling, storage, processing, and transportation of fissionable materials and the long-term management of nuclear waste. Criticality safety is the practice of ensuring that adequate protection is provided against an accidental self-sustaining or divergent fission chain reaction. Criticality safety systems have been performed for a Nuclear Fuel Fabrication Plant producing nuclear fuel elements for nuclear research reactors with low enriched Uranium up to 20%. The precipitation process will be occurred in the precipitator tank to obtain Ammonium- Diuranate (ADU) from Uranyl Florid (UO₂F₂). A proposed Logic Control Safety System (LCSS) was designed to stop and shut down the Process in the Precipitator Tank during abnormal conditions. Standby Liquid Control Safety System (SLCSS) is proposed as a safety related system designed for automatic initiation of Boron solution injection into the Precipitator tank during abnormal conditions to prevent the criticality accident. A Criticality Accident Alarm System (CAAS) was installed as part of criticality safety management for use in reducing the radiation workers could be exposed to in the rare case of a criticality accident. A case study was applied for a real fuel manufacture plant. The results show that the safety system was effective in prevention of criticality accident during abnormal operation.

KEYWORDS: *criticality safety, effective multiplication factor.*

1 INTRODUCTION

The objectives of criticality safety are to prevent a self-sustained nuclear chain reaction and to minimize the consequences of this if it were to occur. The criticality safety analysis should be used to identify hazards, both internal and external, and to determine the radiological consequences. The criticality safety calculations makes recommendations on how to ensure sub-criticality in systems involving fissile materials during normal operation, anticipated operational occurrences, and, in the case of accident conditions [1].

Sixty criticality accidents were occurred in the world. These are divided into two categories, 22 accidents those that occurred in process facilities and 38 accidents those that occurred during critical experiments or operations with research reactor. Process facilities carrying out operations with fissile material avoid criticality accident through physical and administrative controls. These controls are intended to prevent critical or near-critical configurations from ever occurring in the facility. The plant produces nuclear fuel element for research reactors has been operated with enriched uranium up to 20% enrichment. In the design of equipment, the type of criticality calculation and control to be used must be considered. Once the control method is established, the process and equipment must be designed to meet the safety limits and conditions for safe process. Basically, the plants may be designed using mass, concentration, volume, geometry control and combination [2].

In this work a new safety control system was designed based on the nuclear criticality calculations for nuclear fuel fabrication plant producing nuclear fuel elements for nuclear research reactors with low enriched uranium. We proposed more safety control and measurements for a general fuel fabrication plant with a certain defined mixing container to prevent the criticality initiation during the fuel processing. Also subcriticality calculations were performed using MCNP code.

2 GENERAL PROCESS DESCRIPTION

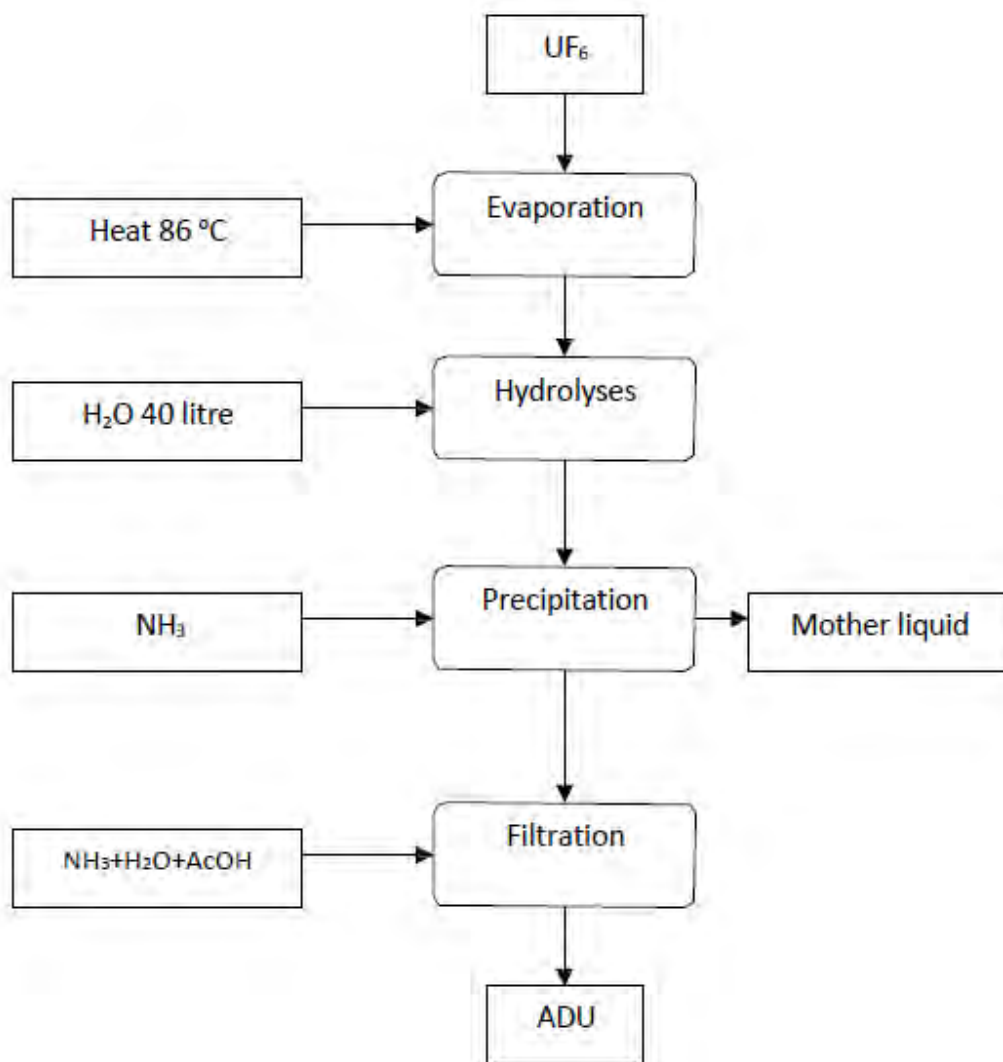
2.1 Wet Process (UF₆-ADU Conversion Process)

In the wet process or ammonium diuranate (ADU) process, the UF₆ with enriched Uranium is 20% is vaporized and transferred to reaction vessel, hydrolyzed with water, and neutralized with NH₄OH to form a slurry of ADU in an aqueous solution of ammonium fluoride and ammonium hydroxide. The ADU is recovered by centrifuging and then is clarified, dried, and calcined to form UO₂ or U₃O₈ powder. Figure 1 are a flow diagram and sheet for the conversion process to convert UF₆ to ADU [3].

The 4 steps of process are:

- 1- Vaporization process – conversion of a UF₆ solid into a gaseous state by adding heat for UF₆ Cylinder.
- 2- Hydrolysis process – a chemical process by which the oxygen or hydrogen in water combines with an element, or some element of a compound, to form a new compound.
- 3- Precipitation – formation of finely divided solids in a chemical reaction.
- 4- Separation – remove or separate solid particles ADU from the liquid effluent.

Figure 1: Flow diagram of UF₆ – ADU conversion process



3 PROPOSED DESIGN FOR SAFE STANDBY LIQUID CONTROL SAFETY SYSTEM (SLCSS)

The sub-criticality of a system depends on many parameters related to the fissile material, for example, mass, concentration, geometry, enrichment or density. It is also affected by the presence of other materials, for example, moderators, absorbers and reflectors. Ensuring sub-criticality may be realized through the control of an individual parameter or a combination of parameters, e.g. by limiting mass or by limiting both mass and moderation. The means for controlling these parameters is ensured either by engineered and/or by administrative measures [1].

Neutron poisoning (e.g. boron) is employed when the process requires the use of large volume equipments whose geometry cannot be made safe such as the precipitator tank, or when it is necessary to provide neutron isolation between equipments. Significantly larger limits are possible if soluble neutron absorbers are present in such solutions. Experience has shown that operations involving the use of such absorbers can be performed both safely and economically. Neutron-absorbing materials are most effective for thermal neutrons [1].

Standby Liquid Control Safety System (SLCSS) is proposed as a safety related system designed for normal or automatic initiation of soluble neutron absorbers (boron solution) injection into the Precipitator tank. The mainly purpose of SLCSS applications is to assure subcriticality for normal and credible abnormal conditions over the operating life of precipitator tank. This system consists of:

- a) High-pressure accumulator containing concentrated boron solution as.
- b) Injection line with actuated valves.
- c) Control system coupled to the process operating set points.
- d) Cover gas pressure regulation system.

A schematic diagram of the process in the SLCSS is presented in Figure 2. The SLCSS accumulator tank is modeled as a single control volume with pipeline for liquid draining. High pressure injection of boron- solution into the bypass region of the mixer tank. The accumulator tank is connected to the mixer through valves and control logic based on system operation set points. Actuation of the SLCSS is integrated to the mixer operating conditions.

The control logic of SLCSS has been implemented into system software (Rule Based Method). The time delay associated with the signal transmission and value actuation must be specified. Also, we can use Borated water (chemical shim) to transfer the process into sub-critical state. The negative reactivity or boron concentration required for sub-critical state will be estimated.

The criticality accident alarm systems are based on groups of detectors, or sensors, that measure the total (neutron + gamma) dose rate, and a processing cabinet of these measurements, which operates sound and light alarms specifically associated with a criticality accident. These alarms are triggered as soon as the total dose and the dose rate reach predetermined thresholds. The detectors have been designed so as to minimize the risk of false alarm and are moreover able to provide informations about the criticality accident (development over time, evaluation of doses, etc.) that can be used for the emergency response.

When the alarms are triggered, the signal initiating automatically and SLCSS will be operate and the valve V1 will be open automatically as in Figure 3 to discharge the uranium solution from the precipitator tank (unsafe geometry) to collecting trays (subcritical geometry). If valve V1 is not open, the safety system sends another signal for valve V2 to open automatically to poured the boron solution from the boron solution tank into the precipitator tank to stop the reactions and shutdown the system as shown in Figures 3, 4.

Figure 2: Process flow sheet UF6-ADU conversion process with proposed safety logic control safety system (SLCSS)

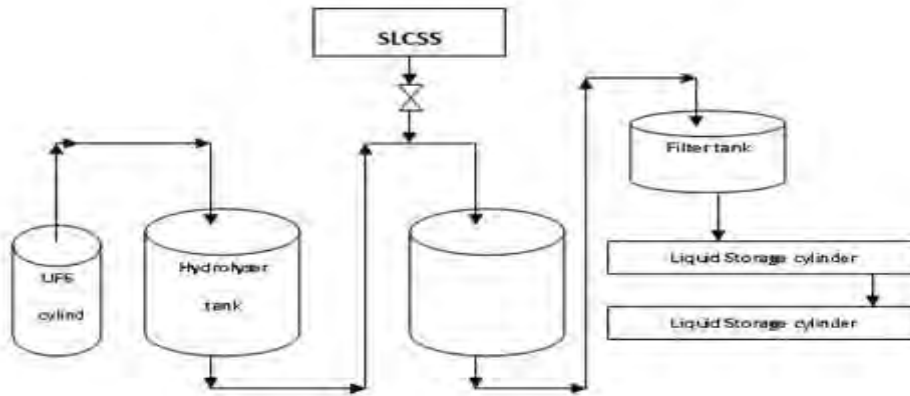


Figure 3: Block diagram for precipitator tank with SLCSS and collecting tray

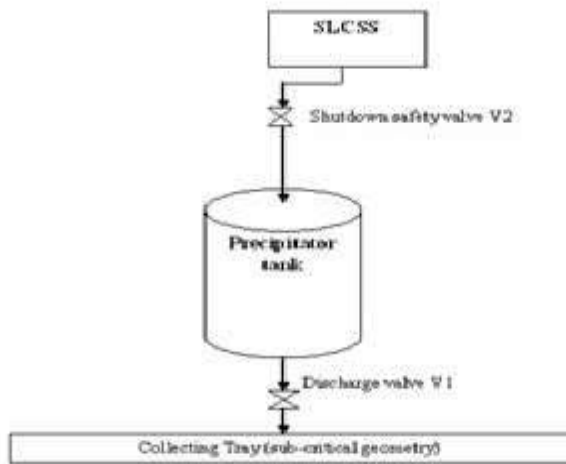
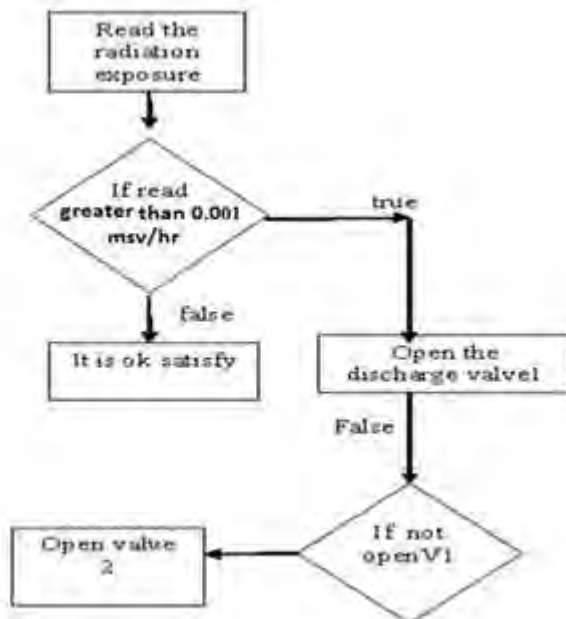


Figure 4: Flow chart of the criticality safety program for the precepitator tank



4 CALCULATION METHODOLOGY, RESULTS AND DISCUSSION

MCNP is a general Monte Carlo N-Particle transport code. It has the capability of transporting neutrons, electrons and photons. In this work the transporting of neutrons is considered. These features make it possible for MCNP to simulate different types of fissile systems, e.g. a nuclear reactor or a nuclear fuel container, and obtain information such as k_{eff} . The neutron energy regime is from 10^{-11} MeV to 20 MeV, and the photon and electron energy regimes are from 1 keV to 1000 MeV. The capability to calculate k_{eff} eigenvalues for fissile systems is also a standard feature MCNP provides four types of boundary conditions that are accepted for performing criticality safety analyses. The default boundary condition is a vacuum where neutrons leaving enter a region of zero neutron importance [4].

4.1 Multiplication Factors in Collecting Trays under glove boxes

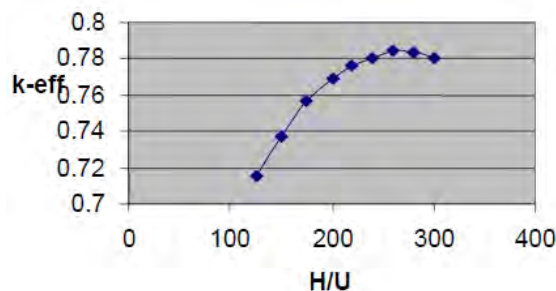
The purpose of three independent collecting trays to collect the spilled of fissile solution when the event of liquids spill inside UF₆-ADU conversion glove box. Another purpose of collecting trays, to receive ADU solution from the precipitator tank if any abnormal conditions introduce the criticality accident. These three collecting trays with subcritical geometry (thickness = 6.7 cm, equivalent to 0.75 times of the critical thickness for a homogenous solution of Uranium enriched at 20%), with volume about of 85 liters.

In order to ensure and verify that these trays are geometrically safe. A system consisting of a 6.7 thick tray with infinite surface, reflected by 20 cm water, was calculated. The composition of the solution which fills the tray corresponds to the composition of a UO₂F₂-HF-H₂O solution. Considered corresponds to hypothetical spilling of the solution contained in hydrolyser tank, containing 40 liter water and 24.95 kg UF₆.

The volume occupied by this solution is 45 liter, which would take up about half the volume of the one collecting tray. Therefore, the solution height would be half the safe thickness. The concentration of the solution is about 400 gU/l is above the critical concentration (60gU/l for 20% enriched Uranium), the solution is very sub-moderated. As its moderation degree is H/U = 60 and the optimum moderation degree has been calculated as H/U = 240. Figure 5 shows the effective multiplication factor will be increase with increasing the H/U in the collecting trays.

Assuming the maximum quantity of Uranium involved in a liquids spill to the collecting trays corresponds to the full load of a UF₆ cylinder (24.95 kg UF₆). To fill the collecting trays 85 liters water should be added to the UF₆ mass contained in a UF₆ cylinder. This solution concentration is about 200 gU/l, and its moderation degree is H/U=125. The system was calculated with different solution moderation degree as shown in Figure 5.

Figure 5: The effective of multiplication factor as a function of the H/U for solution UO₂F₂-HF-H₂O in collecting trays infinite plate 7 cm thick



4.2 Calculation of the Boron Concentration in the Borated water Tank

Chemical shim affects the reactivity of a thermal reactor primarily by changing the value of the thermal utilization. The worth of a given concentration of borated water can be computed from the next Equation.

$$\rho_w = \frac{\sum_{aB}}{(\sum_{aF} + \sum_{aM})}$$

Where \sum_{aB} , \sum_{aF} , and \sum_{aM} are, respectively, the macroscopic thermal average cross sections of the boron, fuel, and moderator. The final formula for shim worth,

$$\rho_w = 1.92C \times 10^{-3} (1 - f_0)$$

To calculate ρ_w :

$$\rho_w = \frac{(K_{final} - k_{initial})}{k_{final}}$$

$$\rho_w = \frac{(1 - 0.8)}{1} = 0.2 \quad \rho_w = 20\%$$

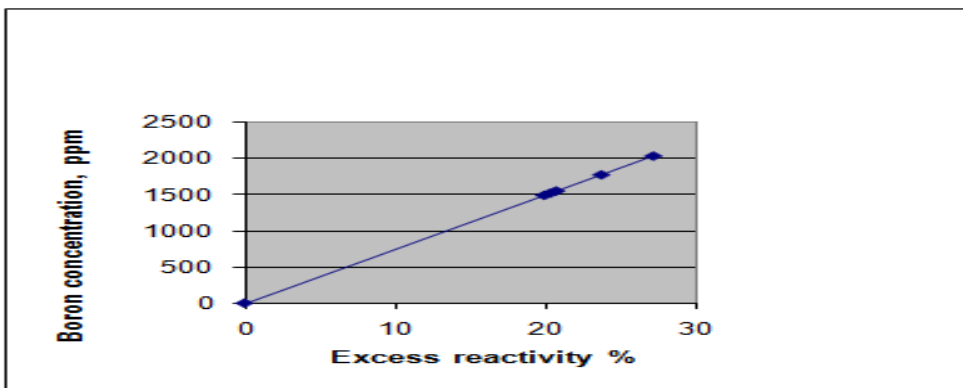
$$C = \frac{\rho_w \times 10^3}{1.92(1 - 0.93)}$$

Where c: is the concentration of the boron in the solution.

$$C = 1488 \text{ ppm} = 1488 \text{ mg/l} \quad C = 1.488 \text{ g/l}$$

$$\text{when: } \rho_w = 27.27\% \quad C = 2029.2 \text{ mg/l} \quad C = 2.2922 \text{ g/l}$$

Figure 6: Boron concentration required in borated water tank with excess reactivity



5 CONCLUSION

A new design for SLCSS to mitigating or preventing the criticality of nuclear fuel fabrication plant was illustrates.

The criticality safety for a nuclear fuel fabrication plant was studied and analyzed with MCNP-4B code.

The effective of multiplication factor was determined for UF₆-ADU conversion process for normal operation and abnormal conditions.

The results indicated that the k_{eff} is subcritical values with SLCSS.

6 ACKNOWLEDGEMENTS

The authors wish to thank the Egyptian Atomic Energy Authority, for some data guidance.

7 REFERENCES

- [1] E. D. Clayton, 1979, Anomalies of Nuclear Criticality Safety, PNL-SA-4868, Battelle Pacific Northwest Laboratory, Richland, Washington.
- [2] Los Alamos National Laboratory, LA 13638, A Review of Criticality Accidents, 2000 revision.
- [3] Hade Elsayed, M.K.Shaat, M.E.Nagy and Saed Agamy, Criticality Calculations for a Typical Nuclear Fuel Fabrication Plant with Low Enriched Uranium, the 15th IGORR (International Group on Research Reactors) Conference combined with IAEA TM, 03_1008, Oral Presentation, Safety of RR, Korea, October 13-18, (2013).
- [4] Briesmeister, Judith F. (Ed.), MCNPTM-A General Monte Carlo N-Particle Transport Code, Los Alamos National Laboratory, LA- 7396, (1996).

Study on the transfer of Polonium-210 from soil and sediment to cattle in a catchment area influenced by gold mining

Immanda Louw*

NECSA, P O Box 582, Pretoria 0001, Republic of South Africa.

Abstract. The longer-lived radionuclides of the three naturally occurring series are likely to accumulate in sediments during the formation of peat and exist in the environment for elongated periods, and can cause internal exposure to humans if used for agricultural purposes and accordingly through ingestion of foodstuffs grown in the affected areas (e.g. milk, meat, vegetables). Due to mining- and mineral processing industries in the Gauteng region of South-Africa the presence of natural occurring radionuclides (NORM) in the soil and sediment in the entire catchment area of the Wonderfontein spruit is likely. Recent developments regarding environmental impact assessments for radioactivity have precipitated the need for information on the transfer of natural occurring radionuclides to non-human biota, such as cattle. The objective of this study was to determine activity concentrations of one of the main dose forming radionuclides, Polonium-210, in biota thus providing insight into the behaviour of this radionuclide. Samples of water, soil, sediment, grass, meat and intestines of slaughtered cattle, were collected from a location in the Wonderfontein spruit catchment area which showed elevated levels of NORM. The samples were analysed at the radio-analytical laboratory of the South African Nuclear Energy Corporation.

KEYWORDS: *transfer factors; natural occurring radionuclides; mining industry.*

1 INTRODUCTION

In the last decade the interest in the radiological assessments of the discharges of natural occurring radionuclides has increased in terms of both current releases from industrial sites and from the presence of historical contaminations in the soil. Assessments are complicated by the widespread presence of these nuclides in the environment. The ERICA integrated approach to the assessment and management of environmental risks for ionising radiation provides a number of databases for selected organisms from aquatic and terrestrial ecosystems [1]. Information on activity concentrations and transfer is limited for radionuclides from the Uranium-238 and Thorium-232 decay series, and notably, for ^{210}Po [2]. The radionuclides ^{210}Po and ^{210}Pb are known to constitute an important component of internal doses to organisms [3]; it is therefore important to gain more information on the behaviour of these nuclides.

The Wonderfontein spruit (WFS) flows through the richest gold mining region in the world and has subsequently been exposed to pollution for more than a century [4]. Consequently, sediments and soil in specific areas in the WFS catchment contains elevated levels of natural radionuclides from the uranium decay series. High concentrations of radionuclides in gold mine tailings facilities present a health hazard to the environment and people living near the area. Due to different migration processes, these radionuclides can be transported via fodder into a cow and cow's milk, which is an important foodstuff for humans.

Accumulation of radionuclides in the tissue of livestock is important when considering dose to consumers of these animal products. Due to the relatively high consumption of milk, it is important to measure the activity concentration of natural radionuclides in milk and to quantify the transfer of natural radionuclides through the food chain from soil via fodder to milk. Radionuclide uptake is also important when considering dose to biota itself, and there is a need for uptake data for livestock suitable for general use in biota dose assessments and for specific use in dose assessment models. Whereas some studies concerning natural radionuclide activity concentrations and uptake in food, including beef and milk, have been published worldwide [5,6], there is a lack of data which enable the

* Presenting author, e-mail: immanda.louw@necsa.co.za

calculation of transfer parameters for natural radionuclides in beef and milk [7,8]. No published radionuclide uptake data of fauna in South Africa in scientific journals could be found.

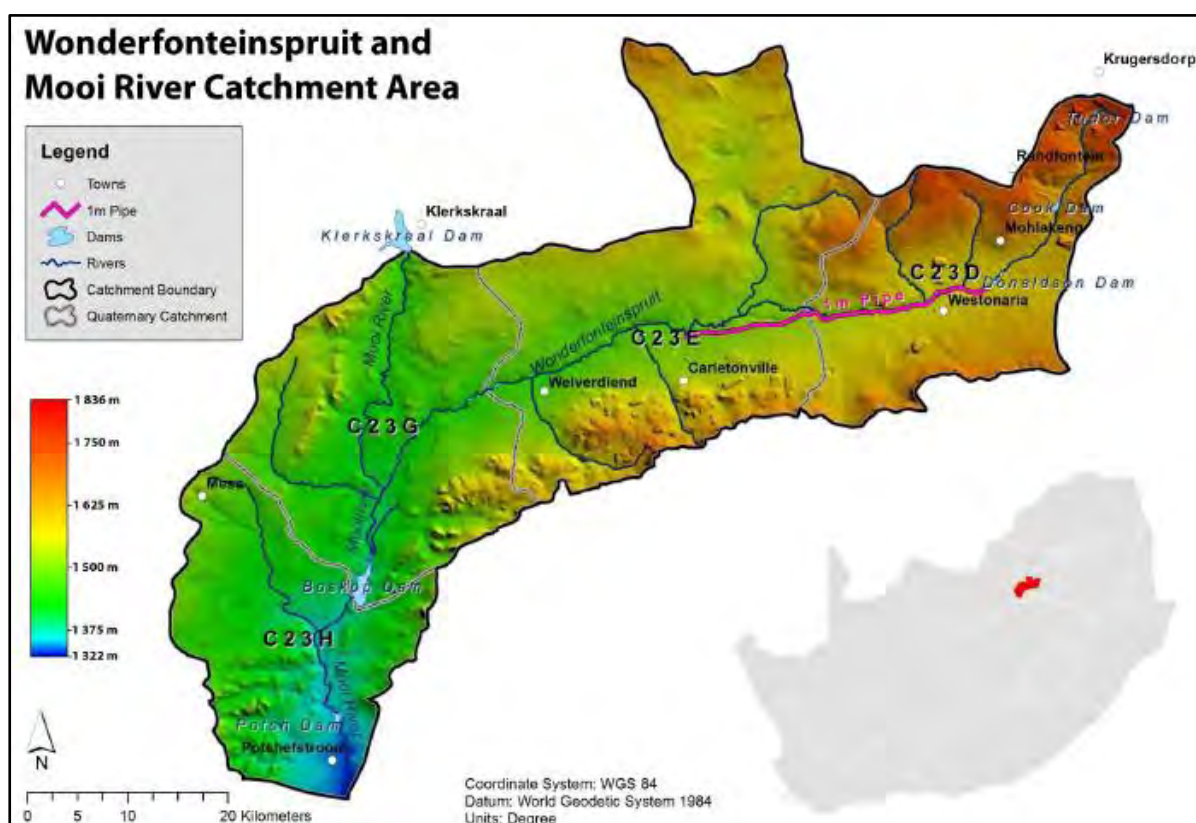
The objective of this study was to determine activity concentrations of ^{210}Po in biota from the catchment area and from this to obtain information on the behaviour of ^{210}Po in environmental systems including pathways to humans. A further objective was defined as exploring the efficacy of selected transfer models for ^{210}Po . This work was undertaken primarily because few data exist of the concentrations of natural radionuclides in edible farm animal tissues.

2 MATERIAL AND METHODS

2.1 Field site and sampling

The WFS catchment area (see Fig.1), located in close proximity to gold-mining activities in South Africa, was identified as study area since elevated levels of uranium in certain locations within the catchment area have been observed in a number of studies [9,10,11].

Figure 1: Map of the WonderfonteinSpruit and surrounding area [9].



Water, sediment, soil, grass, milk and cattle tissue samples were collected on a farm in the WFS area. Background samples were collected from a farm located along the Mooi River, which has not been impacted by mining activities. Water was sampled at two sites along a 1 km stretch of the WFS. Sediment samples were collected from a dam on the farm. One soil sample was collected next to the dam. The grasses found along the dam are actively grazed by the cattle throughout the year, and the cattle feed sample was collected here. A second soil sample was collected at a site consisting of wetlands. Liver, muscle tissue (meat) and bone samples were collected from cattle slaughtered at a local abattoir. The farm produces “natural beef” and, as such, all feed (hay and pasture grasses) are grown on the premises. This enabled the characterization of intake of Po feeds as well as soil ingestion assuming specific consumption rates. Milk was collected from two cows also fed only by hay and

pasture grown on the farm. Milk and cattle issue samples can be considered as potential food for humans. Cattle tissue types include muscle (flesh) as representing the dominant tissue likely to be ingested and also internal organs (liver) that have the potential of being ingested.

Samples were refrigerated and taken to the radio-analytical laboratories of the South African Nuclear Energy Corporation (RadioAnalysis) for analysis. Due to high analysis costs, a limited number of samples of each type were analysed

2.2 Sample preparation

The water samples were filtered using 0.45 µm membrane filters, and then acidified. Soil and sediment samples were dried at 80 °C to constant weight, sieved and homogenized. The grass, beef, bone and milk samples were weighed and dried at 100-110 °C to constant weight, milled and homogenized prior to analysis. The drying temperature was kept relatively low in order to prevent losses of volatile polonium. The grass sample was not washed due to the fact that cattle ingest pasture with adhering soil and the transfer of radionuclides could not be assessed properly if the samples are washed.

For analysis of ^{210}Po , samples were dissolved using an open vessel microwave digestion system. Approximately 1 g of sample was digested for 20 minutes at 100 °C with concentrated nitric acid and hydrogen peroxide. Nitric acid was added periodically during digestion with peroxide being added in the final stages to obtain total dissolution. ^{209}Po was added as yield tracer in the initial stages of the dissolution. After digestion, the samples were evaporated on a hot plate and the final digest was dissolved in 0.5 M hydrochloric acid for radiochemical analysis.

2.3 Radioanalytical measurements

For ^{210}Pb analyses (^{210}Po assumed to be in equilibrium), sediment and soil samples were adjusted to a specific counting geometry for analysis on an HPGe gamma detector system with an ultra-thin beryllium window for low energy counting. Absorption corrections were made for each sample by counting a collimated absorption source.

The procedure for the radiochemical separation of polonium is based on the procedure developed by Flynn [12]. After addition of 0.5 g hydroxylammonium chloride, polonium was pre-concentrated from the solution, acidified with hydrochloric acid, by spontaneous electro deposition onto a silver disc at 80 °C for 4 hours. The alpha activities of ^{209}Po and ^{210}Po were then measured with α -spectrometry. The detection limit obtained for ^{210}Po for a 24 hour counting time and chemical recovery of 70% was better than 0.3 Bq.kg⁻¹ (dry weight) using 1 g of sample.

3 RESULTS AND DISCUSSION

3.1 Activity Concentrations

Activity concentrations of ^{210}Po in soil, sediment, water, grass, cattle tissue and milk samples are shown in Table 1. The activity concentration of ^{210}Po in grass, measured as it is the known food source for cattle in the area, fall in the range as noted from earlier studies for oats and rye [13], and was also similar to the measured concentration in a background sample. As is well known most of the natural radioactivity in leafy plants and grass is ^{210}Po as a result of direct deposition of ^{222}Rn daughters from atmospheric precipitation. Where grass for hay is dried in the sun, it is further exposed to atmospheric deposition of ^{210}Pb and ^{210}Po . This may explain the high concentrations.

The concentration of ^{210}Po in water used to irrigate the crops was very low compared to other biota. This may indicate that the majority of ^{210}Po uptake in cattle feed is due to the radon concentration in the air generated from emanation of the uranium rich deposits in the area concerned and not from the irrigation process as such. The ^{210}Po concentrations in the sediment and soil samples were relatively

high and varied a lot between samples. It is precisely for this reason that it is better to use individual soil concentrations in the calculation of (tissue/soil) concentration ratios rather than averages. The concentration in sediment was however lower than the mean activities reported for 38 sediment samples in the NNR study [11] and those reported in a previous study conducted at RadioAnalysis [14].

Table 1: ^{210}Po activity concentrations in biota from the Wonderfonteinspruit catchment area ($\text{Bq}\cdot\text{kg}^{-1}$ fresh weight)

Sample	Activity ($\text{Bq}\cdot\text{kg}^{-1}$ FW)			Dose ($\text{mSv}\cdot\text{a}^{-1}$)
	This study	Previous data	UNSCEAR	
Water	0.00035 ± 0.00035			0.00025
	0.0165 ± 0.0030			0.012
Sediment	103 ± 12	730 ± 20 [11]		
	215 ± 21	270 ± 20 [14]		
	94.6 ± 10.7			
Soil in wetland	179 ± 18			
Soil next to dam	88.4 ± 11.2			
Cattle feed	5.36 ± 0.05	5.64 ± 0.36 [13]		0.090
		9.55 ± 0.93 [13]		
Feed (background)		5.98 ± 0.63 [13]		
Meat	3.32 ± 0.80	$0.115\text{-}0.250$ [13]	0.06 [15]	0.120
	5.07 ± 0.44			0.183
Liver	52.1 ± 3.3	13.1 ± 0.75 [13]		1.88
Bone	2.53 ± 0.84			
Milk	0.0830 ± 0.0418	0.162 ± 0.075 [13]	0.015 [15]	0.012
Milk (Background)	0.0127 ± 0.0037			0.002

Activity concentrations of ^{210}Po in the muscle of the cattle were high for both samples and much higher than values previously reported for cattle from farms in the same area [13]. Slightly lower concentrations were found in the bone sample. Elevated levels of ^{210}Po were found in the liver sample, which can be expected since internal organs are known to accumulate ^{210}Po [15]. Therefore, a higher level of ^{210}Po transfer to cattle was expected than may be predicted based on the mean activity concentration of the top 10 cm of soil. The activity concentration of ^{210}Po in the milk sample was lower than the previously reported value [13], but higher than the milk samples from a background area and the average value of $0.015 \text{ Bq}\cdot\text{kg}^{-1}$ reported by UNSCEAR [16].

3.2 Annual ingestion dose from milk and meat consumption

It has been found in a previous study [17] that the contribution of ^{210}Po to the overall dose due to ingestion of foodstuffs, was about 20-40% and as high as 80% for intestines, such as kidney and liver. Therefore considering only ^{210}Po will give a good indication of the expected dose due to ingestion. The calculated annual dose due to ^{210}Po for adults consuming meat, milk and water from the farm where the samples were collected, are given in Table 1. The dose conversion factor for ingestion exposure in $\text{Sv}\cdot\text{Bq}^{-1}$ and the consumption rates as prescribed by the South African National Nuclear Regulator [18] were used in the calculations (see Table 2).

The estimated dose was less than $0.25 \text{ mSv}\cdot\text{a}^{-1}$ for all samples, except for the liver. It must be noted that a consumption rate of 30 kg was assumed in the calculation for the dose from the liver sample, which is a very conservative approach, since it is very unlikely that any person will eat 30 kg of liver

originating from this specific farm. Since it is well-known that internal organs accumulate ^{210}Po , exposure can be reduced by dietary choices, such as avoiding the consumption of these animal organs. However, the high accumulation of ^{210}Po in liver is of concern when considering the impact on the cow itself. The dose from meat was also relatively high compared to the milk and water samples. The calculated dose due to ingestion of milk collected in the vicinity of the WFS was 0.012 mSv.a^{-1} which is slightly higher than the milk from the reference location, which was 0.002 mSv.a^{-1} . It is a very conservative approach to assume that all milk consumed comes from the specific farm, since milk producers sell raw milk to dairies where it is mixed with other milk and most people consume milk and milk products bought from shops and not directly from the farmers.

Table 2: South African default parameters for Polonium [18]

Parameter	Value	Unit
Ingestion Dose coefficient for adult age group (DCF)	1.2E-06	Sv.Bq^{-1}
<i>Annual Consumption</i>		
Water	600 (730)	L.a^{-1}
Milk	120 (250)	L.a^{-1}
Beef	30 (100)	kg.a^{-1}
<i>Transfer</i>		
Transfer Soil – Feed (F_v)	1.2E-01 (1.0E-01)	
Transfer to beef (F_f)	5.0E-03	d.kg^{-1}
Transfer to milk (F_m)	2.1E-04 (3.0E-03)	d.L^{-1}
<i>Beef or milk cow daily consumption</i>		
Water	75	L.d^{-1}
Dry feed	16 (25)	kg.d^{-1}
Soil ingestion	1.25	kg.d^{-1}
Wet:Dry mass ratio pasture/grass	0.20 (0.10)	

Previous NNR parameters shown in parenthesis [19]

Table 3: Calculation of dose to humans from ^{210}Po in cattle feed via the meat and milk pathways

Parameter	Calculation	NNR, 2013 [18]	NNR, 1997 [19]
Activity feed (Bq.kg^{-1}) wet	Measured	5.36	5.36
Activity feed (Bq.kg^{-1}) dry	Activity feed (Bq.kg^{-1}) wet X wet:dry ratio	26.8	53.6
Intake by cow (Bq.d^{-1})	Activity dry (Bq.kg^{-1}) X consumption (kg.d^{-1})	429	1340
Activity meat (Bq.kg^{-1})	Intake (Bq.d^{-1}) x F_f (d.kg^{-1})	2.14	6.70
Activity milk (Bq.kg^{-1})	Intake (Bq.L^{-1}) x F_m (d.L^{-1})	0.09	4.02
Human: Intake from meat (Bq.a^{-1})	Activity meat (Bq.kg^{-1}) x consump (kg.a^{-1})	6.43E+01	6.70E+02
Human: Intake from milk (Bq.L^{-1})	Activity milk (Bq.L^{-1}) x consump (L.a^{-1})	1.08E+01	1.01E+03
Total intake (Bq.a^{-1})	Intake meat + Intake milk	7.51E+01	1.68E+03
Dose due to ^{210}Po (Sv.a^{-1})	Total intake (Bq.a^{-1}) x DCF (Sv.Bq^{-1})	9.02E-05	2.01E-03

The dose for humans from cattle feed, via the milk and meat pathways, was calculated to be 0.09 mSv.a^{-1} . The default NNR transfer parameters in Table 2 were used in the calculations shown in Table 3. These parameters have been revised in 2013 to be more realistic and less conservative [18]. Using the 1997 parameters the dose was calculated as 2 mSv.a^{-1} .

3.3 Transfer from feed to animal products

Transfer coefficients (TC), F_m ($d.L^{-1}$) for milk and F_f ($d.kg^{-1}$) for other animal products describe the transfer from feed to animal products. F_m represents the fraction of the element ingested daily that is secreted per liter of milk (day per liter) and F_f represents the fraction of an animal's daily intake of a radionuclide that is transferred to 1 kg of the animal product at equilibrium or at the time of slaughter. TC values are fairly constant for a radionuclide and an animal during a constant feeding period. By knowing the typical TC value and the concentration of the nuclide in feed, the activity in meat can be assessed. Using this approach the expected activity concentrations in meat and milk were calculated from the measured ^{210}Po activity in the feed samples using the NNR default transfer factors in Table 2. The calculated concentrations shown in Table 3 compared fairly well with the actual measured values. However, the concentration in one of the meat samples as well as the liver was much higher than predicted from transfer. An appropriate system-specific TC can be obtained by calculating the ratio between the measured concentrations in the meat ($Bq.kg^{-1}$) to the activity consumed by the animal ($Bq.d^{-1}$). TC values for ^{210}Po were calculated from the measured activities in the meat and milk and the amount of feed consumed daily. The calculated TC values and other published values are given in Table 4. It can be seen from the results that the TC value for milk was comparable to published results and those of meat and liver higher than published values.

Table 4: Transfer factors (F_v), Concentration ratios (CR) and Feed transfer coefficients (F_m , F_f) for ^{210}Po [xE-04]

	This study	[19]	[18]	[8]	[20]	[21]	[6]	[22]	[1]
Beef (F_f); $d.kg^{-1}$	77-118	50	50	50		30			
Liver (F_f); $d.kg^{-1}$	1215					800			
Milk (F_m); $d.L^{-1}$	1.94	30	2.1	0.89 – 3		3	2.3	2.3	
Soil-Feed (F_v)	1500-3045	1000	1200	220-10000	412	230	1610		
Soil-Beef CR	185-576								27.8
Soil-Liver CR	2351-4784								

3.4 Transfer from soil to feed (plant-soil concentration ratios)

The uptake of radionuclides by plants from soil (sediment) is described as the *Transfer Factor*, F_v i.e. radionuclide concentration in the plant (dry weight) per radionuclide concentration in the soil in $Bq.kg^{-1}$. Calculated soil-to-feed transfer factors are presented in Table 4. Table 1 shows activity concentration in $Bq.kg^{-1}$ wet weight, so it was necessary to convert these data to dry weight activity for the purposes of the CR calculation by applying the wet:dry weight conversion factors. The calculated transfer values varied from 0.15 to 0.30 which compared well with published values and those recommended by the NNR [18]. Predicted activity concentrations in feed using the NNR default value was 10.6 – 21.5 $Bq.kg^{-1}$ (dry weight), which compared well with the measured activity concentration of 26.8 $Bq.kg^{-1}$.

3.5 Transfer from soil to muscle

The *Concentration Ratio (CR)* describes accumulation in the plant or animal i.e. the ratio of the activity concentration of a radionuclide in $Bq.kg^{-1}$ fresh or dry mass in the animal to initial activity concentration of the radionuclide in water or soil. CR values are used in models to predict impact on non-human biota and are commonly available in databases. The soil-muscle concentrations for ^{210}Po , calculated for the all possible combinations of the measured concentrations, varied from 0.02 to 0.06 for beef muscle. as shown in Table 4. The concentration ratio for liver (0.2 to 0.5) was about a factor 10 higher than for muscle.

The default transfer parameters used in biota dose assessment software such as ERICA were used to estimate the concentration of ^{210}Po in muscle tissue from the soil concentration. The estimated concentration in meat using the CR in ERICA was 0.24-0.50 Bq.kg⁻¹ which is about 1-2 orders of magnitude lower than the measured values. Application of CRs appears therefore to have limited value. The advantage of using soil-tissue CRs is that it is independent of the route of exposure (i.e. ingestion or inhalation). It is however reliable only if there is a definite linear dependency of the tissues concentrations on the soil concentration. Therefore transfer coefficients are most often used to predict activity concentration in animal tissues.

4 CONCLUSION

This study provides activity concentrations and concentration ratio values for livestock from a mining area with elevated NORM concentrations in soil. The data set is however limited in scope and replication numbers and highlights the need for additional studies to better define these values.

Despite the relatively high activity concentrations in the soil and sediment on this farm located in the Wonderfonteinspruit area, consumption of any of the animal products analysed in this study, will result in a dose of less than 0.2 mSv.a⁻¹. The only concern is the high dose which may result from the liver sample.

There are good correlation between the transfer coefficients for ^{210}Po in the feed-animal pathway derived from this study and the default parameters recommended for use by the NNR for milk and beef. Use of the default parameter of beef to predict transfer to liver will result in an underestimated activity concentration. The calculated transfer factors for soil-plant transfer compare well with published values and those recommended by the NNR. Predicted activity concentrations in feed using the NNR default value compares well with the measured activity concentration in the feed sample. Soil-to-muscle CR values are higher than ERICA tool reference values. Equilibrium based CRs appear to have limited applicability with regards to the prediction of activity concentration of ^{210}Po in livestock, based on measurement of soil concentrations only. The results highlights the need for appropriate system-specific transfer parameters to underpin the dose assessment models being used to assess the impact of ionising radiation on livestock.

5 ACKNOWLEDGEMENTS

The author wishes to thank the personnel of the radio-analytical laboratory at Necsas for their assistance in performing the measurements.

6 REFERENCES

- [1] Brown, J.E., Alfonso, B., Avila, R. Et al., 2008. The ERICA tool. *J. Environ. Radioact.*, 99, 1371-1383.
- [2] Brown, J.E., Gjelsvik, R., Roos, P., et al., 2006. Levels and transfer of Po-210 and Pb-210 in Nordic terrestrial ecosystems. *J. Radioanal. Nucl. Chem.*, 102, 430-437.
- [3] Gomez-Ros, J.M., Prohl, G., Taranenko, V., 2004. Estimation of internal and external exposures of terrestrial reference organisms to natural radionuclides in the environment. *J. Radiol. Prot.*, 24, A79-A88.
- [4] Durand, J.F., 2012. The impact of gold mining on the Witwatersrand on the rovers and karst system of Gauteng and North West Province, South Africa. *J. African Earth Sciences*, 68, pp. 24-43.
- [5] Johansen, M.P., Twining, J.R., 2010. Radionuclide concentration ratios in Australian terrestrial wildlife and livestock: data compilation and analysis. *Radiat. Environ. Biophys.*, 49, 603-611.
- [6] Strok, M., Smodis, B., 2012. Transfer of natural radionuclides from hay and silage to cow's milk in the vicinity of a former uranium mine. *J. Environ. Radioact.*, 110, 64-68.

- [7] Fresenko, S., Howard, B.J. Isamov, N., et al., 2007. Review of Russian language studies on radionuclide behaviour in agricultural animals: part 2. Transfer to milk. *J. Environ. Radioact.*, 98, 104-136.
- [8] IAEA, 2010. Handbook of Parameter values for the prediction of radionuclide transfer in terrestrial and freshwater environments. Technical report series no.472, IAEA, Vienna. [Online] Available at: http://www-pub.iaea.org/MTCD/publications/PDF/trs472_web.pdf.
- [9] Coetzee, H., Winde, F., Wade, P.W., 2006. An assessment of sources, pathways, mechanisms and risks of current and potential future pollution of water and sediments in gold-mining areas of the Wonderfontein spruit Catchment. WRC Report No. 1214/06, Water Research Commission, 2006 [Online] Available at: <http://www.wrc.org.za>.
- [10] DWA, 1999. Report on the Radioactivity Monitoring Programme in the Mooi River (Wonderfontein spruit) Catchment. Report no N/C200/00/RPQ/2399, Institute for Water Quality Studies: Department of Water Affairs and Forestry, Pretoria. May 1999. [Online] Available at: https://www.dwa.gov.za/iwqs/radioact/mooi/index_pdf.html.
- [11] NNR, 2007. Radiological Impacts of the Mining Activities to the Public in the Wonderfontein spruit catchment area. Technical Report No. TR-RRD-07-00006. Unpublished report.
- [12] Flynn, W.W., 1968. Determination of low levels of polonium-210 in environmental materials. *Anal. Chim. Acta.*, 43,221-227.
- [13] Louw, I., Faanhof, A., Kotze, D., 2009. Determination of Polonium-210 in various foodstuffs after microwave digestion. *Radioprotection*, 44:5, 89-95.
- [14] Ramatlape, N.I.I., Faanhof, A., Kotze, D., et al., 2010. Analysis of sediments for NORM and radiocesium using gamma spectrometry and gas-flow proportional counting. Proceedings of the International Youth Nuclear Congress, Cape Town, 12-18 July 2010.
- [15] Bunzl, K., Kracke, W. Kreuzer, W., 1979. Pb-210 and Po-210 in liver and kidney of cattle. *Health Phys.*, 37:4, 320-330.
- [16] UNSCEAR, 2000. United Nations Scientific Committee on the Effects of Atomic Radiation, Sources and Effects of Ionising Radiation, Vol I, United Nations, New York
- [17] Louw, I., Faanhof, A., Kotze, D., et al., 2011. A first order assessment of the potential radiological impact of foodstuffs grown in a catchment area influenced by mining and mineral processing industries. *Radioprotection*, 46:6, S213-S222.
- [18] NNR, 2013. Regulatory Guide; Safety Assessment of radiation hazards to members of the public from NORM activities, RG-002. National Nuclear Regulator, South Africa.
- [19] NNR, 1997. Guideline on the assessment of radiation hazards to members of the public from mining and minerals processing facilities. LG 1032. Council for Nuclear Safety, Centurion, South Africa.
- [20] Pietrzak-Flis, Z., Skowronska-Smolak, M., 1995. Transfer of Pb-210 and Po-210 to plants via root system and above-ground interception. *Sci. Tot. Environ.*, 162, 139-147.
- [21] Ewers, L.W., Ham, G.J., Wilkins, B.T., 2003. Review of the transfer of naturally occurring radionuclides to terrestrial plants and domestic animals. Report NRPB-W49, National Radiological Protection Board, United Kingdom.
- [22] Howard, B.J., Beresford, N.A., Barnett, C.L., et al., 2009. Radionuclide transfer to animal products: revised recommended transfer coefficient values. *J. Environ. Radioact.*, 100, 262-273.

Release Fractions from Airborne Fluid and Slurry Spills

Judith Ann Bamberger^{a*}, John A. Glissmeyer^{a+}

^aPacific Northwest National Laboratory, P.O. Box 999, Richland, WA 99354 U.S.A.

Abstract. Release fractions are commonly used to make conservative estimates of emissions from processes and are applied to characterize industrial operations to safeguard workers and public. Release fractions cannot be derived theoretically; they must be measured. Appropriate measurements are limited. This paper describes tests that were conducted to provide large-scale release fraction data for estimating releases from three operations proposed for waste remediation at the Hanford Site in Richland, Washington. Experiments were conducted to measure release fractions of three processes: 1) pipe discharge of liquid and slurry in free fall into a liquid or slurry, 2) jet transfer of contents to the other side of the tank either impacting the tank wall or falling into the fluid pool, and 3) high pressure fan jet striking a steel plate or simulated waste from a small stand-off distance. The tests were conducted without forced ventilation in an enclosed prototypic ¼-scale model of a 3785 m³ (1 million gallon) tank in use at the Hanford Site for storage of radioactive waste. Aerosol releases were characterized based on filter samples of aerosol collected near the process stream, tank wall, and tank top to determine release fraction at engineering scale. Particle size distribution measurements were analysed to determine whether the particles were in the respirable range. The release fractions for the top of the unventilated tank ranged from 9×10^{-7} to 6×10^{-4} depending on the process simulated. The particle size distribution was determined to be log-normally distributed with geometric mean diameters ranging from 3 to 8 µm. Thus, all particles are conservatively considered to be “respirable.”

KEYWORDS: *aerosol generation; release fraction; water spill; slurry spill; high-pressure jet.*

1 INTRODUCTION

Waste mobilization and retrieval processes are implemented to remediate nuclear waste stored in 22.9-m (75-ft) diameter 3785-m³ (1 million-gallon) underground storage tanks at the Hanford Site in Washington State. These processes are developed based on the characteristics of the waste to be retrieved and other operational constraints. These processes have the potential to generate aerosols or suspend solids during operation. The purpose of this study was to evaluate the aerosol generation performance of several types of fluid transport processes that could be considered for future implementation [1]. These processes included: 1) Discharging liquid or slurry from the mouth of a vertically oriented 5-cm- (two-in.-) diameter pipe. The discharging material was in free-fall from the mouth of the pipe near the top of the tank into a liquid or slurry pool at the bottom of the tank, a distance of 3.48 m (11.4 ft). 2) The jet from a nozzle transferring liquid or slurry waste from one side of the tank to the other. The discharging liquid was aimed at the opposite side of the tank from the nozzle and either impacted the tank wall or fell into a liquid or slurry pool in the bottom of the tank. 3) A high pressure fan jet of liquid striking a steel plate or simulated waste from a stand-off distance of a few cm (in.).

These experiments built on research conducted at Pacific Northwest National Laboratory (PNNL) in the 1980s to characterize aerosols generated by releases of powders and solutions by Ballinger et al. [2-4] and Sutter et al. [5] and are summarized in the US Department of Energy Handbook [6]. More recently, experiments to determine aerosol generation during pipe leaks have been conducted at PNNL led by Phillip Gauglitz [7-11]; a method was developed to determine generation rate of aerosol droplets from transient droplet concentration data within chambers. These experiments led to development of a conservative aerosol generation rate correlation appropriate for a wide range of slurries and salt solutions.

* Contact e-mail: Judith.Bamberger@pnnl.gov; BambergerJ@asme.org

+ Contact e-mail: JonGliss@charter.net

2 METHOD

The three aerosol generation processes, measurement methods, and experiments are described.

2.1 Aerosol Generation Processes

Three processes identified as potential sources of aerosol generation during in-tank operation were investigated to determine release fractions.

2.1.1 Cutting Jet

Cutting jets are mounted on an articulated arm or crawler and are used for cutting, dislodging, or cleaning solids or slurry from surfaces. The jet configuration used to define this experiment includes five jets mounted in a semicircle directed downward. The jets are commercially available wash jets (Spraying Systems Company of Wheaton Illinois, ¼ MEG 2505). Tests conducted at the Hanford cold test facility by others showed that the preferred pressure for cutting jet operation is 2.07 MPag (300 psig). The proposed jet system can operate at pressures up to 8.27 MPag (1200 psig). The effective stand-off distance for the cutting jets ranges from 2.5 to 12.5 cm (1 to 5 in.) based on the deployment configuration. The fan jet has a spray angle of 25 degrees. For this evaluation a single jet mounted in line with a pressure gage was used to model the cutting jet process as is shown in Figure 1a.

Figure 1: Examples of jets



a) Cutting jet

b) Crawler showing transfer jet

c) Transfer jet in test tank

2.1.2 Transfer Jet

The transfer jet nozzle is mounted on a crawler as shown in Figure 1b. The transfer nozzle configuration tested was mounted on the side of the tank as is shown in Figure 1c. Fluid transfer process is operated at relatively low flow rates and pressures and is used to spray fluid from the crawler location to a collection location near a retrieval pump or other retrieval device.

2.1.3 Transfer Jet: Flow from an Open Pipe

Transfers of fluid or slurry from tank to tank occur through nominal 5 cm (2 in.) diameter pipes or 5 cm (2 in.) hose in hose configurations. Some transfers may be conducted using nominal 7.6 cm (3 in.) diameter pipe. The process flow rate range is 0.0032 to 0.0038 m³/s (50 to 60 gpm) for hose in hose transfers, 0.0032 to 0.0063 m³/s (50 to 100 gpm) for 5 cm (2 in.) pipe transfers, and 0.0032 to 0.0101 m³/s (50 to 160 gpm) for 7.6 cm (3 in.) pipe transfers. The nozzle configuration evaluated is shown in Figure 1c.

2.1.4 Aerosol Generation Experiment Configuration

All aerosol generation characterization tests were conducted in a ¼-scale model of a waste tank that provided an enclosed structure [12]. The tank is a ¼-scale model of a 22.9 m diameter, 3785 m³

Hanford double-shell tank. Three segments of the tank dome were installed; the remaining quadrant of the tank was closed with a plastic tarp. The enclosure prevented aerosol from entering or leaving the tank test chamber. Fluid or slurry was pumped from the mix tank through the nozzles into the test tank. Figure 1c shows the arrangement of the test tank with the top rim of the tank, part of the dome and one of the test nozzles. The air samplers clustered near the top of the tank are shown in Figure 2. The locations of the experiment components within the test tank are summarized in Table 1.

Figure 2: Location of instrumentation near top of tank.



Table 1: Location of hardware and sampling equipment in the test tank

Item	Location	Radial	Angular	Elevation
		R=0 At tank center (m)	$\theta = 0$ At north (degrees)	Z=0 At tank floor (m)
Sampler				
Sampler 1	Top of tank	0.31	188	3.51
Sampler 2	Top of tank	0.31	230	3.35
Sampler 3	Top of tank	0.31	230	3.35
Sampler 4	Side of tank	2.87	158	1.52
Sampler 5	Side of tank	2.87	186	1.52
Sampler 6	In tank space	1.40	155	1.22
Dust Monitor	Top of tank	0.31	188	3.51
Optical Particle Counter (OPC)	Top of tank	0.31	188	3.35
Jets				
	Orientation			
Discharge pipe	Vertical	2.60	8	3.48
Transfer jet	Horizontal	2.44	175	2.44
Cutting jet	Vertical	1.22	153	3.35
Tank Dimensions				
Tank height	--	--	--	2.44
Dome height	--	--	--	1.07
Riser height	--	--	--	0.15
Total height	--	--	--	3.66
Tank radius	--	2.86	--	--
Domed area	--	--	188.5 to 360 to 98.5	--
Plastic covered	--	--	98.5 to 188.5	--

The cutting jet was powered using a portable gasoline driven pressure washer that produced pressure up to 22.1 MPag (3200 psig). The unit was instrumented with pressure gages to measure the pressure at the unit and at the nozzle. An Ingersoll Rand Standard Pump Division centrifugal pump was used to circulate fluid between the mix tank and the nozzles being evaluated in the test tank. The pump has a capacity of 0.0095 m³/s (150 gpm) and 1.90 MPag (275 psig). The mix tank was used to supply fluid to this pump. After the mix tank was emptied, the fluid or slurry was pumped back into the mix tank to provide the desired number of operating cycles. A compressed air driven transfer pump was used to move fluid from the test tank to the mix tank. The transfer pump was powered by a 0.779 sm³/s (1650 scfm), diesel driven, portable air compressor. A digital video camera mounted on the tank walkway around the perimeter of the tank was used to film the process during the tests.

2.2 Measurement Methods

Two methods were used for monitoring air concentration in the test tank during the test runs: collecting air samples on filters and qualitatively monitoring particle size and concentration in near real time with an optical particle counter (OPC). Samples of the airborne material were collected during the background run and the process simulations. The samples were collected on 25-mm diameter mixed cellulose ester membrane filters. The samples were contained in open-face filter holders which were connected by flexible tubes to personal sampling pumps located outside the tank. The filter holders were placed to collect samples at four locations in the tank as listed in Table 1. Only the three air samplers at the top of the tank were expected to measure aerosol at a location approximating that where exhaust air is drawn from the full scale tanks.

At the end of a test, the air samplers were retrieved and packaged for transport. In the lab, the cassettes were removed from the filter holders and dried for thirty minutes in an oven at about 90°F (32 °C). The cassettes were allowed to equilibrate to room temperature and were reweighed. For analysis, the filters were removed from the cassettes and placed in known quantities of deionized water to determine the fluorescent dye content. After several hours, the water was analyzed to determine the content of fluorescent dye as compared to prepared standards. Each test was analyzed as a batch. Standards, field blanks, and process blanks were analyzed with each batch of air samples.

The estimated aerosol release fraction was calculated for each sample according to Equations 1 and 2. The quantity of dye in the sample was obtained from the fluorimetry results for each sample. The dye in the process was obtained from analyses of process water samples and measurements of the process water. The tank volume was calculated based on tank geometry, and the sample volume was calculated from the flow rate and elapsed time.

$$\text{Release fraction of liquid} = \frac{\text{dye in sample}}{\text{dye in process}} \cdot \frac{\text{tank volume}}{\text{air sample volume}} \quad (1)$$

$$\text{Release fraction of solids} = \frac{\text{solids in sample}}{\text{solids in process}} \cdot \frac{\text{tank volume}}{\text{air sample volume}} \quad (2)$$

The OPC categorized particulate into one of six size brackets based on the amount of laser light scattered by a particle that is equivalent to that of a spherical calibration particle made of polystyrene latex. The OPC was operated throughout each testing day and for all test runs.

2.3 Experiments

The experimental test matrix evaluated three processes: cutting jet, transfer jet, and flow from an open pipe, using two fluids: water and slurry. In addition, the cutting jet impacted two surfaces: steel and simulant. Examples of the three types of experiments are shown in Figure 3. The processes were operated at several flow rates that are listed in Table 2. Based on the capacity of the mix tank, experiments to evaluate the transfer jet and the tank transfer were conducted as a series of sequential runs to provide an adequate sampling time.

3 RESULTS

This section describes the characteristics of the aerosol created by the processes simulated in the test tank. The results presented and discussed include the real-time aerosol concentration, particle size distribution, and the release fractions.

3.1 Aerosol Concentration

Aerosol concentration was measured using an optical particle counter. With each test run, the OPC data showed a sharp increase in aerosol concentration from the background level and a gradual decline in aerosol concentration at the conclusion of the process simulation. The particle count data were

converted to the volume (or mass) of aerosol in each particle size interval. Plots for each test (see Bamberger and Glissmeyer [1]) show that when a process is repeated rapidly enough the concentration of airborne material continues to ratchet upward and the concentration does not decrease back to background during the cycles, either because the tank was not ventilated or because sufficient time had not elapsed in between operations.

Figure 3: Examples of jet operations



3.2 Particle Size

The particle count data from the OPC was converted to a volume (equivalent to mass for homogenous particles) within each size bracket. The data were reasonably well represented by a unimodal (single peak) distribution [1]. In most cases, the secondary fine particle mode had only a minor contribution to the particle volume distribution. The distribution parameters are the geometric mean diameter (GMD) and the geometric standard deviation (GSD). The GMD remained about the same for the 5-cm- and 1.43-cm-diameter nozzles. When the high pressure spray was tested, the GMD decreased.

3.3 Release Fraction

The release fraction results are tabulated in Table 2 and listed by location in the test tank for each process simulated. The fluorimetry-based release fractions represent the release of the liquid fraction of the process slurry. There is an entry in the table for each air sampler unless the sampler pump malfunctioned and no data was obtained for that sampler.

The results for Run 7 are for the cutting jet striking bare steel. The cutting jet may be used to scarify solid waste that is otherwise not sufficiently mobilized by other dislodging mechanisms. If the water-based cutting jet actually strikes bare steel, it is not striking waste, and waste is not being released at that particular time. Consequently, a measured release fraction from this run is not actually applicable to waste retrieval. The results from Runs 8 and 9 are the appropriate release fractions to use for this purpose. The process simulation only contained a solids component for Runs 8 through 12. Release fractions for solids suspension were obtained for only a third of the possible instances because the solids measurement method was not as sensitive as that for the liquid fraction. Agreement between the liquid and solid release fractions was variable but always within a factor of 3. However, in the one case (Run 9) where both release fractions were measurable at the top of the tank, the results showed excellent agreement among the three samplers.

Table 2: Release fractions

Run	Process	Background			Peak		Release Fraction Measurements from Fluorescent Tracer in Process Water and from Dry Solids (in parentheses)			Bounding Release Fraction
		GMD μm	GSD μm	GMD μm	GSD μm	Tank Top	Tank Wall	Near Process Stream	At Tank Top	
1	Background	6.0	1.7	N.A.	N.A.	--	--	--	--	
Pipe Discharge										
2	Liquid discharge 0.0022 m ³ /s	6.6	1.8	7.5	1.4	0.69, 0.80, 0.93 x 10 ⁻⁶	0.55, 1.2 x 10 ⁻⁶	2.2 x 10 ⁻⁶	9 x 10 ⁻⁷	
3-4	Liquid discharge .00662 and 0.0113 m ³ /s	6.2	1.7	6.8	1.4	N.A.	N.A.	N.A.	N.A.	
11	Slurry discharge 0.00271 m ³ /s	4.0	2.3	6.7	1.4	0.43, 1.5, 1.7 x 10 ⁻⁶	2.1, 2.4 x 10 ⁻⁶	2.1 x 10 ⁻⁶	2 x 10 ⁻⁶	
12	Slurry discharge 0.00789 m ³ /s	6.9	1.6	6.4	1.4	3.1, 3.7, 4.1 x 10 ⁻⁶	5.0 x 10 ⁻⁶	4.5 x 10 ⁻⁶	4 x 10 ⁻⁶	
Transfer Jet										
5	Liquid discharge 0.00202 m ³ /s	7.4	1.7	7.0	1.4	0.48, 3.2 x 10 ⁻⁶	3.6, 5.0 x 10 ⁻⁶	4.1 x 10 ⁻⁶	3 x 10 ⁻⁶	
6	Liquid discharge 0.00360 m ³ /s	8.0	1.4	7.2	1.3	N.A.	N.A.	N.A.	N.A.	
10	Slurry discharge 0.00145 m ³ /s	6.5	1.6	5.0	1.6	1.8, 2.1, 2.1 x 10 ⁻⁶	2.5, 2.7 x 10 ⁻⁶ (3.5, 6.8 x 10 ⁻⁶)	1.6 x 10 ⁻⁵ (4.4 x 10 ⁻⁵)	2 x 10 ⁻⁶	
Cutting Jet										
7	Jet on steel at low pressure	8.1	1.4	7.1	1.3	1.0, 5.6 x 10 ⁻⁴	0.12, 6.3 x 10 ⁻⁴	4.0 x 10 ⁻⁴	6 x 10 ⁻⁴	
8	Jet on simulant at low pressure	5.4	1.6	4.0	1.5	5.5, 7.7 x 10 ⁻⁵	N.A.	1.4 x 10 ⁻⁴ (1.3 x 10 ⁻⁴)	8 x 10 ⁻⁴	
9	Jet on simulant at high pressure	6.4	1.4	3.2	1.5	6.0, 6.0, 8.1 x 10 ⁻⁵ (6.6, 6.6, 7.9 x 10 ⁻⁵)	8.8, 9.1 x 10 ⁻⁵ (3.9, 3.9 x 10 ⁻⁵)	8.0 x 10 ⁻⁵	8 x 10 ⁻⁵	

4 CONCLUSION

The bounding release fraction results for this study are listed in Table 2. This bounding release fraction summary focuses on the values obtained from measurements taken at the top of the tank which is the location from which ventilation air may be drawn. The liquid fraction results are presented because this method of measurement (dye tracer) was more sensitive than that used for the solids fraction (solids loading). These results range over nearly two orders of magnitude. It is noted that the height of the test tank is lower than that of the full scale tank by a factor of 4, but the tests were not conducted to provide the release fraction as a function of height.¹⁾ The release fractions calculated based on samples obtained near the point of the process or fluid stream ranged from the same to as much as an order of magnitude higher than the release fractions obtained from measurements taken near the tank top at an elevation of 3.35 m (11 ft).

4.1 Recommendations

The release fraction measurements could be reported with all significant digits; however, there are simplifications made in simulating processes and significant spatial and orientation differences between the individual sampling locations. Release fractions are commonly used to make conservative estimates of emissions from processes. Usually, rather gross assumptions are made in such estimates, such as the total failure of abatement equipment and the use of maximum inventory values. Consequently, it is common practice to report bounding release fraction values with single digit accuracy.

5 ACKNOWLEDGEMENTS

This work was funded by the US Department of Energy Office of Environmental Management and conducted for CH2MHill Hanford Group Inc. under direction of Lucinda Penn.

6 REFERENCES

- [1] Bamberger, J.A., Glissmeyer, J.A., 2004. Release Fraction Evaluation. PNNL-14545. Pacific Northwest National Laboratory, Richland, Washington.
- [2] Ballinger, M.Y., Hodgson, W.H., 1986. Aerosols Generated by Spills of Viscous Solutions and Slurries. NUREG/CR-4658. Pacific Northwest Laboratory, Richland, Washington.
- [3] Ballinger, M.Y., Buck, J.W., Owczarski, P.C., et al., 1988. Methods for Describing Airborne Fractions of Free Fall Spills of Powders and Liquids. NUREG/CR-4997. Pacific Northwest Laboratory, Richland, Washington.
- [4] Ballinger, M.Y., Sutter, S.L., Hodgson, W.H., 1987. New Data for Aerosols Generated by Releases of Pressurized Powders and Solutions in Static Air. NUREG/CR-4779. Pacific Northwest Laboratory, Richland, Washington.
- [5] Sutter, S.L., Johnston, J.W., Mishima, J., 1981. Aerosols Generated by Free Fall Spills of Powders and Solutions in Static Air. NUREG/CR-2139. Pacific Northwest Laboratory, Richland, Washington.
- [6] U.S. Department of Energy Handbook, 2013. Airborne Release Fractions / Rates and Respirable Fractions for Nonreactor Nuclear Facilities Volume 1 – Analysis of Experimental Data. DOE-HDBK-3010-94. U.S. Department of Energy, Washington, D.C.
- [7] Schonewill, P.P., Gauglitz, P.A., Bontha, J.R., et al., 2012. Large-Scale Spray Releases: Initial Aerosol Test Results. PNNL-21333, WTP-RPT-217 Rev. 0. Pacific Northwest National Laboratory, Richland, Washington.
- [8] Mahoney L.A., Gauglitz, P.A., Blanchard, et al. 2012. Small-Scale Spray Releases: Orifice Plugging Test Results. PNNL-21361. Pacific Northwest National Laboratory, Richland, Washington.

¹⁾ Height influences release fractions in two competing ways: 1) greater height of a spill is likely to increase

aerosol generated and 2) greater height from the source of aerosol of generation to the potential receptor decreases concentration due to particle depletion mechanisms.

[9] Mahoney, L.A., Gauglitz, P.A., Kimura, M.L., et al., 2013. Small-Scale Spray Releases: Initial Aerosol Test Results. PNNL-21367 Rev. 1. Pacific Northwest National Laboratory, Richland, Washington.

[10] Schonewill, P.P., Mahoney, L.A., Gauglitz, P.A., et al., 2013. Small-Scale Spray Releases: Additional Aerosol Test Results. PNNL-22402, Rev. 0. Pacific Northwest National Laboratory, Richland, Washington.

[11] Daniel, R.C., Gauglitz, P.A., Burns, C.A., et al., 2013. Large-Scale Spray Releases: Additional Aerosol Test Results. PNNL-22415, WTP-RPT-221 Rev.0. Pacific Northwest National Laboratory, Richland, Washington.

[12] Bamberger, J.A., Bates, J.M., Waters, E.D., et al. 1993. System Design Specification for the ¼-Scale Tank and Ancillary Equipment. PNL-8120. Pacific Northwest Laboratory, Richland, Washington.

Basic Characterization of a Radioactive Facility and Evaluation of Risk Agents

Carneiro, J. C. G. G., Alves, A. S., Sanches, M. P., Rodrigues D. L., Levy, D. S^{*}, Sordi, G. M. A. A

Instituto de Pesquisas Energéticas e Nucleares (IPEN/CNEN-SP)
Av. Prof. Lineu Prestes, nº 2242 - Cidade Universitária
05508-000 São Paulo, Brasil.

Abstract. This is an exploratory and descriptive study with qualitative and quantitative approaches to investigate the basic characterization of a Brazilian radioisotope production facility through ample knowledge of the workplace, workforce, task performed and identification of present risk agents in labor environment. The studied sample was composed by 102 workers distributed in eight work processes. Data were collected from April 2013 to July 2014 by applying questionnaire forms and complemented by interviews and observations. The descriptive statistical analysis included ANOVA test and non-parametric tests, among others. For the purpose of this study, there was adopted a significance level of 5% ($p < 0.05$). The analysis of socio-demographic variables demonstrated that male gender predominated in total sample (74.5%) and the mean age of the workers was (51.8 ± 1.7) years. The largest percentage of the responders (70.6%) was technician-level workers. Regarding task-related exposure, there was considered that all groups presented the same exposure profile. At the workplace, there were identified 17 risk agents, including physical, chemical, biological, ergonomic and accident risks. The workforce was categorized into 3 risk groups according to relative frequency distribution of the occupational risks. Among the sixteen qualitative variables studied at the workplace, only three of them did not demonstrate relative frequency. The only variable that showed association with the three risk groups was the possibility of the contact with ionizing radiation. The study provided an overview of the perception of occupational risk at the facility. According to the results obtained by statistical analysis, most of the qualitative variables presented statistically significant association ($p < 0.001$) related to the occurrence of occupational risks. Even though the workers may be potentially exposed to different risk agents, the ionizing radiation was the main physical risk factor observed in this facility.

KEYWORDS: *occupational risk; basic characterization; workers profile; qualitative assessment.*

1 INTRODUCTION

The occupational risk assessment is a structured and systematic process, which depends on the correct identification of probable risk factors and agents, through qualitative and/or quantitative evaluation of worker exposure [1].

The first step in workplace exposure risks assessment requires the execution of a basic characterization that enable the qualitative analysis, which comprises the collection and appropriate structure of subjective information about the workers and their work environment. Moreover, an analysis of the socio-demographic variables was carried out for the purpose of a better understanding of the sampling distribution [2-4].

There is a significant difference between processes involving workers of a Brazilian radioisotopes production facility and processes involving workers of other professional categories. Relevant particularities considered to this study comprise the exposure to different risk agents according to their nature: physical (ionizing radiation), chemical (chemical substances involved in the processes), biological (contaminated objects), ergonomic (stress-causing situations) and accidents (fires and explosions) [5-7].

The main purpose this study was to carry out the basic characterization of a Brazilian radioisotope production facility through ample knowledge of the workplace, workforce, task performed and identification and evaluation of occupational risk agents in the workplace.

* Presenting author, e-mail: denise@omicron.com.br

2 METHOD AND MATERIALS

The population of the studied Brazilian radiopharmacy facility is composed of 204 workers: 102 federal public employees (50%), 57 contractors (27.94%) and 45 students / trainees (22.06%). Nevertheless, the studied sample was limited to public employees, which represented 50% of total facility population.

The development of this study comprised a detailed evaluation process, covering the basic characterization of the workplace, workgroups and the identification of the probable occupational risks related to execution of workers' tasks [6]. The exploratory analysis involved descriptive statistical analysis of qualitative variables related to the workplace.

From April 2013 to July 2014 a variety of methods were used to gather both quantitative and qualitative data through a self-completed questionnaire, interviews and direct observations. The respondents of the questionnaire were the managers of each workgroup at the facility. The structured questionnaire was based on work processes involving materials used to new radiopharmaceuticals research and production, workplace conditions, personal and collective protection equipment and identification of provable risk agents related to the workers' tasks.

The software's Statistical Package for Social Science (SPSS) version 17, Minitab 16 and Microsoft Excel 2010 were used for statistical analysis [8, 9]. Initially, qualitative and quantitative variables were studied through descriptive statistics, considering frequency and distribution of a particular event.

The statistical methods comprised nonparametric tests (Equality of two proportions, Chi-square and Yates correction), ANOVA test, descriptive measures of location (mean, median and quartiles) and dispersion (standard deviation and coefficient of variation). Moreover, it was used a P value of 5% to determine statistical significance. Therefore, all confidence intervals were constructed at a 95% statistical confidence level [10-12].

3 RESULTS

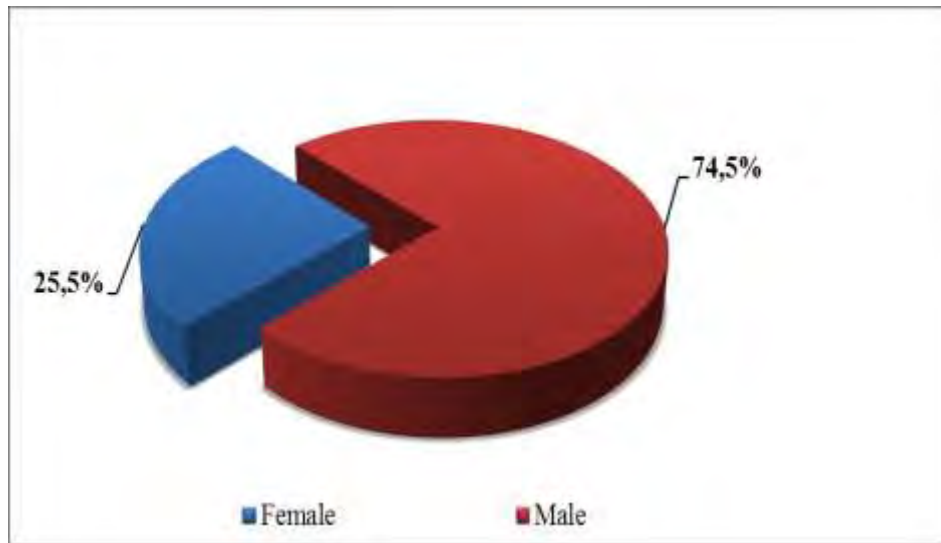
3.1 Basic characterization – Evaluation of occupational exposure

Based on subjective information obtained by questionnaire about workplace, workforce and risk agents, the 102 responders were distributed into eight work processes: 27 workers in production of primary radioisotopes (representing 26% of the total sample), 8 workers in production of labeled compounds (8%), 2 workers in production of lyophilized kits (2%), 24 in Quality Control (23%), 4 in Quality Assurance (4%), 5 workers in Research & Development of methods and Innovation (5%), 25 in infrastructure team (24%) and 8 in Radioprotection team (8%).

3.1.1 Workers profile – analysis of sociodemographic variables

The equality of two proportions test was used to determine the distribution of the relative frequency (percentage) of socio-demographic variables, such as gender, educational level and age. Figs. 1 and 2 illustrate the distribution of workers according to gender and educational level respectively.

Figure 1: Distribution of workers according to the gender



The analysis of sociodemographic variables showed a predominantly male-gender population in the sample (74.5%).

The results of distribution related to the educational level variable (Fig.2) show that 72 workers have technical level, representing the majority of the sample, about (70.6%) of total respondents.

Figure 2: Distribution of sample according to the educational level

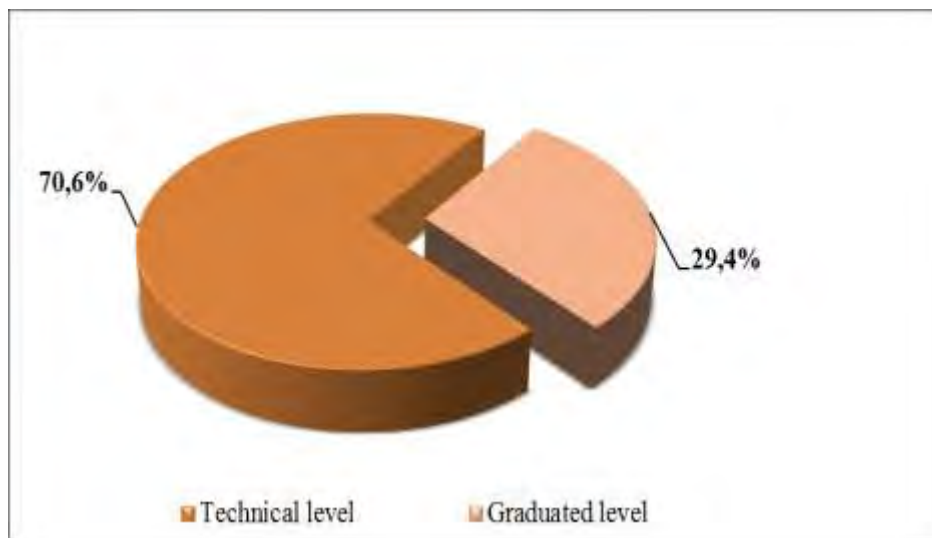


Table 1 shows the complete descriptive analysis for the age variable.

The average age of workers was about (51.8 ± 1.7) years. Table 1 demonstrates that the standard deviation (8.6) and the CV of 17% can be considered low (<50%) when compared to the average. These indicators demonstrate low variability and consequently indicate the homogeneity of data.

Table 1: Complete descriptive analysis for the age variable.

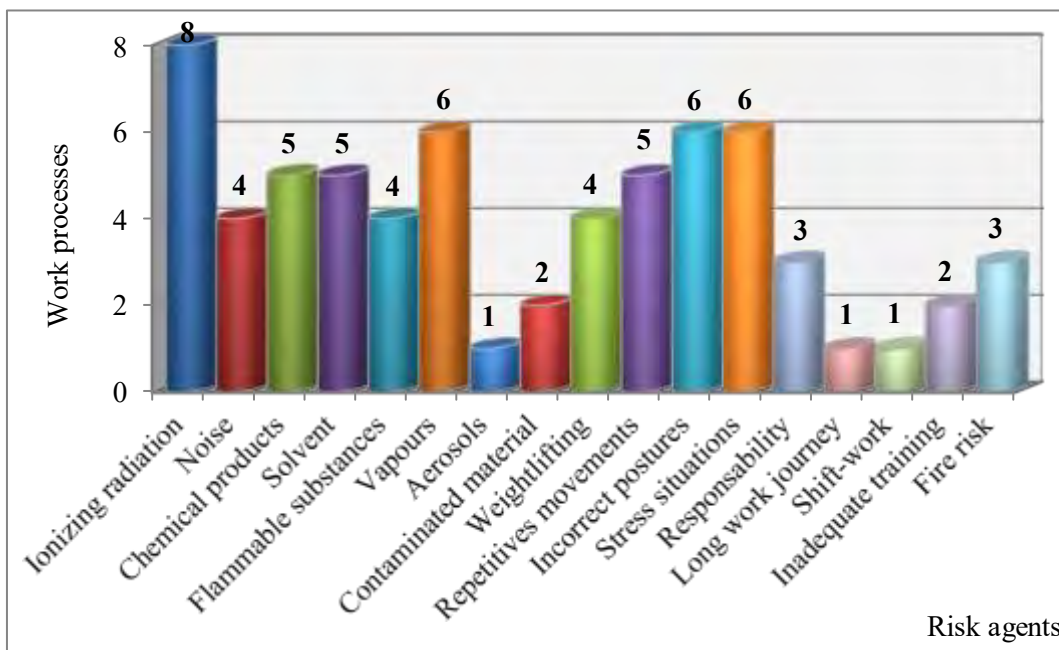
Descriptive analysis	Age
Mean	51.8
Median	52
Standard deviation	8.6
Coefficient of variation (CV)	17%
1° Quartiles (Q1)	49
3° Quartiles (Q3)	57
Minimum	24
Maximum	69
Number of workers (sample)	102
Confidence interval (CI)	1.7

3.1.2 Qualitative assessment of occupational risk agents

The questionnaire used in this research enabled to identify seventeen occupational risk agents at the facility, considering the workplace, work processes and manipulations of materials.

Fig. 3 shows the seventeen risk agents identified at workplace, as well as their frequencies in the eight work processes.

Figure 3: Identification of risk agents related to work processes



As observed among the work processes, ionizing radiation is the most common risk agent, followed by vapors agents, incorrect ergonomic postures in workplace and stress work-related situations. Whereas workplace is a radioactive facility, the possibility of exposures to ionizing radiation is inevitable, due to the influence of the radiation fields from the production of radioisotopes and radiopharmaceuticals products.

3.1.3 Homogeneous exposure groups (HEGs)

Workgroups presenting the same profile of exposure to a specific range of occupational risk agents are called homogeneous exposure groups (HEGs). Based on a systematic assessment of the subjective information collected during the basic characterization of the facility, it was carried out a survey that enabled the determination of HEGs.

Even though the facility counts on eight different work processes, it was observed that two different profile groups are exposed to the same agent risks. As a matter of fact, due to similar characteristics of performance tasks, the production of the primary radioisotopes group and labeled compounds group are occupationally exposed to the same agent risks with similar frequency.

Therefore, there were considered for this study seven HEG s: **production** (primary radioisotopes and labeled compounds), **lyophilized reagents** (kits), **quality control**, **quality assurance**, **research**, **infrastructure** and **radioprotection**.

3.2 Quantitative-qualitative assessment of occupational risks

The only risk agent able of quantification in this study was the ionizing radiation. Therefore, a statistical analysis was performed in order to estimate which of the identified risks agents (qualitative variables) could be associated with the occurrence of the occupational risks in established HEGs.

Initially, nonparametric statistical test as “equality of two proportions” was applied to the analysis and characterization of the relative frequencies distribution.

The qualitative dependent variable occupational risk has been characterized according to its relative frequency in each HEG.

Frequency analyses were performed for the occupational risks identified according to their type (physical risk, chemical, biological, ergonomic and accident), making possible to classify them into three main categories of risk (risk groups 1, 2 and 3). These three groups are exposed to similar work-related risk types. Table 2 presents the analysis of frequencies performed by the equality of two proportions test among the three risk groups.

Table 2: Relative frequency distribution of the variable occupational risk among the risk groups.

Group	Occupational risk	Number of workers (N)	Frequency (%)	p-value
Risk 1	Physical, ergonomic and accident	29	28.4	0.020
Risk 2	Physical, chemical and ergonomic	45	44.1	Ref.
Risk 3	Physical, chemical, biological, ergonomic and accident	28	27.5	0.013

Note: p-value considered statistically significant was $p < 0.05$.

P value Ref. (reference): the response prevalent level or the one that shows the highest frequency. This was used only when the variable presented three or more response levels.

According to Table 2, risk group 2 is composed by HEGs, production, reagents and radioprotection, and showed the highest percentage (44.1%). Risk group 1 is composed by HEGs, quality assurance and infrastructure and showed a percentage similar to risk group 3, consisting by HEGs of the quality control and research. This group is exposed to five types of risk (physical, chemical, biological, ergonomic and accident).

3.2.1 *Relative frequency distribution of the qualitative variables*

The relative frequencies of the qualitative variables could be analyzed based on questionnaire results obtained by equality of two proportions test. The data analyze showed that the sixteen qualitative variables were related to the workers' tasks: radionuclides used in the radiopharmaceuticals production, mode of decay, physical aspects, chemicals products handling, temperature, presence of noise, presence and possibility of contact with ionizing radiation, handling and storage of dangerous chemical products, chemical contaminants dispersed in the air (vapor), biological material handling, biological contaminants dispersed in the air (aerosols), probability of fires or explosions, inadequate lighting, physical workload (manual weightlifting and long work journey), mental workload (responsibility) and stressful situations.

According to variables data analysis, only three of them - extremes temperature, biological contaminants dispersed in the air (aerosols) and inadequate lighting – did not present relative's frequencies. These variables were not selected by the respondents.

The results of the relative frequencies analysis (13 variables) were used to measure the statistical association between occupational risk (dependent variable) and its possible agents and factors (other qualitative variables). In this analysis, there were used the chi-square test and Yates correction test. Even so, the Yates correction test was only applied in the case results were smaller than 5 responses.

Based on the results of the thirteen analyzed variables, it was observed that only two of them (physical form of the radionuclides and stressful situations) did not present a statistically significant association degree. The remaining eleven variables did present a significant statistical association degree with the risk groups, presenting percentage values over 60%.

Regarding the results, risk group 1 showed statistically significant degree of association ($p < 0.001$) only with two variables: presence and possibility of contact with ionizing radiation (100%) and probability of fire or explosion (86%).

Risk group 2 demonstrated a significant association with eight variables: radionuclide, type of emission, chemical products, presence and possibility of contact with ionizing radiation, noise, chemical products handling, physical and mental workload. Results showed association of 100% with the physical workload.

Risk group 3 presented a significant degree of association with all variables, with percentage over 80% in all cases except for mental workload variable.

The only variable that showed significant association with all three groups was the presence and possibility of contact with ionizing radiation.

The statistical analysis of p-values indicates that only two variables showed a significance level of p-value < 0.05 . These variables are: physical form ($p = 0.937$) and stress situation ($p = 0.275$). Thus, these two variables are not statistically associated with the identified occurrences of occupational risk in the workplace. Therefore, the statistical analysis provided eleven risk agents associated with the occurrences of occupational risk among the HEGs.

3.3 Descriptive statistical analysis of the sociodemographic variables related to occupational risk

The ANOVA test was applied to compare the mean age among the three risk groups (Risk 1, 2, 3). Table 3 shows the descriptive analysis between the age variable and risk groups.

Table 3: Comparison of age and risk groups

Descriptive analysis	Risk groups		
	Risk 1	Risk 2	Risk 3
Mean	53.8	51.9	49.4
Median	56	52	49
Standard deviation	9.3	6.9	10.0
Coefficient of variation	17%	13%	20%
Minimum	24	30	27
Maximum	69	67	65
Number of workers	29	45	28
Confidence interval	3.4	2.0	3.7

According to the results from Table 3, there is no difference between the mean age among the three risk groups, even in the case of risk group 1 (workers exposed to physical risk, chemical and ergonomic) which presents the highest average of 53.8 years. Then, workers' age is not the factor that influences the occurrence of the risk.

Yates correction test was applied to analyze the variables "gender" and "educational level". Table 4 shows the statistical association degree between the occurrence of occupational risk in the workplace and gender (female and male), as well as the association degree between the occurrence of occupational risk in the workplace and educational level (technicians or graduate).

Table 4: Association degree of the risk groups with the variables: gender and educational level;

Variables	Risk 1		Risk 2		Risk 3		Total		p-value	
	N	%	N	%	N	%	N	%		
Gender	Female	6	21	9	20	11	39	26	25	0.144
	Male	23	79	36	80	17	61	76	75	
Educational level	Technical	21	72	34	76	17	61	72	71	0.387
	Graduated	8	28	11	24	11	39	30	29	

Note: p-value significance level adopted ($p < 0.05$)

N: number of workers.

As shown in Table 4, neither the gender nor the educational level of workers present statistically significant association with the risk (p -values > 0.05) and both variables bring similar percentages.

4 CONCLUSIONS

This study allowed to carry out the basic characterization of a Brazilian radioactive facility and enabled to identify seventeen occupational risk agents present at workplace. The main physical risk agent observed among them was the ionizing radiation, probably due to the daily handling of radioactive materials.

The quantitative and qualitative approach carried out through the use of statistical methodology and subjective information allowed to find out the real conditions of workplace, work processes and exposure of workers.

The strategy for decision-making for workers' monitoring was founded on HEGs workgroups, which presented similar exposures to risk agents.

Based on this study, our recommendation for future actions is that the homogeneous exposure groups and risk agents must be periodically analyzed and modified whenever necessary, taking into account

that each new evaluation of the risk agents in the workplace should be carried out from the basic characterization phase.

5 REFERENCES

- [1] GARDINER. K.; HARRINGTON. J.M. *Occupational Hygiene*. Third Edition. Blackwell Publishing. 2005. Massachusetts. USA.
- [2] FILHO. A.S.; FANTAZZINI. M.L. Estratégia de amostragem: gestão das exposições na higiene ocupacional. *Revista de Higiene Ocupacional*. v. 9. n. 20. p. 5-9. 2010.
- [3] PULLEN. E.L. *Using a comprehensive exposure assessment strategy to assess workplace health risks*. In: APOSHO 26 (Asia Pacific Occupational Safety and Health Organization) & Australasian Safety Conference 2011 - Enhancing Safety Across Culture. 21 a 24 November. 2011. Perth - Western Australia. *Proceedings...* Perth: APOSHO 26 & Australasian Safety Conference. 2011.
- [4] MENDES. R.. *Patologia do Trabalho*. Ed. Atheneu 2º edição. São Paulo - Brasil (2007).
- [5] BRASIL. Portaria SSST n.º 25. de 29 de dezembro de 1994 do Ministério do trabalho e emprego. *Norma Regulamentadora NR 9 – Programa de Prevenção de Riscos Ambientais*. 1994.
- [6] BRASIL. Portaria SIT n.º 13. de 21 de junho de 2007 do Ministério do trabalho e emprego. *Norma Regulamentadora NR 17 – Ergonomia*. 2007.
- [7] BRASIL. Portaria N.º 25. de 29 de dezembro de 1994 da Secretaria de segurança e saúde no trabalho. *Mapa de Risco*. 1994.
- [8] IBM SPSS SOFTWARE. SPSS Statistics Base 17.0 User's Guide.” <http://www.jou.ufl.edu/archive/researchlab/SPSS-Statistics-Base-Users-Guide-17.0.pdf>. (2014).
- [9] “MINITAB 16 Statistical Software.” http://www.minitab.com/uploadedfiles/documents/readme/minitab_16_readme_en.pdf. (2014).
- [10] REIS. E.. *Estatística Descritiva*. Edições Silabam. Lda. Lisboa - Portugal (1991).
- [11] SPIEGEL. M. R. *Estatística*. 3ª ed. Makron Books (Coleção Schaum). São Paulo - Brasil (1993).
- [12] LANE. D. M.. “Online Statistics Education: A Multimedia Course of Study. Rice University.”

Supervision of German miners at small underground construction sites of old mining to prevent high radon exposures

Jörg Dehnert

Saxon State Office for Environment, Agriculture and Geology, Pillnitzer Platz 3,
01326 Dresden, Germany.

Abstract. More than 40 underground construction sites have been supervised by the radiation protection authority in Saxony in recent years. The paper deals with stories of underground supervisions to share the experiences with authorities and miners to improve the underground radiation protection. A new Express- Air Screen-System (EAS) for miners was developed to shut off radon rich parts of galleries in 20 minutes only.

KEYWORDS: *radon exposure; radiation protection measure; miner; ventilation; air screen; mine air current.*

1 INTRODUCTION

The Ore Mountain and the Vogtland Mountain are located in the eastern part of Germany. Mining started shortly after the year 1168. Today about 250 miners of seven enterprises carry out repair works at 60 small and changing underground construction sites of old mining throughout the year. The miners are protected against high radon exposures by some radiation protection measures such as ventilations, air screens and staff rotations. However, some of them still have annual exposures up to 20 mSv; measured by passive radon dosimeters. Reasons for this include the high radon potential in old mining and the natural density driven mine air current through the galleries. Mine air currents are able to change the directions during the day depending on outdoor temperatures.

2 SUPERVISIONS

More than 40 underground construction sites have been supervised by the radiation protection authority in Saxony in recent years. Supervision usually includes continuous measurements of radon activity concentrations, time-solved by one minute using an AlphaGUARD PQ 2000PRO. Some insufficient or failed radiation protection measures were found during the inspections. Instructions were given to improve the underground radiation protection immediately. The instructions include but are not limited to switching on mine fans, extending air tubes and building air screens.

3 EXPERIENCES TO SHARE

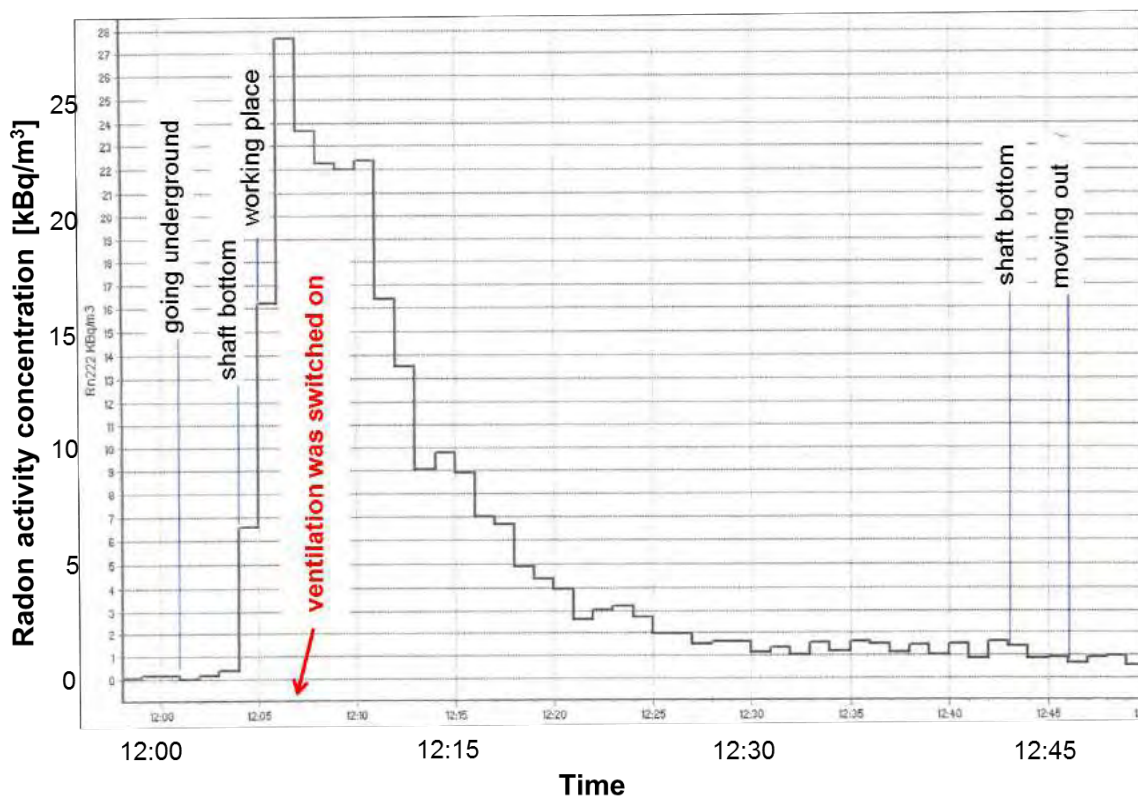
This paper deals with stories of underground supervisions to share the experiences with authorities and miners to improve the underground radiation protection.

3.1 Story no. 1

Miners carried out repair works in the morning at an underground construction site. The ventilation was switched off because the miners felt that the natural density driven mine air current was bringing enough fresh air through the shaft to the working place. However, the mine air current changed the direction in the noon because of the higher temperature outside. Radon activity concentration of 27 kBq/m³ was measured by the radiation protection authority during inspection of the site. The ventilation was switched on immediately to bring fresh air via tubes to the working place. The radon activity concentration at the working place decreased in 15 minutes from 27 kBq/m³ to 3 kBq/m³ and finally reached lower than 1 kBq/m³ (Fig. 1).

Conclusion: Do not switch off ventilations without real time measuring of radon activity concentrations at working places.

Figure 1: Radon activity concentration during inspection of an underground working place



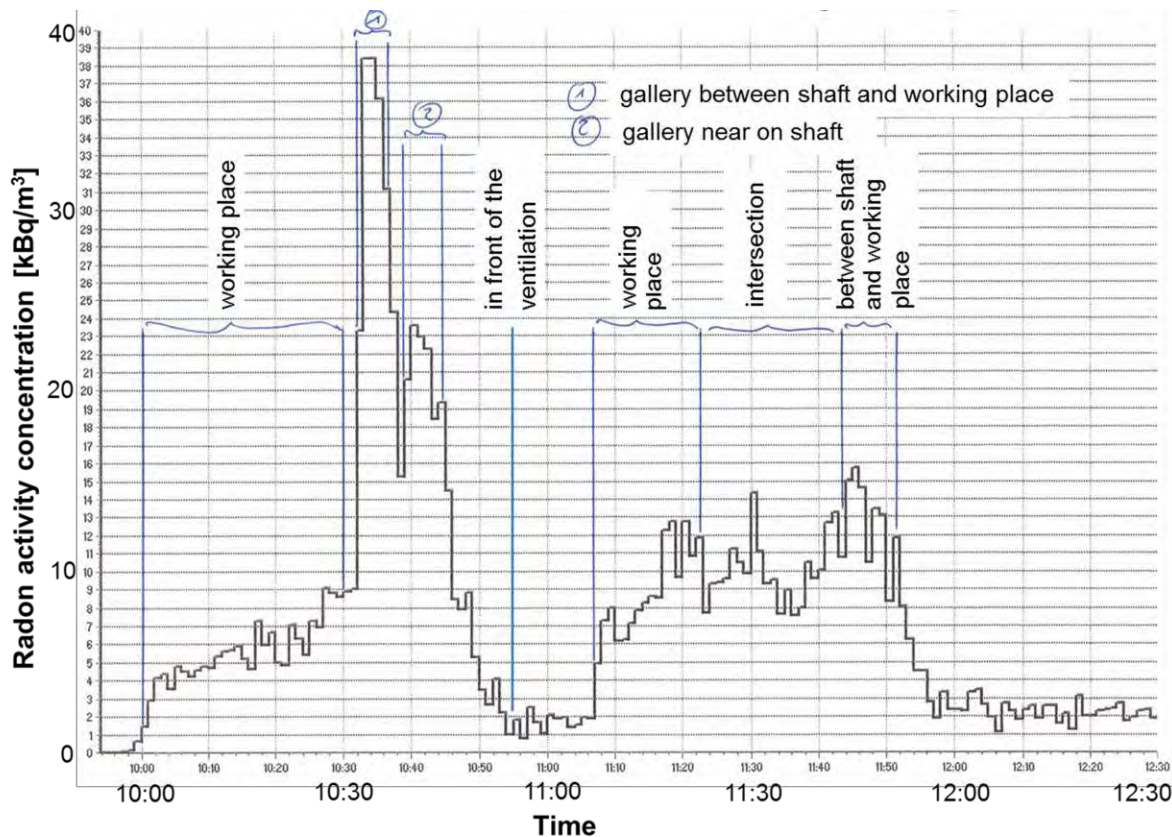
3.2 Story no. 2

Miners worked at an underground construction site. The ventilation was switched on and it carried fresh air via a tube through the shaft into the working gallery. Radon activity concentration of 4 kBq/m³ increasing with time up to 9 kBq/m³ was measured by the radiation protection authority during a inspection of the working place (Fig. 2). What was going on? Two small galleries were also connected to the main gallery. The radon activity concentration in the galleries amount to 38 kBq/m³ and 23 kBq/m³. The ventilation caused low pressure in the gallery along the tube between the working place and shaft. Old air with a lot of radon moved from the two galleries into the main gallery. The radon rich old air was mixed with the fresh air of the ventilation. Radiation protection measures were necessary. Two air screens were built to shut off the two small radon rich galleries. After that the radon activity concentration decreased at the working place from around 10 kBq/m³ to 300 Bq/m³.

Conclusion: Shut off radon rich galleries by air screens.

3.3 Story no. 3

During winter time three miners carrying passive radon dosimeters had effective doses of 2.2 mSv, 3.0 mSv and 7.9 mSv in three months. The enterprise which the miners worked for applied for a low notional dose for the miner with the high effective dose of 7.9 mSv. The radiation protection authority found out, that the two miners with lower doses worked underground in a ventilated working space. The miner with the higher dose worked on the surface the whole quarter. He worked most of the time at roadworks and five days in a pithead building and carried out material transports between the surface and the gallery. A strong natural density driven and radon rich mine air current moved out at the pithead building. The door of the pithead building was closed most of the time because it was

Figure 2: Radon activity concentration during inspection of an underground working place

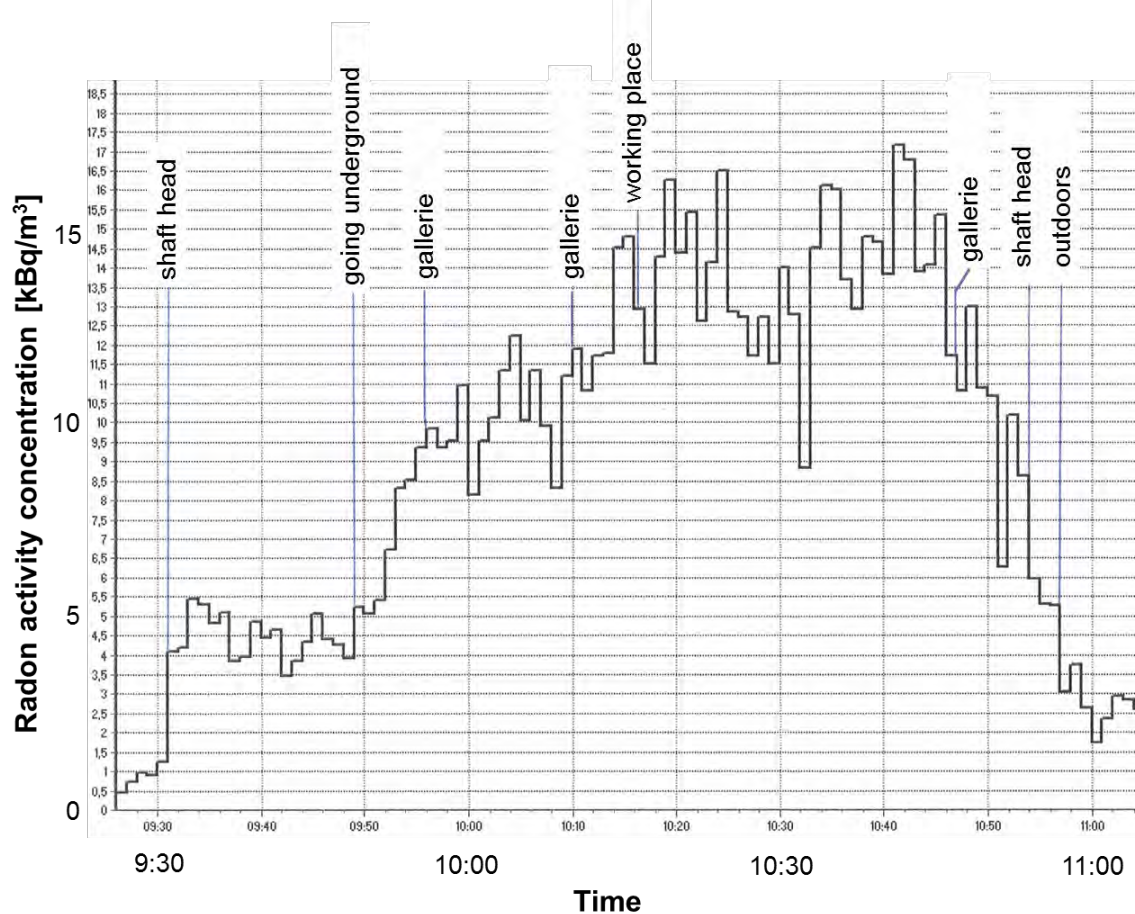
cold outside. The miner worked five days at the surface breathing the mine air without any radiation protection measures. The dose of 7.9 mSv was a real dose. The application for a notional dose was rejected.

Conclusion: Do not work in the discharge air in pithead buildings.

3.4 Story no. 4

Miners carried out repair works in a 270 meter deep shaft during winter. They reconstructed the shaft from the surface to the bottom. The ventilation was switched on and carried fresh air via a pipeline to the working place in the shaft. A radon activity concentration of 13.6 kBq/m³ was measured by the radiation protection authority during inspection at the working place 100 meter above surface (Fig. 3). What was going on? A strong natural density driven and radon rich mine air current moved from different galleries through the shaft towards the surface. Fresh air was moving through a long pipeline connecting the shaft to the working place. The pipeline consisted of tubes with length of 10 meters. The working place relocated few meters downward few times in a month. The pipeline was extended with 10 meter long tubes from time to time depending on the position of the working place. However, the working place was too far from the end of the pipeline. Fresh air was blowing in the shaft and moved backwards after few meters to move out together with the natural density driven mine air current. The fresh air from the pipeline didn't reach the miners. Radiation protection measures were necessary. In this case a radiation protection measures is to use shorter 5 meter long tubes for extending the pipeline to stay closer to the ventilation.

Conclusion: Do not work out of range of ventilation.

Figure 3: Radon activity concentration during inspection of an underground working place

3.5 Story no. 5

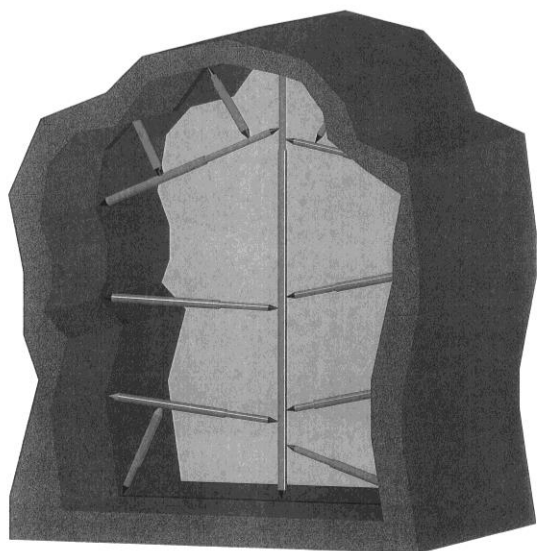
A miner carrying a passive radon dosimeter had an effective dose of 20 mSv in a quarter. The enterprise which the miner worked for applied for a low notional dose for the miner. The radon dosimetry works with reference dosimeter. The miner did not store the personal radon dosimeter together with the reference dosimeter off-time. He took his helmet including the radon dosimeter at home and stored both during holidays for five weeks in the basement at his own house. A radon activity concentration of 4 kBq/m³ was measured in the basement. The radon dosimetry for the quarter was wrong. The application for a notional dose was accepted.

Conclusion: Do not forget to store the radon dosimeter together with the reference dosimeter off-time.

4 EXPRESS - AIR SCREEN - SYSTEM

A new Express- Air Screen-System (EAS) for miners was developed as a result of all the experiences (Fig. 4). The EAS is a lightweight, modular and reusable construction kit of interlocking telescopic aluminum tubes, plastic foils of different sizes and glue foam to shut off radon rich parts of galleries in 20 minutes only. The EAS will help to reduce the radon exposures of miners at small construction sites of old mining in the future.

Figure 4: First idea (left) and prototype installed in a wooden model of an underground gallery (right) of the Express - Air Screen - System (EAS) for miners



5 CONCLUSION

Conclusions to improve the underground radiation protection of miners at construction sites in old mines include:

- (a) Do not switch off ventilations without real time measuring of radon activity concentrations at working places.
- (b) Shut off radon rich galleries by air screens.
- (c) Do not work in discharge air in pithead buildings.
- (d) Do not work out of ranges of ventilations.
- (d) Do not forget to store the radon dosimeter together with the reference dosimeter off-time.

6 ACKNOWLEDGEMENTS

I would like to thank Jens Stopp (Aluminium und Verwaltungs GmbH Stopp) for producing the Express- Air Screen-System and Bernd Schönherr (Bergsicherung Schneeberg GmbH) for underground testing the Express- Air Screen-System.

Analysis of Gamma-Ray Skyshine Contribution to Dose Rates Exterior to an Above-Ground Waste Storage Facility Using Radiation Transport Models

Jenelle Mann^{a*}, Norbert Zoeger^b, Roman Koppitsch^b, Alexander Brandl^a

^aColorado State University, Fort Collins, CO 80523, U.S.A.

^bNuclear Engineering Seibersdorf, Seibersdorf, Austria

Abstract. Skyshine is radiation that is initially directed vertically and is scattered toward the ground at distances that are often far from the source. The scattered skyshine radiation has lowered energy with a characteristic energy spectrum exhibiting pile-up at low energies, typical of photons scattered multiple times in a semi-infinite/infinite medium. Although the photons have a lowered energy, the skyshine radiation reaches much farther distances from the source than radiation laterally directed that passes through shielding. Skyshine has been observed at high-energy particle accelerators, medical accelerators, nuclear reactors, industrial radiography, and waste storage facilities. Guidelines for calculation of skyshine radiation have been established for accelerator facilities, but skyshine radiation has not received similar attention in other radiation protection fields. In this research, the skyshine radiation exterior to a waste storage facility is analysed using Monte Carlo n-Particle Transport eXtended (MCNPX) code. The facility analysed is an above-ground waste storage facility that houses 9996 200-L radioactive waste barrels. The repository has concrete shielding on three sides of the facility, but has minimal roof shielding. In an initial investigation of dose rates exterior to the storage facility, a peak in the dose rate profile was observed for the three sides of the facility with shielding. The sources of the peak were analysed by varying building materials, using different void regions, and analysis of energy spectra. The dose rates exterior to the repository were analysed with and without the facility structure to determine the dose rate profile resultant from the source geometry. Dose rates resultant from just the source geometry continuously decreased, confirming that the observed dose rates were due to scattering within or through the facility structure. The analysis using void regions allowed for the determination of the fraction of the dose rate transmitted through the roof and walls.

KEYWORDS: *scattering; shielding; skyshine; photon dose.*

1 INTRODUCTION

The focus of this research is on the dose rate with distance from an extended source behind shielding. When dose rates were initially modeled for a waste repository using Monte Carlo N-Particle Transport (MCNP), dose rates did not consistently decrease as expected for r^2 law for a point source or r^{-1} for a plane source [1]. Instead, modeled dose rates peaked at a distance from the repository; skyshine is investigated here as a contributor to the peak in the dose profile.

Skyshine is radiation that is initially directed vertically and is scattered back to ground at distances far from the source. The resulting scattered radiation has a lowered energy than the source radiation, but reaches distances much farther from the source than laterally directed radiation that passes through shielding. The result is elevated fluence rates at distances far from the source, making skyshine a concern for onsite workers and populations far from the source. Skyshine was initially observed for high-energy particle accelerators [2], but has also been reported for medical accelerators [3] [4] [5] [6], hot cells [5], industrial radiography [7], nuclear reactors, and waste storage facilities [8].

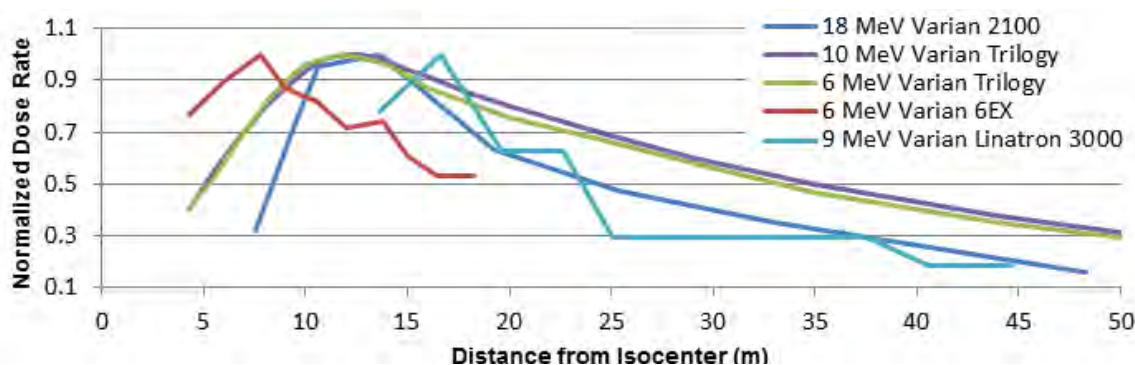
The theoretical calculation of skyshine radiation levels is computationally extensive, making analysis difficult [5] [9] [10]. The most rigorous approach to calculating skyshine radiation is Monte Carlo simulations (such as Monte Carlo N-Particle Transport or MCNP). Guidelines for calculating skyshine for accelerator facilities have been established by the National Council on Radiation Protection and Measurement (NCRP) in Report 51 [11] and 151 [12]. However, skyshine radiation dose rates observations at a 6 MeV Varian Model 6EX Accelerator [6], 6 MeV Varian Trilogy Linear Accelerator [3], a 10 MeV Varian Trilogy Linear Accelerator [3], and a 18 MeV Varian 2100 C

* Presenting author, e-mail: jenelle.e.mann@gmail.com

Accelerator [4] were inconsistent with NCRP Report 51 and 151 methodologies. NCRP Report 51 and 151 empirical formulas predicted a continuously decreasing photon dose rate, while the observed dose rate at the Varian accelerators (regardless of energy) peaked at a distance tens of meters away from the accelerator at a much higher dose rate than calculated [6] [4] [3]. When the experimental skyshine dose rates from a 9 MeV, a 15 MeV, and a 21 MeV electron accelerator skyshine were compared to MCNP and NCRP Report 51 methodology, MCNP dose rate values were much closer to measured values and overestimated the dose rate [10].

In a thorough review of the existing literature, it was observed for most situations that the skyshine dose peaks with distance from the source [13] [3] [6] [4] [10] [7]. The peak location is dependent on the field size [3] [6] and collimator (gantry) angle [13]. For larger field sizes and larger collimator angles, the peak is observed closer to the source [6] [13]. While the relationship between field size and dose rate at a given distance can be modeled by a second order polynomial [6]. Figure 1 contains a graph of several accelerator skyshine dose rate profiles as a function of distance [3] [6] [4] [7].

Figure 1: Accelerator Skyshine Dose Rate with Distance from Isocenter [3] [6] [4] [7]

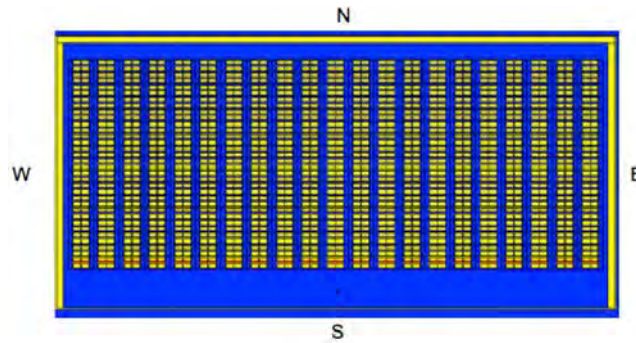


The energy spectrum and dose rate profile has also been studied for a cobalt-60 source multi-radionuclide radioactive waste buried in underground trenches [14] [8]. The energy spectrum exhibited a pile up of photons at low energies, resulting in a distinct low energy line, characteristic of photons scattered multiple times in an infinite or semi-infinite media [14] [13]. The low energy line is independent of source energy and is solely dependent on the properties of the medium; for air, a distinct low energy line at 72 keV was observed [14] [14] [8]. In all cases, a distinct low energy line of 72 keV was observed [14] [8]. A similar low energy peak was observed by Lagutina et al. for multiple collimation half angles [13]. Additionally, the mean skyshine energy has been reported to be between 120 and 250 keV based on IPEM Report 75 [15].

Skyshine has received a lot of attention of particle accelerators, but has not received similar attention in other field of radiation protection. Here, skyshine is analyzed for an extended source of waste barrels arranged for storage at an interim waste storage facility. The waste storage facility analyzed is based on the Austrian Interim Radiological Waste Storage facility, administrated by Nuclear Engineering Seibersdorf at the Austrian Institute of Technology. The barrels are stored in a crate geometry in a facility with minimal roof shielding. Skyshine dose rates and energy spectrum with distance are analyzed using MCNPX up to 500 m.

2 MATERIALS AND METHODS

The waste repository analyzed is an above ground waste repository stores low and intermediate level conditioned waste. There are 9996 200-L waste barrels stored back to back in a crate geometry to allow easy access to the tops of each drum. The walls and roof are 0.2 m thick with additional concrete shielding of 0.7 m present on the west, north, and east sides of the waste repository. The waste drum crate geometry is located 1 m away from the west, north, and east walls; while the crate geometry is located 5.25 m away from the south wall to allow for maneuverability of a crane. Figure 2 contains a bird's eye view of the waste repository generated using Visual Editor (VISED) [16].

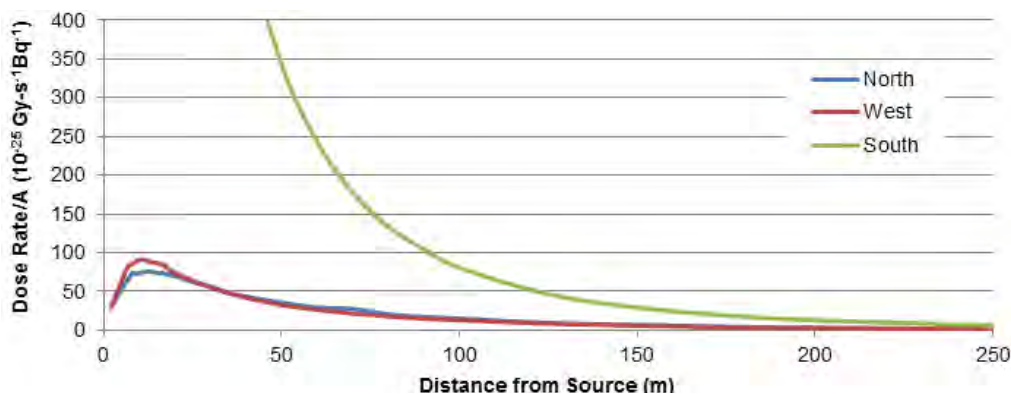
Figure 2: Overhead View of Waste Repository generated using VISED [16]

The waste repository was modeled using Monte Carlo N-Particle Transport Extended (MCNPX) [17]. The contents of each drum were modeled as homogeneous concrete with an evenly distributed cobalt-60 source. Cobalt-60 was chosen due to its high energy photons.

Dose rates were calculated using f5 detector tallies with the ICRP 74 fluence to dose rate conversion factors [18]; while energy spectra were analyzed using a f5 detector tally with multiple energy bins. Dose rates were analyzed at various distances with and without the repository structure for the north, south, and west side to distinguish contribution due to source structure. Additionally, dose rates were analyzed at various heights to determine influence of scattering angle. Void regions for the roof and walls were also used to determine contribution of scattering through walls versus scattering through the roof. Finally, energy spectra were simulated to compare spectra to expected skyshine spectra.

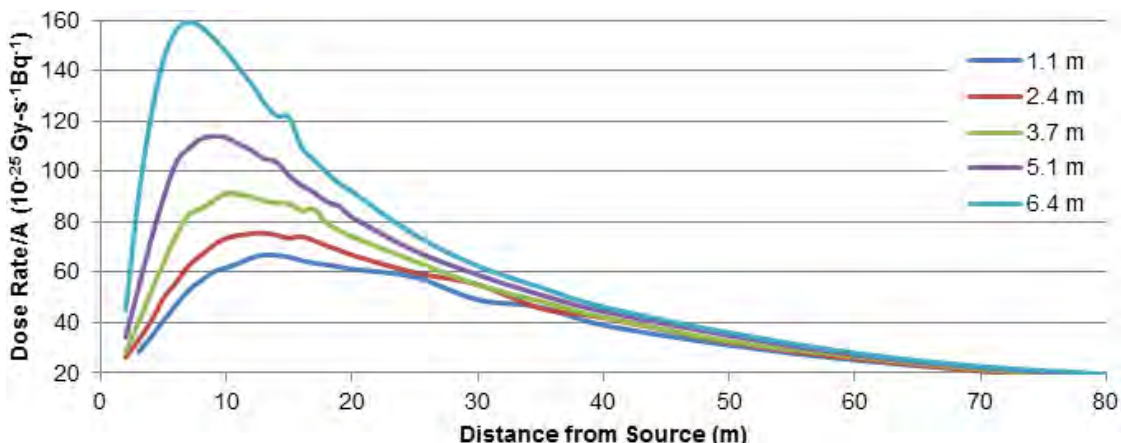
3 RESULTS AND DISCUSSION

The dose rate profile with distance away from the facility for the north, west, and south sides were previously analyzed. It was initially anticipated that that dose rate would consistently decrease with distance, however for the north and west sides of the repository (where additional shielding was present) the dose rate exhibited a peak several meters from the repository. Figure 3 contains the typical dose profile for the north, west, and south sides of the repository at a vertical height of 2.26 m.

Figure 3: Typical Dose Profile at 2.26 m

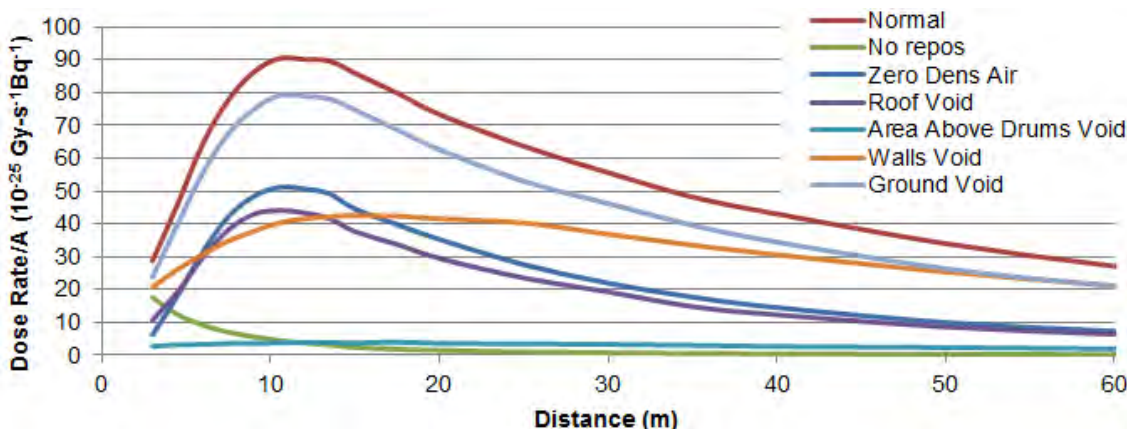
The dose rate profiles for the north, west, and south sides were also analyzed at different vertical heights. Due to the similar trends observed between the north and west side dose rate profiles (as seen in Figure 3), only the west side will be discussed. For the west side of the repository, higher detector points exhibited a more rapid rise in dose rate accompanied with a larger peak dose rate. Changes in the dose rate profile could be due to the distance traveled through the atmosphere, scattering angle, and building materials. A graph of the dose profile for the west side of the facility is in Figure 4. The dose profile for the south side for all heights has a similar shape to Figure 3, but has a different starting dose rate. The initial dose rate is largest for the height of 3.7 m, corresponding to the drum midline.

Figure 4: Dose Profile at Different Heights for West Side



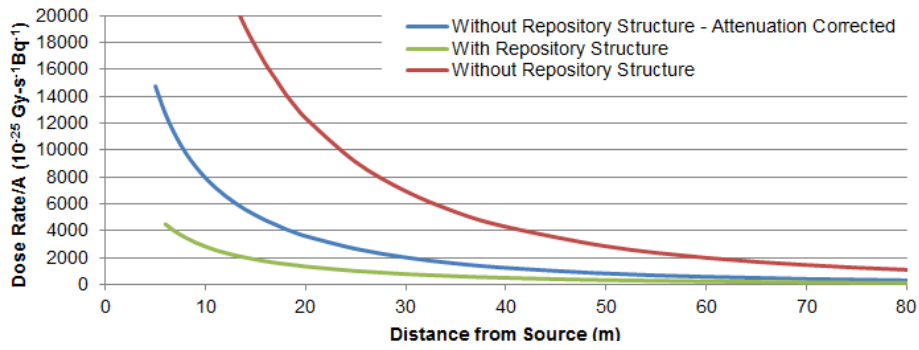
To determine the origin of features in the dose profiles rate profile, several geometry modifications were made and the dose rate profile was compared to one with no modifications. The structure of the repository was removed to determine contribution to the dose rate profile from the source geometry. The air outside of the repository was set to zero density, preventing interactions in air outside of the repository to determine contribution from scattering in source and repository structure. Additionally void regions were used on the roof, area above drums, walls, and ground to prevent photons from being transmitted through the respective regions. The resulting dose rates for the west side for a set of geometry modifications are in Figure 6.

Figure 5: Dose Rates for West Side using Geometry Modifications



When no repository structure is present, the dose rate decreases continuously, indicating that the peak in the dose rate profile is due to structures surrounding the source. Void regions for the walls and area above the drums create the most significant changes, indicating that the majority of scatter occurs in the area directly above the drums and in the walls of the repository. The dose rate profile for the south side was analyzed with and without the repository structure. The dose profile without the repository structure was corrected for attenuation to show differences in shape of the profiles. The profiles are shown in Figure 7. Even when the dose rate profile without the repository structure is attenuation corrected, it exhibits a higher dose rate at distances closer to the repository. This indicates that additional effects from the repository structure exist than just attenuation.

Figure 6: Dose Rates for the South Side With and Without Repository Structure



In addition to analyzing dose as a function of distance from the repository, the dose rates were analyzed as a function of vertical height. The profiles were analyzed with and without the repository structure. The vertical dose profile for the West side is in Figure 7 and the vertical dose profile for the South side is in Figure 9. The height of the drum set labeled on the graphs at 6.3 m, and the height of the waste storage facility is noted at 8.3 m.

Figure 7: Vertical Dose Profile for the West Side

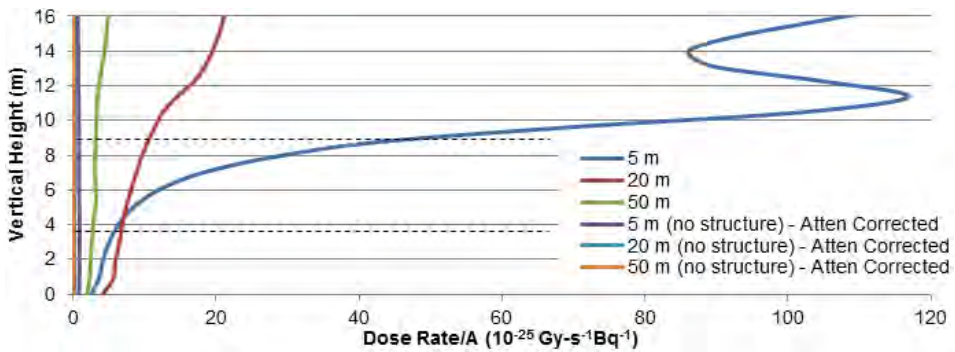
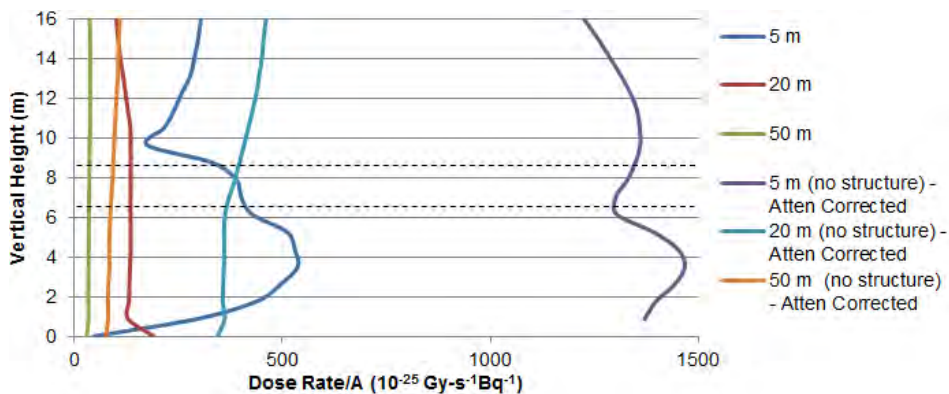


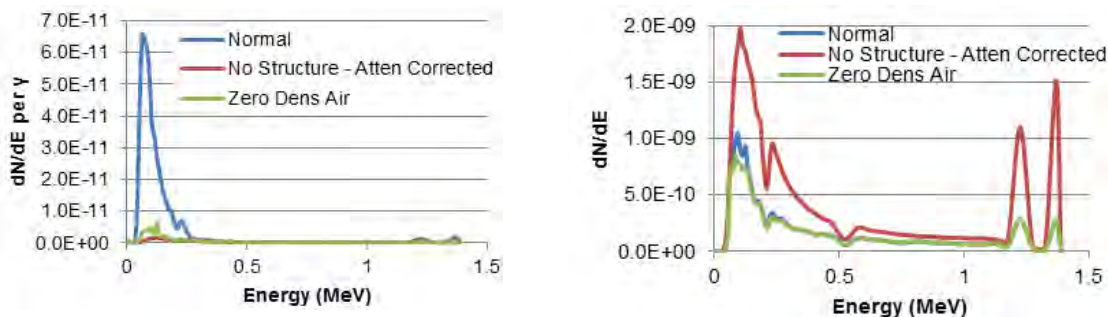
Figure 8: Vertical Dose Profile for the South Side



The dose rate for the west side continues to increase with vertical distance when the repository structure is present until heights much higher than the waste repository, while dose rates for the south side is more rounded with an initial peak around the middle of the drum set. For both sides, the dose rate exhibits a second rise in dose rate above the drum sets, indicating presence of scattered radiation. The dose rate profiles close to the repository structure show more variation, while dose rates further away are flatter. For the west side, the attenuation corrected dose profiles are much less than the profiles with the repository structure, indicating contributions that are not due to source structure. However, for the south side attenuation corrected dose profiles with no repository structure are larger than with the repository structure, similar to observed in Figure 7.

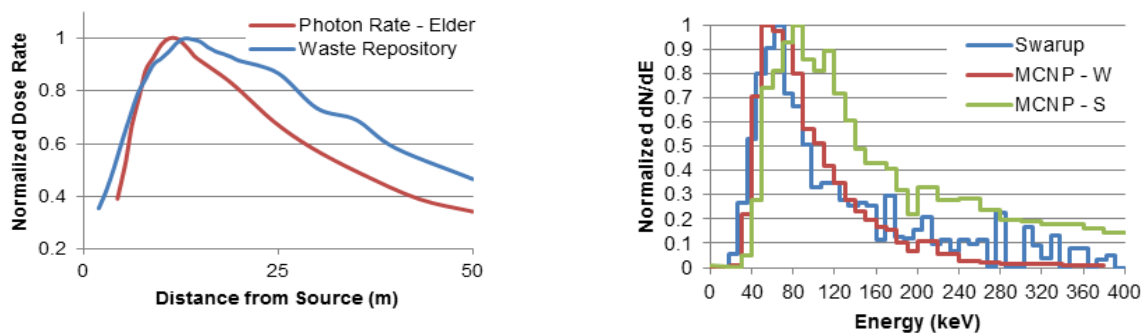
The energy spectrum for the west and south sides for the repository were also analyzed when the repository structure was present, no repository structure was present, and the air was set at zero density. The energy profiles are in Figure 10 at a distance of 2 m from the repository. All energy spectra have a low energy peak, consistent with multiple scatter in air. For the south side for all scenarios, there is a significant contribution from the full energy of the Cobalt-60 photons, while they only contribute to the energy spectrum for the west side when no structure is present.

Figure 9: Energy Profile at 2 m of West side (L), South Side (R)



The dose rate profile of the west side of the repository was compared to the dose rate profile from accelerator skyshine observed by Elder (Figure 1) for an 18 MV medical accelerator in Figure 11 [3]. The low energy peak in the energy spectrum was also compared to the skyshine energy spectrum observed by Swarup and is in Figure 11 [14]. The dose profile from the waste repository has a similar shape to that observed by Elder for accelerator skyshine. Additionally, the low energy peak for the west side compares well to the low energy peak observed by Swarup. The low energy peak for the south side is wider and less prominent than that observed by Swarup and on the west side of the repository.

Figure 10: Comparison of Dose Rate Profile [3] (L) & Energy Spectrum [14] (R) to Skyshine



4 CONCLUSION

Trends in the dose rates analysed outside of a waste repository followed closely to observed skyshine dose rates outside of a medical accelerator building, for the sides of the repository that contained shielding. The contributions to the dose rate were analysed further through the use of void regions, determining that the peak in the dose rate profile of the west side is not due to the source geometry, but rather the materials surrounding the source. Dose rate profiles were analysed at several heights, and for the west side, as detector tally height increased the dose rate increased more rapidly and reached a larger maximum. The changes in the dose rate profile at different heights, is likely due to scattering angle and less attenuation of photons at higher altitudes.

The analysis of the energy spectrum showed that the largest contributor to photon fluence for the west side was low energy photons, consistent with multiple scattered photons, as expected from skyshine. While for the south side, the two cobalt-60 peaks still were a major contributor to photon fluence.

5 ACKNOWLEDGEMENTS

In the development of this project, I would like to acknowledge Nuclear Engineering Seibersdorf for providing this project and repository drawings. I would also like to thank Rafe McBeth for running the MCNP files on the CSU cluster and assisting in debugging code. In addition, I want to thank Thomas McLean and Dave Seagraves at LANL for their help on developing a repeated source structure.

This publication was supported by Grant Number T42OH009229-06 from CDC NIOSH Mountain and Plains Education and Research Center. Its contents are solely the responsibility of the authors and do not necessarily represent the official views of the CDC NIOSH and MAP ERC.

6 REFERENCES

- [1] Parson, J., Brandl, A., Zoeger, N., et al., 2013. Dose rate profile surrounding a repository. ASMI 2013 15th International Conference on Environmental Remediation and Radioactive Waste Management, Brussels.
- [2] Thomas, R.H., 2001. The history and future of accelerator radiological protection. *Radiation Protection Dosimetry*, vol. 96, no. 4, 441-457..
- [3] Elder, D., Harmon, J., Borak, T., 2010. Skyshine radiation resulting from 6 MV and 10 MV photon beams from a medical accelerator. *Health Physics Society*, vol. 99, no. 1, 17-25.
- [4] McGinley, P.H., 1993. Radiation skyshine produced by an 18 MeV medical accelerator. *Radiation Protection Management*, vol. 10, no. 5, 59-64.
- [5] Rindi, A., Thomas, R.H., 1975. Skyshine - a paper tiger?, *Particle Accelerators*, vol. 7, 23-39.
- [6] Gossman, M., McGinley, P., Rising, M., et al., 2010. Radiation skyshine from a 6 MeV medical accelerator. *Journal of Applied Clinical Medical Physics*, vol. 11, no. 3, 259-264.
- [7] Metzger, R., Van Riper, K., Jones, M., 2005. Ford Motor Company NDE facility shielding design. *Radiation Protection Dosimetry*, vol. 116, no. 1-4, 236-238.
- [8] Swarup, J., 1979. Photon spectra of gamma-rays back-scattered by infinite air. Part I: area-skyline. *Indian Journal of Pure and Applied Physics*, vol. 17, no. 6, 381-384.
- [9] Hertel, N., Sweezy, J., Shultis, J.K., et al., 2005. A comparison of skyshine computation methods. *Radiation Protection Dosimetry*, vol. 116, no. 1-4, 525-533.
- [10] Chaocheng, K., Quanfeng, L., Huaibi, C., et al., 2005. Monte Carlo method for calculation the radiation produced by electron accelerators. *Elsevier*, vol. 234, 269-274.
- [11] NCRP, 1977. NCRP Report No. 51, Pergamon Press, Washington.
- [12] NCRP, 2005. Structural Shielding Design and Evaluation for Megavoltage X- and Gamma-Ray Radiotherapy Facilities. NCRP Report No. 51, NCRP, Bethesda.
- [13] Lagutina, I., Mashkovich, V.P., Stroganov, A., et al., 1989. Skyshine from photon radiation. Plenum Publishing Corporation, 118-124.
- [14] Swarup, J., 1980. "Photon Spectra of Gamma Rays Backscattered by Infinite Air II. Skyshine, *Nuclear Instruments and Methods*, vol. 172, 559-566.
- [15] Institute of Physics and Engineering in Medicine, 2006. The Design of Radiotherapy Treatment Room Facilities. Report No. 75. IPEM, York.
- [16] Schwarz, A., Schwarz, R., Carter, L., 2008. MCNP/MCNPX Visual Editor Computer Code.
- [17] MCNPX Team, 2008. Monte Carlo N-Particle eXtended. LANL, Los Alamos.
- [18] ICRP, 1996. Conversion Coefficients of use in Radiological Protection against External Radiation. ICRP.

Use of Real-Time Radon Progeny Monitors in Uranium Mines

John Takala^{a*}, Andre Boucher^b, Mikhail Ioffe^c, Kari Toews^a

^aCameco Corporation, 1131 Avenue W South, Saskatoon SK, Canada.

^balphaNUCLEAR, 1131 Avenue W South, Saskatoon SK, Canada.

^cCameco Corporation, Technology Group, 1 Eldorado Place, Port Hope, ON, Canada.

Abstract. In high-grade uranium mines radon progeny is major component of workers' radiation dose and also highly variable, both temporally and spatially. Real-time monitoring of radon progeny concentrations, which provides a simple and clear feedback to workers, is a very important to effectively control radon progeny exposures. Cameco has used alphaNUCLEAR PRISM radon progeny monitors at its underground uranium mines for over two decades for this purpose. The capabilities and limitations of the monitors will be reviewed and how they have been integrated into the overall radiation protection program will be reviewed.

KEYWORDS: *radon progeny monitoring; uranium mining.*

1 INTRODUCTION

Underground mines can be challenging work environments for people and equipment and in uranium mines there is a need to have reliable information about radon progeny concentrations. Cameco has used continuous radon progeny monitors made by alphaNUCLEAR for over two decades as part of its radiation monitoring program. These units are connected to a light system that provides prompt feedback to workers of radon progeny concentrations, are robust enough to survive in an underground environment, and are portable, so they can be easily moved as work place locations change. These continuous radon progeny monitors have been integrated into the radiation work practices to help ensure workers respond consistently to upset conditions to ensure exposures to radon progeny are well controlled.

Cameco purchased alphaNUCLEAR Ltd in 2001 to ensure the ongoing availability of units when the original owner of the company decided to retire. The company alphaNUCLEAR Ltd is run as a fully owned subsidiary of Cameco and supplies continuous radon progeny monitors to customers around the world. In addition, the company supplies radiation monitoring devices, primarily focused on exploration/geology applications.

2 ALPHANUCLEAR PRISM MONITORS

The alphaNUCLEAR Prism radon monitoring unit is made up of several interconnected subsystems housed in a ruggedized case. The unit has an airflow pump that draws ambient air through a filter. The air flow is determined by measuring the differential pressure across a calibrated restrictor. The alpha activity on the filter is counted in ten minute intervals with a silicon charged-particle detector that has a collimator to improve energy discrimination. The signals from the alpha detector are fed into a multichannel analyzer to enable energy discrimination of the alpha particles into four broad energy levels. This data is sent to a microprocessor, which calculates the concentrations of radon progeny, radon gas, and thoron gas. The microprocessor also controls the air pump, the warning light system, the light test circuit, monitors battery status, executes low power controlled shutdown and supports the display and memory interface.

The radon progeny results are sent to a display module that is a 2 line x 20 character transreflective LCD display, which provides easy viewing in all lighting conditions. The unit can run on either ac power or batteries. The power supply and battery charger are isolated from each other when AC power is present. This system provides the flexibility to use several types of batteries depending on the end users requirements and ensures that the backup battery is fully charged and maintained in a proper manner. Battery run times range from 12 hours for lead acid battery to over two days with

lithium battery formulations. In the event of AC power loss the unit seamlessly switches over to battery operation until AC power is restored.

The latest generation of alphaNUCLEAR Prism monitors can be attached to several different types of external warning light systems; they all have three lights (i.e. green, yellow, and red) and the lights can be individually programmed to go on and off to varying thresholds of either radon progeny, radon or thoron gas. One of the light systems comes with an integrated external device controller, which can be used to control devices such as ventilation fans or access doors. The units can store 100+ years of data and the data can be retrieved from the units in a csv file format for subsequent analysis.

Figure 1 shows two styles of light systems that can be attached to the Prism monitors. In the photograph on the left with two lights, there are two Prism units, one upwind and another downwind of a work location.

Figure 1: Two Styles of light systems with Prism monitors



The Prism units calculate the concentrations of progeny of ^{222}Rn and ^{220}Rn . The method is based on counting alpha particles from the progeny collected on the filter by passing the mine air through. The detector counts α -particles in four energy intervals shown in Table 1; however, only channels 1 to 3 are used.

Table 1: Energy intervals for counting α -particles

Channel	Energy, MeV	^{222}Rn Progeny	^{220}Rn Progeny
1	1.8 – 6.5	^{218}Po	^{212}Bi
2	6.5 – 8.2	^{214}Po	^{216}Po
3	8.2 – 9.0		^{212}Po
4	> 9.0		

The algorithm for calculating the specific activities of ^{222}Rn and ^{220}Rn and Working Levels is based on the general solution of Bateman equations for nuclear transmutations [1, 2]. Decay equations for radon isotopes in the alphaNUCLEAR algorithm were modified compared to Bateman's equations to include the rates of release for radon (Q_{Rn}) and thoron (Q_{Th}) into mine air, which were assumed to be constant through the length of the tunnel but changing with time. The algorithm also includes the age of air t , which characterizes the amount of time for the air to travel through the tunnel to the sampling point. Analytical solutions for the specific progeny activities were obtained using Laplace transformation and expressed as functions of the release rate of the corresponding radon isotope, Q , and the age of air, t , at the sampling point. The decay rate constants for both ^{222}Rn and ^{220}Rn and their progeny, which are used in the calculations, are well known.

Alpha activities of the progeny of ^{222}Rn and ^{220}Rn on the filter can be calculated using analytical solutions to the system of differential equations that describe the rates of their deposition and decay. These solutions were obtained using Laplace transformations similar to the Bateman equations. The initial conditions typically correspond to starting the monitor with a clean filter. Using these solutions, equations were obtained for the alpha count rates in channels 1 to 3, which depend on three unknown parameters to be determined, i.e. the rates of release Q_{Rn} and Q_{Tn} and the age of air, t . Provided that the count rates are known, the system of three non-linear equations can be solved to determine Q_{Rn} , Q_{Tn} and t . Using these parameters, the Working Level (WL) at the sampling point is calculated and displayed in real time. If the WL exceeds a pre-set limit, an alarm is triggered.

The data log for on-line processing represents a matrix of alpha counts collected in the three data channels, which are shown in Table 1, over a specified period of time, typically several minutes. This data log is stored in memory of the unit and it may be used for data analysis later.

There are a number of challenges the algorithm needs to overcome. The alpha counts collected over each sampling interval represent random numbers that are distributed around mean values that are related to the specific activities of radon and thoron progeny. The random distribution of alpha counts, which are measured by the Prism detector, results in statistical errors in determining the values of parameters Q_{Rn} , Q_{Tn} and t . With the exception of the initial period of collecting data starting with a clean filter, the activities on the filter at any given time include the contributions from previously collected progeny, which need to be accounted for. The statistical errors in determining parameters Q_{Rn} , Q_{Tn} and t for a given sampling interval propagate further and contribute to errors in determining these parameters in subsequent measurements. However, as the progeny collected on the filter prior to the current sampling interval is decaying, the effect of those errors diminishes.

Relative statistical errors are larger at low count rates and this may result in collecting over a particular sampling interval a data set that has no physical meaning. Examples of such data sets might include detecting zero alpha particles in channels 1 and 3, and collecting one count in channel 2, which is possible, taking into account the statistical nature of radioactive decay and the mechanism of progeny transport by attaching to dust or aerosol particles. Therefore, it is desirable to increase the duration of sampling, especially at low count rates. However, employing long sampling intervals would increase the response time and cause delays with alarming the workers in case of sudden release of radon.

The algorithm implemented in the Prism detectors uses self-adjusting duration of sampling intervals. At low alpha count rates the duration of sampling increases to reduce the statistical errors. As the count rates increase, which reduces the relative error, the duration of sampling decreases to reduce the response time. It was demonstrated by processing simulated data logs with a random (Poisson or normally distributed) noise and by testing in the radon chamber and in the mines that the algorithm is stable and gives results that are consistent with the WL values measured independently.

The algorithm requires one calibration parameter to account for the efficiency of counting alpha particles, which is determined by calibrating each instrument in a radon chamber. The WL readings are calculated in real time and displayed by the end of each sampling interval.

The units are calibrated in radon chamber run by alphaNUCLEAR Ltd. The radon chamber is a 34 m³ walk-in room. The Prism units are calibrated with a 48-hour job run. The recommendation of the manufacturer is to have a formal calibration on an annual basis; typically the counter efficiency varies by less than 5 percent over a year. In addition, a flow check is recommended to be performed by the end user on a semi-annual basis; typical variations in the flow rate are less than 10 percent.

3 USE OF CONTINUOUS RADON PROGENY MONITORS

The primary use of the Prism units are as a warning system to enable workers to respond in a timely manner to upset conditions. This is important in underground uranium mines as radon progeny levels can vary by several orders of magnitude in short periods of time. It is not uncommon for the source of the problem to be remote from the work location, so there may be no visible indication of a problem other than the warning lights of the Prism. If needed, the stored data on the units can be helpful at reconstructing the details of upset situation. At Cameco facilities the devices have not been used for any official dosimetry purposes. The primary reason for this is that the additional level of effort needed to validate the accuracy of individual workers' exposures with an area-based system is not warranted, particularly because the company has other approved dosimetry programs for radon progeny (e.g. personal alpha dosimeters).

The placement of Prism units in the mine needs to balance a number of factors including occupancy rate, visibility, ventilation air flows, potential interferences from mining activities (e.g. blasting), and availability of electrical services. Typically the units are located near active work areas, along main travel ways at strategic points, at entrances to levels and major sections of a mine, and locations with a known high radon source. In practice, 40 to 60 units are typically deployed at Cameco's underground mines and this provides sufficient coverage.

As noted in the description of the units, they are connected to green-yellow-red light panel system to alert workers to changing conditions. The light system is programmable and can be set to the specific needs of the end user. At Cameco operated facilities the colour-code system has been harmonized with the radiation protection program through a code of practice that sets out a number of pre-determined actions at specific radon progeny concentrations. This coordination of the warning light system with the radiation protection program ensures a consistent response to changing radon progeny concentrations. Table 2 provides a summary of the actions to be taken.

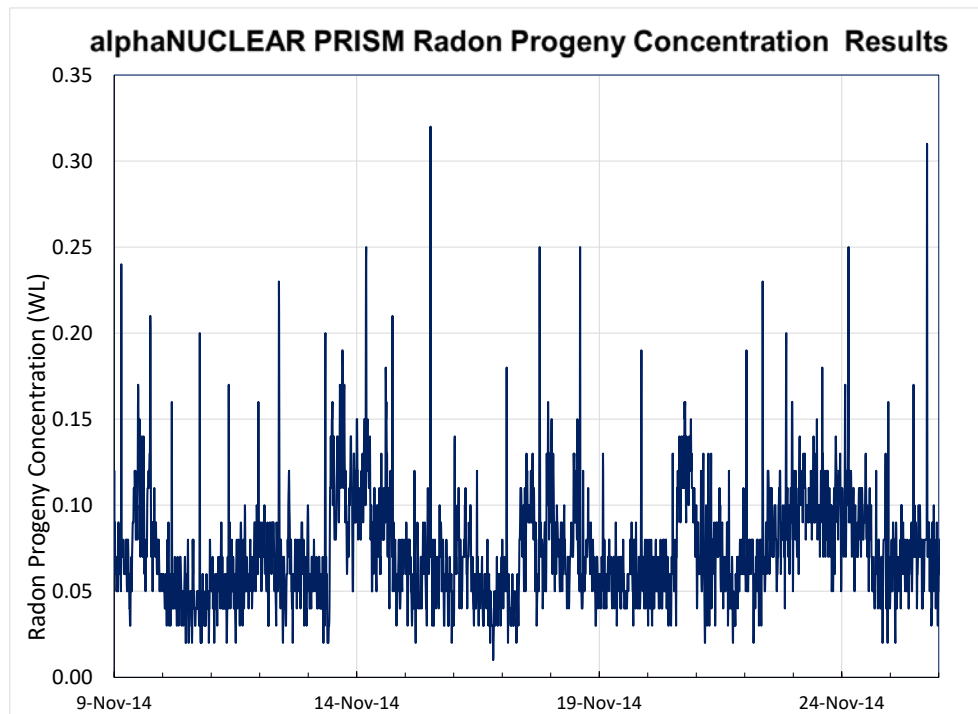
Table 2: alphaNUCLEAR PRISM Lights and Radiation Code of Practice

Radon Progeny Concentration	Prism Light(s)	Summary of Actions When Area Active
$\leq 2.08 \mu\text{J}/\text{m}^3$ (0.10 WL)	Green	1. Continue normal operations
>2.08 to $5.2 \mu\text{J}/\text{m}^3$ (>0.10 to 0.25 WL)	Green & Yellow	1. Workers(s) investigate and take corrective actions. 2. If condition persists for > 24 hours restrict access to the area
>5.2 to $10.4 \mu\text{J}/\text{m}^3$ (> 0.25 to 0.50 WL)	Yellow	1. Workers(s) investigate and take corrective actions. 2. If condition persists for > 6 hours restrict access to the area
>10.4 to $20.8 \mu\text{J}/\text{m}^3$ (> 0.50 and ≤ 1.00 WL)	Yellow & Red	1. Workers(s) investigate and take corrective actions. 2. If condition persists for > 2 hours restrict access to the area
$> 20.8 \mu\text{J}/\text{m}^3$ (>1.00 WL)	Red	1. Workers (s) immediately leave area and restrict access. Inform supervisor and RD. 2. Post radiation warning and RWP Required signs 3. RD to investigate and take appropriate corrective actions.

Because the Prism units provide an update to radon progeny concentrations every 10 minutes, in situations with high radon progeny concentrations (i.e. $> 20.8 \mu\text{J}/\text{m}^3$ or 1.0 WL) workers are warned to leave the area promptly and thus avoid potentially high-exposure incidents. This is an important tool in keeping exposures ALARA. Workers are trained on how to respond to the Prism lights and have come to rely on the units to provide them with the level of assurance that radon progeny concentrations are acceptable.

Figure 2 shows actual results from a Prism monitor in an underground uranium mine. There are both short term and longer term fluctuations apparent in the data. During this period of monitoring the Prism lights would have been primarily green (i.e. < 0.10 WL or $2.08 \mu\text{J}/\text{m}^3$) and periodically been green-yellow indicating an elevated concentration of radon progeny, which was corrected within the time prescribed by the radiation code of practice. This helps to illustrate how providing the feedback of actual conditions to the workers enables them to take corrective actions in timely manner and control their radon progeny exposures.

Figure 2: Radon Progeny Concentrations in Underground Mine



4 CONCLUSION

The alphaNUCLEAR Prism units, which provide continuous monitoring of radon progeny concentrations, are a very important tool in controlling radon progeny exposures in dynamic environments, such as underground uranium mines. The units are robust and reliable in the challenging conditions of underground mines. Linking the warning light system to a system of standardized corrective actions provides consistent guidance to the workforce and helps them control their radon progeny exposure.

5 REFERENCES

- [1] Bateman, H. 1910. Solution of a system of differential equations occurring in the theory of radioactive transformations, Proc. Cambridge Philos. Soc., 15, p. 423-427.
- [2] Cetnar, J. 2006. General solution of Bateman equations for nuclear transmutations. Annals of Nuclear Energy, 33, p. 640-645.

Verification of main shielding bodies at Atucha-2 during full power operation

Martín Brizuela, Felipe Albornoz, Eliana Cuello

INVAP S.E. Comandante Luis Piedra Buena 4950, 8400 San Carlos de Bariloche, Río Negro, Argentina.

Abstract. Atucha-2 (CNA-2) is a 745 MWe Siemens-designed PHWR that has recently begun full power operation. While its construction began as early as 1981, several problems (mainly due to Argentina's financial problems at the time) caused the project to be virtually stopped from 1994 to 2006. The country's nuclear plan was re-launched that year, and the reactor achieved first criticality on June 2014. Finally, operation at full power started on February 2015. As part of the different stages of the commissioning process, the main shielding bodies were routinely checked at different power levels. A final and comprehensive survey was done at full power, by sweeping the plant's shielding at all reactor building levels in order to verify its adequacy and also to properly identify any possible hot spots. Around 200 Radiation Base Points were identified, measured and recorded. It was found that the main shielding bodies are adequate, both in general and also considering the particularities of individual penetrations. In most cases, dose rates that are comparable to the background level or slightly above it are recorded. This work will discuss the experience of measuring and verifying the main shielding bodies at CNA-2, describing the difficulties found due to the long delay in building the plant, and the recommendations given from the lessons learned during this study.

KEYWORDS: *Atucha-2; commissioning; full power; shielding verification.*

1 INTRODUCTION

The "Néstor Kirchner" Nuclear Power Plant (commonly known as Atucha-2) is a 745 MWe Siemens-designed PHWR that began full power operation during February 2015. While its construction began as early as 1981, financial problems caused the project to slow-down during the late '80s, and eventually to be virtually stopped during 1996. At the moment of the work's suspension, more than 90% of the civil work was already completed and many of the main nuclear components were at the construction site, but they were only partially assembled.

The country's nuclear plan was re-launched in 2006. Due to the extended delay in its construction, the original engineering team was mostly dismantled, and a great effort had to be dedicated to recover a team of engineers and technicians able to complete the remaining tasks and to start with the commissioning of the reactor. The reactor achieved first criticality on June 2014, and operation at full power started on February 2015.

As part of the tasks completed when the reactor reached full power, a comprehensive survey was prepared and executed, in order to measure the dose rate behind the main shielding bodies in the plant when the reactor is at full power, and thus identify all the potential hot spots that might arise.

2 GENERAL METHODOLOGY

The externally homogeneous shielding sections might be weakened for several reasons:

- (a) Thickness is not adequate, resulting in a higher dose rate than expected.
- (b) There are points of radiation leakage from where some radiation is emerging.
- (c) There are voids in the concrete created during the formwork's filling operation.
- (d) Lack or insufficient sizing of compensating shielding (for instance, steel slabs), that should have been embedded in the concrete.
- (e) The steps of removable floor and other sections are not adequate.

Concerning the penetrations, the emerging radiation leakage due to them can be several orders of magnitude higher than the radiation emerging after traversing the bulk of the shield itself. Possible causes of leaks through penetrations might be, among others:

- (a) Missing pieces in the dedicated shielding.
- (b) Elements added or modified at the last minute or during assembly of the sets.
- (c) Poor design of some parts or the whole.
- (d) The penetrations for piping, cables, etc., are usually filled with lead wool or lead shots, but it is usually impossible to perfectly compensate for the missing shielding.

The procedure prepared to check the shielding bodies of the reactor and of the primary and moderator cooling systems follows the recommendations in [1]. Based on the drawings for the different levels and sections of the reactor building, the shields (both vertical and horizontal), are divided into sections clearly demarcated on those drawings. For each section, the expected main radiation source on that section is identified. With the appropriate measuring instruments, a systematic sweep on the surface of the shield is made, looking for the point with the highest dose rate.

The vertical shields (walls, doors, etc.) were measured in contact up to a height of ~2 m, while for the horizontal shields (floors) the measurements were done at a height of 1 m. In vertical shields, according to the original design of Siemens, it was expected to find, above 2 m height, a large number of piping penetrations with dose rates higher than the background level. A careful scanning was performed in the area around each set of penetration or penetrations belonging to a given shielding section.

In each section the point of highest dose rate was recorded and identified by sticking a sticker with the corresponding RBP (Radiation Base Point) number. At that point, the dose rates due to gammas and to neutrons are measured, both at contact and at 1 m away from the shield's surface. In those cases where other points of high dose rates were identified in the same section, the numbering of the RBP added correlative letters (i.e. RBP15A, RBP15B, etc.).

A significant interference was expected to occur in many rooms of building level +0.50 m due to the operation of the Fuel Loading Machine (FLM), which is all the time performing different loading/shuffling/unloading operations with fresh and irradiated fuel elements above the reactor lid. Therefore the operating status and position of the FLM was also recorded for those shielding sections potentially affected by the operation of the FLM, so as to later cross-check the measured dose rates.

The measuring team consisted of three persons, carrying a gamma radiometer, a teletector, and a neutron monitor, all with valid calibrations.

3 RESULTS

The procedure was executed during the last week of February 2015. Around 200 RBP's were identified, measured and registered. RBP's stickers were placed accordingly on each shielding measurement section, and sometimes additional stickers were used to identify individual points where a particularly high dose rate (as compared to the dose rate measured in the majority of the shielding section considered) was measured.

The measurement team was permanently informed about the reactor power and the position and load of the Fuel Loading Machine. Reactor power was most of the time at about 100% of nominal power, although during some few hours it stayed at 80% of nominal power. Based on INVAP's experience and considering the position of the RBP's that were measured during that time, it is perfectly valid to renormalize those results to full power. The Fuel Loading Machine was most of the time performing fuel permutations while the measurements were taken. It often contained at least one irradiated fuel element.

Fig. 1 illustrates the position of some few of the RBP's measured, where higher than background dose rates were found. Fig.2 contains four pictures taken at those positions while performing the measurements. A description of findings at each one of these points follows.

Figure 1: Vertical and horizontal sections of Atucha-2 showing some of the RBP's measured locations

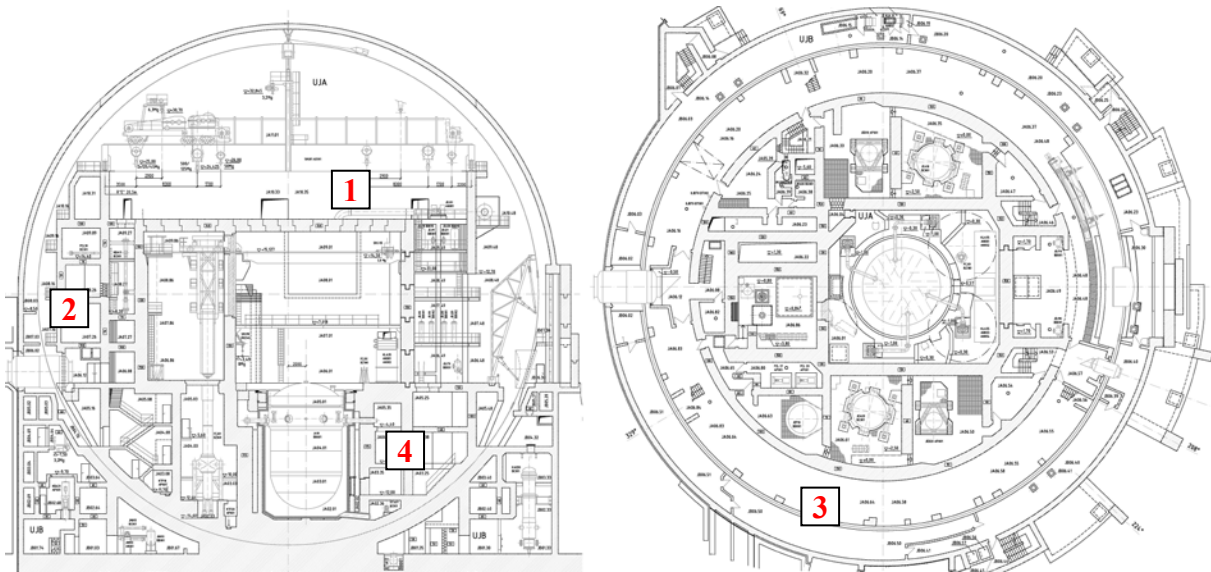


Figure 2: Some selected RBP's: 1=live steam line above Steam Generator in level +18.80 m; 2= rupture valve at level +5.00 m; 3= penetrations belonging to level +0.50 m; 4= door giving access to components of the moderator system in level -12.00 m



3.1 RBP at position 1, level +18.80 m

At this level all the area covered by slatted and concrete-removable floor was verified. The most significant RBP was located at the elbows of the live steam pipes of both Steam Generators. The gamma dose rate measured was around $10 \mu\text{Sv/h}$. No neutrons were detected. The gamma source was probably due to the decay of ^{16}N in the activated D_2O that enters the primary side of the Steam Generators.

3.2 RBP at position 2, level +5.00 m

The measured gamma dose rate in contact with a pressure release device (a rectangular "window", located 2.5 m above the floor level), was 150 $\mu\text{Sv/h}$. No neutrons were detected. At the inner side of the pressure release device, piping carrying activated coolant is located.

3.3 RBP at position 3, level +0.50 m

Two different penetrations for piping of auxiliary systems (inactive). However, these penetrations point to the Steam Generators located at the inner side of the shielding. The measured gamma dose rates close to the penetrations are 50 $\mu\text{Sv/h}$ and 150 $\mu\text{Sv/h}$. These pipes are located 2.4 m and 3.0 m above the floor level.

3.4 RBP at position 4, level -12.00 m

The measured dose rate in contact with this door was similar to background level. No neutrons were detected. This is a thick heavy concrete door, where no hot spots due to leakage through slits were detected. However, next to this door, going down a staircase parallel to that shown in the picture, there is another, unshielded, door that conducts to the same room as the previous one. The contact dose rate at this second position was 5 mSv/h. Neutrons were also detected, resulting in 12 $\mu\text{Sv/h}$ in contact. Gammas are due to ^{16}N from activated moderator, and neutrons are probably due to photoneutron reactions produced by the energetic ^{16}N gammas and deuterium. These measurements are consistent with the original classification of these staircases, implying that the original designer knew about the expected high dose rates here.

A common door (unshielded) is, a priori, a weird design solution, considering that next to it there is the mentioned large and heavy Rigel large door. A shielded door, with a few cm of lead, would have not been enough either, due the expected high intensity radiation in that location. However, further inspection of the access to these doors shows that the unshielded door is the only possible escape route for level -12.0. Thus, we think the designer had considered setting this unshielded door at level -12.0 as an emergency door and, because there is no enough space for an access labyrinth at this level (since the steel sphere is too close to the wall at this level), they set the geometry of the access in such a way that the labyrinth is formed considering the staircase access and walls and the corridors at different levels.

4 CONCLUSIONS

All measured shields are adequate, considering both the bulk shields and the individual penetrations. For most of the shielding sections evaluated, the measured dose rate values were similar to the background dose rate, or slightly above it.

In several of the evaluated sections, at different levels, piping penetrations and pressure release devices were found, with contact dose rates between 50 $\mu\text{Sv/h}$ to 150 $\mu\text{Sv/h}$. All these penetrations are located above 2 m from the corresponding floor level. In consequence, the routine tasks at floor level would result in low doses. The plant operator should assess whether to take any additional action or not. These points were identified in situ with its corresponding sticker RBP. In principle, the designer contemplated that the classification of a given room was valid only up to 2 m high, thus admitting that above that height, higher dose rates could be found.

5 REFERENCES

- [1] ANS-6.3.1-1987 Program for Testing Radiation Shields in Light Water Reactors (LWR). American Nuclear Society, 555 North Kensington Avenue, La Grange Park, Illinois, USA.

Newcomers, new build – the industry view

Marcel Lips^{a*}

^aGoesgen Nuclear Power Plant, P O Box, CH-4658 Daeniken, Switzerland.

Abstract. Nuclear safety has many facets (plant design, human factors, training, attitude, culture, radiological protection, emergency preparedness, and so forth). It is advisable to strive for a balance between all of them. Exchanging expertise between all safety influencing areas is a key point in developing nuclear safety. Maintaining operational experience throughout an “NPP life”, covering almost one century from the beginning of planning to the end of decommissioning, engaging several generations of workers and passing through different steps in the development must be considered carefully. Within that long time period a NPP might undergo different eras of societal and political tendencies, which could give raise to some concerns. Switching from a nuclear promoting into a phase out milieu, to find oneself in life extension programs shortly after and finally to be faced with immediate plant closures is frustrating for the employees. Such a back and forth will lead to the departure of personnel, demotivation and loss of knowledge as one of the safety aspects. Comparable circumstances will arise when equitable market access is suddenly denied and one has to compete against subsidised competitors, having the chance to get access to the market at less than zero cost. Developing nuclear safety is a common goal of Governmental Bodies, Authorities and operators. As such, operators should have the right to be involved in the implementation of new regulations. Especially practicability issues should be discussed in advance to strive for excellence in safety, in which radiological protection is only one facet of the big picture and in some cases even a minor one. Similar reflections can be made when discussing the role of nuclear power within the upcoming global challenges for the electric power supply. Is radiation the key issue – like it seems to be today – or is radiation just one facet?

KEYWORDS: *new build; nuclear industry; safety; stability; stakeholders.*

1 INTRODUCTION

An investment into a nuclear facility is a long-term commitment. Such an investment calls for a certain degree of political stability and equitable market access to achieve a high certainty of prosperity, which at the end is one of the conditions for safe operation. But safety of course is more than that, it’s a far-reaching subject and should always be the main operator’s focus.

In some parts of the world “nuclear” is discussed very controversy and emotionally. The severe incidents/accidents in Three Mile Island, Tschernobyl and Fukushima are part of the causes oppressing all the big nuclear advantages. Safe operation, openness and stakeholder-involvement are key factors in regaining trust. Without trust, public acceptance won’t be gained and nuclear projects might be rejected by public votes or delayed in time judicially with corresponding impacts on economy.

The nuclear industry has many stakeholders but is at the same time a stakeholder itself. Implementing recommendations, regulations and new findings must happen in a practicable way. The industry sees the necessity to be involved thereby, in order to strive for optimal safety.

In the following chapters the main needs of the nuclear industry are briefly discussed.

2 SAFETY

Safety is a societal desire. Each industry, each company and each individual should be aware of that. Depending on complexity, potential for damage or even soft factors (gut feeling), safety has more or less facets. In the nuclear field the following

* Presenting author, e-mail: mlips@kkg.ch

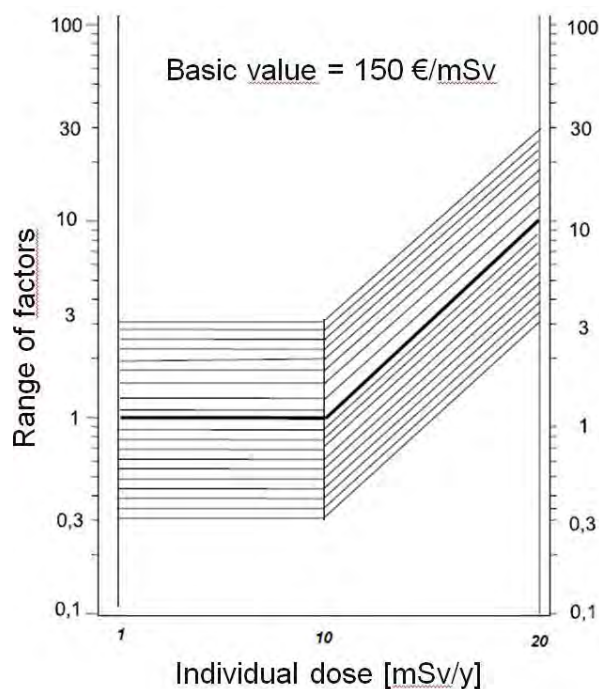
- a profound assessment of possible impacts to installations
- the corresponding plant designs
- human factors
- man-machine interfaces
- training and qualification
- general attitude
- safety culture
- radiological protection
- emergency preparedness
- quality management
- leadership
- and so on

are part of an overarching safety. Finding the right balance between all these safety influencing factors is crucial. Overemphasizing one aspect could have significant safety influence elsewhere or severe economic impact and so should give raise to some concerns, this especially when individuals are tending to tackle problems a little too narrow-mindedly within their own area of expertise. If for example we decide to install cameras in some parts of a plant in order to give up routine walk downs, we might save some micro Sieverts for the staff – having done “a good radiological protection job”. However we probably miss the opportunity to include audible plant inspection aspects. An upcoming pump bearing failure is detectable by means of noise changes and can be fixed prior to a bigger damage, which might have a negative impact on safety.

Exchanging expertise, developing an ability to include different safety influencing factors into a safety assessment and accepting that optimal overarching safety might not be the optimal solution for an individual aspect are really essential.

Depending on the situation, each of these individual safety facets might have a different degree of influence. Radiological protection for example may play a minor role during normal plant operation (including outages). Maintenance of safety systems cannot be omitted for dose saving reasons and the cost for corresponding optimization is limited. According to a cost-benefit analysis [1], which in recent years has been adopted and redefined by industry radiological protection professionals (see Figure 1), the cost for saving a Person-mSv is in the range from 50 to 4'500 € per Person-mSv.

Figure 1: Currently used cost-benefit analysis in radiological protection



Bearing in mind that average annual individual doses are about 1 mSv or less for employees and contractors in nuclear power plants, justified cost for significant dose reductions is well below the cost of only one full power production day.

On the other hand a beyond design accident with a huge activity release may have significant radiological consequences to a huge number of members of the general public. Investments to comply with international recommendations [2] and to reduce the risk of such potential radiation exposures might be mainly driven by radiological protection considerations.

3 THE NUCLEAR CENTURY

Initially life times of nuclear power plants have been assumed to be around 40 years. Because of safety upgrades, preventive maintenance, aging management and life extension programs many utilities decided to extend plant life times up to 60 years. Today first applications for a life time of even 80 years are underway. Including the time span from the beginning of planning to the end of decommissioning, a nuclear power plant life covers around one century. Several generations of workers (suppliers and operators) will be involved, challenging the knowledge transfer. The plant will pass through different steps in the development. When most of the existing plants were designed, digital process control technique for example did not exist or was not available in corresponding reliabilities. Analog technology is still widely spread in the plants, but engineers and workers are no longer educated in these fields. Plant suppliers – having wide experience – might disappear and the availability of classified spare parts is no longer guaranteed.

With this in mind, the development of in-house knowledge in all essential fields is absolutely essential for survival and plant safety. It enables the knowledge transfer to the next generations of workers as well. Not only operators are faced with these problems, it touches the regulatory bodies (including their experts) during their supervisory activities as well.

4 POLITICAL STABILITY

Building and commissioning a nuclear power plant will cost a few billion dollars. The pay back of such an investment is normally a long-term issue. Therefore, once the decision is taken to install nuclear capacities, an investor will need some guarantees that the social and political environment is stable enough to allow the amortisation of the investment. Switching from a nuclear promoting into a phase out milieu, to find oneself in life extension programs shortly after and finally to be faced with immediate plant closures – as happened in one European country – will not motivate a company to invest into a nuclear facility. Furthermore, it is frustrating for the employees and will lead to the departure of personnel, demotivation and loss of knowledge as one of the nuclear safety aspects.

Comparable circumstances will arise when equitable market access is suddenly denied. Cost optimizing programs are always necessary in a competitive market and can be implemented without safety deductions. But if selective competitors are subsidized to an extent, which allows them to sell power at zero or less than zero cost, the market will go off the rails. It's a question of time how long unsubsidized market players or whole industries will survive or will give raise to some safety concerns.

5 THE ROLE OF NUCLEAR

In chapter 2 safety issues have briefly been addressed. The system boundary of this reflection was the plant itself and a potential affected area around the plant in case of an accident.

In a wider view, additional safety aspects should play a role when talking about nuclear. A nuclear facility contains a certain amount of potential hazard. Consequences in case of an accident are huge but “limited as seen from a global scale and perspective”. Greenhouse gas emissions are low and the demand of natural resources is small. Fossil fired plants have limited potential hazards, but consume a vast amount of natural resources. Furthermore, they contribute to greenhouse gas emissions and climate change affecting humans globally as well as flora and fauna. Similar factors can be derived for each

technique used or planned for power production (wind, solar, geothermal, hydro, etc.). An overarching safety assessment against these factors is not commonly used, and if available, often overruled by policymakers, societal demands or misinformation preventing a comprehensive analysis of global safety aspects.

6 THE INDUSTRY AS A STAKEHOLDER

As a nuclear industry there is a need to maintain relations to many stakeholders (owners, suppliers, municipalities, authorities, etc.). All of them contribute in a certain way to plant safety, enhancing trust building in operators. Typical for that is the change in mind set of a region getting a new nuclear facility. Initially, an adverse attitude predominates. After some time local residents are getting familiar with the facility, its operation and safety decision making process, leading to a more positive attitude.

Utilities are implementers of recommendations, regulations, lessons learned, etc. Implementation of new recommendations must happen in a practicable way using the existing operator's knowledge. So in a way utilities are stakeholders for regulatory bodies as well. Without involvement of practitioners there is a risk that not all aspects which may have negative impact on safety are taken into account during the implementation process. Furthermore, when practitioners are involved, acceptance and comprehension of new regulations – especially for far-reaching ones – are much better. In some countries utilities are well involved in the process, in other countries they are more or less excluded. For the latter case there is a need for improvement.

7 CONCLUSION

To ensure optimal plant safety during the whole nuclear power plant life, a close collaboration between involved bodies is required. It is necessary to assess and balance safety issues over a wide base, always considering the developments being in progress over the decades. Counting on stable political situations and fair market access is an indispensable need for investors. If just one of these basic needs is missing, safety will not achieve its optimum.

8 REFERENCES

- [1] IAEA Bulletin Vol. 22 No. 5/6, 1980. Cost-Benefit Analysis and Radiation Protection. Vienna. https://www.iaea.org/sites/default/files/publications/magazines/bulletin/bull22-5/225_605041322.pdf
- [2] IAEA, 1999. INSAG-12 „Basic Safety Principles for Nuclear Power Plants“ 75-INSAG-3 Rev. 1. Vienna.

Lanthanides Patterns as a Nuclear Forensic Signature from a Uranium Mine in South Africa

Manny Mathuthu^{*}, Ntokozo Khumalo, Malayita M Baloyi, Refilwe N Maretela

North-West University (Mafikeng), Center for Applied Radiation Science and Technology (CARST), Mmabatho, 2735, South Africa.

Abstract. The lanthanides are Rare Earth Elements (REE) that exhibit consistent patterns under varying geochemical conditions. Therefore they can be used as signatures to determine the chemical and physical change that has occurred on a uranium ore since it was mined and processed. This work described the analysis of water samples taken from a mine drilling core. This water, which is used to cool the drilling machine, is called *fixture water*. It thus carries small representative particles of the uranium ore before processing by acid leaching or precipitation. The REE Fingerprint results presented here suggests that uranium is embedded in Phosphorite deposit in Apatite & fluorapatite minerals. The uranium is recovered from phosphoric acid, while lime used for precipitation of impurities and magnesia is used for precipitation of uranium. The uranium isotopic signature has a graph of $^{207}\text{Pb}/^{204}\text{Pb}$ versus $^{207}\text{Pb}/^{206}\text{Pb}/^{208}/^{206}\text{Pb}$ almost defining a 45° slope with $^{207}\text{Pb}/^{204}\text{Pb}$ values *distinctively ranging from 12 % wt to 18.5 % wt*.

KEYWORDS: *isotopic ratio; lanthanides patterns; fixture water; REE.*

1 INTRODUCTION

1.1 Nuclear terrorism

Nuclear trafficking arose predominantly during the early 90s with the first case reported in 1991 in Italy and Switzerland as well as the Soviet Union. Later more cases were reported in Germany, Czech Republic, Hungary and other central European countries [1]. However, in 1992, the IAEA illicit trafficking database revealed that there were about 11 cases of smuggled Highly Enriched Uranium or plutonium specifically in Russia and Europe. Consequently, questions concerning the origin, trafficking route and intended use of the nuclear or radioactive material were raised. The International Atomic Energy Agency [2] defined nuclear forensics as: *the analysis of intercepted illicit nuclear or radioactive material and any associated material to provide evidence for nuclear attribution*. The goal of nuclear forensics analysis is to identify forensic indicators in prohibited nuclear and radiological samples or the surrounding environment.

Basically nuclear forensic is the branch of science which is associated with the analysis or characterization of seized nuclear or radioactive material based on chemical and isotopic composition, age dating and physical parameters in determining the origin of the interdicted radiological nuclear material. Despite the development of nuclear security and safety by the IAEA, nuclear forensic has discouraged and in some cases, prevented nuclear terrorism as well as illicit trafficking of nuclear or radioactive material [3]. Nevertheless, during those early 1990s nuclear forensic was not a remarkable tool until nuclear terrorists attacked New York City and Washington in September 2011 [4].

*Corresponding author: Manny.Mathuthu@nwu.ac.za ntokozohkhums@gmail.com ; maxon@live.co.za ; rnmaretela@gmail.com

1.2 Nuclear Forensic Signatures

Signatures are the features of a given sample of nuclear or radioactive material that allows one to differentiate one material from other nuclear or radioactive material. These include physical characterization, elemental, isotopic and chemical composition. ICP-MS Total Quantity method provides one vital technique which is applied to determine signatures of interdicted radiological nuclear material. These signatures are found in the concentration levels of Lanthanides, also called Rare Earth Elements (REE) in a given nuclear material, where they are residual trace amounts or contaminants of the uranium extraction process [5]. REE exhibit coherent behavior during different geo-processes and consistent fractionation [6]. Elemental signatures include the detection of major, minor as well as trace elements in the material. Each of these has a contribution towards obtaining a signature for instance major elements define the identity of the nuclear material, minor elements helps to define the function of the material and lastly, trace elements indicates a certain process. REE and Isotopic Signatures of the material include the discovery of fission or neutron capture products, which designate that the material has been in a nuclear reactor and are a representative fingerprint for the type and operating conditions of a given reactor [5]. Isotopic signatures also include decay products from the parent material which can be used to date the age of the material [7, 8]. Molecular isobaric interferences and matrix suppression are the major challenges in low level lanthanide determination.

2 MATERIALS AND EXPERIMENTAL METHODS

2.1 Sample preparation

The samples used in this study consisted of mine water used in cooling the drilling machine, waste water from the processing plant and soil samples from the mine tailing. It was observed that the slurry from the plant is deposited on the tailing dam in paddocks. Fig 1 shows an example of a tailing with paddocks at different drying stages. The samples were preserved for later preparation and analysis in the Laboratory. Exactly 1 g of each sample was weighed into a Microwave digester vial and then digested according the Aqua Regia method [9]. All the reagents were of Suprapur analytical grade (by Merk, Darmstadt, Germany).

Figure 1: Tailing dam showing sampling points according to the paddocks.



2.2 Instrumentation

The spectrometric analysis was carried out using the Perkin Elmer ICP-MS 300Q equipped with dual detectors. The optimized operating parameters are summarized in Table 1 below.

Table 1: Optimum operating parameters for the Perkin Elmer ICP-MS 300Q.

Forward Power (W)			
Dead Time (ns):	35	Cooling gas flow rate (mLmin ⁻¹):	10
Read Delay (sec):	15	Auxiliary gas flow rate (mLmin ⁻¹):	1
Number of Sweeps:	1000	Nebulizer gas flow rate (mLmin ⁻¹):	1
Number of Readings:	1	Solution uptake rate	
Number of Replicates/reading:	3	Sampling time (s):	10
Dual Detector Mode:	Dual		
Measurement Unit:	cps		
Torch Z Position (mm):	-1.00		

2.1.1 ICP-MS Methodology

Soil, water and vegetation sample digestion protocol follows that commonly known as Aqua Regia digestion Method using a Multiwave 3000, Anton Paar microwave oven manufactured by Perkin Elmer. Water samples were analysed using the ICP-MS stated above. The NeXION 300Q, Perkin Elmer Inductively Coupled Plasma Mass Spectrometer (ICP-MS) calibration uses Dual Detector Calibration Solution as the Atomic Spectrometric Standard. Specifications are:

10 milligrams per litre of Al, Ba, Ce, Co, Cu, In, Li, Mg, Mn, Ni, Pb, Tb, U and Zn [10].

3 RESULTS AND DISCUSSIONS

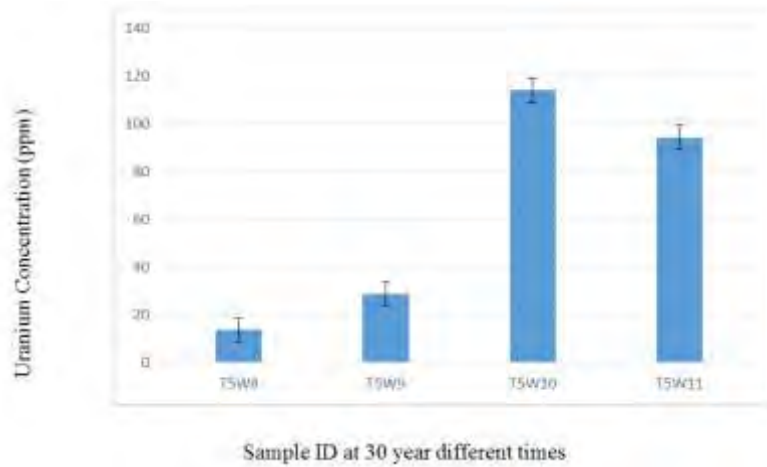
The ICP-MS is already configured by the Manufacture to auto correct for isobaric interferences from elements like Ba. Table 2 shows the concentration of the heavy elements excluding the REE (Lanthanides).

3.1 Heavy metal patterns

Table 2: Concentration (ppm $\pm 1\sigma$) of heavy metals per tailing with lanthanides at trace levels

Sample ID	As	Pb	Cu	Th	U	Zn
T1E1	1.102	0.129	0.491	0.044	0.682	0.546
T1E10	0.876	0.105	0.516	0.088	1.365	0.357
T1E11	0.444	0.086	0.634	0.048	0.227	1.148
T2E1	0.493	0.068	0.352	0.03	0.535	0.479
T2E11	0.767	0.075	0.365	0.043	0.697	0.351
T2E12	2.092	0.281	0.716	0.044	0.227	0.268
T2E13	0.592	0.086	0.517	0.045	0.843	0.437
T3W6	0.011	0.001	0.007	0.003	75.725	0.011
T3W7	0.002	0.002	0.006	0.001	0	0.008
T3W8	0.023	0.001	0.007	0.001	0	0.007
T4W1	0.016	0.001	0.006	0.003	0	0.003
T4W2	0.009	0.004	0.011	0.001	0	0.012
T4W6	nd	nd	nd	nd	10.535	nd
T4W7	nd	nd	nd	nd	46.294	nd
T4W10	nd	nd	nd	nd	67.031	nd
T4W12	0.009	0	0.002	0	3.844	0.001
T5W8	0.015	0.001	0.003	0.001	13.545	0.002
T5W9	0.068	0.001	0.006	0.001	28.87	0.005
T5W10	0.053	0.008	0.015	0.002	114.044	0.016
T5W11	0.006	0.001	0.009	0.002	94.225	0.008
SVW1	0.02	0.001	0.003	0	0	0.007
SVW2	0.017	0.001	0.005	0	0	0.007

Figure 2: Variation of U with Time showing U discharged as waste at different decades.



From sample ID T5W8- T5W11, the uranium concentration increased up to T5W10. These samples were collected at various sedimentation level of the tailing with an estimated time difference of 30 years, see Figure 2. The purpose was to determine the changes in the Processing technology over decades and also which factors affected the extraction of uranium. The tailing is disused now for more than 30 years. It is noticeable that in the early years of gold extraction, (i) uranium price was not conducive for Au and U processing, (ii) the technology used for gold processing was not cost-effective for uranium. From the currently active tailings (T1E, T3E & T3W) the uranium left in the waste in minimal due to improved processing technology.

Figure 3: Chondrite normalized REE patterns for Mine samples. REEs in order of A. (Chondrite data: Anders and Grevesse, 1989).

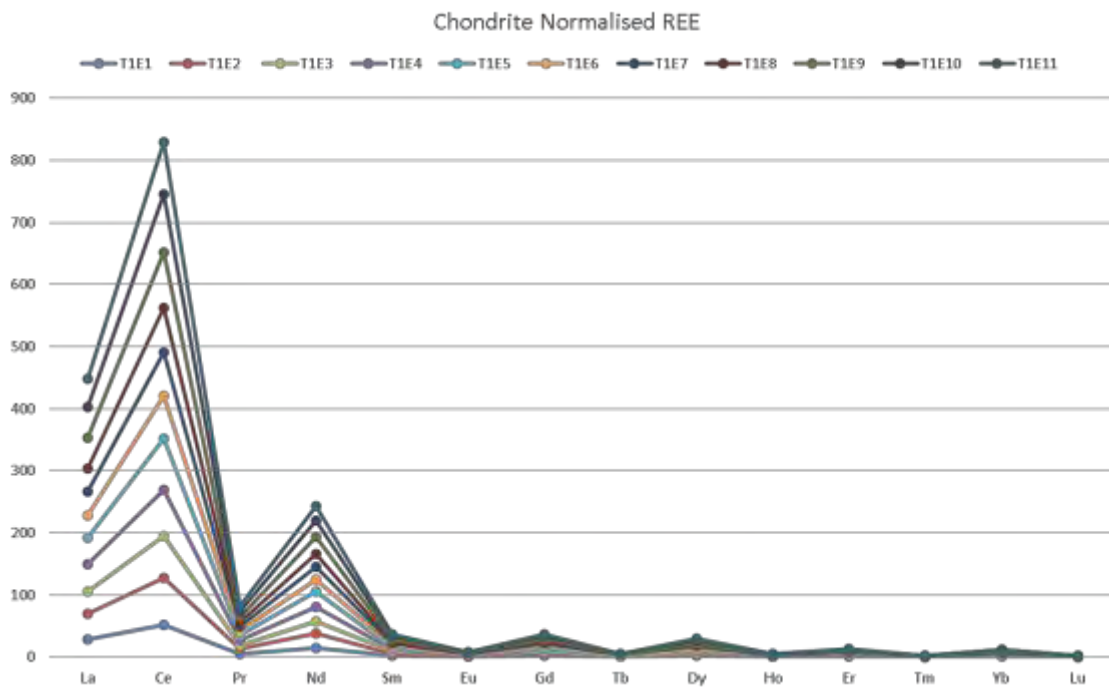
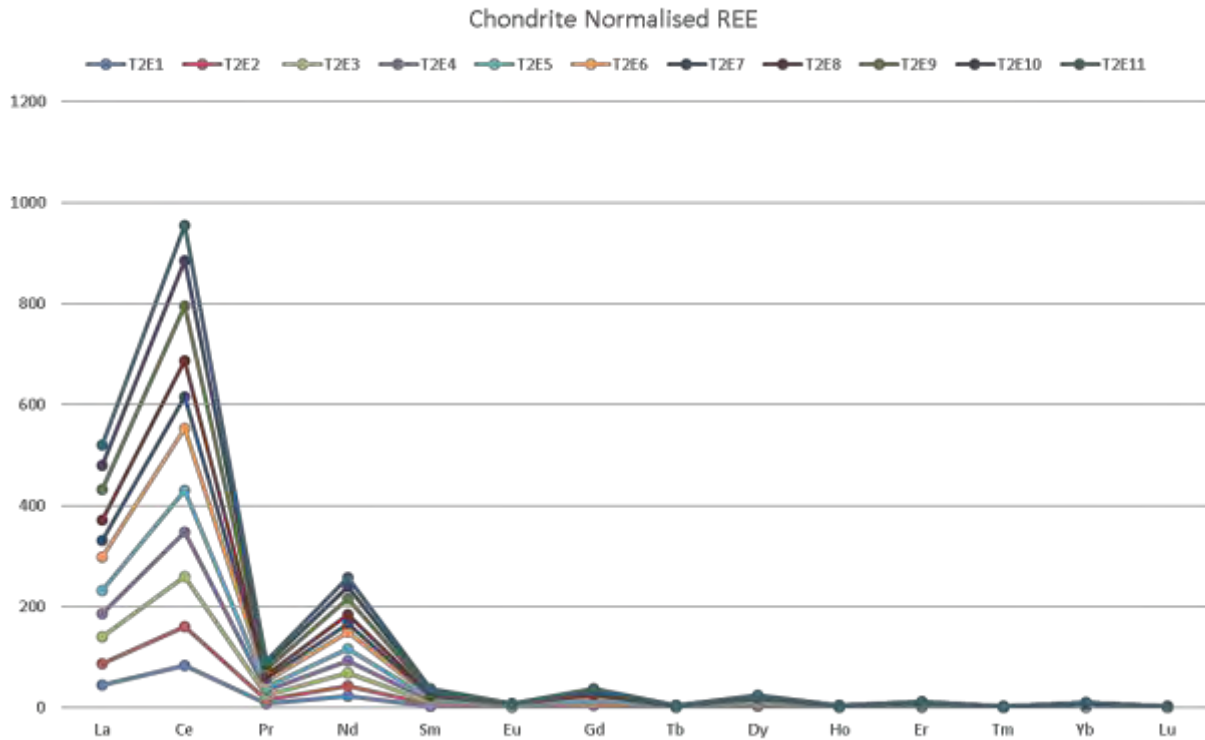


Figure 4: Chondrite normalised REE patterns for Mine samples. REEs in order of A. (Chondrite data : Anders and Grevesse, 1989).



During the processing of the ore, fingerprint is lost. However, Rare earth elements (REE) or Lanthanides, are used to determine the original deposit. Fig 3 & 4 show that La, Ce, (Pr) & Nd have high signatures for U in each mining point. This agrees with observations by Keegan et al. [11] and Dai et al. [6]. Impurities of Ca, Fe, W and Pb were found in urinites and this is normally the characteristic of vein type hydrothermal deposit. The increase of uranium in the T5W samples suggests:

- ❖ Time scale for technology development over years
- ❖ Poor processing methods
- ❖ Poor price of uranium at that time

4 CONCLUSION

The REE fingerprint results presented here suggests that uranium is embedded in Phosphorite deposit in Apatite & fluorapatite minerals. The uranium is recovered from phosphoric acid, while lime used for precipitation of impurities and magnesia is used for precipitation of uranium. Rare Earth Elements (REE) are good signatures of the original deposit [12]. Ca, Fe, W and Pb were impurities found in urinites and this is normally the characteristic of vein type hydrothermal deposit.

In Fig 9, Lead (Pb) isotope ratios for SA gold mine has $^{207}\text{Pb}/^{204}\text{Pb}$ values ***distinctively ranging from about 12 % wt to 18.5 % wt***. This is distinctively different from UK, Germany, Poland, Italy, and Spain [13].

5 ACKNOWLEDGEMENTS

- ❖ Authors would like to acknowledge the International Atomic Energy Authority for sponsoring this Project under CRP J2003.
- ❖ We also acknowledge the NRF-KIC (UID - 104086 & 10487) for providing full sponsorship to this IRPA14 Conference.

6 REFERENCES

- [1] K. Mayer, M. Wallenius, and T. Fanghänel, "Nuclear forensic science—from cradle to maturity," *Journal of Alloys and Compounds*, vol. 444, pp. 50-56, 2007.
- [2] IAEA, "International Atomic Energy Agency Vienna. Technical Guidance Nuclear Forensics Support Reference Manual. ," *IAEA Nuclear Security Series no. 2.*, vol. 2, p. 1 150, 2006.
- [3] I. D. Hutcheon, M. J. Kristo, and K. B. Knight, "Nonproliferation Nuclear Forensics," ed: Glenn Seaborg Institute, Lawrence Livermore National Laboratory.
- [4] M. J. Kristo, "Chapter 21 - Nuclear Forensics," in *Handbook of Radioactivity Analysis (Third Edition)*, M. F. L'Annunziata, Ed., ed Amsterdam: Academic Press, 2012, pp. 1281-1304.
- [5] Z. Varga, R. Katona, Z. Stefanka, M. Wallenius, K. Mayer, and A. Nicholl, "Determination of rare-earth elements in uranium bearing materials by inductively coupled plasma mass spectrometry," *Talanta*, vol. 80, pp. 1744 - 1749, 2010.
- [6] S. Dai, J. Yang, C. R. Ward, J. C. Hower, H. Liua, T. M. Garrison, *et al.*, "Geochemical and mineralogical evidence for a coal-hosted uranium deposit in the Yili Basin, Xinjiang, northwestern China," *Ore Geology Reviews* vol. 70, pp. 1-30, 2015.
- [7] M. Kristo, D. Smith, S. Niemeyer, and G. Dudder, "Model action plan for nuclear forensics and nuclear attribution," *Lawrence Livermore National Laboratory.[2004]*. URL: <https://ereports-ext.llnl.gov/pdf/305453.pdf> (access date: 15.01. 2010), 2004.
- [8] M. Wallenius, K. Mayer, and I. Ray, "Nuclear forensic investigations: Two case studies," *Forensic Science International*, vol. 156, pp. 55-62, 1/6/ 2006.
- [9] C. Kamunda, M. Mathuthu, and M. Madhuku, "Assessment of Radiological Hazards from Gold Mine Tailings in Gauteng Province, South Africa.016, 13(1), 138; <http://dx.doi.org/>," *Int. J. Environ. Res. Public Health* vol. 13, pp. 138 -148, 2016.
- [10] S. G. Dlamini, M. Mathuthu, and V. M. Tshivhase, "Radionuclides and toxic elements transfer from the princess dump to water in Roodepoort, South Africa," *Journal of Environmental Radioactivity*, vol. 153 pp. 201-205, 2016.
- [11] E. Keegan, M. J. Kristo, M. Colella, M. Robel, R. Williams, R. Lindvall, *et al.*, "Nuclear forensic analysis of an unknown uranium ore concentrate sample seized in a criminal investigation in Australia," *Forensic Science International*, vol. 240 (2014) pp. 111–121, 2014.
- [12] O. Morton-Bermea, M. T. Rodríguez-Salazar, E. Hernández-Alvarez, M. E. García-Arreola, and R. Lozano-Santacruz, "Lead isotopes as tracers of anthropogenic pollution in urban topsoils of Mexico City," *Chemie der Erde - Geochemistry*, vol. 71, pp. 189-195, 5// 2011.
- [13] L. Balcaen, L. Moens, and F. Vanhaecke, "Determination of isotope ratios of metals (and metalloids) by means of inductively coupled plasma-mass spectrometry for provenancing purposes — A review," *Spectrochimica Acta Part B* vol. 65, pp. 769–786, 2010.

A Review of Gamma Cell 220 Research Irradiator External Dose Rates

Michael Shannon, Ryan Howell*, Spencer Mickum, Robert Rushton

Hopewell Designs, Inc. Alpharetta, GA.

Abstract. Historically, the radiation processing and high dose rate application sectors relied on research irradiators for calibration, characterization and other research activities. These systems were nominally self-contained devices capable of laboratory-based operations. A mainstay legacy irradiation system used internationally for high dose rate activities is the Gammacell 220 which is a self-contained, dry storage research irradiator developed in the late 1950s by Atomic Energy of Canada Limited. This system is capable of irradiating samples within a 20.47 cm tall by 15.49 cm diameter cylindrical chamber at Co-60 activities approaching 8.88E14Bq (nominally, 17.5 kGy/hr). The present work takes a fresh look at the external dose rates operators are exposed to during routine operations with the Gammacell 220. The study includes development of several high-fidelity Monte Carlo models utilizing the Los Alamos National Laboratory MCNP N-particle transport code (MCNP6). Several model and measurement cases were completed and compared to published work. This paper will review the legacy results and present the results of the current study.

KEYWORDS: *Gammacell 220; external dose rates; transient beam; MCNP6; dose uniformity ratio.*

1 INTRODUCTION

The traditional role of high dose rate irradiation systems is currently widening to support an expanding realm of research and development activities. Since a mainstay legacy irradiation system, the Gammacell 220, has been discontinued, the need exists for a turn-key solution to fill the role of this legacy system. Thus several performance parameters for the Gammacell 220 were investigated in order to provide direction for future developments in order to meet the needs of the high dose rate irradiation community. This article describes the developments underway by addressing the external dose rate levels around the irradiation system and examining the irradiation field parameters within the irradiation chamber of the Gammacell 220. High-fidelity Monte Carlo models utilizing the Los Alamos National Laboratory MCNP N-particle transport code (MCNP6) have been developed to investigate perturbations in the systems geometric orientations during routine operation. The centerline dose rate and dose uniformity ratio (DUR) within the 20.47 cm tall by 15.49 cm diameter cylindrical chamber for a source activity of 8.88E14 Bq, equally divided among 48 ⁶⁰Co pencil sources, have been determined through simulation and presented to optimize the visualization of dose to samples within the chamber.

2 METHODS

2.1 Configuration of Gammacell 220

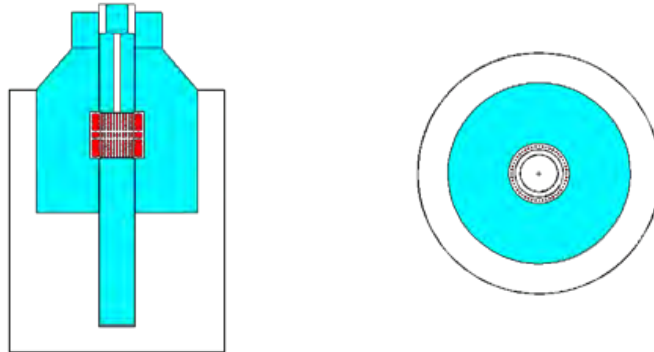
The Gammacell 220 high dose rate research irradiator was developed as the premier standalone irradiation system for maintaining optimal dose uniformity. Irradiation uniformity within the chamber is achieved by accommodating up to 48 double encapsulated ⁶⁰Co pencil gamma sources in a concentric ring around the irradiation chamber, as shown in Fig. 1. The sources are shielded from the operators by approximately six thousand pounds of lead providing 25.4 cm thick shielding [1]. An additional lead collar 16.51 cm deep is mounted on top of the main lead shield to provide shielding for the transient beam occurring when the relatively unshielded volume of the sample chamber moves through the main lead shield.

From the loading position at the top of the system, the inner plug and the top shielding drawer move vertically through the center of the main shield to align the irradiation chamber directly in the center of the source cage. Common practice for operation of the Gammacell 220 is to set a timer to delay the movement of this transition until the operators move away to a safe distance to avoid radiation dose from the transient beam. There is a sufficient transit dose delivered to the irradiation chamber during

* Presenting author, e-mail: ryan.howell@hopewell designs.com

this transition that can exceed 10% of the desired delivered dose, depending on exposure time and dose rate [2]. Additionally, due to the geometry of the system, the bottom of the chamber always receives a transient dose several times that seen at the top of the chamber.

Figure 1: The Gammacell 220 system is shown simulated in the MCNP software for (left) a vertical cross-section and (right) a horizontal cross-section at the source centerline with the ^{60}Co pencil gamma sources visible in a concentric ring around the irradiation chamber.



2.2 Monte Carlo Simulation

A parametric study was completed using Monte Carlo models of the Gammacell 220 design to determine the external dose rates in all possible geometric configurations. In order to quantify the ambient dose around the Gammacell 220, to examine the transient dose during operation, and to obtain the dose uniformity ratio within the irradiation chamber, the radiation transport code MCNP6 was used to develop several high-fidelity models of the irradiation system. Previous publications have found MCNP simulations to match experimental data with relative error of less than 3% [3, 4].

In this study, external measurements of the Gammacell 220 were compared with simulated results in order to validate the models. Then perturbations to the irradiation system were simulated in order to determine the expected radiation fields present surrounding the system during the vertical transition of the chamber. The simulations used weight windows [5] and the density reduction method [6] as the variance reduction techniques to minimize the relative error of the deep penetration radiation transport. Tally meshes with 1,000,000 voxels were placed across the simulation geometry in order to determine the dose rate in mSv/hr at all locations. Furthermore, mesh tallies were applied within the irradiation chamber allowing the determination of the dose uniformity profile and centerline dose rate.

3 EXTERNAL AND TRANSITION DOSE RATES

Discrete simulated measurement points around the Gammacell 220 geometry were analysed from the tally mesh results in order to reflect the realistic measurement results seen from moving an ion chamber at an interval of 24 equally spaced points around the geometry in the vertical and horizontal planes. As shown in Fig. 2, the dose rates in the polar plot on the left at 90° are associated with the dose rate directly on top of the Gammacell 220. The results in the horizontal plane in the polar plot on the right were taken through the center of the chamber and the midplane of the surrounding ^{60}Co sources. To simplify the model and simulation, the thin steel exterior shielding of the Gammacell 220 was modelled as a cylinder surrounding the main lead shielding and all simulated data points were averaged with the five surrounding nearest tally mesh values at a distance of 5 cm away from the external surface of the Gammacell 220 lead shielding.

This approach of simulating measurement points was mirrored after perturbing the geometry of the system to reflect the motion of the inner plug as the irradiation chamber is lowered into the irradiation position. As shown in Fig. 3, the radiation field dose rates are linearly scaled between the white areas representing radiation fields below 0.05 mSv/hr and the red areas representing fields greater than 0.5 mSv/hr. The corresponding polar plots of the dose rate are located directly below the radiation field map for each transition position.

Figure 2: The diagonal axis on the below polar plots show the dose rate in mSv/hr for simulated measurements with the chamber lowered in the irradiation position (left) in the vertical plane from one side of the system, over the top to the other side with the top of the system located at 90° and (right) in the horizontal plane around the circumference of the system at the centerline of the sources.

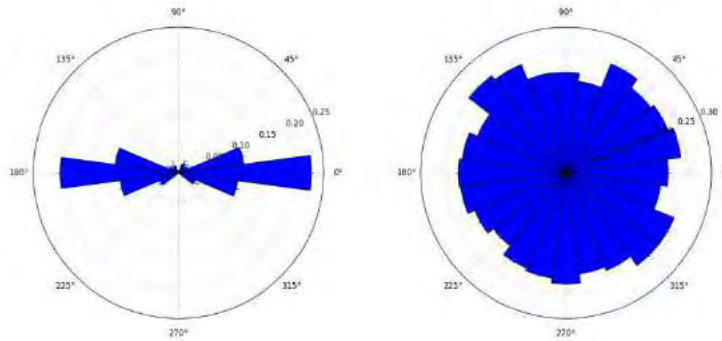
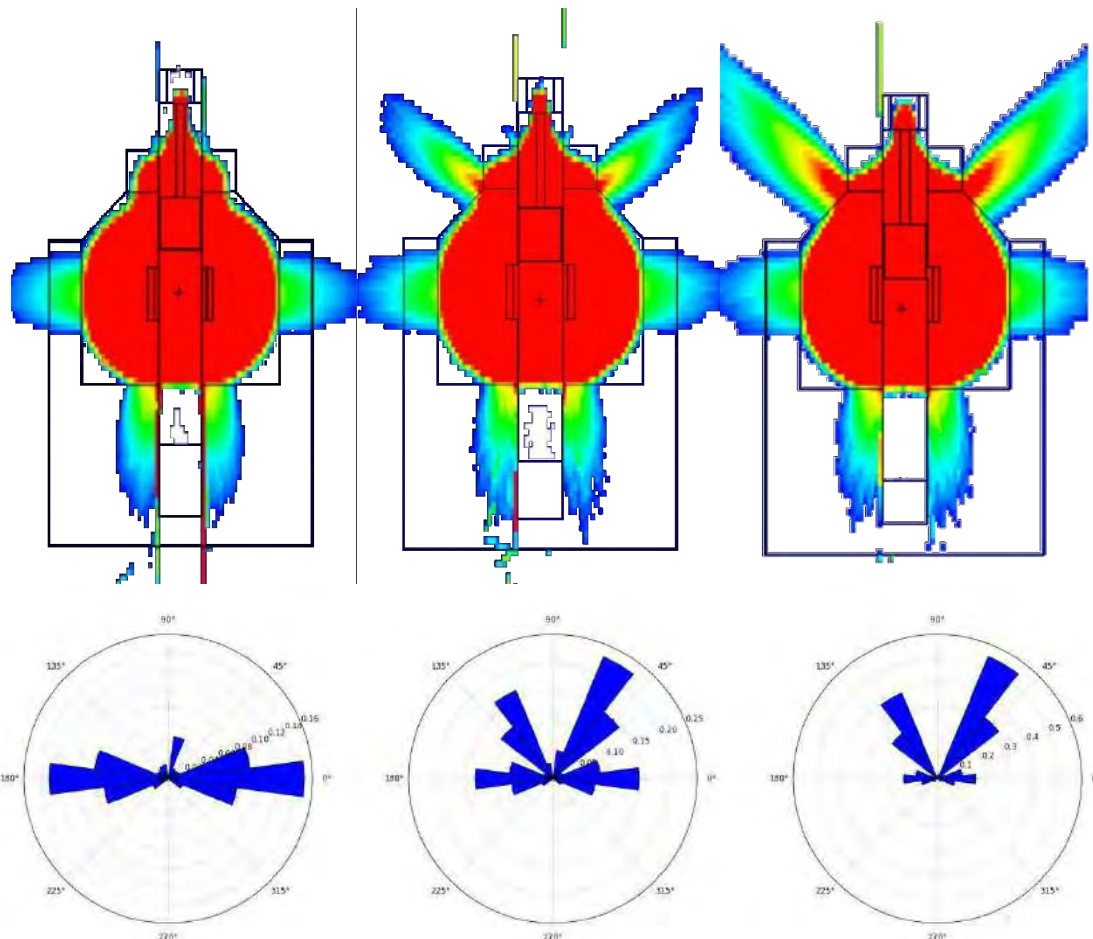


Figure 3: Vertical plane simulated dose rates in mSv/hr of the transition of the irradiation chamber, shown descending from left to right, as the chamber descends from the loading position towards irradiation position. Below each dose map is a corresponding polar plot of the simulated measurement.



During this transition, the dose rate surrounding the top region of the Gammacell 220 increases by more than 30 times, due to the transient beam of radiation passing through the relatively unshielded chamber as it descends towards the sources. While these levels are only raised during the transition of the chamber, the importance of the lead collar is highlighted by the large degree of radiation greater than 0.5 mSv/hr shown within the collar during the transition. Additionally, as the unshielded chamber displaces the inner plug inside the source cage, the dose rate around the circumference of the system increases from approximately 0.15 mSv/hr in the loading position to approximately 0.22 mSv/hr in the irradiation position due to the movement of the inner plug away from the sources.

4 INTERNAL DOSE RATES

The tally mesh results were configured to discretize the spatial radiation flux inside the irradiation chamber in order to determine the transition dose ratio, as shown on the left in Fig. 4. The transition dose ratio is defined as the centerline dose rate in the center of the chamber in the irradiation position relative to the current position as the chamber is moved from the irradiation position (transition position 1) to the loading position (transition position 10). On the right of Fig. 4, the transition dose ratio is shown to drop off slowly as the chamber is moved away from the sources. The chamber center is still receiving around 10% the maximum dose after it has moved half way along its transition away from the sources. Even though the timeframe for this transition can be less than 7 seconds [1], short irradiation periods can result in overdoses and add uncertainty to the overall dose delivered.

Figure 4: Analysis of the discretized radiation flux within the irradiation chamber (left) is used to calculate the transition dose ratio inside the chamber when moving from the irradiation position (1) to the loading position (10) (right).

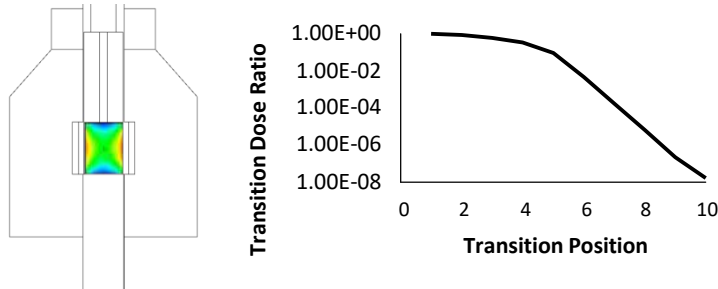
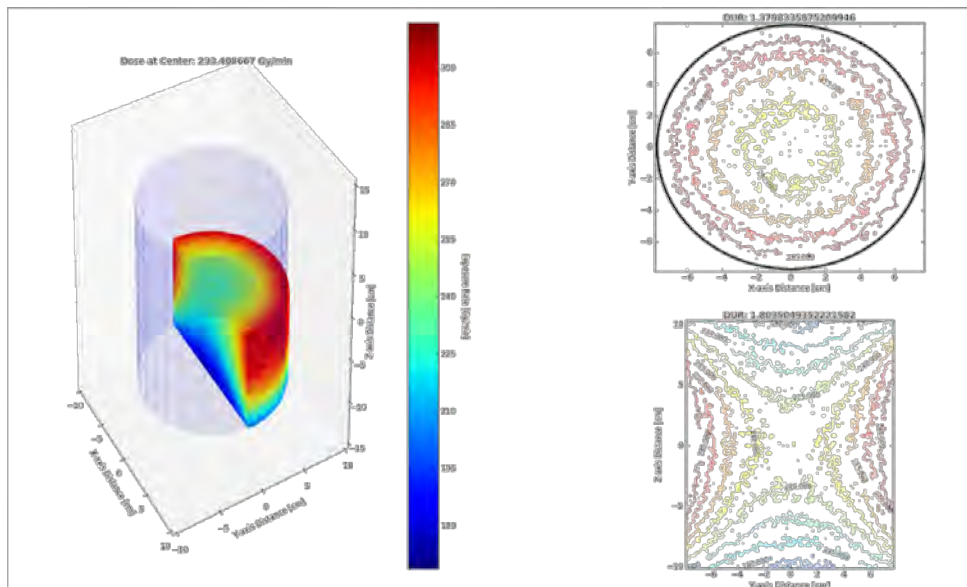


Figure 5: Dose uniformity ratios for the isodose profile of radius verses height (lower right) was determined to be 1.8 and the DUR for the horizontal plane within the irradiation chamber through the center of the sources (upper right) was 1.4. The centerline dose rate at the chamber center as shown in the 3D dose map (left) was determined to be 233.4 Gy/min.



The discretized mesh was analyzed to determine the dose uniformity ratio, the ratio of the highest dose in the chamber to the lowest dose, while in the irradiation position. Furthermore, the mesh analysis allowed for multiple orientations of the dose uniformity within the chamber to be visualized. By selectively isolating individual planes of the three-dimensional mesh, the isodose contour plot was generated for the Gammacell 220 showing contour lines of along the radius of the chamber with respect to the height of the chamber, as shown in the lower right side of Fig. 5.

Additional isodose profiles were generated including: a horizontal plane through the midsection of the sources, such as would be seen by a flat plate containing alanine pellets or a sheet of radiosensitive film, and a three-dimensional cross-section of the entire chamber with only the lower quadrant displayed so that the dose change as a function of each of the location parameters may be visualized. The DUR for the chamber was determined to be 1.8, and the DUR for the horizontal plane was determined to be 1.4. These dose maps assume the unlikely occurrence of equal activity in each of the 48 ^{60}Co sources to simplify the simulation design, so they serve to profile only optimal dose expectations within the irradiation chamber. The dose rate at the center of the chamber was determined by averaging the five closest voxels at the center of the chamber together to obtain 233.4 Gy/min.

5 CONCLUSIONS

Analysis of the results of the simulation of the Gammacell 220 with MCNP6 show the average external dose rate around the circumference of the system to be approximately 0.22 mSv/hr at 5 cm away from the surface while the chamber is located in the irradiation position. In the area surrounding the top of the system, the dose rate is seen to increase more than thirty times in magnitude during the transition between loading and irradiation positions, as shown in Fig. 3. This transient beam is concerning both from an operator dose perspective as well as the increased transition dose to the sample being irradiated, which is shown in Fig. 4 to drop off slowly as the chamber is moved away from the irradiation position. While in the irradiation position, the dose uniformity ratio with 48 equal activity ^{60}Co sources totaling $8.88\text{E}14$ Bq has been determined to be 1.8 with a centerline dose rate in the chamber center of 233.4 Gy/min.

6 REFERENCES

- [1] Instruction Manual Gammacell 220 Cobalt 60 Irradiation Unit, 1968. Atomic Energy of Canada Limited, Edition No. 6.
- [2] Christensen, R., Song, C-M., 1981. Magnitude and Position Dependence of Gammacell 220 Drawer Transit Doses, *Health Physics*, Vol. 41, No. 3 (September), pp. 527-533.
- [3] Rodrigues, R.R., Grynberg, S.E., Ferreira, A.V., et al., 2010. Retrieval of Gammacell 220 Irradiator Isodose Curves with MCNP Simulations and Experimental Measurements, *Brazilian Journal of Physics*, 40.1 pp. 120-124.
- [4] Hefne, J., 2000. The Dose Distribution Inside the Irradiation Chamber of the Gamma Cell 220 at KACST Using MCNP4B, *Journal of Nuclear Science and Technology*, Supplement 1, pp. 402-405.
- [5] T. Goorley, et al., 2012. "Initial MCNP6 Release Overview", *Nuclear Technology*, 180, pp. 298-315.
- [6] Sato, S., Nishitani, T., 2007. A study on variance reduction of Monte Carlo calculation with weight window generated by density reduction method, *J. Nucl. Sci. Technol.* Vol. 6, No. 1, pp. 5-9.

Interpretation of Data Collected During Individual Monitoring of Uranium Dioxide Exposure: Collective Dose Assessment

N. Blanchin^{a*}, E. Davesne^b, E. Blanchardon^b, E. Chojnacki^c, D. Franck^b, M. Ruffin^d

^aCEA, Service de Santé au Travail, 13115 Saint-Paul-Lez-Durance Cedex, France

^bIRSN, Laboratoire d'Evaluation de la Dose Interne, IRSN/PRP-HOM/SDI/LEDI, BP 17, 92262 Fontenay-aux-Roses Cedex, France

^cIRSN, Laboratoire Incertitude et Modélisation des Accidents de Refroidissement, IRSN/PSN- RES/SEMIA/LIMAR, BP 3, 13115 Saint-Paul-Lez-Durance Cedex, France

^dCEA, Laboratoire de Biologie Médicale, 13115 Saint-Paul-Lez-Durance Cedex, France

Abstract. Uranium is naturally present in diet, at highly variable levels, leading to detectable activity in excreta, independently from occupational exposure to uranium. The interpretation of bioassay data from individual routine monitoring of workers occupationally exposed to uranium dioxide must therefore take this dietary intake into account to estimate doses. To do so, the bioassay results of a group of workers exposed to UO₂ were compiled along with results of a control group. A Bayesian approach was developed to integrate the alimentary uranium excretion in the calculation of the committed effective dose distribution for the group of workers. Significant differences between the exposed and control populations were found establishing an occupational contamination of the exposed group of workers. Because the variability of uranium alimentary excretion estimated from the control group is high and leads to unreliable individual dose assessment, a collective dosimetric approach was chosen using the Bayesian method to derive best estimate and dose distribution in the worker population.

Declaration of interest

The authors report no conflicts of interest.

KEYWORDS: *Uranium; variability; alimentary intake; internal dosimetry.*

1 INTRODUCTION

During the preparation of nuclear fuel, workers may inhale aerosols of uranium dioxide (UO₂). The monitoring for intakes is usually based on measurement of urine and/or feces samples. However, uranium is naturally present in food and drinking water. Consequently, detectable amounts of natural uranium can be measured in bioassay by modern techniques even in the absence of occupational exposure. Uranium concentration in excreta from dietary intake varies strongly depending on living location and diet (ICRP, 1975, UNSCEAR, 2000, Castellani et al, 2013). For a person occupationally exposed to uranium, bioassays quantify uranium concentration from alimentary intakes to which an occupational contribution may be added. Therefore, to determine if a worker is contaminated by uranium can be very difficult from the bioassay result.

For workplace radiation protection, it is important to differentiate between the dietary background and professional intakes in the interpretation of bioassay measurement of uranium. Castellani and others in the 2nd version of the report “General Guidelines for the Estimation of Committed Effective Dose from Incorporation Monitoring Data (IDEAS guidelines) recommend the use of blank bioassay data obtained prior to the effective work in potentially contaminating area. These blank bioassay samples can be obtained from the worker before or at the beginning of their employment, from non-occupationally exposed workers or from the population living in the area, including some members of the worker's family (Castellani et al, 2013).

Besides these recommendations, different approaches to determine the committed effective dose

resulting from an occupational intake by distinguishing the uranium activity in excreta coming from the diet from the one generated by the occupational contamination are possible:

1. to subtract from the measured activity a reference value of activity coming from the dietary intake determined for the individual,
2. to subtract from the measured activity a mean value of activity coming from the dietary intake determined for an unexposed population,
3. to compare one group of workers exposed to uranium contamination with a group not exposed in order to highlight a significant difference between them,
4. to estimate an annual collective dose if a contamination was highlighted by the precedent approach.

Therefore, the aim of this study is to test the different possible approaches to determine the committed effective dose resulting from an occupational intake by distinguishing the uranium activity in excreta coming from the diet from the one generated by the occupational contamination.

First, the bioassay results of this population were compared with a control population to possibly highlight differences. Then, the individual variability of the bioassay results was estimated for a group of worker not occupationally contaminated by uranium. Finally, an innovative method was developed to determine the committed effective dose received for the group of exposed workers along with its uncertainty.

2 MATERIALS AND METHODS

2.1 Exposed group of workers

The studied group of workers occupationally exposed to uranium is formed by the operators of a unit handling the preparation of UO₂ fuel for nuclear-powered boats/submarines. The follow-up of occupational exposures rely on ambient air monitoring by the use of static air samplers (Cérat, 1994) and on individual monitoring. The individual monitoring routine program of UO₂ exposure follows the recommendations of the ISO 20553 standard of the International Organization for Standardization (ISO) (ISO, 2006) by carrying twice-yearly feces analyses and three-monthly urine analyses. Since 2003, no contamination leading to dose higher than 1 mSv was detected for the studied group of workers.

In case of low exposure, the isotopic composition of low enriched uranium handled in this facility does not help to identify a possible occupational contamination: the increase of excreted activity due to occupational exposure does not significantly modify the isotopic ratio $^{234}\text{U} / ^{238}\text{U}$ which varies naturally between 1 and 5.6 (Remy et Lemaitre, 1990).

In order to allow a statistical interpretation, a bioassay data base of the 474 urine and 274 feces analyses of the exposed population was constituted from the monitoring done between 2004 and 2011. For this population, the detection limits were quantified by the laboratory of medical analyses for each uranium isotope using the method presented by Vivier *et al* (2010). The detection limits vary between 0.1 and 3 mBq for the 3 isotopes in urine and between 0.1 and 9 mBq in feces.

2.2 Selecting a control population

In order to interpret the analysis results for the exposed population in integrating alimentary intake of uranium, to gather reference values of diet uranium excretion was crucial. Therefore, a control population not occupationally contaminated by uranium was selected. This population was formed by workers handling the preparation of Mixed Oxides (MOX) fuel. The MOX powder is a mixture of depleted UO₂ (95.3 % in weight) and plutonium dioxide (PuO₂, 4.7 % in weight) (Ramounet *et al*, 1998) characterized by a plutonium activity higher than 100 times the uranium activity. This group belonging to the same facility as the exposed population, is monitored by the same laboratory of medical analyses through twice-yearly urine analyses until 2001 and through twice-yearly urine and feces analyses since 2002 (Blanchin *et al*, 2005).

As this population is also exposed to UO_2 , it was necessary to be sure that the uranium bioassay was not reflecting an occupational contamination. Therefore, the bioassay for this population was checked very cautiously and some results were excluded of this study:

- Since theoretical fecal excretion for 1 Bq of UO_2 and PuO_2 are almost identical (ICRP, 1997), if plutonium activity measured in the sample is below the detection limit, a MOX contamination is very unlikely and the uranium activity quantified in the same sample most probably comes from diet. Moreover, the follow-up of actual inhalation of MOX powder, the registered uranium activities stay at their usual level even when the plutonium activity was higher than detection limit. Therefore, all fecal analyses of uranium where plutonium activity is below detection limit were integrated in the data base for the control population.
- Concerning urine analyses, a MOX inhalation would generate almost the same activity in urine for plutonium and uranium because theoretical uranium urinary excretion is around 100 times as much as plutonium excretion (ICRP, 1997). Therefore, the only integrated data were routine analyses of uranium for which the plutonium activity was below detection limit.

The bioassay data base for the control population contains 201 urine and 842 feces results obtained between 2001 and 2010 for urine analyses and between 2002 and 2010 for feces. In this study, the data of interest are the analysis results and not their interpretation integrating measurement uncertainties. Therefore, all results below detection limit for the two data bases were transcript as below decision level instead (ISO, 2000).

3 RESULTS

3.1 Comparison of the two populations

In a first time, the percentage of urine measurement results above detection limit was calculated for each control or exposed population. 11 % of the measurement results are higher than the limit of detection for the control population compared to 21 % for the exposed population. This difference is significant ($P < 0.001$).

To comfort if a significant statistical difference exists between the control and the exposed populations, the following data for each population were compared using a statistical Wilcoxon test:

- Fecal measurement results for ^{234}U , ^{238}U and ^{235}U ,
- Urine measurement results for ^{234}U and ^{238}U ,
- Isotopic ratio $^{234}\text{U}/^{238}\text{U}$ for urine and feces measurement results.

For this comparison, only the results above detection limit are used. As only one ^{235}U urine measurement is higher than the limit, no information was obtained from urine analysis of this isotope. From the analysis of the feces measurement results, a significant difference can be highlighted for ^{234}U and ^{238}U ($P = 9.10^{-7}$ for ^{234}U and $P = 0.08$ for ^{238}U). For other result analysis, no difference was identified ($P = 0.3$ for ^{234}U in urine, $P = 0.4$ for ^{238}U in urine, $P = 0.3$ for ^{235}U in feces). The low number of measurement results higher than the limit of detection can explain these results. The comparison of the isotopic ratios determined for the two populations supports even more the conclusion of a significant difference between the population ($P = 0$).

3.2 Reliability of individual bioassay

The variability of uranium excreted activities for the control population was estimated: the standard deviation of the feces and urine measurement results are very high: 52 mBq for ^{234}U , 27 mBq for ^{238}U and 4.6 mBq de ^{235}U in feces, 2.7 mBq for ^{234}U et 3.7 mBq for ^{238}U in urine. These values must be compared with the mean values of 41 mBq for ^{234}U , 28 mBq for ^{238}U and 2.8 mBq for ^{235}U in feces, and 1.7 mBq for ^{234}U , 2.0 mBq for ^{238}U in urine.

Concerning individual variability of alimentary uranium excretion, the standard deviation of the available measurement results was calculated for each person of the control population for whom at least two analyses were made. Their values are gathered and presented as an empirical cumulative probability distribution to identify easily the median and extreme values of standard deviation.

The mean individual standard deviation obtained for feces analysis of ^{234}U is equal to 30 mBq, to be compared with a mean alimentary fecal excretion of 40 mBq. This variability already important can reach 530 mBq for one of the control worker and 10 % of the individuals of the control population have an individual standard deviation higher than 50 mBq. The individual relative standard deviations vary between 16 and 76 % for urine analysis and between 6 and 217 % for feces. Similar results were obtained for the two other isotopes.

3.3 Appropriateness of collective dosimetry

As a significant difference was found from the population comparison and as the only plausible difference between the two groups is the exposure, it could be concluded that the exposed group of workers is occupationally contaminated by uranium. This contamination should be quantified by a dose estimation.

To use bioassay to assess individual dose, a reference value of alimentary uranium excretion must be used and subtracted to the individual bioassay results. This reference value must be precise and accurate to avoid over and under-estimation of intake and of dose. It can be either the mean value of excreted uranium activities measured for unexposed persons or a point estimate of the alimentary excretion of uranium for an individual based on a measurement made before any occupational uranium exposure. However, the use of these reference values is conditioned on the low variability of the excreted activities among a control population, for the first one, and of the individual for the second. From the results presented here, it can be concluded that the variability of alimentary excretion is really important. Therefore, the reliability of the individual bioassay is not sufficient to use them to estimate dose when their value is close to the alimentary uranium excretion. That is why, the risk of over- or underestimation of the dose for an individual is too high to be taken an individual dose assessment.

Hence, a collective approach was chosen to evaluate the dose for this group of workers. This dose assessment will be used for the optimization of the industrial process and of the worker exposure. It will not provide information on individual risk estimate but as the bioassay results of the exposed population cannot be differenced easily from the results of a control population, this risk is likely to be small. The intake and dose estimates confirm the use of collective dose estimation because such low intake cannot be discriminated, at an individual level, from alimentary excretion. The collective dose can be derived from the mean dose by multiplying it by the number of exposed workers.

The probability distributions of intake and dose model the variability of the intake and dose for the whole group of workers. As the intervals between the 5th and the 95th percentiles of these distributions are small, it can be concluded that this collective dose estimate is reliable and a lot more than an individual estimate. Though this method is well suitable for low exposure, in case of high exposure, an individual dose estimate should be preferred at least to determine which workplace is responsible of this contamination.

4 ASSESSMENT OF THE COLLECTIVE DOSE AND ITS ASSOCIATED UNCERTAINTY

4.1 Biokinetic model

To estimate the committed effective dose for the workers exposed to uranium, the possible contamination could occur as a chronic or acute UO_2 inhalation. Considering the time constancy of the process of fuel preparation and the absence of abnormal condition identified by the ambient monitoring, a chronic contamination seems more realistic. However, to assume an acute contamination allows, through a conservative dose estimation, to quantify the influence of the hypothesis on the time

of exposure. Therefore, two scenarii of contamination were used to assess the dose: either an acute contamination at the middle of the monitoring interval of urine analysis (ICRP, 1997) corresponding to 45 days before the measurement, or, a chronic contamination during the whole monitoring interval of 90 days.

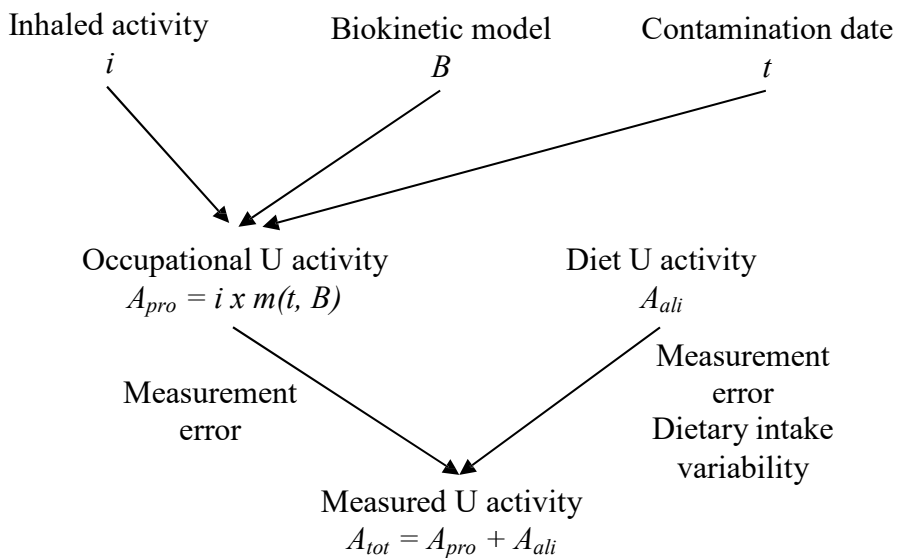
The biokinetic model used is composed of uranium systemic model (ICRP, 1995), gastro-intestinal tract model (ICRP, 1979) and respiratory tract model (ICRP, 1994) of the International Commission on Radiological Protection (ICRP).

The dose coefficients and excretion functions from these models were calculated using Integrated Modules for Bioassay Analysis (IMBA) software (Birchall *et al*, 2007) with reference default values for particle size (Activity Median Aerodynamic Diameter, AMAD = 5 μm; geometric standard deviation, $\sigma_{g\ AMAD} = 2.5$; (ICRP, 1994)). A review allowed determining median absorption parameters for UO₂ (Davesne *et al*, 2014):

- Fraction of deposited activity rapidly dissolved: $f_r = 2.2 \cdot 10^{-2}$;
- Fast dissolution rate: $s_r = 1\ d^{-1}$;
- Slow dissolution rate: $s_s = 5.9 \cdot 10^{-4}\ d^{-1}$;
- Fraction of ingested activity absorbed from guts: $f_A = 4.4 \cdot 10^{-4}$.

4.2 Estimation of mean incorporation, dose and their associated uncertainty

Figure 1: Relationship between inhaled activity and bioassay results



The assessment of the mean intake is done by assuming that all workers have the same exposure. Consequently, the whole bioassay data base of results higher than or below the limit of detection is used to estimate the intake corresponding of the exposure of the group of workers.

The method presented here estimates the likelihood of the mean intake knowing the bioassay results. The inhaled activity activity i is linked to the database A_{tot} of total uranium activity (from diet and occupational activity) A_{to}^j measured in urine and feces for each individual j and for each uranium isotope (Figure 1). However, the uranium activity quantified in bioassay samples A_{tot} is the sum of uranium activities coming from diet A_{ali} and from occupational exposure A_{pro} . For the biokinetic model B and the contamination time t , the uranium activity in bioassay sample coming from occupational activity, A_{pro} , is linked to the inhaled activity i by:

$$A_{pro} = i \times m(B, t)$$

where m is the excretion function. A_{ali} and A_{pro} are subject to inter-individual variability and to measurement uncertainty. To estimate i , these sources of variability must be considered.

In agreement with the version 2 of IDEAS guidelines (Castellani et al, 2013), the uncertainty on urine and feces measurements A_{pro} is assumed to be lognormal with a geometric standard deviation of 1.6 for urine and 3 for feces. These standard deviations are referred as scattering factors (SF). The variability of activity of uranium measured in excreta and coming from diet was fitted using the bioassay results of the control population.

The inhaled activity i the most probable considering the whole database of bioassay results of the exposed population for one isotope was estimated using a maximum likelihood method. The likelihood is the probability to observe the analysis results knowing the biokinetic parameters, the intake and the variability of uranium excretion from diet and occupational exposure and from measurement errors.

This most probable inhaled activity is determined by considering that all the bioassay measurements were made at the end of a monitoring interval of 90 days. To estimate the committed effective dose from the intake of one isotope during one term is done by multiplying the most probable intake by the corresponding dose coefficient. The annual mean committed effective dose is calculated by summing the dose for each isotope and by multiplying this sum by 4 for the 4 terms. This method is particularly conservative because it assumes that all monitoring intervals are independent and does not interact. This is not true because a contamination from a previous intake will lead to measure activity at the next routine measurement.

4.3 Mean intake and dose and their associated uncertainties

By applying the method developed for this study, the probability distributions of the intake and of the dose corresponding to the exposure of the exposed group of workers were calculated. The total median intake is the sum of the median intakes determined for ^{234}U , ^{238}U and ^{235}U : it is equal to 14 Bq for an acute contamination and to 4.7 Bq for a chronic contamination. The total median dose calculated using specific dose coefficients for each isotope is equal to 70 μSv for an acute contamination and 23 μSv for a chronic contamination.

5 CONCLUSION

The aim of this study was to interpret bioassay measurement results obtained by a routine monitoring of UO_2 exposure. A general method was built from these data by comparing the results of an exposed population with the one of a control population. The data gathered for the control population were used to model the alimentary uranium excretion for a group of workers not occupationally contaminated. The variabilities of this excretion for the whole population and for each individual were quantified. They are very important, prohibiting the use of reference values of alimentary excretion to derive dose estimate from a bioassay measurement of an exposed person. The risk of over or underestimation of the dose from an individual bioassay measurement is too large to be taken. As individual interpretation of bioassay is not reliable, a new approach was developed to assess the mean dose received by the exposed workers.

First, the bioassay data of the two populations were compared by a Wilcoxon test. A significant difference was found, suggesting a contamination of the exposed group of workers. Then, a method integrating the different sources of uncertainty and measurement errors allows to estimate the mean intake and dose the most likely and their corresponding variability for the exposed group of workers. The developed method is easily implemented in Excel® for example and can be used for any workplace and exposures as soon as a reliable control population can be provided.

6 REFERENCES

- [1] Birchall A, Puncher M, Marsh JW, Davis K, Bailey MR, Jarvis NS, Peach AD, Dorrian MD, James AC 2007. IMBA Professional Plus: a flexible approach to internal dosimetry. *Radiat Prot Dosimetry* 125(1-4): 194-7.
- [2] Blanchin N, Fottorino R, Grappin L, Guillermin A, Lafon P, Miele A, Ruffin M 2005. Surveillance systématique des expositions aux transuraniens par les analyses radiotoxicologiques des selles. *Radioprotection* 40(2): 231-243.
- [3] Castellani CM, Marsh JW, Hurtgen C, Blanchardon E, Berard P, Giussani A, Lopez MA 2013. IDEAS Guidelines (Version 2) for the Estimation of Committed Doses from Incorporation Monitoring Data EURADOS Report 2013-01.
- [4] Cérat D 1994. EDGAR, retour d'expérience. *Techniques de mesures et de protection* 4: 11-33.
- [5] Davesne E, Blanchardon E 2014. Physico-chemical characteristics of uranium compounds: a review. *Int J Radiat Biol.* 90: 975-988; 2014.
- [6] ICRP (International Commission on Radiological Protection) 1975. Report of the task group on reference man. ICRP Publication 23, Oxford: Pergamon Press.
- [7] ICRP (International Commission on Radiological Protection) 1979. Limits for intake of radionuclides by workers. ICRP Publication 30, Part 1, *Annals of the ICRP* 2(3/4) Oxford: Pergamon Press.
- [8] ICRP (International Commission on Radiological Protection) 1994. Human respiratory tract model for radiological protection. ICRP Publication 66, *Annals of the ICRP* 24(1-3) Oxford: Elsevier Science Ltd.
- [9] ICRP (International Commission on Radiological Protection) 1995. Age-dependent doses to member of the public from intake of radionuclides: Part 3 Ingestion dose coefficients. ICRP Publication 69, *Annals of the ICRP* 25(1) Oxford: Elsevier Science Ltd.
- [10] ICRP (International Commission on Radiological Protection) 1997. Individual monitoring for internal exposure of workers. ICRP Publication 78, *Annals of the ICRP* 27(3/4) Oxford: Elsevier Science Ltd.
- [11] ISO (Standardization International Organization) 2000. Determination of the detection limit and decision threshold for ionizing radiation measurements -- Part 1: Fundamentals and application to counting measurements without the influence of sample treatment. ISO 11929-1:2000.
- [12] ISO (Standardization International Organization) 2006. Radiation protection - Monitoring of workers occupationally exposed to a risk of internal contamination with radioactive material. ISO 20553:2006(E).
- [13] Klein JP, Moeschberger ML 2005. *Survival Analysis: Techniques for Censored and Truncated Data*. New-York, Springer.
- [14] Ramounet B, Verry M, Grillon G, Rateau G, Matton S, Fritsch P 1998. Biokinetics of Pu and Am after inhalation of industrial (U, Pu)O₂ and PuO₂ in the rat: preliminary results. *Radiation Protection Dosimetry* 79: 53-56.
- [15] Remy ML, Lemaitre N 1990. Eaux minérales et radioactivité. *Hydrogeol. Inz. Geol.* 4: 267-278.
- [16] UNSCEAR 2000. Sources and Effects of Ionizing Radiation, Report of the general Assembly with Scientific Annexes, Volume I: Sources. New-York, United Nations.
- [17] Vivier A, Fottorino R, Rousse B 2010. Threshold decision and detection limit: Determination, interpretation and optimization. 2nd part: Application to the urinary uranium alpha spectra, Seuil de décision et limite de détection: estimation, interprétation et optimisation. 2e partie: application aux spectres alpha uranium urinaire. *Radioprotection* 45(3): 345-357.

Monte Carlo analyses for BNCT using near-threshold ${}^7\text{Li}(p,n)$ neutrons Radiation source, shielding, activation, and external exposure

Noriaki Nakao^{a*}, Kazuaki Kosako^a, Noriyosu Hayashizaki^b, Tatsuya Katabuchi^b,
Tooru Kobayashi^{c#}

^aInstitute of Technology, Shimizu Corporation, Koto-ku, Tokyo, Japan.

^bResearch Laboratory for Nuclear Reactor, Tokyo Institute of Technology, Tokyo, Japan.

^cMax Medical Co. Ltd., Yodogawa-ku, Osaka, Japan.

[#]Former institution: Kyoto University Research Reactor Institute, Osaka, Japan.

Abstract. Monte Carlo analyses of shielding, activation, and external exposure were performed using the MCNP5 code for boron neutron capture therapy (BNCT) using the near-threshold ${}^7\text{Li}(p,n)$ neutrons. Neutron and photon radiation sources generated by 1.92-MeV protons at 10 mA were transported through the optimized BNCT target-moderator system and the therapy room. Attenuation profiles of the radiation level in the room and in the shielding walls were obtained. Using the neutron distribution, the residual radioactivity in the components of the target-moderator system and the shielding walls was estimated by the DCHAIN-SP2001 code. The residual radiation distribution in the whole room was also estimated with the thus-obtained residual activities by photon-transport simulation using the MCNP5 code. External exposure of a normal human body during irradiation was also estimated using the MIRD5 computational human phantom. Obtained absorbed doses for organs and tissues by neutrons and photons were converted into units of biological absorbed dose (RBE dose). Finally, the whole-body external exposure of the RBE dose was estimated by using the tissue-weighting factors recommended by ICRP2007 (Pub. 103).

KEYWORDS: *Monte Carlo; shielding; activation; external exposure; BNCT; near-threshold; ${}^7\text{Li}(p,n)$; MCNP; DCHAIN-SP; MIRD; RBE.*

1 INTRODUCTION

Boron neutron capture therapy (BNCT) is a form of radiation cancer therapy that destroys cancer cells using heavy charged particles namely, ${}^4\text{He}$ and ${}^7\text{Li}$ generated by a ${}^{10}\text{B}(n,\alpha){}^7\text{Li}$ reaction with a neutron irradiation. Cancer cells can be selectively destroyed in this therapy since the boron-doped pharmaceutical that is injected into the patient body has characteristics to be accumulated to the cancer cells.

Recently, accelerator-based neutron irradiation systems for BNCT have been widely under development. The threshold of ${}^7\text{Li}(p,n){}^7\text{Be}$ reaction is 1.88 MeV, and near-threshold reactions directly provide epithermal neutrons without complicated or massive moderator systems. To obtain a sufficiently high epithermal neutron intensity, an incident proton intensity of several tens of kilowatts on the lithium target is needed for practical effective therapy. To avoid damage to a solid lithium target, a stable liquid-lithium jet flow has been established instead as the neutron-producing target [1]. Parameters such as the effective thickness of the components around the target system were considered in the optimization [2]. A proton energy of 1.92 MeV was employed on the basis of the optimization analysis for the near-threshold neutrons, and a Gaussian distribution with a 0.02-MeV standard deviation (σ) was assumed for the practical proton beam-energy fluctuation in the case of a radio-frequency quadrupole (RFQ) linear accelerator [2].

For the practical use of near-threshold neutrons for BNCT therapy, spatial radiation distributions around the target and the whole facility during and after the beam operation should be estimated for effective design of the building's shielding structure. When neutron irradiation is used to treat cancer, a potential secondary cancer caused by radiation exposure to normal cells is an inevitable concern. Therefore, the exposure of the normal cells of the whole body during the irradiation should also be estimated. In this study, radiation-transport simulations using the MCNP5 Monte Carlo code [3] were

*Presenting author, e-mail: noriaki.nakao@shimz.co.jp

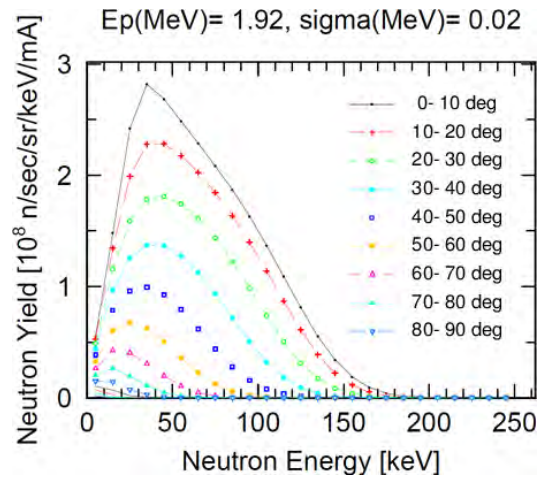
conducted to estimate the spatial distributions of neutrons and photons. In the MCNP simulation, the neutron cross-section library of FSXLIB-J40 [4] (which is based on the JENDL-4.0 library [5]) and the photon library MCPLIB04 [6] were used. Based on the results thus obtained, shielding, activation, and the external exposure were studied in the BNCT facility with near-threshold neutrons.

2 NEUTRON AND PHOTON SOURCES

The angular and energy distributions of neutrons yielded by the ${}^7\text{Li}(p,n){}^7\text{Be}$ reaction in a thick, natural lithium target with near-threshold energy were evaluated by Lee et al. [7]. The computational LIYIELD code [7], which was also developed by Lee et al., was used in this work for the neutron yield estimation for a proton energy of 1.92 MeV with a 0.02-MeV standard deviation. The calculated angular distribution of the neutron energy spectrum is shown in Fig. 1.

Photons generated from ${}^7\text{Li}$ by protons of energies below 1.92 MeV were taken into account in this study. The 0.478-MeV photons were generated from the ${}^7\text{Li}(p,p'\gamma)$ reaction and its yield was estimated by the equation reported by Kiss et al. [8]. Photons with energies of 14.7 and 17.64 MeV were emitted from primary transitions to the first excited and ground states of ${}^8\text{Be}$, respectively. The reaction mainly occurred through a resonance at a proton energy of 0.411 MeV. The thick target photon yield from this reaction at an incident proton energy of 1.92 MeV was estimated to be 3.1×10^{10} ($\gamma/\text{mA}/\text{min}$), based on cross-section data measured by Zahnow et al. [9]. Only the higher-energy photons of 17.64 MeV from the ${}^7\text{Li}(p,\gamma){}^8\text{Be}$ reaction were included in this calculation, since the branching ratios of the two transitions were unknown. Isotropic angular distributions were assumed for 0.478- and 17.64-MeV photons. The photons from the proton-capture reaction with ${}^6\text{Li}$, whose natural abundance is 7.5%, were neglected since the cross-section is ~ 0.002 mb, which is much smaller than those of the ${}^7\text{Li}(p,p'\gamma)$ and ${}^7\text{Li}(p,\gamma)$ reactions.

Figure 1: Angular and energy distributions of neutrons generated by the ${}^7\text{Li}(p,n)$ reaction with an incident proton energy of 1.92 MeV and a standard deviation of 0.02 MeV. The data for angles above 90 degrees, which are also shown in the figure, were negligible.



3 TARGET AND SURROUNDINGS

Fig. 2 shows the vertical cross-sections of the simulation geometry of the target system as well as the upper- and lower-loop tubes of liquid-lithium and the proton-beam duct through the wall. The liquid-lithium jet-flow was sprayed from the upper exit of the loop tube, forming a 0.5-mm-thick film on the curved surface of a 2-mm-thick stainless-steel plate. Insulators, a 30-mm-thick lead shield, and a 24-mm-thick polyethylene bolus were then formed on this layer based on the optimization design of the target system [2]. The loop tubes were covered with the 50-mm-thick lead shields to reduce the residual radiation level after the beam operation due to the activation of the stainless-steel tubes.

Although it was not taken into account in the simulation, a 30-mm-diameter proton beam was assumed to be horizontally transported through the beam duct and irradiated on the surface of the liquid-lithium target. Therefore, the source neutrons and photons described in the previous section were emitted from a 30-mm-diameter area of the proton-incident surface of the lithium target.

4 SHIELDING DESIGN AND PROMPT RADIATION

Fig. 3 shows the shielding structure of the accelerator and therapy rooms in the BNCT facility, which was used as the simulation geometry in a vertical plane parallel to the beam line. This layout was temporarily designed for the BNCT test facility, which was assumed to be built inside the existing building and to be decommissioned easily after the test period. The shielding materials from the inside of the room were a 10-cm-thick layer of undoped polyethylene, a 10-cm-thick layer of boron-doped polyethylene, and a 40-cm-thick layer of iron (80-cm thick at the downstream). These materials were used to attenuate epithermal neutrons, thermal neutrons, and photons, respectively. The thicknesses of the shielding materials were tentatively selected to be thicker to estimate the optimal thicknesses observing the attenuations of various components of the radiation. To obtain good statistics on the Monte Carlo transport simulation of neutrons and photons in the thick shielding, the importance method was used as the optional variance-reduction technique.

Since accelerator-related equipment such as magnets may be located in the wall between the two rooms, a 20-cm (horizontal) by 50-cm (vertical) opening was cut out into the iron shielding on the beam-line level. The floor of the facility was made of concrete. A 10-cm-thick boron-doped polyethylene layer was placed over the entire floor to prevent leaking of neutrons. Moreover, the iron shielding materials on the exterior walls were positioned as much as 20 cm below the floor level to prevent leaking of secondary photons through the concrete floor.

Figure 2: Vertical cross-sectional views of the simulation geometries for the liquid-lithium film and surroundings (left) and its flow loop with surrounding materials (right).

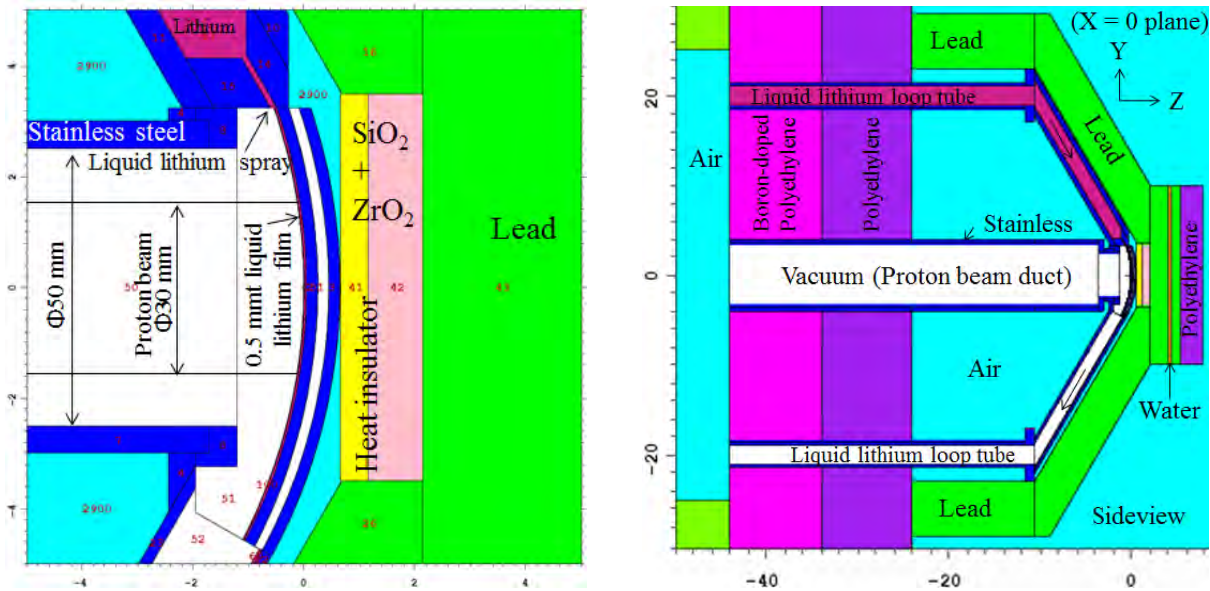


Figure 3: Simulation geometry for the shielding structure of the facility in the vertical plane parallel to the beam line.

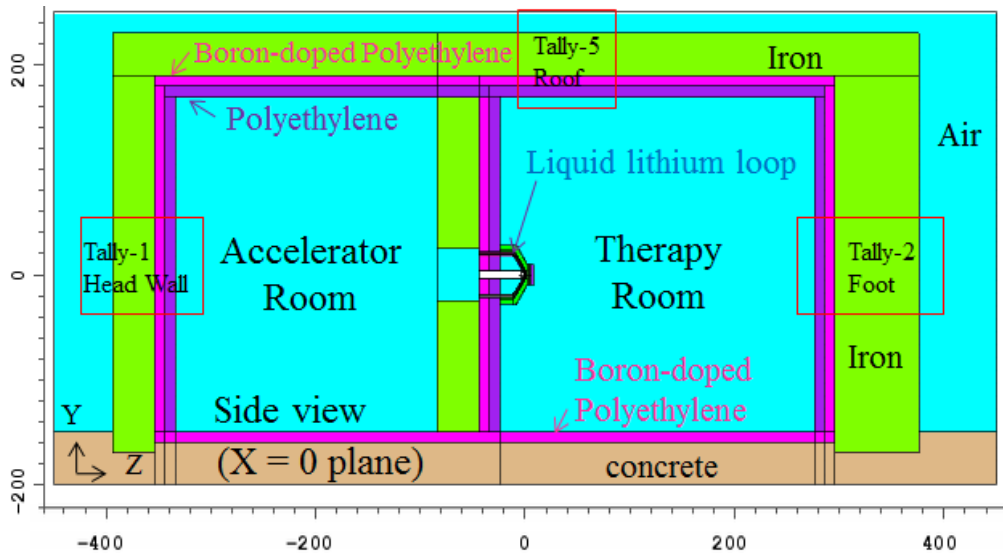


Fig. 4 shows the simulation result of the two-dimensional spatial radiation distributions for neutrons and photons inside and outside of the shield during operation, expressed as an effective dose rate in the unit of $\mu\text{Sv/h}$. Fig. 5 shows the one-dimensional attenuation profiles of the dose rate for various components downstream of the shield wall. The epithermal and thermal attenuations of two types of neutron dose are shown separately, together with the sum of their doses (Total-n) with a boundary energy of 0.25 eV. The photons from neutron-capture (n, γ) reaction and the 0.478- and 17.64-MeV photons from the lithium target as well as the sum of their doses (Total- γ) are also shown in the figure.

Epithermal neutrons are attenuated by about seven orders of magnitude by the 20-cm-thick polyethylene (including 10 cm of boron-doped polyethylene). Thermal neutrons are attenuated by about one and about six orders of magnitude by the undoped and doped polyethylene, respectively. The contributions of the 0.478- and 17.64 MeV photons are negligible compared with those of the neutron-capture photons. These photons are attenuated by about five orders of magnitude through the 40-cm-thick iron.

The dose regulation at the boundary of the radiation-controlled area, 1.3 mSv in 3 months, corresponds to about $2.6 \mu\text{Sv/h}$, assuming a beam-operation period of 500 h over this period. For reference, the $1.0 \mu\text{Sv/h}$ level is shown with the dotted line in the figure. The optimal shielding thickness and materials can be evaluated using the thus-obtained dose-attenuation profiles. Shielding design in actual future facilities should consider the leakage through the shield doors, mazes, and beam-transport ducts.

As shown in Fig. 4, the neutron leakage through the concrete floor to outside the room was lower than the regulated maximum because boron-doped polyethylene was placed on the floor. Moreover, owing to the exterior iron shield placed 20 cm below the floor level, the photon dose rate outside at the floor level was suppressed and was sufficiently lower than regulation.

Figure 4: Simulated two-dimensional spatial distribution of the effective dose rates in the vertical plane for neutrons (upper) and photons (lower) during operation. This figure has been plotted by the graphic tool ANGEL included in the PHITS package [10].

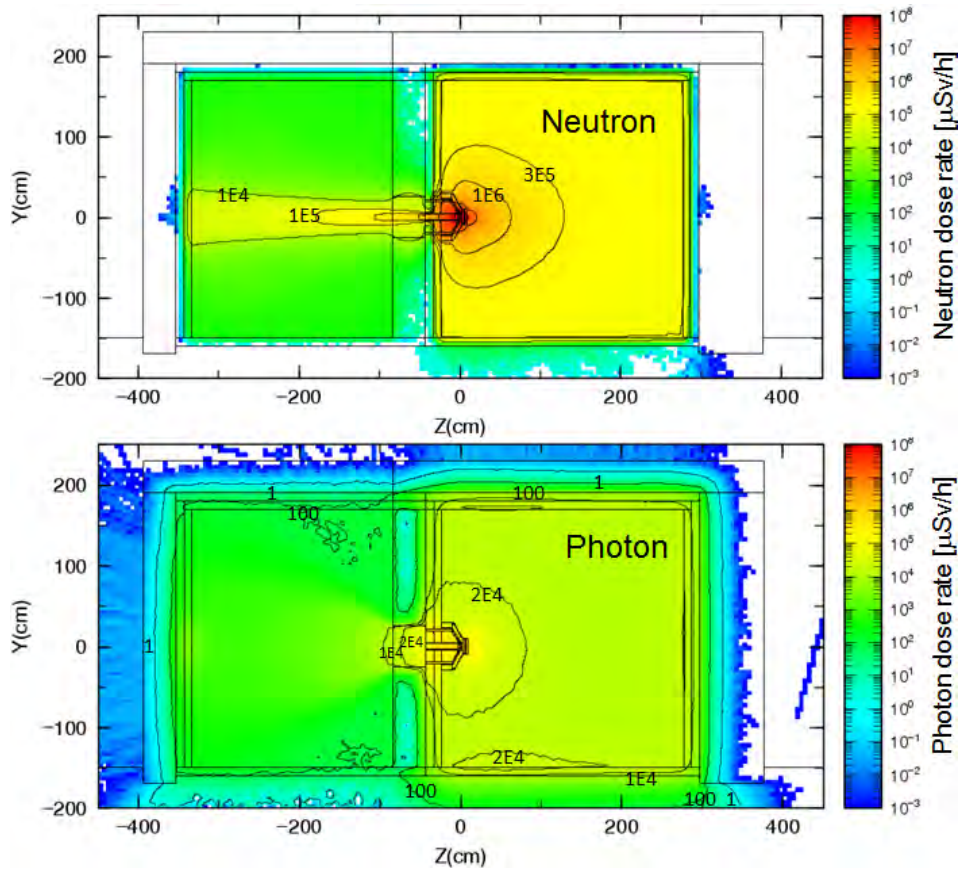
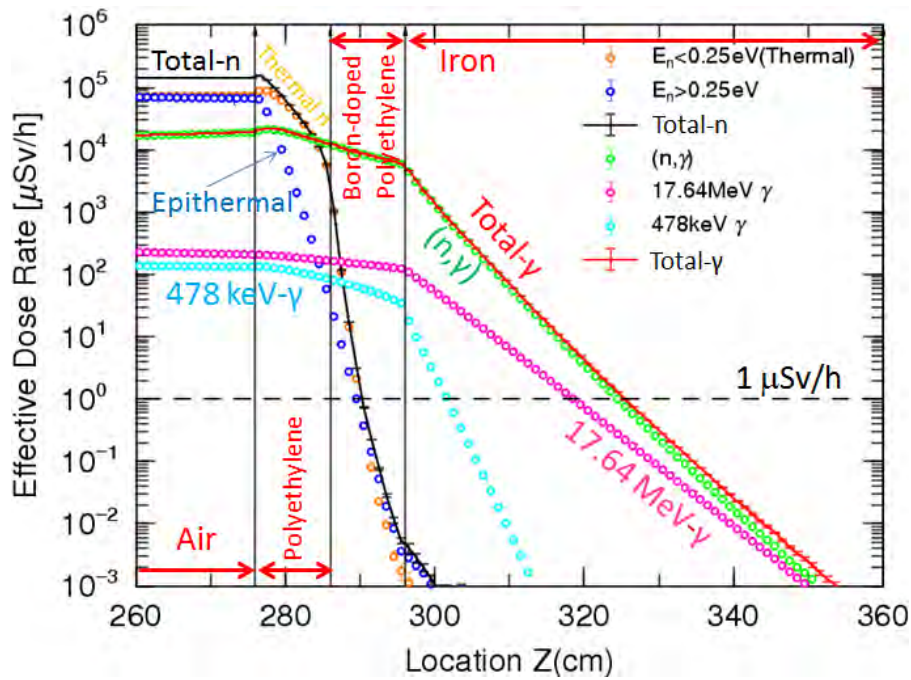


Figure 5: Simulated attenuation profiles of the effective dose rates for various neutron- and photon-radiation components through the downstream wall. This figure has been plotted by the graphic tool ANGEL included in the PHITS package [10].



5 RESIDUAL RADIOACTIVITY AND RADIATION

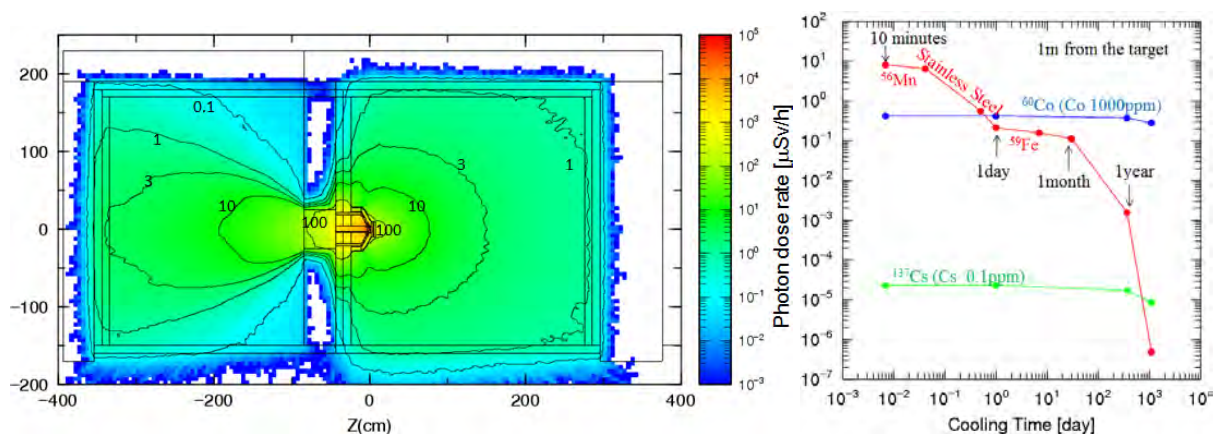
Residual radioactivity in the target and its surroundings after the beam operation was estimated using the high-energy particle-induced activity-computation code DCHAIN-SP2001 [11]. According to this code, nuclear reactions and decays of nuclei in the materials were calculated with output results such as the energy spectra of the neutron flux and material compositions using the MCNP5 Monte Carlo simulation described in Section 4. The condition of the activation calculation is that the irradiation (operation) time was 1 year and the cooling times were 10 min, 1 h, 12 h, 1 day, 1 week, 1 month, 1 year, and 3 years.

Some nuclei, such as cobalt (Co) and cesium (Cs), whose inclusion as impurities has significant effects on activation, were not contained in the stainless steel used in the MCNP5 simulation. Therefore, the activation calculations of Co and Cs were separately conducted with the DCHAIN-SP2001 code. The concentrations in stainless steel assumed in these calculations were 1,000 ppm for Co and 0.1 ppm for Cs. The actual contributions should be re-evaluated by multiplying by factors based on the actually measured concentrations of these impurities.

Using the thus-obtained residual activities at the target and its surroundings, energy distributions of photon flux from the radioactive nuclei in various regions were prepared as an input for the MCNP5 code, and an additional Monte Carlo simulation was conducted for photon transport throughout the whole BNCT facility. The activity distribution in each region was set to be uniform and an isotropic photon emission was assumed.

Fig. 6 shows the two-dimensional distribution of the spatial photon dose rate obtained by the simulation for a 1-h cooling time. Fig. 6 also shows the attenuation profiles of the spatial photon dose rates as a function of the cooling time at 1 m from the target on the beam axis. The dose rate after 10 min of cooling was about 10 $\mu\text{Sv/h}$, mostly due to the produced radioactive ^{56}Mn nuclei (half-life 2.6 hours), and the dose rate continued to be dominant for up to 1 day. ^{56}Mn was generated by the neutron capture of ^{55}Mn in the stainless steel. Without impurities, ^{59}Fe (half-life 44.5 days) was dominant afterwards for up to about 1 year. When considering the impurity of 1,000-ppm Co in the stainless steel, the dose rate due to ^{60}Co would continue to be dominant from about 1 day up to a few years.

Figure 6: Simulated two-dimensional spatial distribution of the photon-dose rate due to residual activity after 1-year operation and 1-h cooling in the vertical plane (left), and one-dimensional photon-dose rates as a function of cooling time (right). These figures has been plotted by the graphic tool ANGEL included in the PHITS package [10].



6 EXTERNAL EXPOSURE FOR PATIENT

To evaluate the external exposure during therapy of all normal tissue in the patient's whole body, the MIRD5 computational human phantom [12] was additionally used in the MCNP5 Monte Carlo simulation. The phantom head surface was placed at a distance of 2 cm from the polyethylene bolus of the target equipment, as shown in Fig. 7. The MIRD5 phantom consisted of three types of body constituents, which were soft tissue (muscles and organs), bone, and lung, and defined the regions of representative organs and tissue as combinations of the smaller cells.

The absorbed dose could be calculated by the MCNP5 Monte Carlo simulation. The physical absorbed dose ($\text{J/kg} = \text{Gy}$) was derived from the energy transfer (MeV/g) from the neutrons and photons in each organ and tissue region. The physical doses of neutrons and photons in each organ and tissue region, along with the statistical error in the simulations, are given in Table 1. The photon dose generally dominates and is significant in organs and tissues because of photons generated by neutron-capture reactions. The relative biological effectiveness (RBE) was used to consider the biological effects of different types of radiation. The RBE dose (Gy-Eq) is given as the physical dose (Gy) multiplied by the RBE factor. In this study, the RBE factors were defined as 1.0 for photons and 2.5 for neutrons.

The method for the effective-dose evaluation recommended by ICRP 2007 [13] was partly used for the evaluation of the whole-body exposure. The effective dose is defined for uniform irradiation from the front of the body and is not suitable for a locally irradiated medical situation. Therefore, by using the calculating method of the tissue weighting average, the RBE dose (Gy-Eq) for the whole body exposure was estimated instead of the effective dose (Sv). The RBE doses for 14 specific organs and tissues, as well as "other organs and tissues" (arithmetic averages of 13 organs) were evaluated and are given in Table 1. Doses at the extrathoracic region of the respiratory tract and lymph nodes in the "other organs and tissues" category could not be obtained, since they were undefined in the MIRD5 phantom. The doses of the red marrow and the bone surface were evaluated using their weight fractions [14] in the bones.

Figure 7: Simulation geometry of the MIRD5 phantom located after the polyethylene bolus.

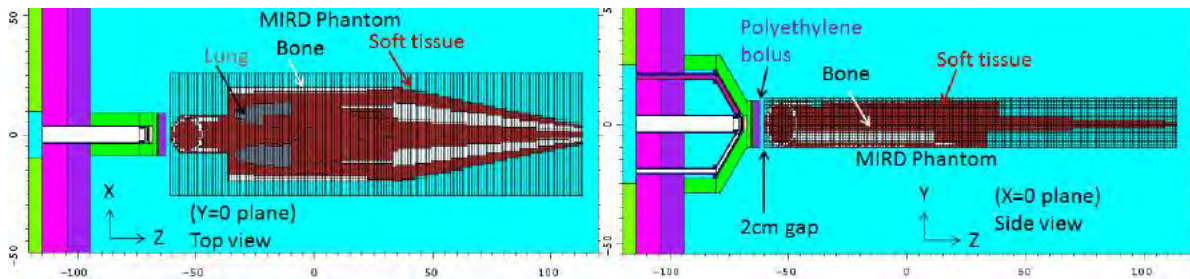


Table 1: Absorbed dose estimated by Monte Carlo simulation and RBE dose for each tissue and organ, and the total tissue-weighting average of the RBE dose.

Tissue, Organ	Mass [g]	Absorbed dose (Physical dose)				RBE dose (Biological dose)						
		Neutron Dose [mGy/h]	Error [%]	Photon Dose [mGy/h]	Error [%]	Total RBE (n2.5, γ :1.0) [mGy-Eq/h]	Tissue, Organ [mGy-Eq/h]	Tissue Weighting w_T				
Lung	938	1.6	0.6	42.2	0.7	46.2	Lung	46.2	0.12			
Stomach	81	0.6	2.4	23.3	2.6	24.8	Stomach	24.8	0.12			
Colon	454	0.4	1.4	17.6	1.4	18.7	Colon	18.7	0.12			
Breasts	148	3.2	1.7	35.9	1.9	44.0	Breasts	44.0	0.12			
Gonad	41	1.2	2.8	17.3	4.3	20.3	Gonad	20.3	0.08			
Thyroid	25	3.0	2.0	128.0	2.1	135.5	Thyroid	135.5	0.04			
Esophagus	66	0.9	1.8	46.4	2.6	48.7	Esophagus	48.7	0.04			
Urinary bladder	45	0.6	2.5	16.6	3.1	18.1	Urinary bladder	18.1	0.04			
Liver	1,920	0.8	1.0	25.8	1.0	27.7	Liver	27.7	0.04			
Brain	1,410	212.0	0.1	1080.0	0.2	1610.0	Brain	1610.0	0.01			
Salivary Gland	82	8.8	0.6	235.0	0.9	257.1	Salivary Gland	257.1	0.01			
Skin Head	531	172.0	0.1	503.0	0.2	933.0	Skin (Mass average)	194.0	0.01			
Body	1,510	2.8	0.5	31.0	0.5	38.0						
Leg	900	1.3	0.5	15.0	0.7	18.2						
Bone Spinal cord (up)	326	7.7	0.7	170.0	1.0	189.2	Red marrow* (Mass average)	126.2	0.12			
Spinal cord (mid)	1,040	1.1	1.2	36.4	1.4	39.1						
Spinal cord (low)	385	0.5	2.7	16.6	2.4	17.9						
Skull	1,370	119.0	0.1	668.0	0.2	965.5	Bone surface* (Mass average)	172.2	0.01			
Jawbone	244	5.9	0.6	166.0	0.8	180.8						
Pelvis	1,120	0.6	1.2	16.1	1.2	17.6						
Leg bones	5,320	0.8	0.7	13.7	0.8	15.6						
Humerus	1,840	2.3	0.5	32.9	0.8	38.7						
Rib	1,890	1.8	0.4	39.5	0.6	44.1						
Clavicle	78	8.0	0.8	90.9	1.3	111.0						
Muscle Head	2,400	36.6	0.1	240.0	0.3	331.5	Muscle	46.6	0.12			
Body	33,600	1.7	0.2	31.4	0.3	35.7						
Leg	18,500	0.9	0.3	15.4	0.5	17.7						
Adrenal	17	0.6	4.3	23.8	5.0	25.3	Others (Arithmetic mean)	46.6	0.12			
Gall bladder	15	0.4	4.3	20.6	4.3	21.7						
Kidney	288	0.6	1.8	20.5	2.0	22.1						
Pancreas	192	0.7	2.4	25.7	2.4	27.3						
Spleen	76	0.4	3.2	23.2	2.8	24.2						
Thymus	21	1.4	2.8	43.2	3.9	46.7						
Uterus	62	0.3	4.2	16.5	3.6	17.3						
Small intestine	371	0.3	2.3	17.6	2.0	18.5						
Heart	767	0.9	1.3	32.6	1.3	34.8						
Oral mucosa	29	7.2	1.1	214.0	1.1	232.1						
Total	78,102									Tissue weighting average	69.9	1.00

The tissue-weighting factor (w_T) in the ICRP 2007 recommendation is given in Table 1. Finally, the tissue-weighting average RBE dose for the whole body was derived as 69.9 (mGy-Eq) for 1-h irradiation at a proton current of 10 mA. Here, the boron-dose contribution was not taken into account because the boron-concentration distribution in the entire body was not clear, and the evaluation of the boron dose in normal tissue remains a task for the future.

7 CONCLUSION

The near-threshold ${}^7\text{Li}(p,n)$ reaction by 1.92-MeV protons (standard deviation 0.02 MeV) provides neutrons with an energy of around 35 keV at peak and around 200 keV at maximum. The optimized target-moderator system was established with a 0.5-mm-thick liquid-lithium flow in the curved stainless-steel plate followed by insulators, a lead shielding, and a polyethylene bolus. Practical radiation analyses for the BNCT facility were performed using the MCNP5 Monte Carlo code. Produced neutrons and photons were successfully shielded by walls consisting of undoped polyethylene, boron-doped polyethylene, and iron shields. Residual radioactivity was also successfully estimated by the DCHAIN-SP2001 code, and residual radiation from the ${}^{56}\text{Mn}$ produced in stainless steel was estimated to be dominant for 1 day, after which the ${}^{60}\text{Co}$ produced in Co impurity was dominant for a few years. External exposure of the human whole body was also simulated using the MIRD5 computing phantom, and the RBE dose of 69.9 (mGy-Eq/h) was estimated. In this study, the simulation method for the BNCT facility was established for the purpose of radiation protection, and the techniques used are expected to be useful for the future upgrades of the BNCT technology.

8 ACKNOWLEDGEMENTS

Authors would like to thank Dr. Ken-ichi Tanaka (Hiroshima Univ.) and Dr. Tatsuhiko Sato (JAEA) for their useful advices during the course of this study. This paper is based on results obtained from a project commissioned by the New Energy and Industrial Technology Development Organization (NEDO).

9 REFERENCES

- [1] Kobayashi, T., Hayashizaki, N., Katabuchi, T., et al., 2014. IEEJ Transactions on Electronics, Information and Systems, 134 (9) 1406–1413.
- [2] Kobayashi, T., Hayashizaki, N., Katabuchi, T., et al., 2014. Near-threshold ${}^7\text{Li}(p,n){}^7\text{Be}$ Neutrons on the Practical Conditions using Thick Li-target and Gaussian Proton Energies for BNCT. Applied Radiation and Isotopes 88, 221–224.
- [3] X-5 Monte Carlo Team, 2003. MCNP – A General Monte Carlo N-Particle Transport Code, Version 5. LA-UR-03-1987, Los Alamos National Laboratory (LANL).
- [4] RSICC, 2003. Data Libraries for MCNP5. CCC-710/MCNP, Oak Ridge National Laboratory (ORNL).
- [5] Shibata, K., Iwamoto, O., Nakagawa, T., et al., 2011. JENDL-4.0: A New Library for Nuclear Science and Engineering. J. Nucl. Sci. Technol. 48(1), 1–30.
- [6] Kosako, K., Yamano, N., Fukahori, T., et al., 2003. The Libraries FSXLIB and MATXSLIB Based on JENDL-3.3. JAERI-Data/Code 2003-011, Japan Atomic Energy Research Institute (JAERI).
- [7] Lee, C. L., Zhou, X. -L., 1999. An Algorithm for Computing Thick Target Differential p-Li Neutron Yields Near Threshold. Proceedings of the 15th International Conference on the Application of Accelerators in Research and Industry, edited by J. L. Duggan and I. L. Morgan (AIP, Woodbury, New York).
- [8] Kiss, A. Z., Koltay, E., Nyako, B., et al., 1985. Measurements of relative thick target yields for PIGE analysis on light elements in the proton energy interval 2.4-4.2 MeV. J. Radioanal. Nucl. Ch. 89(1), 123–141.
- [9] Zahnow, D., Angulo, C., Rolfs, C., et al., 1995. The S(E) factor of ${}^7\text{Li}(p,\gamma){}^8\text{Be}$ and consequences for S(E) extrapolation in ${}^7\text{Be}(p,\gamma_0){}^8\text{B}$. Z. Phys. A 351, 229–326.
- [10] Sato, T., Niita, K., Matsuda, N., et al., 2013. Particle and Heavy Ion Transport Code System PHITS, Version 2.52. J. Nucl. Sci. Technol. 50:9, 913–923.
- [11] Kai, T., Maekawa, F., Kosako, K., et al., 2001. DCHAIN-SP 2001:High Energy Particle Induced Radioactivity Calculation code. JAERI-Data/Code 2001-016.
- [12] ICRP, 1975. Report of the Task Group on Reference Man. ICRP Publication 23.
- [13] ICRP, 2007. The 2007 Recommendations of the International Commission on Radiological Protection. Publication 103. Ann. ICRP 37(2–4).
- [14] ICRP, 2009. Adult Reference Computational Phantoms. Publication 110. Ann. ICRP 39(2).

Nuclear New Build - Disseminating Radiation Safety Culture in the Supply Chain

Peter A Bryant^{a*}, Peter Cole^b

^a Peter A Bryant, Arcadis Consulting (UK) Ltd, The Pithay, All Saints' St, Avon, Bristol, BS1 2NL, United Kingdom.

^b Peter Cole, Radiation Protection Office, University of Liverpool, Liverpool, L69 7ZE, United Kingdom.

Abstract. Across the world we are seeing a resurgence in nuclear new build with a current estimated 160 new reactors planned for construction and an additional 300 proposed. In the UK alone plans are under way for the construction of 4 EPR style reactors, 4 Advanced Boiling Water Reactors (ABWR) and 2 AP1000 style reactors. These reactors are to be operated by 3 newly formed licensees within the UK, a number of which are funded by joint ventures. Central to the success of these nuclear new build ambitions is the embedding of the correct culture into the newly formed organisations to ensure safety is adequately considered at all stages of the design and build process. This front-end loading of the design process with safety, or “Safety Led Design” process is paramount in ensuring a robust, suitable and sufficient design is achieved, whilst demonstrating the risks have been reduced to As Low As Reasonably Practicable (ALARP). In the UK we call this culture “Nuclear Safety Culture” or “Radiation Safety Culture”. The overarching responsibility for embedding this culture falls to the licensee or operator with significant levels of investment being made to provide training to the staff and the associated arrangements to ensure this is acted upon. Due to the large complexity and scale of these new build projects, heavy utilisation of a supply chain is required to support the existing staff (embedded contractors), undertake specialist assessments, undertake design work, procure process plant and equipment, and support construction. With this substantial dependency on the supply chain, how do we ensure that the Nuclear and Radiation Safety Culture is flowed down and embedded into the Supply Chain as well? Do we make it contractual? Do we need to train the Supply Chain? And what is the role of the “Intelligent Customer”? This paper explores these issues with consideration given to the lessons learnt in the UK nuclear new build market, the current solutions being utilised, and how progress might be made in the future.

KEYWORDS: *Safety Culture, New Build, Supply Chain.*

1 INTRODUCTION

Culture in its simplest form is defined as “the way that we do things around here” [1]. Following such global events at Fukushima Daiichi and Chernobyl, safety culture has become the dominant aspect of organisational culture within the high hazard industries such as the Nuclear Sector. Radiation Safety Culture or Nuclear Safety Culture as it is often referred to, is effectively a sub-set of the wider safety culture, focusing on the potential harmful effects associated with the use of radioactive and/or fissile material and ionising radiations. The International Atomic Energy Agency defined Nuclear Safety Culture as the “...human awareness of the significant destructive capability of nuclear power when control is lost, and the recognition that strict attention to safety is essential if the benefits of this form of power are to be obtained” [1].

In the UK plans are under way for the construction of 4 EPR style reactors, 4 Advanced Boiling Water Reactors (ABWR) and 2 AP1000 style reactors. These reactors are to be operated by 3 newly formed licensees within the UK, a number of which are funded by joint ventures.

Central to the success of these nuclear new build ambitions is the embedding of a healthy nuclear safety culture into the newly formed organisations to ensure safety is adequately considered at all stages of the design and build process. This front-end loading of the design process with safety, or “Safety Led Design” process is paramount in ensuring a robust, suitable and sufficient design is achieved, whilst demonstrating the risks have been reduced to As Low As Reasonably Practicable (ALARP). The

* Presenting author, e-mail: p.a.bryant@me.com

overarching responsibility for embedding this culture falls to the licensee and end operator.

Due to the large complexity and scale of these new build projects, heavy utilisation of a supply chain is required to support the existing staff (embedded contractors), undertake specialist assessments, undertake design work, procure process plant and equipment, and support construction.

With this substantial dependency on the supply chain, how do we ensure that the Nuclear Safety Culture is flowed down and embedded into the Supply Chain as well?

In the subsequent sections of this paper we will explore these issues with consideration given to the lessons learnt in the UK nuclear new build market, the current solutions being utilised, and how progress might be made in the future.

2 EMBEDDING SAFETY CULTURE IN A NEW OPERATOR

The ACSNI Human Factors Study Group in the UK defined a positive safety culture as “the product of individual and group values, attitudes, competencies and patterns of behaviour that determine the commitment to, and the style and proficiency of an organisation’s health and safety programmes”[1]. In essence healthy safety culture is created in an organisation by the collective commitment of leaders and individuals to emphasise safety over competing goals, to ensure protection of people and the environment.

The World Association of Nuclear Operators (WANO) defined the “traits of a health nuclear safety culture” [2] into three categories:

- Individual Commitments to Safety
 - Personal Accountability
 - Questioning Attitude
 - Safety Communication
- Management Commitment to Safety
 - Leadership Accountability
 - Decision-Making
 - Respectful Work Environment
- Management Systems
 - Continuous Learning
 - Problem Identification and Resolution
 - Environment for Raising Concerns
 - Work Processes

These can be broken down further into a number of characteristics a few of which are presented in Figure 1.

In the UK a healthy nuclear safety culture is enforced by a system of regulatory control based on a robust licensing process by which Nuclear Operators are granted a licence to use a site for specified activities. As part of the license a set of 36 Standard Conditions are attached, covering design, construction, and operation and decommissioning [3]. These conditions require licensees to implement adequate arrangements to ensure compliance, a number of which by their very nature encourage a positive safety culture.

For instance, License Condition 17 “Management Systems” requires the licensee to establish and implement management systems which give due priority to safety [4]. This is directly linked to the WANO traits of a healthy safety culture along with the “Systematic Approach to Safety” characteristic seen in Figure 1. Similarly License Condition 7 “Incidents on the Site” requires the licensee to make and implement arrangements for the notification, recording, investigation and report of incidents on the site. This directly links to the WANO trait “Problem Identification and Resolution” along with the “Measurement of Safety Performance” characteristic seen in Figure 1.

Figure 1: Healthy Safety Culture Characteristics (adapted from [1], [2])

As mentioned earlier plans are under way in the UK for the construction of the next generation of Nuclear Reactors, all of which are to be operated by 3 newly formed licensees. As these organisations embark on the task of deliver their new build ambitions they will each go through the process of applying for their Nuclear Site License for each site. As part of this application process they will be required to demonstrate to the UK regulators that they have adequate arrangements, or plans to implement adequate arrangements such as to ensure compliance with the standard set of License Conditions. This will ensure a healthy safety culture is present within the organization throughout the design, construction, commissioning and ultimate operation of the new nuclear power stations.

But with the substantial dependency on the supply chain to support the delivery of the nuclear new build ambitions – who enforces “Safety Culture” in the Supply Chain?

3 CONTRACTORS & MANPOWER SUBSTITUTION

Contractors are often used for manpower substitution or for short term additional resources where skills exist within the licensee but are not available. These contractors are normally acting on behalf of the licensee, for instance accepting elements of the design and build or engaging with the regulators and as such are termed “embedded contractors” (EC).

However, it is important that the licensee maintains a core of in-house staff to ensure effective control and management for nuclear safety. Furthermore it is a legal requirement in the UK that the licensee retains overall responsibility for, and control and oversight of, the nuclear and radiological safety and security of all of its business, including work carried out on its behalf by contractors.

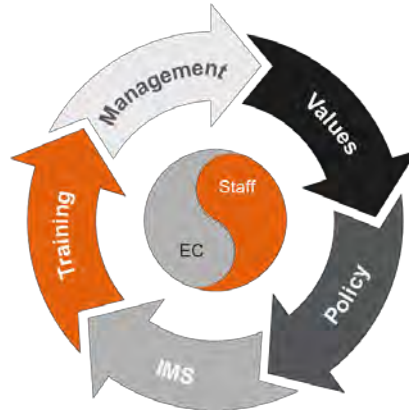
That being said given the scale of the Nuclear New Build ambition in the UK, and resourcing required to fulfil it at various times during the project life cycle it is not unusual to see project teams in these new operators where 50% plus of the total resource is made up by contractors.

Given this heavy dependence on embedded contractors, which as we mentioned earlier are in essence acting on behalf of the licensee, it is important that they are captured under the licensee’s safety culture.

Essentially regardless of being staff or an embedded contractors all individuals carrying out work on behalf of the licensee should have the same individual commitment safety (e.g. personal accountability), with the management providing the same commitment to safety (e.g. a respectful work environment) and use the same Integrated Management System (IMS).

By ensuring a “one team” approach where individuals are treated the same, this encourages a more collaborative working environment. This approach is summarized in Figure 2, showing that regardless of contract type, both staff and embedded contractors should adhere to the same values, follow the same policies, working under a consistent IMS, with adequate training provided and under the correct management and supervision.

Figure 2: Approach to instilling a Healthy Safety Culture in Staff and Embedded Contractors



4 CONSULTANCY SERVICES

Consultancies are often used to provide expert advice within a particular field or to deliver a particular task or package of work. In the Nuclear New Build space this may include providing specialist assessments, such as Safety Assessments or Engineering Assessments.

Ensuring that any consultancy services are delivered to the required quality, and meets the requirements of the licensee is often down to “good” Project and Commercial Management. However, noting the potential nuclear safety implications of some of the packages of work, additional controls are needed to ensure a healthy safety culture is also implemented by the consultancies project team.

The UK Office for Nuclear Regulation (ONR) states that the licensee must “have sufficient competent resource within the licensee organisation to be an ‘intelligent customer’ for any work it commissions externally”.

The concept of the ‘intelligent customer’ was developed by the ONR and has subsequently gained international acceptance. It is defined by the International Atomic Energy Agency as follows [5]:

‘As an intelligent customer, in the context of nuclear safety, the management of the facility should know what is required, should fully understand the need for a contractor’s services, should specify requirements, should supervise the work and should technically review the output before, during and after implementation. The concept of intelligent customer relates to the attributes of an organisation rather than the capabilities of individual post holders’.

It is further broken down into a number of requirements the licensee must be able to demonstrate compliance with as seen in Figure 3.

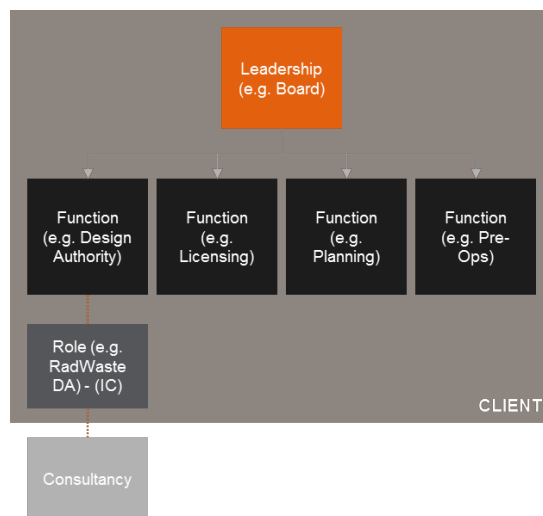
Figure 3: Requirements for an Intelligent Customer



If implemented correctly the ‘intelligent customer’ role will ensure that the consultancy are familiar with the nuclear safety implications of their work and interact with the licensee in a well-coordinated manner.

Those work streams which may impact nuclear safety should be clearly identified within the licensee’s organisational structure allowing a clear identification to those roles linked to the ‘intelligent customer’ capability. Those individuals within the licensee holding these roles, whether embedded contractors or staff, should undergo the appropriate training, to ensure they understand the requirements placed on them, along with the processes and procedures they should follow as part of the licensee’s IMS.

Figure 4: Example Organisational Structure



It should be remembered that the intelligent customer relates to the attributes of the licensee rather than the capabilities of individual post holders, this is closely tied to the traits of a health safety culture.

As mentioned earlier the successful delivery of consultancy services is also dependent on “good” Project and Commercial Management. In itself this can be heavily dependent on an individual managing a contract, and can be a skill that takes time to learn. However, by ensuring a robust set of processes in place within the licensee IMS for the management of consultancy services this can help instil a ‘good’ approach to Project Management. These processes may include:

- A well-defined procurement process ensuring that work with any safety significance is only awarded to companies with suitable (and verified) competence, safety standards, management systems, culture and resources. For example this may require the company being awarded the work to demonstrate that their members of staff are suitable qualified and experienced. In the UK such proof may come in the form of Chartership, such as Chartered Radiation Protection Professional (**CRadP**), which provides confirmation the individual has been independently assessed in a particular field as professionally competent through education, training and professional practice.
- Process for ensuring that any package of work to be contracted out is well-defined, including a task breakdown, required deliverables and any processes or procedures the consultancy is expected to follow. This should be defined early on, if not prior to commencing the package of work to avoid the need for unnecessary re-work.
- An appropriate review and acceptance process for the particular type of work whether it is a report or computational analysis. This should include the need for an independent review/assessment as required.
- A single point of contact for the management of each contract. This will help ensure clear and proactive communication between the licensee and consultancy, and this is key to ensuring a right first time approach.
- A lessons learnt process, ensuring appropriate feedback is sought after the close out of a project and any learning taken on board.

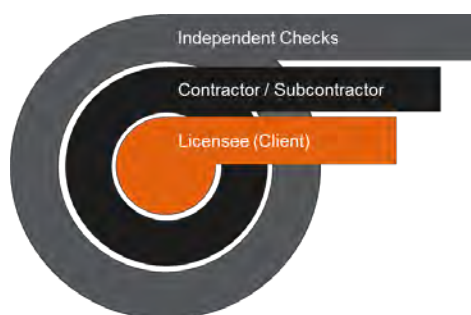
The role of the ‘intelligent customer’ capability along with project and commercial management processes will ensure the work is carried out to the required level of safety and quality in practice.

5 DESIGN, MANUFACTURE AND CONSTRUCT OR PROCURE CONTRACTS

Design, Manufacture, Construct or Procure based contracts are usually related to the construction of a be-spoke piece of process plant and equipment (PP&E) or the procurement of a piece of commercial off-the-shelf equipment. These contracts are normally undertaken within the Supply Chain Organisation and following the Supply Chain Organisation’s own internal management system.

The integrating of a healthy nuclear safety culture can be achieved using a very similar approach to consultancy services, however on a larger scale. Furthermore, due to the volume of contracts which will be awarded during the design and build of a new nuclear power station it will become increasingly difficult for the licensee to maintain a close level of supervision, as such increasing dependency will be placed on the contractual and commercial management.

Figure 4: Levels of Defence



The role of the ‘intelligent customer’ remains essential in understanding what is being procured/manufactured, the requirements on the PP&E, the supervision of the work being undertaken, and the review/check of the outputs/deliverables both during and after implementation. However the level of contractual and commercial management is likely to increase, this may include:

- A requirement for the Supply Chain Organisation to produce a Safety and Environmental Management Plan. This may include an overview of how they will ensure the correct culture is maintained including management systems and how sub-contractors are managed. Additionally, it should define the point of contact within the supply chain organisation that is driving safety into the project. The management plan will in essence summarise how the Supply Chain Organisation will implement the traits of a healthy safety culture into their own delivery team.
- Auditing of the Supply Chain Organisation, as required, to ensure the Safety and Environmental Management Plans are be adequately implemented and periodically reviewed and updated as required.
- Depending on the Safety Significance of the Contract, independent checks of the Supply Chain Organisation’s work, the level of detail of these checks would also be driven by the Safety Significance. This will help provide additional levels of defence against complacency as demonstrated in Figure 4.

In essence, by implementing the increased levels of contractual management it allows the ‘intelligent customer’ to become a pseudo-regulator ensuring the Supply Chain Organisation has adequate arrangements such as to ensure compliance with the contract, and ensure a healthy safety culture is present within the organisation.

6 INSTALLATION CONTRACTS

In addition to the Design, Manufacture, Construct or Procure based contracts there may be an additional requirement for the Supply Chain Organisation to construct or install equipment on the proposed reactor site. In these cases, in addition to those requirements discussed in Section 5 extra consideration should be given to:

- Induction and Training of Supply Chain Organisation Staff whilst working on the reactor site to understand and follow the Licensee’s Processes and Procedures and the hazards they may encounter on site.
- Management of the Supply Chain Organisation Staff by the Licensee Organisation.

Consideration must also be given to treating the Supply Chain Organisation Staff in the same manner as Embedded Contractors as detailed in Section 3, thus ensuring the same values are adhered to and as such the same healthy safety culture adopted.

Throughout construction and installation works on-site there is important for the licensee staff to ensure it maintains its “questioning attitude” in particular noting that there will be various Supply Chain Organisations bringing materials and equipment on site, a number of which could have an implication on safety (e.g. radiography sources).

7 SUMMARY AND CONCLUSIONS

Across the world we are seeing a resurgence in nuclear new build with a current estimated 160 new reactors planned for construction and an additional 300 proposed. In the UK plans are under way for the construction of 4 EPR style reactors, 4 ABWR style reactors and 2 AP1000 style reactors.

Central to the success of these nuclear new build ambitions is the embedding of the correct culture to ensure safety is adequately considered at all stages of the design and build process. Overarching responsibility for embedding this culture falls to the licensee or future operator. However, due to the large complexity and scale of these new build projects, heavy utilisation of a supply chain is required.

When sourcing work from contractors this should be informed by the licensee's policy and IMS that takes into account the nuclear safety implications of those choices. How a healthy safety culture is embedded into the supply chain is dependent on the type of contract.

When using embedded contractors or when staff from the supply chain are working on the licensee's premises it is important to create a "one team" approach. This encourages a more collaborative working environment where both the licensee and supply chain staff adhere to the same values, follow the same policies, working under a consistent IMS, with adequate training provided and under the correct management and supervision.

Where work packages are contracted out or equipment designed, manufactured or procured, the role of the 'intelligent customer' should be emphasised to ensure the licensee has a clear understanding and knowledge of the product or service being supplied. This coupled with 'good' project and contractual management will ensure the work/product is carried out/produced to the required level of safety and quality in practice.

Regardless of contract type it is important that all individuals avoid complacency and continuously challenge existing conditions, assumptions, anomalies and activities. It is through this that we can demonstrate a commitment to safety in your decisions and behaviours.

8 ACKNOWLEDGEMENTS

The authors gratefully thank the Society for Radiological Protection for providing funding to attend the 14th Congress of the International Radiation Protection Association.

9 REFERENCES

- [1] IAEA, 2002, Safety Culture in Nuclear Installations, Guidance for use in the enhancement of safety culture, IAEA-TECDOC-1329, International Atomic Energy Agency, Vienna.
- [2] WANO, 2013 WANO Principles, Traits of a Health Nuclear Safety Culture, PL 2013-1, World Association of Nuclear Operators.
- [3] ONR, 2015, Licensing Nuclear Installations, 4th Edition, Office for Nuclear Regulation, UK.
- [4] ONR, 2016, Licence Condition Handbook, Office for Nuclear Regulation, UK.
- [5] ONR, 2013, Licensee Core and Intelligent Customer Capabilities, Nuclear Safety Technical Assessment Guide, NS-TAST-GD-049 Revision 4, Office for Nuclear Regulations, UK.

On the ingestion of Cs-137 at Volincy municipality in Belarus about 30 years after the Chernobyl accident

Peter Hill*, Petro Zoriy, Herbert Dederichs, Burkhard Heuel-Fabianek, Jürgen Pillath

Forschungszentrum Jülich GmbH, S, D-52425 Jülich, Germany.

Abstract. From 1991 to 1993 the German Chernobyl Project has achieved a total of 317.000 mobile in-vivo measurements in regions affected by fall-out after the Chernobyl Accident. This included measurements in Korma county (Belarus). The deposition of Cs-137 in Korma County varies locally very much. Different exposure situations can be studied within a small area. Therefore the county has been selected for a follow-up study, which since 1998 investigated the long-term evaluation of population dose. This paper reports especially on the most recent assessments of body burdens in the population of Volincy municipality and the internal dose between 2013 and 2015. During these three years 116, 110 and 117 measurements were performed, respectively. A mean annual dose of 0.10 mSv, 0.11 mSv and 0.07 mSv has been derived from the individual body burdens. This may be compared to the value of 1.6 mSv/a observed in 1999. The internal dose has dropped since then considerably. Presently it is only slightly enhanced over background values and of no special relevance to health. Essential for obtaining this achievement have been several facts. The people got knowledgeable about their actual body burden. The people have been given individual advice. They changed their habits and most lately there have been societal changes furthering the consumption of cleaner food, too.

KEYWORDS: *Chernobyl accident; in-vivo monitoring; long-term assessment; internal dose.*

1 INTRODUCTION

Thirty years ago large parts of Belarus suffered strongly from Chernobyl fall-out. In several studies the Division of Radiation Protection at the national laboratory Jülich(Germany) has been investigating the long-term development of population dose in Korma County (Belarus) (e.g. [1] and references given therein). We report on the most recent results of body burdens and internal doses, which were measured during the 2013 to 2015 field missions at the municipality of Volincy. Korma County is situated approx. 70 km north of the city of Gomel/Belarus and about 200 km from the Chernobyl NNP. The municipality Volincy is more forestial in its nature. The ecological half-live of Cs-137 in forests is known to be long [2].

First German mobile in-vivo measurements in Korma county took place in 1992. Since 1998 a van type mobile in-vivo monitoring laboratory has been used to assess body burdens of Cs-137. The calculation of dose is based on dose factors directly related to body burdens since more or less a chronic incorporation can be assumed.

In 1999 body burdens of Cs-137 at Volincy were still quite high [3]. Individual advice provided by the measuring team led to a changed attitude towards the consumption of contaminated food. Over the time body burdens dropped significantly. In the three years from 2013 to 2015 a total of 107, 110 and 117 persons were measured, respectively. Presently the internal dose is only slightly enhanced over and of no special relevance to health.

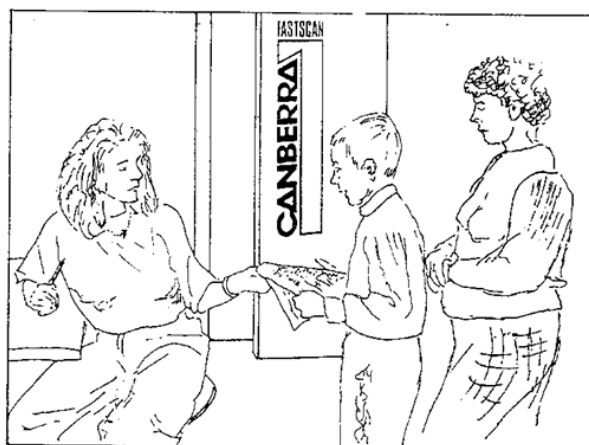
2 THE GERMAN CHERNOBYL PROJECT

To support the former Soviet government under the leadership of Gorbachov the Federal Republic of Germany initiated the German Chernobyl Project. With funding from the Federal Ministry of Environment the National Laboratory Jülich organized from 1991 to 1993 four field missions to the contaminated regions of Russia, Belarus and the Ukraine. Many German institutions and individuals were involved. The aim was to reduce existing anxiety in the population by obtaining and communicating objective information on the radiological situation. The population did trust in the work of German experts but did not trust too much in the measurements of their own scientists.

* Presenting author, e-mail: p.hill@fz-juelich.de

Field missions covered several aspects of assessing the radiological situation [4]. Environmental monitoring included the measuring of soil samples and area dose rates. Also food samples provided by the population have been assessed. Some direct measurements of external dose have been performed. In one village thyroids have been screened by medical experts. The main effort however went into the mobile in-vivo monitoring of the population. Up to 8 mobile laboratories with up to 20 whole-body counters and incorporation monitors were used to perform within 3 years 317.000 incorporation measurements in 240+ settlements ranging from small villages to towns. Both the body burden of Cs-134 and Cs-137 were assessed. Five and more years after the accident the incorporation originated from ingestion, i.e. the contamination of food stuff. The population was very concerned about their children. The first-ever whole-body counter designed especially for babies and toddlers was developed [5] and used for the smallest of the children.

Figure 1: People were informed about the result immediately after the measurement ([4])



Very essential was the immediate information of the people on their body burdens, which was given in writing (Fig.1). Less than 2% of the measurements showed body burdens which were higher than the international annual dose limit of 1 mSv accounted for. But even those were within the range of effective doses allowed for occupational radiation workers. More information is given in [4] and references therein.

In 1992 and 1993 Korma County was included in the assessment. The mobile in-vivo monitoring laboratory was located in Korma itself. Interested inhabitants of the villages had to come into town for measurement. Mean annual internal doses of 0.09 mSv and 0.08 mSv were found, which does not really reflect the radiological situation in some of the villages.

3 LONG-TERM EVALUATION OF POPULATION DOSE – THE KORMA PROJECT

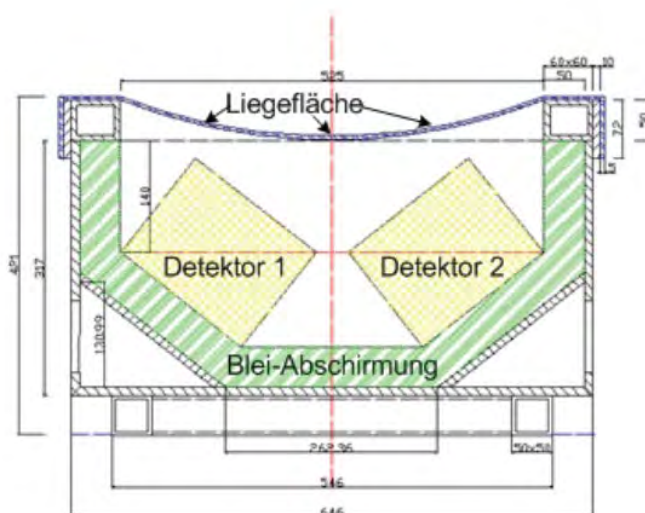
In some follow-up studies the situation had been further investigated in highly contaminated regions. One of them, the Korma Project, concentrated since 1998 on the long-term evaluation of population dose. Korma County is situated approx. 70 km north of the city of Gomel/Belarus and about 200 km from the Chernobyl NNP. There are areas of comparatively low contamination, but also confiscated zones. These areas are close together and different exposure situations could be studied as e.g. villages with lower and more elevated contaminations. In the recent years investigations focused on the municipality of Volincy.

The municipality of Volincy is quite remote, since it can be reached only by a road passing through the confiscated zone of Strumen. It is situated in the forest belt of Korma County. Though there is some agriculture it can be considered to have a more forestial character. It consists of six settlements. Three of them are inhabited, namely Volincy, Kljapin and Klapinskaya Buda. Settlements in the permanent controlled zone had been abandoned with the exception of two families who returned to Koljud in 2005.

3.1 Methods

A van type mobile in-vivo monitoring laboratory has been used to measure Cs-137 body burdens. The design was based on a Mercedes Sprinter van, which is able to carry the weight of the heavily shielded whole-body counter. The latter one is a bed-like type (Figure 2). To fit in the van it is kept short in length. For adults, youth and larger children the lower part of the legs will dangle and are shielded from the detectors. Smaller children, toddlers and babies will fit completely onto the bed. The shielding consists of lead bricks (50 mm thick) and has a total weight of 0.8 metric tons. Two large NaJ-detectors (40cm x 10cm x 10 cm) are positioned in the back of the measured person. Data acquisition and analysis is PC-based (notebook).

Figure 2: Sectional drawing of the whole-body counter [1].



For efficiency calibration a brick phantom [6] has been utilized, which can represent children as well as adults. Efficiency factors for adults have been used in data acquisition and weight-dependent correction factors have been applied. The measuring time has been 1 minute. Typically for Cs-137 a limit of detection (LOD) of 100Bq can be achieved.

3.2 Ingestion dose obtained in the years 2013 - 2015

From 2013 to 2015 the measurement of body burdens continued in the three settlements of Volincy, Kljapin and Klapinskaya-Buda. All measurement results were immediately communicated to the measured persons or the caretakers. The local school is located at Kljapin. Figure 3 shows a group of children waiting in front of the school to be measured. Over the three years the interest of the population was persisting, as can be seen from the number of persons taking part in the measurements (table 1).

Table 1: The number of persons measured during the years 2013 to 2015 [7].

year	Volincy	Klapinskaya-Buda	Kljapin	Total
2013	73	14	20	107
2014	72	14	24	110
2015	78	16	23	117

Figure 3: A group of children queuing up at Kljapin for the measurement ([7]).

Internal doses have been calculated from measured body burdens for each person individually. The calculation is based on dose factors directly related to body burdens since more or less a chronic incorporation can be assumed. They were derived from age-dependent dose factors given in ICRP67 [8]. For those who are younger than 17 years old the dose factors were extrapolated for each year of birth. It had further to be assumed that for conversion to annual dose a seasonal factor of one can be applied at the time of measurement (autumn).

Table 2: The mean annual internal doses obtained for the municipality and its settlements [7].

year	Volincy	Klapinskaya-Buda	Kljapin	Municipality Volincy
2013	0.10 mSv/a	0.07 mSv/a	0.09 mSv/a	0.10 mSv/a
2014	0.11 mSv/a	0.08 mSv/a	0.06 mSv/a	0.10 mSv/a
2015	0.07 mSv/a	0.05 mSv/a	0.06 mSv/a	0.07 mSv/a

The mean internal doses obtained for the years 2013 to 2015 are presented in table 2 for all three settlements together with the values for the municipality as a whole. For the latter a more detailed statistical analysis is given in table 3. In all three years the maximum values for the internal dose obtained have been below 1 mSv/a. This had been different in the past (see chapter 3.3). In 2013 and 2014 the mean internal dose is double as high for persons above the age of 35. This difference levels out in 2015.

Table 3: Statistical analysis of the internal doses at the municipality Volincy [7]. All values are given in the unit mSv/a.

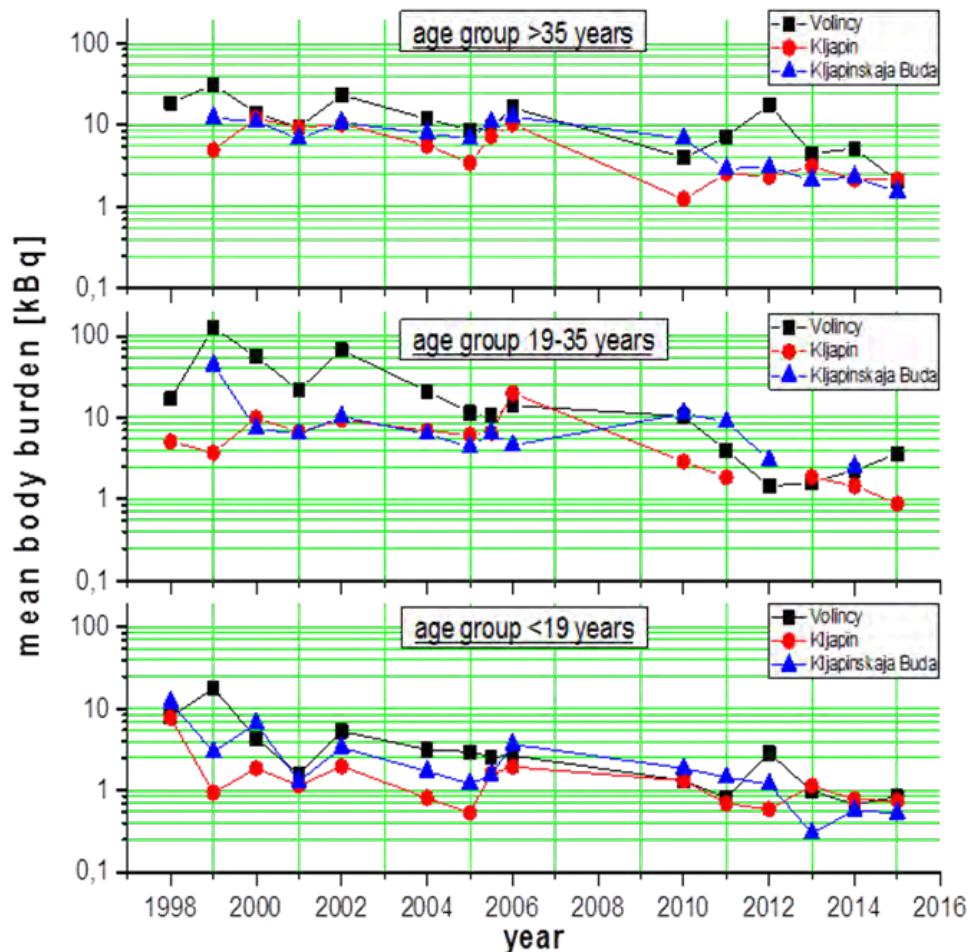
	2013	2014	2015
Arithmetic mean	0.10	0.10	0.07
Maximum value	0.80	0.66	0.80
Standard deviation of mean value	0.12	0.13	0.10
95%- quantile	0.31	0.42	0.18
5%-quantile	0.00	0.00	0.00
Arith. mean <19 y	0.06	0.04	0.05
Arith. mean 19-35y	0.07	0.08	0.09
Arith. mean >35 y	0.13	0.16	0.08

3.3 The long-time evolution of internal dose

In this section information communicated before (e.g. [1], [3]) is updated to include the newly available data. Since 1998 about 560 different inhabitants of Volincy municipality had their body burdens and internal doses assessed. Many of them participated in the measurements several times. More than 2600 mobile in-vivo measurements had been performed in the three settlements investigated. Actually there have been quite some more measurements than that (31 more merely in 2015). However inhabitants of other settlements have been excluded from the later detailed analysis of the results. There are also no data points available for the years 2003, 2007, 2008 and 2009 since there have been no field missions.

Figure 4 shows the evolution of the mean body burdens with time. It proved to be useful to distinguish three different age groups: firstly all children and youths being up to 18 years old, secondly young adults between the age of 19 years and the age of 35 years and thirdly the persons being older than 35 years.

Figure 4: Evolution of body burdens with time [7].



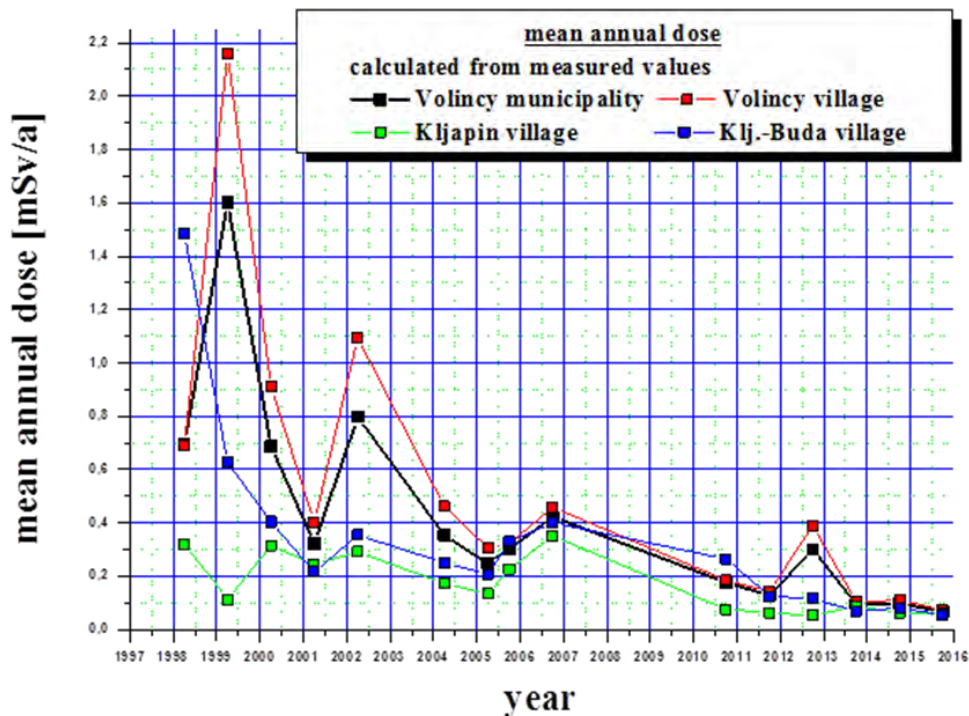
Whereas for the age group of 19-35 years old in the other two settlements the mean body burden is comparable to other adults, at Volincy up to the 4-5 fold has been observed in some years. It seems that members of this age group were in this place especially careless in consuming forest products and contaminated meat. After thorough individual counsel mean values in 2005 and 2006 finally had been closer to those of the older adults. By 2015 all differences have been leveled out.

Completely different is the situation in the age group of younger people. Children and teens usually receive meals at school. There normally 'clean' foodstuff is used. It seems that additional meals consumed at home do not create any considerable ingestion and the body burden is quite low. Even when parents eat food from the contaminated forest and occasionally even some piece of wild boar they forbid this food to their children.

The body burdens in Volincy village have been higher than in the other two villages. From a maximum in 1999 over the time body burdens dropped significantly and stabilized at reasonable values.

In figure 5 the evolution of the mean annual internal dose is shown without regard to a differentiation of age groups. Please note that the numerical value of the year in the x-axis marks the beginning of the year. As with the body burdens the highest values of the dose have been observed in 1999 for Volinc village. This is mainly due to the high influence of the age group of the 19-35 years old on the mean values.

Figure 5: The evolution of the mean annual dose with time [7].



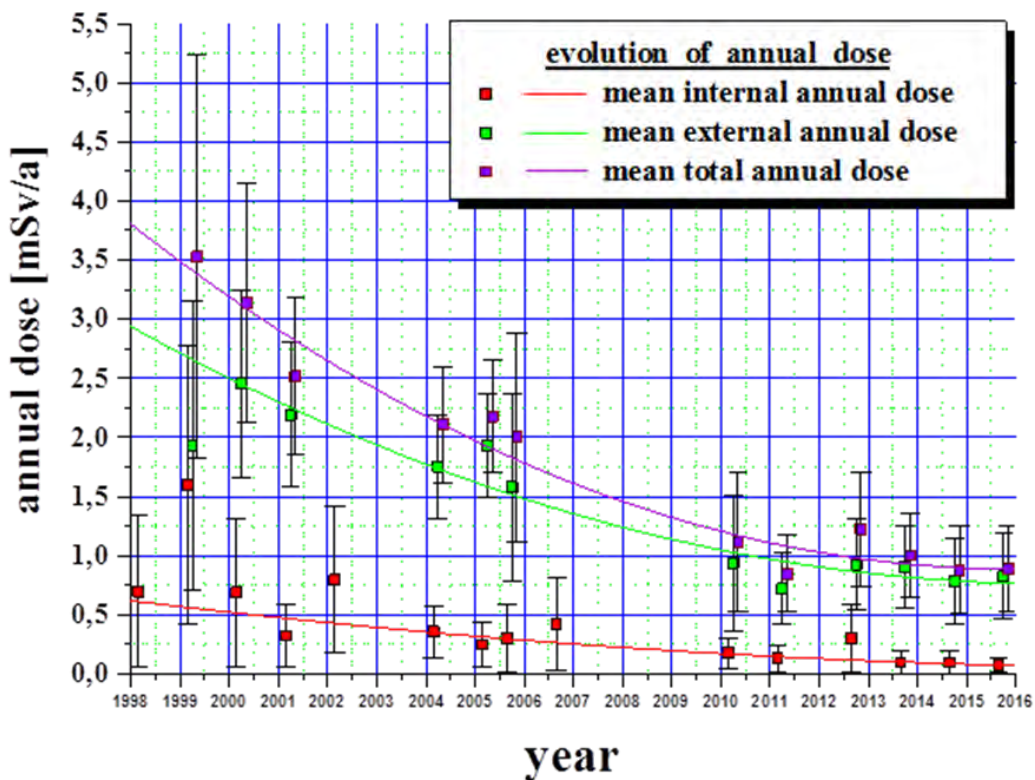
Due to the measurements people became knowledgeable about their internal contamination. This and individual counsel provided by the German team led to a changed attitude towards the consumption of contaminated food. Till spring 2001 the internal dose had significantly dropped. Then people were told, that it would not be possible to continue the measurements. However, some funds were found for another field mission in spring 2002. Meanwhile the ingestion dose had again increased by almost a factor of three in Volincy village and about 50% in the other two villages. The changed attitude had not yet been stabilized sufficiently. A slight increase in autumn 2006 affected all villages and may be connected to a especially large harvest of mushrooms and the end of the mushroom season correlating with the field mission.

At Kljapinskaya-Buda the mean internal dose has a much smoother curve shape than in Volincy, but is also dropping down from high values. At Kljapin the progression of the dose curve is rather flat at an already low level. Since the school is located some of the inhabitants are employed there and most likely have access to some on the road clean food.

Since autumn 2010 mean internal doses have been dropping slowly at generally reasonable levels and in 2015 are at the same level for all villages. Recent societal changes further the consumption of clean food. Presently there is only one cow left in Volincy and people buy milk products in a shop. The supply of clean food from outside the contaminated zone has increased, especially since road conditions have changed to the better and a new bridge over the Sotch has replaced the old one on the road to Korma town.

To evaluate the long-term development of population dose besides the internal dose the external dose has to be considered. During the field missions also information on the external dose has been gathered. More details are given in references [1], [3] and [7]. Figure 6 shows the evolution of population dose in Volincy municipality. The external dose governs the total dose. It has been determined in a very conservative approach. Therefore the population dose given may be considered as an upper limit to the true dose. Nonetheless it can be seen, that the mean annual dose has dropped to values below the general annual dose limit of 1 mSv/a.

Figure 6: The evolution of mean annual dose for Volincy municipality [7].



4 SUMMARY

Radiological long-term assessments have been performed between 1998 and 2011 in a region in Belarus contaminated by fall-out from the Chernobyl accident. The internal radiation exposure of the inhabitants in the municipality of Volincy (Korma County) has been followed-up and experienced a significant decrease from a very high level (table 4).

Table 4: The decrease of internal doses at Volincy municipality [7].

year	Mean internal dose (mSv/a)	Maximum (mSv/a)
1999	1.6	24
2015	0.07	0.80

Through in-vivo monitoring measurements people have become knowledgeable about their actual body burden. In addition to the measurements, a relationship based on mutual trust allowed to offer the inhabitants individual counsel on how to reduce internal contamination. Recent societal changes also further the consumption of clean food. Presently the internal exposure is only slightly enhanced over background values and of no special relevance to health. Taking into account the contribution of external dose the mean annual dose dropped below 1 mSv/a.

5 ACKNOWLEDGEMENTS

Funds from the Walter-Gastreich-Foundation are gratefully acknowledged. The authors like to thank Valerie Majewski and Tamara Bislukova from the Korma County Hospital for their hospitality and strong support. A special thank is due to the members of the 2013 to 2015 field missions, namely Frank Bast, Thomas Gorgels, Wolfgang Marquardt, Edith Preuß-Offermann. Also the essential contribution to the earlier stages of work by Ralf Hille, Jürgen Höbig, Reinhard Lennartz and Heinz Preiß has to be mentioned.

6 REFERENCES

- [1] Dederichs, H., Pillath, J., Heuel-Fabianek B, et al., 2009. Langzeitbeobachtung der Bevölkerung in radioaktiv kontaminierten Gebieten Weißrusslands – Korma-Studie. Schriften des Forschungszentrums Jülich, Reihe Energie&Umwelt: Vol.31. Jülich: Forschungszentrum Jülich GmbH; 2009. ISBN: 978-3893365623 (in German).
- [2] Dederichs, H., Pillath, J., Lennartz, R., et al., 2004. The time-dependent effect of the biological component of Cs-137 soil contamination. *Kerntechnik* 69, 58-65.
- [3] Dederichs H., Heuel-Fabianek B., Hill P., et al., 2011. Long-term development of incorporation dose at Korma County (Belarus) after the Chernobyl accident. Proc. Third European IRPA Congress, 14-18 June 2010, Helsinki, Finland, P10-26, pp. 1711-1720; Electronic publication, August 2011. Retrieved 2016-05-12 from: <http://www.irpa2010europe.com/pdfs/proceedings/S10-P10.pdf>.
- [4] Hille, R., Hill, P., Heinemann, K., et al., 1996. The Impact of the Chernobyl Accident – an Evaluation from the German Perspective. *Berichte des Forschungszentrum Jülich, Jül-3186*. Jülich: Forschungszentrum Jülich GmbH, ISSN 0944-2952.
- [5] Hill, P., 1993. A Whole Body Counter for Babies and Toddlers. In: Proc. FS-SFRP Joint Seminary 'Environmental Impact of Nuclear Installations', Fribourg/Switzerland, 15th - 18th September 1992, Radioprotection, Special Issue, (ed. H. Voelkle, S. Prêtre), Les Ulis CEDEX 1993, ISBN-2-86883-183-6, p. 543-546.
- [6] Kovtun, A.N., Firsanov, V.B., Fominykh, V.I., et al., 2000. Metrological Parameters of the Unified Calibration Whole-Body Phantom with Gamma-emitting Radionuclides. *Radiation Protection Dosimetry* 89, 239-242.
- [7] Zoriy, P., Dederichs, H., Pillath, J., et al., 2016. Langzeitbeobachtung der Bevölkerung in radioaktiv kontaminierten Gebieten Weißrusslands – Korma-Studie.II (1998-2015). Schriften des Forschungszentrums Jülich, Reihe Energie&Umwelt: Vol.315. Jülich: Forschungszentrum Jülich GmbH; 2016. ISBN: 978-3-95806-137-8 (in German; English version in the making).
- [8] ICRP, 1994. Age-dependent doses to members of the public from intake of radionuclides - Part 2 Ingestion Dose Coefficients. ICRP Publication 67. *Ann. ICRP* 23 (3-4).

In preparation for future reduction of the dose limit for the lens of the eye – an assessment at Swedish nuclear facilities

V. Nilsson^{a1}

^aSwedish Radiation Safety Authority, SE-171 16 Stockholm, Sweden.

Abstract. The International Atomic Energy Agency adopted the reduced dose limit for eye lens in *Radiation Protection and Safety of Radiation Sources: International Basic Safety Standards, General Safety Requirements Part 3 No. GSR Part 3 (Interim)* in September 2011 followed by GSR Part 3, in July 2014. Reduction of the dose limit to the lens of the eye followed the recommendation of the International Commission on Radiological Protection in its *Statement on Tissue Reactions* in April 2011. The *Council Directive 2013/59/EURATOM of 5 December 2013 laying down basic safety standards for protection against the dangers arising from exposure to ionising radiation*, is to be complied with by all Member States by 6 February 2018. In process of preparing *Implications for Occupational Radiation Protection of the New Dose Limit for Lens of the Eye*, IAEA TECDOC 1731, 2013, it became obvious that more information was needed concerning equivalent doses to the lens of the eye at Swedish nuclear facilities. The Swedish Radiation Safety Authority initiated an assessment of the conformity of dosimeters used to measure dose to the lens of the eye at Swedish nuclear facilities in April 2013. The assessment included a survey regarding the types and levels of radiation present at the facilities in question, in/on the systems, and doses during different types of tasks performed. The area and/or extent of operations can vary greatly between the different facilities. Results indicate that a need might exist for implementing a programme for monitoring dose to the lens of the eye, in accordance with the guidelines given in ISO 15382:2015 (E) *Radiological protection -- Procedures for monitoring the dose to the lens of the eye, the skin and the extremities*, for certain work places and certain fields of work at Swedish nuclear facilities.

1 INTRODUCTION

In April 2011, in its *Statement on Tissue Reactions*² [1] the International Commission on Radiological Protection (ICRP) issued new recommendations for a reduced dose limit for the lens of the eye for occupational exposure in **planned exposure situations**. ICRP recommended a dose limit for equivalent dose to the lens of the eye of 20 mSv in a year, averaged over defined periods of five years, with no single year exceeding 50 mSv.

The International Atomic Energy Agency (IAEA), following the recommendation of the ICRP, adopted the reduced dose limit for the lens of the eye in *Radiation Protection and Safety of Radiation Sources: International Basic Safety Standards, General Safety Requirements Part 3 No. GSR Part 3* in September 2011, [2], and in July 2014, [3].

In the process of preparing *IAEA TECDOC 1731 Implications for Occupational Radiation Protection of the New Dose Limit for Lens of the Eye* [4] it became obvious that more information concerning the existing doses to the lens of the eye at nuclear facilities was needed.

The *Council Directive 2013/59/EURATOM of 5 December 2013 laying down basic safety standards for the protection against the dangers arising from exposure to ionising radiation (EU BSS)* [5], including the reduced dose limit for the lens of the eye, was adopted in December 2013. The new directive is to be complied with by all Member States by 6 February 2018.

The Swedish Radiation Safety Authority (SSM) initiated an assessment of the conformity of dosimeters used to measure dose to the lens of the eye at Swedish nuclear facilities in April 2013.

The aim of the assessment is to ensure correctness of results when it comes to dosimetric methodology, accurateness of measurements and conclusions drawn. The aim is also to ensure compliance with the future reduced dose limit for the lens of the eye at Swedish nuclear facilities. A

¹ Author, e-mail: Virva.Nilsson@ssm.se

² ICRP ref 4825-3093-1464

system and a programme for monitoring dose to the lens of the eye is to be in place, if and/or when needed, by the time when the EU BSS is to be complied with. A plan for future needs to exist at the facilities, regarding monitoring of dose to the lens of the eye, also in case when the area and/or extent of the operations at the facility will change.

2 DESCRIPTION OF THE ASSESSMENT

In process of preparing *IAEA TECDOC 1731 Implications for Occupational Radiation Protection of the New Dose Limit for Lens of the Eye* [4] it became obvious that more information concerning the existing doses to the lens of the eye at nuclear facilities was needed.

Eight Swedish nuclear facilities or licensees are participating in this assessment, as presented in Fig. 1:

- Three nuclear power stations in operation, a total of ten reactor units:
 - Three boiling water reactor (BWR) units in Forsmark,
 - Three BWR units in Oskarshamn, and
 - One BWR and three pressurized water reactor (PWR) units in Ringhals.
- One nuclear power station to be decommissioned, a total of two BWR units in Barsebäck.
- One licensee, AB SVAFO, dealing with decommissioning services and waste management operating, among other sites, in Ranstad and Studsvik.
- One licensee, SKB, managing and disposing of all radioactive waste from Swedish nuclear power plants operating both in Forsmark and Oskarshamn.
- One licensee, Studsvik Nuclear AB, dealing with advanced technical services to the international nuclear power industry in such areas as waste treatment, consultancy services and fuel and materials technology operating in Studsvik.
- One nuclear fuel fabrication plant, Westinghouse Electric Sweden, dealing with nuclear services and nuclear automation as well operating in Västerås.

Figure 1: Location of Swedish nuclear facilities or licensees.



The area and/or extent of operations varies greatly between facilities or licensees.

Each facility or licensee was to assess:

- radiation fields present at their facility/within the area of operation,
- critical tasks where significant equivalent dose to the lens of the eye might be obtained,
- critical occupational categories that might obtain significant equivalent dose to the lens of the eye when executing their tasks, and
- effectiveness of personal protective equipment (PPE) used in order to protect the eyes at the facility/within the area of operation.

3 CONDUCTING THE ASSESSMENT

Swedish nuclear facilities, or licensees participating in this assessment decided to cooperate in developing a methodology, with Vattenfall Research and Development (VRD) acting as coordinator. The assessment methodology and results have been presented at ISOE European Symposium in Bern in April 2014 by L. Bäckström [6].

The most accurate method for monitoring the equivalent dose to the lens of the eye, according to *IAEA TECDOC 1731*, [4], is to measure the personal dose equivalent at 3 mm depth, $H_p(3)$, with a dosimeter calibrated on a phantom representative of the head and worn as close as possible to the eye. Monitors and dosimeters for other quantities may be used according to [4]. The use of other quantities, though, might be questionable according to Behrens and Dietze [7].

Further, in order to ensure an appropriate individual monitoring, monitors and/or dosimeters should comply with internationally agreed performance requirements. During the period of conducting the assessment dosimeters designed for measuring $H_p(3)$ were not widely available.

As in many countries, $H_p(3)$ has not yet been implemented in legal metrology in Sweden, and only $H_p(0.07)$ and $H_p(10)$ are used for monitoring radiation exposure of workers in accordance to *Radiation Protection 73, Technical recommendations for monitoring individuals occupationally exposed to external radiation* [8]³. These recommendations have since been revised in 2009, in *Radiation Protection 160, Technical recommendations for monitoring individuals occupationally exposed to external radiation* [9]⁴. The revision of the Swedish regulations is on-going, but has not yet been completed. Therefore, revised recommendations in accordance to [9] have not yet been implemented, either.

The dosimeter chosen by Swedish nuclear facilities for conducting the assessment was a $H_p(3)$ calibrated thermoluminescent dosimeter from Public Health England (PHE) Personal Dosimetry Service (PDS), EXTRAD™, together with a polytetrafluoroethylene (PTFE) filter. The dosimeter has been type tested by PHE, as accounted for in *Type testing of a head band dosemeter for measuring eye lens dose in terms of $H_p(3)$* , [10].

A number of tests were conducted by the Swedish nuclear facilities, or licensees, in order to confirm compliance with *SSM's regulations concerning basic provisions for the protection of workers and the general public in practices involving ionising radiation*, [11]. Irradiations for the tests were carried out at the Physikalisch-Technische Bundesanstalt (PTB) in Germany. Both photon and beta radiation qualities used in irradiations were chosen to be those representative of energies most common at the facilities.

4 RESULTS

4.1 Calculations

As part of the assessment a series of calculations based on the facilities' activity inventory were executed to estimate equivalent dose to the lens of the eye from photon and beta radiation fields [6].

The estimates regarding photon radiation were calculated with MicroShield software. For calculation of the estimates regarding beta radiation MCNP5 software was used. A number of cases involving ion exchange resins and surface contamination were calculated. The calculations resulted in dose estimates and a number of recommendations for in situ measurements.

³ Available at: <https://ec.europa.eu/energy/sites/ener/files/documents/rp73.pdf>

⁴ Available at: <https://ec.europa.eu/energy/sites/ener/files/documents/160.pdf>

Two kinds of situations were identified as most likely to result in higher equivalent doses to the lens of the eye. The first situation involved personnel working on contaminated open systems at nuclear power plants in operation and where the source of radiation originates from deposited oxide layers (CRUD⁵). The second kind of situation identified personnel at nuclear fuel fabrication plants preparing uranium powder and performing control tasks.

For personnel whose trunk, but not the eyes/head, could be shielded, the dose to the lens of the eye might not be correctly assessed by a trunk dosimeter.

When performing tasks on open systems at nuclear power plants in operation, dealing with heavily surface contaminated objects and/or ion exchange resins the personnel is most often being exposed to mixed radiation fields.

According to the calculations, in beta radiation fields present at the facilities, the PPE provides good protection for the eyes/head. In photon fields, according to the calculations, and as expected, the PPE does not provide any protection for the eyes. According to the calculations, in photon fields, the material of PPE could, in some cases, slightly enhance the dose to the eye lens.

4.2 In situ measurements

A reference group, per facility, or licensee, was chosen. The test groups chosen at the facilities consisted of radiation protection technicians, mechanics, welders, laboratory engineers, operators preparing uranium powder, as well as personnel working with waste management, insulation, cleaning/decontamination, melting contaminated metal and servicing control rod drive mechanisms. Some of these groups of personnel had been identified as most likely to receive a significant dose to the lens of the eye by the results of the calculations.

In situ measurements were conducted during the period October–November 2013.

According to *SS-ISO 15382:2015 (E), Radiological protection - Procedures for monitoring the dose to the lens of the eye, the skin and the extremities* [12], monitoring of dose to the lens of the eye shall be undertaken if an equivalent dose in a single year exceeds 15 mSv, or, if in consecutive years, more than 6 mSv per year to the lens of the eye is likely to be received. The latter would correspond to an equivalent dose in excess of 0.5 mSv in consecutive months per year to the lens of the eye. For equivalent dose levels expected to be lower than these values, a survey is sufficient to demonstrate that the above levels are not exceeded.

The highest equivalent dose over one month to the lens of the eye for one individual during the period of in situ measurements was 2.9 mSv. The dose measured by the trunk dosimeter for the same individual, over the same month was 2.3 mSv. The individual in question performed decontamination work at a nuclear power plant in operation.

Results from in situ measurements, in cases where the equivalent dose to the lens of the eye, over one month, was equal to or exceeded 0.5 mSv, as well as tasks performed by individuals in question, during the period October–November 2013 are presented in Table 1 below.

⁵ Chalk River Unidentified Deposits

Table 1: Equivalent doses, equal to or exceeding 0.5 mSv over one month to the lens of the eye, during the period of in situ measurements.

Facility	October		November		Tasks performed during the period
	[mSv]		[mSv]		
	$H_p(3)$	$H_p(10)$	$H_p(3)$	$H_p(10)$	
Forsmark	0.6	1.3	0.6	0.5	Oct: Mechanical work in the containment Nov: Handling liquid waste
Oskarshamn	2.9	2.3	1.2	1.1	Oct: Decontamination work Nov: Radiation Protection work
Ringhals	1.0	1.4	0.6 (3 pers.)	1.0, 0.8, 0.3	Oct: Mechanical work, valve overhaul Nov: Decontamination work (2 pers.), cleaning work (1 pers.)
Studsvik	1.5	1.5	0.8	0.7	Oct: Melting contaminated metal (steam generator tubes) Nov: Waste handling
Westinghouse	0.6	0.3	0.7	0.5	Oct: Preparing uranium powder Nov: Control of fuel assemblies

In situ measurements confirmed that, in beta radiation fields present at the facilities, the PPE provides good protection. There was no indication that, in photon fields, the material of PPE could slightly enhance dose to the lens of the eye, as was indicated by calculations [6].

5 DISCUSSION AND CONCLUSIONS

According to *SS-ISO 15382:2015 (E), Radiological protection - Procedures for monitoring the dose to the lens of the eye, the skin and the extremities* [12], monitoring of dose to the lens of the eye shall be undertaken if an equivalent dose in a single year exceeds 15 mSv, or, if in consecutive years, more than 6 mSv per year to the lens of the eye is likely to be received. The latter would correspond to an equivalent dose in excess of 0.5 mSv in consecutive months per year to the lens of the eye. For equivalent dose levels expected to be lower than these values, a survey is sufficient to demonstrate that the above levels are not exceeded.

SSM is currently reviewing the assessment reports delivered by Swedish nuclear facilities in cooperation with VRD.

Results from the in situ measurements show that at nuclear power plants in operation, at waste treatment facilities and at nuclear fuel fabrication plants a risk exists, that equivalent dose to the lens of the eye, in consecutive years, might exceed 6 mSv per year for certain occupational categories of personnel and/or tasks. A test period of monitoring equivalent doses to the lens of the eye of possible risk groups more closely is planned to be implemented at these facilities.

In situ measurements have continued at nuclear power plants in operation in order to achieve a wider picture of some occupational categories, possible risk groups who might need regular monitoring of the equivalent dose to the lens of the eye, both during operation and during outage.

In a number of cases a trunk dosimeter can be considered to provide a good enough estimate for equivalent dose to the lens of the eye at Swedish nuclear facilities. In certain cases a dosimeter calibrated for $H_p(10)$, and even $H_p(0.07)$ complemented with a filter, can provide a good enough estimate for the assessment of equivalent dose to the lens of the eye.

Guidelines are in place at the facilities concerning the correct use of PPE. For beta radiation fields present at the facilities PPE provides good protection.

At some of the facilities area and/or extent of operations is to be expanded in the future. Nuclide vectors have been developed in order to assess and evaluate the tasks and occupational categories to

undergo test periods of monitoring equivalent doses to the lens of the eye, prior to extending or introducing new areas of operation.

The aim of this assessment is to ensure compliance with the reduced dose limit for equivalent dose to the lens of the eye at Swedish nuclear facilities as well as to confirm the compliance with *SSM's regulations concerning basic provisions for the protection of workers and the general public in practices involving ionising radiation* [11]. A system and a programme for monitoring equivalent dose to the lens of the eye is to be in place, if and/or when needed, by the time when the EU BSS is to be complied with in February 2018. A plan for future needs to exist at the facilities for monitoring equivalent dose to the lens of the eye, in case the area and/or extent of the operations at the facility will change.

6 REFERENCES

- [1] ICRP, 2011, Statement on Tissue Reactions, International Commission on Radiological Protection.
- [2] IAEA, 2011, Radiation Protection and Safety of Radiation Sources: International Basic Safety Standards, General Safety Requirements Part 3 No. GSR Part 3 (Interim), International Atomic Energy Agency, Vienna.
- [3] IAEA, 2014, Radiation Protection and Safety of Radiation Sources: International Basic Safety Standards, General Safety Requirements Part 3 No. GSR Part 3, International Atomic Energy Agency, Vienna.
- [4] IAEA, 2013, Implications for Occupational Radiation Protection of the New Dose Limit for Lens of the Eye, IAEA TECDOC 1731, International Atomic Energy Agency, Vienna.
- [5] EC, 2013, Council Directive 2013/59/EURATOM of 5 December 2013 laying down basic safety standards for protection against the dangers arising from exposure to ionising radiation, European Commission, Brussels.
- [6] Andgren, K., Bäckström, L., 2014, Equivalent dose to the lens of the eye at nuclear facilities and shielding factors for protective eye wear – measurements and calculations, ISOE Symposium, Bern.
- [7] Behrens, R., Dietze, G., 2010, Monitoring the eye lens: which dose quantity is adequate? *Physics in Medicine and Biology* 55, pp. 4047-4062.
- [8] EC, 1994, Radiation Protection 73, Technical recommendations for monitoring individuals occupationally exposed to external radiation, Report EUR 14852 EN, European Commission, Luxembourg.
- [9] EC, 2009, Radiation Protection 160, Technical recommendations for monitoring individuals occupationally exposed to external radiation, Final Report of Contract TREN/07/NUCL/S07.70121, European Commission, Luxembourg.
- [10] Gilvin, P. J. et al., 2013, Type testing of a head band dosimeter for measuring eye lens dose in terms of Hp(3), *Radiation Protection Dosimetry*, pp. 1-7.
- [11] SSM, 2008, SSMFS 2008:51, Swedish Radiation Safety Authority's regulations concerning basic provisions for the protection of workers and the general public in practices involving ionising radiation, Swedish Radiation Safety Authority, Stockholm.
- [12] SIS, 2015, SS-ISO 15382:2015 (E), Radiological protection - Procedures for monitoring the dose to the lens of the eye, the skin and the extremities, Swedish Standards Institute, Stockholm.

Findings of radiological events in the Centre of Isotopes in Cuba

Zayda Haydeé Amador Balbona*

Centre of Isotopes, Ave. Monumental y carretera La Rada, Km 31/2, San José de Las Lajas, Mayabeque, Cuba.

Abstract. It is internationally recognized that sharing the findings of radiological events is a useful tool to prevent their recurrence. This paper aims to summarize the lesson learned in the Centre of Isotopes (CENTIS), the highest radioactive facility and the main carrier of radioactive materials in Cuba in the period covering 1997-2015. Specific potential accident scenarios are assessed by identifying maximum radioactive inventories, operational procedures, room dimensions and ventilation system parameters and transport of RAM. The dose constraints are taken as a reference, considering the achievement of ALARA principle. Spills of ^{131}I in controlled zone are mainly registered. It has been not reported any incident in about three thousand and half road shipments carried out. Results show an important contribution of the human factor in radiological events and for this reason, the promotion of a safety culture plays a key role.

KEYWORDS: *Radiological events; production of radiopharmaceuticals; emergency preparedness and response.*

1 INTRODUCTION

The Centre of Isotopes (CENTIS) of the Republic of Cuba is located in a rural area about 30Km to the southeast of Havana. The facility itself consists of five buildings and 6E-02 Km² of property. Unsealed radioactive sources are handled in a building with an area of 3500 m². There is also a building for treatment and storage of radioactive wastes; witch has an area of 260 m². CENTIS is also the main consignor and carrier of the radioactive material in Cuba.

There is a prevalence of excepted and type A packages in about 250 shipping by year. Planning and preparedness for response to radiological occurrences are established in the Emergency Plan and operating procedures, in order to ensure a minimum damage to workers, public and facilities.

Since 1997 has been maintained a radiological event database (RED), taking into account a classification system [1], as a useful tool for the feedback process. The purpose of this paper is to share our findings from radiological events during 1997-2015 in CENTIS.

2 METHOD

2.1 Assessment of hazards

2.1.1 Radiological occurrences

The following potential radiological events for CENTIS are identified considering some reports from analogues radioactive facilities [2-3] and the international experience:

*Presenting author, e-mail:zabalbona@centis.edu.cu

- a) fires in radioactive material warehouses and fumehoods,
- b) liquid release of radioactivity,
- c) loss of the shielding of a radiation source,
- d) loss of containment,
- e) road transport accident with fire and severe damage to type A packages,
- f) loss or robbery of a radioactive material.

Maximum radioactive holdings and estimated exposure time are considered in dose assessment. Point sources are assumed for external exposure, because distances of 1-2m are selected.

For calculate hand equivalent doses ($H_p(0.07)$) and committed effective dose ($E(50)$), plane sources are assumed. Room dimensions, ventilation system parameters and a protection factor of 20 [4] for respiratory protective device are used to estimate $E(50)$. First responders are equipped with full-face masks and combined filters. The following issues reported in [5] are used re-suspension factor of $1E-04m^{-1}$; rates external exposure for point sources and rate contamination skin doses for uniform deposits. The radionuclide committed effective doses per unit intake by inhalation are taken from [6-7]. Skin transfer factor equal to $1E-03 A/m^2$ [8] and an hour exposure time to hands are adopted due to broken gloves during operations.

Two fire scenarios at CENTIS are identified shipping/receiving area with spreading to adjacent radiopharmaceutical storage facility and radioactive waste warehouse. It is supposed that there are some type A packages in the radiopharmaceutical warehouse, with authorized maximum total activities. Annual radioactive inventory in the waste warehouse is assumed. In both cases the source term (activity by radionuclide in the airborne discharges) is calculated using Flew and Lister's methodology [9], but considering the release fraction per radionuclide (R_f) suggested by McGuire [10]. Release package fraction is adopted from [8] for the first scenario.

We assume airborne releases during half hour and to ground level. Gaussian plume model for atmospheric dispersion is applied with the standard deviation expressed according to the Pasquill's categorization scheme of weather conditions [11]. All pathways of exposure for critical group, except milk ingestion, are considered to a distance of 200m from the source. Milk is obtained to 200-250m from the emission point. The occurrence of fires in fumehoods with tritium and carbon are included too, since welding operations of bulb to distillation facility are executed. It is adopted that a fraction equal to $5E-05$ of HT up taken activity is converted to HTO in human body [12].

Loss of the shielding of a radiation source is only considered for ^{99}Mo during input operation to hot cell, because its solution is containment in a polyethylene bottle.

The loss of containments with 0.16TBq of ^{131}I , 12GBq of ^{125}I and 22.7GBq of ^{32}P in the workplaces of controlled area is evaluated and for 0.37TBq of 3H , but in supervised area. For worker is adopted 1 min of exposure and in the case of emergency of first-responders five times this figure. We consider that human mistake is the cause of liquid radioactive waste discharge with $4.4E+07Bq$ of ^{131}I in a volume of $6m^3$ from drainages treatment system. This is diluted in one order due to its mixing with sewer waters and passing through a filtration system [13].

The ^{131}I concentration at downstream distance of 500m is reduced by a factor of 1000 [13-14] and equal to $7.3E+03 Bq/m^3$. This release occurs during 30min.

For road transport accident with fire and severe damage to type A packages, the Gaussian plume model is also adopted, but using neutral meteorological conditions. The basic hypotheses are as follows: point source release to ground level, open downwind surface (no obstacles), release fraction of $1E-02$ [8] and release time of 30 min. First responder's exposure is evaluated to 2m from source and for 15min. It is supposed the permanency of an infant during an hour at distance of 100m from the place of accident since establishing the cordoned area 100m around the vehicle.

2.1.2 External occurrences

The natural events that can happen at CENTIS' site are earthquakes, tornados and hurricanes. The earthquakes do not have a dispersive force enough to cause a significant emission of radioactive material to the environment. Their fundamental radiological consequence is the overturn and rupture of recipients with a located contamination of surfaces [15]. Another possible consequence is the break of buried pipes of special wastewaters system [16]. It is supposed that this break happens in the lowest point and the pipe with $5.1E-02$ m of diameter is filled in 30 percent of its capacity. This contains a waste with low activity ($370MBq/m^3$) and about $0.4m^3$. This spill is completely absorbed; because of the land has a very low permeability. Nevertheless, dilution of this activity in the underground waters has an insignificant contribution to dose for public. The probability of occurrence of the probable maximum tornado in the location is very low ($3.5E-05/year$). The reach and magnitude of the conventional damages will be dominant on any radiological consequence to public, since radioactive material is diluted in the great volume of air [15]. The probability of maximum hurricane in site is low. Its effect is diminished through preventive measures. Radiological consequences will not exist for public since limited radioactive inventory and a high dilution with hurricane's winds.

The aircraft fall has a very low probability ($1E-08/year$). Explosion and fire associated with this event would destroy the building of plant. The described methodology for the atmospheric release of radioactivity due to fires in the radioactive material warehouses, are also performed for this case.

2.2 Emergency preparedness and response

2.2.1 Emergency Plan

The potential hazards related to the relevant practices are considered in the Emergency Plan [1] as well as 2 conditions for plant's operation (working hours and free time). There are established control and protection actions for each case. This plan has been revised taking into account [18-19].

Suitable sets of individual protective means are guaranteed. Dose rate and dose monitors are annually verified in the Second Calibration Laboratory of Cuba. Superficial contamination monitors are tested every two months.

Initial training of staff covers evaluation of instructions and procedure for each kind of occurrence. The review of learned lessons from incidents is included in a periodic training programme.

Four emergency full-scale exercises are made with simulation of fires and communications checks with offsite response organizations [20]. Emergency Plan and procedures are revised after exercises and each two years. Lessons learned from this exercises in 1999, 2000, 2004, 2007, 2009, 2011, 2013 and 2015 represent a feedback process to improve emergency response for CENTIS and off-site authorities.

2.2.2 Review of occurrence reporting data

In the period, covering 1997-2015 is collected following sub-set of radiological event's data: date, occurrence's description, cause (human mistake or equipment failure), classification for occurrence and measured exposure and classification, in a database (RED). Those events increase occupational exposure are classified as incidents [1].

The number of occurrences gathered per month (ORN) is used as indicator data. This indicator empirically appears to fit the "Poison" model. For this reason, a control chart, type c-chart and its periodical exam are used as a tool for taking of decisions and actions, as it is recommended in [21].

These following issues are calculated: average of ORN (Avg), the standard deviation (sigma) as the square root of Avg and the Upper Control Limit (UCL) as the adding of three times sigma to Avg. The analysis of baseline data to look for trends and determine how to detect a significant event is also based on the criteria from Reference [21]. For this reason are determined the total points in a row outside of one sigma above the Avg and in a row outside of two sigma above Avg. As examples, a c-chart for those biannual periods with major values of ORN is created.

In order to take into account the radiological impact and efficacy of the first responders' actions, the number of incidents per year is another indicator used when analyzing trends. Temporal distribution of maximum values of dosimetric magnitudes (effective dose (E), hand equivalent dose (Hp (0.07)) and lens equivalent dose (Hp(3))) are plotted on a graph. These and radiological exposure from incidents are compared.

2.2.3 Dose assessment in emergency response

The employment of electronic direct reading personal dosimeter DOSICARD (Eurisys Mesures, France) and EPD MK2+ (Thermo Scientific, United Kingdom) are reported very good experiences. With these dosimeters are measured personal deep equivalent dose Hp(10) from 1 μ Sv up to 10 mSv and rate doses to 1 Sv/h. They have light and sound alarms. It low register level and alarms haven been very useful when new practices are evaluated and control the most risk operations.

Radiobioassay in vivo is performed for gamma-beta emitters. A Wallac 1409 model is used for in vitro monitoring of ^{32}P , Tritium and ^{90}Sr , with a liquid scintillation universal cocktail (INSTAL-GEL). The reported uncertainties are less than 20 percent.

3 RESULTS

3.1 Assessment of hazards

The calculated activity of airborne releases due to a fire of the radiopharmaceuticals and radioactive wastes warehouses are shown in Table 1 and Table 2 shows the projected doses. There are some doses less than recording levels. These results allow us conclude that there is not necessary to relocate the public [4]. It was necessary improvements in the control of radioactive materials and it was installed a new physical protection system with access cards and TV cameras.

Table 1: Airborne releases by a fire, simulated in the warehouses of radiopharmaceuticals and radwastes.

Radionuclide	Total activity (Bq)		Rf		Release activity (Bq)	
	warehouse	radwastes warehouse	warehouse	radwastes warehouse	warehouse	radwastes warehouse
¹³¹ I	2.96E+11	1.5E+10	1E-03	1E-02	2.96E+08	1.5E+08
¹²⁵ I	9.30E+10	2.1E+10	1E-03	1E-02	9.30E+07	2.1E+08
³² P	2.27E+10	9.3E+08	1E-05	1E-04	2.3E+05	9.3E+04
⁹⁹ Mo	1.90E+12	7.4E+10	1E-05	1E-04	1.90E+07	7.4E+06
³ H	-	2.0E+13	-	1E-01	-	2.0E+12
¹⁴ C	-	9.3E+10	-	1E-01	-	9.3E+09

3.2 Review of occurrence reporting data

In the RED have gathered a total of 165 abnormal occurrences in the period 1997-2015 and 23 of them were classified as incidents. This means that 86.14% of them were classified as alert situation [1]. Nevertheless, there is no reported radiological event in the transport of radioactive material.

The findings of these events are the 54% of these are due to human mistake, there are 26 spills in 18 years of handling ¹³¹I, the maximum average rate of the event per month is of five during 2001-2002.

In spite of these, three of these took place in 2006-2007 (to see in Figure 1). The permanency of worker in a local with Technetium generator drove the maximum value of E and a later detection of the spill of type A package with a 278GBq of ¹³¹I in its a absorbent material inside the container, implied in 2011 the highest registered value of E(50) (to see Table 3).

Table 2: The worker, first responders and public projected exposures in CENTIS.

Occurrence	Worker		First responders		Public	
	E (mSv)	E (mSv)	Hp (0.07) (mSv)	E (mSv)	Ht (mSv)	
Fires	1E-02	16.1	584	2E-01	4.00	
Liquid release	-	-	-	6E-03	1E-01	
Loss of shielding	8E-01	-	-	-	-	
Loss of containment	3E-01	1.5	27	-	-	
Transport accident	-	7	-	3E-02	3E-01	

Incident of the maximum contribution to Hp(0.07) take place during the opening a package with 14.8GBq of ^{90}Sr with spill in controlled zone in 2006. The highest value of Hp(3) was in 2003 due to a bad distribution of workload in Technetium generators' elution. The annual limits are maintained [6]. Fires and liquid release of radioactivity did not occur. The projected value S for all operations in CENTIS [7], has not overcome.

The major account of ORN in the biannual period 2006-2007 was collected on June 2007. As can be determined in Figure 1, for this case there is one point outside of the UCL and this represents a significant shift [23]. Two spills, five important contaminations of personnel and external exposure due to execution of operations without shielding were registered in that month. Besides, there are 9 points in a row all above Avg for 2006 and 8 points for 2007. There are 6 points outside one sigma plus the Avg and 3 points above the line of 2 sigma plus Avg for the last year. This behavior involves more significant changes than for those events belongs to 2006.

Taking into account the above mentioned about the statistical data we could conclude that 2001 and 2007 are the most significant years over all studied period. There is a coincidence of some factors as changes of suppliers for ^{131}Ina and other materials. The number of radiological incidents per year is presented in Figure 2. As can be appreciated, a maximum figure of five incidents is registered in 2001 and 2002.

The maximum values of annual occupational exposure in the last twenty years are shown in Table 3. The highest values of workers and first responder's doses are 2.23mSv as E, 0.7mSv as E(50) and 50.49mSv as Hp(0.07). These values are acceptably low.

Fires and liquid release of radioactivity did not occur. Incident of the maximum contribution to E and Hp(0.07) take place during the opening a radioactive package with 14.8GBq of ^{90}Sr in controlled zone in 2006.

We can conclude there is no a good agreement between radiological impact of incidents and the highest values of occupational exposure. The origin of these is failing to the safety procedures for some worker. These situations have been detected when we have been received the registers from dosimetric service.

Figure 1: Control chart of radiological occurrences for 2006 and 2007.

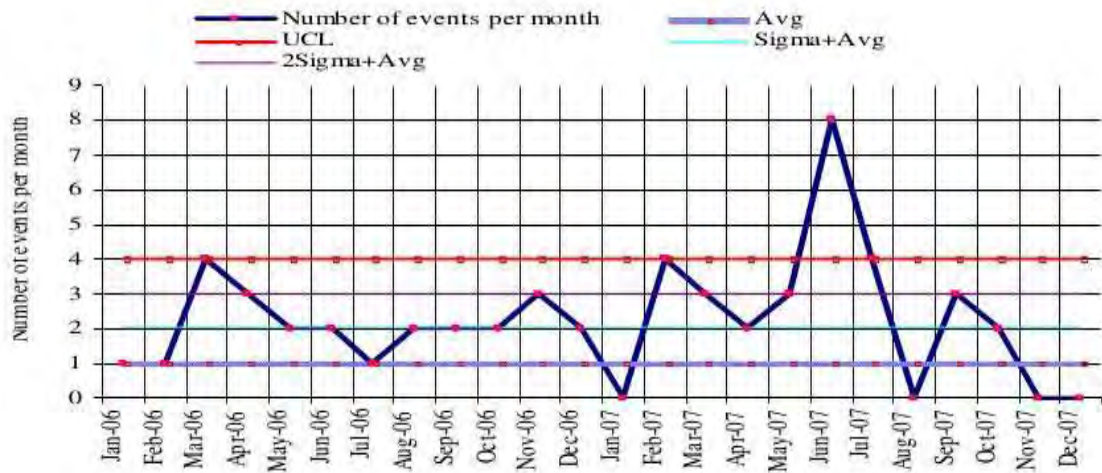


Figure 2: Number of radiological incidents per year in CENTIS.

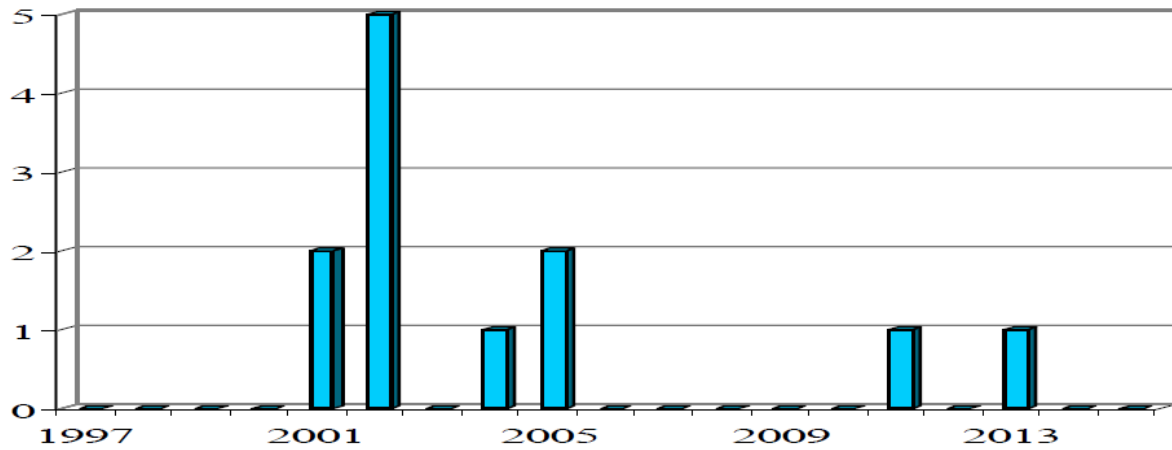


Table 3: Maximum values for dosimetric quantities and their respective dose constraints.

	E	Hp(0,07)	Hp(3)	S
	(mSv)	(mSv)	(mSv)	(man-mSv ⁻¹ y)
Dose constraints	12	200	15	200
1996	4.73	8.15	Not controlled	24.97
1997	4.02	8.56		16.38
1998	10.27	17.85	2.60	39.49
1999	4.85	49.38	4.38	30.50
2000	25.77	65.43	1.27	53.65
2001	3.22	117.97	1.90	35.49
2002	7.06	97.94	8.47	62.47
2003	5.89	91.47	12.09	74.75
2004	4.17	73.41	5.14	26.49
2005	6.52	145.17	5.89	35.22
2006	6.09	232.71	3.49	22.25
2007	2.96	117.70	3.86	16.51
2008	4.28	168.38	2.18	18.34
2009	5.32	172.49	4.85	42.07
2010	5.14	60.68	3.85	55.19
2011	9.13	194.6	12.05	98.26
2012	12.56	116.59	9.95	95.39
2013	13.23	159.23	7.49	77.43
2014	5.46	97.00	5.40	46.95
2015	6.68	125.14	8.75	57.48

4 CONCLUSIONS

In spite of assessed potential radiological events for CENTIS, findings reflect a human factor is generally a contributor to radiological events and the annual activity of education and training and the promotion of a safety culture plays a key role. The most likely events are radioactive spills.

External events have a low influence to safety, but if these events involve a fire in radioactive material warehouses, their consequences will be more significant.

The majority of the registered events has a low radiological impact and for this reason has been classified as alert situations. Only 13.9 % of them are incidents.

The implantation of the envisaged control and protection actions has been effective. Findings from operational experience and maintained infrastructure have contributed to CENTIS' emergency response capabilities.

5 REFERENCES

- [1] Cuban Nuclear Regulatory Authority, Guide for Preparedness and Response to Radiological Emergencies, Resolution No. 18/2012, Havana, (2012).
- [2] United States Nuclear Regulatory Commission, Source-Term Development for Evaluation of Emergency Preparedness Needs for Non-reactor Facilities, Health Physics, Vol. 50, N. 3, New York (1986) 399-403.
- [3] Amersham Corporation, Emergency Preparedness at a Non-Fuel Cycle Facility, 24th Annual Meeting of the Health Physics Society, Albuquerque (1989) 3-15.
- [4] British Standards Institution, Guide to Implementing an Effective Respiratory Protective Device Programme, BS 4275, London, (1997).
- [5] D. Delacroix, J. P. Guerre, P. Leblanc and C. Hickman, Radionuclide and Radiation Protection Data Handbook, Radiation Protection Dosimetry, Vol. 98 No. 1, Nuclear Technology Publishing, (2002).
- [6] European Commission, Food and Agriculture Organization of The United Nations, International Atomic Energy Agency, International Labour Organization, OECD Nuclear Energy Agency, Pan American Health Organization, United Nations Environment Programme, World Health Organization, Radiation Protection and Safety of Radiation Sources: International Basic Safety Standards, General Safety Requirements Part 3, IAEA Safety Standards Series No. GSR Part 3, Vienna (2014).
- [7] International Atomic Energy Agency, Assessment of Occupational Exposure Due to Intakes of Radionuclides, Safety Guide RS-G-1.2, Vienna (1999).
- [8] International Atomic Energy Agency, Advisory Material for the IAEA Regulations for the Safe Transport of Radioactive Material, 2012 Edition, SSG-26, Vienna (2014).
- [9] Flew, E.M., Lister, B.A.J., Assessment of the Potential Release of Radioactivity from Installations at AERE, Harwell, Implications for Emergency Planning. Handling of Radiation Accidents, Proceeding of IAEA' Symposium, Vienna (1969).
- [10] McGuire, S.A., A Regulatory Analysis on Emergency Preparedness for Fuel Cycle and Other Radioactive Material Licensees, Rep. NUREGF 1140 (Draft), USNRC, Washington DC (1985).
- [11] International Atomic Energy Agency, Atmospheric Dispersion Models for Applications in Relation to Radionuclide Releases, IAEA-TECDOC-379, Vienna (1986).
- [12] United States Department of Energy, Primer on tritium safe handling practices, DOE Handbook DOE-HDBK-1079-94, Washington D.C. (1994).
- [13] Santana R., Project of Hydraulic and Sanitary of the Centre of Isotopes, Havana (1989).
- [14] State Committee For Economical Collaboration, Basis of Design for Hydraulic and Sanitary, Havana (1986).

- [15] United States Nuclear Regulatory Commission, Preliminary Screening of Fuel Cycle and By- Product Material Licenses for Emergency Planning, NUREG/CR-3657, USNRC, Washington DC (1985).
- [16] International Atomic Energy Agency, Environmental Monitoring in Emergency Situations, Safety Series N° 18, IAEA, Vienna (1966).
- [17] Centre of Isotopes, Radiation Protection Department, Emergency Plan, DSR.DOC.002, Havana (2014).
- [18] Food and Agriculture Organization of the United Nations, International Atomic Energy Agency, International Labour Organization, OECD Nuclear Energy Agency, Pan American Health Organization, United Nations Office for the Co-Ordination Of Humanitarian Affairs, World Health Organization, Preparedness and Response for a nuclear or radiological Emergency, Safety Standards Series No. GS-R-2, IAEA, Vienna (2002).
- [19] International Atomic Energy Agency, Criteria for Use in Preparedness and Response for a Nuclear or Radiological Emergency, General Safety Guide, No. GSG-2, Vienna (2011).
- [20] International Atomic Energy Agency, Manual for First Responders to a Radiological Emergency, IAEA-EPR-First Responders Emergency Preparedness and Response, Vienna (2006).
- [21] International Atomic Energy Agency, Preparation, Conduct and Evaluation of Exercises to Test Preparedness for a Nuclear or Radiological Emergency, EPR-EXERCISE (2005) Emergency Preparedness and Response, Vienna (2005).
- [22] Perez S, Gatti A.M., Reyes R, Radiological Safety and Protection in the design of the centre of production radiopharmaceuticals and labelled compounds of Cuba, Nucleus No. 24, p. 36-44, Havana (1998).
- [23] Unites States Department of Energy, Project Hanford Management System Docs Online, Generating and Using Control Charts, HNF-PRO-4294, (2005).

Occupational Exposure in Production of Radiopharmaceuticals and Labeled Compounds in Cuba

Zayda Haydeé Amador Balbona, Miguel Antonio Soria Guevara

Centre of Isotopes, Radiation Protection Department, Ave. Monumental y Km. 3_{1/2}, carretera La Rada, Havana, Cuba.

Abstract. The purpose of this paper is to assess the occupational exposure from radiopharmaceuticals production and labeled compounds in the Center of Isotopes of the Cuban Republic. Data belong to the period covering 1996- 2015 are processed. Percentage annual distributions of E, Hp(0.07) and Hp(3) are showed. Annual mean values of these dosimetric magnitudes are plotted. Bioassay results are processed. ALARA principle implemented and maintained considering qualitative and quantitative analysis, as it is required. There are 63- 98% of the monitored workers for E, 80-100% for Hp(0.07) that received lower than 10% of the annual exposure limits. In the case of Hp(3), since 2011 we have been taken the dose constrain of 15 mSv and the exposures are maintained lower than this value. Before this year also we had this behavior. The maximum value registered for S is 98.3 man-mSv y⁻¹ and this occurs in 2011. In spite of this, the maximum handling activity of ⁹⁹Mo was in 2012 and a two years later for ¹³¹I. The most identified useful tools are the use of electronic dosimeters, an additional shielding for the collection of radwastes and the internal shielding components in hot cells. A dose reduction obtained is between 10-27 percent. It is demonstrated, the exposure of workers related with radiopharmaceuticals production in Cuba is acceptable low.

KEYWORDS: *Occupational exposure; radiation safety; production of radiopharmaceuticals; ALARA principle.*

1 INTRODUCTION

During the period covering 1996-2015, the Center of Isotopes (CENTIS) of the Cuban Republic has produced radiopharmaceuticals and labeled compounds with ²⁰¹Tl, ¹³¹I, ³²P, ⁹⁹Mo/^{99m}Tc, ¹²⁵I, ⁹⁰Y, ¹⁸⁸Re and ¹⁵³Sm. Analysis of processing data from individual radiological surveillance and of handling radioactive inventory for radioisotopes of higher contribution to occupational exposure are presented in this paper. There are shown the main findings in ALARA principle application. Results reflect exposure of workers has been maintained below of the applicable dose constrains in the majority of cases.

2 METHODS

2.1 Processing data from registers of occupational exposure

As a part of radiation protection programme is implanted individual radiological surveillance. Through credit dosimetry, are controlled during 18 years the effective doses (E) of a total of 896 workers and 47 as annual average. Among 1996-2000 in our country exists film dosimetry, control period of three months and minimum detection level was 200 µSv. Nevertheless, since 2001 is used TLD dosimetry and control period is monthly, with 100 µSv as minimum detection level.

The reported uncertainty is less than 20 %. Determinations of the committed effective dose (E(50)) are including for controlled workers. Average distributions of effective dose (E), equivalent dose to the hands (Hp (0.07)) and equivalent dose to the lens (Hp(3)) are analyzed among intervals of their annual limits [1] as: <10%, ≥10% y <30%, ≥30% y <60% y ≥60% y <Annual Limit (AL). The effective collective dose (E) is calculated as: $S = \sum E_i N_i$ [2], where E_i is the annual mean E for a group i and N_i is the amount of persons in this group. There is S determined for each group of workers and the total staff. The contribution to annual total S of S for $E \geq 2$ mSv is calculated as a percent.

2.2 Analysis of handling radioactive inventory

Registers on the operation of opening packages [3] with solutions of ^{131}I , ^{99}Mo and ^{32}P are analyzed, because these radionuclides are the most contribution to occupational exposure. Their activities are calculated. For Radiopharmacy group is evaluated its distribution of S, since this group handling that inventory, with respect to the rest of staff and its relation with activities of these radioisotopes.

2.2 ALARA principle application

The principle ALARA (as low as reasonably achievable) is used taking into account quantitative and qualitative analysis in function of the case [5]. For assessment exposure by operation and the control the most risk, are used electronic dosimeters DOSICARD from Eurisys Mesures (France) and EPD MK2+ de Thermo Scientific (United Kingdom). With these dosimeters are measured personal deep equivalent dose Hp(10) from $1\mu\text{Sv}$ up to 10 mSv and rate doses to 1 Sv/h. They have light and sound alarms. It low register level and alarms haven been very useful when new practices are evaluated and control the most risk operations.

In the other hand, operations in hot cell for Molybdenum are evaluated to reduce exposure during operations, with additional shielding and considering the recollection of radioactive wastes during elution of generators. Recently introduce a new shielding in hot cell for Technetium and increase shielding inside the first cell.

In the same way, was introduced additional shielding of 18 mm of lead for transfers of samples and products in the controlled area for the used glove box for the labeled compound with ^{131}I . Also were introduced containers of bigger shield of Pb for handling highest activities of ^{131}I in controlled zone.

For reduce Hp(0.07) from beta emitters, which are more use in the last 5 years, it is necessary evaluate the use of syringe protectors and these are introduced in practices [5].

In spite of it is not possible to evaluate their contribution to reduce occupational exposure, the education activities are organized firstly every two years and annually for the last five years. The analyzing of human behavior in the risk is a main purpose of recent training activities.

3 RESULTS

In Tables 1 and 2 are shown the percent distribution of E and Hp(0.07). As it can see, 63-98% of the monitored workers for E and 80-100% for Hp(0.07) receive less than their annual limits of exposure [1].

For Hp(3) up to 2010 we were applied the old annual limit (150 mSv) and 100% of monitored workers received less than 10% of this. Nevertheless, since 2011 we have been adopted a new annual limit of 20 mSv by year [1] and the dose constraint of 15 mSv. The exposures are maintained lower than last value. In Figure 1 are plotted annual mean values for E and Hp(3). The same is presented in Figure 2 for Hp(0.07). The maximum values are in 2005 and 2008.

To reduce occupational exposure, we applied some measures. For instance, when will handle beta emitters, as ^{32}P and ^{90}Y , we introduce the use of syringe protector of 5 mL and 10 mL. This allows with shielding of 5 mm of Lucite obtain a reduction of rate dose in contact equal to $8.59\text{E}-03$ (reduction factor) [5].

The relationship between the mean value of E and E(50) during the studied period is 6 to 72 %. In the last case this was a radiological incident with the raw material of ^{131}I since a spill of solution in its container was not rapidly detected and implied exposure to an a worker. This situation took place in 2011.

Table 1: Percent distribution of workers by range of the annual effective dose received.

Range of E	E < 2 mSv	(2 ≤ E < 6) mSv	(6 ≤ E < 12) mSv	(12 ≤ E < 20) mSv
1996	77	13	0	0
1997	82	6	0	0
1998	75	14	0	0
1999	66	17	0	0
2000	63	13	0	3
2001	74	5	0	0
2002	47	32	3	0
2003	62	19	0	0
2004	77	5	0	0
2005	73	7	2	0
2006	81	4	2	0
2007	78	2	0	0
2008	98	3	0	0
2009	90	10	0	0
2010	72	28	0	0
2011	78	12	10	0
2012	70	25	3	2
2013	77	17	4	2
2014	91	9	0	0
2015	89	11	4	0

Table 2: Percent of workers by range of Hp(0.07).

Range of Hp(0.07)	Hp(0.07) < 50 mSv	(50 ≤ Hp(0.07) < 150) mSv	(150 ≤ Hp(0.07) < 300) mSv	(300 ≤ Hp(0.07) < 500) mSv
1996	100	0	0	0
1997	100	0	0	0
1998	100	0	0	0
1999	100	0	0	0
2000	83	17	0	0
2001	88	12	0	0
2002	86	14	0	0
2003	84	16	0	0
2004	86	14	0	0
2005	80	20	0	0
2006	85	12	3	0
2007	86	14	0	0
2008	83	14	3	0
2009	93	5	2	0
2010	98	2	0	0
2011	94	2	4	0
2012	90	10	0	0
2013	98	0	2	0
2014	94	6	0	0
2015	96	4	0	0

Figure 1: Values of annual mean effective dose and equivalent dose to lens.

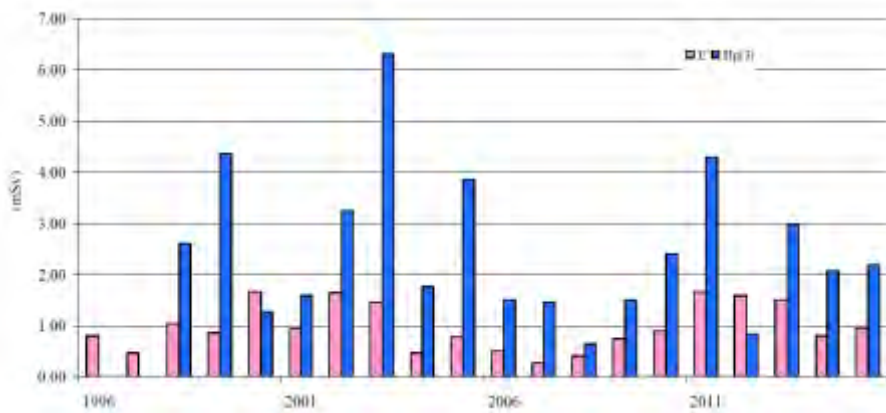
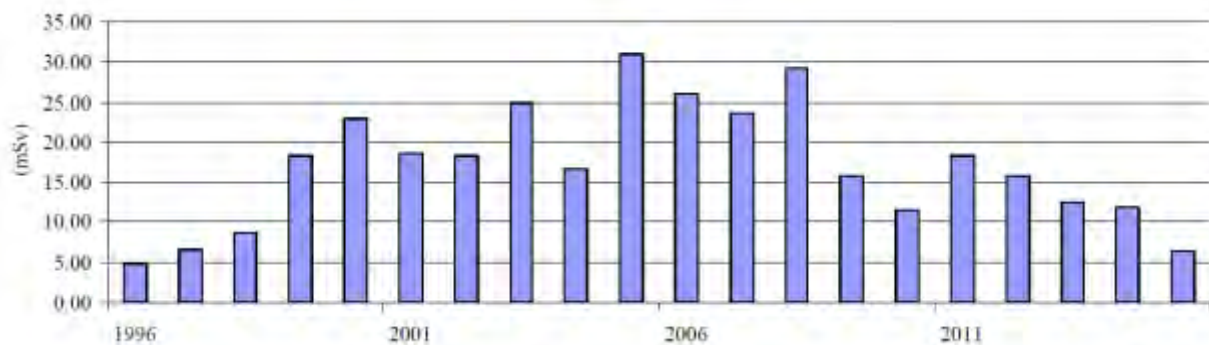


Figure 2: Values of annual mean equivalent dose to hands.



4 DISCUSSIONS

The relationship between the maximum annual value of dosimetric quantities and their respective dose constrains can be observe in Table 3. There we can see that only in four cases maximum values of E and Hp(0.07) are higher than their respective dose constrains. These cases are investigated and safety measures were adopted for eliminate their recurrence. In 1996 and 1997 it is indicated as not controlled (NC) for Hp(3).

The highest values appear in year 2000 for E, 2006 for Hp(0.07) and 2003 for Hp(3). It should be appreciated that dose constrains are overcome in these two first moments. A worker of the group of Quality Control made all of the elution of generators and received an effective dose of 25.77 mSv in

2000, value superior of the limit as average for 5 years [1]. The work load was redistributed and a shielding of lead with 5 cm was situated. In the second case the procedure of intervention in hot cell with ^{131}I was analyzed. There was an incorrect manipulation for part of worker and this is the cause of the highest value of Hp(0.07). When these values are compared with the project occupational exposure in normal conditions for maximum of E equal $5\text{-}8\text{ mSv y}^{-1}$ [6], we can appreciate in table 3 that there are between 3 to 26 mSv y^{-1} . The highest value was obtained in quality control activity of Technetium generators, which procedure was rectified due to this case. In the other hand, the most reiterative value is around 4 mSv y^{-1} .

The use of internal shielding of 3 cm of lead for conditionings solution of Molybdenum in the hot cell of allows reducing in 27% the exposure of operator [7]. After the production of Technetium generators began, in 2004 are introduced new measures ALARA like the use of shielding of 6 mm of lead for radioactive wastes receipts and additional shielding in the bench where the generators are eluted [8]. There is a 10 % of reduction of exposure of staff. For this work the direct reading dosimeters DOSICARD was very useful because rate dose and Hp(10) were measured for each operation and their resulting reductions were registered. The employ of electronic dosimeters is allowed to operators to control time and distances from radioactive sources and indeed reduce their exposure. The using containers of bigger shield of Pb for handling highest activities of ^{131}I in controlled zone allowed reducing in one order Hp(10) and Hp(0.07).

Table 3: Values of maximum of dosimetric magnitudes and their doses constraints.

	E (mSv)	Hp(0,07) (mSv)	Hp(3) (mSv)
Dose constraints	12	200	15
1996	4.73	8.15	NC
1997	4.02	8.56	
1998	10.27	17.85	2.60
1999	4.85	49.38	4.38
2000	25.77	65.43	1.27
2001	3.22	117.97	1.90
2002	7.06	97.94	8.47
2003	5.89	91.47	12.09
2004	4.17	73.41	5.14
2005	6.52	145.17	5.89
2006	6.09	232.71	3.49
2007	2.96	117.70	3.86
2008	4.28	168.38	2.18
2009	5.32	172.49	4.85
2010	5.14	60.68	3.85
2011	9.13	194.6	12.05
2012	12.56	116.59	9.95
2013	13.23	159.23	7.49
2014	5.46	97.00	6.95
2015	6.68	125.14	8.75

Figure 3 shows values of S and amount of monitored workers (MW). We can conclude that the last dose not determinate the value of S in the majority of the years. Table 4 reflects collective dose (S) by group of workers and it is between (15 and 98) man-mSv y⁻¹. The more exposed groups are Radiopharmacy and Quality Control, and their S for E equal and higher than 2 mSv is (9-81.7) % of the total annual value of S. The beginning of production of Technetium generators in 2003 is the cause of values of S registered equal a 75 mSv-hombre y⁻¹. In 2010, the increase of handling activity of ¹³¹I conducted to maximum value of S for the studied period equal 98.3 man-mSv y⁻¹. This is less than the initially projected value (it is 200man-mSv y⁻¹ for all the operations of production of radiopharmaceuticals and labeled compounds [6]).

In Table 5 are shown handling activities of ¹³¹I, ⁹⁹Mo and ³²P, which are the radioisotopes with the most contribution to occupational exposure during 20 years in CENTIS, and the collective dose for all staff. This means that it is for the total of monitored workers.

Mean annual handling activities for ¹³¹I, ⁹⁹Mo and ³²P are 7.84 TBq, 47.3 TBq and 0.199 TBq, respectively. Maximum activities registered in 2013 y 2012, except for ³²P, that was in 2000. The annual increases of annual activities of ¹³¹I were in 1998, 2001, 2004, 2007 and 2009-2014. The production of Phosphate of Sodium (³²P) began in 1999 and its increases presented in 2000 and during 2007-10, 2013 and 2015. It is appreciated in Figure 4 that there is a superior deviation on mean value of S of the Radiopharmacy group in 2002-2003, 2005, 2009, 2011-2013, due to increase of handling activities before analyzed with the highest contribution to exposure of the production of Technetium generators.

Figure 3: Collective dose vs. monitored workers (MW).

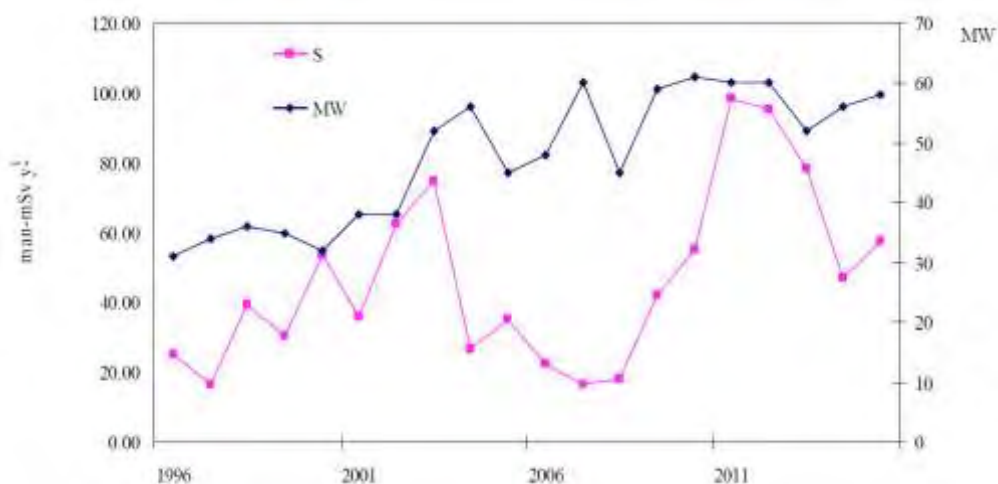


Table 4: Collective dose received by group of workers.

Group of workers	S (man-mSv)				
	Radiopharmacy	Quality Control	Development	Metrology	Radiation protection
1996	9.11	12.23	0.83	0.00	0.93
1997	5.19	5.51	0.64	1.53	1.19
1998	20.04	11.68	0.71	0.97	2.36
1999	18.80	6.59	0.00	1.45	3.43
2000	12.09	29.01	0.47	1.74	3.37
2001	12.88	5.86	0.82	3.77	4.26
2002	24.54	16.52	1.28	5.87	6.28
2003	29.09	22.88	1.49	7.95	4.69
2004	16.33	6.17	0.53	1.14	1.07
2005	19.94	9.46	0.88	1.95	1.45
2006	15.32	5.09	0.36	0.47	0.00
2007	9.76	5.21	0.63	0.16	0.55
2008	13.45	1.73	0.41	0.82	0.83
2009	27.29	6.27	2.70	2.35	1.42
2010	21.62	9.28	8.05	7.02	3.70
2011	56.33	26.98	4.44	12.112	4.58
2012	66.03	18.04	4.06	2.56	3.01
2013	52.66	8.40	3.78	5.10	3.27
2014	27.72	9.88	1.09	1.80	3.52
2015	32.31	6.39	0.29	4.37	4.92

Figure 4: Annual collective dose (S1) and mean collective dose for the group of Radiopharmacy (Sm1).

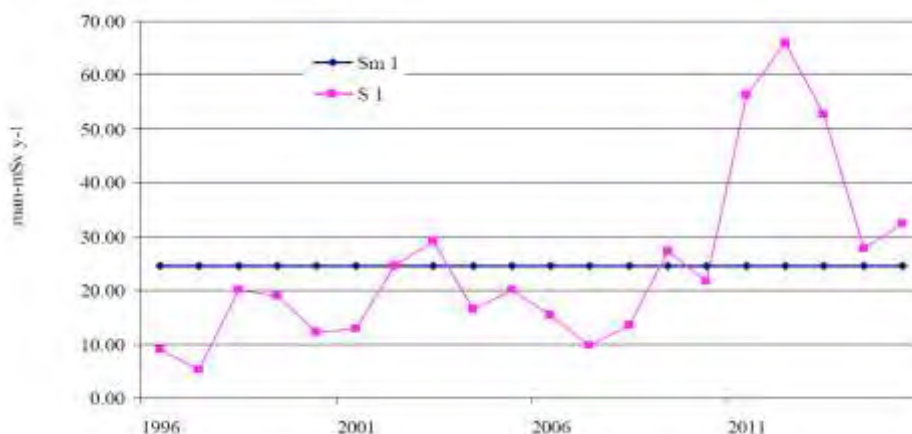


Table 5: Handling activities and collective dose for the total staff by year.

Year	Handling activity ¹³¹ I (Bq y ⁻¹)	Handling activity ⁹⁹ Mo (Bq y ⁻¹)	Handling activity ³² P (Bq y ⁻¹)	S (man-mSv y ⁻¹)
1996	No handling	3.20E+11		24.97
1997	7.33E+11	5.92E+11	No handling	16.38
1998	4.90E+12	5.39E+11		39.49
1999	4.87E+12	6.60E+11	1.19E+10	30.50
2000	4.84E+12	5.35E+11	3.64E+11	53.65
2001	4.88E+12	1.38E+12	3.43E+11	35.49
2002	4.60E+12	1.59E+12	2.35E+11	62.47
2003	3.94E+12	1.49E+13	2.35E+11	74.75
2004	4.71E+12	2.73E+13	1.93E+11	26.49
2005	4.08E+12	2.77E+13	9.75E+10	35.22
2006	3.28E+12	2.29E+13	5.45E+10	22.25
2007	4.91E+12	2.52E+13	8.27E+10	16.51
2008	4.33E+12	2.32E+13	2.03E+11	18.34
2009	5.76E+12	4.01E+13	2.24E+11	42.07
2010	7.09E+12	3.19E+13	3.17E+11	55.19
2011	1.05E+13	3.19E+13	3.12E+11	98.26
2012	1.54E+13	4.42E+14	1.68E+11	95.39
2013	1.86E+13	6.79E+13	2.65E+11	77.43
2014	2.13E+13	6.77E+13	1.16E+11	46.95
2015	2.02E+13	1.19E+14	1.58E+11	57.48

5 CONCLUSIONS

The production of radiopharmaceuticals and labeled Compounds in Cuba show good experiences in the control of occupational exposure, useful for analogue facilities. Analyzing data from radiological surveillance of workers of CENTIS we can appreciate that annually 63-98% of monitored workers for E, 80-100% for Hp(0.07) receive less than the 10% of annual limits of exposure. Since 2011 we have been adopted a new annual limit of 20 mSv by year and the dose constraint of 15 mSv for Hp(3). The exposures are maintained lower than last value. The Radiopharmacy and Quality Control groups are the most exposure, their personal receive E same o higher than 2 mSv, represents the 9-60 % of the total staff.

The highest value of the collective dose for all of practices for production of radiopharmaceuticals and labeled compounds is $98.3\text{man}\cdot\text{mSv}\cdot\text{y}^{-1}$, which is less than about 0.49 times the initially projected value. Measures adopted for the application of the ALARA principle have allowed a reduction between 10 and 27 % of occupational exposure.

The use of electronic dosimeters, the internal shielding in hot cells and the use of shielding for recollection of radioactive wastes have reported the main benefits. In the other hand, shielding of 5 mm of Lucite allows a reduction factor of $8.59\text{E}\cdot 10^{-3}$ of Hp(0.07) for beta emitters, which are a frequent employ since 5 years ago. The education activities have some important contribution to this objective in spite of this it could not be evaluated.

6 REFERENCES

- [1] European Commission, Food and Agriculture Organization of The United Nations, International Atomic Energy Agency, International Labour Organization, OECD Nuclear Energy Agency, Pan American Health Organization, United Nations Environment Programme, World Health Organization, Radiation Protection and Safety of Radiation Sources: International Basic Safety Standards, General Safety Requirements, IAEA Safety Standards Series No, GSR Part 3, Vienna (2014).
- [2] Centre of Isotopes, Radiation Protection Department, Manual of Radiation Safety, DSR.DOC.001, Havana, Cuba (2011).
- [3] International Commission on Radiological Protection. The 2007 Recommendations of the International Commission on Radiological Protection. ICRP Publication 103 (2007).
- [4] International Atomic Energy Agency, Optimization of Radiation Protection in the Control of Occupational Exposure, Safety Series No. 21, Vienna (2004).
- [5] Torres Berdeguez M.B., Ayra Pardo E., Falcon L., Doses Rate in Contact with Plastic Syringes of 1, 2 and 5 mL for Different Beta and Gamma Emitter Radionuclides, 12th International Congress of the International Radiation Protection Association, IRPA 12, Buenos Aires, Argentina (2008).
- [6] Perez S., Gatti A.M., Reyes R., Radiological Safety and Protection in the Design of the Centre of Production of Radiopharmaceuticals and Labeled Compounds in Cuba, Journal Nucleus N. 24, p.36-44, Havana, Cuba (1998).
- [7] Perez Pijuan, S., Gonzalez Fernandez, A., Radiological evaluation for preoperational test of Technetium Generators and its application to reduce occupational, Memories of the 1rst Symposium on Applications of Nuclear Technical in Agriculture, Industry and Health, Section III Dosimetry, Havana (1997).
- [8] Centre of Isotopes, Radiation Protection Department, Safety Report, Havana, Cuba (2013).

Estimation of air born radioactivity induced by 8GeV class electron LINAC accelerator

Yoshihiro Asano^{a*}

^aSpring-8 Center/RIKEN 1-1 Koto Sayo Hyogo, 679-5148 Japan

Abstract. Air born radio-activities induced by high energy electrons from 6 to 10GeV have been estimated by using analytical methods and Monte Carlo codes. The experiments using a gas monitor with NaI(Tl) scintillator have been performed with the air of dump room of SACLA, X-ray free electron laser facility with 7.8 GeV electrons.

KEYWORDS: *induced activity; air born; Monte Carlo; photo-nuclear reaction; PHITS; SACLA.*

1 INTRODUCTION

Recently, many synchrotron radiation facilities and X-ray free electron laser facilities are designed and constructed or under operation such as SACLA[1]. In designing of these facilities, the estimation of induced activity of air is required as well as the shielding design to get the license and agreements of the stakeholders. Especially, a large amount of high energy electrons always injected into the dump at X- ray free electron laser facilities so that the estimation of the activity concentration of exhausts must be required even the electron machines, fundamentally. To obtain the data, the saturation activity methods [2] or the calculation data presented by Mao[3] have been employed so far. However, these data are too conservative in many cases or without considering the contribution of high energy neutron due to over the giant resonance energy photons. On the other hand, Monte Carlo simulation codes with photo- nuclear reactions including giant resonance, quasi-deuteron, and π -production processes such as FLUKA[4] 2011.2c.3 is now available. In addition to the FLUKA and others such as MCNPX [5], recently the upgrade PHITS code [6] can simulate the photo-nuclear reaction process, and now the ability of the simulation is expanded up to 1 TeV gamma-ray energy without restriction to use so there are no problems to check its simulation results. PHITS has been mainly used for particle and heavy ion transport simulation until now, therefore PHITS simulations have been performed with taking around the SACLA beam dump for instance in comparisons with the calculation results by using analytical methods. And the experiments with the gas monitor using NaI(Tl) scintillator are also compared with these calculation data.

2 X-RAY FREE ELECTRON LASER FACILITY “SACLA”

The SPring-8 Angstrom Compact free-electron LAsER, SACLA, is the now one of two operating X- ray free-electron laser facilities, and can produce shorter than angstrom wavelengths of X-ray laser. SACLA is based on three new technologies: one is the low-emittance thermionic CeB₆ electron gun; another is c-band accelerators with gradient of over 35MV/m; and the third is in-vacuum type undulators with a short period length of 18 mm. The Linac can produce electrons of up to 10 GeV energy with repetition rates of 60 Hz and 0.5nC/pulse. Three beamlines are now under operation and each beamline has the beam dump as illustrated in Fig.1 and five beamlines to be constructed to be pulse by pulse operation with different electron energy by the switching magnet in the near future. The electron beam is injected into the dump with inclination of 20 degrees, and the generated X-ray laser beams go straight to another separated area by a thick concrete wall for experiments [7]. The beam dump has a double cylindrical structure, and the core (inner cylinder) is made of graphite with the bottom of copper; the outer is made of 40 cm thick iron. These dumps are within the dump room under the ground surrounded ordinary concrete with the plates of

* Presenting author, e-mail: asano@spring8.or.jp

iron at the top to reduce the skyshine neutron dose as shown in Fig.2. Each dump room has no ventilation system with the air volume of $1.21 \times 10^7 \text{ cm}^3$, and small portion of opening to guide the electron beam to the dump and some other instruments such as optical tracking system (OTR) to control the beam trajectory so that the dump room is not isolate from the undulator hall completely.

3 ESTIMATION OF INDUCED RADIOACTIVITY IN DUMP ROOM

3.1 Analytical methods

Induced radioactivity in air is produced by photo-neuclear reaction such as (γ, n) reaction and neutron absorption reaction such as $^{40}\text{Ar}(n, \gamma)^{41}\text{Ar}$.

(1)Radioactivity concentration due to photo-neuclear reaction is estimated by using saturation activity method as follows,

$$S_{Ai} = \lambda_i \cdot A_{AS}(i) \cdot P \cdot X_m \cdot F_l \tag{1}$$

where $S_A(i)$, $A_{AS}(i)$, and $\lambda(i)$ are the production rate ($\text{GBq} \cdot \text{h}^{-1}$), the saturation activity ($\text{GBq} \cdot \text{kW}^{-1} \cdot \text{m}^{-1}$), and the decay constant (h^{-1}) of i nucleus, respectively. P , X_m , and F_l are electron beam loss power (kW), the photon traversable distance within air (m), and the ratio of the contribution of electron beam loss to induced activity. The concentration of air activity during the irradiation can be expressed as follows,

$$Q \frac{dC_i}{dT} = S_{Ai} - \lambda_i \cdot Q \cdot C_i - q \cdot C_i \tag{2}$$

$$C_i = \frac{S_{Ai}/Q}{\lambda_i + q/Q} \cdot [1 - \exp\{-(\lambda_i + q/Q) \cdot T\}] \tag{3}$$

where Q , q , and C_i are the volume of room air (m^3), the volume of air ventilation ($\text{m}^3 \cdot \text{h}^{-1}$), and the activity concentration of i nucleus ($\text{GBq} \cdot \text{m}^{-3}$). T is the irradiation time (h).

Figure1: Illustration of the SACLA beamlines. The electron generated by the gun are accelerated by the L-band and S band tubes to be about 1 GeV to transport to the deflector cavity. Accelerated electrons are distributed to each beamline by a switching magnet and go through the long undulator to produce X-ray laser. After that electrons are turned out to the dump.

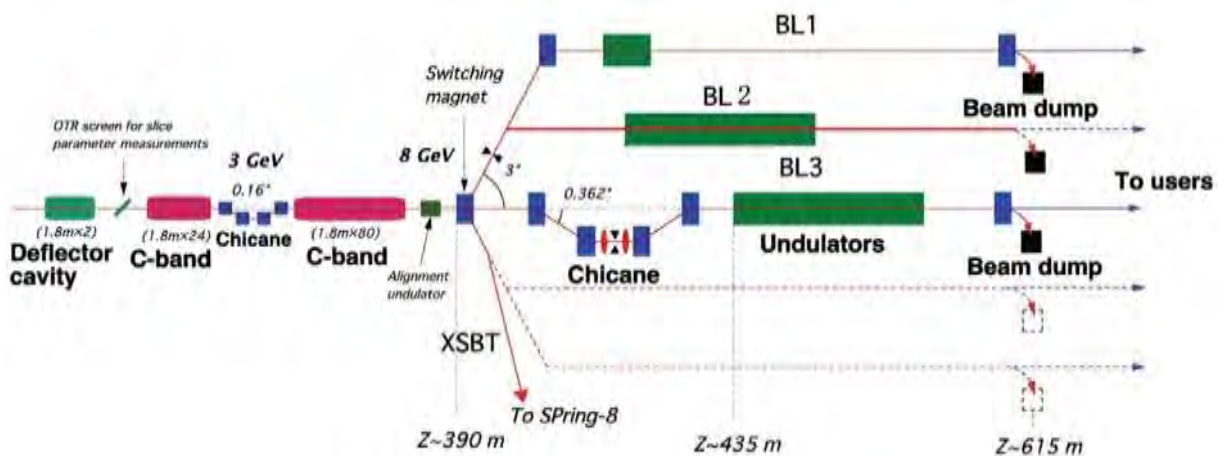
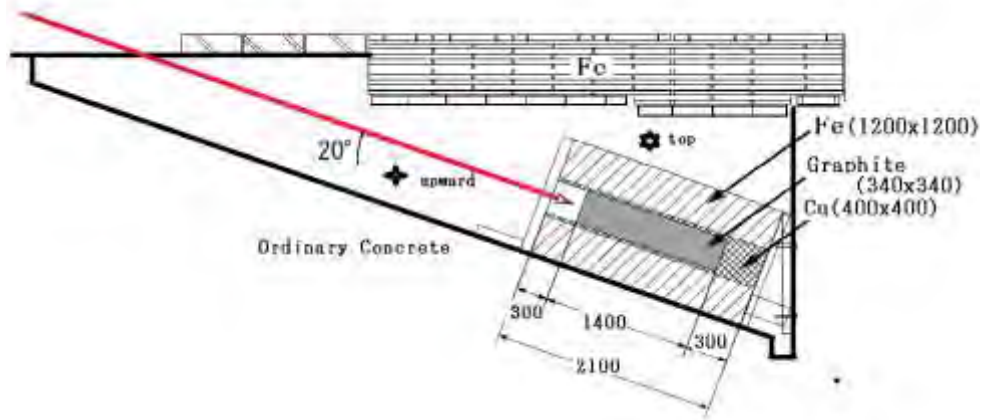


Figure 2: Cross sectional view of SACLA beam dump.



(2) Air activity concentration due to neutron absorption reaction can be estimated as follows,

$$S_{Ai} = \lambda_i \cdot 10^{-24} \cdot \sigma \cdot N \cdot Y \cdot e \cdot X_{cm} \cdot F_1 \cdot 10^{-9} \quad (4)$$

where σ , N , and Y , are the neutron absorption cross section (cm^2), the number of atom (cm^{-3}), and the neutron yield per electron (neutrons/electrons), respectively. e and X_{cm} are the electron loss rate (s^{-1}) and the neutron traversable distance within air (cm), respectively. Another indexes are same as formula (1). Neutron yields can calculate using the Mao's formula [3], and $3.3 \times 10^{-5} (\text{e}^{-1} \cdot \text{MeV}^{-1})$ and $1.4 \times 10^{-4} (\text{e}^{-1} \cdot \text{MeV}^{-1})$ for graphite and iron thick targets. No ventilation system are employed for the dump rooms so that $q=0$ and $Q=1.21 \times 10^7 \text{ cm}^3$. Based on the EGS5[8] simulation, 0.01 is employed for F_1 , and 0.5m for X_m . 30nC/s is assumed for accelerated electron charge. Saturation activities $A_{AS}(i)$ are listed in the reference[2]. For the neutron capture cross section, σ , we employed the ^{40}Ar average cross section of JENDL-4.0 [9] in assumption of Maxwellian spectrum, 0.660 barn.

3.2 Monte Carlo simulation code PHITS

PHITS can calculate the activated nuclei due to photo-nuclear reaction, neutron absorption, and others processes by using DCHAIN-SP in the code package. For photo-nuclear reaction process, PHITS employs the GEM model [10] for giant resonance region with JENDLE/PD-2004 cross section library [11], the quantum molecular dynamics (JQMD) model [12] for the dominant region of quasi-deuteron disintegration process, and the JAM [13] model for high energy reason up to 1 TeV. For the neutron absorption process, FENDL/A-2.0 [14] is employed for the cross section library.

4 EXPERIMENTS

Illustration of the gas monitoring system is shown in Fig.3, and the cylindrical air chamber was used. 76.2 mm ϕ x 76.2mmH NaI(Tl) scintillation detector was employed and set the centre of the air chamber. The diameter and height of the air chamber which used are 540 mm and 519 mm, respectively. The capacity of the roots blower is 0.6 m^3/min . The diameter of pipes and length from the dump room to the air chamber are 19mm ϕ and 20 m so that the average retention time at the chamber and flow time from the dump room are 12 sec and 0.6 sec, respectively. The counting efficiency of the gas monitor was measured by using a ^{137}Cs standard radioisotope to set four points (bottom, in and outside the air chamber wall, and contact the detector wall), and compared to the PHITS calculation showing good agreement within 2%. After that, the efficiencies of air activities depending on the photon energy were simulated, and Fig.4 shows the photon flux distribution in case of 1 photon/ cm^3 with 0.511 MeV photons. The photon energy dependence of the efficiency is shown in Fig.5 including the size of the air chamber.

Figure 3: Illustration of the gas monitoring system. D and H are diameter and height of air chamber, respectively.

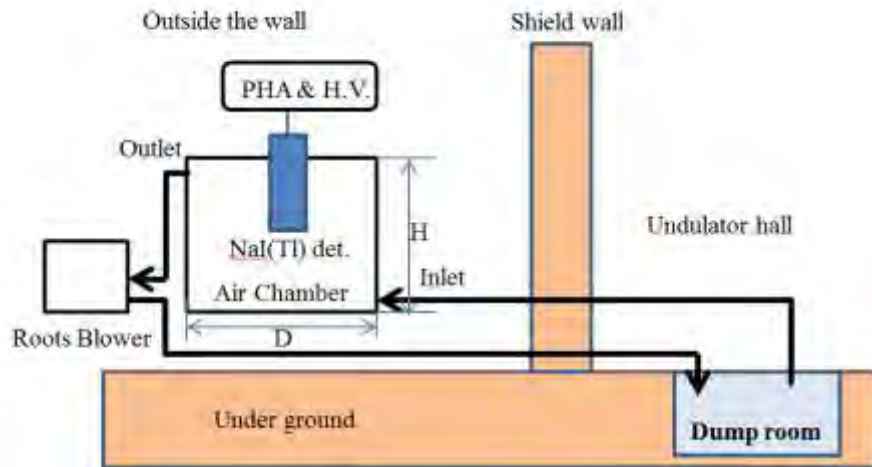


Figure 4: Calculation results of the photon fluence distribution at the case of 1 photon/cm³ with 0.511 MeV energy. The size of the air chamber is 540 mm diameter and 519 mm height.

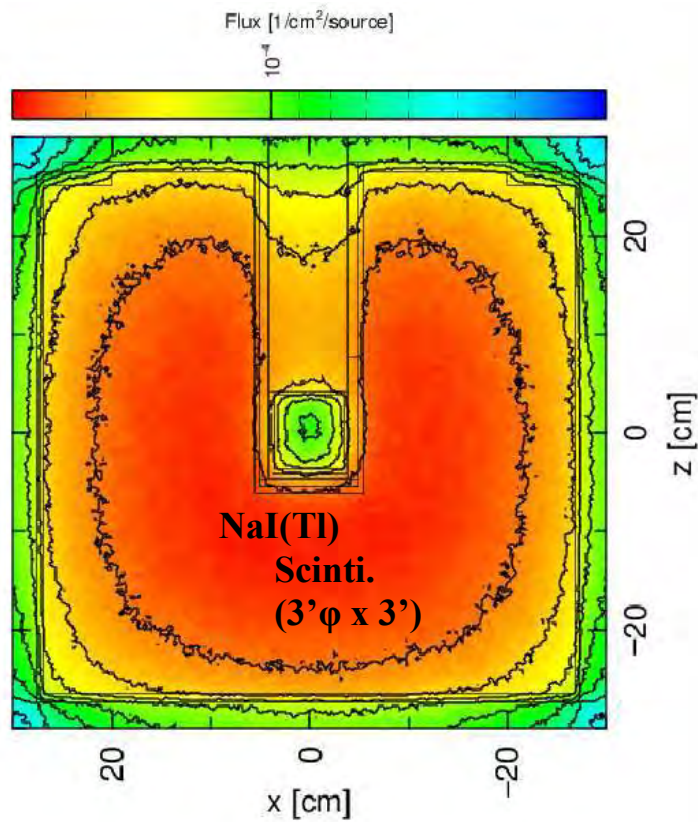
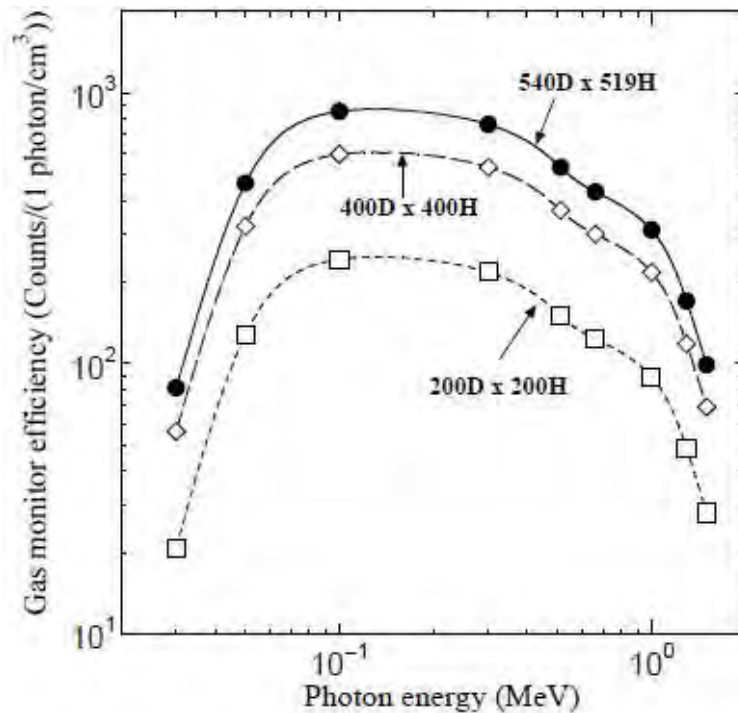


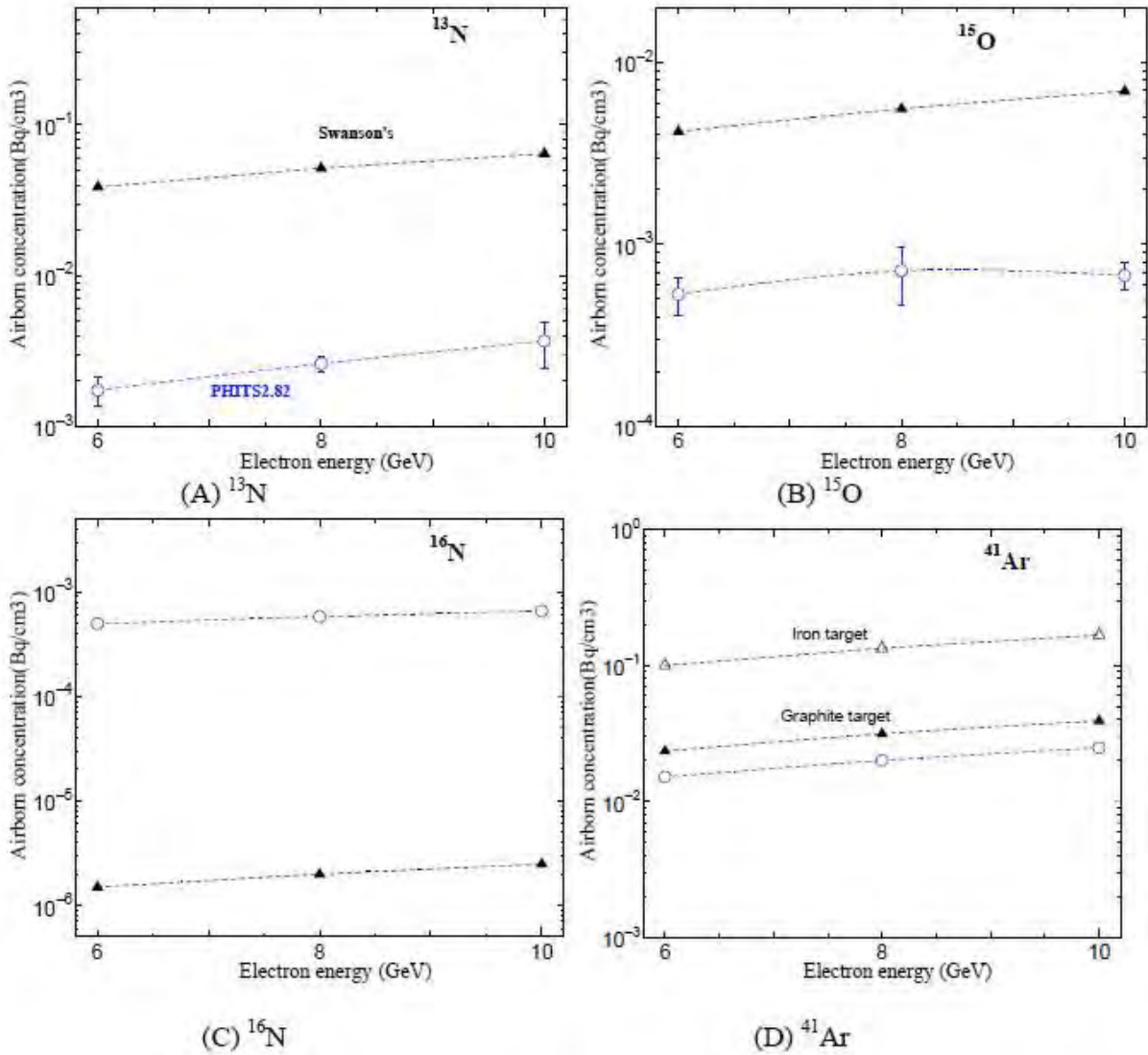
Figure 5: Counting efficiency of the air gas monitor depending on the photon energy and the size. (D and H are the diameter and the diameter and height, respectively.)



5 RESULTS AND DISCUSSION

Figure 6 shows the calculation results of main induced air activity concentrations for (A) ^{13}N , (B) ^{15}O , (C) ^{16}N , and (D) ^{41}Ar due to 6, 8, and 10 GeV electron energy. In these cases, the concentrations are indicated just after 7 hours electron irradiation into the dump. For ^{13}N , and ^{15}O , Swanson's saturation radioactivity method indicates about 10 times or more higher values in comparison with PHITS simulation results. On the other hand, PHITS simulation results of ^{16}N concentration are very high in comparison with that of Swanson's. One of reasons for this difference is that the saturation radioactivity seems incorrect as indicated in reference [2], $(20 \times 10^3 \text{ Bq} \cdot \text{m}^{-1} \cdot \text{kW}^{-1})$, which we used. However, ^{16}N production process can be considered the $^{15}\text{N}(n, \gamma)^{16}\text{N}$, and $^{18}\text{O}(\gamma, np)^{16}\text{N}$ reactions so that the ^{16}N production process is not simple photo-nuclear reaction such as $^{14}(\gamma, n)^{13}\text{N}$, and $^{16}\text{O}(\gamma, n)^{15}\text{O}$ reactions. The ^{41}Ar production process is $^{40}\text{Ar}(n, \gamma)^{41}\text{Ar}$ neutron capture reaction, and the results of the PHITS simulation show good agreement with the values of Graphite target using Mao's equations for neutron yields within factor 2. However, the PHITS simulations for the concentration of the ^{41}Ar seem to be higher estimation because the experiments of the measurements for the air radioactivity concentration could not detect it as shown in Fig.7 in comparison with the back ground spectrum without air flow. During these measurements, the electrons injected into the dump with $0.23 \pm 0.1\%$ C/pulse and repetition rate of 30Hz. Obviously, positron emitters such as ^{13}N , ^{15}O , and ^{11}C were detected, and ^{41}Ar was not detected clearly. The concentrations are listed in Table 1 with the detection limits of this air monitoring system. The measured values are normalized from 6.9 nC/s electron charge during measurements to 30nC/s of the full power so that the ^{41}Ar concentration was measured to be less than $5.5 \times 10^{-3} \text{ Bq/cm}^3$ at the full power of SACLA. The ^{16}N and ^{41}Ar concentrations are measured to be less than $5.5 \times 10^{-3} \text{ Bq/cm}^3$ at the full power of SACLA. The ^{16}N and ^{41}Ar concentrations are measured to be less than $5.5 \times 10^{-3} \text{ Bq/cm}^3$ at the full power of SACLA. The ^{16}N and ^{41}Ar concentrations are produced mainly due to neutron absorption reaction so that the neutron spectra in the dump room are important. Simulated neutron spectra in the dump room are shown in Fig.8 at the top (\star) and the upward (\blacklozenge) of the dump. The positions are also indicated in Fig.2. In the figure, the spectrum at the inverse direction of the electron trajectory (upward) reasonably slants to be lower energy than that at the top of the dump.

Figure 6: Induced air radioactivity concentrations at the dump room depending on the electron energy with the 30nC/s injected into the dump. (A): ^{13}N , (B): ^{15}O , (C) ^{16}N , (D): ^{41}Ar . Black triangles are the results using Swanson's formula, and full and open triangles are the graphite and iron targets, respectively. Blue open circles indicate the results using PHITS 2.82.



The ratios of the total photo-neutron production cross sections for ^{14}N , ^{18}O (air) and ^{12}C and ^{56}Fe (dump) are shown in Fig.9 between the JENDL evaluated photo-nuclear data (PHITS) and the data that FLUKA used based on the experiments. However, even the total cross sections, it is much different each other, especially air material. For the shielding or induced radioactivity estimations, it is required the double differential cross sections of neutron production depending on the photon energy, therefore, the experimental data of the double differential neutron cross sections are strongly required.

Figure 7: Output distribution of the PHA of the air gas monitor with NaI(Tl) scintillation detector. Blue dots are the data during the sampling of dump room air with the electron charge of 6.9 C/s, and black dots are without air flow.

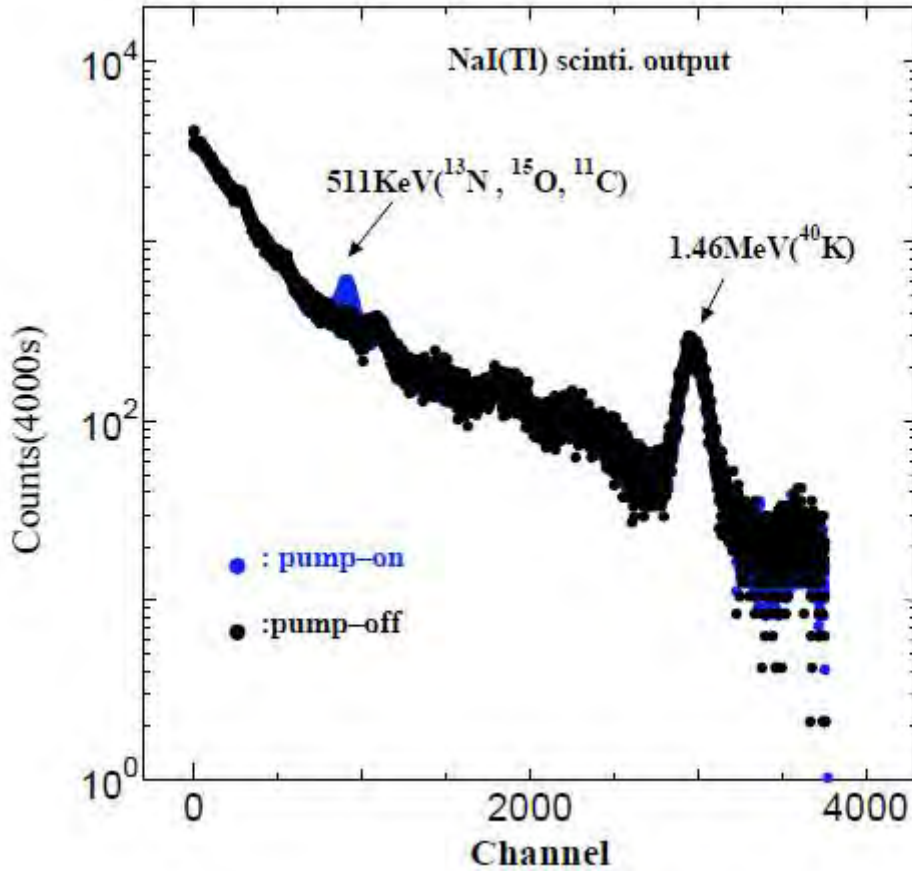


Table 1: Air activity concentration in dump room during the 7.8 GeV electron injection with the detection limit of the air monitoring system.

Nuclei	Detection limit	Measurement results*
Positron emitter(¹³ N & ¹⁵ O)	7.1×10^{-4} (Bq/cm ³)	2.2×10^{-2} (Bq/cm ³)*
⁴¹ Ar	1.3×10^{-3} (Bq/cm ³)	$< 5.5 \times 10^{-3}$ (Bq/cm ³)*

(*) normalize the electron charge from 6.9 to 30 nC/s

Figure 8: Photo-neutron spectra at the top and upward of the dump as shown in figure2 due to 8 GeV electrons bombarded into the SACLA dump.

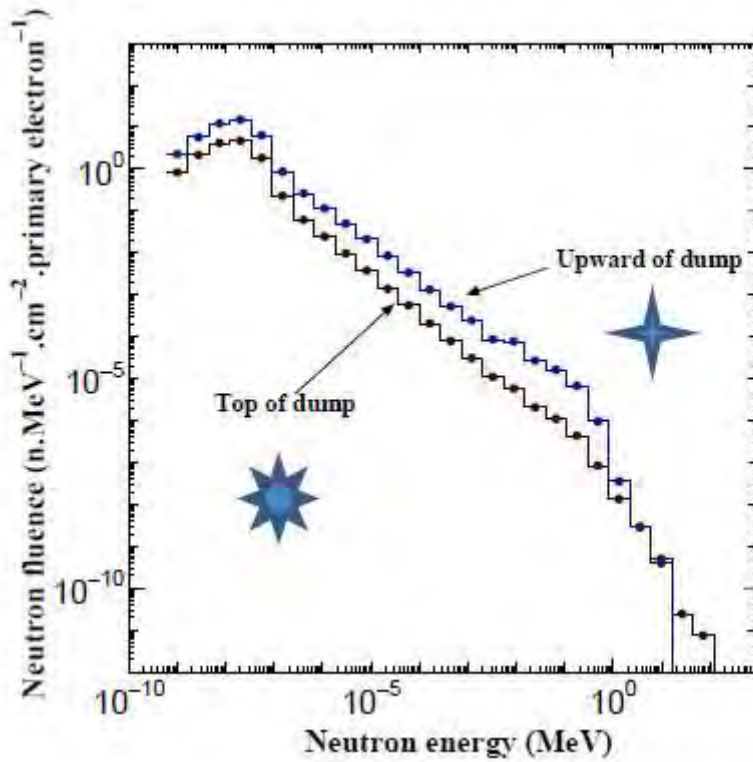
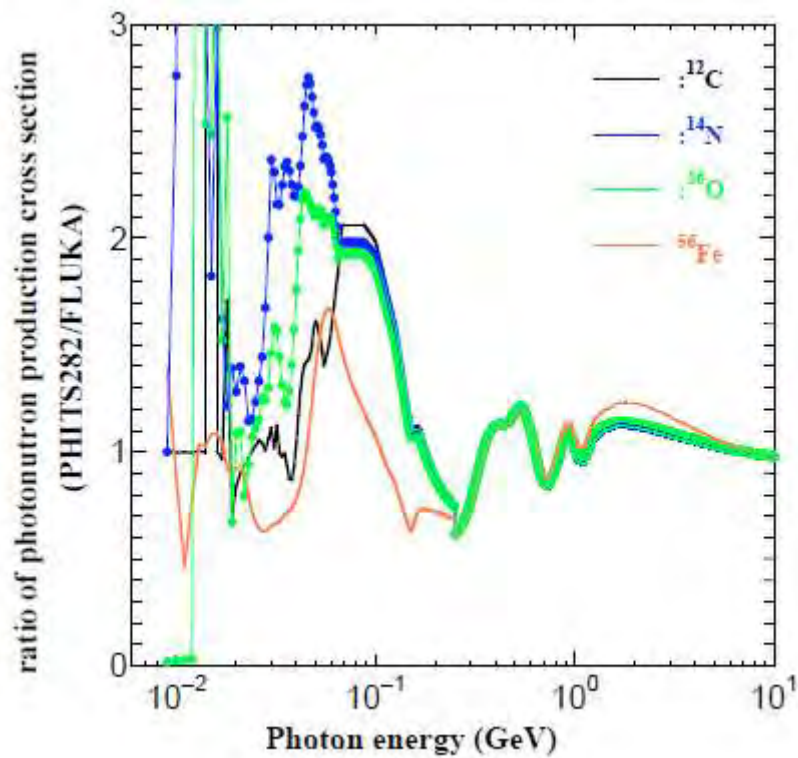


Figure 9 The ratio of the total photo-neutron production between the data of PHITS and the data FLUKA used.



6 SUMMARY

Air activity concentrations in the dump room of SACLA induced by high energy electron have been estimated by using analytical methods and Monte Carlo code, and measured by the gas monitor with NaI(Tl) scintillation counter. As the results,

- (1) The estimation using Swansons' radioactivity saturation method indicates conservative values for air born nuclei except ^{16}N .
- (2) For ^{13}N concentrations, the results of PHITS are lower than that of Swansons' analytical method within about factor 10.
- (3) The concentration of ^{16}N by the analytical method indicates lower values and large differences each other because another reactions such as $^{15}\text{N}(n,\gamma)^{16}\text{N}$ and $^{18}\text{O}(\gamma,np)^{16}\text{N}$ must be considered.
- (4) For ^{41}Ar , the results between PHITS and analytical method with an graphite target show good agreement within about factor 2. But the experiments did not detect it. So it needs to check each process carefully, especially photo-neutron production process.
- (5) It is much different between PHITS photo-neutron production cross section and that of another code, even the total photo-neutron production cross sections. So it is very important to obtain the experimental data of the double differential cross section (DDX) of photo-neutron production for radiation shielding and induced activities estimation.

7 ACKNOWLEDGEMENTS

The author thanks to Dr. T.Sato and his PHITS developer team for valuable discussion and good information service.

8 REFERENCES

- [1] Tanaka, H., et al., 2012 .A compact X-ray free electron laser emitting in the sub-angstrom region, *Nature photonics.Letters* DOI10.1038 141, pp. 1-5.
- [2] Swanson, W.P., 1996. Radiological safety aspects of the operation of electron linear accelerators: IAEA Tech. reports No.188
- [3] Mao, S., et al., 2005. Giant dipole resonance neutron yields produced by electrons as a function of target material and thickness: *Health Physics* 70
- [4] Ferrari, A., et al., 2005. FLUKA:a multi-particle transport code: CERN 2005-10 (2005),INFN/TC_05/11,SLAC-R-773
- [5] Pelowitz,D.B., et al.,2011 "MCNPX 2.7.0 Extensions", LA-UR-11-02295
- [6] Sato, T., et al., 2013. Particle and Heavy Ion Transport Code System PHITS,version 2.52:J.Nucl. Sci.Technol. 50;9 913-923
- [7] Asano, Y., Itoga,T., 2014. Radiation shielding and safety systems of SPring-8 angstrom compact free electron laser, SACLA. *Progress in Nuclear Science and technology* v.4 (186-190)
- [8] Hirayama,H. Namito Y, Bielajew, A.F.,et al.2005," The EGS5 Code system", SLAC-R-730, KEK- Report 2005-8
- [9] Shibata K., et al.,2011, JENDL-4.0:A new library for nuclear science and engineering, J. Nucl. Sci. Technol. 48 (1) 1-30
- [10] Furihata,S. et al., 2001, The GEM code-a simulation program for the evaporation and fission process of an excited nucleus., JAERI-Data/Code 20012 -015
- [11] Kishida N. et al., 2004. JENDL photonuclear data file., *Proceedings of the Int. Conf. on Nuclear Data for Sci. & Tech.* 2004 Sep. Santa Fe
- [12] Niita K. et al., 1995 Analysis of the (N,xN) reactions by quantum molecular dynamics plus statistical decay model. *Phys. Rev. C* (2620-2635)
- [13] Niita K. et al., 2001. High energy particle transport code NMTC/JAM. JAERI-Data/code 2001-007
- [14] Pashchenko A.B.,1996. Summary report for IAEA Consultant;Meeting on Selection of Evaluations for the FENDL/A-2 Activation Cross Section library, INDC(NDS)-341 IAEA

Principles of Formation of Risk Groups for Occupational Diseases for Workers of Facilities Using Nuclear Energy during Obligatory Medical Examinations in the Russian Federation

Andrey Kretov, Andrey Bushmanov, Alexander Samoilov

Burnasyan Federal Medical Biophysical Center of Federal Medical Biological Agency, Moscow, Russia

Abstract. Working environment of employees of facilities using nuclear energy (ionizing radiation, noise, vibration, industrial aerosols and other) are the cause of obligatory medical examinations of the workers in accordance with Russian regulations. System of obligatory medical examinations in Russian Federation provides work of the medical commission in the conditions: limited, paid by the employer, the list of medical examination; a limited time; high intensity of the process of medical examination. Existing methodology for assessing the risk of occupational disease include a thorough analysis of a significant number of the important factors of the working environment, which in turn excludes the use this methodology by medical commissions in the course of the mandatory medical examination. Considering the above described features of the mandatory medical examination in the Russian Federation, specialists of Burnasyan Federal Medical Biophysical Center of Federal Medical Biological Agency were developed principles of formation of risk groups for development of occupational disease during medical examinations: strict compliance with the regulatory framework; using information available in the course of medical examination; minimum time costs; the simplicity of the method (possibility of using the medical commissions of any level). Following these principles, on the basis of analysis of 27 863 cases of the medical examination of persons working in hazardous working conditions, including ionizing radiation, was developed the Method of formation of risk groups for occupational disease during medical examinations, which includes benchmarking of the 3 factors: conditions of work, length of work, results of medical examinations. Method allows to allocate 4 groups with varying degrees of risk, contains recommendation for each group and allows the employer to assess the legitimacy of diagnose of occupational diseases or quality of the investigation of working conditions.

PREDO – A Strengthened Dose Assessment for Routine Discharges by Swedish Nuclear Installations

Anna Maria Blixt Buhr^a, Helene Alpfjord^b, Rodolfo Avila^c, Roman Bezhenar^d, Robert Broed^c, Anna Fermvik^a, Eva Grusell^e, Kenneth Häggkvist^b, Vladimir Maderich^d, Veronika Rensfeldt^c, Synnöve Sundell-Bergman^a, Cor W.M Timmermans^f, Stefan Willemsen^f, Govert deWith^f

^aVattenfall AB, SE-169 92 Stockholm, Sweden

^bSwedish meteorological and hydrological institute (SMHI), SE-601 76 Norrköping, Sweden

^cFacilia AB, Gustavslundsvägen 151C, SE-167 51 Bromma, Sweden

^dUkrainian Center of Environmental and Water Projects (UCEWP), Glushkov av., 42, Kiev 03187, Ukraine

^eSweco Environment AB, Hospitalsgatan 22, SE-611 32 Nyköping, Sweden

^fNuclear Research and Consultancy Group (NRG), P.O. Box 9034, 6800 ES, Arnhem, The Netherlands

Abstract. In order to harmonize with the upcoming national legislation in Sweden, a robust and transparent methodology for assessing radiation doses to the public is developed. The methodology is specific for routine releases of radionuclides to air and water from the Swedish nuclear installations (Ringhals NPP, Forsmark NPP, Oskarshamn NPP, Barsebäck NPP, SKB interim storage for spent fuel, Studsvik Nuclear AB and AB SVAFO, and the Westinghouse Electric Sweden AB fuel fabrication) has been developed within the PREDO project (PREdiction of DOses from routine releases of radionuclides to the environment). The assessment endpoints are radionuclide dose factors (committed effective annual doses in Sv per year per Bq per year releases), together with intermediate results such as radionuclide concentrations in environmental media. Assessments have been done for different representative individuals (adult, child, infant) identified from an exposure pathway analysis within an area of 10 km radius from the release points. The airborne dispersion was simulated with the Gaussian plume model, the SMHI Dispersion 3, former LSAM. Five-year weather data statistics was utilized to derive time-averaged surface air concentrations and deposition fields. For each site, impacted terrestrial land use objects of different types (cropland, pasture land, lake, forest, garden plot) have been identified and radioecological and dosimetry models, implemented in Ecolego, have been used to assess the environmental transfer of radionuclides and doses to man. Releases to the marine environment were modelled by the customized box-model Poseidon and validated with experimental data from the operator's environmental monitoring program. The transfer of radionuclides to marine organisms was simulated with a dynamic food chain model that considers the food web structure with different trophic levels of organisms. The water exchanges of coastal boxes were obtained from data provided by the national weather institute or from simulations with the 3-dimensional hydrodynamic software THREETOX. Available site specific data have been utilized to the greatest extent possible in deterministic as well as probabilistic simulations with the models using Ecolego.

Improvement of the Dose Estimation in Case of an Occupational ^{241}Am Incorporation Event

Anna Pántya, Andor András, Tamás Pázmándi, Péter Zagyvai

Hungarian Academy of Sciences Centre for Energy Research, Budapest, Hungary

Abstract. An occupational incorporation event occurred at the Radioactive Waste Treatment and Disposal Facility of Püspökszilág, Hungary in December 2013. Internal contamination due to ^{241}Am was discovered by a regular routine whole body counting measurement at the Centre for Energy Research, two days after the contamination. For preliminary calibration a home-made chest phantom was applied simulating uniform lung activity distribution by ^{241}Am point sources located in different positions within the lung volume of the phantom. Dose consequences of the incorporation were calculated by using dose coefficients from ICRP publications and the MONDAL-3 computer code. Later great efforts have been made to improve the accuracy of the results. In order to carry out a more precise calibration, efficiency for lungs and liver measurements were performed with the Lawrence Livermore National Laboratory (LLNL) chest phantom provided by the International Atomic Energy Agency. Individual chest wall thicknesses were also determined and taken into consideration. In the long term ^{241}Am is a bone-seeking isotope. As it enters the human skeleton skull measurements were also performed. Efforts have been made using physical and numerical skull phantoms in order to be able to interpret the skull measurements. Since detection of internal contamination by direct in vivo measurement is much less sensitive than bioassay of excreta, activity concentration of ^{241}Am was determined in urine samples with various methods. If activity of ^{241}Am was below the detection limit of gamma-spectrometry, samples were analysed by radiochemical separation followed by alpha-spectrometry and ICP Mass Spectrometry. For more accurate dose estimation physical and chemical parameters of the incorporated radionuclide (absorption type, particle size, etc.) were investigated and more sophisticated computer codes (IMBA, IDEA System) were used for the evaluation of incorporation monitoring data. Primary purpose of the presented work was to increase the accuracy of the methods and measurements used for the evaluation of this incorporation event in order to improve the reliability of dose estimation.

Argentinian Intercomparison on Interpretation of Data from Internal Exposure Sceneries for Dose Assessment

Ana Rojo, Nancy Puerta, Sebastian Gossio, Inés Gomez Parada

National Regulatory Authority, Buenos Aires, Argentina

Abstract. Internal dosimetry intercomparisons are essential for the verification of the models applied and the results' consistency. To that aim, in 2014 a National Intercomparison Exercise was organized and coordinated by the Internal Dosimetry Laboratory of the Nuclear Regulatory Authority of Argentina. Four simulated internal exposure sceneries were set out, each one of them with a particular complexity, covering intakes of ^{131}I , ^{137}Cs and Tritium. The IDEAS Guidelines, developed by the European Internal Dosimetry Working Group (WG 7) (EURADOS), was proposed in this intercomparison as suggested protocol for dose assessment. The participants included four Technical Support Officers (TSO) from nuclear power plants and atomic centres. This paper shows a complete analysis of the participant's reported results based on IDEAS Guidelines criteria. The performance of the laboratories was obtained applying z-score statistical analysis. The assigned values for intake and effective dose were defined from reported results of the Latin American intercomparison organized by ARN in 2013. All participants solved the four proposed cases with a high grade of accepted results.

Economic Losses of the Nuclear Industry Related to Loss of Workers Occupational Disability for Medical Reasons

Alexander Samoilov, Andrey Bushmanov, Andrey Kretov

Burnasyan Federal Medical Biophysical Center of Federal Medical Biological Agency, Moscow, Russia

Abstract. In the last years the enterprises of the Russian nuclear industry have stably maintained a low level of occupational diseases: not more than 120 cases per year, that is less than 1.5% of occupational diseases in the Russian Federation. Among the nuclear industry workers the occupational diseases due to the ionizing radiation exposure are rather rare (0.8% of total occupational diseases in this group of workers) and result from working in poor conditions at the early period of development of the field. Nowadays, Russia is implementing measures to prevent not only occupational diseases, but also diseases which hinder the continuation of professional activities using ionizing radiation sources. In the presented work we examined the results of periodic medical examinations of 70 000 nuclear workers engaged in work with ionizing radiation sources, including the rate of medical contraindications (number of employees with medical contraindications, per 100 employees). The study shows that during 2011 - 2014 the frequency of the revealed medical contraindications among the workers of the nuclear industry has ranged from 2.5 to 3.22 cases per 100 employers. The dominating groups of diseases that hinder continuation of the work with ionizing radiation sources include cardiovascular diseases, diseases of the respiratory system and the musculoskeletal system. The analysis of these data allows to formulate and propose the measures aimed to identify and reduce the risks and to prevent the development of the main types of medical contraindications. As the result it would ensure the prevention of disability of qualified and experienced specialists and, consequently, will prevent related economic losses. The calculated economic losses of the nuclear industry associated with the costs of necessary training of new workers in order to replace the suspended highly skilled professionals can achieve up to \$ 200 million per year. The proposed measures of prevention of medical contraindications among professionals working with ionizing radiation sources can prevent up to 30% of the total economic losses of the nuclear industry.

3A vii Safety and Risk Assessment Safety Assessment for Non-Reactor Facilities

Bethany Louise Cawood

NESCA, Pretoria, South Africa

Abstract. A safety assessment for a non-reactor facility is done using the procedure set out in IAEA-TECDOC-1267 Procedure for conduction probabilistic safety assessment for non-reactor nuclear facilities. There are however a number of constraints for existing facilities that can complicate the process. Complications such as: a lack of design information for an existing facility; a lack of documentation on design changes; adapted work procedures; changes in regulatory requirements during the lifespan of the facility. These are just some of the challenges that has to be overcome in the compilation of a representative safety assessment. Finding a way to fit the available information with the regulatory requirements in a sensible way to prove that the facility is still operating safely is a challenge to nuclear safety analyst and engineers in the licensing environment.

RadProtect[®] Increases Survival Rate in Novel Murine Slow and Low (S&L) Irradiation Model

Chia-Hung Chen, Jen-Ling Wang, Wei-Chuan Liao, Chau-Hui Wang, Tzu-ying Hung, Alan Liss

Original BioMedicals Co., Ltd., Tainan City, Taiwan

Abstract. People moving into a radiation/nuclear event area, such as first responders, will need the traditional acute radiation syndrome (ARS) drugs such as Neupogen and other therapies. However, it is also important to develop radioprotectant to provide protection from irradiation damage and increase the chance to survive the exposure. RadProtect[®], a novel polyethylene glycol micelle formulation of amifostine, is being developed as a radioprotectant for prolonged, slow and low dose rate (S&L) exposure with the intent of protecting first responders in the event of a nuclear emergency. Non-sedated mice were administered RadProtect[®] or amifostine 90 minutes prior to being exposed to a cumulative 8.3 Gy by X-ray irradiation. The low dose rates of 0.035 Gy/min were achieved under normal operation of the RadSource RS-2000 with an increased thickness of the Cu filter. X-ray exposures were conducted for four consecutive hours. The primary efficacy endpoint of RadProtect[®] was survival through 30 days post irradiation; secondary endpoints included objective numerical scoring of ARS severity (posture, coat, and behavior), and histopathology. Results show that animals treated with RadProtect[®] had a 93.3% survival rate at 30 days post irradiation compared to 40% survival in Excipient-treated animals and 50% survival in amifostine-treated animals irradiated at 8.3 Gy. The median survival of RadProtect[®]-treated, amifostine-treated animals and control animals was not calculable (> than 30 days), Day 28 and Day 22, respectively. Treated animals exhibited a reduced magnitude of severity and a delay in expressing ARS symptoms as measured by numerical scoring. Histopathology evaluations indicate that RadProtect[®] provided significant protection from lesions caused by X-ray exposure in comparison to control animals. Overall, in mice RadProtect[®] appears to have a strong radioprotective effect on survival and ARS injury when administered 90 minutes prior to irradiation.

Development of Mesh-Type ICRP Reference Phantoms and its Implications

Chan Hyeong Kim

Hanyang University, Seoul, Republic of Korea

Abstract. The ICRP Committee 2 has launched a new research project to develop a set of mesh-type ICRP reference phantoms, by converting the current voxel-type ICRP-110 reference phantoms into high-quality mesh format, to overcome the limitations of the current voxel-type ICRP reference phantoms. The limitations of the current reference phantoms include that these voxel-type reference phantoms do not properly model very small, complicated, and thin tissues such as the lens of the eyes and the skin, resulting in dose errors for weakly penetrating radiation; cannot represent the thin target tissues (10-300 microns) of the respiratory or alimentary tract organs, requiring additional stylized phantoms for dose coefficient calculations; and are not deformable in nature and cannot be deformed for posture change, which becomes a critical limitation when it comes to emergency exposure situations requiring reference phantoms with different postures for dose coefficient calculations. The objective of the new research project is to produce exact replica of ICRP-110 reference phantoms in a high-quality mesh-format to address these problems. The developed phantoms will include continuous and fully-enclosed surfaces for the skin, stomach, gall bladder, and urinary bladder; include the thin target layers in the alimentary and respiratory tract organs; and will include detailed and more accurate models for skeletal system, eyes, lymphatic nodes, blood vessels, and hands. The developed phantoms will be also deformable. The presentation will introduce the project in general, explaining the motivation, objective, current progress, preliminary results, and implications of the success.

Devaluation of Rhinoceros Horn through Nuclear Techniques

Charles Kros, Jan Rijn Zeevaart, Arnaud Faanhof, Frikkie de Beer, Deon Kotze, Dave Hudson-Lamb, Frederik Botha, Gawie Nothnagel

NECSA, Pretoria, South Africa

Abstract. South Africa is home to 83% of Africa's rhinoceroses and 73% of all wild rhinoceroses worldwide and an important country for rhinoceros conservation. However, the poaching of rhinoceroses has reached a crisis point, and if the killing continues at this rate, population decline could be expected in 2016-2018, meaning rhinoceroses could go extinct in the very near future. The total number of rhinoceroses poached in South Africa during 2014 increased to 1215 as the number of people arrested for rhinoceroses poaching-related offences climbed to 34. Several attempts have been made to stem poaching, ranging from implants of electronic signal devices to possible colouring impregnation or even poisoning of horns. A research project is currently being undertaken at Necsa to investigate the use of in situ labelling of rhinoceros horn through neutron activation. The primary purpose of radioactive labelling techniques is to enable the detection of poached rhinoceros horn at border control points through radiation monitoring. This paper will discuss the options considered and presents results of the investigation to date.

The Radiological and Health Impacts to the Residents of the Tudor Shaft Informal Settlement

Dawid de Villiers^a, Gert Liebenberg^a, Rean Swart^b, Rietha Oosthuizen^c, Juanette John^c, Hanlie Liebenberg-Enslin^d, Didintle Modisamongwe^d, Grant Walters^e

^aSciRAD Consulting (Pty) Ltd, Hartbeespoort, North-West, South Africa

^bNuclear Liabilities Management, Necsa, Pelindaba, Gauteng, South Africa

^cCouncil for Scientific and Industrial Research, Climate Studies, Modelling and Environmental Health Research Group, Pretoria, Gauteng, South Africa

^dAirshed Planning Professionals (Pty) Ltd, Midrand, Gauteng, South Africa

^eDepartment of Environmental Affairs, Pretoria, Gauteng, South Africa

Abstract. The residents of the Tudor Shaft Informal Settlement are exposed to mine waste in that the settlement lies in very close proximity of abandoned gold and uranium tailings facilities. A radiological public safety assessment and a health assessment were conducted to determine the current impact to the residents of the Tudor Shaft, as well as the impacts when the tailings are to be removed while the people remain at the site (this represents a worst case scenario in case the people cannot be relocated). The source-pathway-receptor assessment methodology as well as the applicable data that was utilised, are described. Finally, the results of both the radiological and health assessments (in terms of exposure to particulate matter equal to or smaller than $10 \mu\text{m}/\text{m}^3$ and the radionuclides) are presented and discussed.

Mathematical Modeling of the Aging Process of the Containment Spray Injection System using the Fault Tree Method

Diogo da Silva Borges, Deise Diana Lava, Maria de Lourdes Moreira, Antonio Cesar Ferreira Guimarães

Instituto de Engenharia Nuclear, Rio de Janeiro, Rj, Cidade Universitária, Brazil

Abstract. This paper presents a contribution to the study of aging process of the Containment Spray Injection System (CSIS) in commercial plants of Pressurized Water Reactors (PWRs). The motivation for write this work emerged from the current perspective nuclear. Numerous nuclear power plants worldwide have an advanced operating time. This problem requires a process to ensure the confiability of the operative systems of these plants, because of this, it is necessary a methodologies capable of estimate the behavior of a system during the normal time operation of a plant. In addition to the safety factors involved, such methodologies can to be used to search ways to ensure the extension of the life cycle of nuclear plants, which inevitably will pass by the decommissioning process after the operating time of 40 years. This process negatively affects the power generation, besides demanding an enormous investment for such. Thus, this paper aims to present modeling techniques and sensitivity analysis, which together can generate an estimate of how components, which are more sensitive to the aging process, will behave during the normal operation cycle of a nuclear power plant. With the results obtained and the use of mathematical techniques will be presented a set of equations capable to predict system behavior from its creation to the consideration of total failure, which can be translated as the end of the activities of a facility. To this end, will not be considered the process of replacement or repair of components.

Determination of the Detection Efficiency of ^{131}I in Thyroid using Monte Carlo Method

Dayana Ramos Machado, Yoan Yera Simanca, Gladys M. López Bejerano, Nancy Acosta Rodriguez

Centre for Radiation Protection and Hygiene, La Habana, Cuba

Abstract. Monte Carlo Method was the base to estimate the detection efficiency of ^{131}I of the identiFINDER ultra detector in “thyroid” geometry. The suitability of the calibration methodology is discussed using a comparison of the results of the Direct Monte Carlo Method and the Transfer Monte Carlo Method calculations with the values of experimentally calculated efficiency. Transfer Monte Carlo Method was the elected methodology because of the differences with the real detection efficiency stay below 10%. In the simulations, the geometric parameters of the detector were found using a tomography study. The arrangement detector – point source was simulated to obtain the correction factors for preset distances, and the arrangement detector – thyroid phantom was simulated to obtain of the detection efficiency curve in function of the distance for ^{131}I . In order to validate the proposed methodology the Internal Dosimetry Laboratory of the Centre for Radiation Protection and Hygiene participated in a regional intercomparison exercise of measured activity estimation in thyroid, for the estimation were used the traditional calculation methodology as well as the methodology base on Monte Carlo Method, the results were satisfactory in both cases. As a final result, the curves of detection efficiency for the measurement of ^{131}I in the thyroid gland was obtained without using physical phantoms, replacing the current lack of it.

Uranium Aerosols in Nuclear Fuel Manufacturing

Edvin Hansson^{a,b}, Håkan Pettersson^a, Christine Fortin^c, Mats Eriksson^{a,d}

^aLinköping University, Linköping, Sweden

^bWestinghouse Electric Sweden AB, Västerås, Sweden

^cCarl Zeiss SAS, Marly-le-Roi, France

^dSwedish Radiation Safety Authority, Stockholm, Sweden

Abstract. Internal exposure from inhalation of uranium aerosols is essential to consider in nuclear fuel manufacturing. In-depth knowledge about the aerosol source term is required to carry out risk assessments. Cascade impactor sampling in the operator breathing zone was carried out at a light-water fuel manufacturing plant. The sampled aerosols were analyzed using scanning electron microscopy coupled with energy dispersive spectrometry. Imaging showed remarkable variations in aerosol morphology at the different workshops (conversion, powder preparation and pelletizing). A presence of very large particles (up to $\sim 100 \times 50 \mu\text{m}^2$) in the operator breathing zone was verified. Spectrometric analysis of the aerosols showed varying uranium mass fractions, indicating variable densities. Uranium particles frequently contained nitrogen, fluorine (conversion workshop) and iron (pelletizing workshop). Morphology and elemental composition will affect particle aerodynamics and solubility in lung fluid. The study suggests a very complex aerosol source term for the evaluation of internal exposure.

The Future Free Electron Laser Facility SwissFEL from a Radiation Protection Point of View

Eike Hohmann, Roland Luescher, Elisa Musto, Albert Fuchs, Sabine Mayer

Paul Scherrer Institute, Villigen, Switzerland

Abstract. SwissFEL is a new X-ray free-electron laser large-scale facility, currently under construction at the Paul Scherrer Institute (Switzerland), whose aim is to produce FEL pulses covering the wavelength range 1 Å to 70 Å (0.1–7 nm). The facility has a total length of 720 m and comprises an injector part, a linear accelerator (linac) part, and two undulator sections terminating in two beamlines; the injector, linac and the undulator sections as well as the experimental stations are located underground, in the ground floor of a two-storey building. The linac is foreseen to accelerate electrons with a pulsed time structure up to an energy of 7 GeV, and its commissioning is scheduled for spring 2016. A series of infrastructure buildings will be located on the top floor above the accelerator section. The area above the undulator section is accessible by the public leading to new challenges for the dose surveillance. The shielding of the facility was designed in an early phase of the project based on assumptions regarding different modes of operation, beam losses and accident scenarios. Additional experience from measurements in a test injector facility, operated at a maximum energy of 300 MeV serving as the principal test and demonstration plant for the SwissFEL project, partly changed and influenced these assumptions. The presented studies describe the final layout of the facility including the impact of infrastructure feedthroughs, beam stopping devices and ventilations shafts from a radiation protection point of view and the lessons learned during the project progress. In addition, measures like local shielding, scenarios and beam parameters defined to be in compliance with guidance values according to Swiss radiological protection regulations will be shown.

Assessment of Beam Dump Activation for RAON Heavy Ion Accelerator in Korea

Eunjoong Lee^a, Cheolwoo Lee^b, Sungchul Yang^b, Young-Ouk Lee^b, Kyeongjin Park^a, Gyuseong Cho^a

^aKorea Advanced Institute of Science and Technology, Daejeon, Republic of Korea

^bKorea Atomic Energy Research Institute, Daejeon, Republic of Korea

Abstract. The RAON accelerator will provide primary beams on a fragmentation target in In-Flight (IF) separator system, and unreacted primary beam will be removed by the beam dump system. During the operation, the beam dump components will be activated by the unreacted primary beam. The estimation of the induced radioactivity in an accelerator facility is particularly important for maintenance interventions and final disposal of radioactive waste. In this study, the radioactivity of the radionuclides produced in the beam dump components and residual dose rate induced by the radionuclides are quantified. The induced radioactivity was estimated by two codes which MCNPX 2.7 and SP-FISPACT 2010. MCNPX is a particle transportation code and FISPACT is an activation analysis code. The track information of the primary beam was scored by the MCNPX and activation analysis was carried out by the SP-FISPACT. The dose rate also measured via MCNPX utilizing the gamma-rays emitted from the radionuclides that calculated by the FISPACT. For the primary beam, ^{238}U , ^{16}O , ^{48}Ca , ^{86}Kr and ^{112}Sn were evaluated. The maximum primary beam energy for ^{238}U beam is 400 MeV/u, 590MeV/u for ^{16}O , 550MeV/u for ^{48}Ca , ^{86}Kr and ^{112}Sn . The beam powers are 400kW for all particles. The beam dump consists of three components, titanium (Ti), water and stainless steel (ST304). The outside diameter is 60 cm and titanium shell was set to 1mm. The depth of water chamber is 10 cm. The activity calculation was performed for 5000 hours of irradiation time that expected operation time in a year. After the irradiation, activity was estimated at several cooling times up to 1 year which 1 s, 10 m, 30 m, 1 h, 8 h, 1 d, 1 w, 30 d and 1 y. As a result, quantitative information about the radioactivity in the beam dump of the IF facility in RAON accelerator complex was obtained through the simulations. Activities of the radionuclides and dose rates were estimated. With the ^{238}U as a primary beam, 191, 253 and 129 types of radionuclides were produced in titanium, water and ST304. During the operation, the dose rate was increased up to 0.2 Sv/hr and decreased after shutdown. As well as ^{238}U beam, activation results of the ^{16}O , ^{48}Ca , ^{86}Kr and ^{112}Sn beams also quantified.

Area Monitoring on Nuclear Fuel Cycle Facilities

Elizabeth Renteria, Paula Nuñez, Analia Saavedra, Nestor Fruttero, Allan Segato

Nuclear Regulatory Authority, Buenos Aires, Argentina

Abstract. Several uranium compounds are handled, stored and processed according to rules and safety standards in Nuclear Fuel Cycle Facilities in Argentina. The main risk in the facilities dedicated to manufacture fuel elements with natural or enriched uranium below 1% enrichment, is the exposure to internal contamination. The protection of workers that handle radioactive powders requires the adoption of protective measures in order to reduce the possibility of intake radioactive material through inhalation, skin hurts or contaminated surfaces. Suitable conditions of working areas from health physic point of view are verified through the inspection program implemented by the Control Fuel Cycle Facilities Department of the regulatory body. In this paper, the dominant risks associated to natural uranium fuel fabrication facilities together with the design and operational protective measures adopted are discussed. In addition, inspection activities, their frequency and reference values applied and the results of the monitoring program for the last three years period are summarized. Finally, the calibration techniques and detection limits calculations for inspection equipment available are presented.

How Spanish Nuclear Power Plant have Implemented Lessons Learned from the Fukushima Accident in the Radiation Protection Field

Eduardo Sollet

Cofrentes NPP, Valencia, Spain

Abstract. This presentation will cover the different improvements that Spanish Nuclear Power Plants have implemented after the Fukushima accident in the radiation protection field such as: new radiation protection instrumentation to cover emergency dose rates up to 10 Sv/h, new procedures to define radiation protective measures during the early phase to evaluate the magnitude of the accident, new emergency dose levels, new building to manage the accident in case of control room evacuation, new meteorological tower to be able to estimate the potential impact of the gaseous releases, new procedures to handle potential radioactive liquids and to reduce the amount of the gaseous releases, and dedicated training before the voluntary acceptance of emergency doses greater than 50 mSv.

Setting up an Occupational Radiation Protection Program in NORM Industry: A Case Study in Mining Industry in the Democratic Republic of the Congo

Francois Kazadi Kabuya^a, Vincent Lukanda Mwamba^a, Leonard Woto Makontsh^a, Robert Lwamba Ilonda^b

^aRegional Centre for Nuclear Studies (CRENK), Commissariat Général à l’Energie Atomique (CGEA), Kinshasa, The Democratic Congo

^bAPKAT, Commissariat Général à l’Energie Atomique (CGEA), Lubumbashi, The Democratic Congo

Abstract. Monitoring measures to assess the need for setting up an occupational radiation protection programme in some Co and Cu mines operating in the Katanga Province were conducted. In order to identify suitable mining activities potentially requiring a regulatory control and determine the appropriate regulatory approach, the study implied identifying the radionuclides of interest, the potential pathways of worker’s exposure and the most potentially exposed workers. γ portable survey meters and γ spectrometry system were used to implement area monitoring and to determine NORM activity concentrations in ore rocks samples and concentrates minerals in both open and underground pits. Although radiation doses to workers were as high as 25mSv in some areas of concerned mines, mean doses were calculated and found to be below the regulatory limits in some mines and exceeding exemption levels in some others. As a result, approximately 38% of mines required implementation of workplace monitoring and individual monitoring. Due to underground mining activities, 22% of assessed mines required monitoring for both external exposure and internal exposure. Other major findings included lack of awareness about radiological risks and inadequate knowledge of regulatory infrastructure in place. Government commitment to ensuring safety and security in mining sector through a strong regulatory body has been found to be a key factor to a successful implementation of occupational radiation measures in mines.

KEYWORDS: *occupational; exposure; radiation workers; NORM; ores.*

Monitoring and Mapping of Radon Concentration within Ghana Atomic Energy Commission

Francis Otoo^{a,b}, Emmanuel Ofori Darko^{a,b}, Massimo Garavaglia^c, Concettina Giovani^c, Silvia Pividore^c, Bentil Aba Andam^b, Geoffrey Emi-Reynolds^{a,b}, Lucas Piccini^c

^aRadiation Protection Institute, Ghana Atomic Energy Commission, Accra, Greater Accra, Ghana

^bSchool of Nuclear and Allied Sciences, University of Ghana, Accra, Greater Accra, Ghana

^cPhysics Department, Agency for Environmental Protection, Udine, FVG, Italy

Abstract. The health hazard associated with radon has been the subject of discussion in many fora. Given the importance of health as one of the most vital areas of social concern, a series of studies have already been conducted by leading experts and agencies which discuss mainly the health hazards related to radon concentration. The Surgeon General of the United States has warned that radon is the second leading cause of lung cancer in the United States apart from smoking cigarette. The Ghana Atomic Energy Commission (GAEC) is a workplace of long occupancy for workers where measurements of indoor radon is of equal importance for an adequate risk assessment. Objective: Monitoring and mapping of Indoor radon concentration within the premises of Ghana Atomic Energy Commission Materials and Method: In this study, CR-39 Solid State Nuclear Track Detectors were used. Radon survey was carried out. The radon detectors were exposed in workplaces such as laboratory, offices and conferences halls, of GAEC. After exposure of the radon dosimeters, the radon sensitive plastic pieces inside the Radopot were collected and sent to Physics Department of Agency for Environmental Protection, Udine, Italy for the analysis. The RadoSlide with the chips was then mounted on the etching carousel and chemically etched in the thermostatic bath with 36 ml of 96 % diluted acetic acid and 4000 ml of distilled water. The latent tracks formed on the detectors were scanned and counted with the RadoMeter 2000 system, consist of digital optical microscope with 40 times optical magnification lens which can read 47 mm² surface area divided into 144 fields. The tracks density measured was then used to calculate the activity concentration of the radon given as $(C_{Rn}) = \frac{E_0 \rho_m}{\rho_0 t}$. Where, ρ_0 is the calibration factor of detector (track/cm²d/(Bq/m³), ρ_m is the measured surface density of tracks on the exposed detectors (tracks/cm²), E_0 exposure dose during the calibration process (Bqh/m³) and t is the exposure time. Result and Discussion: The study values for radon concentration ranging from the offices (11.42 - 537.05 Bq/m³), laboratory (17.59 - 140.54 Bq/m³) and conference rooms (110.62 - 229.37 Bq/m³), with the credit union association (CUA) of GAEC recorded elevated value of 537.05 Bq/m³ which 5 times greater than action levels proposed by World Health Organization (WHO) and 3 times greater than highest values of conferences rooms. This is due to poor ventilation in the rooms while the lowest value from office was obtained from wooden structure with very good ventilation as compared to other offices. Average radon concentration increase from conference halls to laboratories. This can be attributed to the number of rooms monitored, since the offices recorded the highest number as compared to the conference halls and laboratories. Conclusion: Generally, radon levels were found to be low with most of the measurements recorded maximum value far less than the recommended action levels proposed by WHO and other international organizations. The CUA and other ground floors recorded radon levels higher than action levels proposed by the WHO.

GIS Mapping and Background Ionizing Radiation (BIR) Assessment of Solid Mineral Mining Sites in Enugu State, Nigeria

Avwiri Gregory, Agbalagba Ezekiel, Osimobi Jude, Ononugbo Patience

University of Port Harcourt, Choba, Rivers State, Nigeria

Abstract. A study of the external background ionizing radiation (BIR) levels in eight solid mineral mining sites in Enugu State have been carried out using two Digilert radiation monitors Radalart-50 and Radalart-100. Thirty- two readings of four each were taken at different solid mineral sites of the state following standard procedure. The measured BIR levels obtained ranged from 0.012mR/hr in Nkpologwu Silica mining site to 0.028mR/hr in clay mining site in Enugu-Ekulu with an average of 0.018 ± 0.004 mR/hr, while the corresponding calculated equivalent dose rate ranged from 1.0mSv/yr to 2.35mSv/yr with a mean value of 1.51 ± 0.04 mSv/yr. The result obtained indicates that the average exposure level of the studied area is 38.5% higher than the international standard. This suggests the possibility of the presence of radionuclide in the solid minerals mined in Enugu state. However, the values obtained may not cause immediate health challenge to miners and those engage in commercial activities around these mining sites in Enugu, but may result to long term health side- effects to residence and miners who put in over twenty- five years in the job. From the forgoing, it is recommended that control mechanism be adopted for the members of the public, residence, commercial traders and miners working in these sites as well as to protect the environment.

KEYWORDS: *BIR assessment; GIS mapping; solid mineral; Enugu State.*

Using a Portable Neutron Generator in an Open Field: The Radiation Protection Assessment

Gian Marco Contessa^a, Nadia Cherubini^a, Alessandro Dodaro^a, Luigi Lepore^b,
Giuseppe Augusto Marzo^a, Sandro Sandri^a

^aENEA - Italian national agency for new technologies, energy and sustainable economic development, Rome, Italy

^bUniversity of Rome "Sapienza", Rome, Italy

Abstract. In view of the experimental activities with a portable D-T neutron generator, which produces 14 MeV neutron beam, the characterization of the emission of the generator was carried out for ensuring adequate safety conditions in terms of operational radiation protection. The neutron generator is used for inspection of samples in which is suspected the presence of fissile or fertile material or explosives. Its use implies the operation to be conducted in an open field, where the radiological protection of workers and public has to be provided with distance-from-the-source and light shielding systems only. In the current study the minimum requirements for the shielding and the distance of workers and other people are assessed, considering the actual operation parameters in terms of neutron yield, energy, working load and so on. This study is the basis for initiating the licensing process in Italy. The safety assessment is performed using the standard method of calculation indicated by the US NCRP publications and the results are validated by comparison to simulations obtained by means of the stochastic code for radiation transport MCNPX 2.5.0, which reproduces the operational conditions the neutron generator should operate in. The simulation model allows the user to reproduce the emission of the generator according to different settings of the accelerator voltage, beam current, pulse frequency and duty factor. The related results include the dose rates for different shielding geometries and compositions. Radiation protection indications for workers and population will be provided. A practical field application of the generator will be described and discussed.

Testing of Burn-up Calculation Method based on Chebyshev Rational Approximation with IAEA-ADS Benchmark

Guangyao Sun, Wending Fan, Lijuan Hao, Binhang Zhang, Jing Song, Pengcheng Long, Liqin Hu

Key Laboratory of Neutronics and Radiation Safety, Institute of Nuclear Energy Safety Technology, Chinese Academy of Sciences, Hefei, Anhui, China

Abstract. Based on the CAD-based Monte Carlo program for integrated simulation of nuclear system SuperMC, the burn-up calculation program was studied based on CRAM method. The combine of transport and burn-up calculation was inner coupling which will friendly for the user and obviously save the total calculation time. At the same time, several advance methods include the scoring massive tallies method based on tally assist tree, parallel calculation based on data decomposition, etc. were used in this study to speed up the calculate time. Series benchmark burn-up cases were used to verify the correctness of program including IAEA-ADS. IAEA-ADS benchmark is a sub-critical Thorium based reaction, which uses ^{233}U as fuel, ^{232}Th as breeding material and Pb as reflect layer. The geometry module of this reaction is a 320x640 cm R-Z cylinder, including 5 material regions and an isotropic outside neutron source in the middle of the system. In this study, the results were agreed well with TTA method and international calculation results, including the component of nuclide and Keff during each burn-up cycle, and shown the correctness of method developed in this paper.

Assessment of Occupational Exposure of ‘Conflict Mineral’ Artisanal Mine Workers via Radiogenic and Dosimetric Characterization of High Background Radiation Area (HBRA) Columbite-Tantalite (Coltan)

Hudson Angeyo Kalambuka^a, Leon Ntihakose^b, Jayanti Patel^a, David Maina^c

^aDepartment of Physics, University of Nairobi, Nairobi, Kenya

^bDepartment of Physics, Kigali Institute of Science & Technology, Kigali, Rwanda

^cInstitute of Nuclear Science & Technology, University of Nairobi, Nairobi, Kenya

Abstract. We report on the dosimetric study of extraction and processing of coltan in selected regions of Rwanda utilizing a dose meter and gamma-ray spectrometry. The study was motivated by the need for evidence-based development of a radiological regulatory framework for artisanal mining of conflict minerals in high background radiation areas, which is widespread in Eastern Africa. Measured absorbed dose rates varied 518.34 - 796.92 nGy h⁻¹, 522.4 - 820.7 nGy h⁻¹ and 563.8 - 845.7 nGy h⁻¹ in Muhanga, Ruli and Ngoma respectively, the values being 11 times higher than world average. Measured dose rates were twice higher than those computed based on measured activities, indicating the significance of gamma dose from radioactive dust and radon. PCA differentiated extracted from processed coltan accurately on the basis of the dosimetric characteristics. Calculation of effective doses according to exposure pathways and working scenarios showed that total effective doses vary 0.0173 - 0.272 mSv y⁻¹ in Muhanga, 0.013 - 0.525 mSv y⁻¹ in Ruli and 0.022 - 0.255 mSv y⁻¹ in Ngoma: inhalation of ore dust accounts for 98 % of the exposure. Processing of coltan was found to enhance the concentration of ²³²Th and ²³⁸U by factors of 3 and 2 respectively.

Towards a Novel Modular Architecture for CERN Radiation Monitoring

Hamza Boukabache, Michel Pangallo, Nicola Cardines, Gael Ducos, Antonio Bellotta, Ciarán Toner, Daniel Perrin, Doris Forkel-Wirth

European Organization for Nuclear Research, CERN, Meyrin, Switzerland

Abstract. CERN has the legal obligation to protect the public and the people working on its premises from any unjustified exposure to ionising radiation. In this context, radiation monitoring is one of the main concerns of the Radiation Protection Group. After 30 years of reliable service, the ARCON (ARea CONtroller) system is approaching the end of its lifecycle, which raises the need for new, more efficient radiation monitors with a high level of modularity to ensure better maintainability. Based on these two main principles, new detectors are currently being developed that will be capable of measuring very low dose rates down to 50nSv/h, whilst being able to instrument radiation over an extensive range of 8 decades without any auto scaling. To reach these performances, CROME (CERN Radiation MONitoring Electronics), the new generation of CERN radiation monitors, is based on a versatile architecture that includes new read-out electronics developed by the instrumentation and logistics section of the CERN radiation protection group as well as a reconfigurable system on chip capable of performing complex processing calculations. Beside the capabilities of CROME to continuously measure the ambient dose rate, the system generates radiation alarms, interlock signals, drives alarm display units through a field bus and provides long-term, permanent and reliable data logging. The measurement tests performed during the first phase of the development show very promising results that pave the way to the second phase: the certification.

KEYWORDS: *radiation monitoring system; sub-femtoampere; nanosievert; modularity.*

Radiation Protection Dosimetry (2017), Vol. 173, No. 1-3, pp. 240–244

doi:10.1093/rpd/ncw308

Assessment of Internal Dose due to Intake of Food for Determination of Representative Person in Normal Operation of Nuclear Power Plant

Hyungjoon Yu, Insu Chang, Jungil Lee, Jang-Lyul Kim, Bonghwan Kim

Korea Atomic Energy Research Institute, Daejeon, Republic of Korea

Abstract. In the process of optimization of radiation protection for the nuclear facility, the assessment of dose to the public should be performed for demonstrating compliance with the dose constraint. A group of the public is composed with various individuals who have different characteristics such as ages, genders, occupations, dietary habits, hobbies, etc. therefore it is necessary to define a specific individual for the assessment of dose. The International Commission on Radiation Protection defines 'representative person' in the publication 101A. Among the factors taken account of determination of representative person, notable consideration is applying the probabilistic approach for the dose assessment. In a probabilistic assessment of dose, the representative person should be defined such that the probability is less than 5% that a person drawn at random from the population will receive a higher dose. In this work, internal dose to the public due to intake of food contaminated from the gaseous effluent in normal operation of nuclear power plant was assessed in compliance with the ICRP's guidelines for determining representative person. For the probabilistic assessment, the dose to the public were calculated with iterations of evaluating gaseous dispersion to the environment and the available statistical data such as food consumption rate. The spatial distribution of ground concentration of radionuclides within 10 km radius from the Shin-kori nuclear power plant in Korea was evaluated with according to 16 points compass rose. By considering the transfer rate of radionuclides from ground to vegetables, to livestock, to meat and to milk, the radioactive concentration in the food were calculated. Then the food consumption rate of Korean and the internal dose coefficients were applied for calculating dose from intake. By combining the census of the population who lives in relevant sections, the distribution of the number of population according to the dose was derived. The 95th percentile value at the data of population according to the dose could represent person who exposed higher dose in the population group.

Practical use of Graph Theory to Reduce the Individual Doses of the Employees Working in Areas with High Background Radiation

Ilia Kudrin, Ivan Mazur, Konstantin Chizhov, Victor Kryuchkov

State Research Center - Burnasyan Federal Medical Biophysical Center of Federal Medical Biological Agency, Moscow, Russia

Abstract. A significant employees number of radiation-dangerous objects exposed to radiation not only at a fixed workplace, but also moving through Industrial site, for example, at the facilities for processing spent nuclear fuel, facilities for temporary storage of radioactive waste, and so on. This presentation is about applying the techniques developed based on graph theory, in order to minimize external doses from individual staff whose work is connected with the movement through the territory with high background radiation. The initial data uses the measurements of ambient dose rate with coordinates. For interpolation dose at any point on the ground we use kriging method. On the basis of these data, a graph is created in the form of a regular grid. As the weight of each graph's edge we use the dose that employee may receive when moving along this edge, taking into account its probable speed of movement, the grid spacing and the interpolated values of the dose rate. Method of dose minimization is selected from the classical methods developed in the theory of graphs, and depends on the task associated with the movement of workers in the territory. In the conditions of the problem may include a set of constraints, such as moving only existing roads, bypassing several fixed points, passing through each road only once, minimizing the dose to undergo mandatory for certain road network. Such problem conditions may arise during the automated radiation monitoring in the contaminated area, decontamination area, and others. The above approaches can be applied to different exposure situations (planned, existing and emergency). The above-mentioned methods are implemented in software and improved as part of the Russian-Norwegian agreements at the Russian enterprise at work on radioactive waste management. While applying these methods and comparing dose estimates calculated by the tracks of employees proposed by specialists of the company, and on alternative tracks calculated by the program, in the latter case, the projected doses were reduced by 20-30%.

Development and Implementation Experience of Information-Analytical System of Radiation Safety of Workers

Ivan Mazur, Ilia Kudrin, Chizhov Konstantin, Kryuchkov Viktor

State Research Center - Burnasyan Federal Medical Biophysical Center of Federal Medical Biological Agency, Moscow, Russia

Abstract. This presentation describes the experience of the development, important milestones and organizational features of implementation of information-analytical system of radiation safety of the workers on the example of Operator and Regulator concerns. The Operator in this case is an enterprise, a branch of the Russian Federation national nuclear corporation "Rosatom", that is the North-West Centre for radioactive waste management "SevRAO". This organization is located in north-west Russia, engaged in the temporary storage of radioactive waste and spent nuclear fuel. The Regulator is the Federal Medical and Biological Agency of Russia, particular the Inter-regional management № 120. The information-analytical system is designed to provide a structured data acquisition and analysis in order to ensure interaction between the regulator and operator. The system also provides a range of analytical tools to assist in decision making. The presentation touches as the creation of the technical features of the system, and organizational issues related to its implementation and use. This system is implemented and improved as part of the agreement between the Burnasyan Federal Medical Biophysical Center and the Norwegian Radiation Protection Authority.

Recent Developments in Occupational Exposure Reduction in Nuclear Power Plants

Jason Harris^a, David Miller^b

^aPurdue University, West Lafayette, IN, USA

^bUniversity of Illinois, Urbana, IL, USA

Abstract. Since the development of commercial nuclear power, measures have been taken to reduce exposure to occupational workers and the public. Although occupational exposures are at their lowest levels to date internationally, new issues challenge this fact. Some plants built in the 1970's and 1980's are reaching the end of their operation and are preparing for decommissioning. Others are extending their operating lifetimes. In both situations, material degradation and other aging issues are leading to higher source terms and thus higher occupational exposures. Also, staff at new plants is dealing with the growing pains associated with understanding operations at these facilities. Regardless, plants have continued to incorporate technologies and procedures to help reverse this trend of increasing occupational exposure. The purpose of this presentation is to highlight some of the recent developments in the commercial nuclear power industry to help reduce occupational exposure. New technologies, such as the use of specialized resins, robots, and novel telemetry, will be discussed. Changes in operational philosophies and workforce practices will also be summarized.

Practical Impacts of NORM Standards on Mining and Minerals Processing

Jim Hondros

JRHC Enterprises Pty Ltd, Adelaide, Australia

Abstract. The international standards for the management of NORM remain complex and sometimes contradictory and have the potential to result in wide ranging impacts in many mining and minerals processing operations around the world. The IAEA framework for managing NORM is based on a logical graded approach, which aims to ensure that the actual risks of radiation remain in perspective and that control is commensurate with the magnitude of risk. However, at a practical level, the application of the NORM standards is generally simplified, resulting in 1Bq/g being seen and used as a de facto limit. Even though mechanisms generally exist in national regulations for assessing the impacts of materials with natural levels of radioactivity from uranium and thorium above 1Bq/g, they are generally not used. This is because accurate impact assessments are difficult, and sometimes subjective, and a single figure is much easier to use. There are consequences of this simplification; with the most important being that it undermines attempts to ensure that radiological hazards and risks remain in perspective with other health, safety and environmental hazards and risks. In practice, the simplification of the standards leads to additional unnecessary project and operational costs or operating constraints in licences. The intent of the IAEA NORM standards is a graded approach to radiation protection based on actual risk. This paper provides real world examples of cases where the intent of the NORM standards has been lost due to simplification. The paper also provides some suggestions for improvement.

Radiation Protection in the South African Mining and Minerals Extraction Industries

James Larkin

University of the Witwatersrand, Johannesburg, South Africa

Abstract. For a number of different reasons both the gold mining and uranium mining industries in South Africa have been contracting over the past couple of years, with a knock – on effect for the extraction industries. This has led to the loss of many jobs across these sectors, including a number of technical positions. This has had a detrimental effect of the provision of radiation protection within these industries. Often times now an RP position within a company has been combined with other positions such as occupational hygienists or ventilation officers. The professional body that represents radiation protection professionals, itself is going through a number of significant changes trying to bring itself in line with international bodies of a similar nature. With the imminent start of the nuclear new build in South Africa, there is an urgent need to retool and train new entrants to the profession of radiation protection so that the mineral wealth of South Africa can be safely developed to the benefit of the whole nation.

Improved Approach to Estimate Fission Product Inventory using TRITON in SCALE 6.1 for a Nuclear Reactor with Gadolinium Burnable Poison

Jaehoon Song, Kyoyoun Kim

Korean Atomic Energy Research Institute, Deajeon, Republic of Korea

Abstract. The fission products inventory evaluation in a nuclear power plant or research reactor is a very important in view of license procedure, environment emission of radioactive isotope and a basis source term of reactor BOP design. The numerical computer code like ORIGEN2.2 has been used to evaluate fission products inventory of nuclear power plant. However, the usage of the ORIGEN2.2 has a limitation in view of restricted libraries and it do not reflect system geometric effect. First, the built-in cross section libraries are BWR(enrichment: 2.75wt%~3.4wt% / burnup: up to 40,000MWd/MTIHM), PWR(enrichment: 3.2wt%~4.2wt% / burnup: up to 50,000MWd / MTIHM), CANDU, HTGR and so on. Second, it could not reflect the effect from highly burning isotopes because the code regards whole reactor core or system as a point. In order to figure out above mentioned limitation to calculate fission products inventory in the case of a fuel with inherent properties and geometric features, TRITON procedure introduced in SCALE 6.1 code package is selected. TRITON makes cross sections data on user specified system using ENDF/b-VII, BULGE and a various build-in libraries considering with self-shielding resonance. After then neutron transport calculation is performed using NEWT(t-newt) and time dependent depletion calculation is also performed using origen-s(t-delp). In order to consider the burnable poison effect such as Gadolinium, several "MULTIRESION" card is used in TRITON input. In the 'MULTIREGION' card, equivalent radius reflecting burnable poison rod is considered with coolant regions. In view of geometric features, ten concentric circles are described in the model and 0.5 GWd/MTU burnup step is used during beginning of cycle. Those manners are to consider the effect that burnable poison is quickly eliminated at beginning of cycle. Through the comparison of multiplication factors increasing with burnup(time) between TRITON and McCARD, it confirmed that TRITON result is well agreed with McCARD within 100pcm and using depletion library generated from TRITON, fission products inventory calculation is performed.

The Field Characterization Around the High Energy X-ray Cargo Screenings

Kamil Szewczak, Katarzyna Woloszczuk

Central Laboratory for Radiological Protection, Warsaw, Poland

Abstract. The work presents results of radiological measurements around the high energy X-ray cargo screening units. The aim of work was to assess the occupational exposure for the staff involved in screening procedures as well as for the persons uncontrolled exposure inside the screening vehicle. The performed research covers the measurements around nine different X-ray machines working with the radiation at energy from 1 MeV to 9 MeV. In addition during the measurements around the 9 MeV accelerator the neutron check-measurements using Berthold LB6411 probe were realized as well. For the electromagnetic component the active method using high sensitive ionization chamber and passive method based on TL detectors were involved. Basing on the obtained results for single scanning procedure the estimation of the annual effective dose for staff as well as the total effective dose for the uncontrolled exposure person were presented.

Occupational Exposure during Fusion Research on PF-1000 Unit

Kamil Szewczak^a, Sławomir Jednorog^b

^aCentral Laboratory for Radiological Protection, Warsaw, Poland

^bInstitute of Plasma Physics and Laser Microfusion, Warsaw, Poland

Abstract. The work presents results of radiological measurements and effective dose assessment for persons working in fusion research using the biggest plasma-focus type unit (PF-1000) operating in the Institute of Plasma Physics and Laser Microfusion in Warsaw. The PF-1000 was considered as a source of neutrons and electromagnetic radiation. As typical the deuterium was used as a working gas in the experiments. In results of D-D reaction the neutron with starting energy 2,45 MeV are emitted. In addition during each discharge strong fluxes of deuterons, electrons and ions are accelerated in the plasma-origin magnetic field. The interaction of the accelerated particles with the unit material provide to emission of electromagnetic radiation. In addition the high energy gamma radiation (23,8 MeV) are emitted as a result of one of output channel of D-D reaction. The work considers the problem of personnel's exposure during plasma discharges and in the period between experimental sessions. Therefore, a distinction was made between the primary radiation appearing during the discharge, and the secondary radiation, which is emitted in the period between the experimental sessions. This secondary radiation is a results of the neutron activation of the constructional material of the vacuum chamber. An assessment of the exposure to the primary radiation was carried out on the basis of dosimetric measurements realized by developed methodology. An impact of the secondary radiation was estimated from activity calculations performed for radioisotopes produced during the activation process. The obtained results were compared with the dose limit specified in the permission for using the PF-1000 facility, as issued by the National Atomic Energy Agency.

Room Submersion Calculations of Noble Gas Dose Rate Coefficients

Ken Veinot^a, Shaheen Dewji^b, Michael Bellamy^b, Keith Eckerman^a, Nolan Hertel^{c,a},
Mauritius Hiller^b

^aEasterly Scientific, Knoxville, TN, USA

^bCenter for Radiation Protection Knowledge, Oak Ridge National Laboratory, Oak Ridge, TN, USA

^cGeorgia Institute of Technology, Atlanta, GA, USA

Abstract. The International Commission on Radiological Protection Publication 116 reports external dose coefficients for voxel phantoms, in so-called standard geometries while dose coefficients for environmental exposures, such as immersion in a cloud of radioactive gas, have been reported broadly in the literature. For environmental exposure scenarios, dose coefficients are typically calculated for persons immersed in a semi-infinite cloud or standing on contaminated ground. In this work, dose coefficients for persons in various sized rooms were calculated using the ICRP reference voxel phantoms positioned in rooms of three sizes representing an office, laboratory, and warehouse. Organ equivalent doses were computed for photons, electrons, and positrons sources, which were uniformly distributed in the room. Additionally, since the voxel phantoms lack the resolution to perform skin absorbed dose calculations appropriate for the depth of the skin, a mathematical phantom was used to compute the skin dose for the three particle types. The computational approach includes bremsstrahlung production in the air inside the room as well as the walls. Results indicate that the smaller room sizes have a significant impact on the dose per unit air concentration compared to the semi-infinite cloud case.

Residual Activity in Lead and Bismuth Materials induced by 100-40 MeV Protons

Leila Mokhtari Oranj^a, Nam-Suk Jung^b, Joo-Hee Oh^b, Hee-Seock Lee^b

^aDivision of Advanced Nuclear Engineering, Pohang University of Science Technology (POSTECH), Pohang, Republic of Korea

^bPohang Accelerator Laboratory, Pohang University of Science and Technology (POSTECH), Pohang, Republic of Korea

Abstract. We present results of the experimental study on the residual activity induced in lead and bismuth by 100-MeV protons. Irradiation was performed at KOMAC linac in Korea. Lead and bismuth targets were irradiated by 100-MeV protons. Lead and bismuth targets were arranged in stacks consisting of lead and bismuth foils at the different depth points of the targets. Aluminum and gold were used to measure the beam intensity of protons. Activation of foils was investigated using gamma-ray spectroscopy. Residual activity of radio-nuclei from $^{nat}\text{Pb}(p,xn)$ and $^{209}\text{Bi}(p,xn)$ nuclear reactions were measured at the different depth points of targets by measurement of individual lead and bismuth foils. The experimental data were compared with Monte Carlo simulations performed by FLUKA, PHITS/DCHAIN, and MCNPX/FISPACT codes in order to verify validity of physical models and data libraries in the codes which is our purpose. A satisfactory agreement between the experiment and the simulations was observed.

Security of Radioactive Materials in Oil & Gas Industry (Compliance & Challenges)

Mohammad Aref

Weatherford, Abu Dhabi, United Arab Emirates

Abstract. Security of Radioactive Materials in Oil & Gas Industry became more and more hot topic and daily challenges because of the incident occurred in some part of the world regarding the attempts of terrorists on developing dirty bombs using these radioactive materials sources. The Oil & Gas Industry Radioactive Materials sources became attractive targets for terrorist because of its small shape engineering design, mobility and normally availability in remote areas. But for the Oil & Gas Industry still the Unique Challenges in Security of Well Logging sources is the frequent transports in-between Base & Drilling Sites. Therefore there is an on-going effort by Oil & Gas companies towards the development of security controls on Radioactive Materials this will include, but limited to: using proper secure transport container and applying special security locking and monitoring system. In this presentation you will learn how effective radiation security management can support the legislations compliance and national security, explain the government and industry partnership relationship on security of radioactive materials, and understand the oil and gas industry security best practices and techniques. I'm trying to explain the specifics security concerns in Oil & Gas Industry from inside point- view and identify the challenges as well as the best practices on applying Security controls on Radioactive Materials on Operations, cover following topics: Application & Characteristics of Radioactive Materials in Oil & Gas Industry; Security Challenges; Industry Best Practices & technique of RAM Security Controls; Shared of lessons Learned.

Egypt Experience with Research Reactors Operation, Nuclear and Radiological Activities Law as a Step for Building Nuclear Power Reactors

Mohamed Goma

Egyptian Society for Nuclear Sciences & Apps, Cairo, Egypt

Abstract. Historically, as Early as 1957 Egypt Atomic Energy Authority (EAEA) was established. Among EAEA scientific departments were Reactors Department and Radiation Protection and civil Defence Department. Furthermore, Egyptian ionizing radiation law was issued in (1960) with EAEA as Reactors regulatory body. Egypt first research reactor ET-RR-1 went critical in 1961, a new project is aimed to upgraded it. Egypt second research reactor ET-RR-2 was operated since 1998, It is currently produce radioisotopes. Egypt is recognized by its Nuclear Engineering Department of Alexandria University. This department is recognized by IAEA as Centre of Excellence .Since 1967 generations of nuclear engineers were qualified as reactor operators not only Egyptian but also for Arab and African Engineers. Egyptian Nuclear power plant Authority (ENPPA) was established in (1977) as centre for studies and training using simulators .ENPPA responsibility was upgraded in 2010 to include build up and operation of nuclear power plants. This upgrading was one important item of law no 7 for year 2010 which deals with nuclear and radiological activities .Other items deals with the establishment of the newly formed Egyptian Nuclear and Radiological Regulatory Authority (ENRRA) as Egypt competent authority. The Egyptian nuclear power program was started as project in mid-sixties. Two sites were examined. The first proposed site was around 30 Km west of Alexandria. Later the second Proposed site was at El Dabaa around 156 Km west of Alexandria. From 1985 till year 2000 it was published in Nuclear News of American Nuclear Society that Egypt is proposing to have 8 NPP units. Due to Chernobyl accident the NPP program was freeze. Then the program was activated after 2010. Currently 4 NPP units to be built in cooperation with Russia.

Direct Measurement of Radium Levels in Waste Water Samples using Portable Medium Resolution Gamma Spectrometers

Michael Iwatschenko-Borho^a, Scott Masiella^b, Richard Oxford^b, James Williams^b

^aThermo Fisher Scientific Messtechnik GmbH, Erlangen, Germany

^bThermo Fisher Scientific RMSI, Oakwood, OH, USA

Abstract. Related to the growing importance of hydraulic fracturing and unconventional drilling (“fracking”) there has been a growing interest in quick and field deployable methods to determine the Radium content in waste water. Traditionally gamma measurements of the Ra-226 content require a 3 to 4 weeks wait time to achieve full in-growth of the Ra-226 progeny and the complete decay of the Ra-224 and Ra-228 progeny. Alternatively high resolution gamma spectroscopy can be applied that directly measures the 186 keV line of the Ra-226 and which requires just a 1 day wait time to account for the Ac-228 in-growth. This paper discusses alternative approaches for a fast decision, whether or not a certain specific activity level is exceeded - without the need of expensive and complex high resolution spectroscopy. Using portable instruments with integrated scintillation detectors such as NaI(Tl) or CsI(Tl) the different timing in-growth and decay behaviour of Ra-224, Ra-226 and Ra-228 progeny is analyzed in a simple process flow. Several variants of the so-called Practical Triage Concept (PTC) are described for both laboratory sample measurements as well as in-situ measurements. A cross comparison of the PTC results to the laboratory results after 3 week wait time is given and shows the benefits and limitations of the triage approach. Furthermore the benefits of in-situ measurements, which help to answer the question regarding the representativeness of the sample and the homogeneity of the activity distribution in the waste container, are discussed.

Practical Application Illustrating Excellence in Radiological Protection at the Koeberg Nuclear Power Station

Marc Maree

Eskom, Cape Town/Western Cape, South Africa

Abstract. The Koeberg Nuclear Power Station (KNPS) is the only nuclear power plant in Africa and is located in the Western Cape Province of South Africa, approximately 30 km north from Cape Town. KNPS produces 4.4% of the electricity generated by Eskom Holdings SOC Ltd (Eskom) and is comprised of two 970 MW pressurised water reactors which were commissioned in 1984 and 1985. The radiation protection programme employed at the KNPS is aligned to International safety principles, recommendations and requirements to maintain public and occupational exposures as low as reasonably achievable (ALARA) during planned exposure situations, emergency exposure situations and existing exposure situations. This presentation provides information about practical applications and practices employed in radiation protection at the KNPS in accordance with the Eskom Radiation Protection and the Safety of Radiation Sources Policy (Eskom RP Policy). The Eskom RP Policy sets out principles and overarching rules which are aligned with the Nuclear Energy Policy for the Republic of South Africa which states that: "In pursuing a national nuclear energy programme there shall be full commitment to ensure that nuclear and radiation safety receives the highest priority to provide for the protection of persons, property and the environment". The presentation addresses excellence in radiation protection employed at the Koeberg Nuclear Power Station relating to: Radiation Protection Rules, Radiation Protection Training, Operational Radiation Protection, Radioactive Waste Management and Emergency Preparedness and Response.

Improvement of Underground Radon Concentrations at a South African Gold Mine

Marc Vermeijs

AngloGold Ashanti, North West, South Africa

Abstract. The management of underground radon concentrations at AngloGold Ashanti, Covalent Water Company became extremely challenging due to a sudden change in underground ventilation conditions experienced at two of our water pumping Shafts. This necessitated the need for a sound approach and the implementation of cost effective solutions to deal with high radon concentrations that were now experienced due to this change. This paper presents the outcome of a project that was initiated where high radon concentrations were managed through a phased implementation process to return ventilation conditions to normal. The project was aimed at systematically reducing radon concentrations at both our water pumping Shafts. This initially required an understanding of the complex underground ventilation conditions as the Mine was recently acquired by AngloGold Ashanti. Ventilation conditions were improved by virtue of installing underground auxiliary fans, walls and doors to ensure that radon concentrations were drastically reduced. The reduction in radon concentrations was achieved and has been sustained. The key to the success of this project was demonstrated by well-structured and planned methodology based on site specific understanding of underground ventilation conditions. Sound ventilation engineering in combination with implementing cost effective solutions is the only way to sustainably reduce and manage underground radon concentrations in a South Africa Gold Mine.

Building Nuclear Security Culture in Morocco

Oumkeltoum Hakam, Abdelmajid Choukri, Taha Laghouazi

University of Ibn Tofail-Institute of Nuclear Materials Management, Kenitra, Kenitra, Morocco

Abstract. Many countries have expressed their interest in building infrastructure to benefit from the nuclear energy and to take advantages from the benefits of nuclear and radioactive materials in different applications. In counterpart, with the increasing threats, states should implement security measures to protect their infrastructure, and prevent non-state actors from acquiring nuclear or radioactive materials. This is why every country is responsible to develop, maintain and implement nuclear security regime which consists at establishing a legislative and regulatory framework, creates institutions to implement nuclear security measures and develop necessary competencies through educational and training programs in addition to international commitment. Furthermore, the role of human factor in increasing the effectiveness and efficiency of nuclear security is very important and therefore nuclear security culture is vital for nuclear security sustainability. Moroccan universities are aware of the role of nuclear security education in promoting nuclear security culture among scientists, technicians and engineers. The University of Ibn Tofail in cooperation with national and international partners developed its nuclear security educational programs and founded the Institute of Nuclear Materials Management Student Chapter (INMM-UIT) to educate the young generation and promote nuclear security culture at the universities and among professionals. We will present in this paper the main achievements of INMM-UIT and point out approaches deployed in order to promote nuclear security culture at national, regional and international level.

The Role of Radiation Protection in Nuclear Forensics: From the Crime Scene to the Laboratory

Philemon Magampa, Gedion Nkosi

NESCA, Pretoria, Tshwane, South Africa

Abstract. Nuclear security events refers to malicious acts (i.e. theft, sabotage, illicit transfer, and unauthorised access) involving nuclear and/or radiological materials as well as nuclear facilities. Nuclear Forensics (NF) refers to measures by which nuclear and/or radiological materials out of regulatory control are categorized, collected, characterized and consequently their origin and route is attributed. NF seeks to provide answers as to what the materials are, whether there is more, whether the law has been broken, who is responsible, was the material diverted, which route did it take? And ultimately prosecution of those responsible. This paper will focus on the radiation safety aspects during the nuclear forensic process as follows: protection of first responders, law enforcement personnel, the public as well as the environment at the crime scene, safe handling and garnering of the materials, safe transportation to the storage area as well as safe laboratory analysis, and safe pre-disposal storage of waste after analysis as well as safe disposal. Radiation Protection or Safety is very key in protecting all people involved during a nuclear security event. NF is a key tool in Nuclear Security as it facilitates nuclear attribution.

EcoMine – A Software Package based on Ecolego to Assess the Radiological Impact of Mining Sites and Activities

Rodolfo Avila^a, Erik Johansson^a, Japie van Blerk^b

^aFacilia AB, Stockholm, Sweden

^bAquisim Consulting Pty Ltd, Centurion, South Africa

Abstract. Mining sites and activities are often associated with radiological impacts to the public from NORM present in the residuals and in releases to the environment during operations. This is not limited to uranium mining, but it is also relevant to other types of mining projects, such as mining of phosphate, heavy mineral, rare earth elements, and metals (e.g., copper and gold). It is commonly the case that the radiological impact from multiple sources of contamination (e.g., tailings storage facilities, waste rock dumps, ventilation shafts), to a variety of receptors under different public exposure conditions need to be considered. The vector of the radionuclide to consider includes natural occurring radionuclides, such as the U-235, U-238 and Th-232 decay chains. The radiological assessment of such situations requires the use of several types of models such as air quality models, groundwater transport models, radioecological and dose assessment models. There is a need for integration of the outputs from all these models and for this purpose we have developed the EcoMine software package. In this presentation we will provide an introduction to the EcoMine software package, which has been developed on the basis of a commercial modelling software, Ecolego (www.ecolego.facilia.se). EcoMine uses as input data the results of air quality modelling (e.g., Radon and PM₁₀ concentrations and dust deposition rates) obtained for each source, to calculate doses associated with different public exposure conditions (e.g., subsistence farming, commercial agriculture, urban settling) by different exposure pathways. The results are obtained for a grid of points in the impacted area that can be seamlessly exported to maps of the radiological impact from all sources and for each particular exposure condition. The radiological impact by the groundwater and surface water transport pathways can also be considered. The usability of EcoMine will be illustrated through examples, which include the Harmony Gold Kusasalethu Operations, located near Carletonville in the North west Province of South Africa.

U and Th Source Term Characterisation in Selected Gold Tailings of the Witwatersrand (South Africa): A Geochemical Modelling and Reaction Network Approach

Robert Hansen^a, Japie Van Blerk^b

^aExigo Sustainability, Johannesburg, Gauteng, South Africa

^bAquisim Consulting, Centurion, Gauteng, South Africa

Abstract. In this study a geochemical reaction modelling and reaction network modelling methodology is used to identify the source terms and evaluate the geochemical behaviour of uranium and thorium in gold mine tailings in the Witwatersrand, South Africa. This study forms part of a larger radiological public safety assessment studies conducted for specific mines in the Free State and Klerksdorp gold mining areas. A number of analytical techniques and methodologies were applied. The numeric geochemical modelling and reaction network development is conducted iteratively and proves to be a useful tool in understanding the geochemical dynamics of U and Th in gold tailings storage facilities. The reaction network for U specifically indicates that the geochemical behaviour of U is governed by the dissolution of pyrite and subsequently uraninite, uranium aqueous complexation and acid neutralisation reactions by carbonates added to ore in the plant process. The study shows that adsorption in Witwatersrand tailings storage facilities are negligible and that dissolution and precipitation reactions dominate U and Th geochemical behaviours. Uranium specifically is shown to leach from the base of the tailings at concentrations between 67 and 95 µg/l. In addition, the study indicates that the spatial nature of the various geochemical zones within the tailings storage facilities may also have important implications for leaching of not only the radioelements, but also the metal, metalloid and anionic contaminants and acidity.

Radiation Protection Research

Rebecca Tadesse

U.S. Nuclear Regulatory Commission, Washington DC, USA

Abstract. This paper/poster will describe four major Radiation Protection Research activities. They are: 1) development of the technical basis for radiation protection regulations, 2) radiation protection computer codes, 3) public health epidemiology studies and 4) doses to the public from patient release research. Current work in the radiation protection regulation arena is the development of a regulatory basis for revisions of regulations to align with the recommendations in the International Commission on Radiological Protection (ICRP) Publication 103. As such, the NRC is sponsoring research in biokinetic and dosimetric models and dose coefficient factors for occupational and public exposure to radionuclides that are based on ICRP Publication 103. The Radiation Protection Computer Code Analysis and Maintenance Program (RAMP) is a program that maintains and develops radiation protection computer codes. The paper will describe RAMP codes that are used for dose assessment and emergency response. One code that will be highlighted is the Radiological Assessment System for Consequence Analysis (RASCAL) emergency preparedness code. This code was used during the Fukushima Dai-ichi event to assess radiation dose. In the area of patient research, will present the literature review performed to document dose to the public from patients' containing Iodine 131. The results of the literature review will be highlighted including next steps that will be taken to ensure that the public is protected from radioisotopes used in patient care.

Radiation Protection Aspects of Uranium In Situ Recovery / In Situ Leach Facilities

Steven Brown

SHB Inc., Centennial, Colorado, USA

Abstract. In Situ Recovery or In Situ Leach (ISR/ISL) uranium facilities, also referred to in the past as “uranium solution mining” have operated since the late 1960s (in US and Russia) and in recent years have been producing almost half of worldwide uranium supplies. In 2013, 47% of world uranium mined was from ISL operations. Most uranium mining in the USA, Kazakhstan and Uzbekistan is now by ISR methods. ISL mining of uranium is also undertaken in Australia, China, and Russia as well. In the next few years ISL operations are likely in Mongolia and Tanzania. The ISR/ISL process for uranium mining and milling involves dissolving the uranium within the ore body itself by circulating groundwater fortified with oxygen and a weak chemical additive (slightly alkaline in US, slightly acidic in Australia and Kazakhstan) into the formation through injection wells, dissolving the uranium “in – situ” and extracting the “pregnant” uranium solution through recovery wells. The final steps in processing (separation via ion exchange {IX} or solvent extraction {SX}, precipitation, drying, and packaging) may be partially or totally carried out at the in-situ facility near to the well fields or an intermediate product (may be shipped to another ISR/ISL facility or a conventional uranium mill for final processing. This paper presents an overview of the ISR/ISL process and the health physics programs developed at a number of commercial scale ISR / ISL Uranium recovery and production facilities in the US as a result of the radiological character of these processes. Although many radiological aspects of the process are similar to that of conventional uranium mills, conventional-type tailings as such are not generated. However, liquid and solid byproduct materials may be generated and impounded. The quantity and radiological character of these byproducts are related to facility specifics. Some special monitoring considerations are presented which are required due to the manner in which radon gas is evolved in the process and the unique aspects of controlling solution flow patterns underground. The health physics and radiation protection programs that were developed at first generation facilities are discussed and contrasted to radiation protection requirements of the current generation and state of the art of uranium ISR/ISL technologies and facilities.

Worker Protection Implications of the Solubility and Human Metabolism of Modern Uranium Mill Products

Steven Brown^a, Douglas Chambers^b

^aSHB Inc., Centennial, Colorado, USA

^bARCADIS Canada, Richmond Hill, Ontario, Canada

Abstract. This paper presents an analysis of the implications of some recent studies performed to characterize uranium products from modern uranium recovery facilities important for worker protection. Assumptions about the solubility (related to the molecular species being produced) of these materials in humans are critical to properly assess radiation dose from intakes, understand chemotoxic implications, and establish protective exposure standards (airborne concentrations, limits on intake, etc.). Recent studies, as well as information in the historical professional literature, were reviewed that address the issue of solubility and related characteristics. These data are important for the design of programs for assessment of both chemical and radiological aspects of worker exposure to the products of modern uranium recovery plants (conventional uranium mills and in situ recovery plants; i.e., ISRs). The data suggest strongly that the oxide form produced by these facilities (and therefore, product solubility) is related to precipitation chemistry and thermal exposure (dryer temperature). Given the peroxide precipitation and low temperature drying methods being used at many modern uranium recovery facilities in the U.S. today, very soluble products are being produced. The dosimetric impacts of these products to the pulmonary system (except perhaps in case of an extreme acute insult) would be small, and any residual pulmonary retention beyond a month or two would most likely be too small to measure by traditional urinalysis sampling or the current state-of-the-art of natural uranium in vivo lung counting techniques. Uranium recovery plants should revisit the adequacy of current bioassay programs in the context of their process and product specifics. Workers potentially exposed to these very soluble yellowcake concentrates should have urine specimens submitted for uranium analysis on an approximately weekly basis, including analysis for the biomarkers associated with potential renal injury [e.g., glucose, lactate dehydrogenase (LDH) and protein albumen]. Uranium facility operators and their regulators need to recognize the importance of the uranium chemotoxicity versus dose relationship in the interest of worker protection.

Dust Management on Tailings Storage Facilities at a South African Gold Mine

SJ van Wyk^b, CF Human^a

^aAngloGold Ashanti, North West, South Africa

^bAgreenco Environmental Projects, North West, South Africa

Abstract. The management of dust from Tailings Storage Facilities (TSFs) remains a challenging issue for environmental managers of mines. The need for a sound approaches and cost effective solutions to deal with dust from TSFs is a pressing matter in the light of mine's social licence to operate and the increasing regulatory air quality environment. The paper present the outcome of a tailings dust mitigation project where dust management objectives have been set by AngloGold Ashanti and mitigation measures are currently being executed through a phased implementation process. Dust suppression efforts prior to 2010 yielded unsatisfactory results for the company and it was therefore decided that a structured approach would be adopted based on a scientific dust management framework. This framework included a complete risk assessment and the development and implementation of a tailings best practice guideline. The process of site specific implementation of a dust mitigation solution requires an understanding of dust mechanics which include the regional climatology, soil properties, geometry of the landscape, existing dust mitigation measures and the legal requirements. When considering a solution cognisance of the Environmental Management Programme (EMP) requirements, scale of implementation, availability of infrastructure, implementation frameworks, cost and community expectations is required. Despite the substantial reduction in dust fallout achieved, the key to the success of this approach is the consistent achievement of the internal compliance target and also the ongoing community satisfaction as they are ultimately regarded the barometer of dust management success. Furthermore, the outcome of this project demonstrates that a well-structured and planned methodology based on a site specific and scientific understanding of tailings dust mechanics in combination with cost effective solutions is the only way to sustainably manage air quality around tailings storage facilities.

Risk of Radon Induced Health Effect: Evaluation Methods and Practical Application

Sergey Kiselev^b, Vladimir Demin^a

^aSRC Burnasyan Federal Medical Biophysical Centre, FMBA, Moscow, Russia

^bNational Nuclear Centre, Kurchatov Institute, Moscow, Russia

Abstract. To support decisions on justification and taking protective measures against radon exposure, methods of radon induced risk assessment are required. The analysis of existing models of the dose-effect relationship (DER) (BEIR VI, Wismuth model, model based on results of joint analysis of European residential radon case-control studies (EU), and the Tomasek model) was carried out. Some features of these models such as discontinuous values of key parameters, including step-like relationship nearby the latent period; the use of a simplified version of the multiplicative risk model; not enough full account of the ES results for the public etc., provided the necessity of developing an improved DER model (model “Radon-14”), and methods for risk assessment of radon human health effects, including the method of estimating exposure doses. The methodology is proposed for use in Russia. The results of risk assessment for various models, radon exposure levels, calendar years, sexes, and smoking status have been analyzed on the basis of the developed model. According to the obtained results, additional mortality due to radon induced lung cancer can reach 20% of the total lung cancer mortality within the territories of the Russian Federation, where radon EEC in dwellings is about 100 Bq / m³. Risk of both radon-induced and spontaneous lung cancer for regular smokers is several times - up to an order of magnitude - higher than for non-smokers. It was shown that the BEIR VI based risk assessments overestimate results (more than twice) in comparison with those based on models “Radon-14” and “Wismuth”.

Comparison of the Efficacy of Neutron Shielding of Aluminum and Polyethylene Composites Containing Micro and Nano-Sized B₄C and Carbon Nanotubes

SMJ Mortazavi^a, Fatemeh Jamali^a, MR Kardan^b, Sedigheh Sina^c, MA Mosleh-Shirazi^a, Jila Rahpeyma^a

^aShiraz University of Medical Sciences, Shiraz, Iran

^bRadiation Application School, Nuclear Science And Technology Institute, Tehran, Iran

^cRadiation Research Center, School Of Mechanical Engineering, Shiraz, Iran

Abstract. Secondary neutron radiation is produced due to the interactions of the galactic cosmic radiation (GCR) and solar energetic particles (SEP) with the walls of the spacecrafts. According to NASA, these secondary radiations have widely been ignored in previous space architectures. NASA confirms that long term human missions (i.e. >90-100 days) beyond low Earth orbit cannot be planned without developing appropriate shielding materials or biological countermeasures to keep the dose to astronauts below current dose limits. In this study, the neutron flux attenuation of new composites containing carbon nanotube and nano and micro- sized B₄C is investigated. After incorporating these materials into the polyethylene matrix, the shielding efficiency of the produced composites was compared to those of pure polyethylene and aluminum through both measurement and MCNPX Monte Carlo simulation. There was a good agreement between measurement and MCNP simulation. Our findings lead us to this conclusion that these composites can be promising shielding materials for space exploration.

Assessment on Occupational Exposure in Malaysia: Practices and Trends

Suzilawati Muhd Sarowi, John Konsoh, Ahmad Bazlie Abdul Kadir

Radiation Safety & Health Division, Malaysian Nuclear Agency, Kajang, Selangor, Malaysia

Abstract. An assessment of occupational exposure due to ionising radiation in Malaysia is regulated under national law, Atomic Energy Licensing Act 1984 (Act 304). Malaysia have developed in assessing of external exposure starts with using film, Thermoluminescence Dosimeter (TLD) and now move to Optically Stimulated Luminescence (OSL). The Secondary Standard Dosimetry Laboratory (SSDL) in Malaysian Nuclear Agency (Nuclear Malaysia) became the Personal Dosimetry Services Provider in the country. In 2011, the lab has collaborated with a private company in management of the dose assessment services. This paper will discuss on the practices of occupational dose assessment on radiation workers in Malaysia as a whole and also in Nuclear Malaysia as the agency is the biggest licensee's holder of national regulatory body. Then, a trends for the dose received by the radiation workers from 2011-2013 will be presented. The results for the dose received by Nuclear Agency's radiation workers show that the null hypothesis (H₀) was accepted which the means of every populations are all equal or not differ significantly and as a whole, no one of radiation workers in Malaysia exceeded the dose limit which is 20mSv/y from 2011-2013.

KEYWORDS: *occupational exposure; assessment; practices; trends.*

Advance Determination of Respiratory Protection Needs when Performing Destructive Work on Structural Materials

Scott Schwahn

Oak Ridge National Laboratory, Oak Ridge, TN, USA

Abstract. A frequent question posed to health physicists is what protective measures are required for drilling, grinding, welding, and cutting activated or contaminated structural materials. There are three questions that are involved in making the decisions: 1. Will there be significant contamination produced? 2. What Personal Protective Equipment (PPE) will be needed to protect the worker from contamination? 3. Will respiratory protection be required? Of the possible protective measures, respiratory protection is certainly the most cumbersome and can contribute to worker fatigue and heat exhaustion; it is also the most difficult of the three questions to be answered. At the Oak Ridge National Laboratory's Spallation Neutron Source, a standard approach was identified to easily determine whether or not respiratory protection will be needed based solely on dose rates from the materials. The previous approach was to make the determination on a case-by-case basis. While the results apply to standard activated materials around the proton accelerator (such as oils, plastics, concrete, aluminium, steel, and copper), the approach can be expanded to other materials and to non-accelerator environments where the radiological source term can be reasonably identified.

Reduction in Doses and Lung Cancer Risks among Canadian Uranium Miners between 1930s and 2013

Tristan Barr^a, Pascale Reinhardt^a, Patsy Thompson^a, Douglas Chambers^c, Ron Stager^c,
Occupational Cancer Research Center^b

^aCanadian Nuclear Safety Commission, Ottawa, Ontario, Canada

^bCancer Care Ontario, Toronto, Ontario, Canada

^cArcadis Senes Canada Inc., Richmond Hill, Ontario, Canada

Abstract. Since the 1930s, doses to Canadian radium and uranium miners have been drastically reduced due to continuous improvements in radiation protection practices. Lung cancer risk from exposure to radon decay products (RDPs) for modern miners is indistinguishable from that of the general population. In 2013, the average internal (0.05 Work Level Month (WLM) which is equivalent to 0.25 mSv) and external effective doses (0.53 mSv) were lower than the public dose limit (1 mSv). In the 1940s, the RDP exposures for Port Radium miners were ~400 WLM/y and higher. In the 1950s, RDP exposure limits (4 WLM) were introduced. Today's effective dose limit for workers is 50 mSv/year with the requirement to implement ALARA (as low as reasonably achievable). Improvements in ventilation, radiation protection practices, and engineered controls have contributed to significantly reduce the average annual RDP exposure to workers in modern mines. A recent update of the Ontario Uranium Miners (OUM) cohort found that the excess relative risk (ERR) for lung cancer incidence (1969-2005) and mortality (1954-2007) are respectively 0.63/100 WLM (95% CI: 0.42-0.84) and 0.64/100 WLM (95% CI: 0.42-0.86). This is lower than the ERR of 1.17/100 WLM (95%CI: 0.2-22.5) estimated by BEIR VI and of 0.89/100 WLM estimated in an earlier study for the same OUM cohort. A feasibility study conducted in 2003 using an ERR of 0.89/100 WLM predicted a single lung cancer mortality in 24000 modern miners (1975-2030). Repeating this study using the measured doses from 2001 to 2013 and the lowered ERR from the updated OUM would predict even fewer lung cancer mortalities. Current lung cancer risks to uranium miners are indistinguishable from the risks to the general Canadian population. This dramatic change in doses and concurrent lung cancer risks for today's miners demonstrates the remarkable effectiveness of the radiation protection framework in Canadian uranium mines.

Operational Health Physics Development Activities Related to Fast Reactor Fuel Fabrication and Pyro-Reprocessing

Ravi T, Akhila R, Krishnakumar D N, Rajagopal V, Jose M T, Venkatraman B, Satyamurthy S A V

Indira Gandhi Centre for Atomic Research, Kalpakkam, Kancheepuram, Tamilnadu, India

Abstract. The main objectives of the Radiochemistry Lab (RCL), at Indira Gandhi Centre for Atomic Research, is to develop advanced fuel fabrication methods, advanced methods of reprocessing, develop methodologies and to understand and predict the chemical behaviour of various types of nuclear fuels, fission products and structural materials through experimental measurements and modeling. The works include development of various types of fuel for the fast reactor and detailed studies related to its physico-chemical characterization. The study also extends to fuel behaviour through post-irradiation measurements and thermodynamic investigations. The feasibility of fuel reprocessing and the recovery of trans-plutonium elements by different methods are also investigated in this lab. Lab scale facilities are available for fabrication of advanced fuels of sphere-pac using sol-gel process and also for the fabrication of sodium bonded metallic fuel. There is a separate facility for the evaluation of spent fuel reprocessing by Pyro electrochemical method and also wet processing using different extractants. The fuel behaviour and characterization of U,Pu mixed oxide microspheres fuel test pins and sodium bonded U-Pu-Zr metal alloy fuel pins is done after irradiation at Fast Breeder Test Reactor. As many of the activities are unique and first of its kind, the radiological safety aspects to be considered are challenging. Health Physics experiences gained from the activities of the fabrication of these advanced fast reactor fuels, to pyro reprocessing for the recovery of transuranium from spent fuel, are outlined in this paper. These include work place monitoring, personnel monitoring, and environmental monitoring. As India is pursuing fast reactor program with various types of fuels such as mixed Pu-U carbides, PU-U oxides and metallic fuel with closed fuel cycle option, the knowledge derived from these laboratory scale operations would serve as valuable input for the proposed future fuel cycle facilities where operations involving large quantities of fissile materials would be handled.

The Information System on Occupational Exposure (ISOE): Trends and Lessons

Tae-Won Hwang^a, Olvido Guzman^b

^aKorea Hydro & Nuclear Power, Daejeon, Republic of Korea

^bOECD Nuclear Energy Agency, Paris, France

Abstract. Since 1992, the Information System on Occupational Exposure (ISOE) has supported the optimization of worker doses in nuclear power plants worldwide. A prerequisite for applying the principle of optimization to occupational radiation protection (ORP) is an appropriate and timely exchange of exposure data and operational experience on dose reduction methods. To facilitate this global approach to work management, the OECD Nuclear Energy Agency (NEA) launched the ISOE programme with the objective of providing a forum for radiation protection experts from nuclear electricity utilities and national regulatory authorities to discuss, promote and co-ordinate international co-operative undertakings for ORP of workers at NPPs. Since 1993, the International Atomic Energy Agency (IAEA) has co-sponsored the ISOE programme, thus allowing the participation from non-NEA member countries. Membership in the ISOE programme is open to nuclear utilities and to radiation protection regulatory authorities. Based on feedback as of June 2015, the ISOE programme included 76 Participating Utilities in 29 countries, and 22 Participating Regulatory Authorities/Organizations from 20 countries. The ISOE database itself contains information on occupational exposure levels and trends at 482 reactor units in 29 countries (401 operating; 81 in cold-shutdown or some stage of decommissioning) covering about 91% of the world's operating commercial power reactors. This paper will present the latest occupational exposure trends and exposure management focus of the world's nuclear power plant regulators and operators as of early 2016.

Protecting Humans and the Environment the Next Hundred Thousands of Years

Ulrik Kautsky, Eva Andersson, Tobias Lindborg, Anders Löfgren, Sara Nordén, Peter Saetre

Swedish Nuclear Fuel and Waste Management Co. (SKB), Stockholm, Sweden

Abstract. A major challenge for the assessment of nuclear waste repositories is to make estimates for the long time scales of 1000 to 100 000 of years. The Swedish Nuclear Fuel and Waste Management Co. (SKB) has recently handed in two applications for repositories. One for a high level repository for spent fuel and one for a low level waste repository for operational nuclear waste. In both assessments the knowledge of the past history of the sites, the last glaciation period to now, and the deduction from the ongoing processes are combined to produce an illustration of future landscapes. This includes variations in the natural ecosystem as well as potential land use of the ecosystems and the potential exposure to humans and the environment. The results from these applications give that humans can be exposed to a variation of several orders of magnitude depending at when and how long releases might occur to the surface. Both the site investigations and the assessment methodology use an ecosystem approach, which facilitates that exposure can be assessed for the environment and humans with the same tools and parameters. The ecosystem approach provides also a rigid framework to describe the conceptual understanding of the transport and fate of radionuclides as well as other toxicants in the area. The ecosystem approach provides that some transfer parameters can be estimated from natural processes rather e.g. empirical concentration factors which is important when addressing these very long time scales.

Assessment of Belarusian NPP for Protection of the Public

Viktoryia Kliaus

Scientific-Practical Centre of Hygiene, Minsk, Belarus

Abstract. The Republic of Belarus is a country embarking into a nuclear power programme. The decision was made to build an NPP which will consist of 2 power units of WWR-1200 reactors 3+ generation in the Ostrovets area Grodno region. The first power unit should start its operation in 2018, the second one – in 2020. The radiological environmental impact assessment was performed at the site selection and at the construction stages and included, among others, an assessment of doses to public in case of normal operation of the NPP and in case of potential emergencies. Transboundary impact to the population of neighbouring countries was also assessed. The result of dose calculation demonstrated that the maximum total effective dose from maximum permissible levels of atmospheric discharges in case of normal operation of the NPP will not exceed 0.2 $\mu\text{Sv}/\text{year}$ for 2 power units. That allowed establishing the Sanitary Protection Zone boundary within site area, based on the established value of dose constraint (100 $\mu\text{Sv}/\text{year}$). The monitoring zone was defined to be 12.9 km. For the assessment of possible consequences of potential emergencies two types of accidents were considered: design basis accident (DBA) and beyond design basis accident (BDBA). Total activities of the accidental releases were 1.1×10^{14} Bq and 1.5×10^{16} Bq respectively. The total effective dose and thyroid dose were estimated. It was found that after the DBA and BDBA at NPP there is no need for evacuation or providing shelter for the public because the highest values of total effective dose will not achieve currently recommended generic criteria (100 mSv in the first 7 days). However, in case of BDBA plans should be made to: recommend to the public to avoid eating potentially contaminated food or milk, perform an environmental monitoring and monitoring of food, water and fodder within 25 km from the NPP, provide food monitoring on the territory about 300 km around the NPP. Thyroid dose in case of BDBA will achieve international criteria (50 mSv in the first 7 days) at the distance 25 km from the site, so it will be a need to make a thyroid blocking. The same protective actions were recommended to the population of neighbouring country living in the vicinity of the NPP. The results of this study were used for the preparation of project documentation for Belarusian NPP.

Development of a Dose Assessment Code for the Radiation Protection of Representative Person in Korea

Won Tae Hwang, Eun Han Kim, Moon Hee Han, Hae Sun Jeong

Korea Atomic Energy Research Institute, Daejeon, Republic of Korea

Abstract. The 2007 recommendations of the International Commission on Radiological Protection (ICRP) have been published in which representative person for radiation protection of the public under the planned exposure situation is introduced. A more detailed description for its compliance has been given by the ICRP as well, but it is not easy task to define representative person because of variety in habits and diets of corresponding residents, and uncertainty in dose prediction. In the Korean regulations, radiological dose assessment of the public is based on maximum exposed individual approach according to the U. S. Nuclear Regulatory Commission (NRC)'s recommendations, although radiation protection quantities of the 1991 recommendations of the ICRP such as effective dose have been introduced. The development of a radiological dose assessment code with representative person approach is in process by taking into account the unique Korean habits and diets. In this manuscript, the authors discuss on how to determine representative person, on how to select a single value from uncertain socio- environmental data, and on how to approach mathematical modelling for major exposure pathways. In addition, comparison tests between a new code introduced representative person approach and a previous code introduced maximum exposed individual approach have been comprehensively carried out. This study would be helpful for the further improvement of the existing Korean regulation guidelines for radiation protection of the public in case of the routine discharge of radioactive materials.

Effect of Particle Size and Percentages of Boron Carbide on the Thermal Neutron Radiation Shielding Properties of HDPE/B₄C Composite: Experimental and Simulation Studies

Zahra Soltani^a, Farhood Ziaie^b

^aHealth Physics and Radiation Dosimetry Research Laboratory, Department of Energy Engineering and Physics, Amirkabir University of Technology, Tehran, Iran

^bRadiation Application Research School, Nuclear Science & Technology Research Institute, Tehran, Iran

Abstract. In this paper the effects of particle size and weight percentage of the reinforcement phase on the absorption ability of thermal neutron by HDPE/B₄C composites were investigated by means of Monte-Carlo simulation method using MCNP code and experimental measurement. The composite samples were prepared using the HDPE filled with different weight percentages of boron carbide powder in the form of micro and nano particles. The samples were subjected to thermal neutron radiation. Radiation shielding efficiency and thermal neutron cross section of the composite samples were investigated and compared with simulation results. According to the simulation, the composites with 2% of B₄C nano particles show the same ability to attenuate thermal neutron in comparison to the composites with 5% of B₄C in micron size. Therefore, to design and construct the shield materials, using the Boron Carbide in nano size form would recommend to have a high performance shielding along with the best safety against radiation. A good agreement was observed between the experimental and simulation results for the composite sample contained 5 wt% B₄C in micro and nano scale. Where, for the sample with 1 and 2 w% of B₄C a significant difference was arisen.